BB
001 II

APOLLO GUIDANCE
AND NAVIGATION NOTES

Part II

Notes 51-100
72, 99, 100 missing
VSM 4-29-65

APOLLO NOTES - PART II

TABLE OF CONTENTS

62.	Trans-Earth Injection Errors	L. Lustick/H. Engel
63.	DSIF Capability on Trans-Earth Trajectory	G. F. Floyd
64.	Capability of the DSIF for Determining In-Plane Orbit Parameters During Ascent	B. Saltzberg
65.	Determination of the Co-ordinates of an LEM on the Moon from DSIF Measurements from One Station	L. Lustick
66.	LLV Landing on a Tilted or Mountainous Lunar Surface	C. H. Dale
67.	Calculation of Covariance Matrices, I	H. Engel/J. Holdsworth
68.	Tracking Error Calculation	H. Engel
69.	An Approximate Technique to Arrive at the DSIF Smoothing Accuracy for Circular or Nearly Circular Orbits--Discussion of Numerical Results	H. Epstein
70.	The LEM as a Recovery Vehicle	H. Dale
71.	Selection of the Optimum Abort Trajectory	R. Roche
72.	The Calculation of Covariance Matrices, II	H. Engel
73.	Some Additional Error Calculations for Determining Three In-Plane Orbit Parameters from DSIF Doppler Measurements	B. Saltzberg
74.	Techniques for Remotely Aligning the LLV IMU from the Attached CM	C. H. Dale
75.	The Fuel Cost of Various Two Boost Ascents	C. H. Dale
76.	Notes on L. S. Pontryagin's Theory of Optimal Processes	L. Horowitz

77.	Calculation of Covariance Matrices for Multiple Uncorrelated Data Sources	J. Holdsworth
78.	DSIF Determination of LEM Altitude Rate	H. Engel
79.	An Approach to Estimating the Allowable Injection Errors for the DSIF Aided LEM Ascent and Rendezvous	C. H. Dale
80.	Correction to Calculation of Covariance Matrices I	J. Holdsworth
81.	Maximum Allowable Injection Errors for a Particular DSIF Aided Rendezvous Scheme	C. P. Siska
82.	Calculation of Covariance Matrices III	H. Engel
83.	Use of Range and Range Rate Data	H. Engel
84.	Notes on L. S. Pontryagin's Theory of Optimal Processes (II)	L. Horowitz
85.	The Equivalence of Data Processing Schemes in a Linearized Error Analysis	J. Holdsworth
86.	Optimal Control Through Hazardous Region in a 3-Dimensional Gravitational Field	L. Horowitz
87.	Rendezvous Aids	G. F. Floyd/H. Enge L. Lustick/C. Siska H. Epstein
88.	Kalman-Schmidt Method for Orbit Determination	Engel
89.	On the Numerical Computation of Optimum Controls	L. Horowitz
90.	Further Examination of Far-Side Relay Trajectories	C. Siska
91.	Minimum-Time Rendezvous	L. Horowitz
92.	Optimum Abort Trajectories	L. Horowitz

93.	Ground System Computation of LEM Orbit	H. Engel
94.	Use of Angle Data	H. Engel
95.	Ground Assistance to LEM, Including Mid-Course Correction	H. Engel
96.	Use of LEM/CM Observations	L. Horowitz
97.	Minimum Boost Velocity Requirement for Far-Side Relay	C. Siska
98.	Multiple Data Sources with Fixed Biases	H. Engel
99.	Preliminary Results of Computer Analyses	H. Engel
100.	Orbit Parameters From Three Stations Using Range and Range-Rate	H. Dale

APOLLO NOTE NO. 51

J. Holdsworth
24 April 1963

THE MAXIMUM LIKELIHOOD ESTIMATORS OF THE PARAMETERS APPEARING IN A CURVE FITTING PROBLEM WHEN BOTH OF THE OBSERVED VARIABLES ARE SUBJECT TO RANDOM ERRORS.

A functional relationship of known generic form is assumed to exist between two variables x and y. The form of the dependence between x and y will, in general, depend upon certain parameters $a_1, \ldots a_M$, thus allowing us to write:

$$y = f(x_i\, a_1,\ a_i, \ldots a_M)\ . \tag{1}$$

We shall assume that we have available a sequence of N observations made upon both the x variate and the y variate. That is, we assume that the available data is a sequence of N ordered pairs $(x_1,\ y_1), \ldots (x_N,\ y_N)$ where the number of data pairs N is assumed to exceed the number M of parameters necessary to specify the curvilinear relation between y and x.

Now if the pairs $(x_i,\ y_i)$ could be observed without error then M such pairs would theoretically suffice to exactly determine the parametric values $a_1, \ldots a_M$. However, the observed values in both x and y are assumed to be contaminated by random noise, thus our problem is to use our observed data in some maximally effective way so that we may obtain good estimates of our parameters.

More precisely we assume that the actual value of x which we observe at time i may be written:

$$x_i = \mu_{x_i} + \xi_i \tag{2}$$

where ξ_i is a zero mean stationary white gaussian process with known

variance σ_1^2, so that the mean value of an x observation made at time i is μ_{x_i} which would be the value actually observed in the absence of contaminating noise.

Similarly we assume that an observation of the y variate made of time i may be written as the sum of a mean component dependent upon the time i plus an error term η_i which is assumed to be a zero mean stationary uncorrelated gaussian noise process with known variance σ_2^2. Thus, we may write:

$$y = \mu_{y_i} + \eta_i \tag{3}$$

Now because of the distortion in our observations due to the noise, Equation (1) will not actually hold for all pairs of observed values x and y. Thus, Equation (1) must be considered a constraining equation relating the expected values of the observations y and x at a particular time i, thus we write:

$$\mu_{y_i} = f(\mu_{x_i}, a_1, \ldots a_M) \ . \tag{4}$$

Thus using Equations (3) and (4) we may write:

$$y_i = f(\mu_{x_i}, a_1, \ldots, a_M) + \eta_i \tag{5}$$

Now because of the uncorrelated nature of our noise sources we find that our data $(x_i, y_i) \ldots (x_N, y_N)$ actually constitute a set of 2 N independent observations whose likelihood function may be written:

$$L(x_i, y_i \mid \mu_{x_1}, \ldots, \mu_{x_N}, a_1, \ldots a_M) = \frac{1}{(2\pi)^N \sigma_1^N \sigma_2^N} \exp -\mathcal{L} \tag{6}$$

where

$$\mathcal{L} = \frac{1}{2\sigma_1^2} \sum_{i=1}^{N} (x_i - \mu_{x_i})^2 + \frac{1}{2\sigma_2^2} \sum_{i=1}^{N} \left[y_i - f(\mu_{x_i}, a_1 \ldots a_M) \right]^2 \tag{7}$$

Inspection of Equation (7) shows that the likelihood function depends upon the parameters $a_1, \ldots, a_M$ which we wish to estimate as well as upon the N unknown nuisance parameters $\mu_{x_1}, \ldots \mu_{x_N}$ in which we have no interest. This, however, is no problem --at least conceptually since the estimators $\hat{\mu}_{x_i}$, $\hat{a}_i$ are those functions of the data which minimize the expression $\mathcal{L}$. That is, we may proceed as though we were interested in estimating the M + N parameters $a_1, \ldots a_M$ and $\mu_{x_1}, \ldots \mu_{x_N}$ by solving the following system of M + N equations in M + N unknowns as functions of the observed data:

$$\frac{\partial \mathcal{L}}{\partial a_k} = 0 = \sum_{i=1}^{N} \left[y_i - f(\mu_{x_i}, a_1, \ldots a_M) \right] \frac{\partial f}{\partial a_k}$$

$$\text{for } k = 1, \ldots M \tag{8}$$

$$\frac{\partial \mathcal{L}}{\partial \mu_{x_i}} = 0 = \frac{1}{\sigma_1^2} (x_i - \mu_{x_i}) + \frac{1}{\sigma_2^2} \left[y_i - f(\mu_{x_i}, a_1, \ldots a_M) \right] \frac{\partial f}{\partial \mu_{x_i}} = 0$$

$$\text{for } i = 1, \ldots N \tag{9}$$

Thus, the simultaneous solution of the system given in Equation (8) allows one theoretically at least to solve for the maximum likelihood estimators of the parameters $a_1, \ldots a_M$ as functions of the observed data alone and not of the nuisance parameters $\mu_{x_1}, \ldots \mu_{x_N}$. Generally the system (Equation 8) will be a rather complicated system of nonlinear algebraic or transcendental equations; however, if digital computing facilities are available the solutions may be numerically obtained by the Newton Raphson method or by applying some other computational technique.

COMPUTATION OF THE ASYMPTOTIC COVARIANCE MATRIX OF THE PARAMETRIC ESTIMATORS

If one is interested in obtaining the covariance matrix of the estimators $\hat{a}_1, \ldots, \hat{a}_M$ then for large samples or long smoothing times

one may proceed in a manner very similar to that employed in Apollo Note No. 43; that is, we may apply a similar linearization technique. Since the technique involved is essentially the same as that employed in Apollo Note No. 43, the computation of the covariance matrix will be briefly sketched below.

As in Apollo Note No. 43, we shall write the estimators $\hat{a}_i$, $\hat{\mu}_{x_j}$ in the following form:

$$\begin{aligned} \hat{a}_i &= a_i + \Delta a_i \\ \hat{\mu}_{x_j} &= \mu_{x_j} + \Delta \mu_{x_j} \end{aligned} \tag{9}$$

In Equation (9) we are decomposing the estimators into the sun of two quantities one of which is the true parametric value, the other term representing the random error component of the estimator. Furthermore, we shall assume that we have a sufficient amount of data so that functions evaluated or expanded about $\hat{a}_i$, $\hat{\mu}_{x_i}$ depend upon the error quantities only up to terms of first order. Thus, we write:

$$f(\hat{\mu}_{x_i}, \hat{a}_1, \ldots, \hat{a}_M) = f(\mu_{x_i}, a_1, \ldots a_M) + \frac{\partial f}{\partial \mu_{x_i}} \Delta \mu_{x_i} + \sum_{k=1}^{M} \frac{\partial f}{\partial a_k} \Delta a_k \tag{10}$$

where the derivatives are evaluated at the parametric values.

Substituting Equation (10) into the system (8) and collecting terms yields the following system of M + N equations which is now a linear system in the random error quantities.

$$\sum_{j=1}^{M} \left(\sum_{i=1}^{N} \frac{\partial f_{(i)}}{\partial a_k} \frac{\partial f}{\partial a_j}(i) \right) \Delta a_j + \sum_{i=1}^{N} \frac{\partial f_{(i)}}{\partial a_k} \frac{\partial f}{\partial \mu_{x_i}} \Delta \mu_{x_i} = \sum_{i=1}^{N} \frac{\partial f_{(i)}}{\partial a_k} \eta_i$$

$$\text{for } k = 1, 2, \ldots M \tag{11a}$$

and

$$\frac{1}{\sigma_2^2}\ \frac{\partial f}{\partial \mu_{x_i}} \sum_{k=1}^{M} \frac{\partial f}{\partial a_k} \Delta a_k \qquad + \frac{1}{\sigma_1^2} + \left(\frac{1}{\sigma_2^2} \left(\frac{\partial f}{\partial \mu_{x_i}} \right)^2 \right) \Delta \mu_{x_i}$$

$$= \frac{1}{\sigma_1^2}\ \xi_i + \frac{1}{\sigma_2^2}\ \frac{\partial f}{\partial \mu_{x_i}}\ \eta_i$$

$$\text{for } i = 1, 2, \ldots N \qquad (11b)$$

Now the system of equations given by (11) is a system of M + N equations in the M + N error quantities $\Delta a_1, \ldots \Delta a_M, \Delta \mu_{x_i}, \ldots \Delta \mu_{x_N}$. However, as we have mentioned before the μ_{x_i} are nuisance parameters in which we have no interest. That is, we desire the covariance matrix of the parametric estimators of interest --not the covariance matrix of all M + N estimators including those of the nuisance parameters.

Fortunately the form of the system (11) allows us to reduce our M by N system of equations in M by N unknowns to a linear system of equations in the desired error terms $\Delta a_1, \ldots \Delta a_M$. To do this we use Equation 11b to write:

$$\Delta \mu_{x_i} = \frac{1}{\frac{1}{\sigma_1^2} + \frac{1}{\sigma_2^2} \left(\frac{\partial f}{\partial \mu_{x_i}} \right)^2} \left[\frac{\xi_i}{\sigma_1^2} + \frac{1}{\sigma_2^2} \frac{\partial f}{\partial \mu_{x_i}}\ \eta_i - \frac{1}{\sigma_2^2} \frac{\partial f}{\partial \mu_{x_i}} \sum_{k=1}^{M} \frac{\partial f}{\partial a_k} \Delta a_k \right] \qquad (12)$$

Substituting Equation (12) in (11a) we obtain the following system of M linear equations in the M random estimator errors $\Delta a_1, \ldots \Delta a_M$.

$$\sum_{j=1}^{M}\left\{\sum_{i=1}^{N}\frac{\partial f_{(i)}}{\partial a_k}\frac{\partial f_{(i)}}{\partial a_j}-\frac{1}{\frac{\sigma_2^2}{\sigma_1^2}+\left(\frac{\partial f}{\partial \mu_{x_i}}\right)^2}\left(\frac{\partial f_{(i)}}{\partial \mu_{x_i}}\right)^2\frac{\partial f_{(i)}}{\partial a_k}\frac{\partial f_{(i)}}{\partial a_j}\right\}\Delta a_j$$

$$=\sum_{i=1}^{N}\left[\frac{\partial f_{(i)}}{\partial a_k}-\frac{1}{\frac{\sigma_2^2}{\sigma_1^2}+\left(\frac{\partial f}{\partial a_{x_i}}\right)^2}\frac{\partial f_{(i)}}{\partial \mu_{x_i}}\right]\eta_1$$

$$-\sum_{i=1}^{N}\frac{\xi_i}{1+\frac{\sigma_1^2}{\sigma_2^2}\left(\frac{\partial f}{\partial \mu_{x_i}}\right)^2}$$

for $k = 1, 2, \ldots M.$ (13)

Note that in Equation (13) we have essentially uncoupled the estimator equations from those involving the nuisance parameters. Again for manipulative convenience we employ matrix notation and write

$$C\,\Delta a = e \tag{14}$$

where Δa and e are M dimensional column vectors and C is an M + N matrix whose elements may be inferred by inspection of the system (13).

For non-singular C we may solve for the estimator error vector and write:

$$\Delta a = C^{-1}\, e \tag{15}$$

Taking the transpose of (15) and using the symmetry of the matrix C we have:

$$\Delta a^T = e^T\, C^{-1} \tag{16}$$

Premultiplying Equation (16) by Equation (15) yields

$$\Delta a \ \Delta a^T = C^{-1} (e \ e^T) C^{-1} \tag{17}$$

Finally as in Apollo Note No. 43, the covariance matrix of the estimators is given by taking the expected value of both sides of the matrix relation (17) or:

$$\text{Cov} (\Delta a \ \Delta a^T) = C^{-1} \ E (e \ e^T) \ C^{-1} \tag{18}$$

Since C is a known matrix, then from (18) we see that it only remains to compute the matrix $E \left[e \ e^T \right]$.

First consider a diagonal term say e_{kk} of $e \ e^T$. Then:

$$e_{kk} = \left\{ \sum_{i=1}^{M} \left[\left(\frac{\partial f_{(i)}}{\partial a_k} - \frac{1}{\frac{\sigma_2^2}{\sigma_1^2} + \left(\frac{\partial f}{\partial \mu_{x_i}} \right)^2} \ \frac{\partial f}{\partial \mu_{x_i}} \right) \eta_i - \frac{\xi_i}{1 + \frac{\sigma_1^2}{\sigma_2^2} \left(\frac{\partial f}{\partial \mu_{x_i}} \right)^2} \right] \right\} \tag{19}$$

Then taking the expected value of both sides of Equation (19) and recalling that ξ_i, η_i are white noise processes which are not cross-correlated we have:

$$E (e_{kk}) = \sum_{i=1}^{N} \left(\frac{\partial f_{(i)}}{\partial a_k} - \frac{1}{\frac{\sigma_2^2}{\sigma_1^2} + \left(\frac{\partial f}{\partial \mu_{x_i}} \right)^2} \ \frac{\partial f}{\partial \mu_{x_i}} \right)^2 \sigma_2^2$$

$$+ \sum_{i=1}^{N} \frac{\sigma_1^2}{\left(1 + \frac{\sigma_1^2}{\sigma_2^2} \left(\frac{\partial f}{\partial \mu_{x_i}} \right)^2 \right)^2} \tag{20}$$

Similarly for an off diagonal from say e_{k_j} where $k \neq j$ we have:

$$e_{k_j} = \left\{ \sum_{i=1}^{M} \left[\left(\frac{\partial f_{(i)}}{\partial a_k} - \frac{1}{\frac{\sigma_2^2}{\sigma_1^2} + \left(\frac{\partial f}{\partial \mu_{x_i}} \right)^2} \frac{\partial f}{\partial \mu_{x_i}} \right) \eta_i - \frac{\partial f}{\partial \mu_{x_i}} \frac{\xi_i}{1 + \frac{\sigma_1^2}{\sigma_2^2} \left(\frac{\partial f}{\partial \mu_{x_i}} \right)^2} \right] \right\}$$

$$+ \left\{ \sum_{i=1}^{M} \left[\left(\frac{\partial f_{(i)}}{\partial a_j} - \frac{1}{\frac{\sigma_2^2}{\sigma_1^2} + \left(\frac{\partial f}{\partial \mu_{x_i}} \right)^2} \frac{\partial f}{\partial \mu_{x_i}} \right) \eta_i - \frac{\xi_i \frac{\partial f}{\partial \mu_{x_i}}}{1 + \frac{\sigma_1^2}{\sigma_2^2} \left(\frac{\partial f}{\partial \mu_{x_i}} \right)^2} \right] \right\} \tag{21}$$

so that the white nature of the noise processes allows us to write:

$$E(e_k e_j) = \sum_{i=1}^{N} \left(\frac{\partial f_{(i)}}{\partial a_k} - \frac{1}{\frac{\sigma_2^2}{\sigma_1^2} + \left(\frac{\partial f}{\partial \mu_{x_i}} \right)^2} \frac{\partial f}{\partial \mu_{x_i}} \right) \left(\frac{\partial f_{(i)}}{\partial a_j} - \frac{1}{\frac{\sigma_2^2}{\sigma_1^2} + \left(\frac{\partial f}{\partial \mu_{x_i}} \right)^2} \frac{\partial f}{\partial \mu_{x_i}} \right) \sigma_2^2$$

$$+ \sum_{i=1}^{N} \left(\frac{\sigma_1}{1 + \frac{\sigma_1^2}{\sigma_2^2} \left(\frac{\partial f}{\partial \mu_{x_i}} \right)^2} \right)^2 \left(\frac{\partial f}{\partial \mu_{x_i}} \right)^2 \tag{22}$$

Thus, finally Equations (21) and (22) give the expressions for the elements of the matrix $E\left[e\, e^T \right]$ as an explicit function of the noise variances and other known quantities. Hence, since the coefficient matrix C is deterministic and known then C^{-1} may be computed and Equations (18), (20) and (22) allow the explicit determination of the asymptotic covariance

matrix of the relevant parameters in the curvilinear relation

$$\mu_y = f(\mu_x, a_1, \ldots a_M). \tag{23}$$

It is perhaps worthwhile noting that the parametric estimators are not necessarily the same as those obtained using a traditional least squares procedure, which is often done in the case where only one observed variate is corrupted by noise. However, if the noise variances are equal and the functional dependence upon the parameters linear, then our estimators are least squares estimators.

It might also be worthwhile to point out that there is nothing sacrosanct about least squares estimators and that from a certain point of view the appropriateness of least squares estimation hinges upon the fact that under certain conditions they turn out to be maximum likelihood estimators or else very closely related to them.

APOLLO NOTE NO. 52

R. Harte/ S. Cushner
24 April 1963

THE USE OF AN EARTH TRACKER FOR EARTH CONTROLLED NAVIGATION AND GUIDANCE OF THE CM VEHICLE IN SEVERE ABORT SITUATIONS

Star-field video transmission has been considered as a method of locating the CM Vehicle and directing its guidance back to earth. Another method of guidance would be the use of an Earth Tracker.

In particular, it is suggested that the earth sensor be a silicon P-N junction device which makes use of lateral photocurrents flowing parallel to the P-N junction rather than the conventionally used transverse currents.

A uniform spot of light focused on the center of the cell produces zero voltage output. Displacement in the x or y axis creates a voltage at the x or y terminals proportional to the degree of displacement.

The device is considered an infrared detector since its peak sensitivity occurs at 0.8μ. About 30 percent of its response, however, falls in the visible portion of the spectrum.

According to manufacturers' specifications, it has a noise equivalent power of 4×10^{-10} watts for a five cycle bandwidth with a 5μ second time constant.

If a zoom type of lens is utilized with varying focal lengths, the field of view can be enlarged to acquire the earth. Once acquisition has been achieved, narrowed fields of view will allow more accurate lock on.

THE TARGET

The earth receives from the sun 0.13 watts/cm^2, which is absorbed and scattered in the atmosphere. The earth's albedo indicates that only 40 percent is reflected and re-radiated into space. Of this

.052 watts cm^{-2}, only 30% fall in the visible and near infrared portions of the spectrum in which the silicon detector operates. Thus, the source radiates .0156 watts cm^{-2}. Treated as a flat circle, radiating into a hemisphere, the energy received in the vicinity of the moon is

$$E = \frac{I T_A A_E}{2\pi R^2}$$

where

I = .0156 watts cm^{-2}

T_A = Transmission of Translunar Space = 1.0

A_E = Area of Earth facing the moon = 1.2×10^{18} cm^2

R = Mean Earth-Moon distance = 3.75×10^{10} cm

$\therefore$ $E = 2.1 \times 10^{-6}$ watts/cm^2

If the lens is a 2" diameter, 2" focal length F/1 system, then the collector area is about 20 cm^2 and 4.2×10^{-5} watts are collected onto the detector. The field of view is 45^o, which should locate an object of 2^o diameter with minimum search.

Since the NEP is approximately 4×10^{-10} watts, the area is approximately 1 cm^2 and we will assume a modulating frequency of 1600 cycles/second. Since a mechanical chopper is not desirable, the electrical output could be commutated and then AC amplified.

$$\text{The system NEP} = \text{cell NEP} \times \sqrt{A\,\Delta F}$$

$$\therefore \quad \text{System NEP} = 40 \times 4 \times 10^{-10} = 1.6 \times 10^{-8} \text{ watts}$$

Thus, the S/N of the full earth is $\frac{4.2 \times 10^{-5}}{1.6 \times 10^{-8}} = 2.6 \times 10^{3}$.

If the earth is in phase, the intensity is reduced as a function of phase angle. Assuming the earth to be a Lambertian diffuse reflector, rather than a back scatterer like the moon, we can assume a regular function and plot S/N as a function of the earth's phase.

Referring to Figure 1., 0^{o} represents the position of new earth, 90^{o} is equivalent to first quarter, and 180^{o} to full earth.

The largest errors in reading the center of earth position, would occur when the earth is in a narrow crescent phase. One day after "new earth," the energy from the crescent is sufficient to give a S/N of over 100 (See Figure 1.). The location of earth's center, however, would be in error by almost an earth's radius. Fortunately, this is about 1^{o}. We can safely say, therefore, that the maximum error achieved in this arrangement is slightly less than 1^{o} or 17 milliradians.

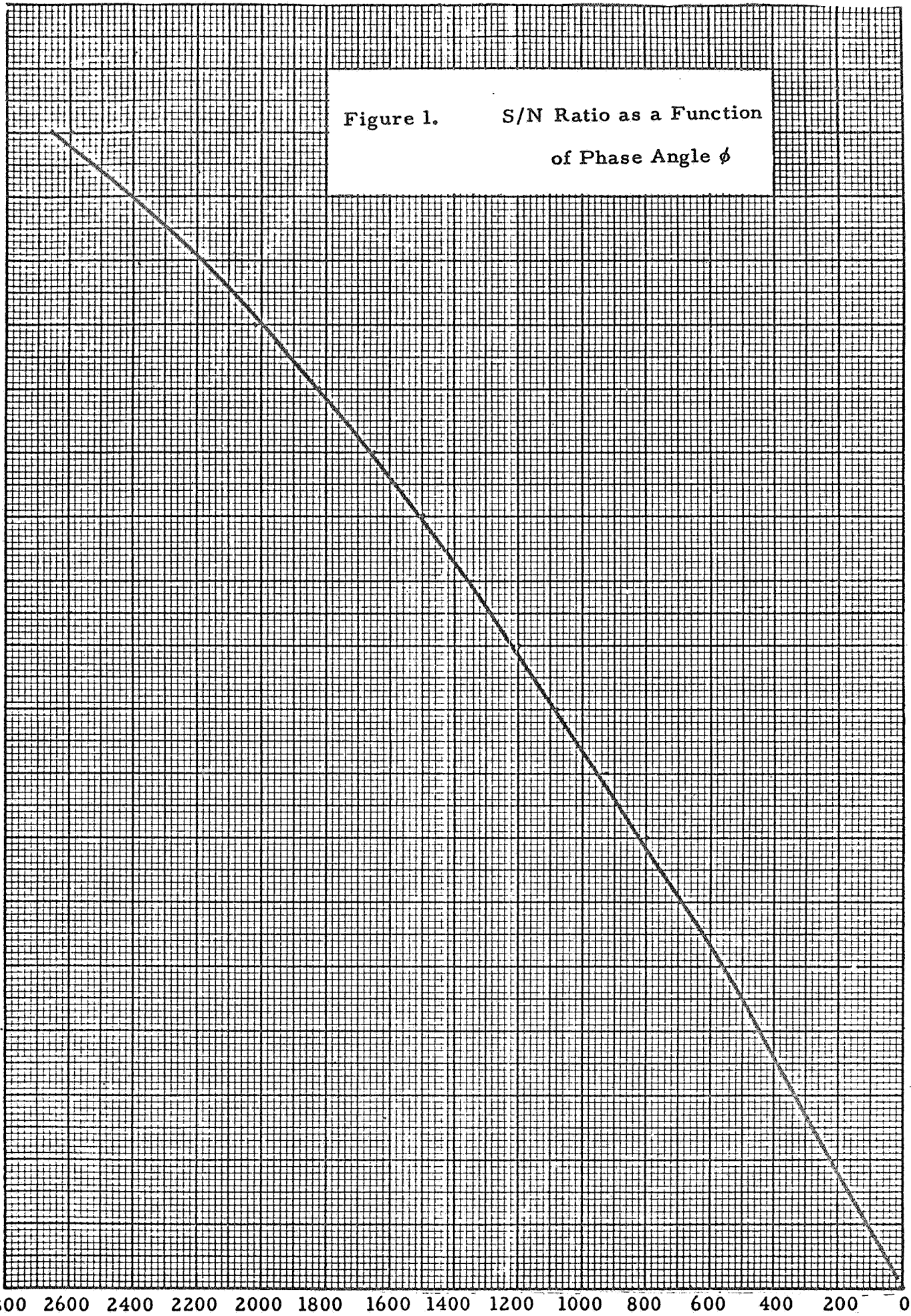

Figure 1. S/N Ratio as a Function of Phase Angle ϕ

APOLLO NOTE NO. 53

G. F. Floyd
25 April 1963

EMERGENCY RE-ENTRY WITH ZERO-LIFT

This note is a reprint of the first part of a paper by Eugene F. Styer of Boeing Airplane Company (Proceedings of the Third Annual West Coast Meeting of the American Astronautical Society), and represents the best summary found by Bissett-Berman of this problem.

As shown, there is a $0.7^{\circ} = \pm .35^{\circ}$ spread between tolerable deceleration and tolerable range dispersion. Therefore, a 1 σ error of $\pm 0.1^{\circ}$ will give a .99% safe zero lift re-entry.

A PARAMETRIC EXAMINATION OF RE-ENTRY VEHICLE SIZE AND SHAPE FOR RETURN AT ESCAPE VELOCITY

*Eugene F. Styer**

The ballistic re-entry vehicle is examined for use in Earth return missions originating from a high geocentric orbit, the Moon or another planet. The acceleration tolerance limit and the minimum angle for direct entry are discussed for various values of the ballistic coefficient. Multiple-pass entry is shown to widen the entry corridor at the expense of time in orbit. The use of a side firing rocket is proposed for "steering" within the entry corridor. Aerodynamic heating, entry loads, and Van Allen radiation are considered for their effect on vehicle design. Preliminary design estimates are given for the weights of a range of ballistic entry bodies designed for direct entry. These vehicles are postulated to return from a space station with one, 10 and 50 astronauts. Selected comparisons are made of the weights of vehicles required to return 10 men to Earth by direct, propulsion braking, and multiple pass techniques.

Introduction

A great deal of attention has been directed at the very complex problem of the return to Earth of a man placed into a near orbit. In this country, the Mercury ballistic re-entry program is in the flight-test stage, and the Dyna-Soar glide re-entry program is well advanced in concept and design.

The implementation of deep space systems will require an extension of our re-entry technology to provide for all missions—military, scientific and commercial. A salient characteristic of return from high Earth orbits, the Moon, and other planets, is that this return is accomplished at or near the Earth's escape velocity—a 40 per cent increase in velocity over the near orbit re-entry case. The Van Allen belts, solar, and cosmic radiations, meteorites, and the hard vacuum of space present added environmental hazards to men and materials.

Some ways of accomplishing superorbital re-entry are diagrammed in Fig. 1. The kinetic energy of the returning vehicle can be dissipated by atmospheric braking in one or several passes, or by the application of propulsion braking. These methods apply with equal validity to ballistic and lifting vehicles.

Much valid attention has been drawn to the use of lifting vehicles for re-entry due to their inherent ability to fly to and land at a specific spot.[1] There are a number of space missions, however, where the lower gross weight and simplicity of a ballistic vehicle will recommend its use.

Strong consideration will be given to the ballistic vehicle for early operations because of limited booster capability and also because of the significantly more complex structural and flight control problems connected with

*Structures Technology Department, Boeing Airplane Company, Aero-Space Division, Seattle, Wash.

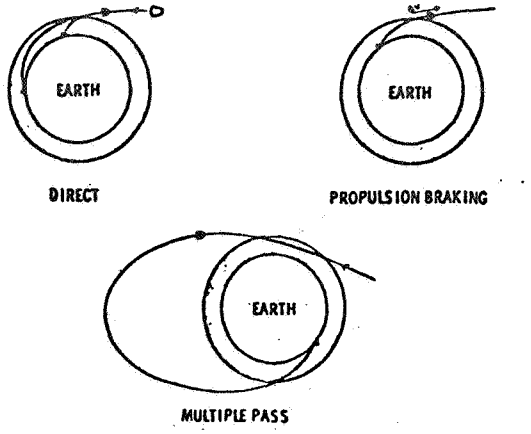

Fig. 1. Methods of re-entry.

glide re-entry. Even when re-entry from space becomes a more established fact, the simplicity, small size, lower weight, and resultant economic advantage of the ballistic or very low L/D vehicle will dictate its use for certain applications. A schematic representation of such a vehicle is shown in Fig. 2.

The present paper indicates design conditions, re-entry weights, and some of the operational factors of manned ballistic vehicles. Preliminary designs and weights are developed for vehicles having capacities of one, 10, and 50 men entering at several values of the ballistic coefficient, $W/C_D A$. These vehicles are compared on the basis that no allowance is made in vehicle layout for equipment or expendables other than that essential to safe entry and touchdown. This series of vehicles is visualized as "shuttle buses" rather than self-contained units for long duration space missions.

Entry Corridor Criteria

Entry limits can be stated in terms of entry angle at a given altitude, where the entry angle (measured positive downward) is the angle between the

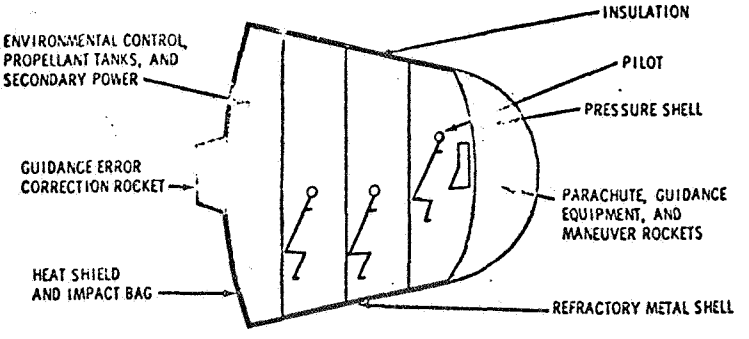

Fig. 2. Entry vehicle.

flight path and local horizontal. Limitations to direct entry are set by vehicle "skip" from the atmosphere, acceleration tolerance of the crew, and structural heating. The minimum entry angle γ_E for direct entry is shown on Fig. 3 as a function of entry velocity and ballistic coefficient. Trajectory data are based on the 1959 ARDC Model Atmosphere,[2] spherical nonrotating Earth, and were obtained by IBM 704 solutions of the entry trajectory equations.[3] Re-entry is defined as starting at an altitude of 400,000 ft. The limiting entry or "skip" angles shown on Fig. 3 are those for which the vehicle will enter and pass through the atmosphere, "climb" back to 400,000 ft and then proceed to touchdown.

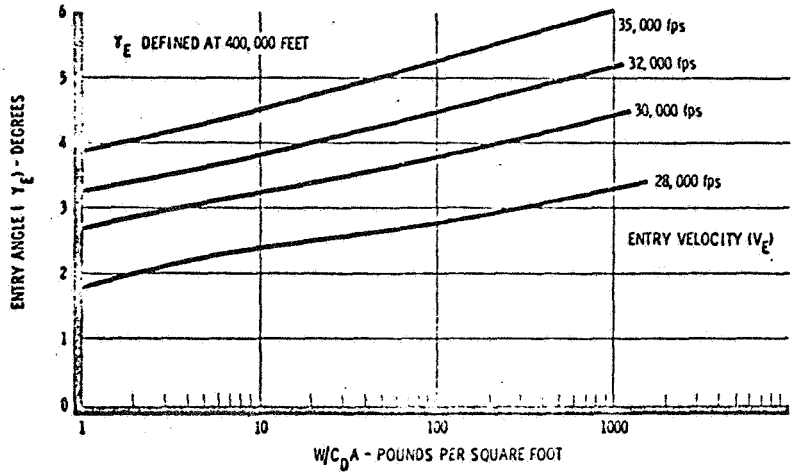

Fig. 3. Minimum angle for direct entry.

The maximum entry angle is dictated by tolerable acceleration when the vehicle design can withstand the accompanying extreme heating rates. Figure 4 illustrates the tolerance limits of magnitude and time of exposure to various g levels where the acceleration vector is oriented as shown.[4] A tolerance limit is very difficult to establish due to the large differences in individual reaction to acceleration. The data shown is for healthy, young males who could be expected to see, think, and exercise at least finger control within the limit shown. It is pertinent here to note that the requirements placed on the pilots for manipulation of controls and equipment monitoring during entry are directly related to the acceptable acceleration level. Relatively passive descent in a ballistic capsule can be accomplished in a more severe acceleration environment than the flying in of a lifting vehicle. The upper curve of Fig. 4 was selected as representative of the acceleration-time history above which irreparable damage would be done to humans.[5]

Multiple-pass entry involves initial atmospheric contact at shallower angles than those shown in Fig. 3. The shallower the angle, the more passes

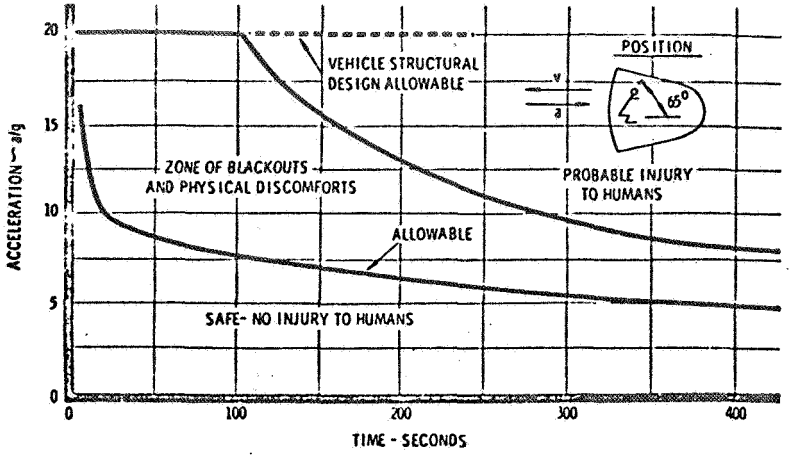

Fig. 4. Acceleration tolerance.

to eventual impact, if the vehicle is left to drag down passively. Should the multiple pass vehicle be designed for the maximum angle (acceleration) conditions noted above, its entry corridor is widened relative to direct entry. The operational factors of guidance accuracy, time of flight, radiation exposure and landing-site predictability would have to be considered in making a selection of the mode of entry which is best for a particular mission.

Trajectory Considerations

For the purposes of this paper, it is assumed that the inertial guidance system in the vehicle has a possible accumulated error of ±0.5 deg from the desired entry angle just prior to entry, and that the system reference can be updated when nearing the Earth to allow prediction of the entry angle to within 0.05 deg (±0.025 deg).

Redirection of the vehicle's velocity vector to an angle within the desired corridor is accomplished with a single rocket which can be fired in any direction, by rotating the vehicle. Due to the 0.05 deg uncertainty in angle, the entry body must not be steered within 0.025 deg of the corridor limits. Operation of the vehicle in this manner will allow the pilot to select an area on the Earth compatible with his entry corridor limits and position information displayed from his guidance system.

Figure 5 illustrates the effect of entry angle on the entry time which becomes important for ablation and heat sink structural systems whose weight increases with entry time. For direct entry, the trajectory is extremely sensitive near minimum γ_E. For example, a change in entry angle of 0.02 deg will change entry time by a factor of 5, and increase total heat by about 50 per cent for a representative vehicle.

No attempt will be made in this paper to present a complete landing-dispersion analysis, but Fig. 6 illustrates the dispersion in miles for the noted

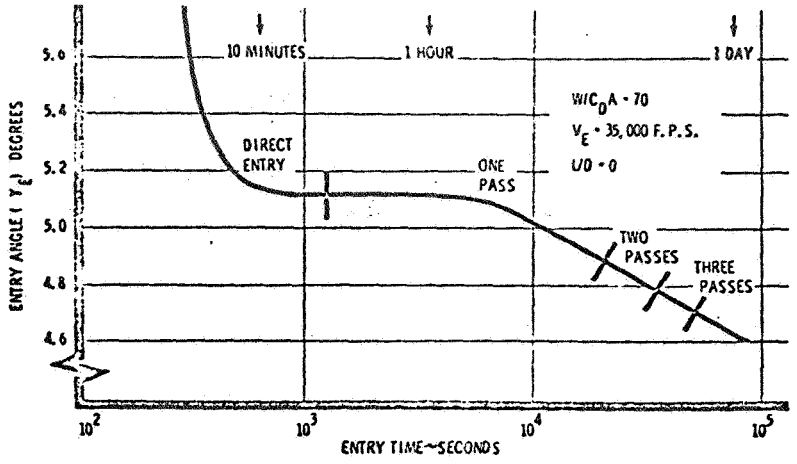

Fig. 5. Entry time.

terminal guidance errors. The dispersion sensitivity is seen to increase greatly toward the skip limit.

The time of flight, heating, and range dispersion sensitivity near the theoretical skip limit suggest an operational procedure whereby a design skip angle would be defined about 0.05 deg steeper than the theoretical skip angle. As an example, Fig. 3 shows a theoretical skip angle of 5.15 deg for V_E = 35,000 ft/sec and $W/C_D A = 70$; the proposed design skip angle would be 5.2 deg.

Figure 7 illustrates the entry corridor for ballistic vehicles entering at 35,000 ft/sec. Shown are the 20-g human damage limit, the acceleration tolerance limit, and the design skip limit which define the corridor within which direct

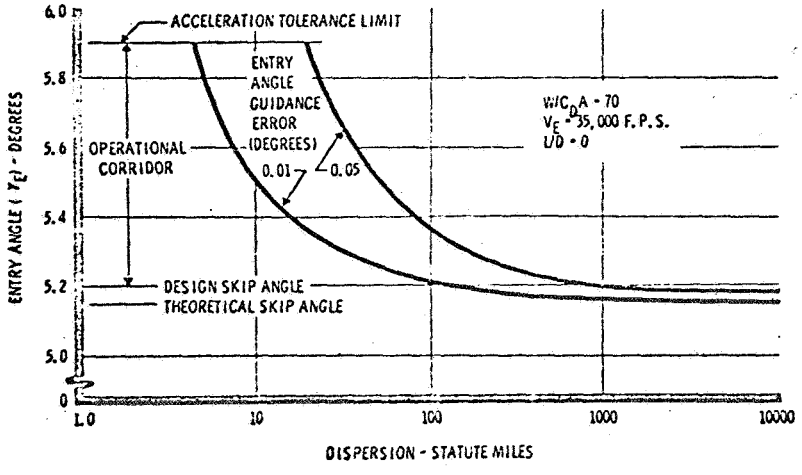

Fig. 6. Landing dispersion.

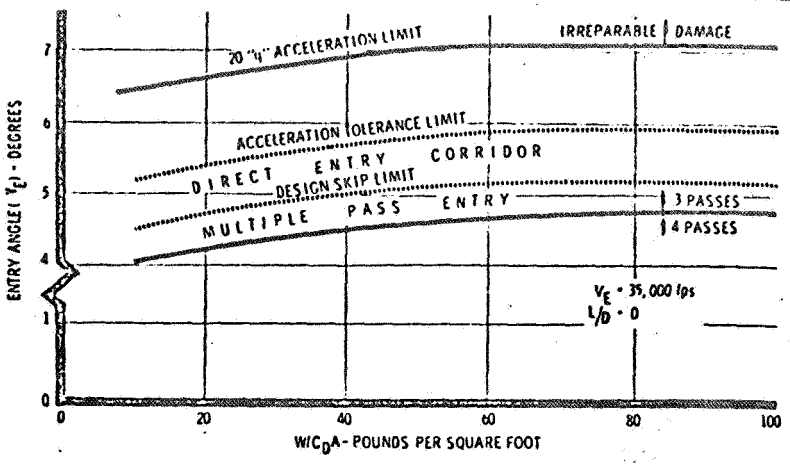

Fig. 7. Entry corridor.

entry vehicles can operate. The operational direct entry corridor is seen to be about 0.7 deg wide.

An entry corridor of 0.7 deg might seem to present a formidable navigation job; however, recent papers[6,7] indicate that extensions of present-day techniques will not only permit such entry but offer the possibility of navigation within the corridor, as mentioned above. For example, a one-mile CEP for a 5000-mi-range ballistic vehicle requires angular flight path control to ±0.014 deg.[6]

Also shown on Fig. 7 are the entry angles which define the boundary between three and four passes around the Earth before landing. For a $W/C_D A = 70$, a manned vehicle designed to operate between the acceleration tolerance limit and the four pass limit has an operational corridor of 1.2 deg.

Structural heating can define corridor limits when the peak heating rate, total heat, or particular heating history are critical factors due to weight, material availability, or processing restrictions.

Figure 8 indicates the limits to range control, measured from start of entry, for a specific ballistic vehicle making a direct entry. This figure shows that the range may be varied from a minimum of 900 mi at the maximum entry angle to 2040 mi for minimum γ_E. The maximum dispersions associated with these two ranges are 20 and 700 mi, respectively, for a guidance error of 0.05 deg, and 4.5 and 125 mi for an error of 0.01 deg.

Two typical sets of velocity, altitude and deceleration plots are shown as a function of entry time in Figs. 9 and 10. Figure 9 is for $\gamma_E = 5.2$ deg, the design skip limit, and Fig. 10 is for $\gamma_E = 5.9$ deg, the acceleration tolerance limit. The shallow entry takes about 500 sec and has the characteristic two deceleration peaks and tendency to "climb" back out of the atmosphere. The steep entry, on the other hand, takes about 250 sec, has a single (higher) deceleration peak and a steadily decreasing altitude-time history. Shown for reference on Figs. 9 and 10 is the allowable g versus time curve taken from

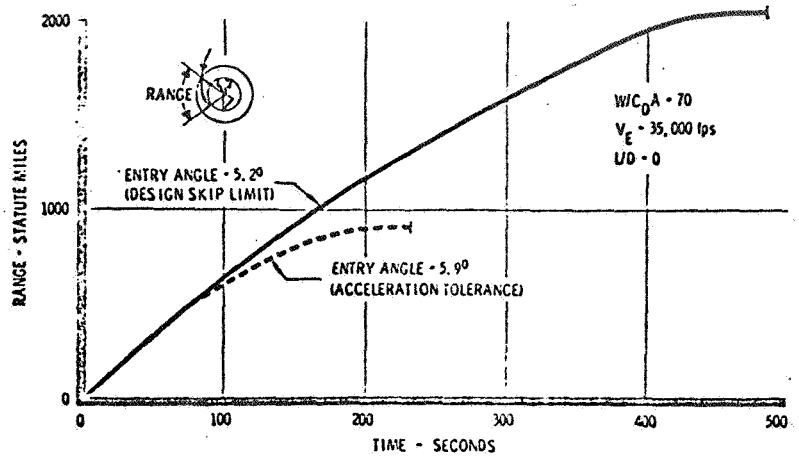

Fig. 8. Entry range.

Fig. 4. As indicated on Fig. 10, limit acceleration occurs at a value less than the peak.

It should be noted that the standard 1959 ARDC Model Atmosphere is used throughout this paper. At the present time an imperfect picture of daily, seasonal and random atmospheric variation exists. Actual re-entry operations will have to consider these variations both from the standpoint of their closer prediction and by allowance in vehicle design.

Aerodynamic Heating

A number of structural schemes are possible for solving the aerodynamic heating problem of a ballistic body decelerating from escape velocity. In general, these can be classed as heat rate systems and total heat systems.

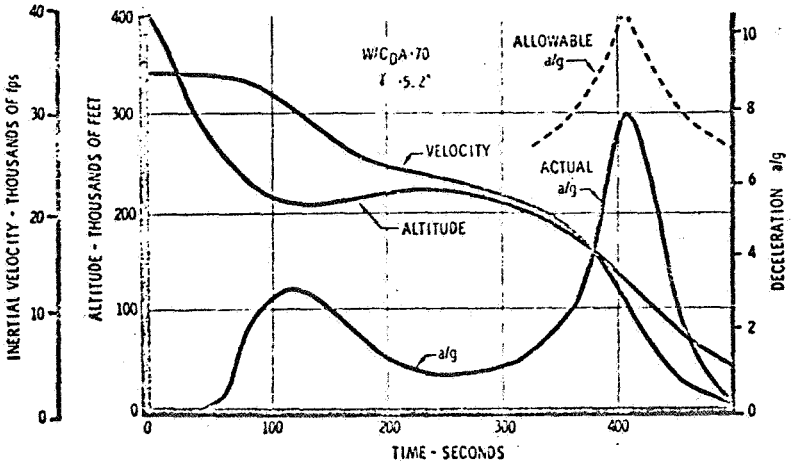

Fig. 9. Design skip limit trajectory.

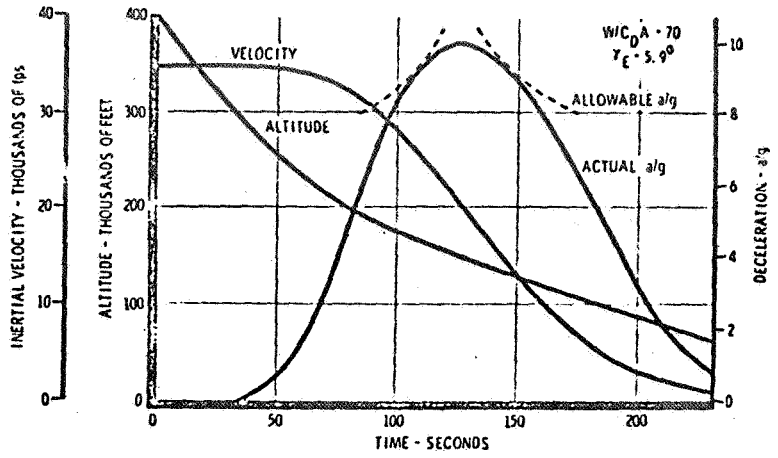

Fig. 10. Acceleration tolerance trajectory.

In the former, a structural material is needed to withstand the surface radiation equilibrium temperature associated with the highest heating rate. The 20-g trajectory would subject the re-entry body to the most severe heating rates. The high temperature outer skin would have to be backed up with insulation (and internal cooling) to provide a workable interior environment.

The total heat system would use a heat-sink material such as beryllium, or ablation materials such as polyethylene or Teflon, to protect the vehicle. For heat-sink materials, the shield is designed so that the integrated heating does not subject the material to excessive surface temperatures. In an ablation system, material is consumed in absorbing the integrated heat load. In both cases the design condition occurs for the long-time trajectory, which is at the design skip limit for direct entry. It should be noted that a very high temperature ablation material, such as quartz, rejects much heat by reradiation and the appropriate design condition may not be the long-time trajectory.

Figure 11 shows the variation of drag coefficient, average heat transfer, and total heat as a function of the nose angle ϕ. Total heating is seen to be minimized for a ϕ of about 20 deg and all vehicles considered in this paper were designed at this point. Heating-rate estimates are based on the methods of Fay and Riddell[8] with some modifications.[9] The aerodynamic heating shown here is convective heating only. Gas-cap radiation for the shapes considered is unimportant at the high altitudes where manned vehicle deceleration takes place.

The major heating problem for the ballistic shape is the heat shield. The conical capsule wall is also subjected to heating. This region is much less severely heated than the heat shield and can be protected by thermal radiation equilibrium cooling.

Ionizing Radiation Considerations

It is desirable at this time to consider the structural requirements for protecting the occupants from Van Allen radiation. Much further definition of the

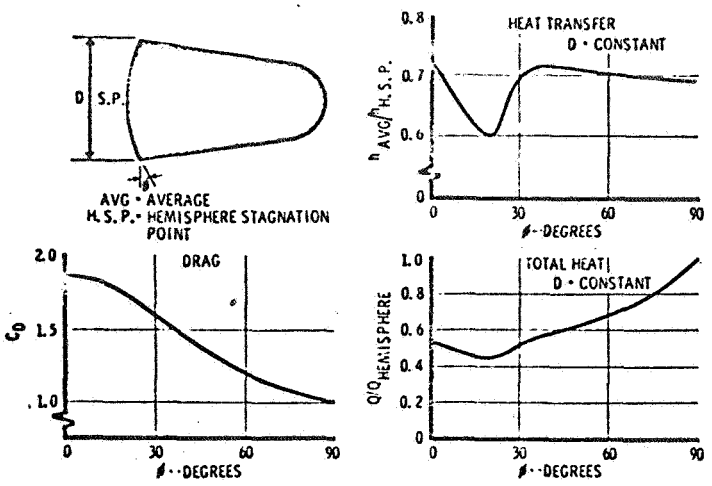

Fig. 11. Entry heating.

type and distribution of this radiation is needed, but preliminary design estimates can be made.

As is well known, the basic data which defined the existence and somewhat the composition of the radiation belts were radiation counter measurements taken by Earth satellites.[10] The radiation contours[10,11] presented by Dr. Van Allen were derived from data taken by a counter shielded with an average value of 1 gr/cm^2. This amount of shielding corresponds to the range of 30 Mev protons. Dr. Van Allen proposes an inner belt spectra[11] which includes a proton flux of 20,000 particles/cm^2-sec having an energy greater than 40 Mev. The outer belt is assumed to be chiefly electrons whose biological significance is low.[13]

Based on the work of Van Allen and others, a differential energy spectra of protons was prepared for the inner belt and shielding requirements estimated.[12,13] The maximum dose rate measured by an unshielded small detector was estimated as 70 rad/hr, which when converted by the RBE (Relative Biological Effect) compatible with the radiation spectra leads to a free-space dose rate of about 440 rem/hr.[13] Shielding requirements included a consideration of Bremsstrahlung energy due to electron flux. These estimates formed the basis of shielding requirements used for the vehicles in this paper.

The above considerations lead to a free-space dosage of 172 rem for a direct entry in the geomagnetic equatorial plane. Shielding, in addition to vehicle structure, needed to reduce whole body dosage to about 12 rem for a direct entry was estimated as 0.2 in. of polyethylene. A thickness of 0.5 in. of polyethylene would reduce the dosage to 6 rem. For comparison, the AEC acceptable emergency exposure is 25 rem, and a proposed one-day maximum exposure is 50 rem.[14]

Inclination of the entry orbit plane with respect to the geomagnetic equator can effect a substantial reduction in total dosage. Figure 12 illustrates this in terms of small detector (free air) dosage for an entry which makes one elliptical pass through the inner Van Allen belt.

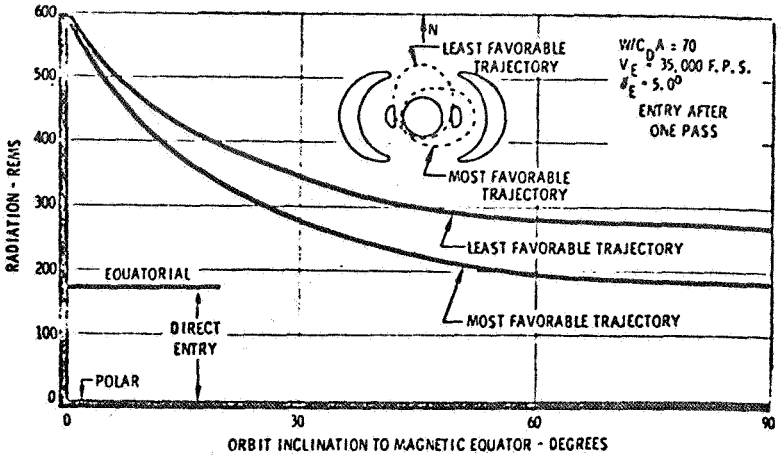

Fig. 12. Van Allen radiation.

REFERENCES

1. Hildebrand, R. B., "Manned Re-Entry at Super-Satellite Speeds," IAS Preprint 60-83, June, 1960.

2. Minzner, R. A., Champion, K. S. W., and Pond, H. L., "The ARDC Model Atmosphere," AFCRC-TR-59-267, Aug., 1959.

3. Jacobsen, W. E., "Determination of Re-Entry Trajectories for Vehicle Structure Evaluation," Structural Analysis Research Memorandum No. 9, Boeing Airplane Company, Jan., 1960.

4. Bondurant, Stuart *et al*, "Human Tolerance to Some of the Accelerations Anticipated in Space Flight," WADC TR 58-156, Apr., 1958.

5. "Space Handbook: Astronautics and Its Applications," House Document No. 86, 86th Congress, 1st Session, 1959.

6. Chapman, Dean R., "An Analysis of the Corridor and Guidance Requirements for Supercircular Entry into Planetary Atmospheres," NASA TR No. R-55, 1959.

7. Freeman, George W., "Limit Cycle Efficiency of On-Off Reaction Control Systems," IAS National Specialists Meeting on Guidance of Aerospace Vehicles, Boston, Mass., May, 1960.

8. Fay, J. A. and Riddell, F. R., "Theory of Stagnation Point Heat Transfer in Dissociated Air," *J. Aero. Sci.*, Feb., 1958.

9. "Handbook for Aerodynamic Heat Transfer Computation, Vol. I.," Document No. D2-5107, Boeing Airplane Company, Jan., 1960.

10. Van Allen, James A., and Frank, Louis A., "Radiation Around the Earth to a Radial Distance of 107,400 KM," *Nature*, Vol. 183, No. 4659, Feb. 14, 1959, p. 430.

11. Van Allen, James A. and Frank, Louis A., "Radiation Measurements to 658,300 KM with Pioneer IV," *Nature*, Vol. 184, No. 4682, July 25, 1959, p. 219.

12. Noyes, J. C. and Brown, W. D., "Shielding Requirements for Radiation Belt Particles," Report No. D1-82-0048, Geo-Astrophysics Laboratory, Boeing Scientific Research Laboratories, Jan., 1960.

13. Dye, D. L. and Noyes, J. C., "Biological Shielding for Radiation Belt Particles," paper to be published in *J. Astronaut. Sci.*

14. Del Duca, M. G., Babinsky, A. D., and Miraldi, F. D., "Integrated Thermo-Dynamic Systems for Manned Space Stations," IAS Manned Space Station Symposium, Los Angeles, Apr. 20, 1960.

APOLLO NOTE NO. 54

G. F. Floyd
29 April 1963

DEFINITION OF $\bar{R}_1(t)$ AND USE FOR DSIF LUNAR ORBIT DETERMINATION

The Function $\bar{R}_1(t)$

For an elliptical orbit we have the usual expressions (see any books on celestial mechanics),

$$\text{Perigee} = R_p = a(1 - e)$$

$$\text{Apogee} = R_a = a(1 + e)$$

$$\text{Energy} = E = -\frac{\mu}{2a} = \frac{V_p^2}{2} - \frac{\mu}{R_p} = \frac{V_a^2}{2} - \frac{\mu}{R_a} \tag{1}$$

$$\text{Orbit Period} = T = \frac{2\pi}{\omega_n} \quad \text{where } \omega_n = \sqrt{\frac{\mu}{a^3}}$$

Combining these we have the alternate forms:

$$\frac{V_p^2 R_p}{\mu} = 2\left(\frac{\mu}{R_p} - \frac{\mu}{2a}\right)\frac{R_p}{\mu} = 2 - \frac{R_p}{a} = 1 + e$$

$$V_p = \sqrt{\frac{\mu}{R_p}(1 + e)}$$

$$\omega_n = \sqrt{\frac{\mu(1 - e)^3}{R_p^3}} \tag{2}$$

with

$$R_a = R_p\left(\frac{1 + e}{1 - e}\right)$$

$$V_a = V_p\left(\frac{1 - e}{1 + e}\right) \tag{3}$$

Then letting (t_p) denote the first time the vehicle reaches perigee, we have for the correct expression:

$$\left.\begin{aligned} \bar{R}\left(t_p + n\frac{\pi}{\omega_n}\right) &= \bar{R}_p \\ \dot{\bar{R}}\left(t_p + n\frac{\pi}{\omega_n}\right) &= \bar{V}_p \end{aligned}\right\} \quad \text{for } n = 0, 2, 4, 6, \cdots$$

$$\left.\begin{aligned} \bar{R}\left(t_p + n\frac{\pi}{\omega_n}\right) &= \bar{R}_a = -\bar{R}_p\left(\frac{1+e}{1-e}\right) \\ \dot{\bar{R}}\left(t_p + n\frac{\pi}{\omega_n}\right) &= \bar{V}_a = -\bar{V}_p\left(\frac{1-e}{1+e}\right) \end{aligned}\right\} \quad \text{for } n = 1, 3, 5, \cdots \qquad (4)$$

Now define $\bar{R}_1(t)$ as:

$$\bar{R}_1(t) = \frac{\bar{R}_p}{1-e}\left[\cos\omega_n(t-t_p) - \frac{e}{2}\left(1+\cos 2\omega_n(t-t_p)\right)\right] + \frac{\bar{V}_p}{\omega_n(1+e)}\left[\sin\omega_n(t-t_p) + \frac{e}{2}\sin 2\omega_n(t-t_p)\right] \qquad (5)$$

with R_p and V_p as given by (2). Also from (5) we have :

$$\dot{\bar{R}}_1(t) = \frac{\bar{R}_p\,\omega_n}{1-e}\left[-\sin\omega_n(t-t_p) + e\sin 2\omega_n(t-t_p)\right] + \frac{\bar{V}_p}{1+e}\left[\cos\omega_n(t-t_p) + e\cos 2\omega_n(t-t_p)\right] \qquad (6)$$

Then evaluating (5) and (6) using (4), we get

For $n = 0, 2, 3, \cdots$,

$$\bar{R}_1 \left(t_p + n\frac{\pi}{\omega_n}\right) = \frac{\bar{R}_p}{1-e}\left(1 + \frac{e}{2}(1+1)\right) = \bar{R}_p = \bar{R}\left(t_p + n\frac{\pi}{\omega_n}\right)$$

$$\dot{\bar{R}}_1 \left(t_p + n\frac{\pi}{\omega_n}\right) = \frac{\bar{V}_p}{1+e}(1+e) = \bar{V}_p = \dot{\bar{R}}\left(t_p + n\frac{\pi}{\omega_n}\right) \qquad (7)$$

While for n = 1, 3, 5, 7, · · ·,

$$\bar{R}_1 \left(t_p = n\frac{\pi}{\omega_n}\right) = \frac{\bar{R}_p}{1-e}\left(-1 - \frac{e}{2}(1+1)\right) = -\bar{R}_p\left(\frac{1+e}{1-e}\right) = \bar{R}_a = \bar{R}\left(t_p + n\frac{\pi}{\omega_n}\right)$$

$$\dot{\bar{R}}_1 \left(t_p + n\frac{\pi}{\omega_n}\right) = \frac{\bar{V}_p}{1+e}(-1+e) = -\bar{V}_p\left(\frac{1-e}{1+e}\right) = -\bar{V}_a = \dot{\bar{R}}\left(t_p + n\frac{\pi}{\omega_n}\right) \qquad (8)$$

Thus

$\bar{R}_1$ and $\dot{\bar{R}}_1$ are correct at any apogee or perigee (9)

To investigate the accuracy of the approximation at in between values of (t) we look at the momentum vector $(\bar{R}_1 \times \dot{\bar{R}}_1)$. Taking the cross product of (5) and (6) and making usual trigometric reductions, we find,

$$\bar{R}_1 \times \dot{\bar{R}}_1 = \bar{R}_p \times \bar{V}_p \left[\frac{1 + \frac{e}{2}\left(\cos 3\omega_n(t-t_p) - \cos\omega_n(t-t_p)\right) - \frac{e^2}{2}\left(1 + \cos 2\omega_n(t-t_p)\right)}{1-e^2}\right] \qquad (10)$$

Thus $(\bar{R}_1 \times \dot{\bar{R}}_1)$ is not the constant $(\bar{R}_p \times \bar{V}_p)$ it should be, and is correct only at apogee and perigee. However, since the area of the orbit ellipse is,

$$\text{Area} = \int_{t_p}^{t_p + \frac{\pi}{\omega_n}} \left| \bar{R} \times \dot{\bar{R}} \right| dt \qquad (11)$$

We have from (10) and (11),

$$\text{Area of Approximation} = (\text{Area Correct})\left(\frac{1 - \frac{1}{2}e^2}{1 - e^2}\right) \approx (\text{Area Correct})\left(1 + \frac{1}{2}e^2\right) \tag{12}$$

For the LEM ascent orbit, $R_a \approx 1100$ n. m. with

$R_p \approx 1000$ n. m. so

$$e = \frac{R_a - R_p}{R_a + R_p} \approx \frac{100}{2000} = \frac{1}{20} = .05 \tag{13}$$

Hence for such orbits

$$\text{Area Approximation} = (\text{Area Correct})\left(1 + \frac{1}{800}\right) \tag{14}$$

and so is a very good approximation on the average as well as being exact in both position and velocity at every perigee and apogee so may be used for arbitrarily long prediction times.

Determination of $\bar{R}_1(t)$ at Long Range From Doppler Measurements

Since $\bar{R}_1(t)$ is very close to $\bar{R}(t)$, we may study the errors in the coefficients of $\bar{R}_1(t)$ since the percent errors relative to $\bar{R}_1(t)$ will be very close to the percent errors in the coefficients of the true function $\bar{R}(t)$. Also we will assume the spacecraft is so far from the earth that the parallax effects caused by motion of the earth station are not useful. The notation is summarized in Figure 1.

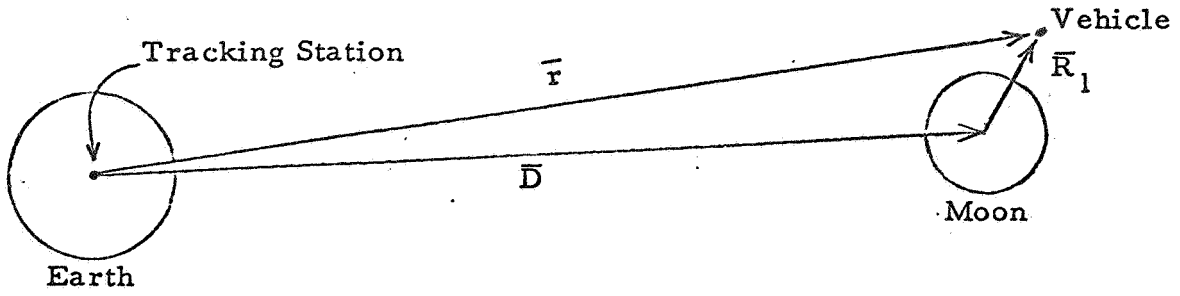

Figure 1.

For the error study we assume the station is at the center of the earth and that $\bar{D}$ is constant and very large. Thus,

$$\bar{r} = \bar{D} + \bar{R}_1$$
$$\dot{\bar{r}} = \dot{\bar{R}}_1 \tag{15}$$
$$\bar{l}_r \approx \bar{l}_D$$

So, for the error study let

$$\boxed{\dot{r} = \dot{\bar{R}} \cdot \bar{l}_D} \tag{16}$$

where the DSIF knows $\bar{l}_D$ exactly.

Using (6) and (2) in (16) we have:

$$\dot{r} = (\bar{l}_{R_p} \cdot \bar{l}_D) \sqrt{\frac{\mu(1-e)}{R_p}} \left(-\sin \omega_n (t - t_p) + e \sin 2\omega_n (t - t_p) \right)$$
$$+ (\bar{l}_{V_p} \cdot \bar{l}_D) \sqrt{\frac{\mu}{R_p(1+e)}} \left(\cos \omega_n (t - t_p) + e \cos 2\omega_n (t - t_p) \right) \tag{17}$$

Now make the following definitions:

$$A_1 \triangleq \sqrt{\frac{\mu}{R_p(1+e)}\left((\bar{I}_{V_p}\cdot\bar{I}_D)^2 + (\bar{I}_{R_p}\cdot\bar{I}_D)(1-e^2)\right)}$$

$$A_2 \triangleq e\,A_1$$

$$\phi_1 \triangleq \omega_n t_p - \tan^{-1}\left[\frac{(\bar{I}_{R_p}\cdot\bar{I}_D)\sqrt{1-e^2}}{\bar{I}_{V_p}\cdot\bar{I}_D}\right] \qquad (18)$$

$$\phi_2 \triangleq 2\omega_n t_p + \tan^{-1}\left[\frac{\bar{I}_{R_p}\cdot\bar{I}_D\sqrt{1-e^2}}{\bar{I}_{V_p}\cdot\bar{I}_D}\right]$$

With these definitions, it is then a matter of straight trigonometry to show that (17) may be written as:

$$\dot{r} = A_1\cos(\omega_n t - \phi_1) + A_2\cos(2\omega_n t - \phi_2) \qquad (19)$$

It is now more convenient to work with normal $\bar{I}_N$ to the orbit plane where:

$$\bar{I}_N \triangleq \bar{I}_{R_p} \times \bar{I}_{V_p} \qquad (20)$$

and since by definition of perigee $\bar{I}_{R_p}$ and $\bar{I}_{V_p}$ are orthogonal, the set $\bar{I}_{R_p}$, $\bar{I}_{V_p}$, $\bar{I}_N$ are mutually orthogonal. Therefore, we have that

$$(\bar{I}_N\cdot\bar{I}_D)^2 = 1 - (\bar{I}_{R_p}\cdot\bar{I}_D)^2 - (\bar{I}_{V_p}\cdot\bar{I}_D)^2 \qquad (21)$$

We can now solve (18) and (2) for the orbit parameters,

$$e = \frac{A_2}{A_1}$$

$$R_p = \frac{\mu^{1/3}(1 - e)}{\omega_n^{2/3}}$$

$$t_p = \left(\frac{\phi_2 + \phi_1}{3}\right) \tag{22}$$

$$A_1 \cos\left(\frac{\phi_2 - 2\phi_1}{3}\right) = \sqrt{\frac{\mu}{R_p(1 + e)}}\ (\bar{I}_{V_p} \cdot \bar{I}_D)$$

$$A_1 \sin\left(\frac{\phi_2 - 2\phi_1}{3}\right) = \sqrt{\frac{\mu(1 - e)}{R_p}}\ (\bar{I}_{R_p} \cdot \bar{I}_D)$$

Thus, in terms of the measurables ω_n, A_1, A_2, ϕ_1 and ϕ_2, we find that,

$$e = \frac{A_2}{A_1}$$

$$R_p = \frac{\mu^{1/3}}{\omega_n^{2/3}}\left(\frac{A_1 - A_2}{A_1}\right)$$

$$t_p = \frac{\phi_2 + \phi_1}{3} \tag{23}$$

$$\bar{I}_{R_p} \cdot \bar{I}_D = \frac{A_1}{(\mu\omega_n)^{1/3}} \sin\left(\frac{\phi_2 - 2\phi_1}{3}\right)$$

$$\bar{I}_N \cdot \bar{I}_D = \sqrt{1 - \frac{A_1^2}{(\mu\omega_n)^{2/3}} + \frac{A_2^2}{(\mu\omega_n)^{2/3}} \cos^2\left(\frac{\phi_2 - 2\phi_1}{3}\right)}$$

To describe the motion of a vehicle in an elliptical orbit we need six numbers. The first two locate the orbit plane by reference to its normal ($\bar{I}_N$). The next four describe the motion in the orbit plane: two for the orbit shape (R_p, e); one for the orientation of the orbit in the orbit plane (i. e. $\bar{I}_{R_p} \cdot \bar{I}_D$); and one for the time location of the vehicle along the orbit (t_p). Of these six descriptors, we then see from (23), that with the Doppler only, we are missing the second direction cosine of $\bar{I}_N$ and so cannot locate the orbit plane. Also since we cannot locate the orbit plane at infinite distance from Doppler only, the ($\bar{I}_{R_p} \cdot \bar{I}_D$) value does not locate $\bar{I}_{R_p}$, (whereas, if we had $\bar{I}_N$, then $\bar{I}_{R_p} \cdot \bar{I}_D$ would be enough). Thus from Doppler only at infinite distance we can know everything except the direction cosine of $\bar{I}_N$ to some known vector lying in the plane normal to $\bar{I}_D$. Thus, we do not know the rotation of the orbit plane about $\bar{I}_D$. This may also be shown by using Euler angles of Figure 2.

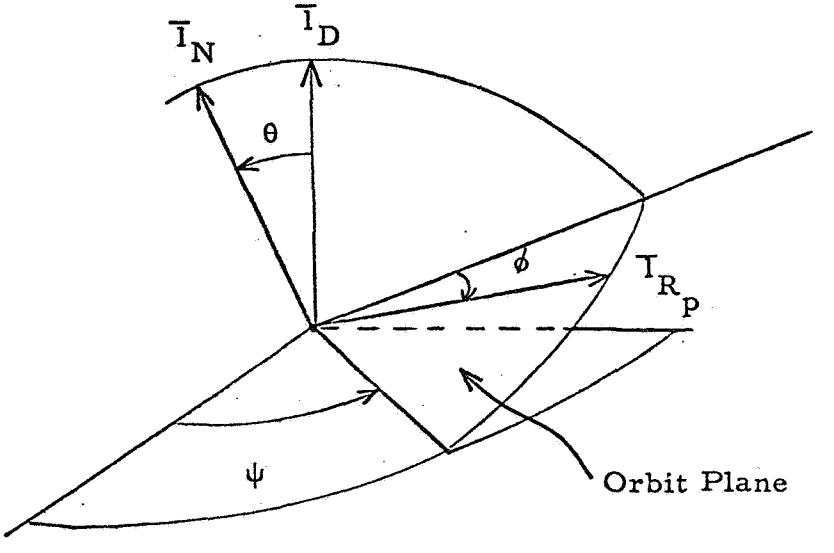

Figure 2.

From the figure

$$\begin{aligned} \bar{l}_N \cdot \bar{l}_D &= \cos\theta \\ \bar{l}_{R_P} \cdot \bar{l}_D &= \cos\phi \sin\theta \end{aligned} \tag{24}$$

Thus with Doppler data we get θ and ϕ but ψ, the rotation of orbit plane about $\bar{l}_D$, is unknown. To summarize then, with Doppler only at infinite distance we know all about the motion in the plane but are missing one piece of information about the orbit plane orientation and this is the direction cosine of $\bar{l}_N$ with a known vector in the plane normal to $\bar{l}_D$.

The smoothing and error study for lunar orbit determination can now be carried out using the form of (19) and this will be done in a later note.

APOLLO NOTE NO. 55

R. Harte
29 April 1963

THE USE OF TELEVISION IN LANDING AN UNMANNED LEM

A television link between LEM and CM/SM is deemed necessary because of the landing site suitability surveillance problem. The television system can also be used to find a suitable landing site which could be a particular mountain peak, crater, or as an ultimate test, an unbeaconed LEM.

The television system may serve as an invaluable aid in terminal navigation and guidance.

As seen from Apollo Note No. 42, the 1σ landing inaccuracy might vary between 2000 feet for the perfectly aligned IMU (at SM/CM separation) and 20,000 feet for a 1^{o} IMU misalignment. If a television camera must cover the 3σ case, then the above two numbers might require a picture width of between 12,000 and 120,000 feet.

It would appear that the problem of bettering the IMU alignment might be neglected if the television system could yield enough information in the 12,000 to 120,000 feet picture to permit terminal maneuvers.

The questions that must be answered, therefore, are:

1. Can a single, stationary television pickup tube see an LEM distinctly if the entire screen must encompass up to 120,000' (60,000' to either side of the optical axis in a horizontal plane at right angles to the optical axis).
2. What is the best frame rate choice.
3. How much degrading of resolution will result from angular displacement of off-axis points in closing toward the lunar surface.
4. Are image intensification techniques necessary or useful.

The assumptions to be used are:

1. Operation is in either sunshine or earthshine.
2. Resolution necessary to distinguish a 20 foot LEM is approximately 5 feet.
3. The transmitting distance never exceeds 150 miles, using omnidirectional antennas.
4. Line of sight is depressed approximately 15° below horizontal.
5. The angular rotation rate of the line of sight will be zero at the intersection of an extension of the LEM velocity vector and the moon. It will be maximum about 45° out-of-track from this point. This critical rate $\omega_{max} = \frac{V}{2R}$ where $V \cong \sqrt{2aR}$ and $a \cong 14$ ft/sec

$$\therefore \quad \omega_{max} = \sqrt{\frac{a}{2R}}$$

To determine the usefulness of television in the described situation, we must first determine the ambient light levels in which they will operate.

In sunlight, the lunar surface receives 0.13 watts cm^{-2}. With an albedo of almost 0.1, this represents a reflected energy level of 1.3×10^{-2} watts cm^{-2}. About 25% of this falls in the visible wave band (0.35μ to 0.70μ). This assumes a panchromatic reflectivity which is reasonable over a restricted bandwidth.

Thus, since there are 900 cm^2 $feet^{-2}$ and approximately 100 lumens $watt^{-1}$ in the visible band, the ambient light level under direct sunlight should be at least 250 foot candles.

The ambient light levels under a full earth are considerably smaller. They can be derived from the formula

$$I_a = \frac{I_{sc} \ \rho_e A_e \ \rho_m K \Delta\lambda}{2\pi R^2}$$

where

I_{sc} = The Solar Constant in watts ft.$^{-2}$ outside of the earth's atmosphere $\cong$ 120 watts/ft.^{2}

ρ_e = Albedo of the earth $\cong$ 0.4

A_e = Area of the earth facing the moon = 1.5×10^{15} ft.^{2}

ρ_m = Albedo of the lunar surface $\cong$ 0.1

K = Conversion factor - watts ft.$^{-2}$ of visible radiation to foot candles $\cong$ 100

R = Earth to moon distance = 1.3×10^9 feet

$\Delta\lambda$ = Amount of radiation in the visible portion of spectrum

$\therefore$ $I_a \cong$ 0.024 foot candles

This value represents full earth light and is reduced as the phase of the earth approaches "new earth."

Special image orthicon tubes are available which will operate in light conditions as low as 10^{-9} foot candles. They leave, however, much to be desired at the low light levels in the way of resolution, perhaps 200 horizontal lines per tube.

There are now, under study, special tubes with as many as 1300 to 1500 lines per inch, with useful tube diameters of 2 inches. These tubes are operated at scan rates from 1 to 20 frames per second. A typical tube has resolution values as follows:

.014 foot candles	750 lines/inch
.0075 foot candles	650 lines/inch
.0035 foot candles	500 lines/inch
.0018 foot candles	300 lines/inch

Thus, even at a first quarter phase earth, with only .012 foot candles of light we can obtain 750 lines inch^{-1}, at 2 inches = 1500 lines.

These tubes, in general, require higher cathode voltages than the standard tubes. They possess either S-10 photocathode surfaces with sensitivities of 60μA per lumen and S-20 surfaces with as much as 100μA per lumen sensitivity.

Assuming that the ambient light level is at least .025 foot candles, we can hope to achieve a total of 2000 lines of video resolution.

If we use a very fast collector lens with a small aperture, we can achieve wide fields of view. For example, Burke and James Catalogue lens No. 12641-A (quartz optics) at $350, is a 25mm focal length lens with a diameter of 30mm. Thus, it is a f/0.87 system which presents a field of view of 90° to the 50mm face plate of the television tube. Each line, then, represents 7.8×10^{-4} radians of angular coverage.

For a given slant range, it is now possible to determine the horizontal extent of lunar surface included in the frame and the ground resolution.

Since the off-axis points move across the screen at a certain angular rate, the resolution will be degraded accordingly. Maximum angular rate occurs at 45° on either side of the optic axis; and, therefore, falls at the very edges of the video frame. If we choose a convenient frame rate, i.e., 10 frames per second, we can determine the angular movement per frame in radians; and when this value is divided by the angular coverage of a single line (7.8×10^{-4} radians), an induced error coefficient is determined. This value when multiplied by the ground resolution determines the maximum value of ground resolution.

Table 1. indicates these calculated values.

Figure 1. plots ground resolution vs. slant range for various positions on the television tube face plate.

Slant Range (feet)	Horizontal Ground Covered in 90° FOV	Ground Resolution No Angular Displacement (feet/line)	Max. Angular Rate (radians/sec)	Max. Displacement In One Frame Radians	Induced Error	Ground Resolution With Maximum Angular Displacement (feet/line)
64,000	128,000 feet	64 feet	.011	1.1×10^{-3}	1.4	90 feet
32,000	64,000 feet	32 feet	.015	1.5×10^{-3}	1.92	61.5 feet
16,000	32,000 feet	16 feet	.020	2×10^{-3}	2.56	41.0 feet
8,000	16,000 feet	8 feet	.030	3×10^{-3}	3.85	30.7 feet
4,000	8,000 feet	4 feet	.042	4.2×10^{-3}	5.4	21.6 feet
2,000	4,000 feet	2 feet	.060	6×10^{-3}	8.2	16.4 feet
1,000	2,000 feet	1 foot	.088	8.8×10^{-3}	11.3	11.3 feet

Table 1.

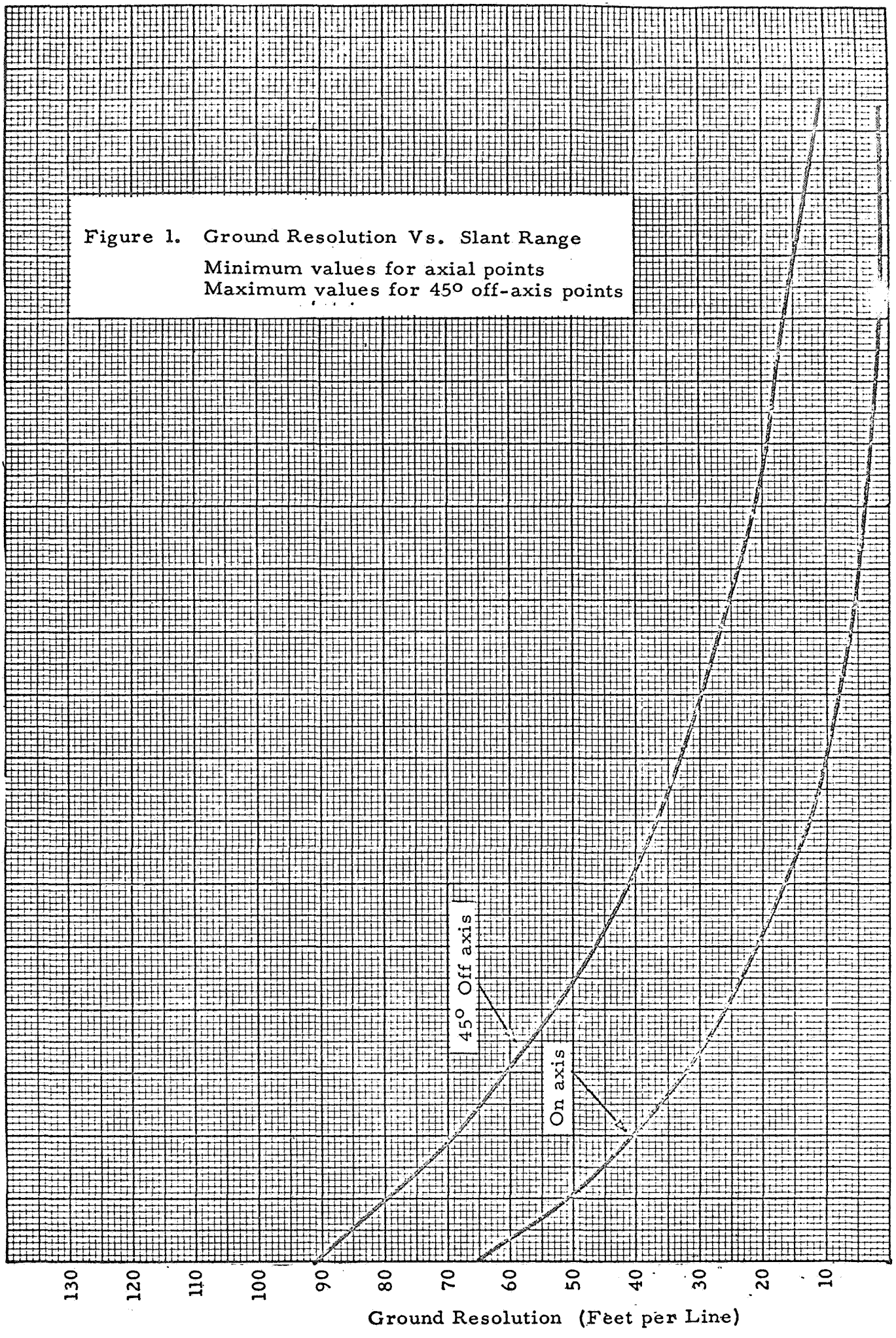
Figure 1. Ground Resolution Vs. Slant Range
Minimum values for axial points
Maximum values for 45° off-axis points
45° Off axis
On axis
130
120
110
100
90
80
70
60
50
40
30
20
10
Ground Resolution (Feet per Line)
1000
2000
4000
8000
16,000
32,000
64,000
Slant Range from LEM to Lunar Landing Point (Feet)

Ground resolution is a geometrical concept, and as has been pointed out in Apollo Note No. 34, human recognition of meaningful data often exceeds geometrically determined values by a considerable degree, expecially straight contours. Thus, if five foot ground resolution is the stated accuracy needed to determine the presence of an unbeaconed LEM, it is very conceivable that the human eye will identify it when geometric values are as high as 15 feet or even 20 feet of resolution.

At a slant range of 20,000 feet or 3.8 miles, 20 feet/line resolution occurs at the center of the screen and 40,000 feet of ground are displayed.

At the edge of the screen, 20 feet/line resolution is not achieved until the slant range is less than one mile (4000 feet). At that range, only 8000 feet of ground are displayed.

We have assumed a frame rate of ten per second. The transmitting bandwidth can be determined from the relationship

$$F_{max} = 1/2\ kmn^2 f \left(\frac{W}{H}\right)\left(\frac{K_v}{K_h}\right)$$

where

F_{max} = Bandwidth

k = An efficiency factor for video transmission which approaches 0.7

m = Ratio of horizontal to vertical resolutions, here, assumed to be 1.0

n = Number of resolution elements per frame = 2000

f = Frame rate = 10/second

$\frac{W}{H}$ = Display tube width over height = 1.0

$\frac{K_v}{K_h}$ = Another resolution efficiency factor $\cong$ 1.0

$\therefore$ $F_{max} \cong$ 14 megacycles

These calculations indicate that while we cannot hope to image as much as 120,000 feet to include all possible cases of 3σ deviations, we can still give considerable coverage.

Light levels are sufficient so that no further intensification of the image is required. Resolution values for slant ranges of several miles are probably adequate to determine the location of an unbeaconed LEM television; therefore, it would appear to be a very useful tool for terminal guidance of the surfacing craft.

APOLLO NOTE NO. 56

G. F. Floyd
1 May 1963

EFFECT OF SMALL BOOSTS ON ACCURACY OF EARTH ORBIT DETERMINATION

While the Apollo spacecraft is in its first earth parking orbit, it is necessary to apply small boosts (about 5 ft/sec), every 18 minutes or so in order to prevent excessive pressures from building up in the S-IV B booster. During this time, the close in ground tracking network is trying to determine the earth orbit exactly in order to calculate the exact boost needed for the translunar trajectory. The problem is then to determine the effect of these small boosts on the accuracy of this orbit determination.

In actual practice these boosts will be applied in essentially known direction and thus a priori knowledge can, of course, be used to good advantage in the orbit determination problem. The general manner by which such information is used is outlined in Note No. 57, but in this note we will neglect this additional information and show that even without it, the ground system should have no real difficulty in keeping track of the new orbit parameters that result with each small boost.

The tracking during earth orbit will be done by the ground based stations. With reference to the Bell Telephone Laboratories report of December 15, 1962, "Apollo, Report on Communications and Tracking System Planning," there are 11 Mercury remote stations plus two ships and the Antigua station for the Atlantic Missile Range, for a total of 14 stations. These stations are, or will be, equipped with FPS-16 radars of two different range capabilities. From Figure 6.3 of this report, we have that the spacecraft will be visible over $30^{\circ} \approx$ 7.5 min of travel for the extended range version and about $30^{\circ} \approx$ 5 min for the standard version. Therefore, we will assume 5 min of tracking while the vehicle is in view of a station with the slant range varying between about 900 and 200 n. mi. On the basis of tests made by General Electric, the FPS-16 appears capable of the following tracking performance:

Azimuth Angle:	$\pm$ 0.1 mil random
Elevation Angle:	0.1 mil bias $\pm$ 0.3 mil random
Angle Servo Bandwidth:	2.5 cps
Range:	50' Bias $\pm$ 10-30 ft random.

The following analysis first develops general smoothing equations for the circular orbit case and then uses the above performance numbers to estimate errors.

A summary of these results is that with the smoothing time available at each station (4 minutes or more), the velocity of the spacecraft can be determined to better than 0.3 ft/sec and position to better than 50 ft. Consequently it does not appear that the necessary venting boosts will cause any particular trouble.

For the analysis we use the notation of Apollo Note No. 31 and write:

$$\overline{R}(t) = \overline{R}_o f(t) + \overline{V}_o g(t) \tag{1}$$

and therefore we may express $\overline{R}(t - \tau)$ in terms of $\overline{R}(t)$ as

$$\overline{R}(t - \tau) = \overline{R}(t) f(\tau) + \overline{V}(t) g(\tau) \tag{2}$$

where $f(\tau)$ and $g(\tau)$ are found from $f(t)$ and $g(t)$ by replacing t by $(-\tau)$. We consider the vector equations:

$$\overline{R}_s(t) = \int_o^T h(\tau)\, \overline{R}_m(t - \tau)\, d\tau \tag{3}$$

$$\overline{V}_s(t) = \int_o^T w(\tau)\, \overline{R}_m(t - \tau)\, d\tau \tag{4}$$

where $\overline{R}_s(t)$ and $\overline{V}_s(t)$ are our smoothed values of range and velocity and $\overline{R}_m(t)$ is the measured value of vector range $\overline{R}(t)$. We note here that if $\overline{R}_t(t)$ is the distance from the earth center to a tracking station and $\overline{r}(t)$ is the measured range of the spacecraft from the tracking station

$$\overline{R}_m(t) = \overline{R}_t(t) + \overline{r}(t) \tag{5}$$

where $\overline{R}_t(t)$ is also changing in inertial coordinates due to the spin of the earth.

Now standard procedure for choosing $h(\tau)$ and $w(\tau)$ is to say that if $\overline{R}_m(t) = \overline{R}(t)$ then the smoothed values should be correct. That is, without noise on the measured values we want no error. Using (2) in (3) and (4) this leads to the equations

$$\begin{aligned} \overline{R}(t) &= \overline{R}(t) \int_o^T h(\tau) f(\tau)\, d\tau + \overline{V}(t) \int_o^T h(\tau) g(\tau)\, d\tau \\ \overline{V}(t) &= \overline{R}(t) \int_o^T w(\tau) f(\tau)\, d\tau + \overline{V}(t) \int_o^T w(\tau) g(\tau)\, d\tau \end{aligned} \tag{6}$$

hence the constraints

$$\int_o^T h(\tau)\, f(\tau)\, d\tau = 1 \qquad \text{and} \int_o^T h(\tau)\, g(\tau)\, d\tau = 0$$

$$\int_o^T w(\tau)\, f(\tau)\, d\tau = 0 \qquad \text{and} \int_o^T w(\tau)\, g(\tau)\, d\tau = 1 \tag{7}$$

To now determine the best functions $h(\tau)$ and $w(\tau)$ we wish to minimize the mean square output of the filters to a noise input. Thus considering the $w(\tau)$ filter we have,

$$\overline{V}_s(t) = \int_o^T w(\tau)\ \overline{N}\,(t - \tau)\, d\tau \tag{8}$$

and considering each component separately we may drop the vector notation and calculate the mean square value as

$$\widetilde{V}_s^{\,2} = \lim_{A\to\infty} \frac{1}{2A} \int_{-A}^{A} V_s^{\,2}(t)\, dt$$

$$= \lim \frac{1}{2A} \int_{-A}^{A} dt \int_o^T w(x)\, N(t - x)\, dx \int_o^T w(y)\, N(t-y)\, dy \tag{9}$$

Letting $w(x)$ be identically zero outside the interval o to T and inverting orders of integration

$$\widetilde{V}_s^{\,2} = \int_{-\infty}^{\infty} w(x)\, dx \int_{-\infty}^{\infty} w(y)\, dy \left[\lim_{A\to\infty} \frac{1}{2A} \int_{-A}^{A} N(t-x)\, N(t-y)\, dy \right] \tag{10}$$

The term in brackets is simply the autocorrelation of the input range noise and will be denoted by $\phi_{NN}(\tau)$ so that (10) becomes

$$\tilde{V}_s^2 = \int_{-\infty}^{\infty} w(x)\, dx \int_{-\infty}^{\infty} w(y)\ \phi_{NN}(x-y)\, dy \tag{11}$$

We now take the case of input noise which has essentially a flat spectrum over the frequencies of interest in our smoothing since at each station we will smooth over the visible time of 5 minutes (smoothing bandwidths of less than 1/300 cps). For such $w(\tau)$, $\phi_{NN}(\tau)$ is essentially an impulse and calling Φ_o the flat low frequency power density of the noise we have upon changing limits back,

$$\tilde{V}_s^2 = \Phi_o \int_o^T w^2(\tau)\, d\tau \tag{12}$$

where

$$\Phi_o \triangleq \int_{-\infty}^{\infty} \phi_{NN}(\tau)\, d\tau \tag{13}$$

and so has the units of ft^2 - sec. We also may clarify our definition of Φ_o in another way by saying that if the input noise has a bandwidth of (b) cycles per second, then the mean square value of the position noise $\tilde{N}^2$ (in ft^2) is related to Φ_o by

$$\tilde{N}^2 = \frac{1}{2\pi} \int_{-2\pi b}^{+2\pi b} \Phi_o\, d\omega = 2\Phi_o b$$

so

$$\boxed{\Phi_o \triangleq \frac{\tilde{N}^2}{2b}} \tag{14}$$

The expression for the mean square position noise output of the filter $h(\tau)$ is just like (12) and is

$$\tilde{R}_s^2 = \Phi_o \int_o^T h^2(\tau)\, d\tau \tag{15}$$

Thus the optimization problem for both $h(\tau)$ and $w(\tau)$ is the same and consists of minimizing the integral of the square of the functions under the constraints (7). The solution to this problem is well known and therefore the procedure will simply be sketched out for completeness.

Assume $w_o(\tau)$ is the optimal function and that $v(\tau)$ is a permissible variation function then for any choice of a small constant e, (either plus or minus), we know that

$$\int_o^T w_o^2(\tau)\, d\tau \leqslant \int_o^T \left[w_o(\tau) + e\, v(\tau)\right]^2 d\tau$$

$$= \int_o^T w_o^2(\tau) + 2e \int_o^T w_o v(\tau)\, d\tau + e^2 \int_o^T v^2(\tau)\, d\tau \qquad (16)$$

Since (e) may be plus or minus, it then follows that for all permissible $v(\tau)$ we must have that

$$\int_o^T w_o(\tau)\, v(\tau)\, d\tau \equiv 0 \qquad (17)$$

The restrictions on $v(\tau)$ follow immediately from the constraints (7) and are that both $w_o(\tau)$ and $\left[w_o(\tau) + e\, v(\tau)\right]$ must satisfy the constraints so

$$\int_o^T w_o(\tau)\, f(\tau)\, d\tau = \int_o^T (w_o + e\, v)\, f(\tau)\, d\tau$$

and

$$\int_o^T w_o(\tau)\, g(\tau)\, d\tau = \int_o^T (w_o + e\, v)\, g(\tau)\, d\tau$$

Thus, the constraints on the permissible variation function are simply that:

$$\int_o^T v(\tau)\, f(\tau)\, d\tau = \int_o^T v(\tau)\, g(\tau)\, d\tau = 0 \qquad (18)$$

To satisfy (17) under the constraints (18) we see that one solution is

$$w_o(\tau) = A\, f(\tau) + B\, g(\tau) \tag{19}$$

where A and B are constants, since with this choice, (17) will be satisfied for all $v(\tau)$ which satisfy (18). In a similar way we find,

$$h_o(\tau) = C\, f(\tau) + D\, g(\tau) \tag{20}$$

where the constants A, B, C, D are found from (7). Thus we have,

$$C \int_o^T f^2(\tau)\, d\tau + D \int_o^T g(\tau)\, f(\tau)\, d\tau = 1$$

$$C \int_o^T gf\, d\tau + D \int_o^T g^2(\tau)\, d\tau = 0$$

$$A \int_o^T f^2(\tau)\, d\tau + B \int_o^T gf\, d\tau = 0$$

$$A \int_o^T gf\, d\tau + B \int_o^T g^2\, d\tau = 1$$

Solving we find,

$$K \triangleq \left(\int_o^T f^2(\tau)\, d\tau \right) \left(\int_o^T g^2(\tau)\, d\tau \right) - \left[\int_o^T g(\tau)\, f(\tau)\, d\tau \right]^2 \tag{21}$$

$$C = \frac{1}{K} \int_o^T g^2(\tau)\, d\tau \tag{22}$$

$$A = D = -\frac{1}{K} \int_o^T g(\tau)\, f(\tau)\, d\tau \tag{23}$$

$$B = \frac{1}{K} \int_o^T f^2(\tau)\, d\tau \tag{24}$$

We can also evaluate the integral of the squares easily from (19), (20) and (7) as

$$\int_o^T h_o^2(\tau)\, d\tau = \int_o^T h_o(\tau) \left[C\, f(\tau) + D\, g(\tau) \right] d\tau = C \tag{25}$$

. . .

$$\int_o^T w_o^2(\tau)\, d\tau = \int_o^T w_o(\tau) \left[A\, f(\tau) + B\, g(\tau) \right] d\tau = B \tag{26}$$

and therefore from (12), (14), (15) and (26) we have using conventional dispersion notation,

$$\tilde{V}_s^2 = \delta_V^2 = \Phi_o \quad B \tag{27}$$

$$\tilde{R}_s^2 = \delta_R^2 = \Phi_o \quad C \tag{28}$$

where B and C are given by (22) and (24).

Returning to the results of Note No.31 we saw that for either short smoothing times or low eccentricities that we can write with only a small signal error,

$$\begin{aligned} f(\tau) &\approx \cos \omega_o \tau \\ g(\tau) &\approx -\frac{1}{\omega_o} \sin(\omega_o \tau) \end{aligned} \tag{29}$$

where we have replaced (t) by $(-\tau)$. Even if we use higher order terms to remove signal errors these simple functions should give very close noise estimates. Evaluating K, B, and C with (29) we find

$$K = \frac{1}{8\omega_o^4} \left[\cos 2\omega_o T + 2\omega_o^2 T^2 - 1 \right] \tag{30}$$

$$A = D = \frac{1}{4\omega_o^2 K} \left[1 - \cos 2\omega_o T \right] \tag{31}$$

$$B = \frac{1}{4\omega_o K}\left[2\omega_o T + \sin 2\omega_o T\right] \tag{32}$$

$$C = \frac{1}{4\omega_o^3 K}\left[2\omega_o T - \sin 2\omega_o T\right] \tag{33}$$

Now evaluating (31), (32), and (33) for small ($\omega_o T$) we find,

$$B \approx \frac{12}{T^3} \; ; \qquad C \approx \frac{4}{T} \; ; \qquad A = D \approx \frac{6}{T^2} \; . \tag{34}$$

so that for small smoothing times, use of (34) in (27) and (28) yields finally, for small $\omega_o T$:

$$\sigma_V \approx \frac{12\,\Phi_o}{T^3}$$

$$\sigma_R \approx \frac{4\,\Phi_o}{T}$$

for small $\omega_o T$. (35)

Returning now to the numbers for the FPS-16, if we assume that they represent maximum errors, then the RMS values will be less. Thus, let the 1σ angle tracking error be 0.2 mils and consider the maximum range case of 900 n. mi. so the RMS position error is 0.2/1000 x 900 x 6080 = 1000 ft along each of the axes normal to the range line and less than 50 ft along so the scaler range error is unimportant. The position noise spectral density is then given by (14) as

$$\Phi_o = \frac{\overline{N^2}}{b} = \frac{10^6}{(2)(2.5)} = 2 \times 10^5 \text{ ft}^2/\text{sec}. \tag{36}$$

Letting the smoothing time, T, be the minimum observation time of 5 minutes or 300 seconds, we get from (35)

$$\sigma_V = \sqrt{\frac{12 \times 2 \times 10^5}{(300)^3}} = 0.3 \text{ ft/sec}$$

$$\sigma_R = \sqrt{\frac{4 \times 2 \times 10^5}{300}} = 52 \text{ ft.} \qquad (37)$$

Since the actual ground system will use the data from all the 14 stations and also the a priori knowledge of the planned on boost direction, the system will actually do better than this by several factors of 2. Thus, we would guess that final errors of more like 1/10 ft/sec and 20 ft are quite possible, so that having to make these boosts should cause no appreciable loss in parking orbit parameter determination accuracy.

APOLLO NOTE NO. 57

G. F. Floyd
3 May 1963

OPTIMUM SMOOTHING WITH IMPERFECTLY EXECUTED COMMANDS

During the return to earth, the DSIF first tracks for a while to estimate the re-entry angle that will result if the vehicle coasts all the way, then periodically commands changes which the spacecraft imperfectly executes, and then the DSIF tracks again to see what happened. With such a process, the question arises as to the best estimate of the re-entry angle using all the data. Since we are trying to estimate some orbit parameter (a), which we know is constant unless we execute a boost, let:

a_n, a_{n+1} = True value of the parameter during smoothing cycles (n) and (n + 1).

$\hat{a}_n$, $\hat{a}_{n+1}$ = Best estimates of a_n and a_{n+1} using all data.

$\hat{a}'_{n+1}$ = Best estimate of a_{n+1} using all data measured after the executed change. (1)

c_n, b_n = Commanded and executed changes at end of n^{th} cycle.

So

$$a_{n+1} = a_n + b_n \tag{2}$$

To maximize the likelihood we will want zero expected errors in the estimators and minimum variance so will want the expected values of all estimators to be the true values. We will assume that on the average, the executed change will equal the commanded. So

$$\bar{b}_n = c_n. \tag{3}$$

We will denote the different variances involved as:

$$\overline{(b_n - c_n)^2} \triangleq \sigma_e^2$$

$$\overline{(\hat{a}_n - a_n)^2} \triangleq \sigma_n^2 \qquad (4)$$

$$\overline{(\hat{a}_{n+1} - a_n)^2} \triangleq \sigma_{n+1}^2$$

$$\overline{(\hat{a}'_{n+1} - a_n)^2} \triangleq \sigma_{new}^2$$

To form $\hat{a}_{n+1}$, we have available $\hat{a}_n$, c_n, $\hat{a}'_{n+1}$ and our a priori knowledge of the variances σ_e^2, σ_n^2, σ_{new}^2, and we will choose $\hat{a}_{n+1}$ to make the expected error zero with a minimum value for σ_{n+1}^2.

Thus let,

$$\hat{a}_{n+1} = \rho\, \hat{a}_n + \rho_1\, c_n + \rho_2\, \hat{a}'_{n+1} \qquad (5)$$

Taking expected values and requiring that these be correct we have,

$$\bar{a}_{n+1} = a_n + c_n = \rho\, a_n + \rho_1\, c_n + \rho_2\, (a_n + c_n) \qquad (6)$$

So that,

$$\rho + \rho_2 = \rho_1 + \rho_2 = 1 \qquad (7)$$

hence

$$\rho_2 = 1 - \rho \quad \text{and} \quad \rho_1 = \rho.$$

Thus for zero mean error, $\hat{a}_{n+1}$ must be of the form:

$$\hat{a}_{n+1} = \rho\, (\hat{a}_n + c_n) + (1 - \rho)\, \hat{a}'_{n+1} \qquad (8)$$

Therefore,

$$\hat{a}_{n+1} - a_{n+1} = \rho(\hat{a}_n + c_n - a_{n+1}) + (1-\rho)(\hat{a}'_{n+1} - a_{n+1})$$

$$= \rho\,(\hat{a}_n + c_n - a_n - b_n) + (1-\rho)(\hat{a}'_{n+1} - a_{n+1}) \tag{9}$$

$$= \rho\,(\hat{a}_n - a_n) + \rho\,(c_n - b_n) + (1-\rho)(\hat{a}'_{n+1} - a_{n+1})$$

Squaring and averaging with zero correlation assumed, we get using the notation of (4):

$$\sigma^2_{n+1} = \rho^2\sigma^2_n + \rho^2\,\sigma_e^2 + (1-\rho)^2\,\sigma^2_{new}$$

$$= \rho^2\,(\sigma_n^2 + \sigma_e^2 + \sigma^2_{new}) - 2\rho\,\sigma^2_{new} + \sigma^2_{new} \tag{10}$$

$$= (\sigma_n^2 + \sigma_e^2 + \sigma^2_{new})\left[\rho - \frac{\sigma^2_{new}}{\sigma^2_n + \sigma^2_e + \sigma^2_{new}}\right]^2 + \frac{(\sigma_n^2 + \sigma_e^2)(\sigma^2_{new})}{(\sigma_n^2 + \sigma_e^2) + \sigma^2_{new}}$$

Thus to minimize σ^2_{n+1} we want,

$$\rho = \frac{\sigma^2_{new}}{\sigma_n^2 + \sigma_e^2 + \sigma^2_{new}} \tag{11}$$

and this choice yields,

$$\boxed{\sigma^2_{n+1} = \frac{(\sigma_n^2 + \sigma_e^2)(\sigma^2_{new})}{(\sigma_n^2 + \sigma_e^2) + (\sigma^2_{new})}} \tag{12}$$

Thus we have the simple result that the variance of the best estimate is the "parallel" combination of two variances. The first is the sum of the variance of the old smoothing data plus the variance in the execution and the second is the variance based solely on new data. Thus the resulting variance is smaller than either and approaches the smaller when one is larger than the other.

APOLLO NOTE NO. 58

C. H. Dale
29 April 1963

LEM TERMINAL LANDING AND THE NECESSITY OF AN INERTIAL PLATFORM

In the Lunar Logistics Vehicle (LLV) mission, the LEM IMU is not available for initial alignment by the crew of the CM. If the IMU is used it would either need be aligned by some technique, or degraded IMU performance would result. A possible solution might exist in command guidance from the CM using a one mil radar. This would surely relieve the IMU of its navigational tasks during the midcourse portion of its descent. The questions to be taken up here are:

What characterizes the terminal descent; and, is an IMU necessary during the terminal descent?

Of the many possible LLV missions, one of the most taxing is the landing near a small, pre-assigned point (such as an un-beaconed LEM). Two pieces of equipment which appear absolutely necessary are a T. V. link and a doppler altimeter. The terminal phase can be considered to start when the T. V. link recognizes the target landing sight. Surely before this no form of terminal navigation can better the midcourse trajectory (with the possible exception of altimeter derived altitude and altitude rate updating).

The terminal portion of the descent trajectory has been studied before and, for the normal LEM, consists of a constant acceleration, gun-barrel path. This near-optimum path is easily defined for the case of no errors. Two non-orthogonal thrust components are present. The first is equal to the lunar attraction and in a downward direction. The second is equal to a constant and is in the direction of the velocity vector which, in turn, is along the line-of-sight to the target landing point. The constant acceleration is chosen by relating the velocity, V, to the range, R.

$$V = \sqrt{2\,a\,R} \qquad (1)$$

A safety margin is present in both R and a. This type of terminal trajectory is shown in Figure 1.

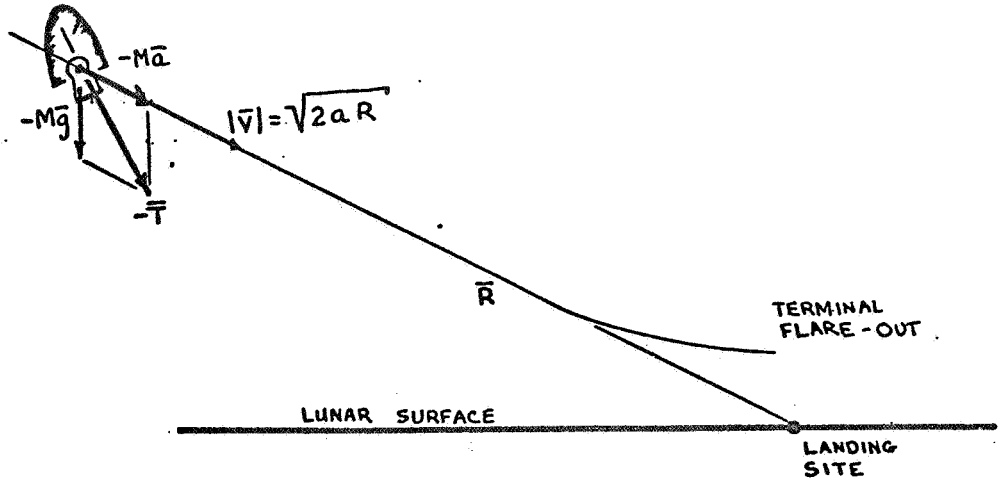

Figure 1.
Landing Maneuver With No Errors

Needless to say, this is an easy maneuver if no errors exist since the thrust acceleration is constant. If a subsequent error is found in R or V, then $|\bar{a}|$ is varied according to Equation (1). It is important to note that the conditions of the midcourse trajectory would be such as to make $|\bar{a}|$ as high as possible, still maintaining a margin of safety. This in turn makes the time of flight remaining as short as possible.

$$t_f = \frac{V}{a} = \frac{2R}{V} \qquad (2)$$

For any given range, R, the flight time is minimized by maximizing both the velocity and the acceleration. The boost velocity, $\bar{V}_b$, is defined as the time integral of the thrust divided by the instantaneous mass.

$$\bar{V}_b = \int_o^{t_f} (\bar{a} + \bar{g})\, dt = \bar{a}\, t_f + \bar{g}\, t_f = \bar{V} + \bar{g}\, t_f \qquad (3)$$

Thus for the situation shown in Figure 1, it is always best to minimize the time-of-flight for any given initial conditions.

When the initial velocity, $\bar{V}$, does not "point" at the desired target, the question arises as to what is the best thing to do about it. A gravity turn trajectory is a perfectly good example of such a trajectory which is also near optimum. In the following analysis it will be assumed that the initial angle between the line-of-flight, $\bar{V}/V$, and the line-of-sight is reasonably small and is due to midcourse navigational errors.

One possible guidance scheme would be to treat the horizontal (x) and vertical (y) components separately but in a fashion similar to Equation (1). That is, a_x and a_y could be chosen such that

$$a_x = \frac{\dot{x}^2}{2x} \quad , \quad a_y = \frac{\dot{y}^2}{2y} \qquad (4)$$

then with no further changes in a_x and a_y, the following short analysis will yield the space trajectory:

$$\dot{x}^2 = 2\, \ddot{x}\, x \qquad (4a)$$

$$\ddot{x} = \frac{d\dot{x}}{dx}\,\frac{dx}{dt} = \frac{d\dot{x}}{dx}\,\dot{x} \qquad (4b)$$

$$\therefore \dot{x}^2 = 2\,\frac{d\dot{x}}{dx}\,\dot{x}\,x \Rightarrow \dot{x} = 2\,x\,\frac{d\dot{x}}{dt} \qquad (4c)$$

Which upon integration gives:

$$x^{1/2} = c_1\,\dot{x} \quad \text{where } c_1 = \frac{x_o^{1/2}}{\dot{x}_o} \qquad (4d)$$

This may be rewritten:

$$\frac{dx}{x^{1/2}} = \frac{dt}{c_1} \qquad (4e)$$

which may be integrated again to give:

$$2\,x^{1/2} = \frac{t}{c_1} + c_2$$

or

$$x = \left(\frac{t + c_1 c_2}{2 c_1}\right)^2 = \frac{1}{x_o}\left(x_o + \frac{\dot{x}_o t}{2}\right)^2 \qquad (4f)$$

From Equation (4a) a similar equation to (4f) may be written in y, thus,

$$\frac{y}{x} = \frac{x_o}{y_o}\left(\frac{y_o + \frac{\dot{y}_o t}{2}}{x_o + \frac{\dot{x}_o t}{2}}\right)^2 = \frac{\dot{y}_o^2 x_o}{\dot{x}_o^2 y_o}\left(\frac{\frac{y_o}{\dot{y}_o} + \frac{t}{2}}{\frac{x_o}{\dot{x}_o} + \frac{t}{2}}\right)^2 \qquad (4g)$$

Now it can be seen that y/x is a measure of the tangent of the line-of-sight. In Equation (4g), it can be seen that if, and only if, $\dot{y}/y_o = x/x_o$ (i.e., if $\bar{V}_o$ is along $\bar{R}_o$) then y/x can remain at a constant value (remember that $\dot{y}_o$ and $\dot{x}_o$ are negative). For $\bar{V}$ initially pitched above the line-of-sight, the trajectory will end up going straight down (arc tan $\frac{y}{x} = 90^o$). And far more serious, if $\bar{V}$ is pitched below $\bar{R}$, at any time, the guidance rule would have the LEM skim in along the lunar surface. This is quite undesirable. With perfect guidance and no errors the time of flight for this scheme is given by Equation (2). However, with an initial error in the direction of $\bar{V}$ two times exist. Similarly to Equation (2):

$$t_{f_x} = \frac{2 x_o}{\dot{x}_o}$$

$$t_{f_y} = \frac{2 y_o}{\dot{x}_o} \qquad (4h)$$

These are the times that $\ddot{x}$ must change from a_x to zero, and separately that $\ddot{y}$ must change from a_y to zero. Since the line-of-flight angle is

close to the lunar surface (14^{o} or so) a small error in $\bar{V}$ will cause a greater percentage change in t_{f_y} than in t_{f_x}. Thus although t_{f_x} will remain quite close to t_f (from Equation (2)), t_{f_y} might get quite a bit larger, and in any case, the longer of the two determines the actual time of flight. Any unnecessary time of flight burns unnecessary fuel according to Equation (3).

Thus a summary of the complaints against the above guidance scheme are:

1. The trajectory is curved (badly so near the end of flight).
2. The guidance scheme must change at either $x = 0$ and/or $y = 0$.
3. A lengthy flight time, which burns fuel, may occur for an initial pitched-up condition.

A related scheme which overcomes many of the problems is discussed in Apollo Note No. 19. Here the horizontal acceleration is picked as before, however, the vertical acceleration is chosen such that a suitable positive y and downward $\dot{y}$ exist when x and $\dot{x}$ reach zero. From Apollo Note No. 19, the terminal values of y and $\dot{y}$ are (when x and $\dot{x} \rightarrow 0$):

$$\dot{y}_f = \left(\frac{2 x_o}{\dot{x}_o} \right) \left(a_y - g \right) + \dot{y}_o \tag{5}$$

$$y_f = \left(\frac{\dot{y}_o + \dot{y}_f}{2} \right) \left(\frac{-2 x_o}{\dot{x}_o} \right) + y_o \tag{6}$$

Then since some $\dot{y}$ remains when x and $\dot{x}$ have gone to zero, the remaining acceleration and velocity will be constrained to the vertical (except for any remaining errors). This is thus a considerably safer scheme.

The guidance rules for this scheme, to reiterate Apollo Note No. 19, can be broken into the following temporal pieces:

1. Pre-terminal: Undefined except that the desire would be to achieve descent initial conditions for the terminal phase. One would assume that this would be close to an optimum boost trajectory.

2. Initial Terminal Descent: Pick a_x such that $\dot{x}_o = \sqrt{2 a_x x_o}$; pick a_y such that a_{total} places the LEM in a favorable vertical descent path ($\dot{y}$ and y) when x and $\dot{x}$ go to zero. See Apollo Note No. 19.

3. Initial Vertical Descent: Align the LEM body axis with the vertical, and at the same time reduce any remaining $\dot{x}$ errors. Do this at a greatly reduced thrust (minimum thrust) until the point on an altitude vs. altitude rate profile is reached where maximum thrust (x 0.9) will bring the LEM to 7.5 ft/sec. downward velocity at a safe minimum altitude (100 to 200 ft).

4. High Thrust Vertical Descent: At high thrust, control y and $\dot{y}$ and keep the vehicle basically vertical.

5. Constant Velocity Descent: Make the vehicle vertical for landing while maintaining thrust equal to the lunar attraction.

This set of guidance rules appears to offer two basic improvements over Equation (4). First, the terminal descent will always be vertical and second, the time of flight will always be shorter because of the reasoning previously presented after Equation(4h). Although, for this scheme $\bar{a}_T$ is constant in space co-ordinates during the initial terminal phase, the trajectory is not necessarily straight. This means that optical sensors will see a rotating line-of-sight to the target. A rotating line-of-sight presents a number of problems. First, it requires the optical sensor to be continually servoed with respect to body axes. Second, field of view and gimbal limitations may result from structural constraints. Third, the expected landing point (by the computer) is not obviously delineated in an optical sensor unless the optical sensor is servoed by computer commands to drive the angular rate to the predicted landing point to zero.

A set of guidance schemes, worthy of consideration, are those

which cause the velocity vector to be aligned with the line-of-sight. Defining σ as the line-of-sight angle (with respect to any space reference), it might thus be desirable to drive $\dot{\sigma}$ to zero which would return the trajectory to that shown in Figure 1. Any such scheme would then drive the LEM to a trajectory which is:

1. Straight, making visual observations (T. V.) easy and gimbal angles predictable and small.
2. Continuous until flare-out or hover.
3. Economical in that the target is reached in the shortest time consistent with a safe design limit on the acceleration.
4. Constant Thrust, in magnitude and direction.

A time proven way of driving the line-of-sight rate, $\dot{\sigma}$, to zero is proportional navigation. Defining $\dot{\gamma}$ as the rate of change of the direction of $\overline{V}$, then

$$\dot{\gamma} = \lambda \dot{\sigma} \tag{7}$$

is proportional navigation where λ is a constant, usually between 2 and 6. An idea of the actual motion of the LEM using proportional navigation can be gained by slightly redrawing Figure 1 to show an initial pointing error. This is done in Figure 2, with the lunar surface taken as an arbitrary angular reference.

In the following figure, e is the angle between $\overline{V}$ and the line-of-sight. The rotation rate of the line-of-sight is equal to the component of velocity perpendicular to the L. O. S. divided by the range.

$$\dot{\sigma} = \frac{V \sin e}{R} = \sqrt{2 a_V / R} \quad \sin e \tag{8}$$

and for small angles

$$\dot{\sigma} = \sqrt{2 a_V / R} \quad e \tag{9}$$

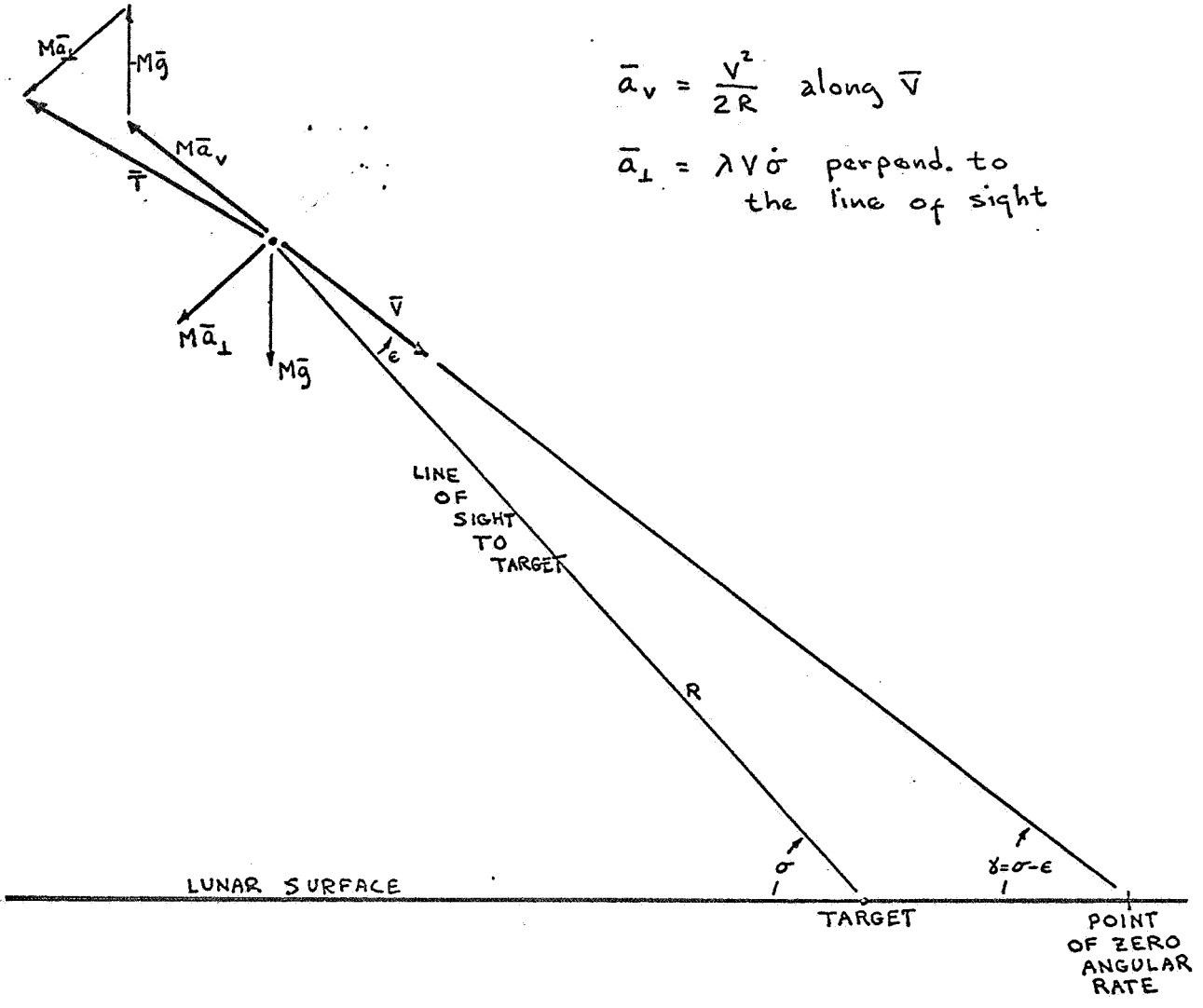

Figure 2.
Landing Maneuver With An Initial Error, e, Under
Proportional Navigation Control

Equation (7) may be rewritten:

$$\dot{\gamma} = (\dot{\sigma} - \dot{e}) = \dot{\sigma} - \dot{e} = \lambda \dot{\sigma} \tag{10}$$

Thus, combining Equation (9) and (10) gives:

$$\sqrt{2 a_V / R}\ e - \dot{e} = \lambda \sqrt{2 a_V / R}\ e$$

or

$$\dot{e} + (\lambda - 1) \sqrt{2 a_V / R}\ e = 0 \tag{11}$$

which may be integrated if the integration time is very short with respect to the flight time; that is, if R can be considered constant. Thus, approximately

$$e \simeq e_o e^{-(\lambda-1)\sqrt{2 a_V / R}\ t} \quad (\text{for } t << t_f) \tag{12}$$

The following is an example calculation which shows that the velocity vector may easily be brought in alignment with the line-of-sight.

The T. V. link should surely be able to recognize the target at five miles range. Given a one mil radar in the CM/SM, the location of the target relative to the LEM should be correct to 0.001 x 100 = 0.1 mile. A 1000 foot error will be assumed. Thus, the initial conditions are assumed to be:

R_o = 5 miles = 30,000 ft.

a_V = 12 ft/sec. $\geqslant V_o = \sqrt{2 a_V R}$ = 850 ft/sec.

t_f = the time of flight = $\frac{V}{a_V}$ = 71 seconds

$e_o = \frac{1000}{30,000}$ = .033 radians

Now by taking five second increments, Equation (12) may be solved iteratively giving the following graph.

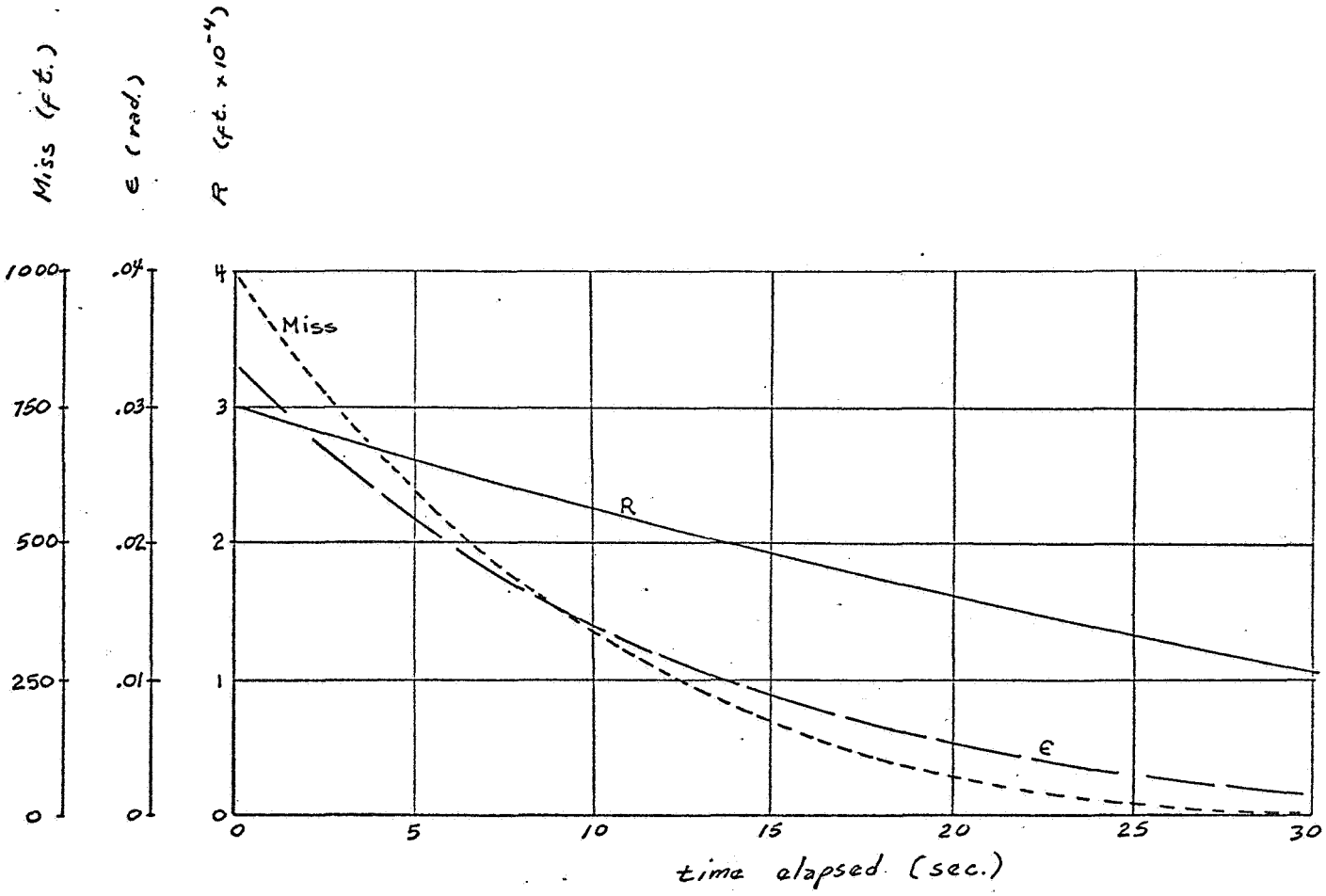

Figure 3.
A Sample Proportional Navigation Trajectory

The terminal portion of the "gun-barrel" trajectory should possibly follow the same reasoning as Apollo Note No. 19. Since only two controllables exist, thrust magnitude and direction, then various phases must exist within which no more than two errors at a time are reduced. During the gun-barrel phase described above, the acceleration component a_V is chosen such that some safe R_f exist when $\dot{R}$ (and thus V) goes to zero. R_f could be 200 feet or so. When some particular range, before R_f, is reached the LEM could change its program to one which made:

1. $\dot{x} = 0$ at $x = 0$ (fixes $\ddot{x}$)

2. a_T remain constant (fixes attitude)

In practice this would cause the LEM to approach a near vertical attitude from a 34 degree nose-up position. The time required to pitch this approximate 40 degrees is roughly two seconds, and during this time the altitude rate should be brought equal to zero. The next phase should bring $\dot{x}$ to zero at $x = 0$ while maintaining $a_y = g$ (or $\dot{y} = 0$ at a roughly predetermined value of y). This situation should allow the LEM to coast towards the target at a constant attitude and altitude which is high enough to not raise a dust cloud and yet is low enough to both obtain excellent ground resolution and T. V. estimates of the ground rates (i. e., $\dot{x}$ and $\dot{z}$). Hopefully this will allow the radar altimeter designers greater latitude. In any case it should not be necessary to roll the vehicle to reduce $\dot{x}$ and $\dot{z}$ to acceptable limits. When $\dot{x} = x = 0$ (or at least a suitable site has been chosen), then the thrust should be brought to a minimum while aligning the vehicle with the vertical. When an acceptable negative $\dot{y}$ is reached the thrust should be set equal to gravity, while again maintaining vertical LEM alignment. Touchdown should follow.

An example of a terminal trajectory is shown in Figure 4. The total time between the termination of the gun-barrel descent and touchdown is 28 seconds (which may be too large or small), and the correspondingly required boost is 159 ft/sec.

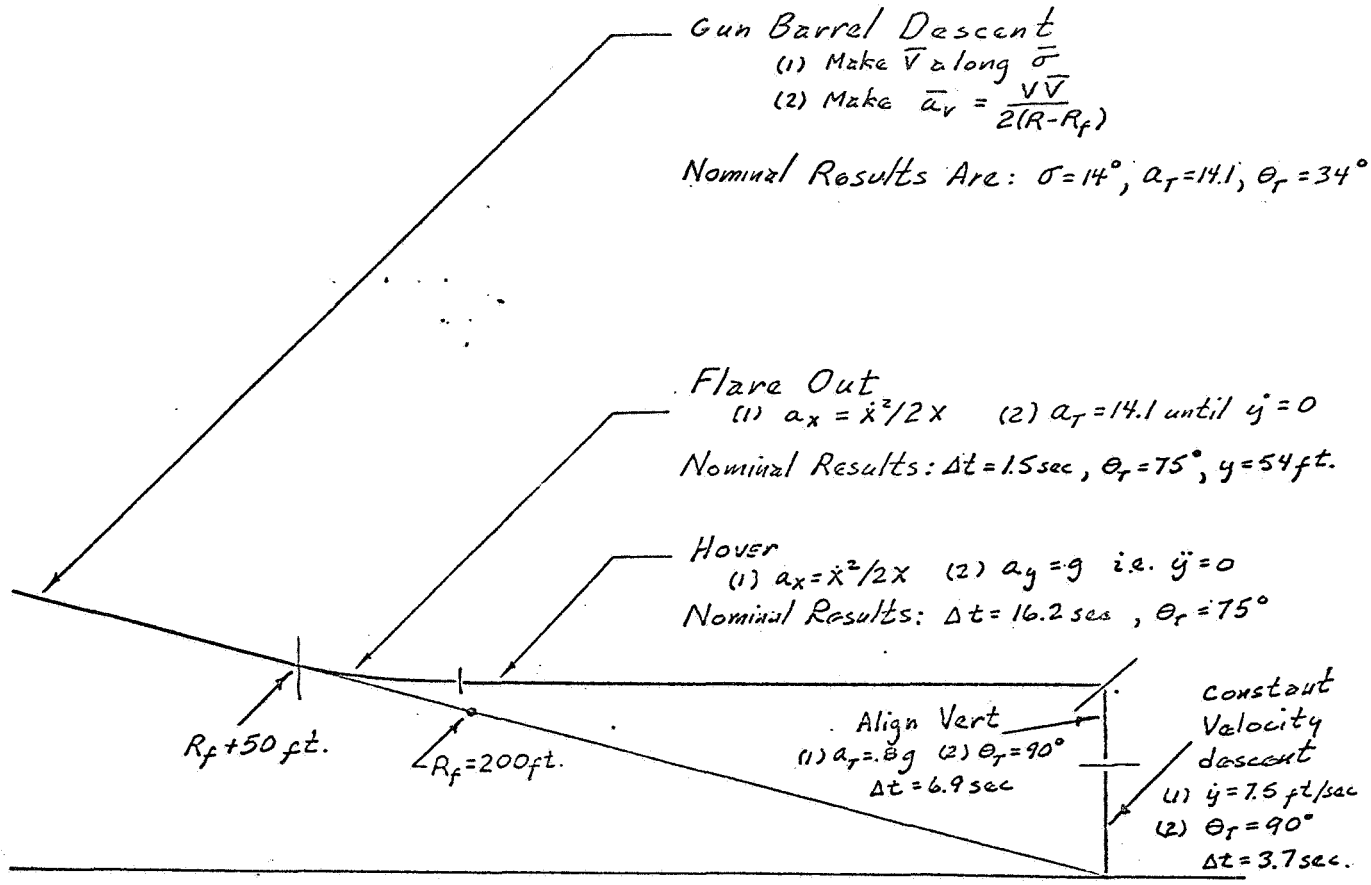

Figure 4.
An Example Terminal Trajectory Starting With A
Gun-Barrel Descent

The remainder of this note will be devoted to the necessity of an IMU in the lunar logistics LEM. The IMU is a set of integrating gyros and accelerometers mounted on a stable platform; it, thus, has the capacity to:

1. Act as an inertial attitude reference.
2. Provide inertial components of position, velocity, and acceleration.
3. Break.

The question of whether an IMU should or should not exist on the lunar logistics vehicle can best be answered by finding the guidance requirements and providing only those sensors which are absolutely necessary. This should provide the most reliable non-redundant set of equipment.

During the initial portion of the terminal descent it seems apparent that radar command guidance (good to 1 mil) is inherently more accurate than inertial guidance as seen from Apollo Note No. 42. An inertial attitude reference is necessary during this phase in order to point the thrust axis and to point a T. V. camera. The thrust direction is not critical since sine errors correspond to a small fuel cost. However, the T. V. camera should probably be pointed to within a degree. Assuming that the target is first seen at ten miles range, then the figure below gives the angular error in the expected line-of-sight as a function of the one sigma error in position.

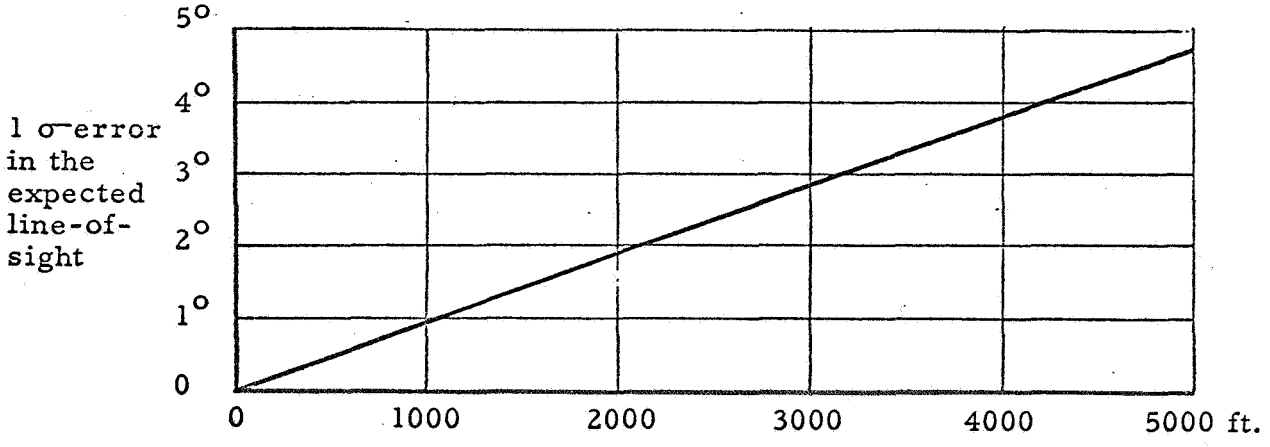

1 σ error in position of LEM upon T. V. location of the target at a range of 10 miles.

Figure 5.
Angular Error in T. V. Axis

Once the T. V. camera sights the target, the camera would be driven to place cross-hairs on the target. The line-of-sight must then be used to remove guidance errors. Given a doppler altimeter (y and $\dot{y}$) and the ability to hold the T. V. cross-hairs close to the target, i. e., measure $\dot{\sigma}$, then the following equations follow from Figure 2:

$$R = y/\sin\sigma \tag{13}$$

$$\dot{R} = (\dot{y} - R\dot{\sigma}\cos\sigma)/\sin\sigma \tag{14}$$

where σ is intended to be the in-plane component of the line-of-sight as measured from an axis on the lunar surface. These equations may be solved for R and $\dot{R}$ if and only if σ may be measured. The question thus arises as to how well σ must be measured in order that a safe and conservative landing may be made. Given a guidance rule along the line-of-sight that sets the thrust, an error in that acceleration will occur due to an error in σ. Thus, if the acceleration along the line-of-sight, a_V, is set equal to $\dot{R}^2/2R$, then

$$\frac{\partial a_V}{\partial \sigma} = \frac{\partial (\dot{R}^2/2R)}{\partial \sigma} \tag{15}$$

and since

$$a_V = \frac{\dot{R}^2}{2R} = \frac{\dot{y}^2}{2y}\cos\sigma + \dot{\sigma}\left[\frac{y\dot{\sigma}}{2}\frac{\cos^2\sigma}{\sin^3\sigma} - \dot{y}\frac{\cos\sigma}{\sin^2\sigma}\right] \tag{16}$$

then

$$\frac{\partial a_V}{\partial \sigma} = -\frac{\dot{y}^2}{2y}\frac{\cos\sigma}{\sin^2\sigma} + \dot{\sigma}\left[\frac{y\dot{\sigma}}{2}\left(\frac{3\cos^3\sigma}{\sin^4\sigma} - \frac{2\cos\sigma}{\sin^2\sigma}\right)\right.$$

$$\left. + \dot{y}\left(\frac{1}{\sin\sigma} + \frac{2\cos^2\sigma}{\sin^3\sigma}\right)\right] \tag{17}$$

The error in a_V when the line-of-sight rate has been driven to zero is given by Equations (16) and (17):

$$\frac{\Delta a_V}{a_V} = \left.\frac{\frac{\partial a_V}{\partial \sigma}\Delta\sigma}{a_V}\right| = -\cot\sigma\ \Delta\sigma \tag{18}$$

$\dot{\sigma} = 0$

For a flight path of $\sigma = 14^{o}$ this is about 7.0% per degree of $\Delta\sigma$. The equation of motion of the descending LEM along the line-of-sight is:

$$\ddot{R} = (1 - n) \frac{\dot{R}^2}{2R} \tag{19}$$

where n is the 7% or so per degree of error in σ. This can be integrated to give

$$\dot{R} = C R^{\frac{1-n}{2}} \tag{20}$$

from which

$$\ddot{R} = \frac{C^2 (1-n)}{2 R^n} = \frac{\dot{R}_o^2 (1 - n)}{2 R_o^{(1-n)} R^n} \tag{21}$$

For negative values of n, $\ddot{R}$ will approach zero as R reaches zero (actually as R reaches some R_f). For positive values of n, $\ddot{R}$ will grow as R diminishes, finally reaching a value limited by the thrust of the LEM. From this critical range on in, the limit acceleration will prevail and the stopping distance, R_f, will be exceeded. It is necessary to design a safe margin and thus an example set of calculations will be used to show the effect of an error in σ (causing the error, n) on the stopping range, R_f.

Given, for example:

R_o = 5 n.mi. (3.04×10^4 ft)

$\ddot{R}$ (planned upon) = 12 ft/sec^2

$\ddot{R}_{ultimate}$ = 110% of 12 ft/sec^2 = 13.2 ft/sec^2

$\therefore \dot{R}_o = \sqrt{2 (12) 3.04 \times 10^4} = 854$ ft/sec

Then from Equation (21) the range, R_1, at which the ultimate of 13.2 ft/sec^2 is reached can be calculated as a function of n where $n = .070 \Delta\sigma^{o}$. At this range, R_1, the error in acceleration is exactly n times the required acceleration to bring the LEM to rest at R_f from the target. Given that this limit acceleration is applied until $\dot{R}$ is brought to zero, then the design point, R_f, will be exceeded by a miss of n R_1. The example is plotted in Figure 6.

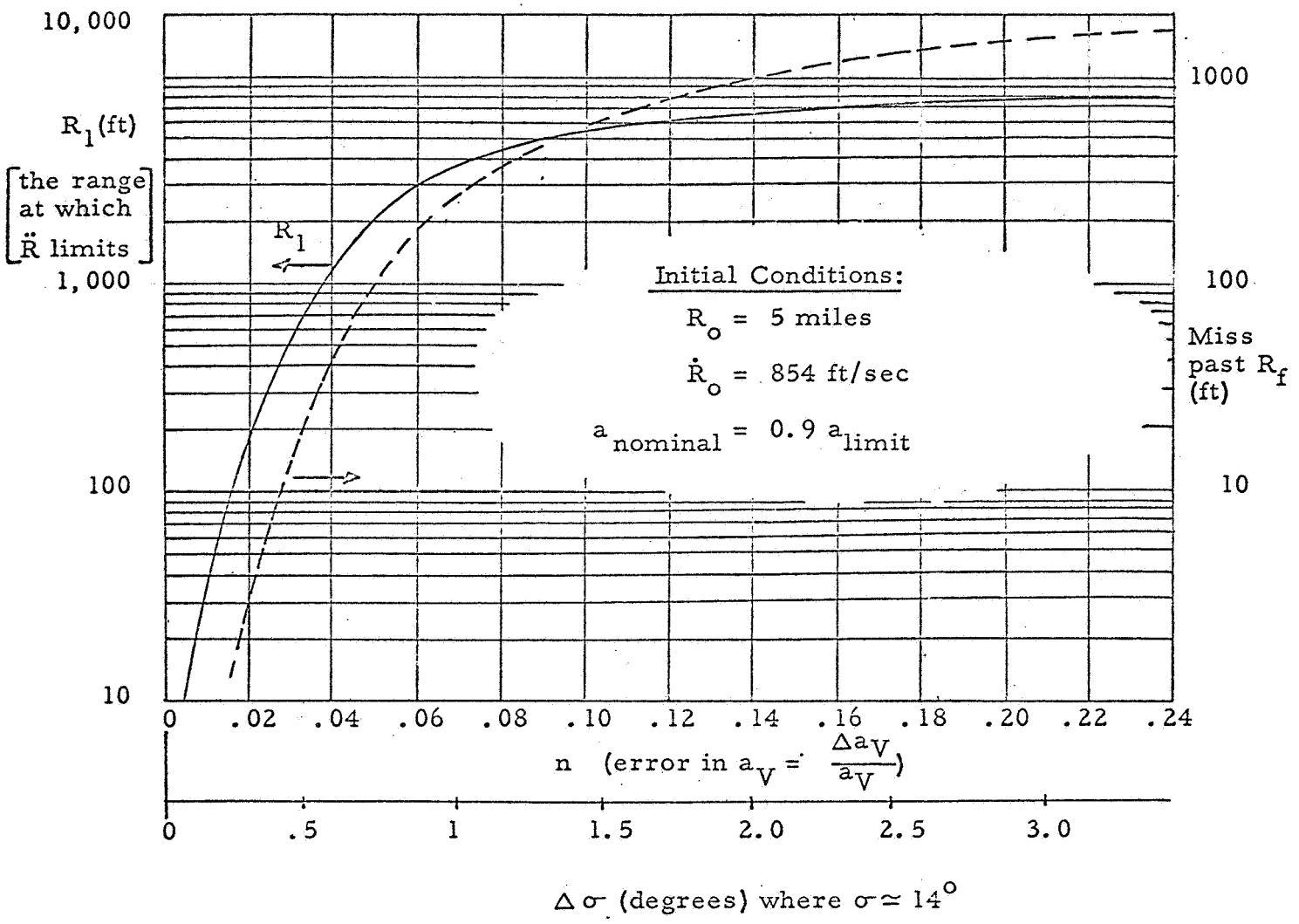

Figure 6.
Sample Terminal Trajectory Showing The Miss Along
R For A Given Error In σ.

From the foregoing example, as shown in Figure 6, it can be inferred that σ should be known to within a degree, and a one-half degree limit would not be out-of-line with safety considerations.

Thus, up to the point of the flare-out, the instrumentation requirements of the lunar logistics vehicle have been shown to be:

1. A doppler altimeter
2. A T. V. link
3. A stable platform good to about one-half of one degree
4. A set of body-mounted rate gyros and accelerometers

It, as yet, has not been shown that an IMU is a good choice as a replacement of (3) and (4) above. However, further analysis of the initial thrusting portion of the synchronous descent and of the very terminal flare-out and hover stages may well suggest an IMU.

APOLLO NOTE NO. 59

H. L. Engel
6 May 1963

PHYSICAL CONSTANTS

Earth

Radius	6.3781×10^3 km
μ	3.99689×10^5 km^3/sec^2
Period	23.93447 hours
ω	7.29116×10^{-5} rad/sec
Axis inclination to ecliptic	23° 26.5'

The precession of the Earth's axis is small enough to be neglected here.

Moon

Radius	1.7373×10^3 km
μ	4.896 km^3/sec^2
Period (sidereal)	27 days 7 hours 43 minutes 11.5 sec.
Period (apparent Earth)	29 days 12 hours 44 minutes 3 sec.
ω	4.236×10^{-7} rad/sec

The Moon's axis of rotation, the normal to the ecliptic, and the axis of Earth-Moon rotation line in a plane, as indicated in Figure 1. This plane rotates westward about the normal to the ecliptic with a period of 18 years, 7 months.

The mean distance from the Earth to the Moon is 385,000 km. The eccentricity of its orbit is 0.0549, and the major axis of the orbit rotates eastward with a period of 8.85 years.

The physical "constants" given here differ according to the source selected, but are suitable for error studies.

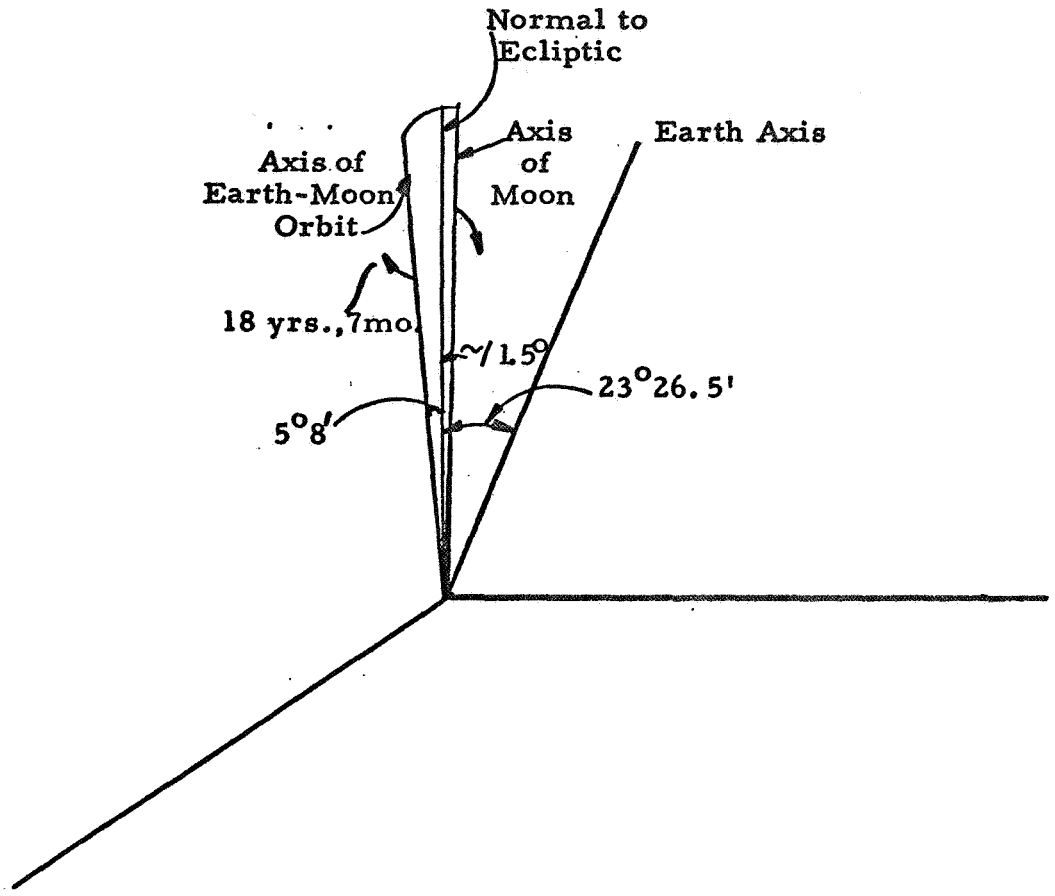
Normal to
Ecliptic
Axis
of
Moon
Earth Axis
Axis of
Earth-Moon
Orbit
18 yrs., 7mo.
~1.5°
23°26.5'
5°8'

Figure 1.

APOLLO NOTE NO. 60

B. Saltzberg
6 May 1963

ERROR ANALYSIS FOR DETERMINING IN-PLANE ORBIT PARAMETERS USING DSIF DOPPLER MEASUREMENTS DURING DESCENT INTO SYNCHRONOUS ORBIT

INTRODUCTION

This note investigates the accuracy with which the DSIF can predict:

1. the altitude of the LEM at perilune, and
2. the angle of the position vector at periline relative to the earth-moon line

The error analysis considers the case of synchronous descent from 100 n. mi. circular orbit. Since descent into synchronous orbit is initiated approximately 90° from perilune, we have examined the accuracy with which the orbit can be determined (and hence the accuracy with which perilune altitude and angle can be predicted) based on doppler data taken during the first 30° after initiation of descent into synchronous orbit.

ANALYSIS

From Apollo Note No. 32 the doppler velocity measured at the DSIF, assuming the earth at infinity, is given by:

$$\lambda f_d = \dot{R} = \left[\dot{r} \sin (\theta + \psi) + r \dot{\theta} \cos (\theta + \psi) \right] \cos \beta \qquad (1)$$

where ψ = angle from earth-moon line to perilune

β = angle between orbit plane normal and normal to earth-moon line

In this error analysis we will assume the orbit plane known, say $\beta = 0$, so that Equation (1) can be written as: (A second angle is required to completely define the orbit plane, but $\dot{R}$ is independent of this angle for the zero parallax case considered here and would have to be determined by other means - See Apollo Note No. 37).

$$\dot{R} = \dot{r} \sin(\theta + \psi) + r\dot{\theta} \cos(\theta + \psi) \tag{2}$$

Using the co-ordinate system chosen in Apollo Note No. 32, we have:

$$r = \frac{a(1 - e^2)}{1 - e \sin\theta} \tag{3}$$

$$r = \frac{r_p(1 + e)}{1 - e \sin\theta} \qquad \text{where } r_p = \text{perigee altitude} \tag{4}$$

Differentiating the logarithm of Equation (4) with respect to time gives:

$$\frac{\dot{r}}{r} = \frac{e \cos\theta}{1 - e \sin\theta}\,\dot{\theta} \tag{5}$$

or

$$\dot{r} = \frac{e \cos\theta}{r(1 - e \sin\theta)}\,r^2\dot{\theta} \tag{6}$$

but

$$H = r^2\dot{\theta} \tag{7}$$

so that

$$\dot{r} = \frac{H e \cos\theta}{r(1 - e \sin\theta)} \tag{8}$$

Using Equation (7) and (8) in Equation (2), we have:

$$\dot{R} = \frac{H}{r}\left[\frac{e \cos\theta}{1 - e \sin\theta} \sin(\theta + \psi) + \cos(\theta + \psi)\right] \tag{9}$$

Simplifying Equation (9), we have:

$$\dot{R} = \frac{H}{r(1 - e \sin\theta)}\Big[e \cos\theta \sin(\theta + \psi) - e \sin\theta \cos(\theta + \psi) + \cos(\theta + \psi)\Big] \tag{10}$$

which reduces to:

$$\dot{R} = \frac{H}{r_p (1+e)} \left[e \sin \psi + \cos (\theta + \psi) \right] \tag{11}$$

but $H = \sqrt{\mu\, r_p (1+e)}$, so

$$\dot{R} = \frac{\mu^{1/2}}{\sqrt{r_p (1+e)}} \left[e \sin \psi + \cos (\theta + \psi) \right] \tag{12}$$

The orbit is now characterized in terms of the parameters r_p, ψ, and e. We will estimate the errors in the determination of these parameters from $\dot{R}$ measurements (i.e., DSIF doppler data) during a 30^o portion of the synchronous descent orbit. The small error approximation gives:

$$\Delta \dot{R} = \frac{\partial \dot{R}}{\partial r_p} \Delta r_p + \frac{\partial \dot{R}}{\partial \psi} \Delta \psi + \frac{\partial \dot{R}}{\partial e} \Delta e \tag{13}$$

where the partial derivatives are:

$$\frac{\partial \dot{R}}{\partial r_p} = - \frac{\dot{R}}{2 r_p} \tag{14}$$

$$\frac{\partial \dot{R}}{\partial \psi} = \frac{\mu^{1/2}}{\sqrt{r_p (1+e)}} \left[e \cos \psi - \sin (\theta + \psi) \right] \tag{15}$$

$$\frac{\partial \dot{R}}{\partial e} = \frac{\mu^{1/2} \sin \psi}{\sqrt{r_p (1+e)}} - \frac{\dot{R}}{2 (1+e)} \tag{16}$$

In order to simplify computation, we will obtain an approximation for the parameter errors by measuring $\dot{R}$ at 3 points on the trajectory. In this error analysis the angle at perilune (ψ) for the synchronous descent is displaced from the earth-moon line in order for the analysis to be meaningful. This occurs because if $\psi = 0$ the DSIF doppler measurement is proportional to $\dot{y}$ only (i.e., no $\dot{x}$ information is

contained in $\dot{R}$) and the resulting simultaneous equations for the parameter errors are not independent. However, this does not imply that it is necessary for perilune to be displaced from the earth-moon line in order to determine the orbit parameters from doppler data. In computing the orbit by processing the doppler data to establish the maximum likelihood estimators of the orbit parameters, the position of perilune relative to the earth-moon line can be completely arbitrary because the likelihood estimators are based on a best fit using time as the independent variable, whereas θ is the independent variable in this simplified error analysis. With time as the independent variable, it is not necessary to have $\dot{x}$ information to estimate the orbit parameters from doppler data.

Error Computation

Denote the doppler velocity measured at three distinct θ values $(\theta, \theta_2, \theta_3)$ by $(\Delta\dot{R}_1, \Delta\dot{R}_2, \Delta\dot{R}_3)$ and write:

$$\Delta\dot{R}_1 = \left(\frac{\partial \dot{R}}{\partial r_p}\right)_1 \Delta r_p + \left(\frac{\partial \dot{R}}{\partial \psi}\right)_1 \Delta\psi + \left(\frac{\partial \dot{R}}{\partial e}\right)_1 \Delta e \tag{17}$$

$$\Delta\dot{R}_2 = \left(\frac{\partial \dot{R}}{\partial r_p}\right)_2 \Delta r_p + \left(\frac{\partial \dot{R}}{\partial \psi}\right)_2 \Delta\psi + \left(\frac{\partial \dot{R}}{\partial e}\right)_2 \Delta e \tag{18}$$

$$\Delta\dot{R}_3 = \left(\frac{\partial \dot{R}}{\partial r_p}\right)_3 \Delta r_p + \left(\frac{\partial \dot{R}}{\partial \psi}\right)_3 \Delta\psi + \left(\frac{\partial \dot{R}}{\partial e}\right)_3 \Delta e \tag{19}$$

where the partial derivatives are evaluated at nominal values of the parameters and at the θ values corresponding to the subscripts.

The solution of Equations (17), (18), and (19) for the parameter errors Δr_p, $\Delta\psi$, Δe, has been carried out numerically for the 100 n. mi. synchronous trajectory with perilune at 50,000 ft. The variance of Δr_p, $\Delta\psi$, Δe, and the correlation coefficient of $\Delta r_p, \Delta\psi$ have been computed.

The computations have been carried out for the case depicted in Figure 1.

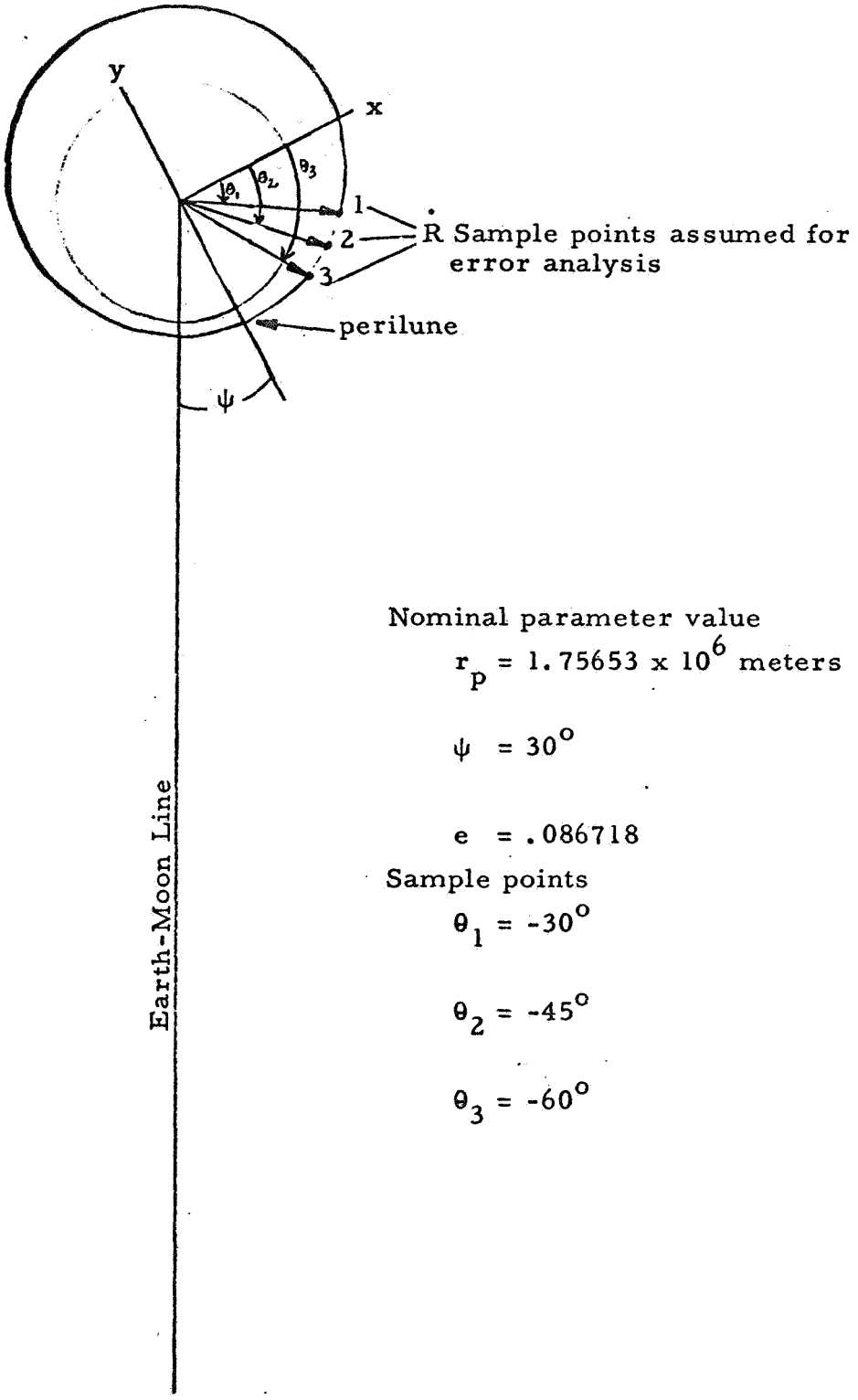

Nominal parameter value

$r_p = 1.75653 \times 10^6$ meters

$\psi = 30^\circ$

$e = .086718$

Sample points

$\theta_1 = -30^\circ$

$\theta_2 = -45^\circ$

$\theta_3 = -60^\circ$

Figure 1.

The computed root-mean-square errors for the case shown in Figure 1 are:

$$\sigma_{r_p} = 2360\ \sigma_{\dot{R}} \text{ (meters)} \tag{20}$$

$$\sigma_{\psi} = 6.03 \times 10^{-3}\ \sigma_{\dot{R}} \text{ (radians)} \tag{21}$$

$$\sigma_{e} = 4.66 \times 10^{-2}\ \sigma_{\dot{R}} \tag{22}$$

where the units of $\sigma_{\dot{R}}$ are meters/sec.

The DSIF accuracy assumed for one minute of smoothing is $\sigma_{\dot{R}} = .02$ meters/sec. This gives:

$$\sigma_{r_p} = 47 \text{ meters} \tag{23}$$

$$\sigma_{\psi} = 1.2 \times 10^{-4} \text{ radians} = 6.9 \times 10^{-3} \text{ degrees} \tag{24}$$

$$\sigma_{e} = 9.3 \times 10^{-4} \tag{25}$$

The correlation between Δr_p and Δ_{ψ}, that is their covariance, $\sigma_{r_p \psi}$, divided by $\sigma_{r_p} \cdot \sigma_{\psi}$ for this case was computed to be:

$$\rho = \frac{\sigma_{r_p \psi}}{\sigma_{r_p}\ \sigma_{\psi}} = 0.111 \tag{26}$$

Approximate error calculations were also carried out assuming that the vehicle was tracked over 60° of its orbit starting approximately

from the time it is emerged from the back-side of the moon to when it is approximately 30^{o} from the earth-moon line. The approximate errors (not significantly different from those of the previous results for tracking over 30^{o} of the orbit) are shown below.

$$\sigma_{r_p} = 2200\ \sigma_{\dot{R}} \tag{27}$$

$$\sigma_{\psi} = 2.95 \times 10^{-3}\ \sigma_{\dot{R}} \tag{28}$$

$$\sigma_{e} = 1.13 \times 10^{-2}\ \sigma_{\dot{R}} \tag{29}$$

$$\rho = 0.555 \tag{30}$$

Again taking $\sigma_{\dot{R}} = .02$ meters/sec for one minute of smoothing, we have:

$$\sigma_{r_p} = 44 \text{ meters} \tag{31}$$

$$\sigma_{\psi} = 5.9 \times 10^{-5} \text{radians} = 3.4 \times 10^{-3} \text{ degrees} \tag{32}$$

$$\sigma_{e} = 2.26 \times 10^{-4} \tag{33}$$

The foregoing results of this error analysis are summarized in the following table.

Table 1.

RMS Error \ Observation Interval	30^{o}	60^{o}
σ_{r_p}	47 meters	44 meters
σ_{ψ}	6.9×10^{-3} degrees	3.4×10^{-3} degrees
σ_{e}	9.3×10^{-4}	2.3×10^{-4}
$\rho_{r_p-\psi}$	0.111	0.555
$\sigma_{\dot{R}}$ (1 minute of smoothing)	.02 $\frac{\text{meters}}{\text{sec.}}$	.02 $\frac{\text{meters}}{\text{sec.}}$

APOLLO NOTE NO. 61

L. Lustick
7 May 1963

DETERMINATION OF SELENOCENTRIC ORBIT PARAMETERS WITH THE DSIF

PURPOSE

The purpose of this note is to estimate the accuracy that the DSIF can establish the selenocentric orbit parameters. In particular, this note examines the hyperbolic orbit relative to the moon (in the lunar sphere of influence) and the accuracy to which the DSIF can determine perilune conditions.

GEOMETRY CONSIDERED

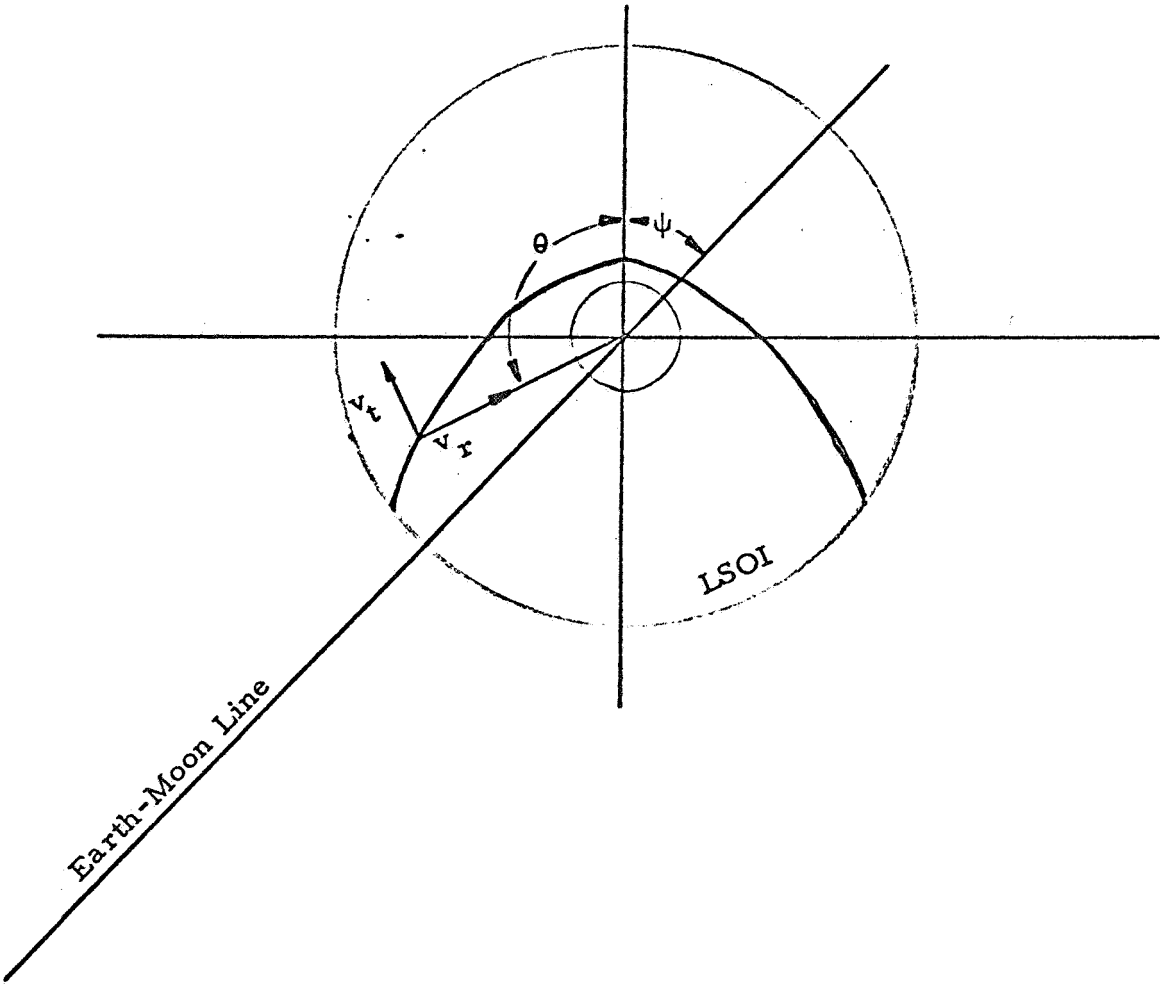

EXPRESSION FOR $\dot{R}$

The DSIF observes an $\dot{R}$ which is the projection of the velocity components relative to the moon (v_t and v_r) on the line connecting the earth and the moon.

$$\dot{R} = v_r \cos(\pi - \theta - \psi) + v_t \cos(\theta - \frac{\pi}{2} + \psi)$$

In terms of e, ψ, and r_p, $\dot{R}$ can be expressed by the equation below (See Apollo Note No. 60).

$$\dot{R} = \sqrt{\frac{\mu}{(1+e)\, r_p}} \left[e \sin\psi + \sin(\theta + \psi) \right]$$

The partial derivatives of $\dot{R}$ with respect to the parameters are presented below:

$$\frac{\partial \dot{R}}{\partial r_p} = - \frac{\dot{R}}{2 r_p}$$

$$\frac{\partial \dot{R}}{\partial \psi} = \sqrt{\frac{\mu}{(1+e)\, r_p}} \left[e \cos\psi + \cos(\theta + \psi) \right]$$

$$\frac{\partial \dot{R}}{\partial e} = - \frac{\dot{R}}{2(1+e)} + \sqrt{\frac{\mu}{(1+e)\, r_p}} \sin\psi$$

ASSUMPTIONS

1. The DSIF is located an infinite distance away from the moon.

2. The error in the determination of $\dot{R}$ with the DSIF is .02 m/sec. This number is consistent with 1 minute of smoothing.

3. The plane of the orbit is equatorial and it is assumed that no errors in the knowledge of the orbit plane exist.

4. The angle θ is used as the independent variable instead of time.

5. The nominal trajectory conditions used in the error analysis are presented below:

$\psi = 30^{o}$

e = eccentricity = 1.38

r_p = perilune radius = 1.92332×10^{6} meters

μ_m = gravitational constant of the moon = 4.899×10^{12} $\frac{m^3}{sec^2}$

ERRORS IN PARAMETERS

The errors in the parameters, r_p, ψ, and e were arrived at by observing $\dot{R}$ at three points on the trajectory and solving for the changes in the parameters indicated. The error equations used are presented below.

$$\Delta \dot{R}_1 = \left(\frac{\partial \dot{R}}{\partial \psi}\right)_1 \Delta \psi + \left(\frac{\partial \dot{R}}{\partial e}\right)_1 \Delta e + \left(\frac{\partial \dot{R}}{\partial r_p}\right)_1 \Delta r_p$$

$$\Delta \dot{R}_2 = \left(\frac{\partial \dot{R}}{\partial \psi}\right)_2 \Delta \psi + \left(\frac{\partial \dot{R}}{\partial e}\right)_2 \Delta e + \left(\frac{\partial \dot{R}}{\partial r_p}\right)_2 \Delta r_p$$

$$\Delta \dot{R}_3 = \left(\frac{\partial \dot{R}}{\partial \psi}\right)_3 \Delta \psi + \left(\frac{\partial \dot{R}}{\partial e}\right)_3 \Delta e + \left(\frac{\partial \dot{R}}{\partial r_p}\right)_3 \Delta r_p$$

The statistical averages presented below were obtained:

σ_{r_p} - standard deviation in perilune radius - meters

σ_{ψ} - standard deviation in location of perilune

σ_e - standard deviation in eccentricity

$\rho_{r_p - \psi}$; $\rho_{r_p - e}$, $\rho_{\psi - e}$ - correlation coefficient between estimated parameters

where:

$$\rho_{xy} = \frac{\overline{xy}}{\sigma_x \sigma_y}$$ x and y have zero mean.

RESULTS

Results were obtained for observation intervals of 30 and 60 degrees. The first observation was taken at conditions when the vehicle first entered the lunar sphere of influence and it equally spaced values of θ thereafter.

Table 1.

Quantity \ Observation Interval	30^o	60^o
σ_{r_p}	1080 meters	330 meters
σ_ψ	.033 degrees 1110 meters	.00675 degrees 227 meters
σ_e	5.35×10^{-4}	2.4×10^{-4}
$\rho_{r_p-\psi}$	.99389	.97779
ρ_{r_p-e}	.98032	.94897
$\rho_{\psi-e}$	.95474	.87893

CONCLUSIONS

If the orbit plane is known, the DSIF capability of determining the in-plane orbit parameters is excellent. Using the smoothed value of $\dot{R}$ at three points and a 60^o observation interval the location of perilune and the altitude at perilune can be determined with approximate errors of 1/4 of a kilometer (1 σ values).

there is no maximum value of f if the x_i can be arbitrarily large. Indeed, the partial derivatives $\frac{\partial f}{\partial x_i} = \alpha_i$, $i = 1, 2, \cdots n$ cannot simultaneously vanish except in the trivial case $\alpha_i \equiv 0$, $i = 1, \cdots, n$. The interesting case occurs when all the x_i are bounded: $a_i \leq x_i \leq b_i$. The above argument on the simultaneous vanishing of the partial derivatives indicates that there is no maximum in the open (i.e., the interior) region of the domain of the x_i. Since f must now have a maximum, we conclude it must occur on the boundary of the domain of the x_i where the derivatives do not exist.

In a heuristic way, we extend this argument to the solution of (3) and thus argue that for fixed t, the optimal controls $u_i(t)$ must assume their extreme values: $|u_i(t)| = 1$. Since this is true for arbitrary t, $u_i(t)$ must have the form of step functions:

$$\boxed{|u_i(t)| = 1} \tag{7}$$

except possibly at a finite number of discontinuities.

Synthesis of Optimal Controls

Following Pontryagin, we refer to the selection of the $u_i(t)$ as optimal control synthesis, and proceed as follows:

For fixed time, call it T, and arbitrary admissible (not necessarily optimal) controls $u_i(T)$, we first assert that the locus of accessible terminal points in phase space, call them $\xi_f(T)$, form a convex set, call it $\Omega(T)$. By a convex set we mean a set of points with the property that the line joining any two points of the set contains only points of the set. Lines, triangles, circles, spheres, ellipsoids are

APOLLO NOTE NO. 62

L. Lustick/H. Engel
10 May 1963

TRANS-EARTH INJECTION ERRORS

The error in reentry dive angle and the miss along the flight path at reentry have been computed.

This was done by finding a nominal trajectory with a flight time of approximately 70 hours from perilune to reentry and a reentry dive angle of approximately 6°, and then calculating the dive angles and reentry points for trajectories in which the initial conditions were perturbed. The differences divided by the perturbations are approximations to the partial derivatives of reentry dive angle and miss with respect to the perturbed quantities.

In this analysis, the CM is assumed to be acted upon by only one body at a time. While in the lunar sphere of influence (LSOI) it is acted upon only by the Moon's gravitational field. Outside of the LSOI it is acted upon only by the Earth's gravitational field.

The planes of the CM trajectory and Earth-Moon rotation are assumed coincident. Only perturbations in this plane are considered.

The coordinates employed are shown in Figure 1. The x and y axes move with the Moon. They are fixed in direction, and the y axis is directed along the Earth-Moon line at the instant that the CM on its nominal trajectory pierces the LSOI. The motion of the CM with respect to the Moon is a conic section in these coordinates.

The counterclockwise angle from the y axis to perilune is $\hat{\phi}$ and the clockwise angle from perilune to the point of piercing the LSOI is $\hat{\theta}$. The velocity of the CM with respect to the Moon at the instant of piercing the LSOI makes an angle $\hat{\gamma}$ with the radius from the Moon, and an angle $\pi - \hat{\alpha}$ with the y axis. The clockwise angle between the line joining the Earth and Moon and the line joining the Earth and CM at intersection with the LSOI is $\hat{\beta}$. The velocity of the Moon at the time of CM piercing the LSOI is in the -x direction.

The perilune speed is

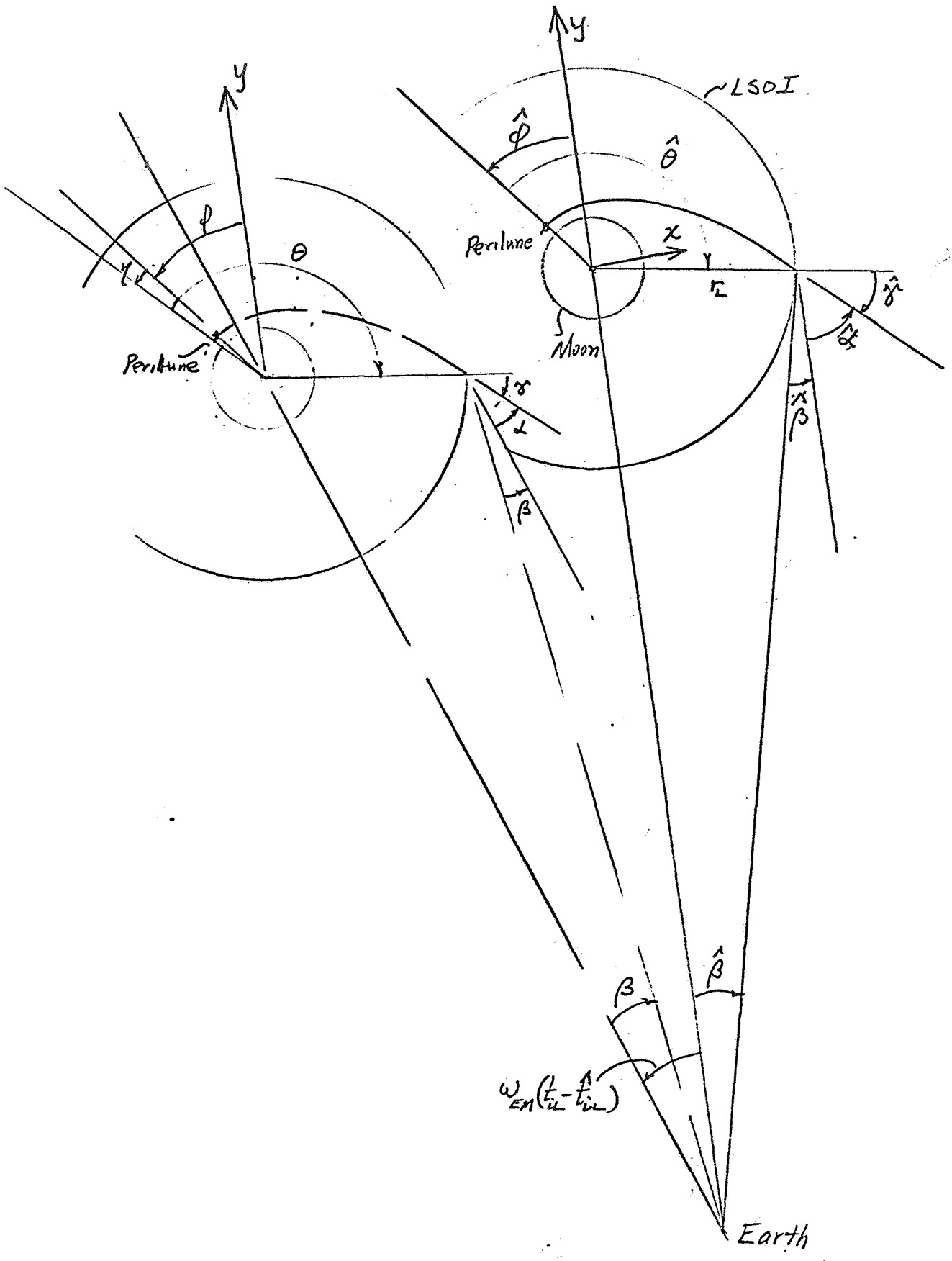

Figure 1.

$$\hat{v}_p = \sqrt{\frac{\mu_m (1 + \hat{e}_m)}{\hat{r}_p}}$$

The speed with respect to the Moon on piercing the LSOI is

$$\hat{v}_L = \sqrt{\frac{2\mu_m}{\hat{r}_p} \left(\frac{1 + \hat{e}_m}{.2} - 1 + \frac{\hat{r}_p}{r_L} \right)}$$

Its component perpendicular to the radius from the Moon is

$$\hat{v}_{\tau L} = \frac{\hat{v}_p \hat{r}_p}{r_L}$$

and its component along the radius from the Moon is

$$\hat{v}_{rL} = \sqrt{\hat{v}_L^2 - \hat{v}_{\tau L}^2}$$

The angles $\hat{\gamma}$ and $\hat{\beta}$ are given by

$$\tan \hat{\gamma} = \frac{\hat{v}_{\tau L}}{\hat{v}_{rL}}, \qquad 0 \leq \hat{\gamma} \leq \pi$$

and

$$\tan \hat{\beta} = \frac{r_L \sin (\pi - \hat{\theta} + \hat{\phi})}{r_{EM} - r_L \cos (\pi - \hat{\theta} + \hat{\phi})}, \qquad \frac{-\pi}{2} \leq \hat{\beta} \leq \frac{\pi}{2}$$

in which r_{EM} is the distance from the Earth to the Moon. Now, if v_m is the speed of the Moon with respect to the Earth, directed counterclockwise, the radial and tangential components of the CM velocity with respect to the Earth at the LSOI are

$$\hat{V}_{RL} = -\hat{v}_L \cos(\hat{\alpha}+\hat{\beta}) - v_m \sin\hat{\beta}$$

$$\hat{V}_{TL} = -\hat{v}_L \sin(\hat{\alpha}+\hat{\beta}) + v_m \cos\hat{\beta}$$

in which

$$\hat{\alpha} = \hat{\phi} + \pi - \hat{\theta} - \hat{\gamma}$$

The distance from Earth at the point of piercing the LSOI is

$$\hat{R}_L = \frac{r_L \sin(\pi - \hat{\theta} + \hat{\phi})}{\sin\hat{\beta}}$$

The angular momentum and energy of the Earth-centered orbit are

$$\hat{H}_E = \hat{V}_{TL}\,\hat{R}_L$$

and

$$\hat{E}_E = \frac{1}{2}\left[\hat{V}_{TL}^2 + \hat{V}_{RL}^2\right] - \frac{\mu_E}{\hat{R}_L}$$

Then the Earth orbit eccentricity and perigee distance are

$$\hat{e}_E = \sqrt{1 + \frac{2\hat{E}_E \hat{H}_E^2}{\mu_E^2}}$$

and

$$\hat{R}_P = \frac{\hat{H}_E^2}{\mu_E(1+\hat{e}_E)}$$

For perigee radius less than the reentry radius, R_F, the dive angle at reentry is given by

$$\tan\hat{\delta}_F = \sqrt{-1 + \frac{2\mu_E R_F}{\hat{H}_E^2} + \frac{2\hat{E}_E R_F^2}{\hat{H}_E^2}}, \quad 0 \leq \hat{\delta}_F \leq \pi/2$$

The angular distance about the Earth from exit from the LSOI to perigee is $\hat{\psi}_{LP}$,

$$\hat{\psi}_{LP} = \sin^{-1}\left[\frac{1 - \frac{\hat{H}_E^2}{\mu_E R_L}}{\hat{e}_E}\right] + \frac{\pi}{2}, \qquad 0 \leq \hat{\psi}_{LP} \leq \pi$$

and the angular distance from reentry to perigee, if reentry occurs, is $\hat{\psi}_{FP}$,

$$\hat{\psi}_{FP} = \sin^{-1}\left[\frac{1 - \frac{\hat{H}_E^2}{\mu_E R_F}}{\hat{e}_E}\right] + \frac{\pi}{2} \qquad 0 \leq \psi_{FP} \leq \pi$$

The angle between exit from the LSOI and reentry is

$$\hat{\psi}_{LF} = \hat{\psi}_{LP} - \hat{\psi}_{FP}$$

In order to compute the time from injection into the trans-earth orbit until piercing the LSOI, the energy and angular momentum of the CM in the LSOI must be known. These are

$$\hat{E}_m = \frac{2\mu_m}{\hat{r}_p}(\hat{e}_m - 1)$$

and

$$\hat{H}_m = \mu_m \hat{r}_p (\hat{e}_m + 1)$$

The time from perilune to piercing the LSOI is

$$\hat{t}_{pL} = \frac{1}{2\hat{E}_m}\left\{\hat{H}_m \cot \hat{\gamma} - \frac{\mu_m}{\sqrt{2\hat{E}_m}} \log_e\left[\hat{u} + \sqrt{\hat{u}^2 - 1}\right]\right\}$$

in which

$$\hat{u} = \left[1 + (\hat{e}_m - 1) \frac{r_L}{\hat{r}_p} \right] / \hat{e}_m$$

The time from piercing the LSOI until reentry is

$$t_{LF} = \frac{1}{2\hat{E}_E} \left\{ \sqrt{-\hat{H}_E^2 + 2\mu_E R_L + 2\hat{E}_E R_L^2} \right.$$

$$+ \frac{\mu_E}{\sqrt{-2\hat{E}_E}} \sin^{-1} \left[\frac{1 + \frac{2\hat{E}_E R_L}{\mu_E}}{\hat{e}_E} \right] - \hat{H}_E \tan \hat{\delta}_F$$

$$\left. - \frac{\mu_E}{\sqrt{-2\hat{E}_E}} \sin^{-1} \left[\frac{1 + \frac{2\hat{E}_E R_F}{\mu_E}}{\hat{e}_E} \right] \right.$$

in which the angles indicated on the right hand side are between $-\pi/2$ and $\pi/2$.

The total time of flight is

$$\hat{t}_T = \hat{t}_{pL} + \hat{t}_{LF}$$

In order to find the nominal orbit, a number of values of $\hat{\phi}$ and $\hat{e}_m$ were selected, and the perigee radius and time of flight determined. See Figure 2. On the basis of these computations, a second run was made and perigee, reentry angle and time of flight plotted as in Figures 3 and 4. Based on these results, a third run was made, yielding in one case a dive angle of 6.09° and a time of flight of 70.415 hours. This was deemed close enough to the desired 6° and 70 hours to be used as the basis for an error analysis.

Using the indicated trajectory as a basis the perilune conditions were perturbed, the new reentry conditions calculated, and the difference between the perturbed and unperturbed reentry conditions divided by the amount of the perturbation to indicate the sensitivity.

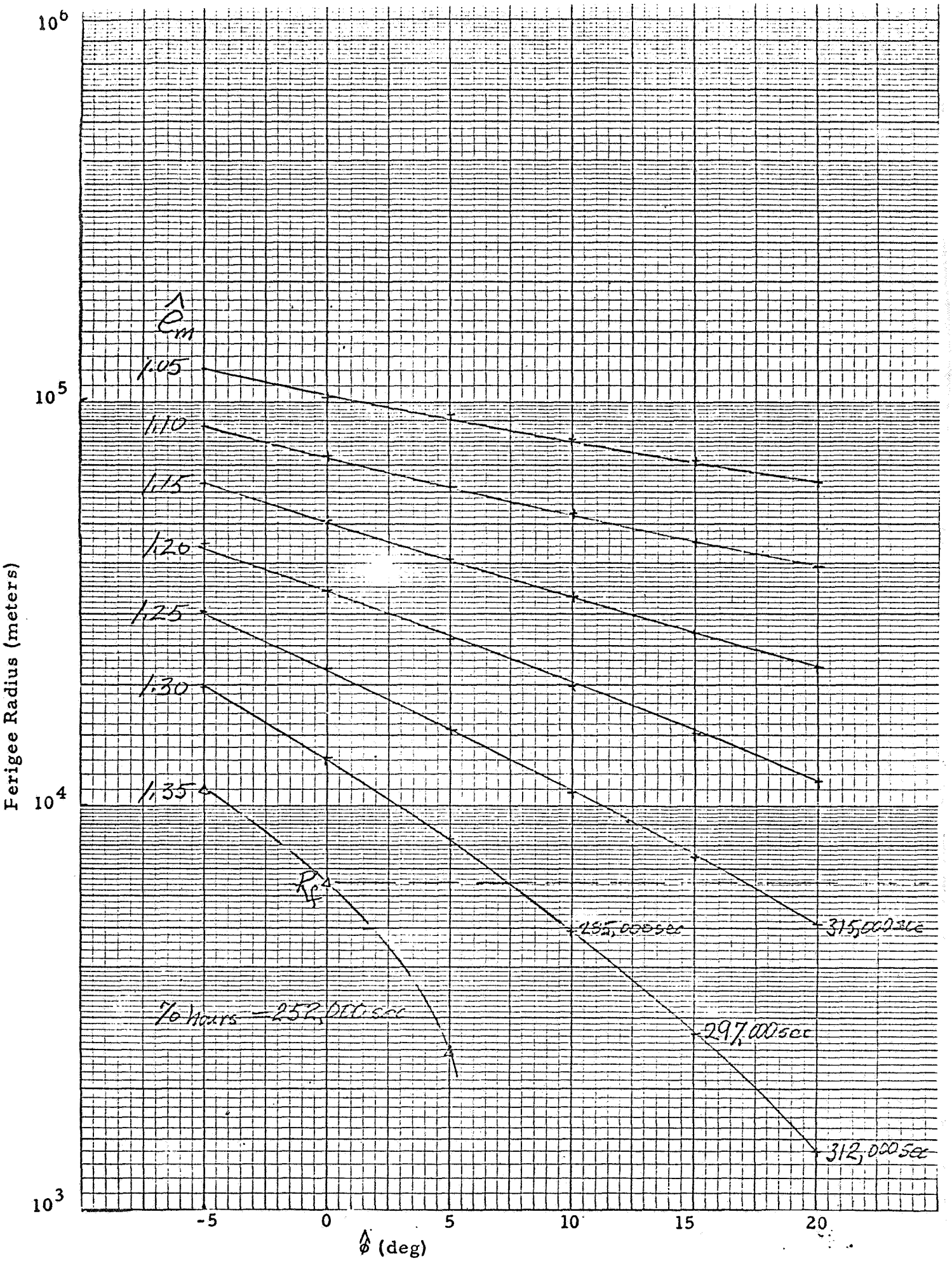
10^6
10^5
10^4
10^3
Perigee Radius (meters)
$\hat{e}_m$
1.05
1.10
1.15
1.20
1.25
1.30
1.35
R_e
195,000sec
315,000sec
297,000sec
312,000sec
7½ Hours = 252,000 sec
-5
0
5
10
15
20
$\hat{\phi}$ (deg)

Figure 2.

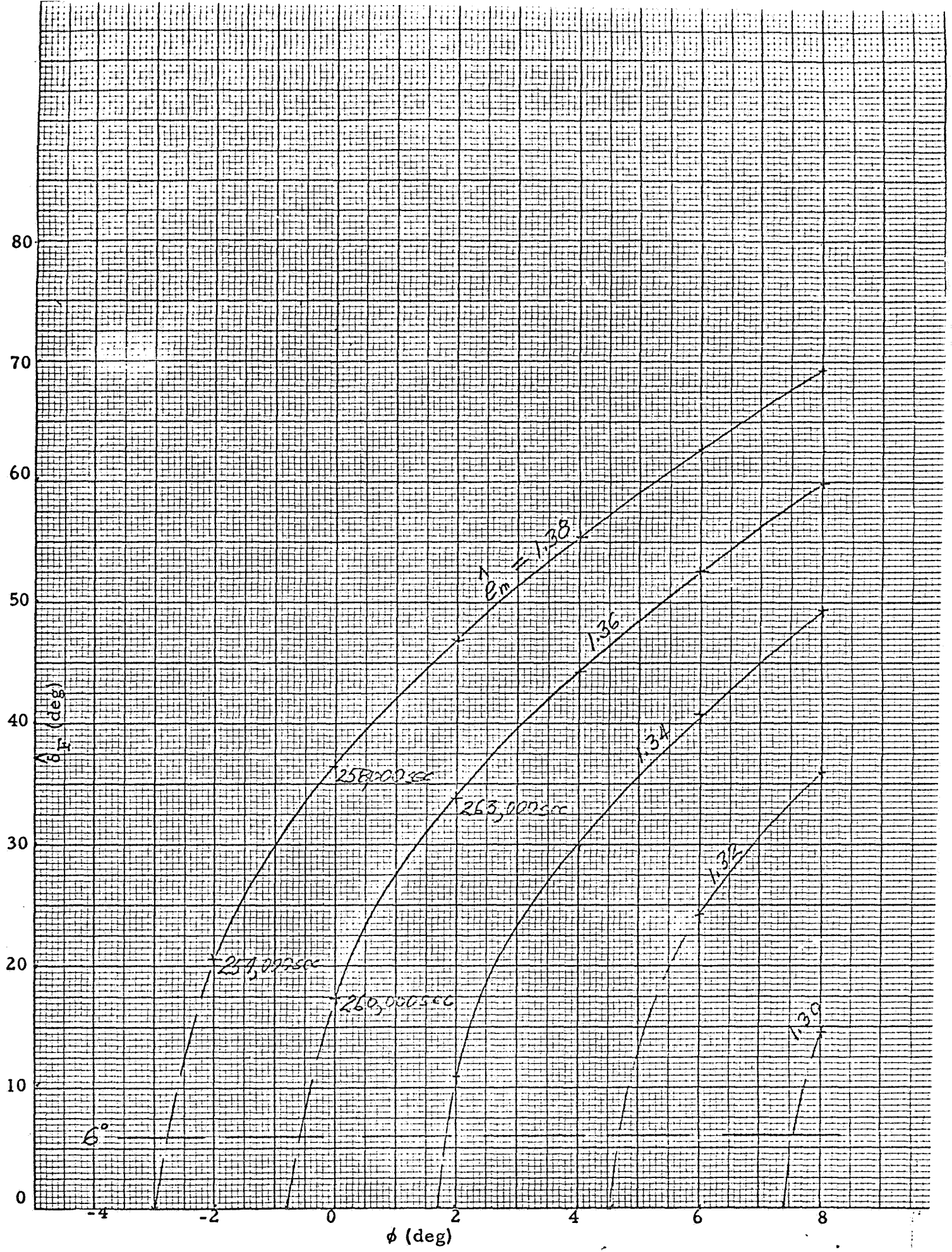
80
70
60
50
40
30
20
10
0
-4
-2
0
2
4
6
8
ϕ (deg)
$\Delta\delta_H$ (deg)
$M_m = 1.38$
1.36
1.34
1.32
1.30
6°

Figure 3.

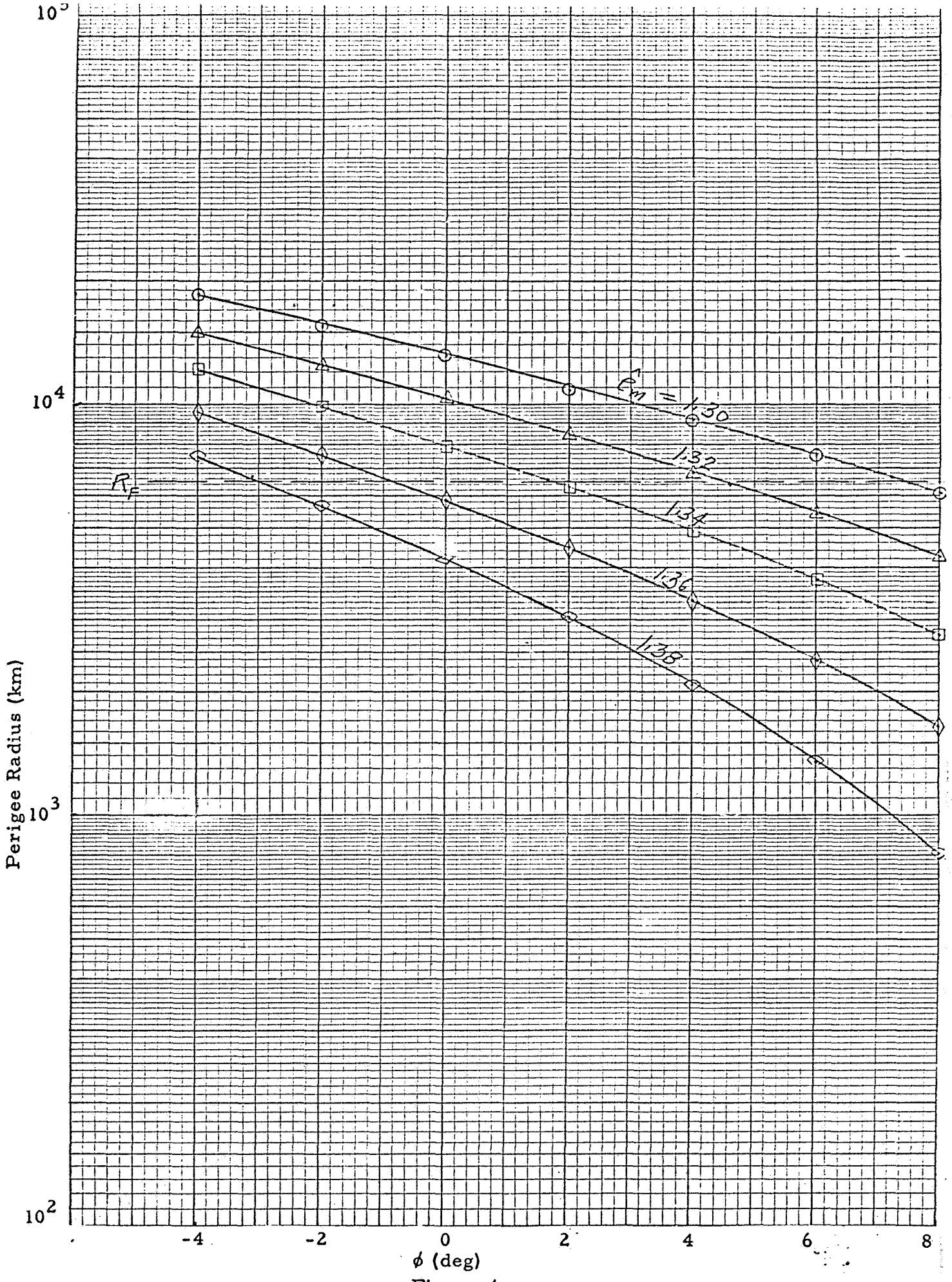
10^5
10^4
10^3
10^2
R_F
$\hat{e}_m = 1.30$
1.32
1.34
1.36
1.38
Perigee Radius (km)
-4
-2
0
2
4
6
8
ϕ (deg)

Figure 4.

The quantities perturbed were radius at injection, ϕ at injection, and the radial and tangential components of velocity at injection.

$$r_i = \hat{r}_p + \Delta r$$

$$\phi_i = \hat{\phi} + \Delta\phi$$

$$v_{r_i} = \Delta v_r - \hat{v}_t \Delta\phi$$

$$v_{t_i} = \hat{v}_p + \Delta v_t$$

On the basis of these new injection conditions, the orbit within the LSOI was computed, using

$$H_m = v_{t_i} r_i$$

$$E_m = \frac{1}{2}\left[v_{t_i}^2 + v_{r_i}^2 \right] - \frac{\mu_m}{r_i}$$

$$e_m = \sqrt{1 + \frac{2E_m H_m^2}{\mu_m^2}}$$

$$r_p = \frac{H_m^2}{\mu_m(1 + e_m)}$$

$$\cos\eta = \frac{1}{e_m}\left[(1 + e_m)\frac{r_p}{r_i} - 1 \right], \begin{cases} -\frac{\pi}{2} \leq \eta \leq \frac{\pi}{2} \\ \operatorname{sgn}\eta = \operatorname{sgn}(\Delta v_r - \hat{v}_p \Delta\phi) \end{cases}$$

Here η is the angle between perilune and injection.

$$v_p = \sqrt{\frac{\mu_m (e_m + 1)}{r_p}}$$

The conditions at piercing the LSOI are computed from the same formulas used in the unperturbed case, but with the perturbed values. It must be remembered, however, that the coordinate system used for the orbit outside the LSOI was based on the location of the Moon at the time the nominal orbit pierced the LSOI, and that ϕ_i was measured relative to this coordinate system. Since the time to piercing the LSOI is different in the perturbed orbit the position of the Earth-Moon line at the time of piercing the LSOI is also different, as indicated in Figure 1, and some angle corrections are necessary. Thus

$$x_i = -1 + \frac{2}{1+e_m}\,\frac{r_i}{r_p} + \frac{e_m - 1}{1+e_m}\,\left(\frac{r_i}{r_p}\right)^2$$

$$t_{pi} = \frac{\operatorname{sgn}\left(\Delta v_r - \hat{v}_p\,\Delta\phi\right)}{2E_m}\left\{H_m\,x_i^{1/2} - \frac{\mu_m}{\sqrt{2E_m}}\log_e\left(u_i + \sqrt{u_i^2 - 1}\right)\right\}$$

in which

$$u_i = \left[1 + (e_m - 1)\,\frac{r_i}{r_p}\right]/e_m$$

The time from perilune to piercing the LSOI is calculated from the same formula at $\hat{t}_{pi}$, using the perturbed values. Then

$$t_{iL} = t_{pL} - t_{pi}$$

$$\alpha = \phi_i + \eta + \pi - \theta - \gamma - \omega_{EM}\left(t_{iL} - \hat{t}_{iL}\right)$$

$$\tan\beta = \frac{r_L \sin(\alpha+\gamma)}{r_{EM} - r_L\cos(\alpha+\gamma)}$$

$$V_{RL} = -v_L\cos(\alpha+\beta) - v_m\sin\beta$$

$$V_{TL} = -v_L\sin(\alpha+\beta) + v_m\cos\beta$$

$$R_L = \frac{r_L \sin(\alpha + \gamma)}{\sin \beta}$$

The dive angle at reentry, the angular motion about the Earth, and the time from piercing the LSOI to reentry are computed as in the nominal case.

The miss must be computed taking into account the difference in Earth coordinates systems in the perturbed and unperturbed cases, so

$$M = \left\{ \psi_{LF} - \beta - (\hat{\psi}_{LF} - \hat{\beta}) + \omega_{EM}(t_{iL} - \hat{t}_{iL}) - \omega_E(t_T - \hat{t}_T) \right\} R_f$$

The results are indicated in Figures 5 and 6 for various perturbations.

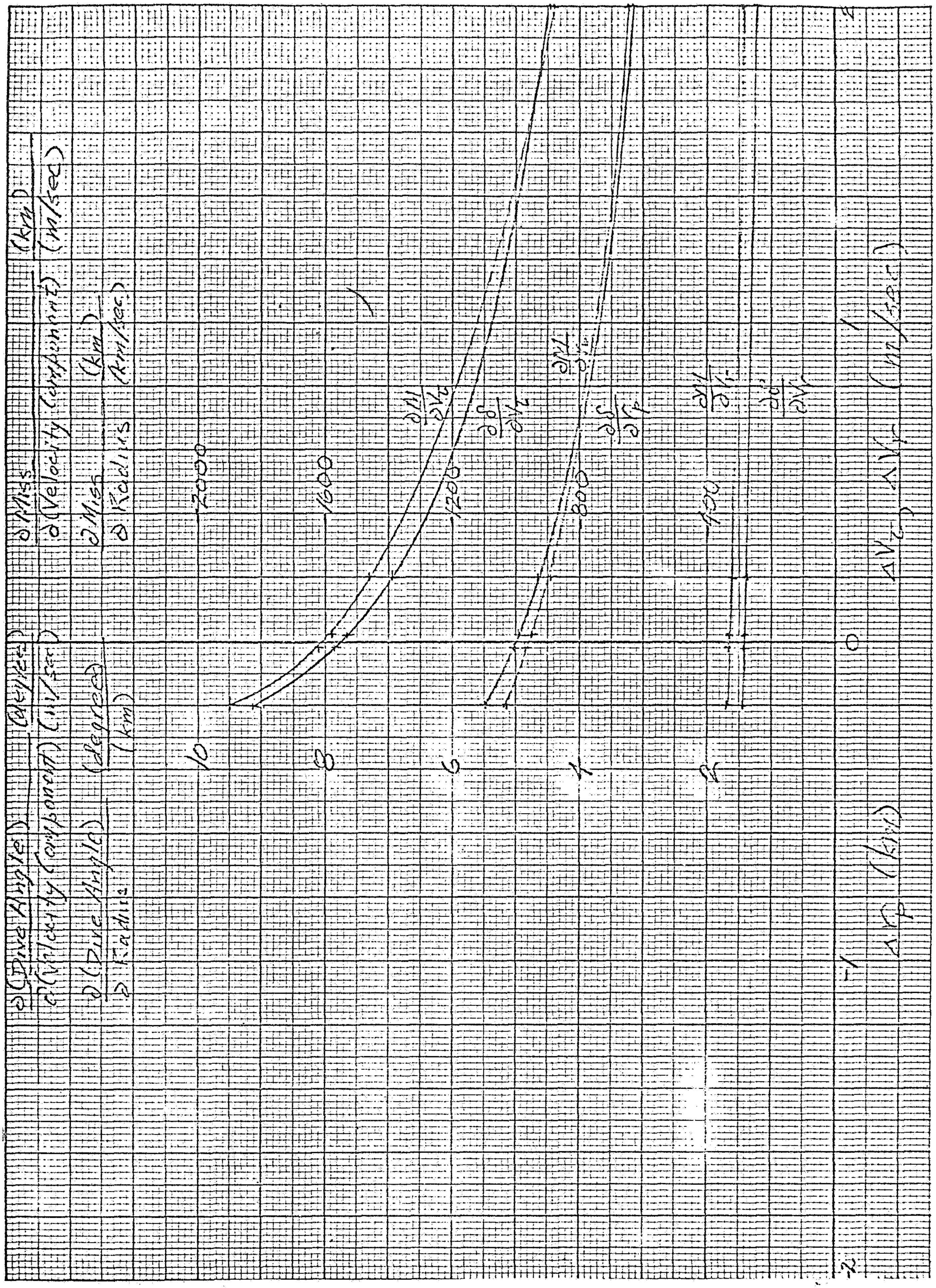

Figure 5.

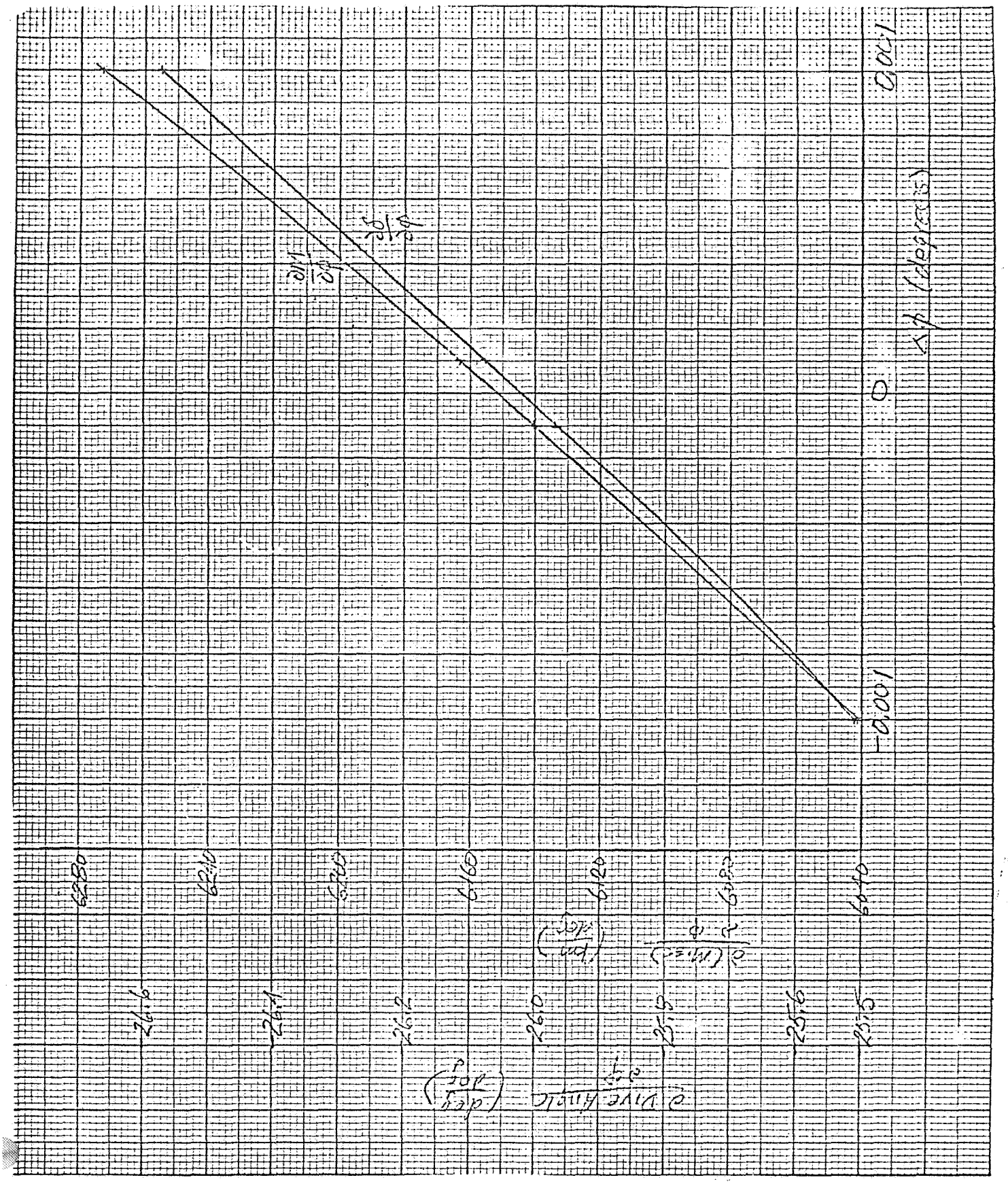

Figure 6.

APOLLO NOTE NO. 63

G. F. Floyd
10 May 1963

DSIF CAPABILITY ON TRANS-EARTH TRAJECTORY

As shown in Note No. 26, the sensitive directions for re-entry dive angle and miss along (range miss) are so close while in the earth's sphere of influence that independent control of the two orbit parameters is impractical. Luckily, however, the results of Note No. 62 show that this high correlation also exists back at lunar injection. At lunar injection we have for the coefficients along the most sensitive direction,

$$\frac{\Delta M_{||}}{\Delta \delta_f} = 220 \text{ km per degree} \tag{1}$$

while after we enter the earth sphere of influence, we have, from page 4 of Note No. 26:

$$\frac{\Delta M_{||}}{\Delta \delta_f} = 210 \text{ km/degree} \tag{2}$$

and the sensitivity ratios are of the same sign. Therefore, the ratios are so nearly the same that midcourse corrections to correct the effect of injection errors or re-entry angle will automatically correct the range miss. Further justification of this conclusion is furnished by the fact that from Note No. 53 we see that the range dispersion with a zero-lift re-entry will be several hundred miles at re-entry angle dispersion of 0.1°. Therefore, there is no gain in holding the re-entry miss much smaller than this value. This result is, of course, fortunate since we can't control the two separately anyhow.

Also as shown in Note No. 26, the sensitivity of the out of plane miss (track miss) is very much lower than that of the re-entry angle. Therefore, if we can measure and control the re-entry angle to 0.1° we will be able to control the track miss to better than a fraction of a nautical mile. Consequently, the following analysis of the DSIF capability on the return trajectory will be devoted entirely to the variance in the re-entry dive angle.

The basic formulas for the variance in the estimated value of (δ_f) from $\dot{n}$ data observed over the range interval R_2 to R_1 are derived in Note No. 5 and the results of a computer evaluation of these formulas is given as $\phi(R_2, R_1)$ of Figure 1 and Figure 2. The variance in (δ_f) related to the plotted function $\phi(R_1, R_2)$ is,

$$\sigma^2(\delta_f) = \frac{\sigma^2(\dot{R})\,(R_2 - R_1)\,\phi\,(R_2, R_1)}{N}$$

where

$$N \triangleq \text{number of samples} = \frac{T(R_2) - T(R_1)}{t_{correlation}}$$

and T(R) is the time-to-go at range R, which is plotted in Figure 3.

The optimum method of combining old and new measurements when there is an intervening imperfectly executed change is derived in Note No. 57, and this method was used in calculating the performance during a typical midcourse correction system for earth return.

In order to determine the limitations of the DSIF, the assumption was made that the CM was under completely manual control with no autopilot and no integrating accelerometers. The execution of the ground derived commands is then accomplished by pointing the spacecraft at the ordered star, spinning it to get spin stabilization (see Note No. 38), and applying the boosts for a commanded time interval. With such crude control, the major error that results would be that of the assumed 10% engine thrust level uncertainty since the errors due to poor directional control arising from unbalanced torques (c. g. shifts or locked over nozzles), were shown in Note 38 to be less than 12° and with the boost ordered in the most sensitive direction (Note 22), these directional errors would result in percentage error of less than 2% which is negligible compared with the 10% magnitude error that would result without a longitudinal integrating accelerometer.

The assumption of very poor execution of the commands puts a real premium on navigation accuracy and short smoothing time in order to keep the midcourse correction fuel requirements within the fuel pad limits. The reason for this is shown in Figure 4 which is a plot of the

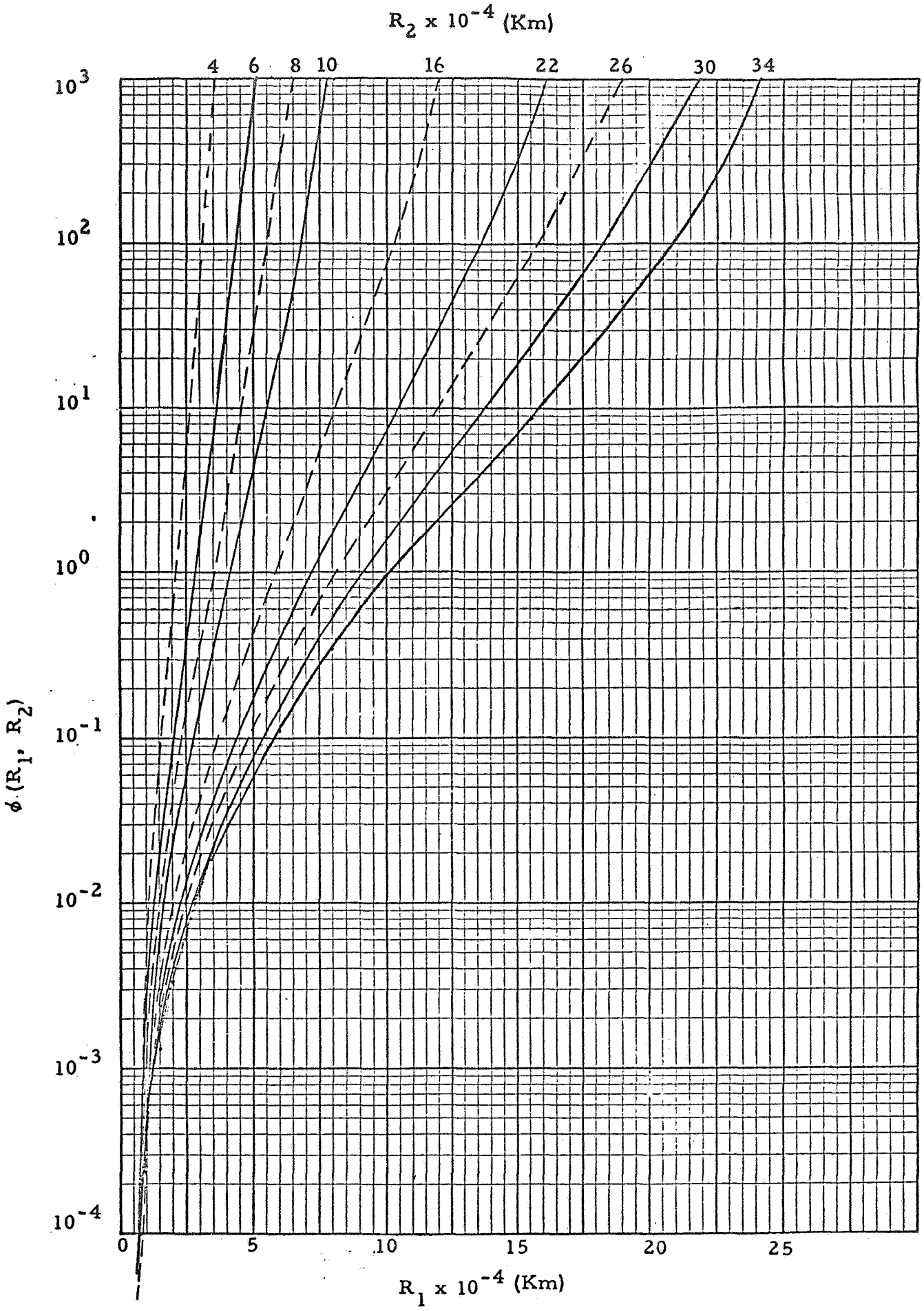
$R_2 \times 10^{-4}$ (Km)
4
6
8
10
16
22
26
30
34
10^3
10^2
10^1
10^0
10^{-1}
10^{-2}
10^{-3}
10^{-4}
$\phi(R_1, R_2)$
0
5
10
15
20
25
$R_1 \times 10^{-4}$ (Km)

Figure 1.

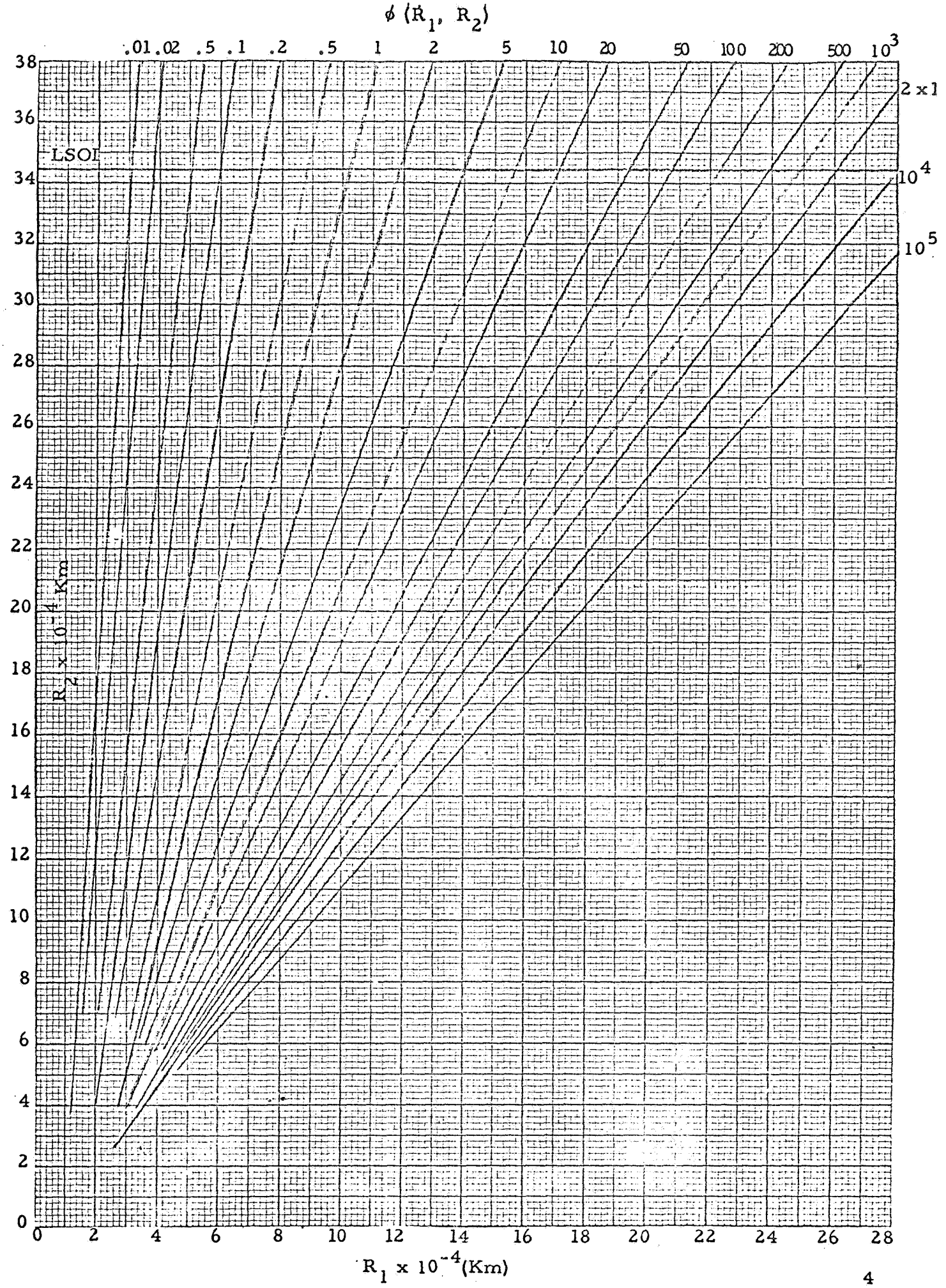
$\phi(R_1, R_2)$
.01 .02 .5 .1 .2 .5 1 2 5 10 20 50 100 200 500 10^3
2 x 1
10^4
10^5
LSOI
$R_2 \times 10^{-4}$ Km
0 2 4 6 8 10 12 14 16 18 20 22 24 26 28 30 32 34 36 38
0 2 4 6 8 10 12 14 16 18 20 22 24 26 28
$R_1 \times 10^{-4}$(Km)

Figure 2.

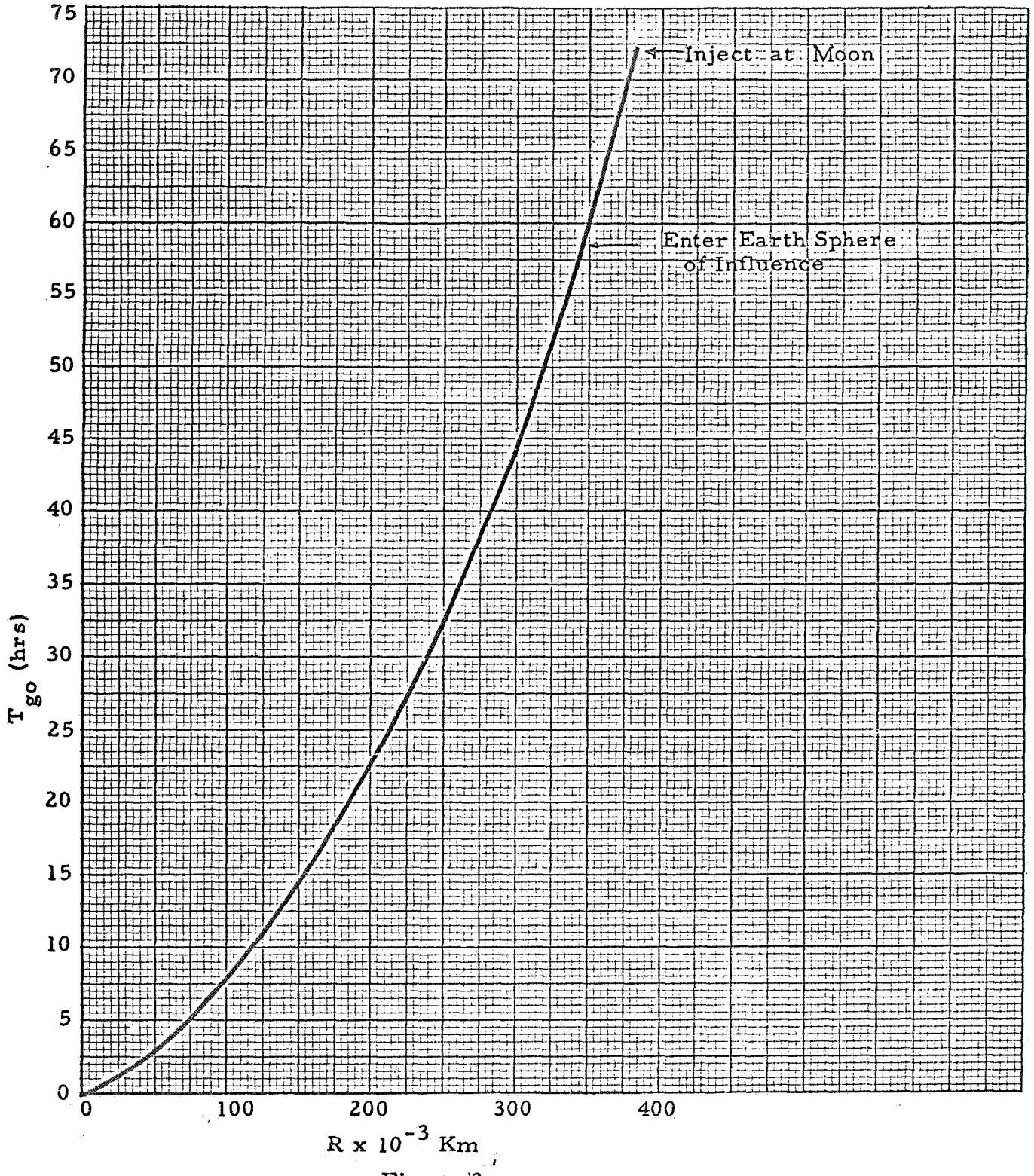
75
70
65
60
55
50
45
40
35
30
25
20
15
10
5
0
T_{go} (hrs)
Inject at Moon
Enter Earth Sphere of Influence
0
100
200
300
400
R x 10^{-3} Km

Figure 3.

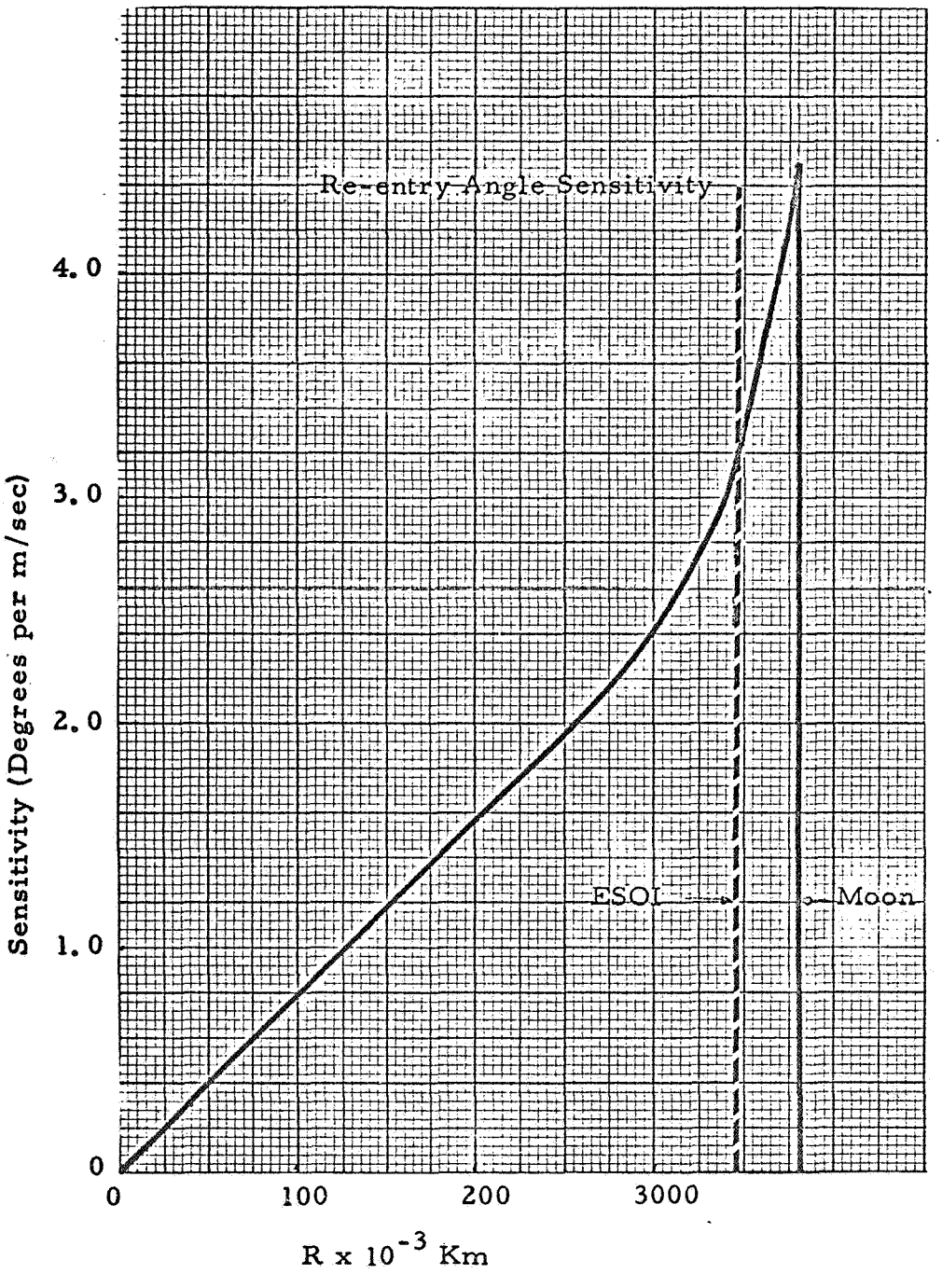
Re-entry Angle Sensitivity
4.0
3.0
2.0
1.0
0
Sensitivity (Degrees per m/sec)
ESOI
Moon
0
100
200
3000
R x 10^-3 Km

Figure 4.

re-entry angle sensitivity coefficient in degrees per meter/sec as a function of range from the earth. At injection the coefficient is 4.5°/m/sec and it very rapidly falls to 3.0°/m/sec as the spacecraft goes through the lunar sphere of influence. Thus even if the injection error could be completely corrected when the vehicle reached the earth sphere of influence, the correction required would be 1.5 times the injection error and with a 10% autopilot the injection error will be $\frac{1}{10} \times 3000 = 300$ ft/sec so the midcourse ΔV required will be at least 450 ft/sec.

No attempt has been made yet to optimize the midcourse correction schedule other than just intuitive guesses at one which will give satisfactory performance. The results with such a "guessed at" program are shown in Table 1.

Table 1.

Time Till Re-entry (hrs)	DSIF 1σ Uncertainty in Re-entry Angle	Correction No.	Commanded Boost ft/sec	Resultant Error in Re-entry Angle (degrees)
72	DNA	Injection	3000	450
50	1.1	1	550	45
36	1.1	2	69	4.6
24	.7	3	10	.8
16	.3	4	2.5	.3
8	.09	5	1.5	.09
2	.02	-	-	-

As the table shows, the capabilities of the DSIF are so good that even with very poor execution of commands, resulting in very large initial errors, large errors in the execution of each command (so that old smoothing data is not useful, see Note 57), the DSIF still can get the spacecraft within the 0.1° tolerance at eight hours to go (spacecraft at 15 earth radii).

It will be noted that five corrections are required. This is not due to DSIF uncertainties but simply because of the large execution error that was assumed. With a 10% execution error, and an initial error of 450°, it would take four perfectly computed corrections to bring the result to .04 whereas with present DSIF accuracy, tracking errors stretch this to only 5. The total midcourse boost needed is 633 ft or about twice the injection error as compared with 450 ft/sec if there were DSIF errors.

In summary, it appears that with DSIF orbit prediction accuracy, it should be possible to make a safe zero lift re-entry with manual execution of the commanded maneuvers. Also it should be emphasized that if there were a single longitudinal integrating accelerometer, the execution error would be reduced by a factor of 5 to the 2% associated with spin stabilization. In this case the re-entry angle error reduction of Table 1 would look much better and reach the $.1^{\circ}$ goal at more than 12 hours out.

APOLLO NOTE NO. 64

B. Saltzberg
14 May 1963

CAPABILITY OF THE DSIF FOR DETERMINING IN-PLANE ORBIT PARAMETERS DURING ASCENT

INTRODUCTION

This note is similar to Apollo Note No. 60 which presented an error analysis for determining the in-plane orbit parameters during descent. In this note, the errors are calculated for the ascent part of the trajectory, assuming that DSIF doppler measurements are made during approximately 30° of the ascent trajectory.

This approximate analysis considers the error in apolune position and the resulting rendezvous miss distance due to the timing error as well as the apolune altitude and angle error. For this error analysis the rendezvous miss distance is defined as the separation between the ascending LEM and the CM when the ascending LEM reaches apolune. The nominal orbits assumed in this analysis are:

1. the CM in circular orbit at 100 n. mi. altitude, and
2. the ascending LEM in the same orbit plane with perilune at zero altitude and apolune at 100 n. mi. altitude, such that the LEM and CM meet at the first approach to apogee.

The nominal values used in the analysis are:

$$r_a = 1.9226 \text{ km}$$

$$r_p = 1.7373 \times 10^3 \text{ km}$$

$$e = \frac{.19}{3.6599} = .05063$$

$$\psi = 30^{\circ}$$

The parameter errors will be estimated by measuring $\dot{R}$ at three points on the trajectory as in Apollo Note No. 60. Using the co-ordinate

system of Apollo Note No. 60, the sample points for the approximate analysis were chosen as:

$$\theta_1 = -165^\circ$$

$$\theta_2 = -180^\circ$$

$$\theta_3 = -195^\circ$$

With a nominal $\psi = 30^\circ$ (see Figure 1 of Apollo Note No. 60), then the last data point ($\theta_3 = -195^\circ$) is approximately 15° ahead of where the ascending LEM would be occluded by the Moon.

ERROR EQUATIONS

The in-plane orbit parameters r_a, ψ, e, are related to the doppler, f_d, as follows:

$$\lambda f_d = \dot{R} = \frac{\mu^{1/2}}{\sqrt{r_a (1 - e)}} \left[e \sin \psi + \cos (\theta + \psi) \right] \tag{1}$$

Just as in Apollo Note No. 60, the small error approximation is used:

$$\Delta \dot{R} = \frac{\partial \dot{R}}{\partial r_a} \Delta r_a + \frac{\partial \dot{R}}{\partial \psi} \Delta \psi + \frac{\partial \dot{R}}{\partial e} \Delta e \tag{2}$$

where the partial derivatives are:

$$\frac{\partial \dot{R}}{\partial r_a} = - \frac{\dot{R}}{2 r_a} \tag{3}$$

$$\frac{\partial \dot{R}}{\partial \psi} = \frac{\mu^{1/2}}{\sqrt{r_a (1-e)}} \left[e \cos \psi - \sin (\theta + \psi) \right] \tag{4}$$

$$\frac{\partial \dot{R}}{\partial e} = \frac{\mu^{1/2} \sin \psi}{\sqrt{r_a (1-e)}} + \frac{\dot{R}}{2 (1-e)} \tag{5}$$

The system of equations whose inverse has been computed for the parameter errors is:

$$\Delta\dot{R}_1 = \left(\frac{\partial \dot{R}}{\partial r_a}\right)_1 \Delta r_a + \left(\frac{\partial \dot{R}}{\partial \psi}\right)_1 \Delta\psi + \left(\frac{\partial \dot{R}}{\partial e}\right)_1 \Delta e \tag{6}$$

$$\Delta\dot{R}_2 = \left(\frac{\partial \dot{R}}{\partial r_a}\right)_2 \Delta r_a + \left(\frac{\partial \dot{R}}{\partial \psi}\right)_2 \Delta\psi + \left(\frac{\partial \dot{R}}{\partial e}\right)_2 \Delta e \tag{7}$$

$$\Delta\dot{R}_3 = \left(\frac{\partial \dot{R}}{\partial r_a}\right)_3 \Delta r_a + \left(\frac{\partial \dot{R}}{\partial \psi}\right)_3 \Delta\psi + \left(\frac{\partial \dot{R}}{\partial e}\right)_3 \Delta e \tag{8}$$

The approximate uncertainty in the time from perilune to apolune due to an error in r_a is:

$$\left.\begin{aligned} T_{p\text{-}a} &= \text{time from perilune to apolune} \\ T_{p\text{-}a} &= \pi \frac{a^{3/2}}{\mu^{1/2}} \end{aligned}\right\} \tag{9}$$

$$\frac{\Delta T_{p\text{-}a}}{T_{p\text{-}a}} = \frac{3}{2} \frac{\Delta a}{a} \tag{10}$$

but

$$a = \frac{(r_a + r_p)}{2} \tag{11}$$

Assuming no error in r_p, we have:

$$\Delta a = \frac{\Delta r_a}{2} \tag{12}$$

and

$$\frac{\Delta T_{p-a}}{T_{p-a}} = \frac{3}{4} \frac{\Delta r_a}{a} \tag{13}$$

The miss along the orbit path due only to the above timing error at apolune is approximately:

$$\Delta S_t = V_a \Delta T_{p-a} = \frac{3}{4} \frac{V_a T_{p-a}}{a} \Delta r_a \tag{14}$$

but

$$V_a = \sqrt{\frac{\mu (1 - e)}{a (1 + e)}} \tag{15}$$

so, using Equation (9)

$$\frac{V_a T_{p-a}}{a} = \pi \sqrt{\frac{1 - e}{1 + e}} \tag{16}$$

and Equation (14) becomes:

$$\Delta S_t = \frac{3\pi}{4} \sqrt{\frac{1 - e}{1 + e}} \Delta r_a \tag{17}$$

For the case $e = .05063$

$$\Delta S_t = 2.2 \Delta r_a \tag{18}$$

Thus, the total miss distance, ΔS, due to an error in r_a is approximately:

$$\Delta S = \sqrt{(\Delta S_t)^2 + (\Delta r_a)^2} = \sqrt{(2.2)^2 + 1} \Delta r_a = 2.4 \Delta r_a \tag{19}$$

The standard deviation and the correlation between the errors in r_a, ψ, and e, assuming one minute of doppler smoothing, are

summarized in the following table. Again, these numbers are based on sampling at 3 points over a 30^{o} sector of the orbit, assuming an effective one minute of smoothing at each of the three sample points as described in the Introduction. (See Figure 1).

TABLE 1.

σ_{r_a}	26 meters
σ_{ψ}	2.04×10^{-5} radians
σ_{e}	8×10^{-5}
$\rho_{r_a-\psi}$	-.949
ρ_{r_a-e}	.959
$\rho_{\psi-e}$	-.80
$\sigma_{\dot{R}}$	.02 meters/sec. (1 minute of smoothing)

The variance in the miss distance (σ_S) at apolune due to errors in r_a, ψ, and T_{p-a} is approximately (assuming $\rho_{r_a-\psi} = -1$ and $\rho_{r_a-T_{p-a}} = 1$)

$$\sigma_S^2 = \sigma_{r_a}^2 + (\sigma_{S_t} - r_a \sigma_{\psi})^2$$

where (from Equation (18))

$$\sigma_{S_t} = 2.2 \sigma_{r_a}$$

thus,

$$\sigma_S = 62 \text{ meters}$$

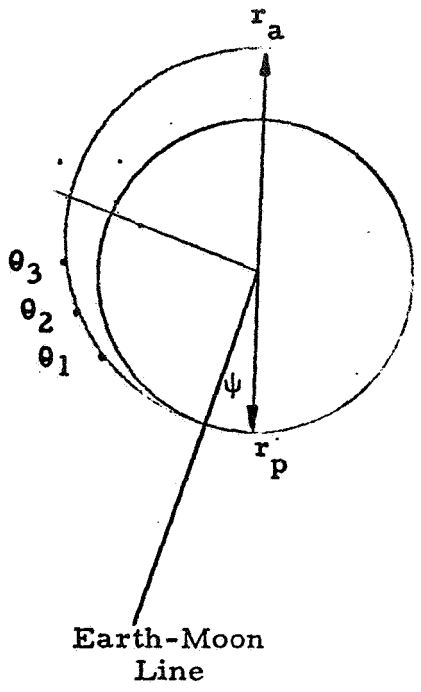

Figure 1.

This error analysis has assumed that the phase, θ, at each of the sample points is known, and the resulting small error in determining the position of the LEM at apolune ($\sim$ 62 meters), suggests that the error in the phase parameter may be the principal source of error in deriving apolune position from DSIF doppler data. Therefore, a more general analysis, taking into account errors in the phase parameter, is being conducted.

APOLLO NOTE NO. 65

L. Lustick
15 May 1963

DETERMINATION OF THE CO-ORDINATES OF AN LEM ON THE MOON FROM DSIF MEASUREMENTS FROM ONE STATION

PURPOSE

The purpose of this note is to indicate the capability of the DSIF to determine the location of an LEM on the lunar surface.

Celestial Geometry

The celestial geometry of earth-moon space is defined in Apollo Note No. 59. The figure below is reproduced from this note and defines the geometry pertinent to the analysis of this report.

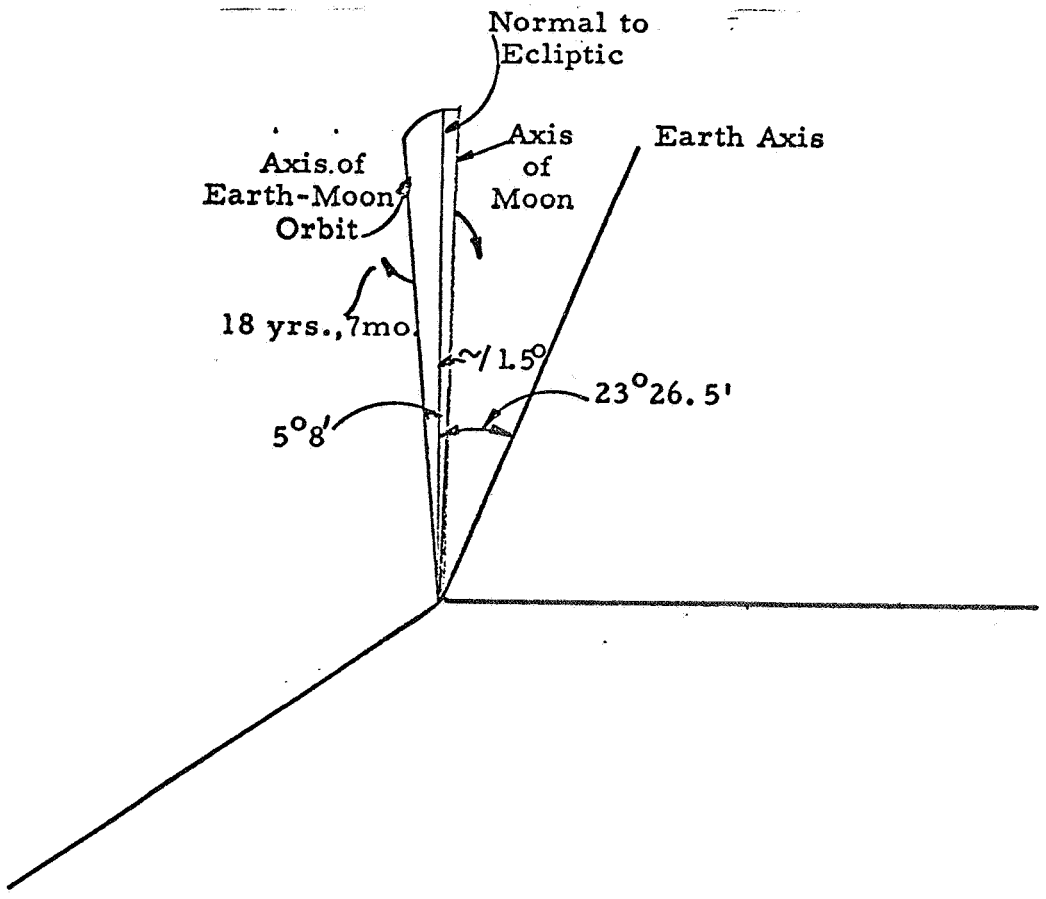

Figure 1.

Expression for the Doppler

Neglecting the eccentricity of the lunar orbit, the expression for the doppler, D, is derived below.

$$D = \frac{(\vec{R} + \vec{r}_m - \vec{r}_E) \cdot \left[\vec{\omega}_{mE} \times \vec{R} + \vec{\omega}_m \times \vec{r}_m - \vec{\omega}_E \times \vec{r}_E \right]}{\left[\vec{R} + \vec{r}_m - \vec{r}_E \right]_{mag.}} \qquad (1)$$

where:

D = Doppler – meters/sec.

R = vector from the center of the moon to the center of the earth

r_E = vector location of tracking station on the earth

r_m = vector location of LEM on the lunar surface

ω_{mE} = angular velocity vector of moon about the earth

ω_m = angular velocity of the moon about its own spin axis

ω_E = angular velocity of the earth about its spin axis

After suitable simplification the expression for the doppler can be written as shown in Equation (2) below:

$$D = \frac{r_m \cdot \left[R \times (\omega_m - \omega_{mE}) + r_E \times (\omega_E - \omega_m) \right] + R \cdot \left[r_E \times (\omega_E - \omega_m) \right]}{\left[R + r_m - r_E \right]_{mag.}} \qquad (2)$$

Since the moon approximately keeps the same face toward the earth, it is reasonable to assume for this error analysis that $R \times (\omega_m - \omega_{mE})$ is negligible. In addition $\omega_E >>> \omega_m$ hence the simplified expression shown in Equation (3) is a reasonable representation of the doppler.

$$D \cong \frac{r_m \cdot \left[r_E \times \omega_E \right] + R \cdot \left[r_E \times \omega_E \right]}{\left[R + r_m - r_E \right]_{mag.}} \qquad (3)$$

since $\left[R + r_m - r_E \right]_{mag.} \cong \left[R \right]_{mag.}$

$$D \cong \frac{r_m \cdot \left[r_E \times \omega_E \right] + R \cdot \left[r_E \times \omega_E \right]}{\cdot \; R_{mag.}} \qquad (4)$$

For purpose of error analysis the partial derivatives of the doppler with respect to the co-ordinates of the location of the LEM on the lunar surface are of interest. (The partial derivatives with respect to the components of the vector r_m).

$$D = \begin{vmatrix} a_1 & a_2 & a_3 \\ b_1 & b_2 & b_3 \\ c_1 & c_2 & c_3 \end{vmatrix} + K$$

where:

a_i are the components of the r_m vector

b_i are the components of the r_E vector

c_i are the components of ω_E vector

$i = 1, 2, 3$

K = value of the scalar $R \cdot (r_E \times \omega_E)$

Since a_1, a_2, and a_3 are functions of the parameters to be estimated, $\hat{\lambda}$ the latitude and $\hat{\theta}$ the longitude of the location of the LEM, the partial derivatives with respect to these parameters can be written as follows.

$$R_{mag.}\ \frac{\partial D}{\partial \hat{\lambda}} = \frac{\partial a_1}{\partial \hat{\lambda}}\Bigg|_1 - \frac{\partial a_2}{\partial \hat{\lambda}}\Bigg|_2 + \frac{\partial a_3}{\partial \hat{\lambda}}\Bigg|_3$$

$$R_{mag.}\ \frac{\partial D}{\partial \hat{\theta}} = \frac{\partial a_1}{\partial \hat{\theta}}\Bigg|_1 - \frac{\partial a_2}{\partial \hat{\theta}}\Bigg|_2 + \frac{\partial a_3}{\partial \hat{\theta}}\Bigg|_3$$

where

$$\Bigg|\ \Bigg|_1 = \begin{vmatrix} b_2 & b_3 \\ c_2 & c_3 \end{vmatrix}$$

$$\Bigg|\ \Bigg|_2 = \begin{vmatrix} b_1 & b_3 \\ c_1 & c_3 \end{vmatrix}$$

$$\Bigg|\ \Bigg|_3 = \begin{vmatrix} b_1 & b_2 \\ c_1 & c_2 \end{vmatrix}$$

Co-ordinates of Pertinent Vectors

The co-ordinate system used is the i, j, k system associated with the celestial sphere. The k axis is normal to the plane of the earth's orbit and the moon center is assumed to lie along the i axis. For purposes of error analysis, the moon is assumed stationary and non-rotating and to lie in the plane of the ecliptic along the i axis.

Location of Tracking Station

$$i \left[r_E \cos\lambda \cos\theta \cos\alpha + r_E \sin\lambda \sin\alpha \right]$$

$$j \left[r_E \cos\lambda \sin\theta \right]$$

$$k \left[- r_E \cos\lambda \cos\theta \sin\alpha + r_E \sin\lambda \cos\alpha \right]$$

α = tilt of earth axis (23° 26.5') toward the moon in the i - k plane

λ = latitude of station (measured from the earth equator)

θ = longitude (measured in the earth's equatorial plane from the i - k plane)

Location of Earth Spin Vector

$$i \left[\omega_E \sin\alpha \right]$$

$$j \left[0 \right]$$

$$k \left[\omega_E \cos\alpha \right]$$

Location of Nominal Point on Lunar Surface

$$i \left[- r_m \cos\hat{\lambda} \cos\hat{\theta} \right]$$

$$j \left[r_m \cos\hat{\lambda} \sin\hat{\theta} \right]$$

$$k \left[r_m \sin\hat{\lambda} \right]$$

Error Analysis

The error analysis was conducted by measuring the doppler from the same station at two different times. The error in the doppler measurement can be related to the error in $\hat{\lambda}$, and $\hat{\theta}$ through the following equations.

$$\Delta D_1 = \left(\frac{\partial D}{\partial \hat{\lambda}}\right)_1 \Delta \hat{\lambda} + \left(\frac{\partial D}{\partial \hat{\theta}}\right)_1 \Delta \hat{\theta}$$

$$\Delta D_2 = \left(\frac{\partial D}{\partial \hat{\lambda}}\right)_2 \Delta \hat{\lambda} + \left(\frac{\partial D}{\partial \hat{\theta}}\right)_2 \Delta \hat{\theta}$$

Solving for $\Delta \hat{\lambda}$ and $\Delta \hat{\theta}$ and statistically averaging, the standard deviation in $\hat{\lambda}$, and $\hat{\theta}$ are presented in the equation below.

$$r_m \sigma_{\hat{\lambda}} = \frac{r_m \sigma_D \sqrt{\left(\frac{\partial D}{\partial \hat{\theta}}\right)_2^2 + \left(\frac{\partial D}{\partial \hat{\theta}}\right)_1^2}}{\begin{vmatrix} \left(\frac{\partial D}{\partial \hat{\lambda}}\right)_1 & \left(\frac{\partial D}{\partial \hat{\theta}}\right)_1 \\ \left(\frac{\partial D}{\partial \hat{\lambda}}\right)_2 & \left(\frac{\partial D}{\partial \hat{\theta}}\right)_2 \end{vmatrix}}$$

$$r_m \sigma_{\hat{\theta}} = \frac{r_m \sigma_D \sqrt{\left(\frac{\partial D}{\partial \hat{\lambda}}\right)_1^2 + \left(\frac{\partial D}{\partial \hat{\lambda}}\right)_2^2}}{\begin{vmatrix} \left(\frac{\partial D}{\partial \hat{\lambda}}\right)_1 & \left(\frac{\partial D}{\partial \hat{\theta}}\right)_1 \\ \left(\frac{\partial D}{\partial \hat{\lambda}}\right)_2 & \left(\frac{\partial D}{\partial \hat{\theta}}\right)_2 \end{vmatrix}}$$

σ_D = standard deviation in the doppler measurement.

$$\frac{\partial D}{\partial \hat{\lambda}} = \frac{r_m r_E \omega_E}{R_{mag.}} \Bigg\{ \sin \hat{\lambda} \cos \hat{\theta} \Big[\cos \lambda \sin \theta \cos \alpha \Big]$$

$$+ \sin \hat{\lambda} \sin \hat{\theta} \Big[\cos \alpha (\cos \lambda \cos \theta \cos \alpha + \sin \lambda \sin \alpha)$$

$$- \sin \alpha (- \cos \lambda \cos \theta \sin \alpha + \sin \lambda \cos \alpha) \Big]$$

$$+ \cos \hat{\lambda} \Big[- \sin \alpha \cos \lambda \sin \theta \Big] \Bigg\}$$

$$\frac{\partial D}{\partial \hat{\theta}} = \frac{r_m r_E \omega_E}{R_{mag.}} \Bigg\{ \cos \hat{\lambda} \sin \hat{\theta} \Big[\cos \lambda \sin \theta \cos \alpha \Big]$$

$$- \cos \hat{\lambda} \cos \hat{\theta} \Big[\cos \alpha (\cos \lambda \cos \theta \cos \alpha + \sin \lambda \sin \alpha)$$

$$- \sin \alpha (- \cos \lambda \cos \theta \sin \alpha + \sin \lambda \cos \alpha) \Big] \Bigg\}$$

$$r_m \sigma_{\hat{\lambda}} = \frac{R_{mag.}}{r_E \omega_E} \frac{\sqrt{\left(\frac{\partial \hat{D}}{\partial \hat{\theta}}\right)_1^2 + \left(\frac{\partial \hat{D}}{\partial \hat{\theta}}\right)_2^2}}{\begin{vmatrix} \left(\frac{\partial \hat{D}}{\partial \hat{\lambda}}\right)_1 & \left(\frac{\partial \hat{D}}{\partial \hat{\theta}}\right)_1 \\ \left(\frac{\partial \hat{D}}{\partial \hat{\lambda}}\right)_2 & \left(\frac{\partial \hat{D}}{\partial \hat{\theta}}\right)_2 \end{vmatrix}}$$

$$r_m \sigma_{\hat{\theta}} = \frac{R_{mag.}}{r_E \omega_E} \frac{\sqrt{\left(\frac{\partial \hat{D}}{\partial \hat{\lambda}}\right)_1^2 + \left(\frac{\partial \hat{D}}{\partial \hat{\lambda}}\right)_2^2}}{\begin{vmatrix} \left(\frac{\partial \hat{D}}{\partial \hat{\lambda}}\right)_1 & \left(\frac{\partial \hat{D}}{\partial \hat{\theta}}\right)_1 \\ \left(\frac{\partial \hat{D}}{\partial \hat{\lambda}}\right)_2 & \left(\frac{\partial \hat{D}}{\partial \hat{\theta}}\right)_2 \end{vmatrix}}$$

where $$\frac{\partial D}{\partial \hat{\lambda}} = \frac{\partial \hat{D}}{\partial \hat{\lambda}} \frac{r_m r_E \omega_E}{R_{mag.}}$$

$$\frac{\partial D}{\partial \hat{\theta}} = \frac{\partial \hat{D}}{\partial \hat{\theta}} \frac{r_m r_E \omega_E}{R_{mag.}}$$

RESULTS

The following conditions were used to evaluate the results.

Station Location

$\lambda = +33^\circ$, $\theta_1 = -45^\circ$

$\lambda = +33^\circ$, $\theta_2 = +45^\circ$

Nominal Conditions on Lunar Surface

$\hat{\lambda} = 0^\circ$

$\hat{\theta} = -30^\circ$

Other Constants

$\omega_E = 7.29116 \times 10^{-5}$ rad/sec.

$r_E = 6.378 \times 10^6$ meters

$r_m = 1.738 \times 10^6$ meters

$R = 385 \times 10^6$ meters

The results consistent with the above parameters and 3 hours of smoothing at each mean-station location are tabulated below:

$$r_m \sigma_{\hat{\lambda}} = 2.804 \times 10^6 \sigma_D = 4.1 \text{ km}$$

$$r_m \sigma_{\hat{\theta}} = 1.1395 \times 10^6 \sigma_D = 1.64 \text{ km}$$

APOLLO NOTE NO. 66

C. H. Dale
20 May 1963

LLV LANDING ON A TILTED OR MOUNTAINOUS LUNAR SURFACE

In Apollo Note No. 58 the assumption of a flat-surfaced moon led to the sufficient requirements of a T. V., platform, and broad-beamed doppler altimeter. It is pointed out in this note that an unknown tilted surface presents the same guidance problem as an error in the platform alignment. The possibility of correcting this problem with a slant range radar is shown to be dependent upon the angular discrimination of the range returns.

Given an LEM (or LLV) in the terminal portion of the descent, the following parameters would be measured:

1. With the doppler altimeter the range and range-rate to the lunar surface may be measured (y and $\dot{y}$).
2. With the platform the direction of the supposedly known normal to the lunar surface may be measured. y and $\dot{y}$ are assumed to be along this direction.
3. With the T. V., the angle, σ, between the lunar surface and the line-of-sight may be measured (with the help of the platform). $\dot{\sigma}$ may also be measured with the help of a drift meter or T. V. link.

With an unknown slope, α, in the lunar surface, the following figure pictures the situation.

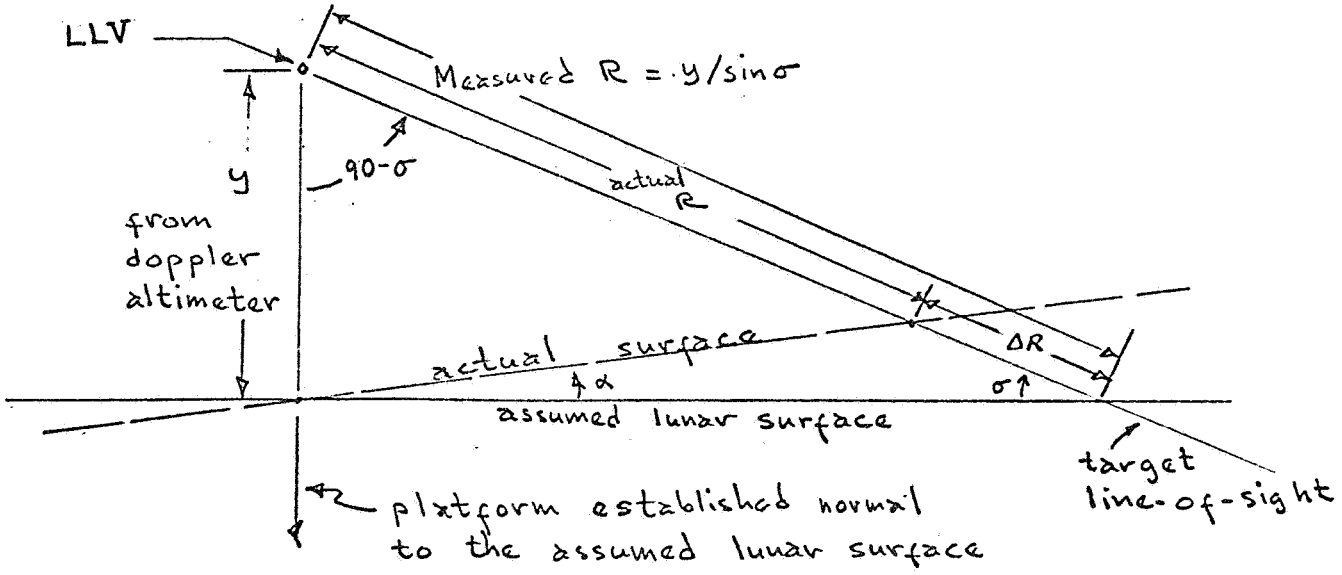

From the law of sines:

$$\frac{y \frac{\cos \sigma}{\sin \sigma}}{\sin \left[180 - (\sigma + \alpha)\right]} = \frac{\Delta R}{\sin \alpha}$$

which may be solved for the error in range, ΔR, caused by an error, α, in the assumed slope of the lunar surface.

$$\frac{\Delta R}{R} = \frac{\sin \alpha \cos \sigma}{\sin (\sigma + \alpha)}$$

This is plotted below:

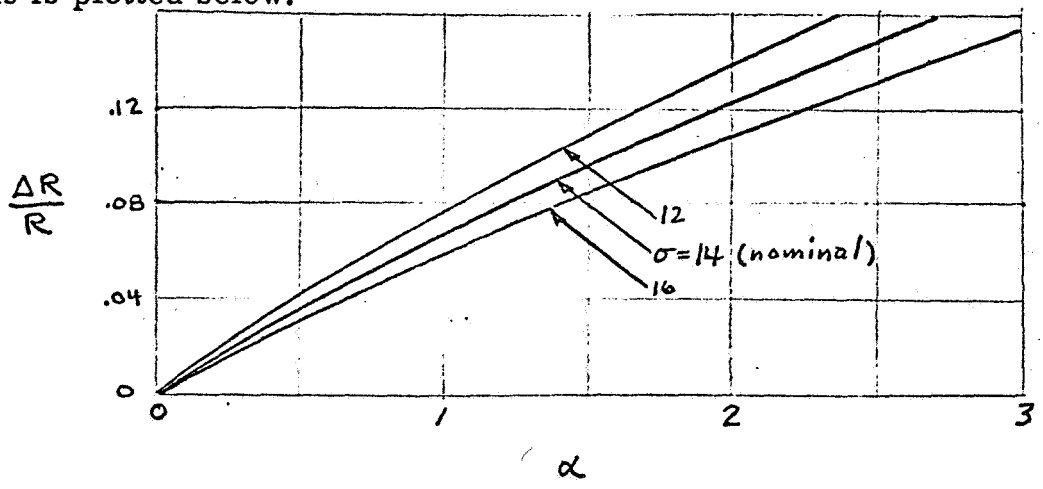

Since the acceleration along $\overline{R}$ is proportional to the measured range, then a one degree error, α, will cause a 7% error in acceleration. From Apollo Note No. 58, it can be seen that the effect of α is identical to an equivalent error in σ. Thus, the plane of the lunar surface near the landing site should be known to within about one-half of one degree. It would thus appear that the system using an altimeter to determine $\overline{R}$ is practical only under the assumption of a well surveyed and flat landing site. Mountainous landing sites would overtax such a system.

A possible fix may consist of returning to the earlier concept of a monopulse, gimbaled, slant-range radar. With such a device

range could be measured extremely accurately with a beacon. If the radar and T. V. are colinear (and possibly welded together on the same gimbals) there exists the possibility that R can be measured to wherever the T. V. is pointing. With poorly controlled target characteristics, it is difficult to estimate the angular resolution capability of such a radar. In order to offer any improvement over the doppler altimeter, the angular resolution of the slant-range radar must be better than one-half of one degree. (From Equation (18) of Apollo Note No. 58).

$$\frac{\Delta a_V}{a_V} = - \cot \sigma \, \Delta \sigma$$

which equals about 7% per degree of error in σ for a 14 degree flight path. It is understood that the presently conceived monopulse radar will have a 4 degree beam. Phased monopulse hopefully will be able to achieve better than one-half of one degree resolution.

APOLLO NOTE NO. 67

H. Engel/J. Holdsworth
22 May 1963

CALCULATION OF COVARIANCE MATRICES, I

In this note, one means for determining the covariance matrix referred to in Apollo Note No. 43 is explored for orbits in the lunar sphere of influence.

It is assumed that the observations of Doppler velocity are measured in a fixed direction -- which is contrary to the actual situation. This assumption, however, permits a simpler formulation of the problem, although it permits the computation of only five orbit parameters. The sixth parameter, orientation of the orbit plane about the line-of-sight, can not be determined in this case.

The distance from the Moon to the vehicle is r,

$$r = \frac{\frac{\mu}{2E}\,(e^2 - 1)}{1 + e\cos(\theta - \theta_p)}$$

in which all parameters are referred to the Moon, $-\theta_p$ is the initial angle from perilune, θ is zero initially and increases as time increases.

The Doppler velocity measured at the DSIF assuming a non-rotating Earth at infinity is given by:

$$\dot{R} = \left[\dot{r}\cos(\theta - \theta_p + \psi) - r\dot{\theta}\sin(\theta - \theta_p + \psi)\right]\cos\beta$$

in which ψ and β are defined as in Apollo Note No. 62. Then,

$$\dot{r} = e\sqrt{\frac{2E}{e^2 - 1}}\sin(\theta - \theta_p)$$

$$\dot{\theta} = \frac{4E^2}{\mu}\sqrt{\frac{(e^2 - 1)^3}{2E}}\left[1 + e\cos(\theta - \theta_p)\right]^2$$

and the eccentric anomaly $\mathcal{E}$ for an elliptical orbit is given by

$$\sin \mathcal{E} = \frac{(1-e^2)^{1/2} \sin (\theta - \theta_p)}{1 + e \cos (\theta - \theta_p)}$$

and

$$\cos \mathcal{E} = \frac{e + \cos (\theta - \theta_p)}{1 + e \cos (\theta - \theta_p)}$$

For the elliptic orbits, then, the time from perilune is:

$$t = \sqrt{\frac{-1}{\mu} \left(\frac{\mu}{2E}\right)^3} \left[\mathcal{E} - e \sin \mathcal{E}\right]$$

For hyperbolic orbits, the corresponding quantity F is given by:

$$\sinh F = \frac{(e^2-1)^{1/2} \sin (\theta - \theta_p)}{1 + e \cos (\theta - \theta_p)}$$

$$\cosh F = \frac{e + \cos (\theta - \theta_p)}{1 + e \cos (\theta - \theta_p)}$$

and the time from perilune is:

$$t = \sqrt{\frac{1}{\mu} \left(\frac{\mu}{2E}\right)^3} \left[e \sinh F - F \right].$$

In this analysis the parameters selected for the covariance matrix were β, ψ, θ_p, E, e and b, where b is an unknown constant Doppler bias. (Note that according to JPL, as reported in Apollo Note No. 17, no significant Doppler bias has been detected). This has proved not to be a very good set of parameters since for small eccentricities the uncertainties in both θ_p and ψ are large, although these uncertainties are highly correlated and future position can be well determined. The high correlation of θ_p and ψ makes the matrix to be inverted nearly singular and results in computation difficulties.

Also, for β close to zero, since β enters R only as cos β, the variance in the estimate of β becomes very large. Nonetheless, the procedure followed was this:

Evalute the necessary partial derivatives:

$$\frac{\partial \dot{R}}{\partial \beta} = -\left[\dot{r} \cos(\theta - \theta_p + \psi) - r\dot{\theta} \sin(\theta - \theta_p + \psi)\right] \sin\beta$$

$$\frac{\partial \dot{R}}{\partial \psi} = -\cos\beta \left[r \sin(\theta - \theta_p + \psi) - r\dot{\theta} \cos(\theta - \theta_p + \psi)\right]$$

$$\frac{\partial \dot{r}}{\partial \theta_p} = -e\sqrt{\frac{2E}{e^2-1}} \cos(\theta - \theta_p)$$

$$\frac{\partial (r\dot{\theta})}{\partial \theta_p} = \frac{2E r^2 \dot{\theta} e \sin(\theta - \theta_p)}{\mu (e^2-1)}$$

$$\frac{\partial \dot{R}}{\partial \theta_p} = \cos\beta \left[\dot{r} \sin(\theta - \theta_p + \psi) + \cos(\theta - \theta_p + \psi) \frac{\partial \dot{r}}{\partial \theta_p}\right.$$

$$\left. + r\dot{\theta} \cos(\theta - \theta_p + \psi) - \sin(\theta - \theta_p + \psi) \frac{\partial (r\dot{\theta})}{\partial \theta_p}\right]$$

$$\frac{\partial \dot{R}}{\partial E} = \cos\beta \left[\cos(\theta - \theta_\beta + \psi) \frac{\dot{r}}{2E} - \sin(\theta - \theta_p + \psi) \frac{r\dot{\theta}}{E}\right]$$

$$\frac{\partial \dot{R}}{\partial e} = \cos\beta \left[\cos(\theta - \theta_p + \psi) \frac{\dot{r}}{e(1-e^2)} + \sin(\theta - \theta_p + \psi) \frac{\mu^2}{2E r^2}\right]$$

Then, the elements of the covariance matrix are determined as sums over N observation instants equally spaced in time.

$$C_{11} = \frac{1}{N} \sum_{k=1}^{N} \left(\frac{\partial \dot{R}_p(k)}{\partial \beta} \right)^2$$

$$C_{22} = \frac{1}{N} \sum_{k=1}^{N} \left(\frac{\partial \dot{R}_p(k)}{\partial \psi} \right)^2$$

$$C_{33} = \frac{1}{N} \sum_{k=1}^{N} \left(\frac{\partial \dot{R}_p(k)}{\partial \theta_p} \right)^2$$

$$C_{44} = \frac{1}{N} \sum_{k=1}^{N} \left(\frac{\partial \dot{R}_p(k)}{\partial E} \right)^2$$

$$C_{55} = \frac{1}{N} \sum_{k=1}^{N} \left(\frac{\partial \dot{R}_p(k)}{\partial e} \right)^2$$

$$C_{66} = 1$$

$$C_{12} = C_{21} = \frac{1}{N} \sum_{k=1}^{N} \frac{\partial \dot{R}_p(k)}{\partial \beta} \frac{\partial \dot{R}_p(k)}{\partial \psi}$$

$$C_{13} = C_{31} = \frac{1}{N} \sum_{k=1}^{N} \frac{\partial \dot{R}_p(k)}{\partial \beta} \frac{\partial \dot{R}_p(k)}{\partial \theta_p}$$

and, in general,

$$C_{ij} = \frac{1}{N} \sum_{k=1}^{N} \frac{\partial \dot{R}_p(k)}{\partial \alpha_i} \frac{\partial \dot{R}_p(k)}{\partial \alpha_j}$$

in which α_i and α_j are the i- and j^{-th} parameters.

After the matrix C_{ij} is evaluated, its inverse is found, and each element value divided by N to obtain the matrix $\left[\frac{\sigma_i \sigma_j \rho_{ij}}{\sigma_{\dot{R}}^2}\right]$ in which $\sigma_{\dot{R}}$ is the standard deviation in the Doppler measurements.

The program is presently being debugged. Results will be presented in another Apollo Note.

APOLLO NOTE NO. 68

H. Engel
22 May 1963

TRACKING ERROR CALCULATION

The standard deviation in the dive angle at re-entry has been calculated as a function of the standard deviation of the Doppler velocity measurements and of the conditions of observation within the Earth's sphere of influence. The DSIF was assumed to be at the center of the Earth. The results are indicated in Figure 1.

Given the re-entry radius R_f, the desired final dive angle δ_f and the orbit energy, the angular momentum is found to be:

$$H = R_f \cos \delta_f \sqrt{\frac{2\mu}{R_f} + 2E}$$

Then, letting

$$b = \frac{2\mu}{H^2}$$

and

$$c = \frac{2E}{H^2}$$

the tangent of the dive angle at any point is found to be:

$$\tan \delta = -1 + b R + c R^2$$

Following the notation of Apollo Note No. 5,

$$\dot{} = \dot{R} = \frac{H}{R} \tan \delta$$

$$a_1 = \delta_f$$

and

$$a_2 = E.$$

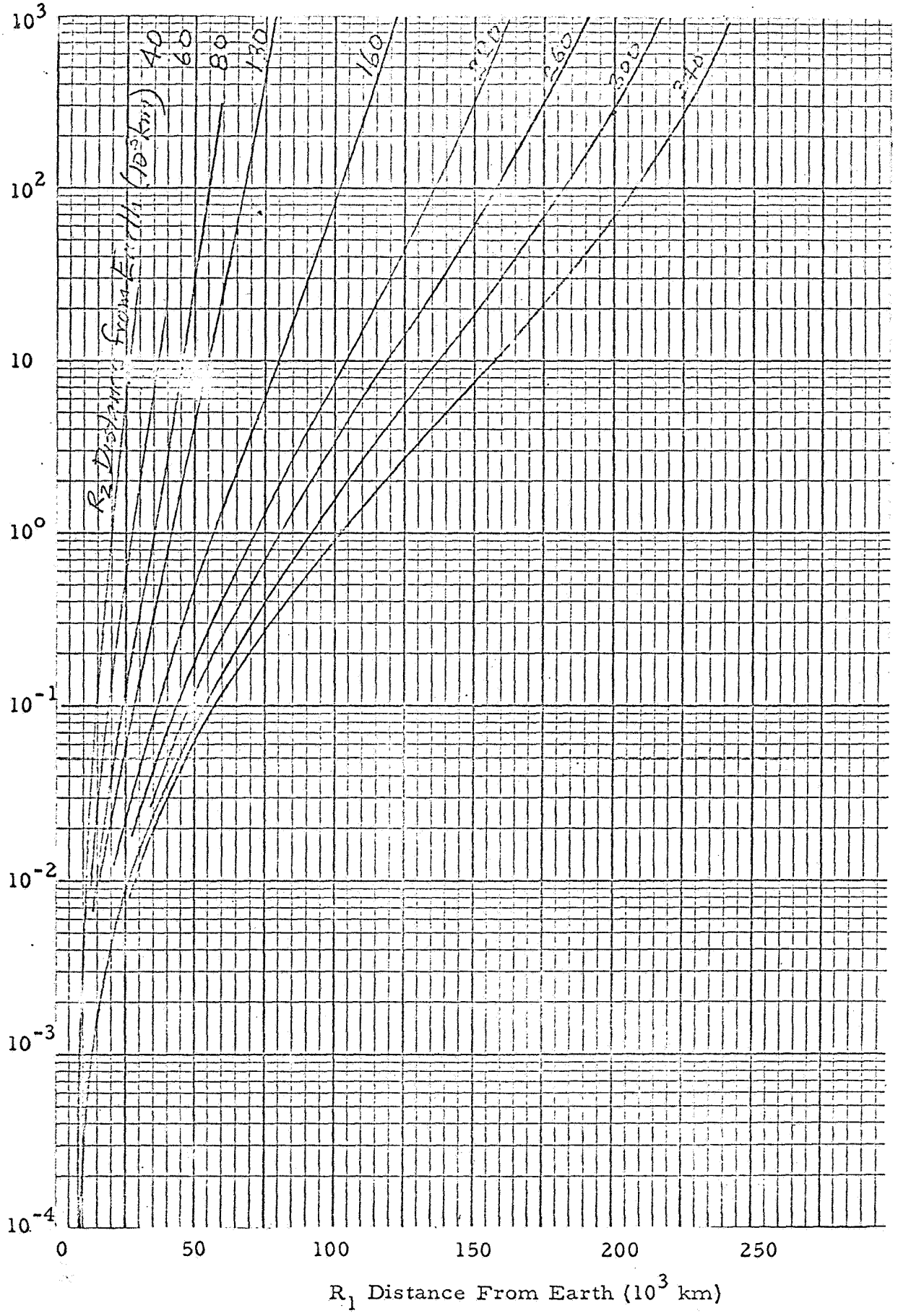
10^3
10^2
10
10^0
10^{-1}
10^{-2}
10^{-3}
10^{-4}
$\frac{\sigma_{\delta_f}^2}{\sigma_{\dot{R}}^2 \Delta R}$
R_2 Distance From Earth (10^3 km)
40
60
80
130
160
220
260
300
340
0
50
100
150
200
250
R_1 Distance From Earth (10^3 km)

Figure 1.

Then,

$$\frac{\partial f}{\partial a_1} = \frac{\partial \dot{R}}{\partial \delta_f} = \frac{H \tan \delta_f}{R \tan \delta}$$

and

$$\frac{\partial f}{\partial a_2} = \frac{\partial \dot{R}}{\partial E} = \frac{R}{H \tan \delta} - \frac{(R_f \cos \delta_f)^2}{H R \tan \delta}$$

Now, the Doppler measurements are made at equal intervals of time, but in this analysis they were assumed to be made at equal intervals of R. As long as $\dot{R}$ does not vary greatly over the interval of the measurements, the only effect of this approach is to change slightly the value of standard deviation in final dive angle obtained. Replacing the summations by integrals, assuming a large number of measurements,

$$C_1 = \frac{1}{R_2 - R_1} \int_{R_1}^{R_2} \left(\frac{\partial f}{\partial a_1} \right) dR$$

$$= \frac{H \tan \delta_f}{R_2 - R_1} \int_{R_1}^{R_2} \frac{dR}{R \tan \delta}$$

$$C_2 = \frac{1}{R_2 - R_1} \int_{R_1}^{R_2} \left(\frac{\partial f}{\partial a_2} \right) dR$$

$$= \frac{H^{-1}}{R_2 - R_1} \int_{R_1}^{R_2} \frac{R dR}{\tan \delta} - \frac{(R_f \cos \delta_f)^2 H^{-1}}{R_2 - R_1} \int_{R_1}^{R_2} \frac{dR}{R \tan \delta}$$

$$C_{11} = \frac{1}{R_2 - R_1} \int_{R_1}^{R_2} \left(\frac{\partial f}{\partial a_1} \right)^2 dR$$

$$= \frac{H^2 \tan^2 \delta_f}{R_2 - R_1} \int_{R_1}^{R_2} \frac{dR}{R^2 \tan \delta}$$

$$C_{12} = C_{21} = \frac{\tan \delta_f}{R_2 - R_1} \int_{R_1}^{R_2} \frac{dR}{\tan \delta} - \frac{\left(R_f \cos \delta_f \right)^2 \tan \delta_f}{R_2 - R_1} \int_{R_1}^{R_2} \frac{dR}{R^2 \tan \delta}$$

$$C_{22} = \frac{H^{-2}}{R_2 - R_1} \int_{R_1}^{R_2} \frac{R^2 \, dR}{\tan \delta} - \frac{2 H^{-2} (R_f \cos \delta_f)^2}{R_2 - R_1} \int_{R_1}^{R_2} \frac{dR}{\tan \delta}$$

$$+ \frac{H^{-2} (R_f \cos \delta_f)^4}{R_2 - R_1} \int_{R_1}^{R_2} \frac{dR}{R^2 \tan \delta}$$

where

$$\int \frac{dR}{R \tan \delta} = - \sin^{-1} \left(\frac{bR - 2}{R \sqrt{b^2 + 4c}} \right) \Bigg]$$

$$\int \frac{R \, dR}{\tan \delta} = \frac{\tan \delta}{c} \Bigg] - \frac{b}{2c} \int \frac{dR}{\tan \delta}$$

$$\int \frac{dR}{R^2 \tan\delta} = \frac{b}{2} \log \frac{\tan\delta}{R^2} \Bigg] + \frac{1}{R} \Bigg] + \left(\frac{b^2}{2} + c\right) \int \frac{dR}{\tan\delta}$$

$$\int \frac{dR}{\tan\delta} = \frac{1}{\sqrt{b^2 + 4c}} \log \frac{2cR + b - \sqrt{b^2 + 4c}}{2cR + b + \sqrt{b^2 + 4c}} \Bigg]$$

$$\int \frac{R^2\, dR}{\tan\delta} = \frac{R}{c} \Bigg] - \frac{b}{2c^2} \log \tan\delta \Bigg] + \frac{b^2 + 2c}{2c^2} \int \frac{dR}{\tan\delta}$$

Let

$$D = C_{11} C_{22} - C_{12}^2 + 2 C_1 C_2 C_{12} - C_1^2 C_{22} - C_2^2 C_{11}$$

The number of measurements N is given by:

$$N\Delta R = R_2 - R_1$$

Letting $\sigma_{\dot{R}}$ be the variation of Doppler measurements,

$$\sigma_{\delta_f}^2 = \frac{\sigma_{\dot{R}}^2}{N} \frac{C_{22} - C_2^2}{D}$$

$$= \frac{\Delta R}{R_2 - R_1} \frac{C_{22} - C_2^2}{D} \sigma_{\dot{R}}^2$$

Finding D required double precision operations on an IBM 7090.

APOLLO NOTE NO. 69

H. Epstein
29 May 1963

AN APPROXIMATE TECHNIQUE TO ARRIVE AT THE DSIF SMOOTHING ACCURACY FOR CIRCULAR OR NEARLY CIRCULAR ORBITS--DISCUSSION OF NUMERICAL RESULTS

This note discusses the numerical results which have been obtained to date on the DSIF smoothing accuracy for circular orbits about the Moon. The following basic assumptions were made in the analysis performed. The analysis itself will be the subject of a future Apollo Note.

1. The moon is considered as a stationary point mass with its mass precisely known.

2. The earth is at an infinite distance from the center of the moon--the zero parallax condition. This includes the premise that the DSIF radar is considered as being located at the center of the earth.

3. The effect of bodies other than the moon on the lunar orbit are negligible. A restricted two-body solution is employed.

4. The DSIF radar has no bias error in its range rate measurement. The (1 σ) accuracy of the DSIF is .015 meters per second for a one-minute sample.

5. Low eccentricity elliptical orbits are taken as represented by a circular orbit with the same period. The orbital period (7570 seconds) assumed corresponds to a 100 nautical mile altitude circular orbit.

6. Linear analysis is adequate.

7. An equatorial orbit is assumed with the angle between the axis of the earth-moon orbit and the axis of the moon taken as 6.5°.

8. The error in DSIF station location is negligible.

9. The sixth orbital parameter is determined by some other means (such as optical data or a priori knowledge of initial injection conditions).

The numerical results are most directly applicable for three situations during cruise portions of the orbit: one, the long term prediction accuracy problem for the CM; two, the comparatively short time prediction accuracy required for the LEM during synchronous descent (nominally 1/4 of an orbit period); and, three, the prediction accuracy of the LEM in its ascent to rendezvous. In each of these situations the nominal orbit is characterized by either a small eccentricity (LEM) or zero eccentricity (CM). The numerical results contained within this note are based on the exact results for a circular orbit.

General Analytical Approach

The approach taken to arrive at the smoothing errors is similar to the approach outlined in Apollo Note No. 31. However, since the situations of interest include prediction and smoothing over long periods of time, the power series for time is abandoned for a power series in terms of eccentricity to arrive at the exact analytical results for a circular orbit. The details of the analysis are quite lengthy and will be accordingly omitted from this note--only numerical results and approach will be given. The set of orbital parameters employed is essentially components of initial position ($\overline{R_o}$) and initial velocity ($\overline{V_o}$) as indicated below.

Type of orbital parameters employed:

1. R_o
2. V_o
3. $\vec{l}_{R_o} \cdot \vec{l}_{V_o}$
4. $\vec{l}_D \cdot \vec{l}_{R_o}$

5. $\vec{I}_D \cdot \vec{I}_{V_o}$

6. $\vec{I}_D \cdot (\vec{I}_{R_o} \times \vec{I}_{V_o})$

where

$$\vec{R}_o = R_o \vec{I}_{R_o}$$

$$\vec{V}_o = V_o \vec{I}_{V_o}$$

$$\vec{I}_D = \frac{\vec{D}}{D}$$ (is the direction along the line between the earth and the moon).

The analysis was performed along the following general lines. The error coefficients in predicted position and velocity was obtained in an earth-based co-ordinate system. These errors were then transformed to an orbit plane co-ordinate system as indicated below.

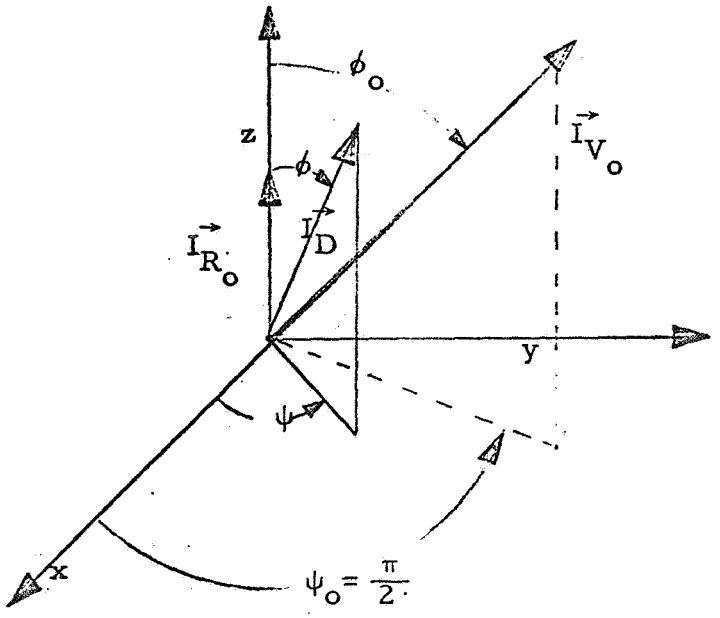

Figure 1. Orbit Plane Co-ordinate System.

For a circular orbit $\vec{1}_{R_o} = \vec{1}_z$ and $\vec{1}_{V_o} = \vec{1}_y$. It is worthwhile to recall that future position and future velocity can be related to present position and present velocity with the aid of scalar time varying functions (see Apollo Note No. 31, Equations (4) and (5)). The scalar functions and required partials were then derived for a low eccentricity orbit. The relationships for a circular orbit can then readily be obtained by taking the limiting form of these expressions for a circular orbit. The zero parallax doppler data then makes it possible to arrive at estimates for the first five parameters indicated in the list of orbital parameters. Then, finally, these parameter estimates can be employed to arrive at the required accuracy in future position and velocity.

To gain a greater insight into the nature of the accuracy obtainable as a function of smoothing interval and prediction interval (and other parameters of interest), it is desirable to treat two special situations that enable reasonably simple analytical expressions to be obtained. For the first situation, the unit vector from the earth to the center of the moon ($\vec{1}_D$) is normal to the direction of the initial velocity vector and will be known as Case I. The second situation occurs when $\vec{1}_D$ is normal to the direction of the initial position vector. The further selection of the center of the smoothing interval as the time origin (at no loss in generality) makes an additional simplification. The final simplification results from the assumption that an adequate number of samples are taken so that the summations involved may be represented by integrals. It is expected that this analysis will indicate critical orientation situations from an accuracy standpoint. The form of the error in future position and velocity components (for the DSIF errors) is then given as:

$$\sigma_R = \frac{\sigma}{\omega_o \sqrt{m}} F_1 (\phi, \psi, \omega_o T_s; \omega_o t_p) \tag{1}$$

and

$$\sigma_v = \frac{\sigma}{\sqrt{m}} F_2 (\phi, \psi, \omega_o T_s; \omega_o t_p) \tag{2}$$

where:

σ_R = appropriate future position error component (x, y, or z)

σ_v = appropriate future velocity error component (x, y, or z)

ω_o = average angular frequency (radians per second)

T_s = smoothing interval (seconds)

t_p = prediction time from the center of the smoothing interval (seconds)

$\omega_o T_s$ = orbit angle smoothing interval (radians)

$\omega_o t_p$ = orbit angle prediction interval (radians)

ϕ, ψ = angles as defined in Figure 1

m = numbers of samples per orbital period taken

F_1, F_2 = appropriate functions of parameters indicated

These equations clearly indicate the scaling laws for prediction accuracy as a function of $\frac{\sigma}{\sqrt{m}}$. The largest permissible value of m is determined by the ratio of the orbital period to the correlation time of the doppler noise. Present estimates by JPL of the doppler noise correlation time is about one minute. This leads to a value of m of about 126 for a 100 n. mi. altitude circular orbit. A present conservative estimate of one minute smoothed range rate accuracy (1 σ) of the DSIF is about .015 meters per second.

A plausibility analysis for the nature of the error is indicated below:

$$\vec{R} = f\vec{R}_o + g\vec{V}_o = f R_o \vec{l}_{R_o} + g V_o \vec{l}_{V_o} \qquad (3)$$

$$\vec{V} = \dot{f}\vec{R}_o + \dot{g}\vec{V}_o = \dot{f} R_o \vec{1}_{R_o} + \dot{g} V_o \vec{1}_{V_o} \tag{4}$$

For a circular orbit with the co-ordinate system of Figure 1.

$$\vec{\Delta R} = (\vec{\Delta R} \cdot \vec{1}_x)\ \vec{1}_x + (\vec{\Delta R} \cdot \vec{1}_y)\ \vec{1}_y + (\vec{\Delta R} \cdot \vec{1}_z)\ \vec{1}_z \tag{5}$$

$$\vec{\Delta V} = (\vec{\Delta V} \cdot \vec{1}_x)\ \vec{1}_x \tag{6}$$

The out-of-plane errors are given by:

$$\frac{\vec{\Delta R} \cdot \vec{1}_x}{R_o} = (\vec{\Delta 1}_{R_o} \cdot \vec{1}_x) \cos \omega_o t + (\vec{\Delta 1}_{V_o} \cdot \vec{1}_x) \sin \omega_o t \tag{7}$$

$$\frac{\vec{\Delta V} \cdot \vec{1}_x}{V_o} = -(\vec{\Delta 1}_{R_o} \cdot \vec{1}_x) \sin \omega_o t + (\vec{\Delta 1}_{V_o} \cdot \vec{1}_x) \cos \omega_o t \tag{8}$$

These equations indicate that the out-of-plane errors are a periodic function of time (a pure sinusoid for circular orbits) and that the position and velocity errors are in time quadrature. (When the position error is a maximum in magnitude the velocity error is a minimum and the converse also holding true). In addition, the percentage accuracy of the maximum errors in position and velocity are the same.

The in-plane error can be written as:

$$\frac{\vec{\Delta R} \cdot \vec{1}_y}{R_o} = \omega_o \Delta g + \frac{\Delta V_o}{V_o} \sin \omega_o t + (\vec{\Delta 1}_{R_o} \cdot \vec{1}_y) \cos \omega_o t + (\vec{\Delta 1}_{V_o} \cdot \vec{1}_y) \sin \omega_o t \tag{9}$$

$$\frac{\vec{\Delta R} \cdot \vec{1}_z}{R_o} = \Delta f + \frac{\Delta R_o}{R_o} \cos \omega_o t + (\vec{\Delta 1}_{R_o} \cdot \vec{1}_z) \cos \omega_o t + (\vec{\Delta 1}_{V_o} \cdot \vec{1}_z) \sin \omega_o t \tag{10}$$

$$\frac{\vec{\Delta V} \cdot \vec{l}_y}{V_o} = \dot{\Delta g} + \frac{\Delta V_o}{V_o} \cos \omega_o t - (\vec{\Delta l}_{R_o} \cdot \vec{l}_y) \sin \omega_o t$$

$$+ (\vec{\Delta l}_{V_o} \cdot \vec{l}_y) \cos \omega_o t \qquad (11)$$

$$\frac{\vec{\Delta V} \cdot \vec{l}_z}{V_o} = \frac{\dot{\Delta f}}{\omega_o} - \frac{\Delta R_o}{R_o} \sin \omega_o t - (\vec{\Delta l}_{R_o} \cdot \vec{l}_y) \sin \omega_o t$$

$$+ (\vec{\Delta l}_{V_o} \cdot \vec{l}_y) \cos \omega_o t \qquad (12)$$

All of the terms involved in Equations 9, 10, 11, and 12 are purely sinusoidal with the exception of the errors associated with Δf, Δg, $\dot{\Delta f}$, and $\dot{\Delta g}$. Even though it is not proved in this note, these last four quantities contain factors which can increase linearly with time in addition to the purely sinusoidal components. Actually for the co-ordinate system employed the linearly increasing terms are modified by sinusoidal functions. These later errors can be directly associated with errors in the period or average angular frequency of the orbit. Where these errors are dominant, the position and velocity errors are consistent with a viewpoint of time uncertainty. This results in essentially an azimuthal error in position and a range rate (referred to center of the moon) error in velocity. Furthermore, Δf and $\dot{\Delta g}$ errors will be essentially in phase and $\dot{\Delta f}$ and Δg will be essential in phase with each other and in quadrature with Δf and $\dot{\Delta g}$. This means that when this type error is dominant, where ΔR_y and ΔV_z are maximum, that ΔR_z and ΔV_y will be minimum and the converse will again hold. On the other hand, when timing errors are relatively unimportant, the y and z components of position or velocity errors will tend to be important

together and the position and velocity errors will be essentially in quadrature.

One last general comment is required pertaining to the asymptotic solution for large orbital periods of smoothing. The r.m.s. smoothing accuracy contains terms which vary inversely with the square root of time and time to the three halves ($\frac{3}{2}$) power. The $\frac{3}{2}$ power can be associated with errors in orbital period. This result is quite similar in nature to the smoothing results for a straight line. Preliminary calculations indicate that for smoothing periods greater than about one or two orbital periods this approximation yields good numerical accuracy. This will be further discussed in the following section.

Some preliminary estimates for very short smoothing interval indicate that the covariance matrix will contain terms which will vary inversely with the $\frac{11}{2}$ power of the smoothing interval for a five parameter set of orbit parameters. This can be considered as the fifth power arising from five parameter and the $\frac{1}{2}$ power associated with the number of smoothing samples available. The numerical values for the covariance matrixes calculation will be included as an Appendix to this note at a later date to facilitate computation of other derived quantities as required.

Discussion of Numerical Results

Tables 1 through 6 indicate the numerical values obtained to this point. The (a) portion pertains to numerical results for the initial velocity perpendicular to the Earth-Moon line (Case I), and the (b) portion to the results for the initial position perpendicular to the Earth-Moon line (Case II). The last column of Tables 1 through 4 (optical error) indicates the ephemeris error associated with an optical (or a priori) error of 100 meters (1 σ) in the determination of the sixth orbital parameter. In Tables 5 and 6, the optical (or a priori) error is indicated by a bracketed quantity to facilitate comparison of the requirements for this error source. In general, if a criterion were established that percentage errors in future range and future velocity were equally important then the results for Case II are more favorable or about the same as those for Case I. For smoothing intervals greater than about one orbital period, no pronounced differences occur (see Tables 3 and 4).

The numerical values of accuracy obtained are good to the point that DSIF station location errors (about 100 meters) and other approximations would need to be taken into account to arrive at the precise value of accuracy obtainable. Tables 1 and 2 and most particularly Tables 5 and 6 indicate the marked decrease in accuracy as shorter smoothing times are employed. The difference in accuracy for predominate error terms between 1/4 orbit period and 1 orbit period smoothing is about a factor of 1000. This demonstrates the severe penalty associated with the determination of many orbital parameters where only short smoothing intervals are available. For example, Table 5 (a) indicates an out-of-plane position error of about 30,000 meters for 1/4 orbit period smoothing and zero prediction time (from the center of the smoothing interval) while Table 3 indicates a corresponding value of about 20 meters for 1 orbit period smoothing. Similar comparisons can be made with other error terms.

An examination of the errors even at zero prediction time, in-plane errors indicate that the errors are probably most sensitive to the accuracy of determination of orbital period, which is somewhat surprising. The indicator is taken in terms of the quadrature relationship between the in-plane components. Recalling that for a circular orbit, the determination of the orbital period for a known and constant mass determines the energy, radius, and speed parameters of the orbit. It, therefore, must cautiously be stated that the orbital period or an equivalent quantity is probably the single most important contributor to errors for circular or near circular orbits. A much stronger dependence is noted for long prediction time.

It further appears that as more exact solutions are found, the necessity for a priori or additional sources for parameter information will be required to achieve high accuracy in time intervals substantially less than 1/4 of an orbital period. Additional sources could involve optical data from the spacecraft or range data from the DSIF. The situation wherein range as well as range rate data is available has not been analyzed to the point. If it is required that the DSIF compute six orbital parameters without a priori information or

additional information sources and that the correlation time of the primary noise source of the DSIF is one minute, it would take a minimum of about six minutes to obtain six independent measurements to establish the six parameters.

CONCLUSIONS

1. Very accurate data pertaining to the CM ephemeris can be made available from the DSIF for all times after the CM has completed a few orbits about the moon during its cruise portion about the moon.

2. It is to be expected that for available smoothing periods of about 10 minutes or less, it will be necessary to make use of a priori information or additional sources of information to arrive at suitable ephemeris accuracy. A possible additional source could be in the form of position data from the DSIF in addition to the range rate data as well as the use of several DSIF stations. Optical or other data from the spacecraft could also be employed. An example of the use of a priori information can be given for the LEM on descent. The location of the LEM prior to the boost into synchronous orbit is known by the CM ephemeris. Knowledge of the boost to be performed might be expected to yield adequate estimates for at least some of the initial conditions. A somewhat analogous situation occurs for the LEM ascent to rendezvous.

3. For the zero parallax situation, no information on out-of-plane errors can be made when the vector from earth-to-center of moon, the initial position vector, and the initial velocity error are co-planar by linear analysis techniques. Parallax is then required to estimate the out-of-plane error by the DSIF alone. The maximum degree of parallax is about 1/2 of a degree from the earth. This would increase the out-of-plane error by about one order of magnitude from the calculated values. The satellite relay technique may also be profitably employed to assist in the determination of the orbital parameter.

4. The requirement that the LEM be visible during its descent to the lunar surface insures that the pessimistic results of Case I

(initial velocity perpendicular to the earth-moon line) for short smoothing times will not be a situation of interest. A modest decrease in the Case II performance seems more rational. A somewhat similar situation occurs during the LEM ascent to rendezvous.

5. The results for a circular orbit may be considered as a conservative, if not pessimistic result, when extended to the LEM ephemeris accuracy with its nominal eccentricity of almost .1.

Table 1. Prediction Accuracy Based on 1/4 Orbit Period of Observation.

Predicted Error Component	Prediction Interval (Orbit Periods)					Optical Error
	0	1	2	5	10	
σ_{R_x} (meters)	28,900	28,900	28,900	28,900	28,900	(0)
σ_{R_y} (meters)	0	34,500	69,000	172,500	345,000	(11.32)
σ_{R_z} (meters)	1,630	1,630	1,630	1,630	1,630	(0)
σ_{v_x} (m/sec.)	.0506	.0506	.0506	.0506	.0506	(.08247)
σ_{v_y} (m/sec.)	.1705	.1705	.1705	.1705	.1705	(0)
$\sigma_{v_{z(I)}}$ (m/sec.)	0	28.67	57.33	143.3	286.7	(.00940)
$\sigma_{v_{z(II)}}$ (m/sec.)	.00381	.00381	.00381	.00381	.00381	

(a) Initial Velocity Perpendicular to Earth-Moon Line

Predicted Error Component	Prediction Interval (Orbit Periods)					Optical Error
	0	1	2	5	10	
σ_{R_x} (meters)	2.114	2.114	2.114	2.114	2.114	(99.36)
$\sigma_{R_{y(I)}}$ (meters)	0	2,664	5,328	13,320	26,640	(11.32)
$\sigma_{R_{y(II)}}$ (meters)	18.56	18.56	18.56	18.56	18.56	
σ_{R_z} (meters)	42.1	42.1	42.1	42.1	42.1	(0)
σ_{v_x} (m/sec.)	1.297	1.297	1.297	1.297	1.297	(0)
σ_{v_y} (m/sec.)	.1509	.1509	.1509	.1509	.1509	(0)
$\sigma_{v_{z(I)}}$ (m/sec.)	0	2.211	4.422	11.06	22.11	
$\sigma_{v_{z(II)}}$ (m/sec.)	.055	.0554	.0554	.0554	.0554	(.0094)

(b) Initial Position Perpendicular to Earth-Moon Line

Table 2. Prediction Accuracy Based on 1/2 Orbit Period of Observation.

Predicted Error Component	Prediction Interval (Orbit Periods)					Optical Error
	0	1	2	5	10	
σ_{R_x} (meters)	396	396	396	396	396	(0)
σ_{R_y} (meters)	0	694.3	1389	3472	6943	(11.32)
σ_{R_z} (meters)	18.8	18.8	18.8	18.8	18.8	(0)
σ_{v_x} (m/sec.)	.04735	.04735	.04735	.04735	.04735	(.0825)
σ_{v_y} (m/sec.)	.01655	.01655	.01655	.01655	.01655	(0)
$\sigma_{v_{z(I)}}$ (m/sec.)	0	.5765	1.153	2.883	5.765	(.0094)
$\sigma_{v_{z(II)}}$ (m/sec.)	.00297	.00297	.00297	.00297	.00297	

(a) Initial Velocity Perpendicular to Earth-Moon Line

Predicted Error Component	Prediction Interval (Orbit Periods)					Optical Error
	0	1	2	5	10	
σ_{R_x} (meters)	.873	.873	.873	.873	.873	(99.36)
$\sigma_{R_{y(I)}}$ (meters)	0	100.4	200.8	502	1004	(11.32)
$\sigma_{R_{y(II)}}$ (meters)	7.66	7.66	7.66	7.66	7.66	(0)
σ_{R_z} (meters)	8.10	8.10	8.10	8.10	8.10	
σ_{v_x} (m/sec.)	.0792	.0792	.0792	.0792	.0792	(0)
σ_{v_y} (m/sec.)	.01087	.01087	.01087	.01087	.01087	(0)
$\sigma_{v_{z(I)}}$ (m/sec.)	0	.0833	.167	.417	.833	(.0094)
$\sigma_{v_{z(II)}}$ (m/sec.)	.01118	.01118	.01118	.01118	.01118	

(b) Initial Position Perpendicular to Earth-Moon Line

Table 3. Prediction Accuracy Based on Orbit Period of Observation.

Predicted Error Component	Prediction Interval (Orbit Periods)					Optical Error
	0	1	2	5	10	
σ_{R_x} (meters)	17.5	17.5	17.5	17.5	17.5	(0)
σ_{R_y} (meters)	0	8.88	17.76	44.4	88.8	(11.32)
σ_{R_z} (meters)	1.76	1.76	1.76	1.76	1.76	(0)
σ_{v_x} (m/sec.)	.0374	.0374	.0374	.0374	.0374	(.0825)
σ_{v_y} (m/sec.)	.0017	.0017	.0017	.0017	.0017	(0)
$\sigma_{v_{z(I)}}$ (m/sec.)	0	.00735	.0147	.0368	.0735	(.0094)
$\sigma_{v_{z(II)}}$ (m/sec.)	.0019	.0019	.0019	.0019	.0019	

(a) Initial Velocity Perpendicular to Earth-Moon Line

Predicted Error Component	Prediction Interval (Orbit Periods)					Optical Error
	0	1	2	5	10	
σ_{R_x} (meters)	.576	.576	.576	.576	.576	(99.36)
$\sigma_{R_{y(I)}}$ (meters)	0	9.94	19.88	49.70	99.4	(11.32)
$\sigma_{R_{y(II)}}$ (meters)	5.06	5.06	5.06	5.06	5.06	(0)
σ_{R_z} (meters)	2.29	2.29	2.29	2.29	2.29	
σ_{v_x} (m/sec.)	.0193	.0193	.0193	.0193	.0193	(0)
σ_{v_y} (m/sec.)	.00195	.00195	.00195	.00195	.00195	(0)
$\sigma_{v_{z(I)}}$ (m/sec.)	0	.00825	.01650	.04125	.0825	(.0094)
$\sigma_{v_{z(II)}}$ (m/sec.)	.00596	.00596	.00596	.00596	.00596	

(b) Initial Position Perpendicular to Earth-Moon Line

Table 4. Prediction Accuracy Based on 2 Orbit Periods of Observation.

Predicted Error Component	Prediction Interval (Orbit Periods)					Optical Error
	0	1	2	5	10	
σ_{R_x} (meters)	14.3	14.3	14.3	14.3	14.3	(0)
σ_{R_y} (meters)	0	2.96	5.92	14.8	29.6	(11.32)
σ_{R_z} (meters)	1.89	1.89	1.89	1.89	1.89	(0)
σ_{v_x} (m/sec.)	.0264	.0264	.0264	.0264	.0264	(.0825)
σ_{v_y} (m/sec.)	.0015	.0015	.0015	.0015	.0015	0
$\sigma_{v_{z(I)}}$ (m/sec.)	0	.00248	.00496	.0124	.0248	(.0094)
$\sigma_{v_{z(II)}}$ (m/sec.)	.0014	.0014	.0014	.0014	.0014	

(a) Initial Velocity Perpendicular to Earth-Moon Line

Predicted Error Component	Prediction Interval (Orbit Periods)					Optical Error
	0	1	2	5	10	
σ_{R_x} (meters)	.407	.407	.407	.407	.407	(99.36)
$\sigma_{R_{y(I)}}$ (meters)	0	2.876	5.751	14.38	28.76	(11.32)
$\sigma_{R_{y(II)}}$ (meters)	3.575	3.575	3.575	3.575	3.575	(0)
σ_{R_z} (meters)	1.697	1.697	1.697	1.697	1.697	
σ_{v_x} (m/sec.)	.01186	.01186	.01186	.01186	.01186	(0)
σ_{v_y} (m/sec.)	.00137	.00137	.00137	.00137	.00137	(0)
$\sigma_{v_{z(I)}}$ (m/sec.)	0	.00239	.00477	.01193	.02387	(.0094)
$\sigma_{v_{z(II)}}$ (m/sec.)	.00421	.00421	.00421	.00421	.00421	

(b) Initial Position Perpendicular to Earth-Moon Line

Table 5. Prediction Accuracy Based on 1/4 Orbit Period of Observation.

Predicted Error Component	Prediction Interval (Orbit Periods)					
	0		.25		.5	
σ_{R_x} (meters)	28,900	(0)*	60.97	(99.4)	28,900	(0)
σ_{R_y} (meters)	0	(11.3)	3664	(0)	17,270	(11.3)
σ_{R_z} (meters)	1,630	(0)	4570	(11.3)	5696	(0)
σ_{v_x} (m/sec.)	.0506	(.0825)	23.99	(0)	.0506	(.0825)
σ_{v_y} (m/sec.)	.1705	(0)	5.480	(.0094)	3.207	(0)
σ_{v_z} (m/sec.)	.00381	(.0094)	1.521	(0)	14.33	(.0094)

(a) Initial Velocity Perpendicular to Earth-Moon Line

Predicted Error Component	Prediction Interval (Orbit Periods)					
	0		.25		.5	
σ_{R_x} (meters)	2.11	(99.4)	1563	(0)	2.11	(99.4)
σ_{R_y} (meters)	18.56	(11.3)	287	(0)	1339	(11.3)
σ_{R_z} (meters)	42.1	(0)	121	(11.3)	605	(0)
σ_{v_x} (m/sec.)	1.297	(0)	.00176	(.08247)	1.297	(0)
σ_{v_y} (m/sec.)	.151	(0)	.301	(.0094)	.385	(0)
σ_{v_z} (m/sec.)	.0554	(.0094)	.0124	(0)	1.114	(.0094)

*( ) indicates effect of optical error.

(b) Initial Position Perpendicular to Earth-Moon Line

Table 6. Prediction Accuracy Based on 1/2 Orbit Period of Observation.

Predicted Error Component	Prediction Interval (Orbit Periods)					
	0		.25		.5	
σ_{R_x} (meters)	396	(0)*	57.1	(99.4)	396	(0)
σ_{R_y} (meters)	0	(11.32)	73.8	(0)	348	(11.32)
σ_{R_z} (meters)	18.8	(0)	63.3	(11.32)	130	(0)
σ_{v_x} (m/sec.)	.0474	(.0825)	.328	0	.0474	(.0825)
σ_{v_y} (m/sec.)	.0166	(0)	.0980	(.0094)	.0772	(0)
σ_{v_z} (m/sec.)	.0030	(.0094)	.0307	(0)	.2884	(.0094)

(a) Initial Velocity Perpendicular to Earth-Moon Line

Predicted Error Component	Prediction Interval (Orbit Periods)					
	0		.25		.5	
σ_{R_x} (meters)	.873	(99.4)	95.43	(0)	.873	(99.4)
σ_{R_y} (meters)	7.66	(11.3)	13.39	(0)	59.6	(11.3)
σ_{R_z} (meters)	8.10	(0)	23.4	(11.3)	28.8	(0)
σ_{v_x} (m/sec.)	.0792	(0)	.000724	(.0825)	.0792	(0)
σ_{v_y} (m/sec.)	.0109	(0)	.01748	(.0094)	.0195	(0)
σ_{v_z} (m/sec.)	.0112	(.0094)	.00674	(0)	.0478	(.0094)

*( ) indicates effect of optical error.

(b) Initial Position Perpendicular to Earth-Moon Line

APPENDIX
COVARIANCE MATRIX

A by-product of the calculation of future position and velocity errors is the covariance matrix for the derived parameters. This matrix can be employed to arrive at the variance in other derived quantities,(i.e., periapsis distance, eccentricity, and energy).

Using the notation that:

$$b = \sum_i \alpha_i a_i \tag{13}$$

a_i = is the i^{th} original derived parameter

α_i = is the i^{th} amplitude co-efficient

for unbiased estimators $\overline{b} = \overline{a_i} = 0$ and

$$\overline{b^2} = \frac{\sigma^2 \sum_i \sum_j \alpha_i \alpha_j D_{ij}}{n\,(\mathrm{Det})} \tag{14}$$

where:

D_{ij} = appropriate co-factor

(Det) = determinant of the original matrix

Aside from notation, this result is derived in Apollo Note No. 43 (see Equation (21)). Numerical values are listed below for smoothing intervals of 1/4, 1/2, 1, and 2 orbital periods for two special conditions. For the first situation the earth-to-moon line is perpendicular to initial velocity direction (Table 7) and for the second situation the earth-to-moon line is perpendicular to the initial position direction (Table 8). The five parameters that may be derived by the DSIF for the zero parallax case imply a fifth order matrix. For these two special situations, the fifth order matrix can be decomposed to a second and third order matrix. The notation employed here will be consistent with the notation to be employed in a future Apollo note dealing with the analysis performed.

An example of the use of these tables will be given below.

It can readily be shown that:

$$\sigma_E = \frac{V_o \sigma}{\cos \phi} \left[\frac{D_{11} + D_{22} + 2 D_{12}}{n \, (\text{Det})} \right]^{1/2} = \omega_o \sigma_H \tag{15}$$

$$\sigma_H = \frac{R_o \sigma}{\cos \phi} \left[\frac{D_{11} + D_{22} + 2 D_{12}}{n \, (\text{Det})} \right]^{1/2} \tag{16}$$

$$\sigma_e = \frac{\sigma}{V_o \cos \phi} \left[\frac{D_{11} + 4 D_{22} + 4 D_{12}}{n \, (\text{Det})} \right]^{1/2} \tag{17}$$

$$\sigma_{R_p} = \frac{\sigma}{\omega_o \cos \phi} \left[\frac{D_{11}}{n \, (\text{Det})} \right]^{1/2} \tag{18}$$

For the earth-moon line perpendicular to the initial position vector, a smoothing interval of 1/4 orbit, σ = . 020 meters/sec., and $\phi = 0$, then,

$$\sigma_{R_p} \sim 56 \text{ meters}$$

$$\sigma_e \sim 2.4 \times 10^{-4}$$

This result can be compared in a later note to the approximate approach taken in Apollo Note No. 60.

Table 7. Covariance Matrix

(Earth-Moon Line Perpendicular to Initial Velocity Direction)

Smoothing Interval (Orbital Periods)	Required Third Order Matrix Terms				
	D_{11}	$D_{11}+2\,D_{12}+D_{22}$	D_{22}	D_{55}	$(\mathrm{Det})_{1\text{-}2\text{-}5}$
1/4	$6.214,665 \times 10^{-4}$	$7.817,825,6 \times 10^{-4}$	$9.824,746 \times 10^{-6}$	$2.524,495 \times 10^{-3}$	$2.442,842 \times 10^{-9}$
1/2	.018,131,17	.069,873,45	.020,717,69	.104,411,65	2.6990×10^{-4}
1	3.4647	.25	4.7147	4.5272	2.9647
2	35.1713	.25	32.4213	26.2338	13.0857

Smoothing Interval (Orbital Periods)	Required Second Order Matrix Terms			
	D_{33}	$D_{33}+D_{44}-2\,D_{34}$	D_{44}	$(\mathrm{Det})_{3\text{-}4}$
1/4	.818,310	1.872,40	.117,88	.407,052
1/2	.5	1.6512	.575,587	.204,968
1	.5	2.5	1	.25
2	.5	2.5	1	.25

Table 8. Covariance Matrix

(Earth-Moon Line Perpendicular to Initial Position Direction)

Smoothing Interval (Orbital Periods)	Required Third Order Matrix Terms				
	D_{11}	D_{12}	D_{22}	D_{44}	$(Det)_{1-2-4}$
1/4	.004, 339, 834	-.018, 167, 777	.080, 897, 564	.077, 632, 433	.000, 025, 680
1/2	.474, 238, 596	-.753, 973, 291	1.238, 676, 348	.854, 411, 888	.037, 904, 819
1	4.714, 703, 3	-4.714, 703, 3	4.964, 703, 3	6.277, 2033	2.357, 351, 65
2	30.921, 313	-29.921, 313	29.171, 313	28.483, 813	14.085, 656

Smoothing Interval (Orbital Periods)	Required Second Order Matrix Terms			
	D_{33}	D_{35}	D_{55}	$(Det)_{3-5}$
1/4	.181, 690, 114	.063, 369, 684	.026, 338, 701	.000, 781, 782, 5
1/2	.5	.575, 586, 819	.802, 347, 274	.069, 873, 451
1	.5	1	2.5	.25
2	.5	1	2.5	.25

APOLLO NOTE NO. 70

H. Dale
27 May 1963

THE LEM AS A RECOVERY VEHICLE

One of the questions within Task No. 2 of this contract is concerned with the ability to align the LEM IMU. It is assumed that the LEM is attached to the CM. A real possibility is that the LLV is neither attached nor near the CM.

Consider a rescue mission requiring the landing of a second, but unmanned, LEM. Since the total LEM life support period will not exceed 48 hours, a rescue vehicle can not start from the earth, travel the nominal 70-hour course, and be of much use. Since lunar orbit missions will exist prior to the first lunar landing mission, it is conceivable that a slightly modified LEM might be stored in lunar orbit to be used in the event of a rescue requirement. Amongst the various special problems is that of IMU alignment (or its equivalent) in the special purpose LEM. Along with this is the problem of getting the rescuing LEM into a geometrically workable position with respect to the CM and the downed LEM.

Two reasonable techniques appear capable of getting the LEM down safely to the moon. Both require a line-of-sight between the rescuing LEM and the CM during the descent. The first consists of using the IMU for the initial and mid-course descent phases, and the T.V. link to the CM for the final descent phase. From Apollo Note No. 42 it can be seen that IMU alignment on the order of a mil or so would be required. The second technique would replace the highly accurately aligned IMU with a CM based radar. A one mil radar would thus be used to get the LEM down to the position where the T.V. link could take over. Unfortunately, both systems use an IMU. Apollo Note No. 58 shows that a platform, correct to about one-half of one degree, is necessary for T.V. lock-on and altitude-to-range conversion. Apollo Notes No. 14 and 27 present a good case

for the IMU during lunar descent. Thus the relevant questions are how well can one align the distant IMU, and would it be better to rely on radar guidance?

No answer appears possible to the first question without an automatic star tracker if one-mil accuracy is to be obtained. If greater than about a degree error may be permitted, a lunar horizon scanner and earth or sun disk tracker may be used. The presently planned LEM utilizes manned star tracking with the stellar telescope mounted rigidly to the IMU. It would thus seem that automatic star tracking is a proper choice for such a vehicle.

The question of using radar guidance can best be answered after looking into the orbit phase problem. Since it would place undue restrictions on the lunar landing mission to do otherwise, one may assume that any particular phase relationship exists between the orbiting LEM and the CM at the outset of a rescue attempt. Since T.V. information will be used in the terminal landing of the rescuing LEM, the phase angle must be small near touchdown. Without expending fuel for orbital transfer, the only way in which initial phase angles may be made to disappear is to have the semi-major axis of the LEM significantly different from that of the CM. For various circular altitudes of the rescuing LEM and for a 100 n. mi. CM, the following chart is a plot of the time between coincidences of the two vehicles.

Since little or no fuel penalty is paid for an increased LEM orbit altitude, (Apollo Note No. 2), it would thus seem that a 400 mile LEM orbit would be suitable.

In the event of a required faster rescue, the control of the rescuing LEM must come from a source other than the CM. It is conceivable that the DSIF or the downed LEM might initiate the rescuing descent. The final terminal descent and landing could then not be controlled by the CM since a favorable line-of-sight might not exist. If the rescuing LEM were equipped with a slant range radar and the downed LEM's transponder were working, the final descent

might follow (Apollo Note No. 19).

It would thus appear that a rescuing LEM mission is quite possible. It would also appear that circular orbits, different in radius from the CM's orbit, should be used. Good arguments can be made for the addition of automatic star tracking equipment for IMU alignment. The IMU is a reasonable equipment choice even in the event of radar guidance. And finally, a slant-range radar (gimbaled or not) would be necessary for extremely quick rescue.

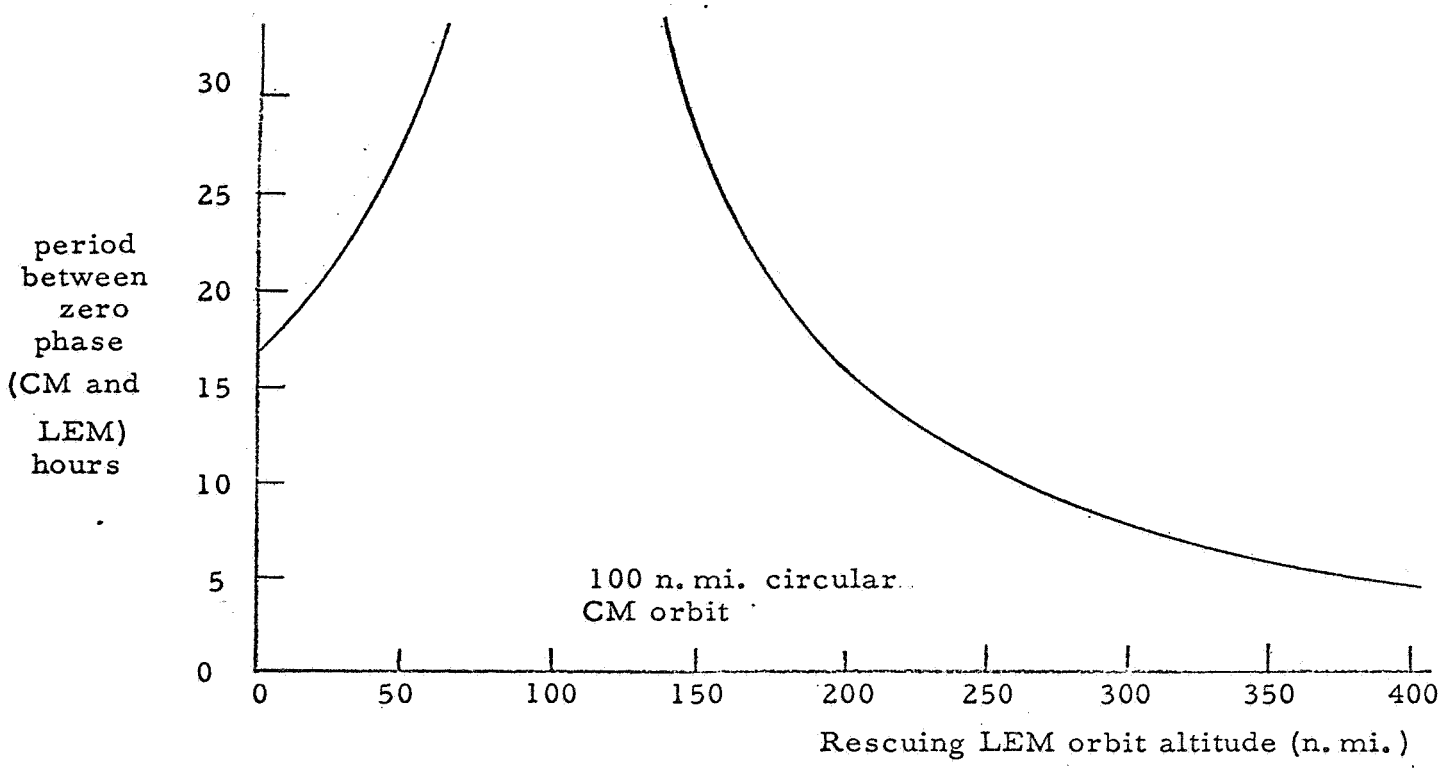

APOLLO NOTE NO. 71

R. Roche
29 May 1963

SELECTION OF THE OPTIMUM ABORT TRAJECTORY

SUMMARY

In this note the problem of how best to select an abort trajectory is considered. A simplified model is used to explore the merit of always choosing the minimum time return subject to the constraints imposed by the spacecraft status. The note is incomplete and suggests only a method of approach--it will be supplemented by subsequent notes.

DEVELOPMENT

When a change occurs in the status of the spacecraft which, without compensatory action, increases the probability of damage to the crew to more than some maximum proscribed value, the decision is made to abandon the normal mission objectives. With the normal mission objectives discarded, it becomes logical to choose as the aborted mission objective the maximization of the probability of safe return of the crew.

The problem now becomes one of choosing from the spectrum of return trajectories which are available to the spacecraft by virtue of its current status, that which best accomplishes this objective.

The spacecraft status factors which directly influence the choice of return trajectory will include:

Capabilities
- Present Position
- Present Velocity
- Total Velocity Change Capability
  a. with reconfiguration
  b. without reconfiguration
- On-Board Navigation Capability
- Ground Support Navigation Capability
- Attitude and Thrust Control Capability (Present and Projected)
- Crew Action Capability
- Re-entry Capability (Structural Integrity)

Problems
- Crew Health
- External Environment, Present and Projected
- Life Support System Status

The return trajectories can be characterized by a number of requirements and a number of attributes.
Namely:

Requirements
- ΔV Required, Total
- Placement and Number of Control Actions Required
- Precision of Control Actions Required

Attributes
- Time to Earth Surface Recovery
- Time to Atmosphere
- Time in Van Allen Belt
- Time in Solar View

There appears to be no firm reason to believe that the spacecraft status factors will be in general independent, i.e., that some event of significant probability will not affect more than one of the status factors.

Thus the general problem of matching capabilities to requirements in such fashion as to best solve the problems with the return trajectory attributes is not one of trivial difficulty. Nor is it clear without more complete formulation that we could recognize the best trajectory selection if we made it.

What seems to be required is a standard rationale for accomplishing this selection, if it is possible to establish one, and with this in mind, we consider a much simpler model than the actual one in the hope of gleaning some general principle which may be applicable to and may simplify the real physical situation.

Consider a spacecraft as an aggregate of m capabilities which are essential to the performance of the mission. Suppose further that some degree of redundancy is provided in each capability so that a failure in one does not in general immediately reduce the capability

but merely reduces the probability that the capability will be retained over some arbitrary period of time Δt.

We will further suppose that the probability of the crew's safe return is given by some function of the probabilities associated with retention of all the capabilities over the mission duration. Specifically we choose the simple relation:

$$P_s = (1 - P_{F_1}) \cdot (1 - P_{F_2}) \ldots (1 - P_{F_m})$$

where P_{F_i} is the probability of complete loss of the i^{th} capability. Thus, P_s is unity if all P_{F_i}'s are zero and goes to zero if any capability is completely lost.

For further simplicity we will assume that the individual capabilities have been designed to have the same P_F's so that:

$$P_s = (1 - P_F)^m$$

We digress a moment to consider the P_F's. If each element of the redundant set which make up a given capability is an aggregate of many sub-elements which have a mean time between failures of t_f independent of the time t, then the probability of r of these sub-elements failing in an interval t is:

$$P_r(t) = \frac{(\tau)^r}{r!} e^{-\tau} \quad ; \tau = \frac{t}{t_f}$$

so that the probability of no failures in the interval is:

$$P'_o(t) = e^{-\tau}$$

and thus the probability of at least one failure is:

$$P'_F = 1 - e^{-\tau}$$

However by virtue of the redundancy, the probability of completely losing the i^{th} capability is:

$$P_{F_i} = P'^{n}_F = (1 - e^{-\tau})^n$$

Thus using this expression for P_F the probability of a safe return will be:

$$P_s = \left\{1-(1-e^{-\tau})^n\right\}^m$$

After some arithmetic:

$$\frac{\Delta P_s}{P_s} = -\,m\,n\,\frac{(1-e^{-\tau})^n}{1-(1-e^{-\tau})^n}\,\frac{\tau\,e^{-\tau}}{1-e^{-\tau}}\,\frac{\Delta t}{t}$$

$$\cong -\,m\,n\,\frac{\tau^n}{1-\tau^n}\,\frac{\tau(1-\tau)}{\tau}\,\frac{\Delta t}{t}$$

$$\boxed{\frac{\Delta P_s}{P_s} \cong -\,m\,n\,\frac{\tau^n(1-\tau)}{1-\tau^n}\,\frac{\Delta t}{t}}$$

Gives the fractional change in safe return probability with fractional changes in time-to-go.

If one element in a redundant set fails at time t' the new probability, P_s, will be:

$$P_{S_2} = (1-P_F)^{m-1} \cdot \left\{1-(1-e^{-\tau})^{n-1}\right\}$$

so that

$$-\Delta P_s = (1-P_F)^m - (1-P_F)^{m-1}\left\{1-(1-e^{-\tau})^{n-1}\right\}$$

$$= (1-P_F)^m\left\{1-\frac{1-(1-e^{-\tau})^{n-1}}{1-(1-e^{-\tau})^n}\right\}$$

or:

$$\left(\frac{\Delta P_s}{P_s}\right)_{;n} = \left\{1 - \frac{1 - (1 - e^{-\tau})^{n-1}}{1 - (1-e^{-\tau})^{n}}\right\}$$

$$\cong 1 - \frac{1 - \tau^{n-1}}{1 - \tau^{n}}$$

$$= \frac{\tau^{n-1} - \tau^{n}}{1 - \tau^{n}}$$

$$\boxed{\frac{\Delta P_s}{P_s} = \frac{\tau^{n}}{1 - \tau^{n}} \cdot (\tau^{-1} - 1) = \frac{\tau^{n}}{1 - \tau^{n}} \frac{1 - \tau}{\tau}}$$

Thus the failure of a critical system element can be compensated for by a reduction in time-to-go provided that:

$$\frac{\tau^{n}}{1-\tau^{n}} \frac{(1-\tau)}{\tau} \leqq \frac{\tau^{n}}{1-\tau^{n}} (1 - \tau)\, m\, n \frac{\Delta t}{t}$$

or:

$$\frac{\Delta t}{t} \geqq \frac{1}{m\, n\, \tau} \quad ;$$

where, reasonably, $m\, n\, \tau \geqslant 1$.

This rather simple and incomplete analysis tends to indicate that in choosing abort return trajectories time may be of the essence because of its over-all effect on the probability of safe return as affected by time rate of change of component failure probabilities.

This suggests that a possible rationale for optimal course selection may be one of minimizing the time-to-go, subject to the extreme value constraints imposed by the status factors such as ΔV_{max}, time in radiation zones, and maneuvering capability, etc. A method for treating problems of this class has been developed by Pontryagin and his colleagues and may have application in this specific problem.

This will be the subject of a future note.

APOLLO NOTE NO. 73

B. Saltzberg
3 June 1963

SOME ADDITIONAL ERROR CALCULATIONS FOR DETERMINING THREE IN-PLANE ORBIT PARAMETERS FROM DSIF DOPPLER MEASUREMENTS

In order to compare the approximate techniques of Apollo Notes 32, 60, 61, and 64 for determining three in-plane orbit parameters with the more rigorous technique for deriving the accuracy of the orbit parameters obtainable with smoothed DSIF doppler data presented in Apollo Note No. 69, the following additional error calculations have been made.

Table 1 presents the variance and covariance values for data smoothed over the same 90° portion of the orbit selected in Apollo Note No. 69. In this case the results of the approximate error analysis are in substantial agreement with the results of the more complete analysis carried out in Apollo Note No. 69.

The first column of Table 2 represents the results of an error analysis for a case similar to that of Table 1, with the single exception that the three orbit parameters estimated are r_p, ψ, and θ instead of r_p, ψ, and e.

The second column of Table 2 represents the errors for the same orbit conditions as assumed in the first column except that data smoothing is conducted over 30° of the orbit rather than 90°. A comparison of the errors in Tables 2 and 3 indicates the high sensitivity of the errors to the length of the smoothing interval (when it is assumed that the initial phase rather than eccentricity is derived from doppler data).* The data shows that increasing

---

* When r_p, ψ, and e are derived from the doppler data as in Apollo Note No. 60, the errors are much less sensitive to increases in the length of the smoothing interval after 30° of smoothing.

the smoothing interval by a factor of 3 (30° to 90°) increases the accuracy of determining perigee, r_p, by a factor of 20, and the angular position accuracy of the earth-moon line relative to perigee by a factor of 35.

The coordinate system chosen for the error analysis is shown below.

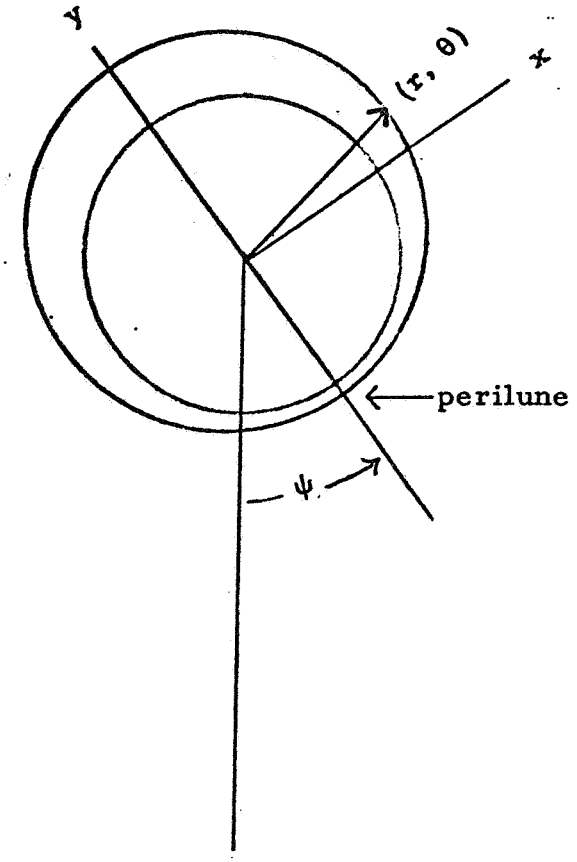

APOLLO NOTE NO. 74

C. H. Dale
11 June 1963

TECHNIQUES FOR REMOTELY ALIGNING THE LLV IMU FROM THE ATTACHED CM

This note discusses four techniques for aligning the IMU in the unmanned, but attached, Lunar Logistics Vehicle from the CM/SM. In order of increasing utility, they appear to be:

1. Utilizing the CM/LEM structure as a common base.
2. Provide a light path between the CM IMU and the LEM IMU.
3. Match accelerometers on the CM IMU and LEM IMU.
4. Star track with the T. V.

Structural Alignment

If reasonably perfect selsyns measure the attitude of the CM with respect to its IMU and the attitude of the LEM with respect to its IMU, then the two IMU's may be aligned to within the flexural deflection of the CM/LLV taken as a solid structure. Estimates of the structural misalignment and flexure of the LEM/CM combination are difficult to come by yet it would not be absurd to assume that the lower bound is one-half of one degree. This is better than is usually attainable in aircraft gun and rocket launcher boresightings. An upper bound of one or two degrees seems reasonable also.

The real problem is not how stiff a structure can be made, but rather how stiff an optimally light structure will be. If, for instance, the mating structure between the CM and LEM can be held flat to within .2 inches and if the opening is big enough for a man (for the LEM case), then a misalignment of about 5 mils could be expected from this source alone.

It seems apparent that structural alignment is a useful tool as an initial rough technique, but as shown in Apollo Note No. 42, further alignment is necessary if the LLV is to inertially navigate to within T. V. range of the lunar touchdown point.

Optical Light-Path Alignment

If a light beam can be directed from one IMU to the other, and back, then extremely good alignment may be accomplished. The major problem with such a technique is inherent in the fact that the light beam must go directly from one navigational base to the other; no structurally attached mirrors can be used to avoid objects that might interfere with a direct line-of-sight. Holes and windows must exist in any in-between structure.

In order to prove simply that the inherent accuracy of this sytem is high without trying to evolve an optimum system, a sample design is shown and analyzed. This design is shown as Figure 1. The system is based upon a light and set of mirrors rigidly attached to

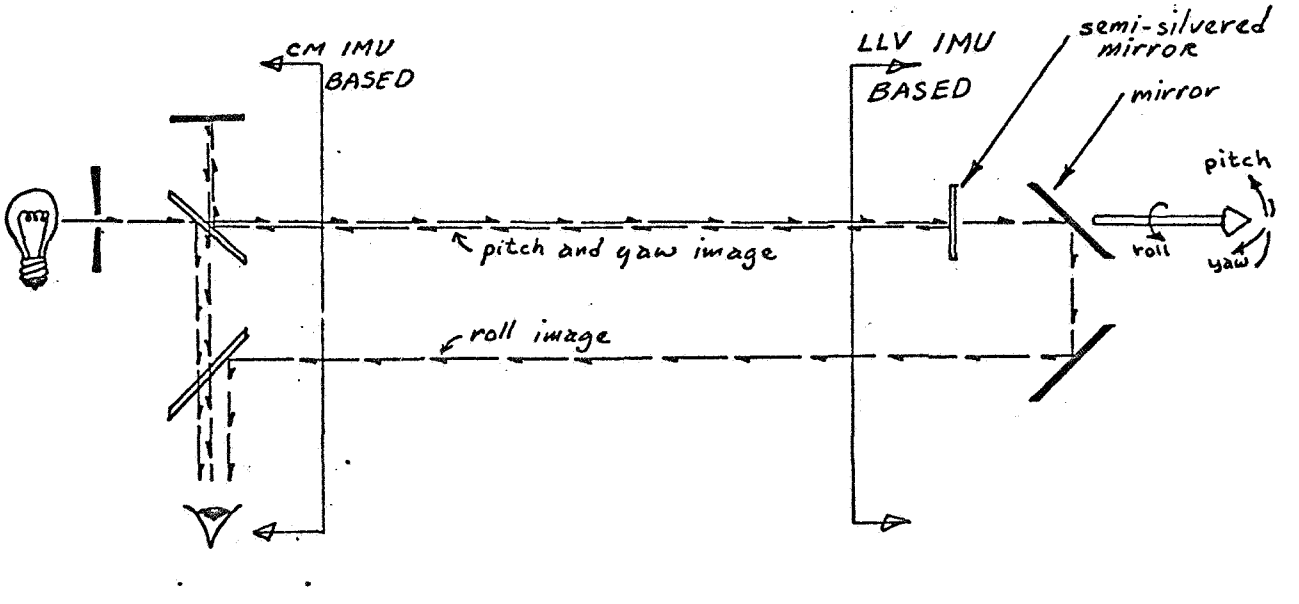

Figure 1. An Example Optical Aligning System.

the navigational base of the CM and a set of 3 mirrors rigidly attached to the navigational base of the LLV. Denoting a triad by pitch, yaw and roll axes, as shown in the figure, the pitch and yaw components may be zeroed first by superposing an outgoing and reflected image.

After this is accomplished, the roll axis may be zeroed through the use of an off-set return light path. It is interesting to note that if all three axes are to be aligned reasonably simultaneously, then such an off-set path must exist. If the initial alignment of one degree is to be used for initial acquisition, then about a ten inch wide path must exist between the CM navigational base and the LLV navigational base. This is not necessarily an easy thing to provide. However, if a ten inch path exists, and if 1/100 inch resolution exists, then one mil roll alignment follows from the figure. Pitch and yaw will far surpass roll alignments unless the craft is rotated through 90° and again aligned to improve the roll alignment.

Accelerometer Matching Alignment

Both the CM IMU and the LLV IMU have a set of accelerometers. The differences in the readings of the two sets of accelerometers can only be due to accelerometer errors and/or a difference in the spatial orientation of the two IMU's. Under the assumption of a thrust acceleration, $\overline{a}$ (the only kind measured by an accelerometer in free fall), the LLV will measure $\overline{c}$ in its co-ordinate system while the CM will measure $\overline{d}$. If enough time elapses such that noise errors are reduced to insignificance then the difference, $\overline{b}$, between $\overline{c}$ and $\overline{d}$ will be due to bias errors in the accelerometers. The transformation, T, between $\overline{c}$ and $\overline{d}$ is thus not length preserving and part of its rotational characteristic can be caused by $\overline{b}$. Three maneuvers, $\overline{a}_i \Delta t$ where $i = 1, 2, 3$, that are non-coplanar will allow the determination of T since

$$\overline{d}_i = T\ \overline{c}_i \qquad i = 1, 2, 3$$

is actually a set of nine equations in the nine unknown components of T.

However, knowing T does not allow an exact solution for the angular difference between the two platforms, since part of the

rotation between $\bar{c}$ and $\bar{d}$ is due to platform misalignment and part is due to $\bar{b}$, the difference in the accelerometer biases between the two IMU's.

With a single maneuver the above equation can not be solved unless the assumption is made that $\bar{b}$ is zero. However, since in the LLV alignment period no maneuvers are required, it would be a good idea to minimize the fuel spent on accelerating for IMU alignment. If one maneuver were made and a computer lengthened $\bar{c}$ or $\bar{d}$ so as to make $|\bar{c}| = |\bar{d}|$ then T is a pure rotation. The expected error in the relative alignment of the platforms will be due to $\bar{b}$ and will be on the order of:

$$e\,\gamma \simeq \frac{a_{bias}}{a}$$

where a_{bias} is the expected bias error in the accelerometers and a is the average thrust acceleration.

It turns out that the main service module engine must be used to acquire reasonable alignment. The expected bias acceleration of the IMU accelerometers is 0.5 cm/sec.^{2}. With CM, SM, and LLV attached and in lunar orbit their combined weight is on the order of 50,000 pounds. If two auxiliary control jets on the LLV could be used along with two jets on the CM, a total thrust of about 400 pounds could be applied resulting in an acceleration of 8 cm/sec.^{2}. This in turn results in an alignment error of about 60 mils. With the main 20,000 pound engine the alignment error might be reduced to about 1.5 mils. This engine, however, burns about 65 pounds of fuel per second. Since times of not too much less than a second are required for turning the engine on and off, this may prove to be a costly technique for IMU alignment. It should be noted however that no additional equipment is necessary and no penalty is placed upon the exact location of the IMU's relative to one another.

Television Star Tracking

The men in the CM uses a telescope on the navigational base to star track and thus align their IMU. Since a T. V. link exists between the LLV and the CM and since the T. V. camera could easily be mounted on the navigational base of the LLV's IMU, then it would seem that it might be appropriate to align both IMU's by star tracking. It is true that a lens, differing in focal length from other requirements, must be used, but a lens turret is not an uncommon concept.

Assuming 1000 lines on a 2 inch T. V. tube, and a 5 inch lens, resolution on the order of one quarter mil is achievable. From Apollo Note No. 36, it would appear that only first or second order magnitude stars might be picked up by such a system. However, this is satisfactory since initial orientation would depend upon structural alignment. This system, with the exception of a possibly needed extra lens, will require no added components.

APOLLO NOTE NO. 75

H. Dale
17 June 1963

THE FUEL COST OF VARIOUS TWO BOOST ASCENTS

The nominal ascent consists of boosting off the lunar surface to a safe perigee altitude of 8 nautical miles. Rendezvous occurs after a central angle from perigee of 160^{o}. This trajectory is near the optimal Hohmann yet allows some out-of-plane correction capability with two boosts.

Assuming no out-of-plane problem, this Note attempts to calculate the additional boost required to make higher energy, safe transfers. The cut-off perigee velocity is always horizontal.

Defining:

μ = lunar gravitational constant = $173.094 \times 10^{12} ft^3/sec^2$

R_m = lunar radius = $5.70267 \times 10^6 ft$

R_p = perigee = $5.75131 \times 10^6 ft$

R_{cm} = 80 n.mi. command mod. radius = $6.18907 \times 10^6 ft$

e = eccentricity

θ = subtended angle from perigee

V, V_p = velocity, perigee velocity

a = semi-major axis

then for the nominal ascent

$$R_{cm} = \frac{a(1 - e^2)}{1 + e\cos\theta} = \frac{R_p(1 + e)}{1 + e\cos\theta} \qquad (1)$$

defines the eccentricity of the trajectory which starts at R_p and meets the CM/SM at R_{cm} after traversing $\theta = 160^{o}$. The required perigee velocity is

$$V_p = \sqrt{\frac{\mu}{R_p}(1 + e)} = 5588.85 \text{ ft/sec} \qquad (2)$$

The horizontal velocity at $R = R_{cm}$ ($\theta = 160^{o}$) is

$$V_h = \frac{V_p R_p}{R_{cm}} = 5193.54 \text{ ft/sec} \tag{3}$$

The CM/SM velocity is

$$V_c = \sqrt{\frac{\mu}{R_{cm}}} = 5288.44 \text{ ft/sec} \tag{4}$$

Thus the change in horizontal speed must be

$$\Delta V_h = V_c - V_h = 94.90 \text{ ft/sec} \tag{5}$$

The change in vertical speed ($\dot{R}$) must be, at rendezvous:

$$\Delta \dot{R} = \dot{R} = V \left[1 - \left(\frac{V_h}{V} \right)^2 \right]^{1/2} = 69.20 \text{ ft/sec} \tag{6}$$

where V is the LEM's total velocity before retroing for rendezvous.

$$V = \sqrt{\mu \left(\frac{2}{R_{cm}} - \frac{1 - \epsilon}{R_p} \right)} = 5194.00 \text{ ft/sec} \tag{7}$$

Thus from equation (5) and (6) the total rendezvous correction is

$$\Delta V_T = \left[(\Delta V_h)^2 + (\dot{R})^2 \right]^{1/2} = 116.30 \text{ ft/sec} \tag{8}$$

The total boost required is then

$$V_{req.} = V_p + \Delta V_T = 5705.15 \text{ ft/sec.} \tag{9}$$

This neglects the boost required to fight lunar gravity during ascent, but for all the cases to be studied that will be a constant since all cases will have at least circular velocity at perigee cut-off. Now since this is the nominal trajectory, all other trajectories may be expressed as an increase or decrease in velocity from this base.

Since all trajectories to be considered have horizontal velocity at ascent cut-off (8 naut. miles altitude), their apogee altitude is enough to determine the cut-off velocity. Thus as a function of the radius of apogee

$$V_p = \sqrt{\frac{2\mu}{R_p}\left(\frac{R_a}{R_a + R_p}\right)} \tag{10}$$

The total velocity upon reaching the CM/SM in its 80 nautical mile orbit is

$$V = \sqrt{2\mu\left(\frac{1}{R_{cm}} - \frac{1}{R_a + R_p}\right)} \tag{11}$$

Equations (3) through (9) may be used to compute the total boost required for ascent and rendezvous as a function of the apogee altitude of the ascent trajectory. The results are shown in the following figure.

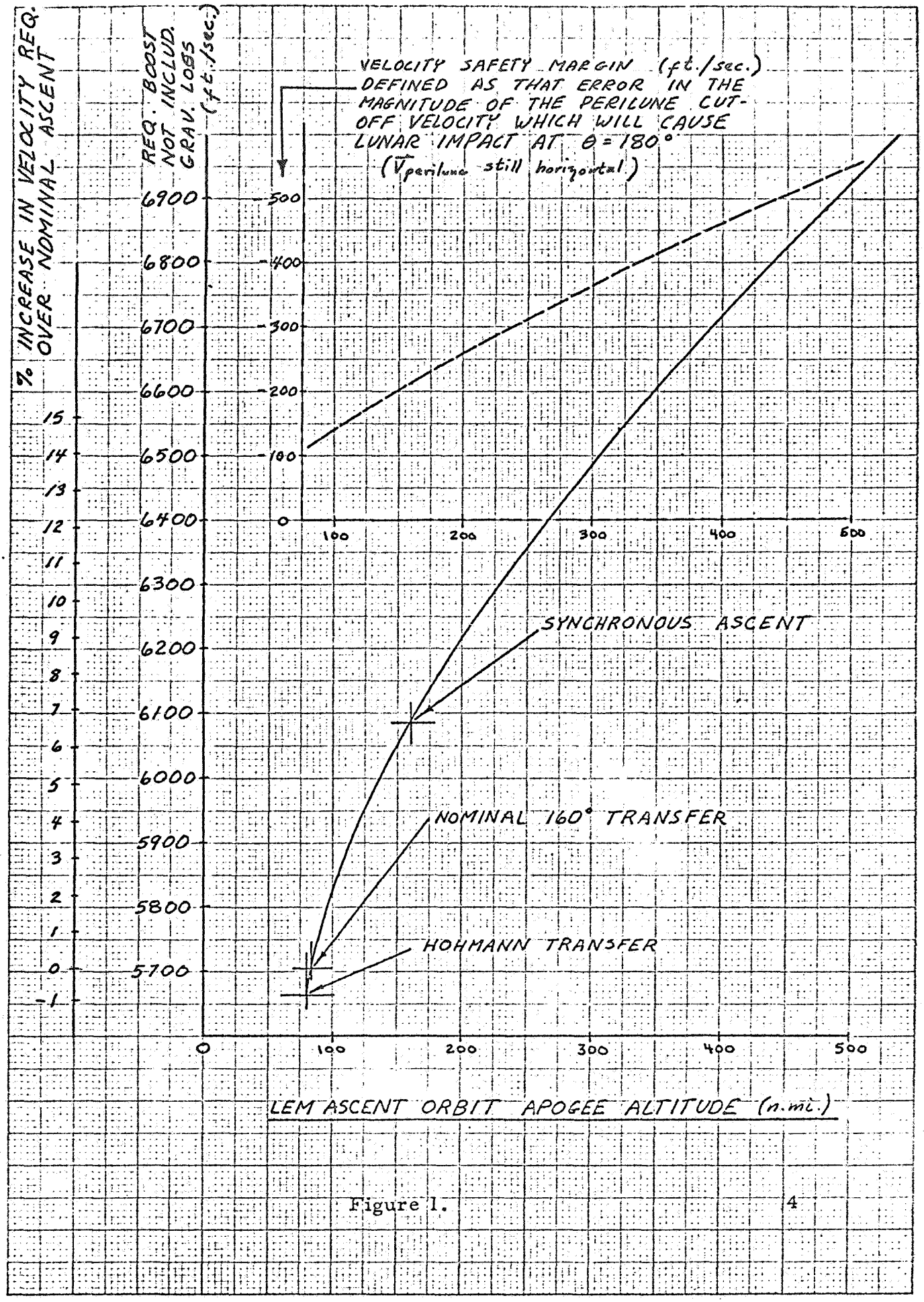

Figure 1.

APOLLO NOTE NO. 76

L. Horowitz
18 June 1963

NOTES ON L. S. PONTRYAGIN'S THEORY OF OPTIMAL PROCESSES

Introduction: Soviet Academician L. S. Pontryagin has proposed an elegant solution to the following problem: from a given set of "control functions" (variable thrust, limited fuel supply, etc.), call them $u_i(t)$, how can the "optimum" $u_i(t)$ be selected such that the time required to transfer a vehicle between two given points is minimized?*

In practical situations, the $u_i(t)$ are all bounded (since the transfer could otherwise generally be accomplished in arbitrarily small time). Initial and final points $\underline{\xi}_o$ and $\underline{\xi}_f$ are given in the "phase space" defined by the problem; i.e., the space spanned by the generalized position and velocity coordinates. The motion of a representative point in this phase space is then given by the equations of motion

$$\dot{x}_i = f_i(x_1, \ldots, x_n, u_1, \ldots, u_r); \quad i = 1, 2, \ldots, n. \qquad (1)$$

Pontryagin's technique involves linearizing the general equations of motion, writing the solution to the resulting simultaneous system of linear, first order differential equations subject to the given initial and boundary conditions, and then selecting the optimal control functions $u_i(t)$ by exploiting the convex properties of the loci of optimal trajectories corresponding to optimal control functions.

Pontryagin's paper considers this problem in fully abstract mathematical formulation; in addition to presenting the completely general abstract solution to the problem, he also provides generalized existence and uniqueness proofs for the solutions obtained.

This paper attempts to motivate Pontryagin's method in a heuristic fashion, and concludes with simple examples of the technique

---

* Theory of Time Optimal Processes in Linear Systems, presented by R. V. Gamkrelidze, Bulletin of the Academy of Sciences of the USSR Vol 2, 1958 - pps 449 - 474.

as applied to elementary linear control problems. No attempt is made to provide rigorous mathematical justification of the development; for this the reader is referred to the original work previously cited.

Formulation of the Problem: We consider a computer whose inputs are position and velocity; we wish to determine optimal control functions $u_i(t)$. The equations of motion are given by (1). We assume the control functions $u_i(t)$ are bounded and piecewise smooth; without loss of generality, the $u_i(t)$ may be taken as normalized: $|u_i(t)| \leq 1$, $t \geq t_o$. Initial position and velocity are given: $x_i(t_o) = x_i^o$; $\dot{x}_i(t_o) = \dot{x}_i^o$. This corresponds to an initial point in "phase space": $\underline{\xi}(t_o) = \underline{\xi}_o$, where $\underline{\xi} = (x_1, \ldots, x_n; \dot{x}_1, \ldots, \dot{x}_n)$. A final condition is also specified: $\underline{\xi}(t_f) = \underline{\xi}_f$ for some t_f. We wish to select the control functions $u_i(t)$ ($|u_i(t)| \leq 1$) so as to minimize t_f. Form the total differential of (1):

$$d\dot{x}_i = \sum_{j=1}^{n} \frac{\partial f_i}{\partial x_j} dx_j + \sum_{k=1}^{r} \frac{\partial f_i}{\partial u_k} du_k . \qquad (2)$$

To effect a linearization of the problem, we assume that the indicated partial derivatives of (2) are all constant: $\frac{\partial f_i}{\partial x_j} = a_{ij}$; $\frac{\partial f_i}{\partial u_k} = b_{ik}$. Integrating (2), the equation of motion can then be written as a simultaneous system of first order, linear differential equations:

$$\boxed{\dot{\underline{x}} = A\underline{x} + \underline{b}_1 u_1 + \underline{b}_2 u_2 + \cdots + \underline{b}_r u_r} \quad ; \qquad (3)$$

with the appropriate initial and final conditions specified. The problem at hand thus reduces to selecting optimal control functions $u_i(t)$ ($|u_i(t)| \leq 1$) so that with motion governed by (3), the transfer time between $\underline{\xi}_o$ and $\underline{\xi}_f$ is minimized.

We note several extensions compatible with (3):

(i) If the equations of motion involve higher order derivatives of the $\underline{x}_i(t)$, a reduction to a larger system involving only first order derivatives can be readily effected by introducing new variables.

Example: $\ddot{x}_1 = a\dot{x}_1 + bx_1 + cu$. Let $\dot{x}_1 = x_2$.

Then the larger system, now of first order, is simply

$$\begin{cases} \dot{x}_1 = x_2 \\ \dot{x}_2 = ax_2 + bx_1 + cu \end{cases}$$

(ii) If a particular control function happens to require that its time integral be bounded, a new system of higher order is readily obtained by differentiation.

Example: $\dot{x}_1 = ax_1 + b \int_0^t u_1(\tau)\, d\tau$.

Differentiating this equation, we have $\ddot{x}_1 = a\dot{x}_1 + bu_1(t)$.

The order of this equation can now be reduced to one by using the technique of (i).

Analogous extensions can be formulated for similar linear systems.

General Solution of (3): If we knew the control functions $u_i(t)$, the general solution to (3) could be obtained as follows:

$$\dot{\underline{x}} = A\underline{x} + \underline{b}_1 u_1 + \cdots + \underline{b}_r u_r \qquad (3)$$

Introduce a new dependent variable $\underline{y} = (y_1, \cdots, y_n)$ so that $y_i = q_{ij}x_j$, $x_i = p_{ij}y_j$, the p_{ij} to be determined. Then

$$\dot{\underline{y}} = P^{-1}AP\underline{y} + P^{-1}\underline{b}_1 u_1 + \cdots + P^{-1}\underline{b}_r u_r, \qquad (4)$$

where P is the matrix of the p_{ij}. If we assume that A is non-

singular (Pontryagin shows that the problem is otherwise over-specified; page 8 of his paper), we can select P so that $P^{-1}AP$ is a diagonal matrix, call it $\Lambda = \{\lambda_{ij}\}$. Then (4) becomes

$$\dot{y}_i = \lambda_i y_i + \sum_j d_{ij} u_j \; ; \quad i = 1, \cdots, n \text{ with solution}$$

$$y_i = e^{\lambda_i t}\left[(y_i)_o + \sum_{j=1}^{r} \int_o^t d_{ij} e^{-\lambda_i \tau} u_j(\tau)\, d\tau \, . \right]$$

Then

$$\sum_{j=1}^{n} q_{ij} x_j = e^{\lambda_i t}\left[\sum_{j=1}^{n} q_{ij} (x_j)_o + \sum_{k=1}^{r} \int_o^t d_{ik} e^{-\lambda_i t} u_k(\tau)\, d\tau \right], \quad (5)$$

which can be solved for the $x_i(t)$. Following Pontryagin, we simplify the ensuing discussion by writing

$$\boxed{\underline{x}(t) = \sum_{\alpha=1}^{n} \underline{\phi}_\alpha(t) \left[x_o^{\alpha} + \int_o^t \underline{\psi}^{\alpha} \cdot (\underline{b}_1 u^1 + \cdots + \underline{b}_r u^r)\, d\tau \right]}, \quad (6)$$

where $\underline{\phi}_1(t), \cdots, \underline{\phi}_n(t)$ generate the fundamental system of solutions to the corresponding homogeneous vector equation $\dot{\underline{x}} = A\underline{x}$, and $\underline{\psi}^1(t), \cdots, \underline{\psi}^n(t)$ are the respective "duals" of the $\underline{\phi}_i(t)$; viz., the fundamental system of solutions to the corresponding "adjoint" equation $\dot{\underline{\psi}}^j = -A' \underline{\psi}^j$, A' the adjoint (viz., the conjugate transpose) transformation of A. We observe that $\underline{\phi}_i(t) \cdot \underline{\psi}^j(t) = \delta_i^j$ since $\left\{\underline{\phi}_i\right\}_{i=1}^{n}$, $\left\{\underline{\psi}^j\right\}_{j=1}^{n}$ solve adjoint systems (we have, without loss of generality, taken the $\underline{\phi}_i$, $\underline{\psi}^j$ to be normalized). A more detailed account of this procedure for solving linear differential systems is included in Appendix II.

Functional Form of the Optimal Controls

We observe that for a linear function f of n independent variables

$$f = \sum_{j=1}^{n} \alpha_j x_j \, ,$$

simple examples of convex sets. For any two points (vectors) $\underline{x}_1$ and $\underline{x}_2$ in a convex set containing the origin, and any $\lambda \geq 0$, $\mu \geq 0$ with $\lambda + \mu = 1$, we have $\underline{x} = \lambda \underline{x}_1 + \mu \underline{x}_2$ is on the line joining $\underline{x}_1$ and $\underline{x}_2$:

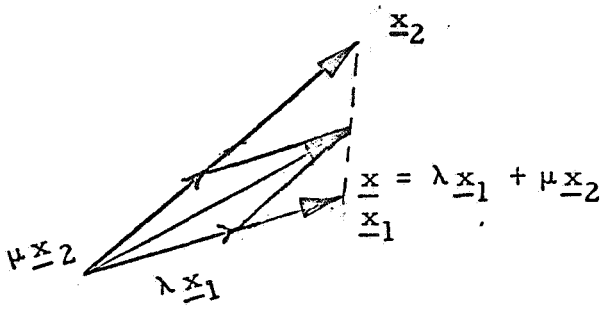

Figure 1.

If u_1 and u_2 are the admissible controls corresponding to $\underline{x}_1$ and $\underline{x}_2$, then $\underline{x}$ is accessible by using the control $\lambda u_1 + \mu u_2$ since by (6),

$$\underline{x}(T) = \lambda \underline{x}_1 (T) + \mu \underline{x}_2(T) = \lambda \sum_\alpha \underline{\phi}_\alpha (T) \left[x_o^\alpha + \int_o^T h^\alpha(\tau)\, u_1(\tau)\, d\tau \right] +$$

$$\mu \sum_\alpha \underline{\phi}_\alpha (T) \left[x_o^\alpha + \int_o^T h^\alpha(\tau)\, u_2(\tau)\, d\tau \right] = \sum_\alpha \underline{\phi}_\alpha (T) \left[x_o^\alpha + \int_o^T h^\alpha(\tau) \left[\lambda u_1(\tau) + \mu u_2(\tau) \right] d\tau \right].$$

Note that $\left| \lambda u_1 + \mu u_2 \right| \leq \lambda \left| u_1 \right| + \mu \left| u_2 \right| \leq \lambda + \mu = 1$, so that $\lambda u_1 + \mu u_2$ is an admissible control. Thus, if $\underline{x}_1(T)$ and $\underline{x}_2(T)$ are two optimal terminal points, we see that the chord of $\Omega(T)$ joining them contains only points of Ω, guaranteeing the convexity of the region. This argument extends inductively to the case of multiple controls.

Note that if $u(T)$ is an optimal control with corresponding optimal trajectory $\underline{x}(T)$, then $u(t)$ is also optimal for all t, $0 \leq t \leq T$.

For if we could get to a point $\underline{x}(T_1)$, $T_1 < T$, in a time $T_1 - \epsilon$ $(\epsilon > 0)$ by using a <u>different</u> control, call it $v(t)$, then we could get to $\underline{x}(T)$ in time $T - \epsilon$ by using $v(t)$ for $0 \leq t < T_1 - \epsilon$, and then $u(t)$ for $T_1 - \epsilon \leq t \leq T - \epsilon$:

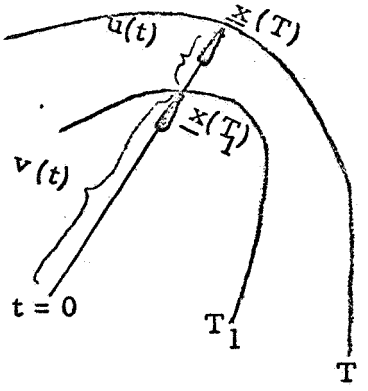

Figure 2.

Since this contradicts the optimal character of $u(T)$, we conclude that $u(t)$ is indeed optimal for all t, $0 \leq t \leq T$.

Having established the convex character of $\Omega(T)$ (the set of all points accessible from $\underline{\xi}_o$ in time T, using admissible controls), we next note that the normal, call it $\underline{\lambda}$, to the boundary of $\Omega(T)$ at $\underline{x}(T)$ forms an angle $\geq \frac{\pi}{2}$ with the incremental vector $\delta \underline{x}(T)$, where $\underline{x}(T) + \delta \underline{x}(T)$ is an optimal terminal point adjacent to $\underline{x}(T)$:

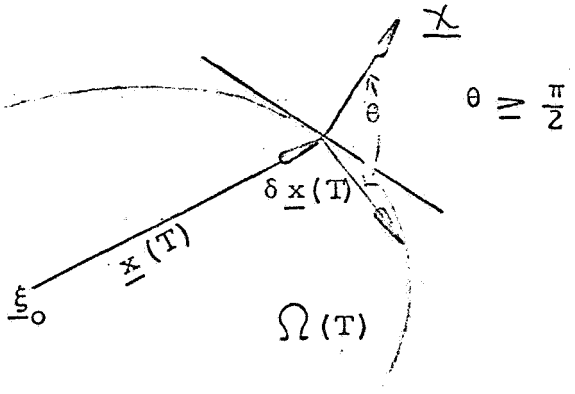

Figure 3.

$$\boxed{\underline{\lambda} \cdot \delta \underline{x} \leq 0} \tag{8}$$

This is an immediate consequence of the definition of convex sets. We note two features of this representation:

(i) Since the boundary of $\Omega(T)$, call it $\partial \Omega(T)$, contains only optimal terminal points (i. e., only endpoints of optimal trajectories corresponding to optimal controls), then the control corresponding to $\underline{x}(T) + \delta \underline{x}(T)$ (call this control $u(t) + \delta u(t)$) must itself be optimal.

(ii) For a monotonically increasing sequence of times T_k ($T_1 < T_2 < \cdots\cdots < T_n$, $k = 1, 2, \cdots\cdots, n$), the corresponding convex sets $\Omega(T_k) \triangleq \Omega_k$ form a nested sequence in the sense of proper set inclusion: $\Omega_1 \subset \Omega_2 \subset \cdots\cdots \subset \Omega_n$.

With these preliminaries established, the crucial matter of determining optimal controls $u_i(t)$ can now be handled. From (6), we know that for any optimal control $u(t)$ (assume there is just one control for the moment), the corresponding trajectory is

$$\underline{x}(t) = \sum_{\alpha = 1}^{n} \underline{\phi}_{\alpha}(t) \left[x_o^{\alpha} + \int_o^t \underline{\psi}^{\alpha} \cdot \underline{b}\, u(\tau)\, d\tau \right]. \tag{6}$$

For an admissible perturbation $\underline{x} + \delta \underline{x}$ with corresponding optimal control $u + \delta u$, we have

$$\underline{x}(t) + \delta \underline{x}(t) = \sum_{\alpha = 1}^{n} \underline{\phi}_{\alpha}(t) \left[x_o^{\alpha} + \int_o^t \underline{\psi}^{\alpha} \cdot \underline{b}\, (u(\tau) + \delta u(\tau))\, d\tau \right]. \tag{9}$$

Subtracting (6) from (9), we obtain

$$\delta \underline{x}(t) = \sum_{\alpha=1}^{n} \underline{\phi}_\alpha(t) \int_o^t \underline{\psi}^\alpha \cdot \underline{b}\, \delta u(\tau)\, d\tau, \tag{10}$$

the equation for the perturbation $\delta \underline{x}(t)$ in terms of the corresponding perturbed control δu. For fixed T, take the dot product of (10) with the unit normal $\underline{\lambda}$ to $\Omega(T)$ at $\underline{x}(T)$:

$$\underline{\lambda} \cdot \delta \underline{x}(T) = \sum_{\alpha=1}^{n} \underline{\lambda} \cdot \underline{\phi}_\alpha(T) \int_o^T \underline{\psi}^\alpha(\tau) \cdot \underline{b}\, u(\tau)\, d\tau$$

$$= \sum_{\alpha=1}^{n} \int_o^T c_\alpha \underline{\psi}^\alpha(\tau) \cdot \underline{b}\, \delta u(\tau)\, d\tau, \quad \text{where } c_\alpha = \underline{\lambda} \cdot \underline{\phi}_\alpha(T).$$

By (8), $\underline{\lambda} \cdot \delta \underline{x}(T) \leq 0$; an inequality holding for every fixed T and every admissible perturbation $\delta u(t)$ of $u(t)$. We conclude

$$\int_o^T c_\alpha \underline{\psi}^\alpha(\tau) \cdot \underline{b}\, \delta u(\tau)\, d\tau \leq 0 \tag{11}$$

and hence that for positive values of $c_\alpha \underline{\psi}^\alpha(t) \cdot \underline{b}$, $\delta u(t)$ must be non-positive, while for negative values of $c_\alpha \underline{\psi}^\alpha(t) \cdot \underline{b}$, $\delta u(t)$ must be non-negative. Since $u(t) + \delta u(t)$ is an admissible control ((i), page 8 of this Note), we have $|u(t) + \delta u(t)| \leq 1$. But by (7), $|u(t)| = 1$ (save possibly at a finite number of discontinuities; following Pontryagin after Lebesgue, we say $|u(t)| = 1$ <u>almost everywhere</u>); further, $|u(t) + \delta u(t)| = 1$ almost everywhere. We conclude

$$\boxed{u(t) = \text{sign}\ \underline{\psi}(t) \cdot \underline{b}, \quad 0 \leq t \leq T}, \tag{12}$$

where the "sign" function is defined by

$$\text{Sign } x = \begin{cases} 1, & x > 0 \\ 0, & x = 0 \\ -1, & x < 0 \end{cases} .$$

Here, $\underline{\psi}(t) = \sum_{\alpha} c_{\alpha} \underline{\psi}^{\alpha}(t) = \sum_{\alpha} \underline{\chi} \cdot \underline{\phi}_{\alpha}(t)\, \underline{\psi}^{\alpha}(t)$.

We now show that $c_{\alpha}(t) = \underline{\chi} \cdot \underline{\phi}^{\alpha}$ is a constant of the entire trajectory, so that the boundary conditions suffice to completely determine the constant c_{α} and hence the control functions $u_i(t)$. First note that $\underline{\psi}(t) \cdot \dot{\underline{x}} \equiv$ constant, since

$$\frac{d}{dt}\left[\underline{\psi}(t) \cdot \dot{\underline{x}}(t)\right] = \frac{d}{dt}\left[\underline{\psi}(t) \cdot (A\underline{x} + \underline{b}u)\right]$$

$$= \dot{\underline{\psi}} \cdot A\underline{x} + \underline{\psi} \cdot A\dot{\underline{x}} + \dot{\underline{\psi}} \cdot \underline{b}u$$

$$= -A' \underline{\psi} \cdot A\underline{x} + \underline{\psi} \cdot A(A\underline{x} + \underline{b}u) + (-A' \underline{\psi} \cdot \underline{b}u)$$

$$= -\underline{\psi} \cdot A^2\underline{x} + \underline{\psi} \cdot A^2\underline{x} + \underline{\psi} \cdot A\underline{b}u - \underline{\psi} \cdot A\underline{b}u \equiv 0$$

so that $\underline{\psi} \cdot \dot{\underline{x}}$ is identically constant. But $\underline{\psi} = \sum_{\alpha} c_{\alpha} \underline{\psi}^{\alpha} = \sum_{\alpha} \underline{\chi} \cdot \underline{\phi}_{\alpha} \underline{\psi}^{\alpha}$, where $\underline{\phi}_{\alpha}\, \underline{\psi}^{\alpha}$ is just the tensor identity element (by the normalization of $\underline{\phi}_{\alpha}$ and $\underline{\psi}^{\alpha}$), so that $\underline{\chi} \cdot \underline{\phi}^{\alpha}$ is identically constant over the entire trajectory.

Hence, (12) is precisely the relation sought after, and the optimal selection of the control functions $u_i(t)$ is completed.

Conclusions: Functions assuming only the values $\pm$ 1 are called "relay functions" in the literature. Pontryagin shows that the relay function solutions obtained in his analysis are unique, and that a physically meaningful problem always possesses unique control functions optimizing the transfer trajectory. Pontryagin's uniqueness proof is based on the fact that the class of all relay functions forms a Hilbert Space (a linear vector space with a "distance function" defined on the space; it has the property that every (infinite) convergent sequence of elements in the space always converges to an element which again belongs to that space), and hence that all (infinite) bounded monotonic sequences of accessible loci Ω_k always converge to limits belonging to the same space.

We note also that the arguments of Appendix II are readily generalized to the case of time-varying elements a_{ij} of the matrix A, so that linear equations (3) with time-varying coefficients can also be solved in this manner.

Unfortunately, most of the Apollo optimizing problems are fundamentally non-linear and hence not directly amenable to Pontryagin's solution. Several devices are available however: many non-linear equations may be converted to linear equations by inspired changes of variables; sometimes techniques are available for converting non-linear equations to infinite systems of linear equations (e.g., Carleman's Method, Adaptive Control Processes by R. Bellman, p. 45). If further study along these lines proves fruitful, the next note will extend this technique to the more general case of non-linear optimization.

APPENDIX I

POSITION SERVO OPTIMIZATION

To apply Pontryagin's theory to a specific problem, we consider the "position servo" problem:

$$\ddot{x}_1 = -a\dot{x}_1 - cx_1 + Mu(t) \qquad \text{(I-1)}$$

$$x_1(0) = x^o_1$$

$$\dot{x}_1(0) = \dot{x}^o_1$$

$$|u(t)| \leq 1$$

$$\left.\begin{aligned} x_1(t_f) &= 0 \\ \dot{x}_1(t_f) &= 0 \end{aligned}\right\} \quad \text{for some } t_f.$$

We wish to select $u(t)$ so as to minimize t_f.

To convert (I-1) to suitable form, introduce the new variable $x_2 = \dot{x}_1$. Then the problem to be optimized is:

$$\dot{x}_1 = x_2 \qquad \text{(I-2)}$$

$$\dot{x}_2 = -ax_2 - cx_1 + Mu(t)$$

$$x_1(0) = x^o_1; \quad x_2(0) = x^o_2 = \dot{x}^o_1$$

$$|u(t)| \leq 1$$

$$x_1(t_f) = x_2(t_f) = 0$$

For a realistic servo problem, we suppose $a \geq 0$ and $a^2 - 4c \leq 0$.
To write (I-2) as a vector equation, we have

$$\underline{x} = \begin{pmatrix} x_1 \\ \dot{x}_1 \end{pmatrix} = \begin{pmatrix} x_1 \\ x_2 \end{pmatrix}$$

$$\dot{\underline{x}} = \begin{pmatrix} \dot{x}_1 \\ \dot{x}_2 \end{pmatrix}$$

$$A = \begin{pmatrix} 0 & 1 \\ -c & -a \end{pmatrix}$$

$$\underline{b} = M \begin{pmatrix} 0 \\ 1 \end{pmatrix}$$

Then,

$$\dot{\underline{x}} = A\underline{x} + \underline{b}u \qquad \text{(I-3)}$$

as in (3), with the indicated boundary conditions $\underline{x}(0) = \underline{x}_o$, $\underline{x}(t_f) = 0$ for <u>some</u> t_f; we wish to select $u(t)$ $(|u(t)| \leq 1)$ so as to minimize t_f.

The corresponding homogeneous matrix equation is

$$\dot{\Phi} = A\Phi \qquad \text{(I-4)}$$

with solution

$$\Phi = \begin{pmatrix} e^{\frac{a+\sqrt{a^2-4c}}{2}t} & 0 \\ 0 & e^{\frac{a-\sqrt{a^2-4c}}{2}t} \end{pmatrix}, \qquad \text{(I-5)}$$

up to arbitrary multiplicative constants.

To obtain Ψ, use (II-6) and obtain

$$\Psi = \begin{pmatrix} e^{\frac{-a-\sqrt{a^2-4c}}{2}t} & 0 \\ 0 & e^{\frac{-a+\sqrt{a^2-4c}}{2}t} \end{pmatrix}; \quad \text{(I-6)}$$

again up to arbitrary multiplicative constants. Next, form the vector $\underline{\psi}(t) = \underline{\chi} \cdot \underline{\phi}_\alpha \underline{\psi}^\alpha$ (where $\underline{\chi}$ is to be determined by boundary conditions; it is the outward normal to the convex set about $\underline{x}_o$). Then by the orthogonality of $\underline{\phi}_\alpha$ and $\underline{\psi}^\alpha$, we have

$$\underline{b} \cdot \underline{\psi}(t) = c_1 e^{\frac{-at}{2}} \sin\left[\sqrt{4c - a^2}\, t + c_2\right] \quad \text{(I-7)}$$

since $\sqrt{a^2 - 4c}$ is purely imaginary. The constants c_1 and c_2 are determined by the boundary conditions (I-2), so that the required control $u(t)$ is given by (12):

$$\boxed{u(t) = \text{sign}\left[c_1 e^{\frac{-at}{2}} \sin\left(\sqrt{4c - a^2}\, t + c_2\right)\right].} \quad \text{(I-8)}$$

R. E. Kopp (Optimization Techniques, edited by G. Leitmann, Academic Press 1962, p. 275) also obtains this result in a slightly different manner by instead considering the Hamiltonian of the system (Pontryagin shows that these two approaches are entirely equivalent, p. 14 of his paper). Kopp plots the "switching sequence" in the

"phase plane" ($\dot{x}_1$ vs. x_1):

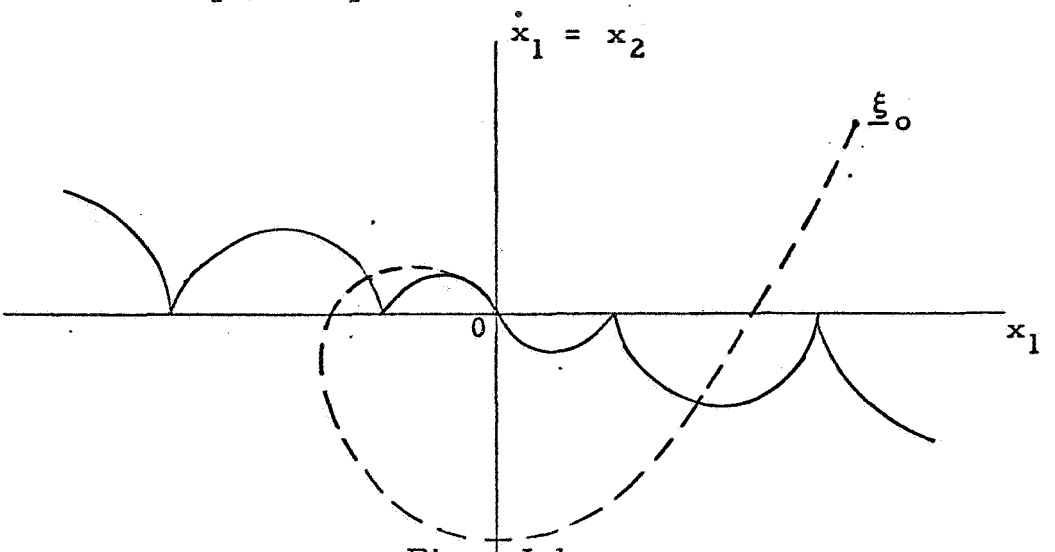

Figure I-1

A typical trajectory from $\underline{\xi}_o$ to the origin is shown in Figure I-1; we note that the optimal trajectory from $\underline{\xi}_o$ must approach the origin along the switching boundary shown in the figure (since it is the only trajectory passing through the "equilibrium point" 0). Finally, we see that the control function u(t) "switches" whenever the trajectory from $\underline{\xi}_o$ crosses the switching boundary, as noted in Kopp's paper.

APPENDIX II

SOLUTION OF LINEAR HOMOGENEOUS DIFFERENTIAL SYSTEMS

To solve

$$\dot{\underline{x}} = A\underline{x} + \underline{b}_1 u_1(t) + \cdots + \underline{b}_r u_r(t), \tag{II-1}$$

where $x = \begin{pmatrix} x_1 \\ x_2 \\ \vdots \\ x_n \end{pmatrix}$, $A = \left\{ a_{ij} \right\}$, $\underline{b}_i = \begin{pmatrix} b_i^1 \\ b_i^2 \\ \vdots \\ b_i^n \end{pmatrix}$

and $\underline{x}(0) = \underline{x}_o$; $\dot{\underline{x}}(0) = \dot{\underline{x}}_o$:

consider first the linear homogeneous system with constant coefficients a_{ij}:

$$\dot{\underline{x}} = A\underline{x} \tag{II-2}$$

By a <u>fundamental matrix</u> for (II-2), call it $\Phi(t)$, we mean an nxn matrix whose columns are linearly independent solutions of (II-2). In this case (a_{ij} <u>constant</u>), the fundamental matrix is simply

$$\Phi(t) = e^{At}, \tag{II-3}$$

since $e^{(t+\Delta t)A} = e^{tA} e^{\Delta tA}$ implies that $\frac{d}{dt} e^{At} = A e^{At}$ making e^{At} a solution of (II-2). Then $\Phi(0) = I$ (the identity matrix) implies that $\det \Phi(t) = e^{t(\mathrm{Tr}\, A)}$, where $\mathrm{Tr}\, A$ is the trace of A

$(\mathrm{Tr}\,A = \sum_{i=1}^{n} a_{ii})$, so that $\Phi(t)$ is indeed a fundamental matrix for (II-2).[1]

The solution of (II-2) with $\underline{x}(0) = \underline{x}_o$ is then

$$\underline{x}(t) = \underline{x}(0)\, e^{At} = \underline{x}(0)\, \Phi(t) \,. \tag{II-4}$$

With Φ the fundamental matrix for (II-2), we observe that $\frac{d}{dt}(\Phi^{-1})$

$$= -\Phi^{-1} \frac{d\Phi}{dt} \cdot \Phi^{-1} = -\Phi^{-1} A$$

or, taking the complex conjugate transpose (denoted by *)

$$\frac{d}{dt}\, \Phi^{*\,-1} = -A^*\, \Phi^{*\,-1}.$$

Comparing this with (II-2), we conclude that $\Phi^{*\,-1}$ is a fundamental matrix for the system

$$\dot{\underline{x}} = -A^* \underline{x} \,. \tag{II-5}$$

Since A is generally real, $A^* = A^T$ (T denotes transposition) for physical applications. (II-5) is called the adjoint to (II-2).

We can now show that it suffices to obtain Ψ from the relation

$$\underline{\phi}_i(t) \cdot \underline{\psi}^j(t) = \delta_i^{\,j} \,, \tag{II-6}$$

[1] See also: Coddington and Levinson Theory of Ordinary Differential Equations (1955) pps 67 - 78)

where $\underline{\phi}_i(t)$ is the "i^{th}" column of Φ and $\underline{\psi}^j(t)$ the "j^{th}" row of Ψ. For we have that

$$\frac{d}{dt}\left(\underline{\phi}_\alpha(t)\cdot\underline{\psi}^i(t)\right) = \dot{\underline{\phi}}_\alpha\cdot\psi^i + \underline{\phi}_\alpha\cdot\dot{\psi}^i$$

$$= A\,\underline{\phi}_\alpha\cdot\underline{\psi}^i + \underline{\phi}_\alpha\cdot\dot{\underline{\psi}}^i$$

$$= \underline{\phi}_\alpha\cdot A^T\underline{\psi}^i + \underline{\phi}_\alpha\cdot\dot{\underline{\psi}}^i$$

$$= \underline{\phi}_\alpha\cdot\left(A^T\underline{\psi}^i + \dot{\psi}^i\right) \equiv 0 \quad \text{by (II-5).}$$

Hence $\underline{\phi}_\alpha(t)\cdot\underline{\psi}^i(t) \equiv$ constant; we lose no generality in normalizing this to the Kronecker delta δ_α^i. A physical example of this process is given in Appendix I.

It is now a straightforward matter to verify by direct substitution that the solution of (II-1) satisfying the indicated initial conditions is

$$\underline{x}(t) = \sum_{\alpha=1}^{n}\underline{\phi}_\alpha(t)\left[x_o^\alpha + \int_o^t \underline{\psi}^\alpha\cdot\left(\underline{b}_1 u^1 + \cdots + \underline{b}_r u^r\right) d\,r\right]. \qquad \text{(II-7)}$$

APOLLO NOTE NO. 77

J. Holdsworth
19 June 1963

CALCULATION OF COVARIANCE MATRICES FOR MULTIPLE UNCORRELATED DATA SOURCES

The purpose of this note is to extend the methods developed in Apollo Notes Nos. 3 and 43 to the case where multiple data inputs are available. The previous notes have covered the case where only one form of data, such as range rate from Doppler measurements, was available. The present note will extend these procedures to the case where range, range rate, and angular data are all available. In the subsequent analysis we shall assume that there is no autocorrelation in any of the three data inputs and that the different types of data are not cross correlated.

As before we shall assume that there are certain parameters a_i, $i = 1, \cdots 6$, which we wish to estimate on the basis of our observed data. We shall also assume that we have available range, range rate, and angular data which we shall denote by $R, \dot{R}$ and θ respectively and that $R, \dot{R}$ and θ may be written as invertible functions of the parameters of interest a_i.

If our measurements could be made with complete accuracy then any six observations would theoretically suffice to allow us to determine the parameters in question. However, the measured data is corrupted by random noise hence we must use our data to obtain estimators $\hat{a}_i$ of the orbit parameters a_i. In reality we are more interested in this note in obtaining an expression for the accuracy or asymptotic accuracy with which the parameters can be estimated rather than the computation of the estimators from the observed data.

As in Apollo Notes Nos. 3 and 43 we assume that we may write the following expressions:

$$R_m = R_c(a_i, t) + n_R(t)$$

$$\dot{R}_m = \dot{R}_c(a_i, t) + n_{\dot{R}}(t) \qquad (1)$$

$$\theta_m = \theta_c(a_i, t) + n_\theta(t)$$

In equations (1) the quantities subscripted m are the measured quantities, the quantities subscripted c refer to the correct functional values if the data were not contaminated by noise and $n_R(t)$, $n_{\dot{R}}(t)$, $n_\theta(t)$ indicates the additive random noise.

As mentioned before we shall assume that the noise processes $n_R(t)$, $n_{\dot{R}}(t)$ and $n_\theta(t)$ are independent, i. e. not cross correlated, zero mean stationary white gaussian processes with variances σ_R^2, $\sigma_{\dot{R}}^2$ and σ_θ^2, respectively. From equation (1) we see that if we have N observations on R, $\dot{R}$ and θ that we may write the following expression for the likelihood function of the data.

$$L = \frac{1}{(2\pi)^{3/2}\sigma_R^N \sigma_{\dot{R}}^N \sigma_\theta^N} \exp -\mathcal{L} \qquad (2)$$

where:

$$\mathcal{L} = \frac{1}{2\sigma_R^2} \sum_{k=1}^{N} \left[R_m(k) - R_c(a_i, k) \right]^2$$

$$+ \frac{1}{2\sigma_{\dot{R}}^2} \sum_{k=1}^{N} \left[\dot{R}_m(k) - \dot{R}_c(a_i, k) \right]^2$$

$$+ \frac{1}{2\sigma_\theta^2} \sum_{k=1}^{N} \left[\theta_m(k) - \theta_c(a_i, k) \right]^2 \qquad (3)$$

As before the maximum likelihood estimators a_i of the parameters a_i are those functions of the data which make the data most probable or maximize the value of the likelihood function. They are obtained by solving the equations

$$\frac{\partial \mathcal{L}}{\partial a_i} = 0 \qquad i = 1, \cdots 6 \tag{4}$$

for the parameters a_i as functions of the observed data R_m, $\dot{R}_m$ and θ_m.

Performing the indicated differentiations and substituting into equation (4) we obtain:

$$\frac{1}{\sigma_R^2} \sum_{k=1}^{N} \left[R_c(a_i, k) - R_m(k) \right] \frac{\partial R_c}{\partial a_i} + \frac{1}{\sigma_{\dot{R}}^2} \sum_{k=1}^{N} \left[\dot{R}_c(a_i, k) - \dot{R}_m(k) \right] \frac{\partial \dot{R}_c}{\partial a_i}$$

$$+ \frac{1}{\sigma_R^2} \sum_{k=1}^{N} \left[\theta_c(a_i, k) - \theta_m(k) \right] \frac{\partial \theta_c}{\partial a_i} = 0 \qquad \text{for } i = 1, \cdots 6 \tag{5}$$

Now the functional forms R_c, $\dot{R}_c$, θ_c are assumed known, as are the observed data points $R_m(k)$, $\dot{R}_m(k)$, $\theta_m(k)$, thus equation (5) is actually a system of 6 equations in the a_i which may be solved as a function of the known data. The solutions $\hat{a}_i$ of this system of equations in terms of the observed data are the maximum likelihood estimators of the orbital parameters a_i.

Now as we have done in the previous notes we shall assume that the smoothing time or number of samples N is sufficiently large so that the following expressions may be written for the maximum likelihood estimators:

$$\hat{a}_i = a_i + \Delta a_i \tag{6}$$

where the Δa_i are sufficiently small so that only first order terms in these random perturbations need be retained in various series expansions. This assumption is always valid for sufficiently large sample sizes and is exactly true whenever the dependence of the functions f_c on the a_i parameters is linear.

Utilizing the above assumptions we may write the following approximate expressions.

$$R_c(\hat{a}_i, k) = R_c(a_i, k) + \sum_{i=1}^{6} \frac{\partial R_c}{\partial a_i}(a_i, k)\Delta a_i$$

$$\dot{R}_c(\hat{a}_i, k) = \dot{R}_c(a_i, k) + \sum_{i=1}^{6} \frac{\partial \dot{R}_c}{\partial a_i}(a_i, k)\Delta a_i \qquad (7)$$

$$\theta_c(\hat{a}_i, k) = \theta_c(a_i, k) + \sum_{i=1}^{6} \frac{\partial \theta}{\partial a_i}(a_i, k)\ \Delta a_i$$

$$\frac{\partial R_c}{\partial a_i}(\hat{a}_i, k) \approx \frac{\partial R_c}{\partial a_i}(a_i, k)\ ,\quad \frac{\partial \dot{R}_c}{\partial a_i}(\hat{a}_i, k) = \frac{\partial \dot{R}_c}{\partial a_i}(a_i, k), \frac{\partial \theta}{\partial a_i}(\hat{a}_i, k) = \frac{\partial \theta}{\partial a_i}(a_i, k)$$

Substituting equation (7) into equation (5) and performing some routine algebra yields the following system of equations which is linear in the random perturbation quantities Δa_i.

$$\sum_{j=1}^{6}\left\{\sum_{k=1}^{N}\left(\frac{1}{\sigma_R^2}\frac{\partial R_c}{\partial a_i}(k)\frac{\partial R_c}{\partial a_j}(k) + \frac{1}{\sigma_{\dot{R}}^2}\frac{\partial \dot{R}_c}{\partial a_i}(k)\frac{\partial \dot{R}_c}{\partial a_j}(k) + \frac{1}{\sigma_\theta^2}\frac{\partial \theta_c}{\partial a_i}(k)\frac{\partial \theta_c}{\partial a_j}(k)\right)\right\}\Delta a_j$$

$$= \sum_{k=1}^{N} \left[\frac{1}{\sigma_R^2} \frac{\partial R_c}{\partial a_i}(k) \left(R_m(k) - R_c(k) \right) + \frac{1}{\sigma_{\dot{R}}^2} \frac{\partial \dot{R}_c}{\partial a_i}(k) \left(\dot{R}_m(k) - R_c(k) \right) \right.$$

$$\left. + \frac{1}{\sigma_\theta^2} \frac{\partial \theta_c}{\partial a_i}(k) \left(\theta_m(k) - \theta_c(k) \right) \right] \qquad \text{for } i = 1, 2, \cdots 6 \qquad (8)$$

In equation (8) it is perhaps worth mentioning that $R_c(k)$, $\dot{R}_c(k)$, $\theta_c(k)$ refer to the nominal value of these quantities at the time of the k^{th} observation, while $R_m(k)$, $\dot{R}_m(k)$, $\theta_m(k)$ refer to the observed data obtained from the k^{th} observation.

Again if we define the estimator error vector Δa by the column matrix

$$\Delta a = \begin{pmatrix} \Delta a_1 \\ \Delta a_2 \\ \Delta a_3 \\ \Delta a_4 \\ \Delta a_5 \\ \Delta a_6 \end{pmatrix} \qquad (9)$$

then using matrix notation we may write the following vector equation:

$$C \Delta a = e. \qquad (10)$$

In equation (10) C is a 6 x 6 matrix whose i, j^{th} element is given by:

$$C_{ij} = \sum_{k=1}^{N} \left[\frac{1}{\sigma_R^2} \frac{\partial R_c}{\partial a_i}(k) \frac{\partial R_c}{\partial a_j}(k) + \frac{1}{\sigma_{\dot{R}}^2} \frac{\partial \dot{R}_c}{\partial a_i}(k) \frac{\partial \dot{R}_c}{\partial a_j}(k) + \frac{1}{\sigma_\theta^2} \frac{\partial \theta_c}{\partial a_i}(k) \frac{\partial \theta_c}{\partial a_j}(k) \right] \qquad (11)$$

Similarly e is a column vector whose i^{th} component is given by:

$$e_i = \sum_{k=1}^{N} \left[\frac{1}{\sigma_R^2} \frac{\partial R_c}{\partial a_i}(k) \left(R_m(k) - R_c(k)\right) + \frac{1}{\sigma_{\dot{R}}^2} \frac{\partial \dot{R}_c}{\partial a_i}(k) \left(\dot{R}_m(k) - \dot{R}_c(k)\right) \right.$$

$$\left. + \frac{1}{\sigma_\theta^2} \frac{\partial \theta_c}{\partial a_i}(k) \left(\theta_m(k) - \theta_c(k)\right) \right]$$

$$\text{for } i = 1, 2, \cdots 6 \tag{12}$$

Now, if the joint distribution of the parametric estimators is non-singular; i. e., if the total probability mass of the estimator distribution does not lie in some subspace of dimension 5 or lower, then equation (10) may be formally solved to yield:

$$\Delta a = C^{-1} e \tag{13}$$

Taking the transpose of both sides of equation (13) and noting that $C_{ij} = C_{ji}$, we obtain:

$$\Delta a^T = e^T C^{-1} \tag{14}$$

Equations (13) and (14) are vector equations. Multiplication of (13) on the right by equation (14) yields the matrix equation

$$\Delta a \, \Delta a^T = C^{-1} e \, e^T C^{-1} \tag{15}$$

Equation (15) is a matrix rather than a vector equation, i. e., the quantities on both sides of equation (15) are 6 x 6 matrices. Moreover, the elements of these matrices are random so that in similar observations over the same smoothing interval we would expect a random variation in the elements.

Since we have assumed large smoothing times the estimators $\hat{a}_i$ of the parameters a_i may be assumed to be unbiased, i. e.

$$E\,\hat{a}_i = a_i \tag{16}$$

or equivalently

$$E\Delta a_i = 0 \tag{17}$$

- a fact which is always asymptotically true for maximum likelihood estimators.

Since the estimators are unbiased the covariance matrix of the estimator errors is obtained by taking the expected value of both sides of equation (15) with respect to the joint distribution of the noise processes. Thus, we may write:

$$\mathrm{Cov}\,(\hat{a}_i,\ \hat{a}_j) = E\left[\,\Delta a\ \Delta a\ T\right] \;= C^{-1}\,E(e\ e^T)\,C^{-1} \tag{18}$$

where E denotes the expected value operator.

Since the matrix C is known and assumed non singular, it follows from equation (18) that we have an expression for our desired covariance matrix once we have computed

$$E\,(e\ e^T) \tag{19}$$

The element in the i, j^{th} position of the matrix $e\,e^T$ is simply $e_i e_j$, where the expression for e_i and e_j is given by equation (12). However, comparison with equation (1) shows that we may write:

$$e_i = \sum_{k=1}^{N}\left[\frac{1}{\sigma_R^2}\frac{\partial R_c}{\partial a_i}(k)\ n_R(k) + \frac{1}{\sigma_{\dot{R}}^2}\frac{\partial \dot{R}_c}{\partial a_i}(k)\ n_{\dot{R}}(k) + \frac{1}{\sigma_\theta^2}\frac{\partial \theta}{\partial a_i}(k)\ n_\theta(k)\right] \tag{20}$$

Now a term on the main diagonal of $e\,e^T$ is of the form e_i^2 where e_i is given by equation (20). Since $n_R(k)$, $n_{\dot{R}}(k)$, $n_\theta(k)$ were assumed to be independent zero mean stationary gaussian random processes then we have the following expressions:

$$E\left[n_R(k)\, n_R(\ell)\right] = \delta_{k\ell}\,\sigma_R^2$$

$$E\left[n_{\dot{R}}(k)\, n_{\dot{R}}(\ell)\right] = \delta_{k\ell}\,\sigma_{\dot{R}}^2 \qquad (21)$$

$$E\left[n_\theta(k)\, n_\theta(\ell)\right] = \delta_{k\ell}\,\sigma_\theta^2$$

and

$$E\left[n_R(k)\, n_{\dot{R}}(\ell)\right] = 0 = E\left[n_R(k)\, n_\theta(\ell)\right] = E\left[n_{\dot{R}}(k)\, n_\theta(\ell)\right]$$

for all k and ℓ, where $\delta_{k\ell}$ is the Kronecker delta function.

Using equations (20) and (21) we see that a main diagonal term of the matrix $E\left[e\,e^T\right]$ is given by:

$$E\,e_{ii} = E\,e_i^2 = \sum_{k=1}^{N}\left[\left(\frac{\partial R_c(k)}{\partial a_i}\right)^2\frac{1}{\sigma_R^2} + \left(\frac{\partial \dot{R}_c(k)}{\partial a_i}\right)^2\frac{1}{\sigma_{\dot{R}}^2} + \left(\frac{\partial \theta(k)}{\partial a_i}\right)^2\frac{1}{\sigma_\theta^2}\right] \qquad (22)$$

for $i = 1, 2, \cdots 6$. Thus, we have an expression for the diagonal elements of $E\left[e\,e^T\right]$.

Now consider an off diagonal element $E\left[e_i\, e_j\right]$ where $i \neq j$. Then again from equations (20) and (21) we may write:

$$E\left[e_{ij}\right] = E\left[e_i\, e_j\right] = \sum_{k=1}^{N}\left[\frac{1}{\sigma_R^2}\,\frac{\partial R_c(k)}{\partial a_i}\,\frac{\partial R_c(k)}{\partial a_j} + \frac{1}{\sigma_{\dot{R}}^2}\,\frac{\partial \dot{R}_c(k)}{\partial a_i}\,\frac{\partial \dot{R}_c(k)}{\partial a_j} + \frac{1}{\sigma_\theta^2}\,\frac{\partial \theta_c(k)}{\partial a_i}\,\frac{\partial \theta_c(k)}{\partial a_j}\right] \qquad (23)$$

Now from equations (22) and (23) we may explicitly calculate the elements of the matrix $E\left[e\, e^T \right]$. Also since the elements of the matrix C are known then C^{-1} is known also which gives us our desired covariance matrix by substitution into equation (18).

However, comparison of the defining equations for the elements of the matrices C and $E\left[e\, e^T \right]$ - i. e., equations (11), (22) and (23) - reveal the interesting fact that

$$E\left[e\, e^T \right] = C. \tag{24}$$

Thus equation (24) allows us to write the following expression for the covariance matrix of the errors in the estimators of the orbital parameters.

$$\text{Cov}\left(\hat{a}_i, \hat{a}_j\right) = C^{-1} \tag{25}$$

CONCLUSION

In this note it will be noticed that there was no systematic bias error assumed in any of the three data inputs. In reality there is reason to suspect that there may be a non-negligible systematic bias error in the range and angle data. The extension of this analysis to cover that situation is straightforward and is more of a notational nuisance than a conceptual difficulty. The interested reader should be able to make the necessary amendments by using the analysis in either Notes 43 or 3 as a guide.

A more serious shortcoming of this note is that using the JPL measuring procedure the range and the range rate data are very strongly cross correlated. As other data collection schemes are under consideration which would probably tend to reduce this cross correlation, it is hoped that the results obtained in this note may be of use in some cases of genuine physical interest.

Since the cross correlation of the data inputs does not unduly encumber the necessary mathematics as long as the individual error

processes may be assumed to be white or uncorrelated, another note will appear shortly extending the current results to the case where appreciable cross correlation exists between the data inputs.

APOLLO NOTE NO. 78

H. Engel
20 June 1963

DSIF DETERMINATION OF LEM ALTITUDE RATE

In an abort situation in which the LEM takes off with a minimum amount of equipment functioning it is important to control the vertical velocity at cut-off. This note examines the ability of the DSIF to provide this information.

The present LEM landing site is 2° 40'N 3° 40'E. The downrange distance to burnout is about 106 km in the westerly direction, so at burnout the LEM is at about 2° 40'N 0°E.

The physical libration of the Moon is about $\pm$ 0.02° in latitude and $\pm$ 0.04° is longitude. The corresponding optical librations are $\pm$ 7.6° and $\pm$ 6.7°.

The Earth subtends a half angle of about 1.5°.

The observed Doppler velocity, omitting the DSIF velocity, is:

$$\dot{D} \stackrel{\circ}{=} v_T \theta - v_r$$

where θ is the angle between the line joining the center of the Moon and the LEM; and the line-of-sight, v_T is the component of velocity tangent to the Moon and v_r is the component of velocity normal to the Moon. The error in $\dot{D}$ is:

$$E(\dot{D}) \stackrel{\circ}{=} v_T E(\theta) + \theta E(v_T) - E(v_r)$$

or

$$E(v_r) = v_T E(\theta) + \theta E(v_T) - E(\dot{D})$$

Now, in the worst possible situation $\theta = 9.1^\circ$ (=7.6° + 1.5°) and the error in θ is approximately

$$E(\theta) = \frac{1}{r} \times \text{Error in downrange distance}$$

$$= \frac{1}{r} E(\lambda)$$

so at burnout at 8 n. m. altitude

$$E(v_r) = 1700 \frac{E(\chi)}{1752 \times 10^3} + \frac{9.1}{57.3} E(v_T) - E(\dot{D})$$

For 10 second smoothing $\sigma(\dot{D})$ is about 4 cm/sec., and $E(\dot{D})$ is negligible. Assume that $E(\chi)$ is 5% of the downrange distance and $E(v_T)$ is 5% of circular velocity, then

$$\dot{E}(v_r) = \left[1700 \frac{106 \times 10^3}{1752 \times 10^3} + \frac{9.1}{57.3} 1700 \right] (0.05) \text{ m/sec.}$$

$$= 5.15 + 13.5 \text{ m/sec.}$$

$$= 18.7 \text{ m/sec.}$$

With a circular speed at 8 n. m. altitude, a vertical velocity error of 34.3 m/sec. is needed to cause impact with the Moon, so it appears that the DSIF can be of use in LEM aborts to assure a safe trajectory.

Table 1 (Errors in r_p, ψ, and e)

Nominal Values

$r_p = 1.75653 \times 10^6$ meters

$\psi = 30^o$

$e = .086718$

$\sigma_{\dot{R}} = .02$ meters/sec (1 minute of smoothing)

RMS Error \ Observation Interval	90^o Sample Points $\theta_1 = 15^o$, $\theta_2 = -30^o$, $\theta_3 = -75^o$
σ_{r_p}	46 meters
σ_ψ	1.25×10^{-5} radians
σ_e	2.7×10^{-5}
$\rho_{r_p - \psi}$	.065
$\rho_{r_p - e}$	.45
$\rho_{\psi - e}$	-.070

Table 2 (Errors in r_p, ψ, and θ)

Nominal Values

$r_p = 1.75653 \times 10^6$ meters

$\psi = 30^o$

$e = .086718$

$\dot{\sigma}_R = .02$ meters/sec (1 minute of smoothing)

Observation Interval / RMS Error	90^o Sample Points $\theta_1 = 15^o$, $\theta_2 = -30^o$, $\theta_3 = -75^o$	30^o Sample Points $\theta_1 = -30^o$, $\theta_2 = -45^o$, $\theta_3 = -60^o$
σ_{r_p}	76 meters	1520 meters
σ_ψ	1.8×10^{-2} radians	6.1×10^{-3} radians
σ_θ	1.8×10^{-4} radians	6.2×10^{-3} radians
$\rho_{r_p-\psi}$	.850	.9996
$\rho_{r_p-\theta}$	-.837	-.9995
$\rho_{\psi-\theta}$	-.998	-.9999

APOLLO NOTE NO. 79

C. H. Dale
26 June 1963

AN APPROACH TO ESTIMATING THE ALLOWABLE INJECTION ERRORS FOR THE DSIF AIDED LEM ASCENT AND RENDEZVOUS

The purpose of this note is to show a single technique for using the DSIF in a reasonably short ascent and rendezvous mission under abort assumptions. The technique is evaluated in one way to show that a maximum of 100 feet per second (2%) error may be allowed in the LEM ascent boost without exceeding the 10% fuel pad.

The basic abort trajectory is shown in Figure 1. The nominal path of the LEM is shown under the assumption of no errors.

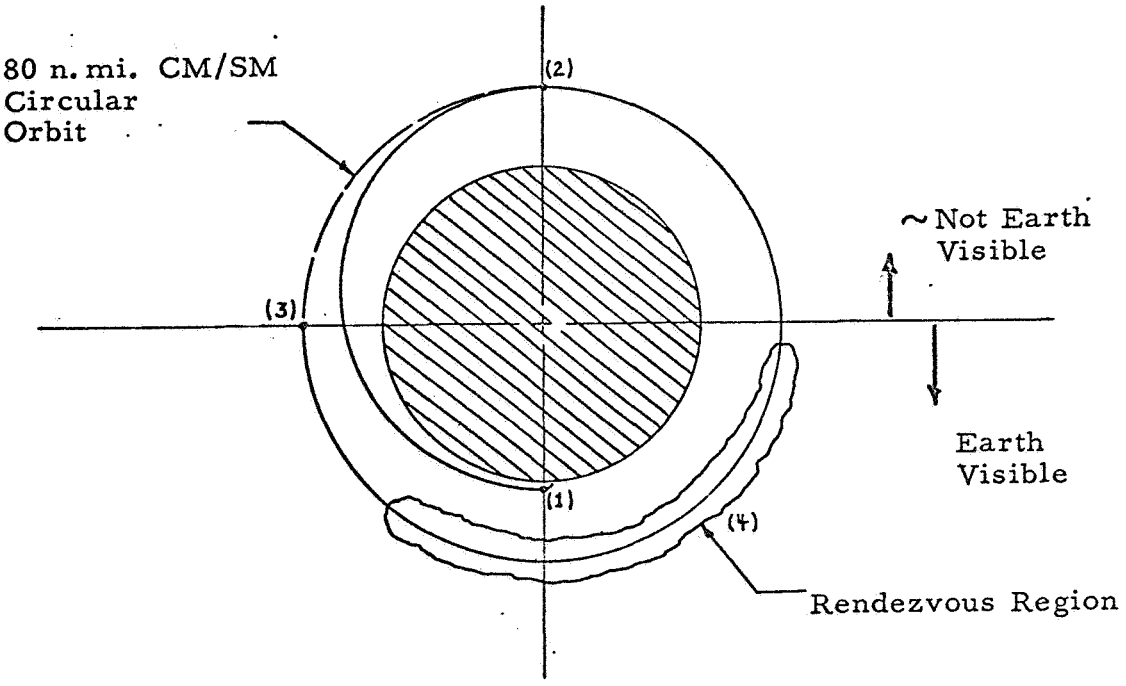

Figure 1. Nominal Abort Trajectory

At point (1), the nominal abort ascent would place the LEM into a Hohmann transfer with perilune 8 miles off the lunar surface.

Since a perilune burnout (5586 ft/sec) is roughly in the center of the Moon, as viewed from the Earth, this would allow about a half hour of DSIF tracking before the LEM disappears behind the Moon. The launch time is designed to place the CM/SM and LEM together at apolune (2). A horizontal injection boost of 97.0 ft/sec. will co-orbit the nominal LEM at (2) with the CM/SM. Even if the CM/SM is nowhere in sight at (2), it is planned to add the horizontal 97 ft/sec. This nominally places the two crafts in synchronism. When the LEM again enters into view, it can be tracked for an additional hour or so until it reaches point (3). At about this time the DSIF should have a good idea of the LEM position and velocity. The errors in the boost at (2) should surely be less than 2 ft/sec., based upon star-oriented thrusting with 1% accelerometers used for cut-off. A boost at (3) can thus be computed (to within 2 ft/sec., DSIF willing) which will bring the two crafts into coincidence in the region (4); docking thus being Earth visible.

This nominally Hohmann transfer is about a percent more efficient than the planned upon 160° ascent (See Apollo Note No. 75). The questions are thus: How much error may be stood at perilune? How large a set of corrective impulses (3) and (4) must be used to make up that error.

Given the actual magnitude of the velocity at ascent engine cut-off, V_1, and the radius of cut-off, r_p, then the semi-major axis of the transfer ellipse, a_1, is:

$$a_1 = \frac{1}{\frac{2}{r_1} - \frac{V_1^2}{\mu}} \qquad (1)$$

The eccentricity for the lowest allowable safe orbit is:

$$e_1 = 1 - \frac{\text{Lunar Radius}}{a_1} \qquad (2)$$

The angular momentum of the transfer ellipse is:

$$h_1 = \sqrt{\mu a_1 (1-e_1^2)} \tag{3}$$

from which the initial flight path angle, β_1, may be defined

$$\sin^2 \beta_1 = \frac{h_1}{\left(V_1 a (1+e)\right)^2} \tag{4}$$

Now the error in the vertical velocity can be defined

$$\Delta R = \frac{dR}{dt}\Big|_1 = V_1 \cos \beta_1 \tag{5}$$

This error is plotted as a function of the error in the magnitude of the perilune velocity in Figure 2.

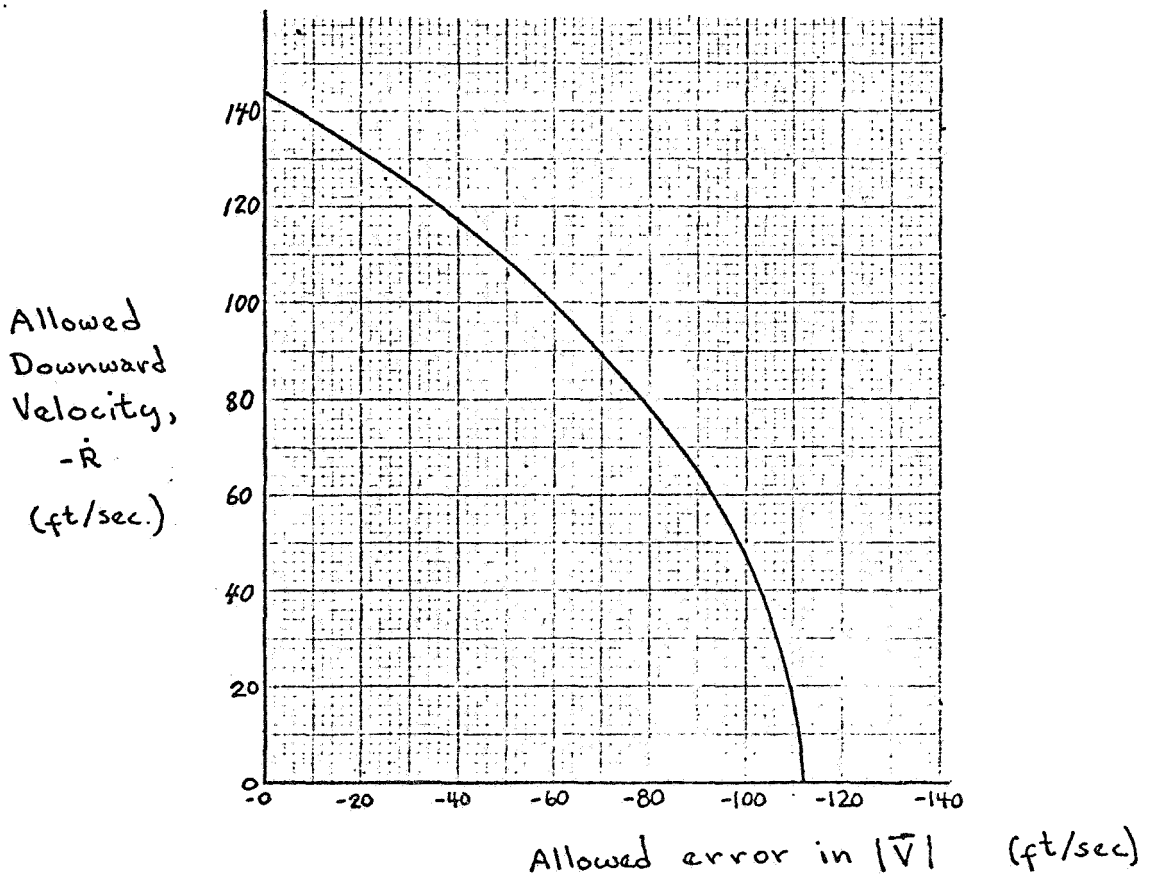

Figure 2 Allowable Ascent Cut-Off Errors to Avoid Lunar Collision

Thus any error less than that shown in Figure 2 will not hit the Moon during a full orbit. The object of the remainder of this note is to calculate the boost required at (3) and (4) for any error such as that shown in Figure 2.

As an example, assume that a horizontal decrement of 100 ft/sec. existed at (1). This would place the LEM in an exactly circular orbit of 8 n.mi. altitude instead of the planned upon Hohmann transfer. Now at point (2) of Figure 1, the LEM is 72 miles below the CM/SM orbit. Since the timing was planned such that the CM/SM and LEM would reach point (2) coincidentally, a phase-lag will exist due to the error at (1). This phase-lag will be due to the difference between the semi-periods of the expected Hohmann transfer and the actual circular orbit at 8 n.mi. altitude. This places the LEM about 170.8 seconds in front of the CM/SM.

Now assuming no other sensors, the LEM would apply a 97.0 ft/sec. horizontal boost at point (2). This boost should not be in error by more than the two percent corresponding to the 100 ft/sec. error at point (1). This can be considered insignificant. The new orbit after the boost at point (2) will have a semi-major axis:

$$a_2 = \frac{1}{\frac{2}{r_1} - \frac{V_2^2}{\mu}} = 5.96407 \times 10^6 \text{ ft.} \qquad (6)$$

This will place the LEM at a new radius at point (3). This radius will coincide with the semi-minor axis of the new orbit.

$$b_2 = \sqrt{r_1 (2a - r_1)} = 5.96027 \times 10^6 \text{ ft.} \qquad (7)$$

which is 42.41 n.mi. off the lunar surface. The eccentricity of this orbit is:

$$e_2 = 1 - \left(\frac{b_2}{a_2}\right)^2 = .03577 \qquad (8)$$

The time between perilune at (2) and point (3) is given by:

$$t_3\ (\text{LEM}) - t_2\ (\text{LEM}) = \sqrt{\frac{(a_2)^3}{\mu}}\ \left[E - e \sin E\right] \tag{9}$$

$$= \sqrt{\frac{(a_2)^3}{\mu}}\ \left[\frac{3\pi}{2} + e_2\right] = 5256.5 \text{ sec.}$$

While the time required for the CM/SM to travel 3/4 of an orbit is 5514.9 sec., thus at point (3), the LEM is leading the CM/SM by:

$$\Delta t = 5514.9 - 5256.5 + 179.8 = 438.2 \text{ seconds.}$$

Since the DSIF has tracked the LEM for all this time, it is assumed to know its position and velocity at point (3),

$$V_3 = \sqrt{\frac{2\mu}{b_2} - \frac{\mu}{a_2}} = 5390.71 \tag{10}$$

The horizontal component of velocity at point (3) is:

$$V_{h_3} = \frac{V_2\, r_1}{b_2} = 5387.29 \text{ ft/sec.} \tag{11}$$

from which the flight path angle is:

$$\cos \beta_3 = \frac{V_{h_3}}{V_3} \Rightarrow \sin \beta_3 = .03577 \tag{12}$$

giving the vertical component

$$V_{v_3} = V_3 \sin \beta = -192.83 \text{ ft/sec.} \tag{13}$$

The commanded boost at point (3) should now place the LEM in an orbit which will reach the circular CM/SM orbit in the region of (4) of Figure 1 at the same time that the CM/SM reaches that same point. One way of doing this is to make point (3) a perilune point of the transfer ellipse. If the 192.83 ft/sec. vertical velocity is removed and the speed increased by 175.29 ft/sec., then the perilune velocity of the transfer ellipse would be 5566 ft/sec. This would just allow coincidence. The required boost to inject at (4) is 327.3 ft/sec. The total boost required would be:

$$V_1 = 5586$$

$$V_2 = 97$$

$$V_3 = 260.6$$

$$V_4 = 327.3$$

$$V_{tot} = 6271.$$

This is almost exactly 10% larger than the nominal 5705 ft/sec., calculated in Apollo Note No. 75. It would thus seem that this technique can cope with errors less than 100 ft/sec., although this example only treated an error in the horizontal direction. Figure 3 is a recapitulation of this example trajectory.

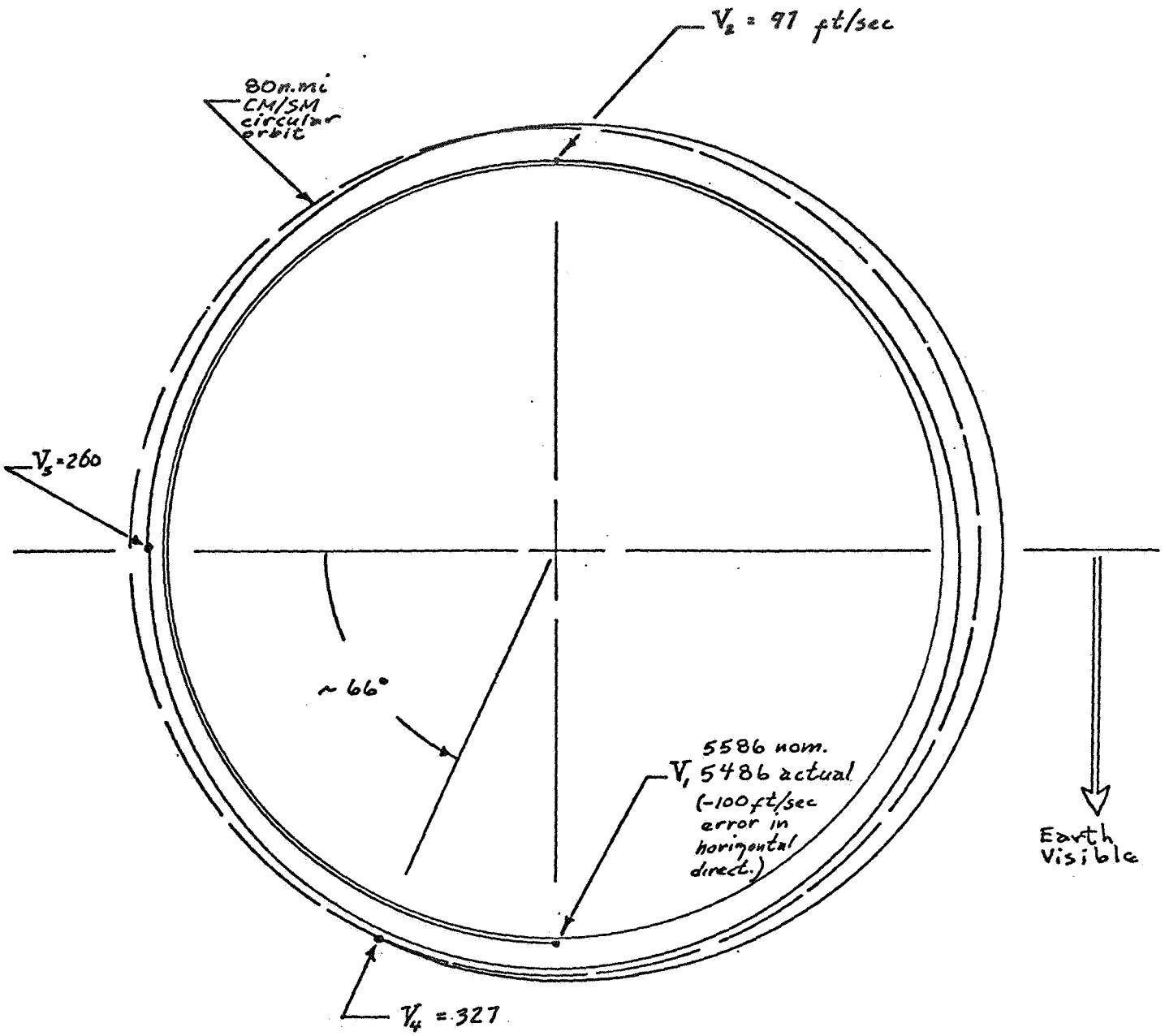

Figure 3 Example Trajectory with Negative 100 ft/sec Initial Ascent Error

APOLLO NOTE NO. 80

J. Holdsworth
15 July 1963

CORRECTION TO CALCULATION OF COVARIANCE MATRICES I

The purpose of this note is to correct an error in Apollo Note No. 67.

In Apollo Note No. 67 the analysis was performed as though the polar angle θ did not depend upon the orbital parameters whose values were to be estimated from the Doppler data. This is not so, however, because of the relationship between the time from perilune and the mean anomaly which appears on Page 2 of Apollo Note No. 67.

In the present note the same orbit parameters will be used as in Apollo Note No. 67 with the exception that instead of considering the energy E we shall employ the semi-major axis, a, of the elliptical trajectory. Thus, the parameters to be estimated are: λ, β, e, θ_o, a, where λ is the angle between moon perilune and the earth moon lines, and β is an angle measuring the rotation of the orbital plane about a line in the earth moon plane which is normal to the earth moon line. The quantities e, θ_o and a are the eccentricity, initial value of the polar angle from perilune and semi-major axis of the vehicle trajectory respectively.

If we assume that the earth and the moon are infinitely distant, then all line-of-sight vectors from the earth to the vehicle are parallel and we may write the following expression for the observed doppler:

$$\dot{R} = \left[- r \dot{\theta} \sin (\theta + \lambda) + \dot{r} \cos (\theta + \lambda) \right] \cos \beta \qquad (1)$$

If the polar angle θ is measured from perilune, we have:

$$r = \frac{a (1 - e^2)}{1 + e \cos \theta} \qquad (2)$$

In addition to the relations (1) and (2), we have the following relationship which implicitly defines the polar angle θ as a function of the parameters a, e, and θ_o.

$$t = \frac{a^{3/2}}{\sqrt{u}} \left[(\zeta - e \sin \zeta) - (\zeta_o - e \sin \zeta_o) \right] \tag{3}$$

In (3), t is the total time, u is the lunar gravitational constant and ζ and ζ_o are the eccentric anomalies at times t and zero respectively. The quantities ζ and ζ_o are given as functions of θ, e and θ_o by the following equations:

$$\begin{aligned} \cos \zeta &= \frac{e + \cos \theta}{1 + e \cos \theta}, \quad \cos \zeta_o = \frac{e + \cos \theta_o}{1 + e \cos \theta_o} \\ \sin \zeta &= \frac{\sqrt{1 - e^2} \sin \theta}{1 + e \cos \theta}, \quad \sin \zeta_o = \frac{\sqrt{1 - e^2} \sin \theta_o}{1 + e \cos \theta_o} \end{aligned} \tag{4}$$

thus, Equations (3) and (4) do implicitly define the polar angle θ as a function of the parameters and time, e. g.,

$$\theta = \theta (a, e, \theta_o, t). \tag{5}$$

To compute the covariance matrix of the estimator errors we need the following quantities:

$$\frac{\partial \dot{R}}{\partial \lambda}, \frac{\partial \dot{R}}{\partial \beta}, \frac{\partial \dot{R}}{\partial \theta_o}, \frac{\partial \dot{R}}{\partial e}, \frac{\partial \dot{R}}{\partial a}.$$

Since λ and β are independent of the in-plane parameters, the first two quantities may be computed immediately from (1) to yield:

$$\frac{\partial \dot{R}}{\partial \lambda} = -\left[r \dot{\theta} \cos (\theta + \lambda) + \dot{r} \sin (\theta + \lambda) \right] \cos \beta \tag{6}$$

and

$$\frac{\partial \dot{R}}{\partial \beta} = \left[r \dot{\theta} \sin (\theta + \lambda) - \dot{r} \cos (\theta + \lambda) \right] \sin \beta \tag{7}$$

Also, since $\dot{R}$ depends only implicitly upon θ_o via θ and Equations (3) and (4) then we may write, after eliminating r, $\dot{\theta}$, and $\dot{r}$,

$$\frac{\partial \dot{R}}{\partial \theta_o} = \frac{\partial \dot{R}}{\partial \theta} \frac{\partial \theta}{\partial \theta_o} \tag{8}$$

Furthermore since:

$$r\dot{\theta} = \sqrt{\frac{u}{a(1-e^2)}} (1 + e\cos\theta) \tag{9}$$

and

$$\dot{r} = e\sqrt{\frac{u}{a(1-e^2)}} \sin\theta \tag{10}$$

we may write the following expression for $\dot{R}$:

$$\dot{R} = \sqrt{\frac{u}{a(1-e^2)}} \left[-(1 + e\cos\theta)\sin(\theta+\lambda) + e\sin\beta\cos(\theta+\lambda) \right] \cos\beta. \tag{11}$$

Thus, from Equation (11), we obtain:

$$\frac{\partial \dot{R}}{\partial \theta} = -\sqrt{\frac{u}{a(1-e^2)}} \cos(\theta+\lambda)\cos\beta \tag{12}$$

By implicitly differentiating Equations (3) and (4) we obtain the following expression for $\frac{\partial \theta}{\partial \theta_o}$:

$$\frac{\partial \theta}{\partial \theta_o} = \left(\frac{1 - e\cos\zeta}{1 - e\cos\zeta_o} \right)^2 \tag{13}$$

Thus, combining Equations (8), (12), and (13), we have:

$$\frac{\partial \dot{R}}{\partial \theta_o} = -\sqrt{\frac{u}{a(1-e^2)}} \left(\frac{1 - e\cos\zeta}{1 - e\cos\zeta_o} \right)^2 \cos(\theta+\lambda)\cos\beta \tag{14}$$

From Equations (11) and (3) and (4), we see that $\dot{R}$ depends upon the parameters e and a both explicitly and implicitly through the angle θ, thus we may expect the calculation of $\frac{\partial \dot{R}}{\partial e}$ and $\frac{\partial \dot{R}}{\partial a}$ to be more difficult. The expressions for the complete partial derivatives of $\dot{R}$ with respect to e and a are given by the following equations, the first

terms of which are to be regarded as formal partials of $\dot{R}$ with respect to e and a from Equation (11) --ignoring the dependence of $\dot{R}$ upon e and a through θ. The second terms properly account for the implicit dependence of $\dot{R}$ upon e and a through θ. The equations are:

$$\frac{\partial \dot{R}}{\partial e} = \left(\frac{\partial \dot{R}}{\partial e}\right)_f + \frac{\partial \dot{R}}{\partial \theta} \frac{\partial \theta}{\partial e} \tag{15}$$

$$\frac{\partial \dot{R}}{\partial a} = \left(\frac{\partial \dot{R}}{\partial a}\right)_f + \frac{\partial \dot{R}}{\partial \theta} \frac{\partial \theta}{\partial a} \tag{16}$$

Since $\frac{\partial \dot{R}}{\partial \theta}$ is given by (12), then (15) and (16) may be evaluated when we have the quantities:

$$\left(\frac{\partial \dot{R}}{\partial e}\right)_f, \left(\frac{\partial \dot{R}}{\partial a}\right)_f, \frac{\partial \theta}{\partial e}, \frac{\partial \theta}{\partial a},$$

where the subscript f denotes the formal partial obtained from (11) by ignorning θ.

From (11), we have:

$$\left(\frac{\partial \dot{R}}{\partial a}\right)_f = -\frac{1}{2}\sqrt{\frac{u}{a^3(1-e^2)}}\left[-(1+e\cos\theta)\sin(\theta+\lambda) + e\sin\theta\cos(\theta+\lambda)\right]\cos\beta \tag{17}$$

$$\left(\frac{\partial \dot{R}}{\partial e}\right)_f = \sqrt{\frac{u}{a(1-e^2)^3}}\left[-(e+\cos\theta)\sin(\theta+\lambda) + \sin\theta\cos(\theta+\lambda)\right]\cos\beta \tag{18}$$

To obtain $\frac{\partial \theta}{\partial e}$ and $\frac{\partial \theta}{\partial a}$ we must differentiate (3) implicitly. That is, consider:

$$F(\theta_o, e, a, t, \theta) = t - \frac{a^{3/2}}{\sqrt{u}}\left[(\zeta - r\sin\zeta) - (\zeta_o - e\sin\zeta_o)\right] = 0 \tag{19}$$

Equations (19) and (4) define θ implicitly as a function of θ_o, e, a, and time t. The quantities $\frac{\partial \theta}{\partial e}$ and $\frac{\partial \theta}{\partial a}$ are then obtained from the standard technique for the differentiation of implicit functions as described, e. g., in Sokolnikoff's Advanced Calculus.[1] That is, we may write:

$$\frac{\partial \theta}{\partial e} = - \frac{\partial F}{\partial e} \Bigg| \frac{\partial F}{\partial \theta} \quad \text{and} \quad \frac{\partial \theta}{\partial a} = - \frac{\partial F}{\partial a} \Bigg| \frac{\partial F}{\partial \theta} \tag{20}$$

which allows the computation of the required derivatives even though (3) may not be analytically inverted to yield an explicit expression for θ as a function of θ_o, e, a, and t.

From (3) and (4):

$$\frac{\partial F}{\partial \theta} = \frac{- a^{3/2}}{\sqrt{1-e^2}\sqrt{u}} \left[1 - e \cos \zeta\right]^2 . \tag{21}$$

$$\frac{\partial F}{\partial a} = - \frac{3}{2} \frac{a^{1/2}}{\sqrt{u}} \left[(\zeta - e \sin \zeta) - (\zeta_o - r \sin \zeta_o)\right] \tag{22}$$

$$\frac{\partial F}{\partial e} = \frac{a^{3/2}}{\sqrt{u}} \left[\frac{(1-e \cos \zeta)\,(1-\cos \theta \cos \zeta)}{(1-e^2)^{1/2} \sin \theta} \right. \tag{23}$$

$$\left. - \frac{(1 - e \cos \zeta_o)\,(1-\cos \theta_o \cos \zeta_o)}{(1-e^2)^{1/2} \sin \theta_o} + \sin \zeta - \sin \zeta_o \right]$$

---

(1) I. S. and E. S. Sokolnikoff, Advanced Calculus, p. 89.

Thus Equations (20) through (23) allow us to complete the calculation of our required derivatives and yield exact expressions for $\frac{\partial \dot{R}}{\partial e}$ and $\frac{\partial \dot{R}}{\partial a}$.

The remainder of the calculation of the covariance matrix of the estimator errors proceeds exactly as described in Apollo Note No. 67, the elements of the inverse of the covariance matrix being given by:

$$C_{i,j} = \frac{1}{N} \sum_{k=1}^{N} \frac{\partial \dot{R}_{(k)}}{\partial \alpha_i} \frac{\partial \dot{R}_{(k)}}{\partial \alpha_j} \tag{24}$$

where:

$$\alpha_1 = \lambda, \alpha_2 = \beta, \alpha_3 = \theta_o, \alpha_4 = e, \alpha_5 = a.$$

To obtain the covariance matrix of the estimator errors, the matrix $C_{i,j}$ is inverted and multiplied by $\frac{\sigma^2}{N}$ where σ^2 is the noise variance of the doppler data and N is proportional to the smoothing time or the number of independent pieces of doppler data.

APOLLO NOTE NO. 81

C. P. Siska
15 July 1963

MAXIMUM ALLOWABLE INJECTION ERRORS FOR A PARTICULAR DSIF AIDED RENDEZVOUS SCHEME

INTRODUCTION

This note examines the problem of LEM rendezvous with the CM under the condition that large injection velocity errors may exist at the end of the first boost phase.

It is assumed that the DSIF can attain precise orbital data on the LEM and consequently assist the LEM in providing the proper steering information to cancel the effects of initial injection errors.

With this in mind, the question arises as to how large a first boost velocity error can be made and still be cancelled within a designed 10% velocity pad. This note examines this question for a particular rendezvous scheme.

RENDEZVOUS SCHEMES

For comparison purposes, the nominal rendezvous scheme is defined as one using a Hohmann transfer with perilune and apolune at 8 and 80 n.m. altitude as shown in Figure 1 (a). Trying to establish a Hohmann ellipse, immediately restricts the maximum injection boost error to around 100 ft/sec., in order to avoid grazing the lunar surface (without additional boost). Consequently, the first boost will be designed to yield an "off design" orbit which is larger than the Hohmann. The programmed rendezvous scheme is shown in Figure 1 (b), and uses three programmed boosts, the second boost correcting to a Hohmann orbit.

When first boost velocity errors exist, the correction scheme will be as pictured in Figure 1 (c). The DSIF will be able to track the first orbit for almost half a revolution (in two segments), and then provide thrust information for the LEM to initiate the Hohmann transfer at

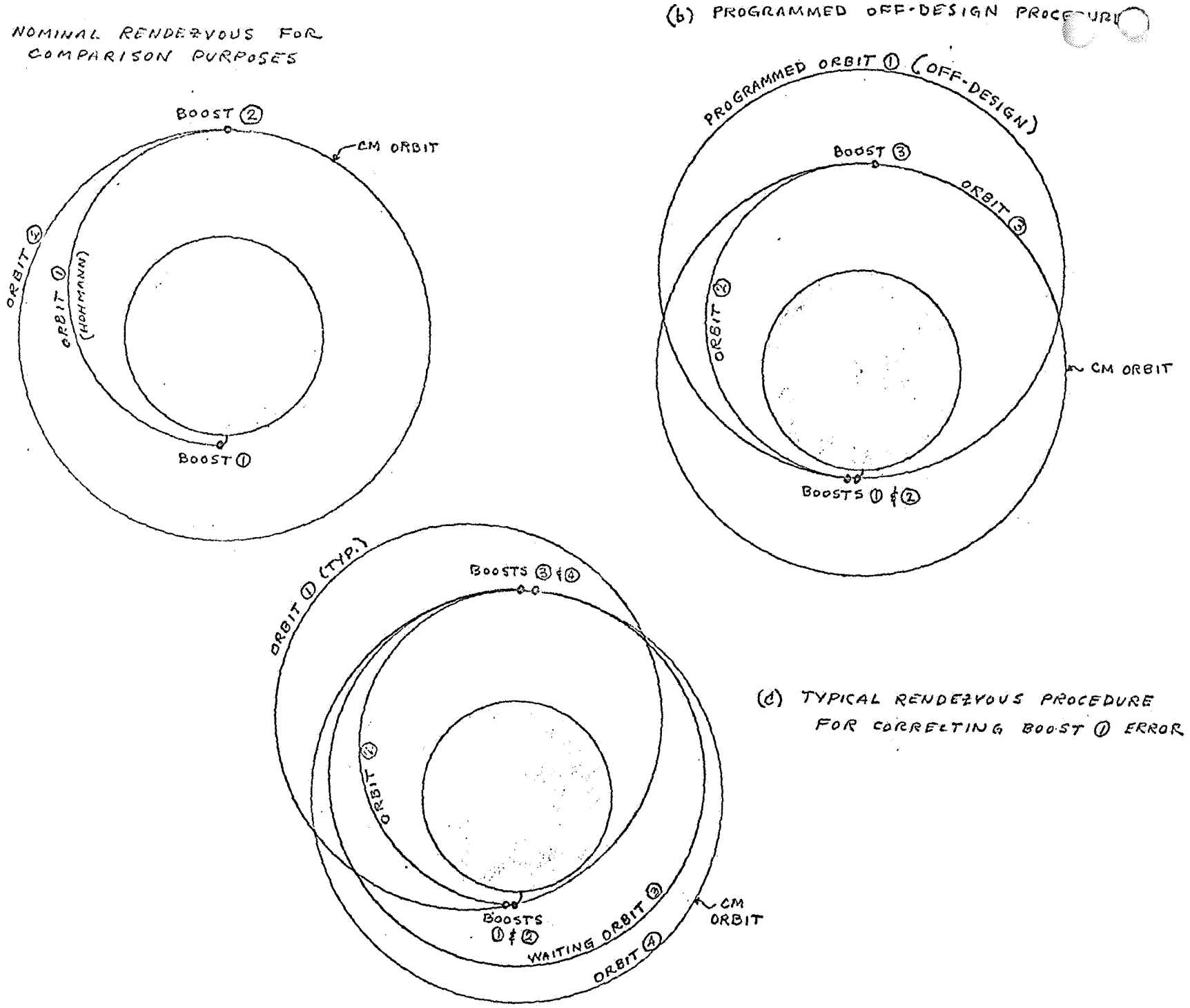

FIG. 1 - SCHEMATIC DIAGRAM OF RENDEZVOUS PROCEDURES

the end of the first revolution. * At the Hohmann apolune, boost three initiates a waiting orbit, so that at the end of exactly N_3 revolutions, the LEM and CM positions coincide and boost four then provides circular orbit velocity.

In the analysis that follows it is assumed boost errors are negligible after the first boost and, therefore, are cancelled out in the final docking procedure. However, if more than one waiting orbit ($N_3 > 1$) is designed into the procedure, then the DSIF can assist in refining the waiting orbit before boost four is applied.

It is noted that since boost two is applied after one full revolution, the programmed "off-design" boost one velocity vector must be horizontal in order to prevent unfavorable bias for upward or downward velocity errors. For example, if boost two occurs after a half revolution, the design boost one velocity can be pitched upward, thereby allowing greater injection errors before the lunar grazing condition occurs.

REQUIRED PERIODS OF WAITING ORBITS

For sake of mathematical simplicity, the following linearized relations will be used in the analysis.

From the energy equation and Kepler's law of periods, we obtain:

$$\frac{a}{R_{CM}} \approx 1 - 2\left(\frac{R_{CM}-R}{R_{CM}}\right) - 2\left(\frac{V_{CM}-V}{V_{CM}}\right) \tag{1}$$

$$\frac{a}{R_{CM}} \approx 1 - \frac{2}{3}\left(\frac{P_{CM}-P}{P_{CM}}\right) \tag{2}$$

and after combining Equations (1) and (2),

---

* If more than one revolution is required for adequate DSIF tracking, the second boost will remain the same but the design lead angle for the CM must be changed appropriately.

$$\frac{P_{CM}-P}{P_{CM}} \approx 3 \left(\frac{R_{CM}-R}{R_{CM}}\right) + 3 \left(\frac{V_{CM}-V}{V_{CM}}\right) \tag{3}$$

where the subscript CM refers to orbital quantities associated with the circular orbit of the Command Module.

The mean relative rate of phase angle change can be written:

$$\dot{\eta} = \bar{\omega} - \omega_{CM} = \omega_{CM} \left(\frac{P_{CM}-P}{P}\right) \tag{4}$$

For the rendezvous scheme under consideration, the required period for orbit three (waiting orbit) in order to make contact with the CM is,

$$N_3 \dot{\eta}_3 P_3 = \eta_o - \dot{\eta}_1 P_1 - \frac{1}{2} \dot{\eta}_2 P_2; \qquad N_3 = 1, 2, \ldots \tag{5}$$

where:

η_o = design phase angle difference between the LEM and CM at the end of boost one.

N_3 = Number of waiting orbits.

Since the subscript 2 refers to the Hohmann orbit, it will henceforth be replaced by subscript H, so that upon combining Equations (4) and (5),

$$\frac{P_{CM}-P_3}{P_{CM}} = \frac{1}{N_3} \left[\frac{\eta_o}{2\pi} - \left(\frac{P_{CM}-P_1}{P_{CM}}\right) - \pi \left(\frac{P_{CM}-P_H}{P_{CM}}\right)\right] \tag{6}$$

We now have to impose a restriction on the magnitude of $\frac{P_{CM}-P_3}{P_{CM}}$ in order to prevent perilunes which lie too near the lunar surface and thus, allow some margin for boost three errors. For convenience, we will restrict orbit three to lie outside the Hohmann, so that:

$$\left(\frac{P_{CM}-P_3}{P_{CM}}\right) \leq \left(\frac{P_{CM}-P_H}{P_{CM}}\right) \tag{7}$$

The maximum value of $\frac{P_{CM}-P_3}{P_{CM}}$ in Equation (6) will occur for the case of minimum $\left(\frac{P_{CM}-P_1}{P_{CM}}\right)$. Designing the initial lead angle η_o with these values assures that Equation (7) will always be satisfied. Thus, the design lead angle is:

$$\frac{\eta_o}{2\pi} = \left(N_3 + \frac{1}{2}\right) \left(\frac{P_{CM}-P_H}{P_{CM}}\right) + \left(\frac{P_{CM}-P_1}{P_{CM}}\right)_{min.} \tag{8}$$

Note that the lead angle is designed for maximum P_1 (the largest orbit), which occurs when the velocity error is co-linear to, and increases the magnitude of the programmed boost one velocity.

Combining Equations (6) and (8), yields:

$$\left(\frac{P_{CM}-P_3}{P_{CM}}\right) = \left(\frac{P_{CM}-P_H}{P_{CM}}\right) + \frac{1}{N_3}\left[\left(\frac{P_{CM}-P_1}{P_{CM}}\right)_{min.} - \left(\frac{P_{CM}-P_1}{P_{CM}}\right)\right] \tag{9}$$

EXCESS VELOCITY REQUIREMENTS

The excess velocity requirement is defined as the total velocity used to accomplish the rendezvous, (see Figure 1 (c)), minus the velocity used for the nominal rendezvous with the Hohmann transfer, Figure 1 (a).

A schematic illustration of Equation (9), shown in Figure 2, enables us to discuss some facets involved in the rendezvous scheme.

First of all, the curve defined by Equation (9) is a simple straight line whose slope is determined by the magnitude N_3. Point A on the curve involves a transfer in which the phase angle difference between the LEM and CM after orbit one is, by design, dissipated in exactly $N_3 + \frac{1}{2}$ Hohmann revolutions. On the other hand, the point B transfer eliminates the difference remaining after orbit one in one-half a Hohmann revolution.

It is evident that waiting orbits between points A and B lie between the Hohmann orbit and the circular orbit of the CM. In these

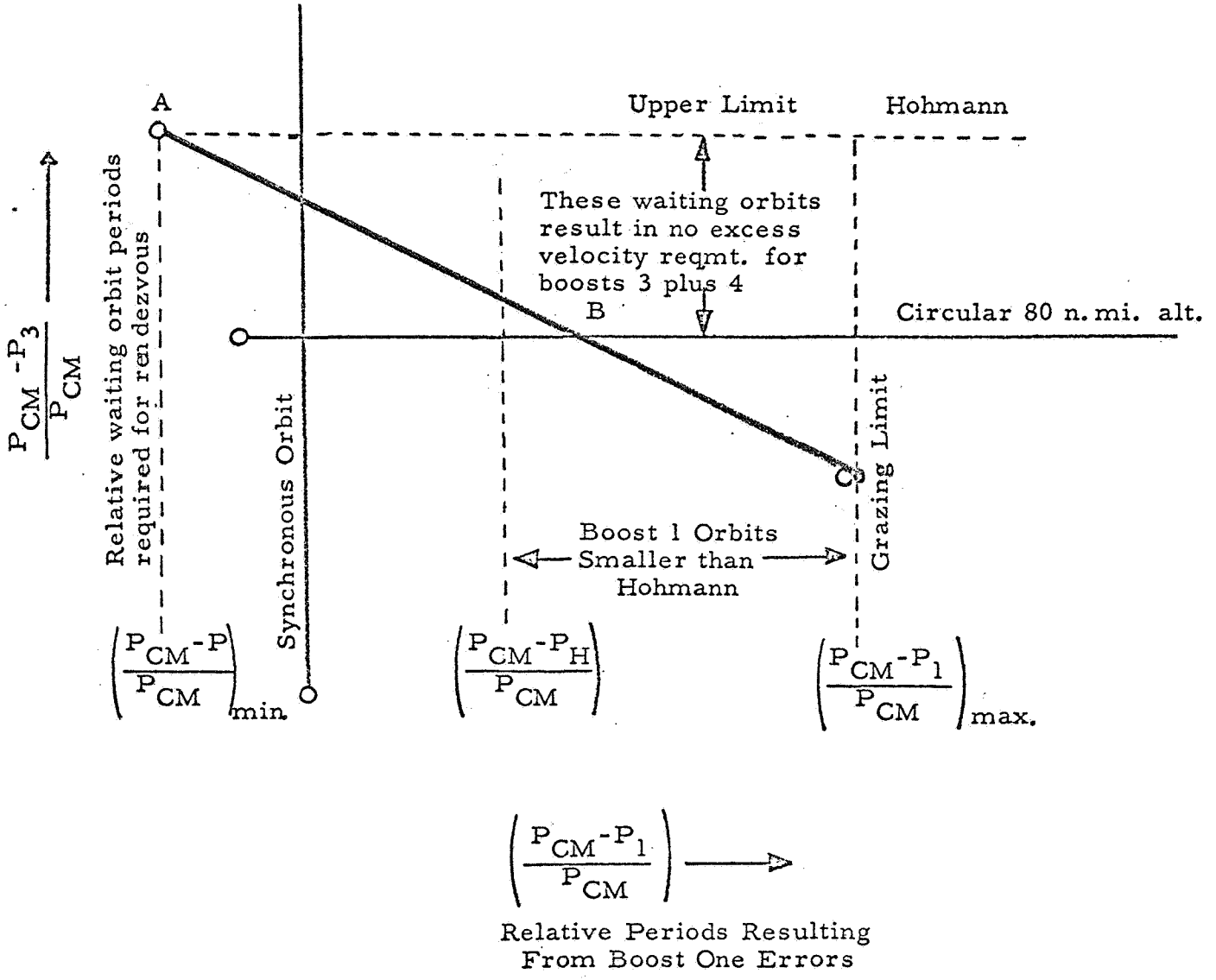

Figure 2. Schematic Relation Involving Required Waiting Orbits and Orbits Resulting From Boost One Errors

cases the sum of velocities generated in boosts three and four is exactly equivalent to the velocity generated in boosting from Hohmann apolune velocity to circular orbit velocity. Consequently, no excess boost velocity is required for this part of the rendezvous. Between points B and C, the waiting orbits lie outside the CM circular orbit and the excess velocity here is $2\,(V_3 - V_{CM})$. Therefore, if $\delta V_{3,4}$ defines the excess velocity requirements for boosts three plus four, we have the conditions,

$$\delta V_{3,4} = 0 \text{ if } \frac{P_{CM} - P_3}{P_{CM}} \geq 0 \tag{10}$$

$$\delta V_{3,4} = 2\,(V_3 - V_{CM}) \text{ if } \frac{P_{CM} - P_3}{P_{CM}} < 0$$

According to Equation (3), therefore, $\delta V_{3,4}$ will increase as boost one errors move one from point B to point C.

On the other hand, the excess velocity requirement associated with boosts one and two is the difference between the sum of the velocities generated by boosts one and two, and the Hohmann perilune velocity V_{HP}. Call this excess velocity $\delta V_{1,2}$. With the aid of the following diagram, one can express this in more concrete terms as:

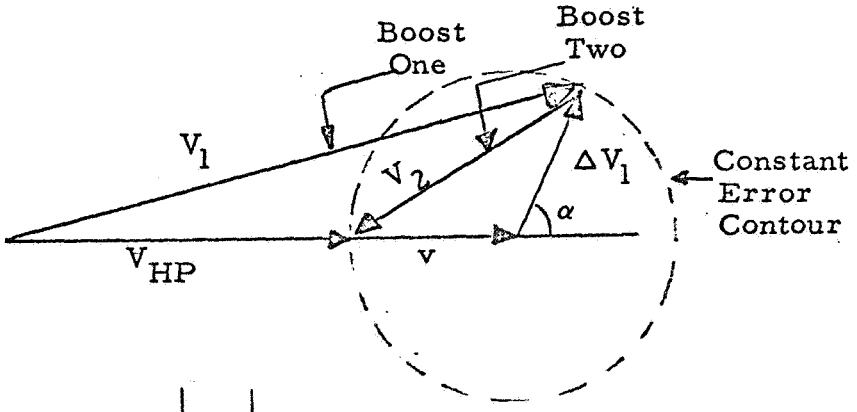

$$\delta V_{1,2} = V_1 + \left|V_2\right| - V_{HP} \tag{11}$$

$$V_1^2 = (V_{HP} + v + \Delta V_1 \cos \alpha)^2 + (\Delta V_1 \sin \alpha)^2 \tag{12}$$

$$V_2^2 = (v + \Delta V_1 \cos \alpha)^2 + (\Delta V_1 \sin \alpha)^2 \qquad (13)$$

where:

ΔV_1 = boost one velocity error

$V_{HP}+v$ = programmed boost one velocity for the "off design" orbit --(See Figure 1(b)).

In the foregoing diagram it is apparent that as V_1 decreases (or equivalently the period P_1), the value of $\delta V_{1,2}$ decreases. Thus, in Figure 2, as one moves from point A to point C on the curve, the value $\delta V_{1,2}$ decreases monotonically.

Summarizing the above discussion, as one moves from point A to B, the total excess velocity required is simply $\delta V_{1,2}$ and thus keeps decreasing in magnitude. In moving from B to C, the total excess velocity is the sum of $\delta V_{1,2}$ and $\delta V_{3,4}$ with the former decreasing and the latter increasing. Since we are interested in determining the maximum excess velocity requirement, it is a question of comparing the values at points A and C only for a given ΔV_1, or, in other words, comparing the two velocity error directions $\alpha = 0, \pi$.

If δV_{tot} denotes the total excess velocity, we therefore have from Equations (10) through (13),

$$\delta V_{tot} (\alpha = 0) = 2 (v + \Delta V_1) \qquad (14)$$

$$\delta V_{tot}(\alpha = \pi) = 2 (V_3 - V_{CM})_{max} + 2 k (v - \Delta V_1) \qquad (15)$$

where: $k = \begin{bmatrix} 0 \ ; \ v \leq \Delta V_1 \\ 1 \ ; \ v > \Delta V_1 \end{bmatrix}$

Using Equations (3) and (9), one can rewrite Equation (15) to read:

$$\delta V_{tot}\,(\alpha = \pi) = 2\left[-\left(\frac{V_{CM}-V_{HA}}{V_{CM}}\right) + \frac{2\Delta V_1}{N_3 V_{CM}}\right] V_{CM} + 2k\,(v - \Delta V_1) \qquad (16)$$

$$\text{with } K = \begin{cases} 0 \;;\; v \le \Delta V_1 \\ 1 \;;\; v > \Delta V_1 \end{cases}$$

For a given ΔV_1, the quantity v in the preceding equations will affect the location of the straight line curve in Figure 2, moving it from left to right and vice versa. The permissible combinations of v and ΔV_1 must never permit the condition to exist in which orbit one intersects the lunar surface. This problem is examined in the next section.

LUNAR GRAZING LIMITATIONS ON FIRST BOOST VELOCITY

The grazing limitation on the first boost velocity components can be obtained from the following energy and momentum relations,

$$\frac{1}{2}\left(V_{1N}^2 + V_{1T}^2\right) - \frac{\mu}{R_M + h_1} = \frac{1}{2} V_{R_M}^2 - \frac{\mu}{R_M} \qquad (17)$$

$$(R_M + h_1)\, V_{1T} = R_M\, V_{R_M} \qquad (18)$$

Combining Equations (17) and (18) yields the limiting hyperbola in the hodograph plane,

$$\frac{V_{1T}^2}{a^2} - \frac{V_{1N}^2}{b^2} = 1.0 \qquad (20)$$

where:

$$a^2 = \left(\frac{\mu}{R_M + h_1}\right) \Big/ \left(1 + \frac{1}{2}\,\frac{h_1}{R_M}\right) \qquad (21)$$

$$b^2 = \left(\frac{\mu}{R_M + h_1}\right) \left(\frac{2h_1}{R_M}\right) \qquad (22)$$

The condition that non-intersecting orbits prevail implies that, for any given v, the maximum value of ΔV_1 must equal the segment of the normal to the hyperbola bounded by the hyperbola and the V_{1T} axis. This is shown graphically in the following diagram.

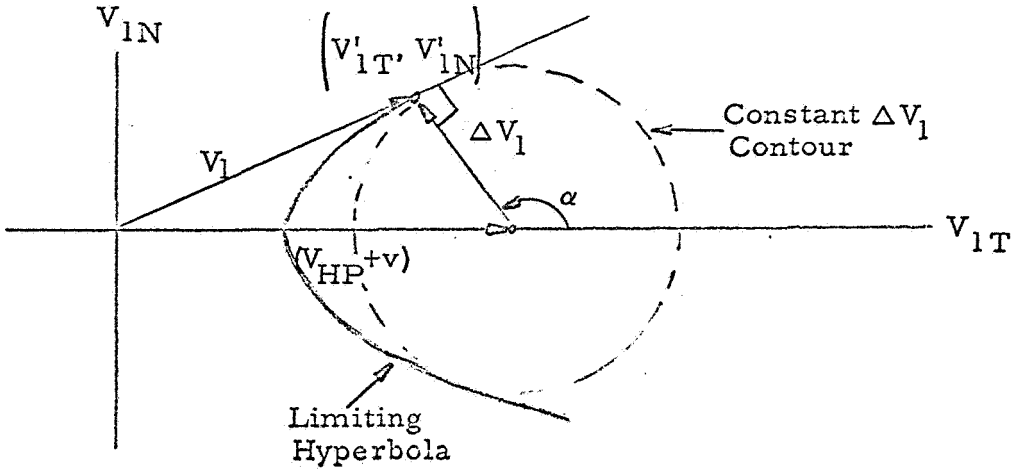

Since the slope of the normal is $-\frac{a^2}{b^2} \cdot \frac{V'_{1N}}{V'_{1T}}$, the value of the subnormal is:

$$(V_{HP} + v) - V'_T = \frac{b^2}{a^2} V'_{1T} \tag{23}$$

which can be written:

$$V'_T = \left(\frac{a^2}{a^2 + b^2}\right)\left(V_{HP} + v\right) \tag{24}$$

Combining Equations (24) and (20), the vertical component of ΔV_1 becomes:

$$V'^2_{1N} = \frac{b^2}{a^2}\left(\frac{a^2}{a^2 + b^2}\right)^2 \left(V_{HP} + v\right)^2 - b^2 \tag{25}$$

Finally, forming ΔV_1 from the components in Equations (23) and (25), we have:

$$\Delta V_1^2 = \left(\frac{b^2}{a^2 + b^2} \right) \left(V_{HP} + v \right)^2 - b^2 \qquad (26)$$

or in terms of the boost one burnout altitude after introducing Equations (21) and (22),

$$\Delta V_1^2 = \frac{2 h_1}{R_M} \left\{ \frac{\left(1 + \frac{h_1}{2R_M} \right)}{\left(1 + h_1/R_M \right)^2} \left(V_{HP} + v \right)^2 - \frac{\mu}{R_M + h_1} \right\} \qquad (27)$$

Since the area of interest is when $\frac{h_1}{R_M} << 1.0$, and also $\frac{v}{V_{HP}} << 1.0$, Equation (27) can be linearized, (by the use of the energy equation for V_{HP}), to yield:

$$\frac{\Delta V_1}{V_{CR_M}} = \sqrt{\frac{h_1}{R_M}} \sqrt{\frac{h_{CM} - 4 h_1}{R_M} + \frac{4 v}{V_{CR_M}}} \qquad (28)$$

where:

h_{CM} = CM circular orbit altitude

h_1 = boost one burnout altitude

$V_{CR_M} = \sqrt{\frac{\mu}{R_M}}$ = circular orbit velocity at lunar surface

Equation (28) gives us the maximum value of ΔV_1 for preventing intersecting orbits with the lunar surface with boost one.

NUMERICAL RESULTS

The solution for the maximum permissible ΔV_1 within the allowable 10% velocity pad can be obtained graphically using Equations (14), (16), and (28).

From Apollo Note No. 75, Figure 1, the difference between the velocity potential for the 10% pad and the Hohmann transfer is $\delta V_{tot} \simeq 620$ ft/sec. Also, from the same note we have:

$\mu = 173.1 \times 10^{12}$ ft^3/sec^2

$R_M = 5.7 \times 10^6$ ft. = 938 n. mi.

$R_{CM} = 6.19 \times 10^6$ ft. = 1018 n. mi.

V_{CM} = 5288 ft/sec. (circular orbit velocity at 80 n. mi. altitude)

In addition there are the following values,

$V_{CR_M} = \sqrt{\frac{\mu}{R_M}}$ = 5510 ft/sec. (circular orbit velocity at lunar surface)

h_1 = 8 n. mi. (boost one burnout altitude)

h_{CM} = 80 n. mi. (circular orbit altitude of CM)

$\frac{V_{CM} - V_{HA}}{V_{CM}}$ = .0177, from Equation (1)

Using the above values, the aforementioned equations are shown graphically in Figure 3.

The $\alpha = 0$ case, where ΔV_1 is directed along the perilune velocity, $V_{HP} + v$, reaches the allowable excess velocity limit first as v increases, and therefore, determines the critical value of ΔV_1. Thus, the programmed "off design" orbit one should have a perilune velocity approximately 120 ft/sec. greater than perilune velocity for a Hohmann, and this allows a maximum boost one velocity error $\Delta V_1 \simeq 190$ ft/sec.

Note that for a Hohmann transfer, (v = 0), the allowable ΔV_1 is approximately 115 ft/sec., and the maximum excess velocity for this rendezvous occurs for the $\alpha = \pi$ case at a value $\delta V_{tot} \simeq 2 \times 132.5 \simeq 265$ ft/sec.

For the values v = 120 and $\Delta V_1 = 190$, Equation (3) indicates that $\left(\frac{P_{CM} - P_1}{P_{CM}}\right)_{min} = -.123$, which from Equation (4) yields a phase angle

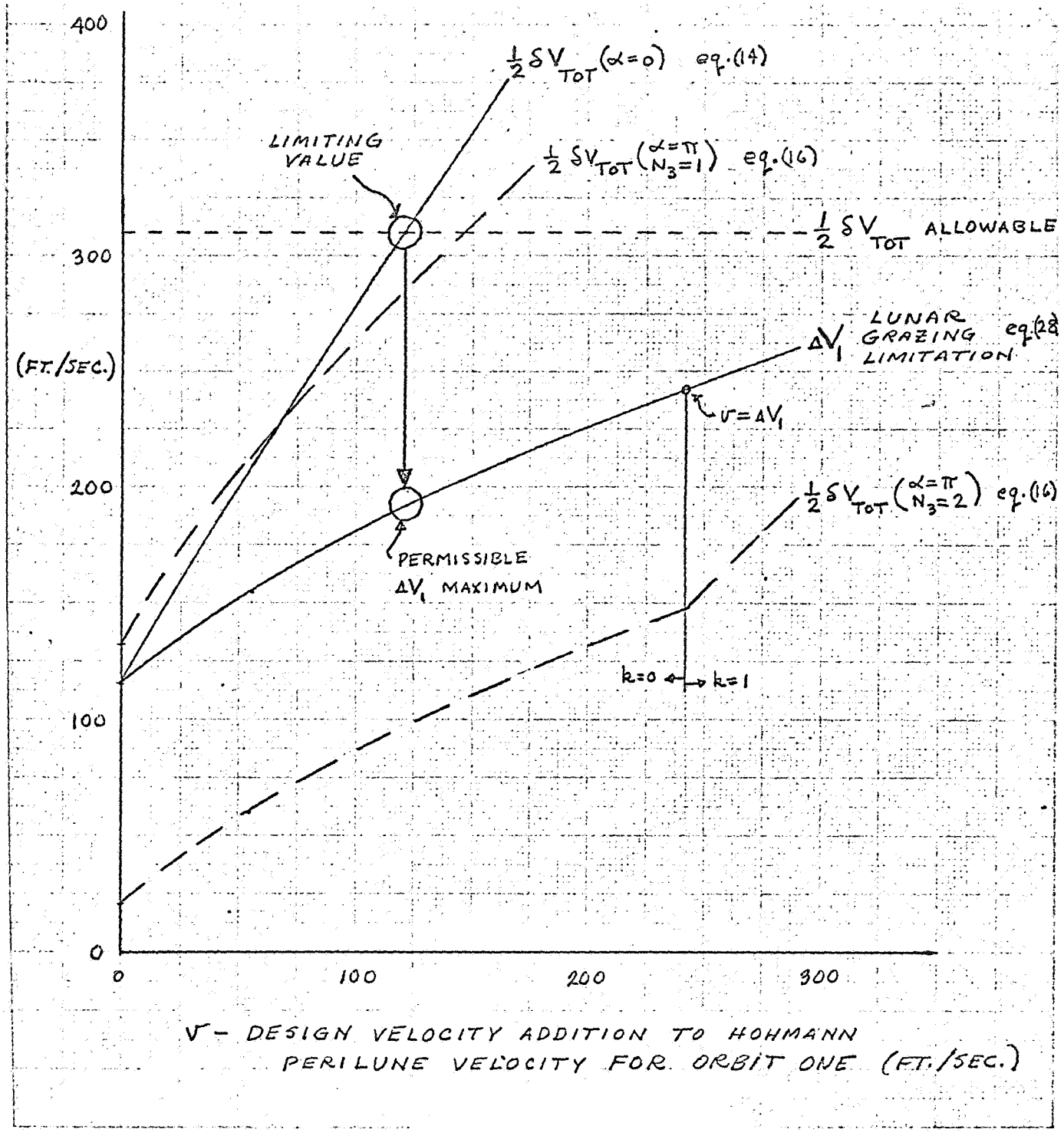

Figure 3. Graphical Solution for Maximum Permissible Boost One Velocity Error

Boost One Burnout Altitude = 8 n. mi.
CM Circular Orbit Altitude = 80 n. mi.

change of -44.3° for this case; that is, the CM gains a maximum of 44.3° on the LEM during orbit one.

Also from Equation (3), we find that the relative Hohmann period $\left(\frac{P_{CM}-P_H}{P_{CM}}\right) = .0531$, and thus from Equation (8), the following lead angles obtain, $\eta_o\ (N_3 = 1) = -15.5^{\circ}$ and $\eta_o\ (N_3 = 2) = 3.6^{\circ}$. Consequently, at the end of boost one, the LEM is leading the CM by 15.5° if one waiting orbit is planned and is trailing by 3.6° if two waiting orbits are planned for the rendezvous.

The maximum rendezvous time from boost one burnout for one waiting orbit is $P_{1\ max} + \frac{3}{2} P_{H'}$ which upon using the above values yields a value $2.543\ P_{CM}$. Since $P_{CM} = 2.04$ hrs., this time is 5.2 hours.

SUMMARY

By programming a boost one perilune velocity 120 ft/sec., greater than Hohmann perilune velocity, the allowable boost one velocity error can be increased from 115 ft/sec. to 190 ft/sec. In this case the maximum excess velocity required to cancel the errors during rendezvous increases from 265 ft/sec. to 620 ft /sec.

The maximum rendezvous time from boost one burnout with one waiting orbit planned is 5.2 hours for the boost one velocity error of 190 ft/sec.

REVISION SHEET NOTE #82

$$\dot{r}_o = a_4$$

$$\frac{\partial (r_o \dot{r}_o)}{\partial a_j} = r_o \frac{\partial \dot{r}_o}{\partial a_j} + \dot{r}_o \frac{\partial r_o}{\partial a_j} = \frac{\partial}{\partial a_j} (a_1 a_4 + a_2 a_5 + a_3 a_6)$$

$$r_o \frac{\partial \dot{r}_o}{\partial a_j} = \delta_{1j} a_4 + \delta_{2j} a_5 + \delta_{3j} a_6 + \delta_{4j} a_1 + \delta_{5j} a_2 + \delta_{6j} a_3 - \dot{r}_o \frac{\partial r_o}{\partial a_j}$$

$$\boxed{a_1 \frac{\partial \dot{r}_o}{\partial a_j} = \delta_{4j} a_1 + \delta_{2j} a_5}$$

The angular momentum H is given by:

$$\overline{H} = (a_2 a_6 - a_3 a_5) \hat{x}' + (a_3 a_4 - a_1 a_6) \hat{y}' + (a_1 a_5 - a_2 a_4) \hat{z}'$$

$$H^2 = (a_2 a_6 - a_3 a_5)^2 + (a_3 a_4 - a_1 a_6)^2 + (a_1 a_5 - a_2 a_4)^2$$

$$2 H \frac{\partial H}{\partial a_j} = 2 (a_2 a_6 - a_3 a_5) \frac{\partial (a_2 a_6 - a_3 a_5)}{\partial a_j}$$

$$+ 2 (a_3 a_4 - a_1 a_6) \frac{\partial (a_3 a_4 - a_1 a_6)}{\partial a_j}$$

$$+ 2 (a_1 a_5 - a_2 a_4) \frac{\partial (a_1 a_5 - a_2 a_4)}{\partial a_j}$$

$$\boxed{H = a_1 a_5}$$

REVISION SHEET NOTE #82

in which ρ_e is the radius of the Earth and ω_e is the Earth's angular rate.

The latitude and longitude of the sub-lunar point on Earth at the instant of the first observation are L and ℓ respectively. The inclination between the plane of the orbit of the Moon about the Earth and the Earth's equator is β, as shown in Figure 1. It must be specified whether the angle γ in that figure is greater or less than $\pi/2$. Then

$$\sin \gamma = \frac{\sin L}{\sin \beta}$$

$$\cos \gamma = \begin{cases} +\sqrt{1 - \sin^2 \gamma} & \text{if } \gamma \leq \pi/2 \\ -\sqrt{1 - \sin^2 \gamma} & \text{if } \gamma > \pi/2 \end{cases}$$

$$\sin (\phi - \ell) = \tan L \cot \beta$$

$$\cos (\phi - \ell) = \frac{\cos \gamma}{\cos L}$$

$$\sin b = -\sin \beta \sin \left(\frac{\pi}{2} - \gamma\right)$$

$$\sin b = -\sin \beta \cos \gamma$$

$$\cos b = +\sqrt{1 - \sin^2 b}$$

REVISION SHEET NOTE #82

$$K_{11} = \cos L \cos \ell$$

$$K_{12} = \cos L \sin \ell$$

$$K_{13} = \sin L$$

$$K_{21} = \cos b \cos (\phi + \nu)$$

$$K_{22} = \cos b \sin (\phi + \nu)$$

$$K_{23} = \sin b$$

$$K_{31} = K_{12} K_{23} - K_{13} K_{22}$$

$$K_{32} = K_{13} K_{21} - K_{11} K_{23}$$

$$K_{33} = K_{11} K_{22} - K_{12} K_{21}$$

$$\tilde{X}_d = K X_d$$

$$\dot{\tilde{X}}_d = K \dot{X}_d$$

The rotation matrix L rotates vector components from the $\tilde{x}\ \tilde{y}\ \tilde{z}$ system to the x' y' z' system. The relative angular positions of these two co-ordinate systems are shown in Figure 2.

$$\cdot L = \begin{bmatrix} \cos\zeta & \sin\zeta & 0 \\ -\sin\zeta & \cos\zeta & 0 \\ 0 & 0 & 1 \end{bmatrix} \begin{bmatrix} 1 & 0 & 0 \\ 0 & \cos\eta & \sin\eta \\ 0 & -\sin\eta & \cos\eta \end{bmatrix} \begin{bmatrix} \cos\xi & \sin\xi & 0 \\ -\sin\xi & \cos\xi & 0 \\ 0 & 0 & 1 \end{bmatrix}$$

REVISION SHEET NOTE #82

Then the vectors $\bar{s}$ and $\dot{\bar{s}}$ are

$$X'_s = \begin{bmatrix} x'_s \\ y'_s \\ z'_s \end{bmatrix} = X' + L\,(\tilde{X}_m - \tilde{X}_d)$$

and

$$\dot{X}'_s = \begin{bmatrix} \dot{x}'_s \\ \dot{y}'_s \\ \dot{z}'_s \end{bmatrix} = \dot{X}' + L\,(\dot{\tilde{X}}_m - \dot{\tilde{X}}_d)$$

$$s^2 = x'^2_s + y'^2_s + z'^2_s$$

$$\frac{\dot{s}}{s} = \frac{1}{s^2}\,(x'_s\,\dot{x}'_s + y'_s\,\dot{y}'_s + z'_s\,\dot{z}'_s)$$

Denoting the partials of X'_s and $\dot{X}'_s$ with respect to a_j by R'_j and $\dot{R}'_j$,

$$R'_j = \begin{bmatrix} \frac{\partial x'}{\partial a_j} \\ \frac{\partial y'}{\partial a_j} \\ \frac{\partial z'}{\partial a_j} \end{bmatrix} = \begin{bmatrix} -y' \dfrac{\partial\,(\theta-\theta_o)}{\partial a_j} + \cos(\theta-\theta_o)\,\dfrac{\partial r}{\partial a_j} \\ x' \dfrac{\partial\,(\theta-\theta_o)}{\partial a_j} + \sin(\theta-\theta_o)\,\dfrac{\partial r}{\partial a_j} \\ \delta_{3j}\,\dfrac{a_5 x' - a_4 y'}{H} + \delta_{6j}\,\dfrac{y'}{a_5} \end{bmatrix}$$

APOLLO NOTE NO. 82

H. Engel
16 July 1963

CALCULATION OF COVARIANCE MATRICES III

This note presents a means for finding the covariance matrix when Doppler observations of a vehicle in an elliptic or circular orbit about a moving Moon are made from a DSIF or MSFN facility on the surface of the Earth. The orbit of the Moon is assumed circular, but an elliptical orbit could be used with just slightly more computation.

The parameters chosen to describe the vehicle orbit are its position and velocity with respect to the Moon at the time of the first observation. This choice of parameters has the advantage that it is possible to obtain expressions for the partial derivatives used in calculating the inverse of the covariance matrix that do not blow up when the orbit eccentricity approaches or equals zero.

The vector from the Moon to the vehicle is $\overline{r}$, the vector from the Earth to the Moon is $\overline{X}_m$, and the vector from the center of the Earth to the observing station is $\overline{X}_d$. The vector from the observing station to the vehicle is $\overline{s}$,

$$\overline{s} = \overline{X}_m + \overline{r} - \overline{X}_d$$

The observed quantity is the rate of change of distance between the observing station and the vehicle, i.e., $\dot{s}$. Now,

$$\dot{\overline{s}} = \dot{\overline{X}}_m + \dot{\overline{r}} - \dot{\overline{X}}_d$$

and

$$\dot{s} = \left(\frac{\overline{s}}{s}\right) \cdot \dot{\overline{s}}$$

Then,

$$\frac{\partial \dot{\overline{s}}}{\partial a_j} = \frac{\partial \dot{\overline{X}}_m}{\partial a_j} + \frac{\partial \dot{\overline{r}}}{\partial a_j} - \frac{\partial \dot{\overline{X}}_d}{\partial a_j}$$

$$= \frac{\partial \dot{\overline{r}}}{\partial a_j}$$

and

$$\frac{\partial \dot{s}}{\partial a_j} = \frac{1}{s}\left[\bar{s}\cdot\frac{\partial \dot{\bar{s}}}{\partial a_j} + \dot{\bar{s}}\cdot\frac{\partial \bar{s}}{\partial a_j} - \dot{s}\,\frac{\partial s}{\partial a_j}\right]$$

$$= \frac{1}{s}\left[\bar{s}\cdot\frac{\partial \dot{\bar{s}}}{\partial a_j} + \dot{\bar{s}}\cdot\frac{\partial \bar{s}}{\partial a_j} - \frac{\dot{s}}{s}\,\bar{s}\cdot\frac{\partial \bar{s}}{\partial a_j}\right]$$

$$= \frac{1}{s}\left[\bar{s}\cdot\frac{\partial \dot{\bar{r}}}{\partial a_j} + \left(\dot{\bar{s}} - \frac{\dot{s}}{s}\,\bar{s}\right)\frac{\partial \bar{r}}{\partial a_j}\right].$$

Terms of the form $\sum \frac{\partial \dot{s}_i}{\partial a_j}\,\frac{\partial \dot{s}_i}{\partial a_k}$ are used in computing the matrix from which the covariance matrix is found.

It is convenient to use different co-ordinate systems in computing $\overline{X}_m$, $\bar{r}$, and $\overline{X}_d$. By co-ordinate rotations $\overline{X}_m$ and $\overline{X}_d$ are expressed in the same co-ordinates as $\bar{r}$ so $\partial\dot{s}/\partial a_j$ can be evaluated.

In the work that follows, the various quantities that must be employed are presented in the sequence in which they are used in actual computations.

The x'y'z' co-ordinate system is right-handed, non-rotating and Moon-centered. x' is directed along the initial position vector $(x'_o, 0, 0)$ of the vehicle, vehicle motion is in the x'y' - plane, and y' is directed so that $\dot{y}'_o$ is positive. The orbit parameters are the components of $\bar{r}_o$ and $\dot{\bar{r}}_o$ in the x'y'z' co-ordinate system; these are x'_o, y'_o, z'_o, $\dot{x}'_o$, $\dot{y}'_o$, and $\dot{z}'_o$, and are called a_1 through a_6 respectively.

Note well that one can not employ the fact that a_2, a_3 and a_6 are zero, until after derivatives are taken; otherwise incorrect results are obtained. For this reason two different expressions for a quantity may be found, one perhaps including a_3, a_5, and a_6, and used for differentiation, and a second expression without a_3, a_5, and a_6 and used for computation. The quantities used for computation are enclosed in boxes.

The initial radius $\bar{r}_o$ is given by:

$$\bar{r}_o = a_1 \hat{x}' + a_2 \hat{y}' + a_3 \hat{z}'$$

in which the caret denotes a unit vector.

$$r_o^2 = a_1^2 + a_2^2 + a_3^2$$

$$2 r_o \frac{\partial r_o}{\partial a_j} = 2 a_1 \delta_{1j} + 2 a_2 \delta_{2j} + 2 a_3 \delta_{3j}$$

$$\boxed{\frac{\partial r_o}{\partial a_j} = \delta_{1j}}$$

in which $\delta_{i,j}$ is the Kronecker delta

$$\delta_{i,j} = \begin{cases} 0 \text{ if } i \neq j \\ 1 \text{ if } i \neq j \end{cases}$$

$$r_o = a_1$$

$$\dot{\bar{r}}_o = a_4 \hat{x}' + a_5 \hat{y}' + a_6 \hat{z}'$$

$$r_o^2 = \bar{r}_o \cdot \bar{r}_o$$

$$2 r_o \dot{r}_o = 2 \bar{r}_o \cdot \dot{\bar{r}}_o$$

$$\dot{r}_o = \frac{\bar{r}_o \cdot \dot{\bar{r}}_o}{r_o}$$

$$= \frac{a_1 a_4 + a_2 a_5 + a_3 a_6}{r_o}$$

$$\dot{r}_o = a_4$$

$$\frac{\partial (r_o \dot{r}_o)}{\partial a_j} = r_o \frac{\partial \dot{r}_o}{\partial a_j} + \dot{r}_o \frac{\partial r_o}{\partial a_j} = \frac{\partial}{\partial a_j} (a_1 a_4 + a_2 a_5 + a_3 a_6)$$

$$r_o \frac{\partial \dot{r}_o}{\partial a_j} = \delta_{1j} a_4 + \delta_{2j} a_5 + \delta_{3j} a_6 + \delta_{4j} a_1 + \delta_{5j} a_2 + \delta_{6j} a_3 - \dot{r}_o \frac{\partial r_o}{\partial a_j}$$

$$\boxed{a_1 \frac{\partial \dot{r}_o}{\partial a_j} = \delta_{4j} a_1 + \delta_{2j} a_5}$$

The angular momentum H is given by:

$$\overline{H} = (a_2 a_6 - a_3 a_5) \hat{x}' + (a_3 a_4 - a_1 a_6) \hat{y}' + (a_1 a_5 - a_2 a_4) \hat{z}'$$

$$H^2 = (a_2 a_6 - a_3 a_5)^2 + (a_3 a_4 - a_1 a_6)^2 + (a_1 a_5 - a_2 a_4)^2$$

$$2 H \frac{\partial H}{\partial a_j} = 2 (a_2 a_6 - a_3 a_5) \frac{\partial (a_2 a_6 - a_3 a_5)}{\partial a_j}$$

$$+ 2 (a_3 a_4 - a_1 a_6) \frac{\partial (a_3 a_4 - a_1 a_6)}{\partial a_j}$$

$$+ 2 (a_1 a_5 - a_2 a_4) \frac{\partial (a_1 a_5 - a_2 a_4)}{\partial a_j}$$

$$\boxed{H = a_1 a_5}$$

$$\boxed{\frac{\partial H}{\partial a_j} = \delta_{1j} a_5 - \delta_{2j} a_4 + \delta_{5j} a_1}$$

The orbit energy E is given by:

$$2E = -\frac{2\mu}{r_o} + a_4^2 + a_5^2 + a_6^2$$

$$\boxed{2E = -\frac{2\mu}{a_1} + a_4^2 + a_5^2}$$

$$2\frac{\partial E}{\partial a_j} = 2\frac{\mu}{r_o^2}\frac{\partial r_o}{\partial a_j} + 2a_4\delta_{4j} + 2a_5\delta_{5j} + 2a_6\delta_{6j}$$

$$\boxed{\frac{\partial E}{\partial a_j} = \delta_{1j}\frac{\mu}{a_1^2} + \delta_{4j} a_4 + \delta_{5j} a_5}$$

If the orbit eccentricity is e, then,

$$r = \frac{H^2}{\mu(1 + e\cos\theta)}$$

and

$$\dot{r} = \frac{\mu e}{H}\sin\theta$$

where θ is the central angle between the vehicle and perilune. Then

$$e\cos\theta = \frac{H^2}{\mu r} - 1$$

$$e\cos\theta_o = \frac{H^2}{\mu r_o} - 1$$

$$\boxed{e\cos\theta_o = \frac{H a_5}{\mu} - 1}$$

and

$$e \sin \theta = \frac{H \dot{r}}{\mu}$$

$$e \sin \theta_o = \frac{H \dot{r}_o}{\mu}$$

$$\boxed{e \sin \theta_o = \frac{H a_4}{\mu}}$$

Then,

$$\boxed{e^2 = (e \cos \theta_o)^2 + (e \sin \theta_o)^2}$$

Also,

$$e^2 = 1 + \frac{2EH^2}{\mu^2}$$

so

$$\boxed{1 - e^2 = -2E \left(\frac{H}{\mu}\right)^2}$$

and

$$\boxed{(1 - e^2)^{1/2} = \sqrt{-2E} \left(\frac{H}{\mu}\right)}$$

$$\frac{\partial e^2}{\partial a_j} = \frac{2}{\mu^2} \left[H^2 \frac{\partial E}{\partial a_j} + E \frac{\partial H^2}{\partial a_j} \right]$$

$$\boxed{\frac{\partial e^2}{\partial a_j} = 2 \left(\frac{H}{\mu}\right)^2 \left[\frac{\partial E}{\partial a_j} + \frac{2E}{H} \frac{\partial H}{\partial a_j}\right]}$$

If the eccentricity is not zero, then θ_o can be found from:

$$\boxed{\theta_o = \tan^{-1}\left(\frac{e \sin\theta_o}{e \cos\theta_o}\right)}$$

and if the eccentricity is zero, θ_o can be arbitrarily chosen as zero. θ_o is always between $-\pi$ and π. In both cases $\sin\theta_o$ and $\cos\theta_o$ are evaluated from θ_o.

Now,

$$\frac{\partial (e \cos\theta_o)}{\partial a_j} = \frac{\partial\left(\frac{H^2}{\mu r_o} - 1\right)}{\partial a_j}$$

$$= \frac{1}{\mu}\left[r_o^{-1}\ \frac{\partial H^2}{\partial a_j} + H^2\ \frac{\partial r_o^{-1}}{\partial a_j}\right]$$

$$= \frac{H}{\mu r_o}\left[2\ \frac{\partial H}{\partial a_j} - \frac{H}{r_o}\ \frac{\partial r_o}{\partial a_j}\right]$$

$$\boxed{\frac{\partial (e \cos\theta_o)}{\partial a_j} = \frac{a_5}{\mu}\left[2\ \frac{\partial H}{\partial a_j} - \delta_{1j}\, a_5\right]}$$

and

$$\frac{\partial (e \sin\theta_o)}{\partial a_j} = \frac{\partial\left(\frac{H\dot{r}_o}{\mu}\right)}{\partial a_j}$$

$$= \frac{1}{\mu}\left[H\ \frac{\partial \dot{r}_o}{\partial a_j} + \dot{r}_o\ \frac{\partial H}{\partial a_j}\right]$$

$$\frac{\partial (e \sin \theta_o)}{\partial a_j} = \frac{a_5}{\mu} \left(a_1 \frac{\partial \dot{r}_o}{\partial a_j} \right) + \frac{a_4}{\mu} \frac{\partial H}{\partial a_j}$$

The sine and cosine of the initial eccentric anomaly $\mathcal{E}_o$ are given by:

$$\sin \mathcal{E}_o = \frac{(1 - e^2)^{1/2} \sin \theta_o}{1 + e \cos \theta_o}$$

$$\sin \mathcal{E}_o = \frac{\sqrt{-2E}}{a_5} \sin \theta_o$$

and

$$\cos \mathcal{E}_o = \frac{e + \cos \theta_o}{1 + e \cos \theta_o}$$

$$\cos \mathcal{E}_o = \frac{e + \cos \theta_o}{\left(\frac{Ha_5}{\mu} \right)}$$

$$\mathcal{E}_o = \tan^{-1} \left(\frac{\sin \mathcal{E}_o}{\cos \mathcal{E}_o} \right)$$

$\mathcal{E}_o$ is always between $-\pi$ and π. The mean anomaly at the initial condition is:

$$M_o = \mathcal{E}_o - e \sin \mathcal{E}_o$$

and the mean motion, n, is

$$\boxed{n = \frac{-2E\sqrt{-2E}}{\mu}}$$

so the time, t_o, from perilune to the initial point, T = 0, is

$$\boxed{t_o = M_o/n}$$

also,

$$\frac{\partial n}{\partial a_j} = \frac{3\,n}{2E}\,\frac{\partial E}{\partial a_j}$$

Then,

$$e \sin \xi_o = \frac{(1-e^2)^{1/2}\,(e \sin \theta_o)}{1 + e \cos \theta_o}$$

$$\frac{1}{e \sin \xi_o} \cdot \frac{\partial (e \sin \xi_o)}{\partial a_j} = \frac{\partial (1-e^2)^{1/2} / \partial a_j}{(1-e^2)^{1/2}} + \frac{\partial (e \sin \theta_o)/\partial a_j}{e \sin \theta_o}$$

$$- \frac{\partial (e \cos \theta_o)/\partial a_j}{1 + e \cos \theta_o}$$

$$\frac{\partial (e \sin \xi_o)}{\partial a_j} = \frac{-e \sin \xi_o}{2(1-e^2)}\,\frac{\partial e^2}{\partial a_j} + \frac{\sin \xi_o}{\sin \theta_o}\,\frac{\partial (e \sin \theta_o)}{\partial a_j} - \frac{e \sin \xi_o}{1 + e \cos \theta_o}\,\frac{\partial (e \cos \theta_o)}{\partial a_j}$$

$$\boxed{\frac{\partial (e \sin \xi_o)}{\partial a_j} = \frac{-e \sin \xi_o}{2(1-e^2)}\,\frac{\partial e^2}{\partial a_j} + \frac{(1-e^2)^{1/2}}{1+e \cos \theta_o}\,\frac{\partial (e \sin \theta_o)}{\partial a_j} - \frac{e \sin \xi_o}{1+e \cos \theta_o}\,\frac{\partial (e \cos \theta_o)}{\partial a_j}}$$

and

$$e \cos \mathcal{E}_o = \frac{e^2 + e \cos \theta_o}{1 + e \cos \theta_o}$$

$$\frac{\partial (e \cos \mathcal{E}_o)}{\partial a_j} = \frac{(1 + e \cos \theta_o)(\partial e^2/\partial a_j + \partial [e \cos \theta_o]/\partial a_j) - (e^2 + e \cos \theta_o)\partial (e \cos \theta_o)/\partial a}{(1 + e \cos \theta_o)^2}$$

$$\boxed{\frac{\partial (e \cos \mathcal{E}_o)}{\partial a_j} = \frac{1}{1 + e \cos \theta_o} \frac{\partial e^2}{\partial a_j} + \frac{(1 - e^2)}{(1 + e \cos \theta_o)^2} \frac{\partial (e \cos \theta_o)}{\partial a_j}}$$

Also, since

$$e^2 = (e \cos \theta_o)^2 + (e \sin \theta_o)^2$$

it follows that

$$e \, de = e \cos \theta_o \, d (e \cos \theta_o) + e \sin \theta_o \, d (e \sin \theta_o)$$

so

$$\boxed{\frac{\partial e}{\partial a_j} = \cos \theta_o \frac{\partial (e \cos \theta_o)}{\partial a_j} + \sin \theta_o \frac{\partial (e \sin \theta_o)}{\partial a_j}}$$

Since

$$\mathcal{E}_o = \tan^{-1} \left(\frac{e \sin \mathcal{E}_o}{e \cos \mathcal{E}_o} \right)$$

it follows that

$$\frac{\partial \mathcal{E}_o}{\partial a_j} = \frac{1}{1 + \tan^2 \mathcal{E}_o} \frac{e \cos \mathcal{E}_o \frac{\partial (e \sin \mathcal{E}_o)}{\partial a_j} - e \sin \mathcal{E}_o \frac{\partial (e \cos \mathcal{E}_o)}{\partial a_j}}{(e \cos \mathcal{E}_o)^2}$$

so

$$e \frac{\partial \xi_o}{\partial a_j} = \cos \xi_o \frac{\partial (e \sin \xi_o)}{\partial a_j} - \sin \xi_o \frac{\partial (e \cos \xi_o)}{\partial a_j}$$

Since

$$M_o = \xi_o - e \sin \xi_o$$

it follows that:

$$\frac{\partial M_o}{\partial a_j} = \frac{\partial \xi_o}{\partial a_j} - e \cos \xi_o \frac{\partial \xi_o}{\partial a_j} - \sin \xi_o \frac{\partial e}{\partial a_j}$$

$$= (1 - e \cos \xi_o) \frac{\partial \xi_o}{\partial a_j} - \frac{\sin \xi_o}{2e} \frac{\partial e^2}{\partial a_j}$$

$$e \frac{\partial M_o}{\partial a_j} = (1 - e \cos \xi_o) \left(e \frac{\partial \xi_o}{\partial a_j} \right) - \frac{\sin \xi_o}{2} \frac{\partial e^2}{\partial a_j}$$

At any time T after the initial observation, the time from perilune is

$$t = t_o + T$$

and the mean anomaly is

$$M = nt$$

The corresponding eccentric anomaly must be computed by solution of the equation

$$M = \xi - e \sin \xi$$

and the values of sin ξ and cos ξ found from ξ.

Then the trigonometric functions of the central angle are

$$\sin\theta = \frac{(1-e^2)^{1/2}\sin\xi}{1 - e\cos\xi}$$

and

$$\cos\theta = \frac{\cos\xi - e}{1 - e\cos\xi}$$

Now,

$$\tan\xi = \frac{\sin\xi}{\cos\xi} = \frac{(1-e^2)^{1/2}\sin\theta}{e + \cos\theta}$$

so

$$\frac{\partial\xi}{\partial a_j} = \frac{1-e\cos\xi}{(1-e^2)^{1/2}}\frac{\partial\theta}{\partial a_j} - \frac{\sin\xi}{2e(1-e^2)}\frac{\partial e^2}{\partial a_j}$$

Then from

$$M = \xi - e\sin\xi$$

it follows that

$$\frac{\partial M}{\partial a_j} = (1 - e\cos\xi)\frac{\partial\xi}{\partial a_j} - \frac{\sin\xi}{2e}\frac{\partial e^2}{\partial a_j}$$

$$= \frac{(1-e\cos\xi)^2}{(1-e^2)^{1/2}}\frac{\partial\theta}{\partial a_j} - \frac{\sin\xi}{2e}\left(\frac{1-e\cos\xi}{1-e^2} + 1\right)\frac{\partial e^2}{\partial a_j}$$

$$e\frac{\partial M}{\partial a_j} = \frac{(1-e\cos\xi)^2}{(1-e^2)^{1/2}}e\frac{\partial\theta}{\partial a_j} - \frac{\sin\xi}{2}\frac{\partial e^2}{\partial a_j} - \frac{\sin\xi(1-e\cos\xi)}{2(1-e^2)}\frac{\partial e^2}{\partial a_j}$$

Now T is not varied when the orbit parameters are so $t - t_o$ should be held constant in taking partial derivatives with respect to the orbit parameters.

$$t - t_o = (M - M_o)/n$$

and

$$\frac{\partial (t - t_o)}{\partial a_j} = \frac{\partial \left[(M-M_o)/n\right]}{\partial a_j} = 0$$

so

$$\frac{1}{n} \frac{\partial (M-M_o)}{\partial a_j} - \frac{M-M_o}{n^2} \frac{\partial n}{\partial a_j} = 0$$

$$\frac{1}{n} \frac{\partial (M-M_o)}{\partial a_j} - \frac{M-M_o}{n^2} \frac{3n}{2\Xi} \frac{\partial \Xi}{\partial a_j} = 0$$

or

$$e \frac{\partial M_o}{\partial a_j} + e \frac{3 (M-M_o)}{2\Xi} \frac{\partial \Xi}{\partial a_j} = e \frac{\partial M}{\partial a_j}$$

Setting the two expressions for $e \frac{\partial M}{\partial a_j}$ equal to one another, we find

$$e \frac{\partial \theta}{\partial a_j} = \frac{(1-e^2)^{1/2}}{(1-e\cos\xi)^2} \left\{ \frac{3(M-M_o)}{2\Xi} e \frac{\partial \Xi}{\partial a_j} + \left(e \frac{\partial M_o}{\partial a_j} \right) + \frac{\sin\xi}{2} \left(\frac{1 - e\cos\xi}{1-e^2} + 1 \right) \frac{\partial e^2}{\partial a_j} \right\}$$

Setting ξ, θ, and M equal to ξ_o, θ_o, and M_o we find

$$e\,\frac{\partial(\theta-\theta_o)}{\partial a_j} = \frac{(1-e^2)^{1/2}}{(1-e\cos\xi)^2}\left\{\frac{3\,(M-M_o)}{2E}\,e\,\frac{\partial E}{\partial a_j}+\frac{\sin\xi}{2}\left(\frac{1-e\cos\xi}{1-e^2}+1\right)\frac{\partial e^2}{\partial a_j}\right\}$$

$$-\frac{(1-e^2)^{1/2}}{(1-e\cos\xi_o)^2}\left\{\frac{\sin\xi_o}{2}\left(\frac{1-e\cos\xi_o}{1-e^2}+1\right)\frac{\partial e^2}{\partial a_j}\right\}$$

$$+(1-e^2)^{1/2}\,e\,\frac{\partial M_o}{\partial a_j}\left\{\frac{1}{(1-e\cos\xi)^2}-\frac{1}{(1-e\cos\xi_o)^2}\right\}$$

$$=\frac{(1-e^2)^{1/2}e}{(1-e\cos\xi)^2}\left\{\frac{3\,(M-M_o)}{2E}\,\frac{\partial E}{\partial a_j}+\frac{\sin\xi}{2e}\left(\frac{1-e\cos\xi}{1-e^2}+1\right)\frac{\partial e^2}{\partial a_j}\right\}$$

$$-\frac{(1-e^2)^{1/2}e}{(1-e\cos\xi_o)^2}\left\{\frac{\sin\xi_o}{2e}\left(\frac{1-e\cos\xi_o}{1-e^2}+1\right)\frac{\partial e^2}{\partial a_j}\right\}$$

$$+(1-e^2)^{1/2}e\left(e\,\frac{\partial M_o}{\partial a_j}\right)\frac{-2\cos\xi_o+e\cos^2\xi_o+2\cos\xi-e\cos^2\xi}{(1-e\cos\xi)^2(1-e\cos\xi_o)^2}$$

$$\frac{\partial(\theta-\theta_o)}{\partial a_j} = (1-e^2)^{1/2}\left\{ \frac{\frac{3(M-M_o)}{2E}\frac{\partial E}{\partial a_j} + \sin\xi\left(\frac{1-e\cos\xi}{1-e^2}+1\right)\frac{\partial e}{\partial a_j}}{(1-e\cos\xi)^2} - \frac{\sin\xi_o\left(\frac{1-e\cos\xi_o}{1-e^2}+1\right)\frac{\partial e}{\partial a_j}}{(1-e\cos\xi_o)^2} + \frac{(\cos\xi-\cos\xi_o)\left(2-e\left[\cos\xi+\cos\xi_o\right]\right)}{(1-e\cos\xi)^2(1-e\cos\xi_o)^2}\left(e\frac{\partial M_o}{\partial a_j}\right)\right.$$

Now since

$$r = \frac{H^2}{\mu(1+e\cos\theta)}$$

and

$$\dot{r} = \frac{\mu e}{H}\sin\theta$$

it follows that

$$\frac{\partial r}{\partial a_j} = 2\frac{r}{H}\frac{\partial H}{\partial a_j} - \frac{r}{1+e\cos\theta}\left[\cos\theta\frac{\partial e}{\partial a_j} - \sin\theta\left(e\frac{\partial\theta}{\partial a_j}\right)\right]$$

and

$$\frac{\partial\dot{r}}{\partial a_j} = \frac{\mu}{H}\left[\sin\theta\frac{\partial e}{\partial a_j} + \cos\theta\left(e\frac{\partial\theta}{\partial a_j}\right)\right] - \frac{\dot{r}}{H}\frac{\partial H}{\partial a_j}$$

Now

$$\sin(\theta - \theta_o) = \sin\theta\cos\theta_o - \sin\theta_o\cos\theta_o$$

$$\cos(\theta - \theta_o) = \cos\theta\cos\theta_o + \sin\theta\sin\theta_o$$

and the components of $\bar{r}$ in the x'y'z' co-ordinate system are:

$$X' = \begin{bmatrix} x' \\ y' \\ z' \end{bmatrix} = \begin{bmatrix} r\cos(\theta - \theta_o) \\ r\sin(\theta - \theta_o) \\ 0 \end{bmatrix}$$

and the components of $\dot{\bar{r}}$ in the same co-ordinates are

$$\dot{X}' = \begin{bmatrix} \dot{x}' \\ \dot{y}' \\ \dot{z}' \end{bmatrix} = \begin{bmatrix} -\frac{H}{r}\sin(\theta - \theta_o) + \dot{r}\cos(\theta - \theta_o) \\ \frac{H}{r}\cos(\theta - \theta_o) + \dot{r}\sin(\theta - \theta_o) \\ 0 \end{bmatrix}$$

The $\tilde{x}\ \tilde{y}\ \tilde{z}$ co-ordinate system is Earth-centered, non-rotating and right-handed with $\tilde{z}$ normal to the plane of the Moon's motion about the Earth and directed at an acute angle to the Earth's angular velocity vector. $\tilde{x}$ is in the direction of the Earth-Moon line at the time of the initial observation. Then the position and the velocity of the Moon with respect to the Earth are given by:

$$\tilde{X}_m = \begin{bmatrix} \tilde{x}_m \\ \tilde{y}_m \\ \tilde{z}_m \end{bmatrix} = \begin{bmatrix} \rho_m\cos\omega_m T \\ \rho_m\sin\omega_m T \\ 0 \end{bmatrix}$$

and

$$\dot{\tilde{X}}_m = \begin{bmatrix} \dot{\tilde{x}}_m \\ \dot{\tilde{y}}_m \\ \dot{\tilde{z}}_m \end{bmatrix} = \begin{bmatrix} -\omega_m \tilde{y}_m \\ \omega_m \tilde{x}_m \\ 0 \end{bmatrix}$$

in which ω_m is the angular rate of the Moon about the Earth and ρ_m is the Earth-Moon distance.

The xyz co-ordinate system is Earth-centered, right-handed and non-rotating. The z axis is in the direction of the Earth angular rotation vector and the x axis is in the plane of the prime meridian at the instant of the first observation. If λ is the observing station latitude (measured positive North) and α is the observing station longitude (measured positive East), then

$$X_d = \begin{bmatrix} x_d \\ y_d \\ z_d \end{bmatrix} = \begin{bmatrix} \rho_e \cos\lambda \cos(\omega_e T + \alpha) \\ \rho_e \cos\lambda \sin(\omega_e T + \alpha) \\ \rho_e \sin\lambda \end{bmatrix}$$

and

$$\dot{X}_d = \begin{bmatrix} \dot{x}_d \\ \dot{y}_d \\ \dot{z}_d \end{bmatrix} = \begin{bmatrix} -\omega_e y_d \\ \omega_e x_d \\ 0 \end{bmatrix}$$

in which ρ_e is the radius of the Earth and ω_e is the Earth's angular rate.

The latitude and longitude of the sub-lunar point on Earth at the instant of the first observation are L and ℓ respectively. The inclination between the plane of the orbit of the Moon about the Earth and the Earth's equator is β, as shown in Figure 1. It must be specified whether the angle γ in that figure is greater or less than $\pi/2$. Then

$$\sin \gamma = \frac{\sin L}{\sin \beta}$$

$$\cos \gamma = \begin{cases} +\sqrt{1 - \sin^2 \gamma} & \text{if } \gamma \leq \pi/2 \\ -\sqrt{1 - \sin^2 \gamma} & \text{if } \gamma > \pi/2 \end{cases}$$

$$\sin (\phi - \ell) = \tan L \cot \beta$$

$$\cos (\phi - \ell) = \frac{\cos \gamma}{\cos L}$$

$$\sin b = -\sin \beta \sin \left(\frac{\pi}{2} - \gamma \right)$$

$$\sin b = -\sin \beta \cos \gamma$$

$$\cos b = +\sqrt{1 - \sin^2 b}$$

$$\sin \nu = \frac{\tan b}{\tan \beta}$$

$$\cos \nu = \frac{\cos\left(\frac{\pi}{2} - \gamma\right)}{\cos b}$$

$$\cos \nu = \frac{\sin \gamma}{\cos b}$$

$$\cos \phi = \cos (\phi - \ell) \cos \ell - \sin (\phi - \ell) \sin \ell$$

$$\sin \phi = \sin (\phi - \ell) \cos \ell + \cos (\phi - \ell) \sin \ell$$

$$\cos (\phi + \nu) = \cos \phi \cos \nu - \sin \phi \sin \nu$$

$$\sin (\phi + \nu) = \sin \phi \cos \nu + \sin \nu \cos \phi$$

The rotation matrix K rotates vector components from the xyz system to the $\tilde{x}\tilde{y}\tilde{z}$ system.

$$K = \begin{bmatrix} K_{11} & K_{12} & K_{13} \\ K_{21} & K_{22} & K_{23} \\ K_{31} & K_{32} & K_{33} \end{bmatrix}$$

$$K_{11} = \cos L \cos \ell$$

$$K_{12} = \cos L \sin \ell$$

$$K_{13} = \sin L$$

$$K_{21} = \cos b \cos (\phi + \nu)$$

$$K_{22} = \cos b \sin (\phi + \nu)$$

$$K_{23} = \sin b$$

$$K_{31} = K_{12} K_{23} - K_{13} K_{22}$$

$$K_{32} = K_{13} K_{21} - K_{11} K_{23}$$

$$K_{33} = K_{11} K_{22} - K_{12} K_{21}$$

$$\tilde{X}_d = K X_d$$

$$\dot{\tilde{X}}_d = K \dot{X}_d$$

The rotation matrix L rotates vector components from the $\tilde{x}\ \tilde{y}\ \tilde{z}$ system to the x' y' z' system. The relative angular positions of these two co-ordinate systems are shown in Figure 2.

$$\cdot L = \begin{bmatrix} \cos\zeta & \sin\zeta & 0 \\ -\sin\zeta & \cos\zeta & 0 \\ 0 & 0 & 1 \end{bmatrix} \begin{bmatrix} 1 & 0 & 0 \\ 0 & \cos\eta & \sin\eta \\ 0 & -\sin\eta & \cos\eta \end{bmatrix} \begin{bmatrix} \cos\xi & \sin\xi & 0 \\ -\sin\xi & \cos\xi & 0 \\ 0 & 0 & 1 \end{bmatrix}$$

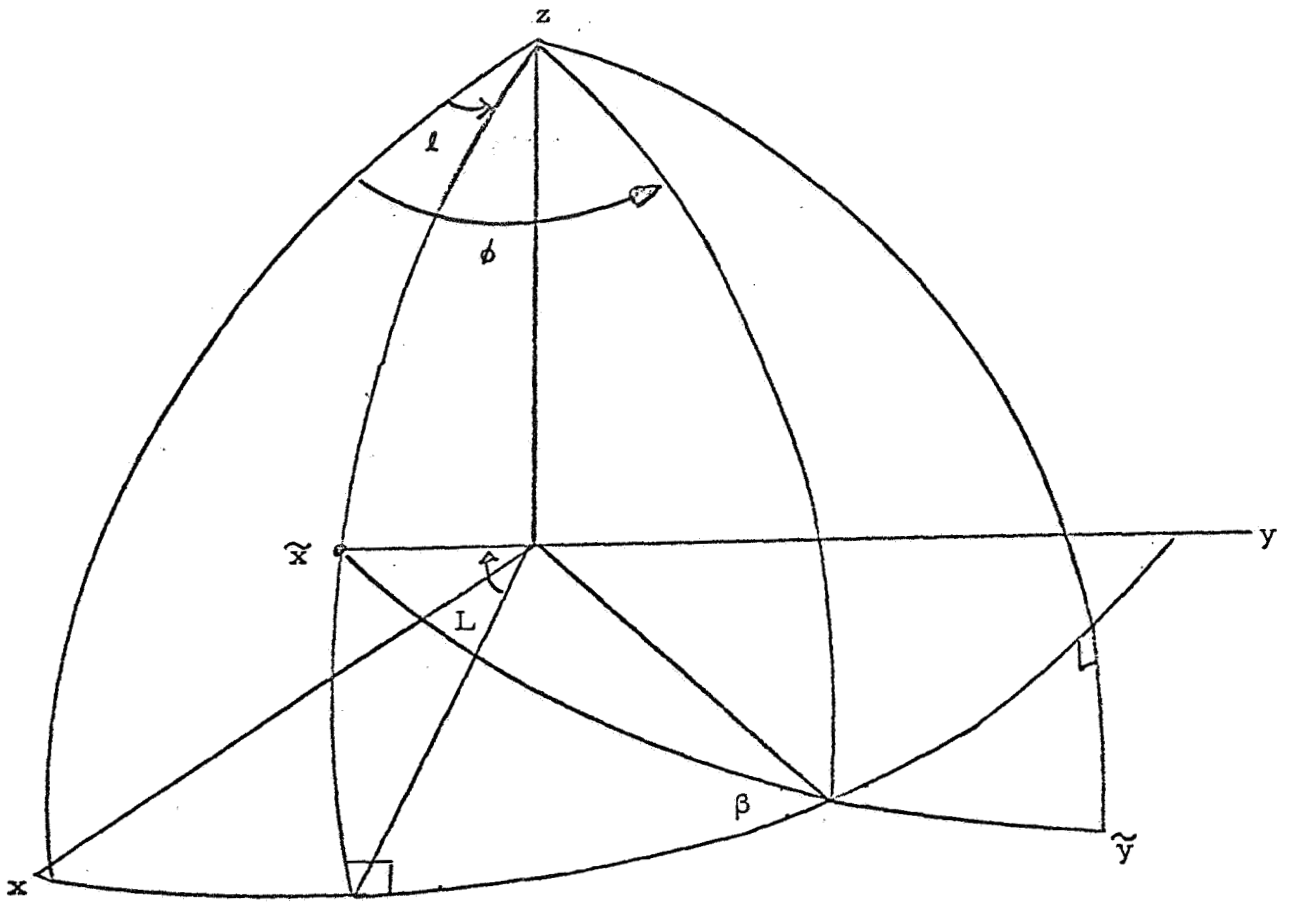

Figure 1.

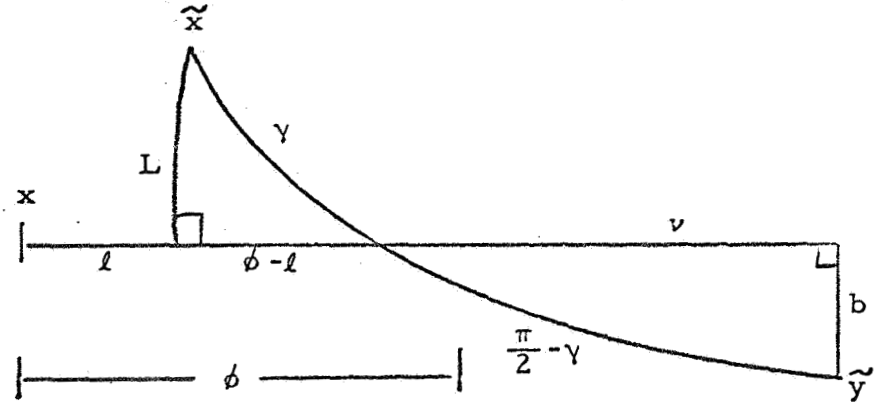

Then the vectors $\bar{s}$ and $\dot{\bar{s}}$ are

$$X'_s = \begin{bmatrix} x'_s \\ y'_s \\ z'_s \end{bmatrix} = X' + L\,(\tilde{X}_m - \tilde{X}_d)$$

and

$$\dot{X}'_s = \begin{bmatrix} \dot{x}'_s \\ \dot{y}'_s \\ \dot{z}'_s \end{bmatrix} = \dot{X}' + L\,(\dot{\tilde{X}}_m - \dot{\tilde{X}}_d)$$

$$s^2 = x'^2_s + y'^2_s + z'^2_s$$

$$\frac{\dot{s}}{s} = \frac{1}{s^2}\,(x'_s\,\dot{x}'_s + y'_s\,\dot{y}'_s + z'_s\,\dot{z}'_s)$$

Denoting the partials of X'_s and $\dot{X}'_s$ with respect to a_j by R'_j and $\dot{R}'_j$,

$$R'_j = \begin{bmatrix} \frac{\partial x'}{\partial a_j} \\ \frac{\partial y'}{\partial a_j} \\ \frac{\partial z'}{\partial a_j} \end{bmatrix} = \begin{bmatrix} -y' \dfrac{\partial\,(\theta-\theta_o)}{\partial a_j} + \cos\,(\theta - \theta_o)\,\dfrac{\partial r}{\partial a_j} \\ x' \dfrac{\partial\,(\theta - \theta_o)}{\partial a_j} + \sin\,(\theta-\theta_o)\,\dfrac{\partial r}{\partial a_j} \\ \delta_{3j}\,\dfrac{a_5 x' - a_4 y'}{H} + \delta_{6j}\,\dfrac{y'}{a_5} \end{bmatrix}$$

and

$$\dot{R}'_j = \begin{bmatrix} \frac{\partial \dot{x}'}{\partial a_j} \\ \frac{\partial \dot{y}'}{\partial a_j} \\ \frac{\partial \dot{z}'}{\partial a_j} \end{bmatrix} = \begin{bmatrix} -\left\{\ \right\}_1 \sin(\theta - \theta_o) + \left\{\ \right\}_2 \cos(\theta - \theta_o) \\ \left\{\frac{1}{r}\frac{\partial H}{\partial a_j} - \frac{H}{r^2}\frac{\partial r}{\partial a_j} + \dot{r}\frac{\partial(\theta - \theta_o)}{\partial a_j}\right\}_1 \cos(\theta - \theta_o) \\ \quad + \left\{-\frac{H}{r}\frac{\partial(\theta-\theta_o)}{\partial a_j} + \frac{\partial \dot{r}}{\partial a_j}\right\}_2 \sin(\theta-\theta_o) \\ \delta_{3j}\frac{a_5\dot{x}' - a_4\dot{y}'}{H} + \delta_{6j}\frac{\dot{y}'}{a_5} \end{bmatrix}$$

Finally,

$$\frac{\partial \dot{s}'}{\partial a_j} = \frac{1}{s}\left\{ X'^{T}_s \dot{R}'_j + \left[\dot{X}'_s - \frac{\dot{s}}{s} X'_s\right]^T R'_j \right\}$$

and

$$NC_{i,j} = \sum_{p=1}^{N} \frac{\partial \dot{s}(T_p)}{\partial a_i} \frac{\partial \dot{s}(T_p)}{\partial a_j}$$

in which T_p ($p = 1, \ldots, N$) are the times of the N measurements, T_p being zero at the initial measurement.

The covariance matrix of the parameters is simply

$$\left[\text{cov } a_i\ a_j\right] = \sigma^2 \left[NC_{i,j}\right]^{-1}$$

in which σ^2 is the mean square Gaussian error in the measurements.

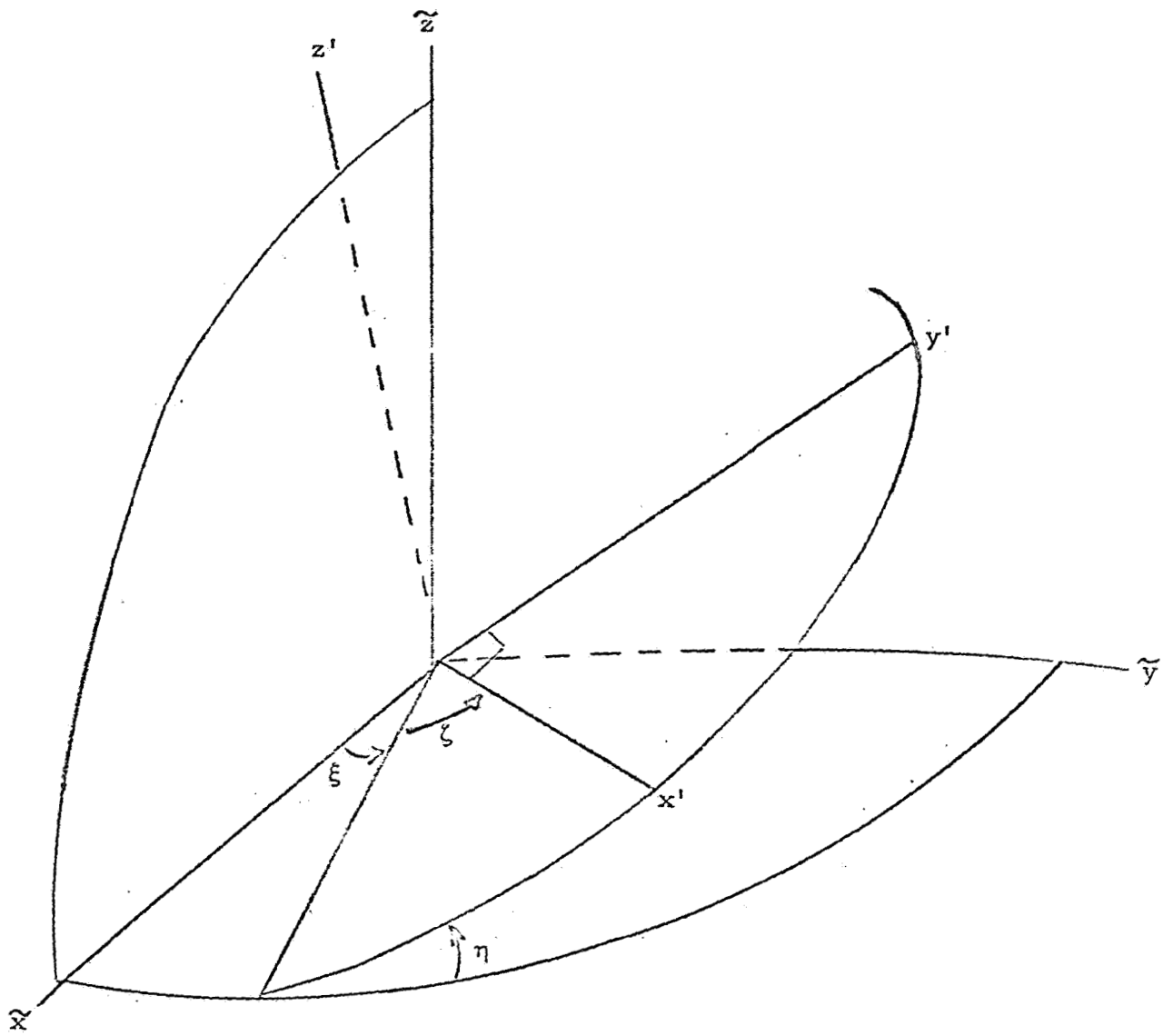

Figure 2.

APOLLO NOTE NO. 83

H. Engel
18 July 1963

USE OF RANGE AND RANGE RATE DATA

Range Only

From Apollo Note No. 43, if the measured quantities, f(t), have a fixed bias, b, and a zero mean stationary Gaussian noise, n(t), impressed, then

$$f_m(t) = f_c(t) + b + n(t)$$

and

$$\text{cov}\,(a_i, a_j) = \sigma^{-2}\,(NC)^{-1} \qquad i,j=1,\ldots,7$$

in which σ^{-2} is the variance of the Gaussian noise,

$$f_c(t) = f_c\,(t,\ a_1,\ldots,a_M, b)$$

$$NC_{i,j} = \sum_{k=1}^{N} \frac{\partial f_c\,(t_k)}{\partial a_i} \frac{\partial f_c\,(t_k)}{\partial a_j} \qquad i,j=1,\ldots,6$$

$$NC_{7,j} = NC_{j,7} = \sum_{k=1}^{N} \frac{\partial f_c\,(t_k)}{\partial a_j} \qquad j=1,\ldots,6$$

and

$$NC_{7,7} = N$$

Now, if the quantity measured is the range from the DSIF or MSFN station to the vehicle orbiting the Moon, then from Apollo Note No. 82,

$$\bar{s} = \bar{X}_m - \bar{X}_d + \bar{r}$$

$$s^2 = \bar{s} \cdot \bar{s}$$

$$s \frac{\partial s}{\partial s_j} = \bar{s} \cdot \frac{\partial \bar{s}}{\partial a_j}$$

$$= \bar{s} \cdot \frac{\partial \bar{r}}{\partial a_j}$$

or

$$\frac{\partial f_c}{\partial a_j} \triangleq \frac{\partial s}{\partial a_j} = \frac{1}{s} \bar{s} \cdot \frac{\partial \bar{r}}{\partial a_j} .$$

Now, expressions for s, $\bar{s}$, and $\frac{\partial \bar{r}}{\partial a_j}$ are available from Apollo Note No. 82, so it is simple (in theory) to determine the covariance matrix of orbit parameters and radar range bias using this note and Apollo Note No. 82.

Range and Range Rate

From Apollo Notes No. 43 and 82, the likelihood function of the data is:

$$L = \frac{1}{(2\pi)^{\frac{N_1+N_2}{2}} \sigma_R^{N_1} \dot{\sigma}_R^{N_2}} \exp(-\mathcal{L})$$

in which N_1 is the number of range measurements, N_2 the number of range rate measurements, and

$$\mathcal{L} = \frac{1}{2\sigma_R^2} \sum_{k=1}^{N_1} \left[R_m(k) - R_c(a_i, k) - b \right]^2$$

$$+ \frac{1}{2\dot{\sigma}_R^2} \sum_{\ell=1}^{N_2} \left[\dot{R}_m(\ell) - \dot{R}_c(a_i, \ell) \right]^2$$

To obtain the covariance of the most likely a_i's and b, set $\partial \mathcal{L}/\partial a_i$ and $\partial \mathcal{L}/\partial b$ equal to zero, and, assuming N_1 and N_2 are sufficiently great, obtain a set of seven equations linear in the random perturbation quantities Δa_i and Δb.

This leads to:

$$C_{i,j} = \frac{1}{\sigma_R^2} \sum_{k=1}^{N_1} \frac{\partial R_c(k)}{\partial a_i} \frac{\partial R_c(k)}{\partial a_j} + \frac{1}{\dot{\sigma}_R^2} \sum_{\ell=1}^{N_2} \frac{\partial \dot{R}_c(\ell)}{\partial a_i} \frac{\partial \dot{R}_c(\ell)}{\partial a_j} \quad ; i,j = 1, \ldots, 6$$

$$C_{7,j} = C_{j,7} = \frac{1}{\sigma_R^2} \sum_{k=1}^{N_1} \frac{\partial R_c(k)}{\partial a_j}$$

$$C_{7,7} = \frac{N_1}{\sigma_R^2}$$

and

$$\text{cov}\,(a_i, a_j) = C^{-1} \qquad i,j = 1, \ldots, 7$$

APOLLO NOTE NO. 84

L. Horowitz
17 July 1963

NOTES ON L. S. PONTRYAGIN'S THEORY OF OPTIMAL PROCESSES (II)

INTRODUCTION

The previous note on this topic (Apollo Note No. 76) sketched Soviet Academician L. S. Pontryagin's method of optimal control synthesis for linear problems. It was shown that optimal controls for this case were step functions assuming their extreme values almost everywhere. The linear position servo problem was then solved to illustrate the technique, and restriction to the linear case emphasized as the factor limiting general applicability of this method.

Further work by Soviet Academician L. I. Rozonoer has generalized this method to the case of non-linear payoff functions by an extension of the Pontryagin theory.* Rozonoer shows that there exists a function H of the state and control variable of the system with the property that its absolute extrema completely characterize optimal selection of the control functions. This paper sketches Rozonoer's results heuristically and shows it a straightforward matter to apply this formulation to non-linear problems. Illustrative examples are given. Finally, it is shown that although formal relations defining optimal controls for non-linear problems can now be written directly, a two-point boundary value simultaneous non-linear differential system has to be solved in general. Thus, it appears that a computer will have to be utilized to generate optimal controls for non-linear cases.

Pontryagin Maximum Principle: Following Apollo Note No. 76, we consider the transfer of a vehicle between two points with boundary conditions specified. Bounded control functions $u_i(t)$ are available to mechanize the transfer—we wish to select the "optimum" controls $u_i(t)$ providing the most "economical" transfer (the criterion for optimality may be economy

* L. I. Rozonoer, Pontryagin Maximum Principle in the Theory of Optimum Systems, Avtomat. i Telemekh. 20, (1959)

of fuel, time, hazard, etc., or even a "weighted" combination thereof). The equations of motion are

$$\dot{x}_i = f_i(x_1, \cdots, x_n; u_1, \cdots, u_r); \; i = 1, 2, \cdots, n, \quad (1)$$

where the x_i are generalized coordinates in the phase space of the problem. We take the bounded control functions $u_i(t)$ as normalized:

$$\left|u_i(t)\right| \leq 1, \quad t \geq t_o .$$

Initial conditions are given:

$$x_i(t_o) = x_i^o$$

$$\dot{x}_i(t_o) = \dot{x}_i^o$$

A final condition is also given:

$$x_i(t_f) = x_i^f$$

$$\dot{x}_i(t_f) = \dot{x}_i^f$$

for some t_f. We wish to select the $u_i(t)$ $\left(\left|u_i(t)\right| \leq 1\right)$ so as to minimize t_f. (This assumes we are interested only in time economy; only a minor modification is needed to minimize (maximize) some other state variable or linear combination thereof).

To illustrate the Pontryagin Maximum Principle, consider first the case of Equation (1), linear in the state variables:

$$\dot{\underline{x}} = A\underline{x} + \underline{b}_1 u_1 + \cdots + \underline{b}_r u_r \quad (2)$$

as in Equation (3), of Apollo Note No. 76. We have already shown that for this linear case, optimal controls are given by

$$\boxed{u_i(t) = \operatorname{sign}\left[\underline{\psi}(t) \cdot \underline{b}_i\right]} \tag{3}$$

as in Apollo Note No. 76 (12). Here,

$$\underline{\psi}(t) = \sum_{\alpha} c_\alpha \underline{\psi}^\alpha(t),$$

where $\underline{\psi}^\alpha(t)$ generate the fundamental system of solutions to the corresponding homogeneous adjoint equation

$$\dot{\underline{\psi}} = -A' \underline{\psi} \tag{4}$$

(A' is the adjoint (conjugate transpose) of A and c_α are constants defined by the boundary conditions).

Following Rozonoer, we can now produce a new function H of the state variables x_i and the control variables u_i which assumes absolute extrema when and only when optimal $u_i(t)$ have been selected. Then, once we know how to write this function H (it will be shown that this is a simple and straightforward matter), we need only locate the zeros of $\frac{\partial H}{\partial u_i}$ to determine the optimal controls. Generalization to the non-linear case will complete the problem.

We first note that $\underline{\psi}(t) \cdot \dot{\underline{x}}(t) \equiv$ constant as shown on page 10 of Apollo Note No. 76. Further,

$$\underline{\psi}(t) = \sum_{\alpha} \underline{\chi}(t) \cdot \underline{\phi}_\alpha(t) \underline{\psi}^\alpha(t)$$

by definition (page 10, Apollo Note No. 76) where $\underline{\phi}_\alpha \underline{\psi}^\alpha$ is the tensor identity element (by the normalization of $\underline{\phi}_\alpha$ and $\underline{\psi}^\alpha$) and $\underline{\chi}(t)$ is the outward normal to the convex set $\Omega(t)$, as illustrated in Figure 3, page 7, of Apollo Note No. 76. It is clear on physical grounds that the angle between the outward normal $\underline{\chi}(t)$ and the velocity vector $\dot{\underline{x}}(t)$ never exceeds $\pi/2$.

$$\boxed{\dot{\underline{x}}(t) \cdot \underline{\psi}(t) = \text{constant} \geq 0} \; . \qquad (5)$$

We now define the function H by

$$\boxed{H = \underline{\psi}(t) \cdot \dot{\underline{x}}(t)} \; ; \qquad (6)$$

by (5), it is a non-negative constant when optimal controls are used (since we are then on the boundary $\partial\Omega$ of $\Omega(t)$ as shown in Figure 3 of Apollo Note No. 76). We can now show that the function H does indeed possess the advertised property; viz., that it assumes an absolute extremum when optimal controls $u_i(t)$ are used. For by using (2) in (6) (assuming only one control $u_i(t)$ for the moment), we have

$$H = \underline{\psi}(t) \cdot A\underline{x}(t) + \underline{\psi}(t) \cdot \underline{b}\, u(t) \geq 0 \; . \qquad (7)$$

By (3), we have already shown that optimal controls require $u(t) = \text{sign}\left(\underline{b} \cdot \underline{\psi}(t)\right)$. Hence, $\underline{\psi}(t) \cdot \underline{b}\, u(t) = \underline{\psi}(t) \cdot \underline{b}\ \text{sign}\left(\underline{b} \cdot \underline{\psi}(t)\right) \geq 0$, so that H does in fact assume an absolute extremum when the optimal $u(t)$ is chosen. This argument extends inductively to the case of multiple controls, so that optimal control synthesis precisely corresponds to maximizing H.

Before proceeding to the non-linear case, we first see how H is formed for the general linear case. Taking the optimization problem (1) with boundary conditions specified, we introduce new variables p_i by

$$\boxed{\dot{p}_i(t) = -\sum_{j=1}^{n} p_j(t)\, \frac{\partial f_j}{\partial x_i}} \qquad (8)$$

(These $p_i(t)$ are just the variables of the adjoint equation (4), since with the matrix A taken as $A = \{a_{ij}\}$ where $a_{ij} = \frac{\partial f_i}{\partial x_j}$; (assumed constant for the linear case). then $A' = a_{ji} = \frac{\partial f_j}{\partial x_i}$; just the transpose of A for the case of real coefficients). Denote the variable to be optimized (the "payoff function", as it is sometimes called) by S. Introducing new

variables if necessary, S can always be written as a linear combination of the state variables x_i:

$$\boxed{S = \sum_{i=1}^{n} c_i \, x_i(T)} \, . \tag{9}$$

Here, T is the time required for execution of the transfer; it may or may not be specified (if T itself is to be optimized, simply introduce the new state variable x_{n+1} by the relation $\dot{x}_{n+1} = 1$; then $S = x_{n+1}$. See page 3 of Apollo Note No. 76 for further illustrations). Since (8) is a first order differential system in the p_i, we are free to impose a boundary condition—the obvious one is

$$\boxed{p_i(T) = -c_i \, ; \quad i = 1, \cdots, n} \quad , \tag{10}$$

where the c_i are given by (9). The function H is then just

$$\boxed{H = \sum_{i=1}^{n} p_i(t) \, \dot{x}_i(t)} \, , \tag{11}$$

precisely as in (6), where $\dot{x}_i = f_i(x_1, \cdots, x_n ; u_1, \cdots, u_r)$ as in (1). Differentiating (11) with respect to p_i yields

$$\boxed{\dot{x}_i = \frac{\partial H}{\partial p_i}} \, . \tag{12}$$

Further, differentiating (11) with respect to x_i yields

$$\boxed{\dot{p}_i = - \frac{\partial H}{\partial x_i}} \qquad \text{by (8)} \tag{13}$$

with the boundary conditions $x_i(0) = x_i^{\circ}$ and $p_i(T) = -c_i$; $i = 1, 2, \cdots, n$. Note that (12) and (13) are precisely Hamilton's equations for the generalized coordinates x_i and p_i.

Application of the Maximum Principle

To apply this principle to a specific problem, we take the case governed by equations of motion linear in the control variables $u_i(t)$:

$$\dot{x}_i = f_i(x_1, \cdots, x_n) + \sum_{k=1}^{r} b_{ik}\, u_k(t)\,; \; i = 1, \cdots, n. \tag{14}$$

Boundary conditions are: $x_i(0) = x_i^\circ$, $\dot{x}_i(0) = \dot{x}_i^\circ$. We take the control functions to be bounded by 1:

$$\left| u_i(t) \right| \leq 1 .$$

By (11), the H-function for this system is

$$H = \sum_{i=1}^{n} p_i\, f_i + \sum_{i=1}^{n} \sum_{k=1}^{r} b_{ik}\, p_i\, u_k \tag{15}$$

Then by the Maximum Principle, optimal controls are achieved by maximizing (minimizing) H, which simply means choosing the u_k so that

$$\boxed{u_k(t) = \operatorname{sign}\left[\sum_{i=1}^{n} b_{ik}\, p_i(t) \right]}, \tag{16}$$

precisely as argued on page 4 of this note. Kopp points out that if $\sum_{i=1}^{n} b_{ik}\, p_i(t)$ happens to vanish identically, then the payoff function

$S = \sum_i c_i\, x_i$ is insensitive to the particular control variable $u_k(t)$.*

Note that the payoff function $S = \sum c_i\, x_i$ appears in the problem through boundary values selected for the adjoint variables $p_i(t)$: $p_i(T) = -c_i$; $i = 1, \cdots, n$, where T is the time required for the transfer.

* Optimization Techniques, edited by G. Leitman, Academic Press, 1962, p. 274.

Generalization to the Non-Linear Case

The proof of the Maximum Principle given in this note rests on the development of optimal controls $u_i(t)$ given by (16):

$$u_k(t) = \text{sign}\left[\sum_{i=1}^{n} b_{ik}\, p_i(t)\right]. \qquad (16)$$

This relation was in turn obtained from the convex properties of the loci of accessible terminal points in phase space, all as argued in Apollo Note No. 76. Fundamental in this argument was the linearization of the equations of motion (3) of Apollo Note No. 76, since this established the convexity of these loci (page 6 of Apollo Note No. 76) and hence (16) of this note.

The basis for this linearization was the truncation of the Taylor Series for f_i:

$$\Delta f_i\,(x_1, \cdots, x_n) = \sum_{j=1}^{n} \frac{\partial f_i}{\partial x_j}\,\Delta x_j + \frac{1}{2}\sum_{k=1}^{n}\sum_{\ell=1}^{n} \frac{\partial^2 f_i}{\partial x_k \partial x_\ell}\,\Delta x_k\,\Delta x_\ell$$

$$+ \cdots\cdots, \qquad (17)$$

where we assume that over sufficiently small intervals of time, the higher order increments $\Delta x_k\,\Delta x_\ell \cdots\cdots$ can be neglected in proving that the Maximum Principle (16) still obtains over each small increment Δt.* Hence, H assumes an extremum at each point of the trajectory and hence holds the extremum everywhere. Thus, a necessary condition for optimization of the payoff function S is always that the H-function attain an extremum with respect to the control vector $\underline{u} = (u_1, \cdots, u_r)$, provided only that the equations of motion are linear in the control functions u_i. No linearity in the state variables x_i is assumed; only the existence of the mixed partial derivatives of (17).

* For a more thorough discussion of this result, see Leitman (loc. cit., p. 260) and Boltyanskii, Theory of Optimal Processes, Izvest. Akad. Nauk S.S.S.R. Ser. Mat. 24, 3 - 43 (1960).

Conclusions

Optimal controls $u_i(t)$ optimizing (1) together with indicated boundary conditions have been shown to be fully characterized by absolute extrema of the H-function (11). This criterion is usable provided only that the equations of motion are linear in the controls (as in (14)) and that the mixed partials of f_i with respect to the state variables exist. Once the H-function is formed (as in (15)), the u_i are selected so as to maximize H. This is the Pontryagin Maximum Principle.

The next Apollo Note on this topic shows how optimum thrust control is obtained for a variable-mass vehicle being transferred between two points in phase space in a three dimensional central gravitational field in such a way as to minimize fuel expenditure. Other problems under consideration include:

(i) Optimum transfer through hazardous regions (Van Allen belts)

(ii) Optimum thrust regulation to obtain desired reentry dive angle

(iii) Optimum transfer with fixed probability of safe return.

APOLLO NOTE NO. 85

J. Holdsworth
22 July 1963

THE EQUIVALENCE OF DATA PROCESSING SCHEMES IN A LINEARIZED ERROR ANALYSIS

The purpose of this note is to demonstrate rigorously the statistical equivalence of certain pairs of data processing schemes under the assumption of a linear propagation of random errors in the estimators of certain orbital parameters.

First, we consider that we are observing a time series $\dot{R}_m(t)$ which may be represented as:

$$\dot{R}_m(t) = \dot{R}_c(a_1, \ldots a_6, t) + n(t) \tag{1}$$

where n(t) is a white stationary zero mean gaussian process with variance σ_n^2. We assume that we know the functional dependence of $\dot{R}_c(a_1 \ldots a_6, t)$ on the orbit parameters a_i. Then, on the basis of N_1 pieces of data $\dot{R}_m(1), \ldots \dot{R}_m(N_1)$, where $N_1 \geq 6$, we compute the maximum likelihood estimates $\hat{a}_1, \ldots \hat{a}_6$ of the parameters $a_1, \ldots a_6$.

Apollo Note No. 43 gives a method for computing the covariance matrix of the errors in the estimators of the parameters as a function of the noise variance σ_n^2 and the number of independent observations N_1. It will be recalled that the analysis in that note was based upon the assumption that the number of pieces of data N_1 was sufficiently large so that the following linearization was valid:

$$\dot{R}_c(\hat{a}_1, \ldots \hat{a}_6, t) = \dot{R}_c(a_1, \ldots a_6, t) + \sum_{i=1}^{6} \frac{\partial \dot{R}_c}{\partial a_i}(a_1, \ldots a_6, t)\, \Delta\hat{a}_i \tag{2}$$

where

$$\Delta\hat{a}_i = \hat{a}_i - a_i.$$

Let $\Delta\hat{a}$ denote the column estimator error vector whose components are: $\hat{a}_i - a_i$ for $i = 1, 2, \ldots 6$. It was shown in Apollo Note No. 43 that

the covariance matrix of the estimator errors is given by:

$$\text{Cov}\left(\Delta\hat{\underline{a}}\,(N_1)\right) = \sigma_n^2\, C^{-1}\,(N_1) \tag{3}$$

where the i, jth element of the matrix C is given by:

$$C_{i,j}(N_1) = \sum_{k=1}^{N_1} \frac{\partial \dot{R}_c}{\partial a_i}(a_1,..a_6,t_k)\,\frac{\partial \dot{R}_c}{\partial a_j}(a_1,..a_6,t_k) \tag{4}$$

Furthermore, if the parameters were estimated on the basis of $N_1 + N_2$ observations we would have

$$\text{Cov}\left(\Delta\hat{\underline{a}}\,(N_1+N_2)\right) = \sigma_n^2\, C^{-1}\,(N_1+N_2) \tag{5}$$

where:

$$C_{i,j}\,(N_1+N_2) = \sum_{k=1}^{N_1+N_2} \frac{\partial \dot{R}_c}{\partial a_i}(a_1,\ldots a_6,t_k)\,\frac{\partial \dot{R}_c}{\partial a_j}(a_1,..a_6,t_k)$$

$$= \sum_{k=1}^{N_1} \frac{\partial \dot{R}_c}{\partial a_i}(a_1,..a_6,t_k)\,\frac{\partial \dot{R}_c}{\partial a_j}(a_1,..a_6,t_k)$$

$$+ \sum_{k=N_1+1}^{N_2} \frac{\partial \dot{R}_c}{\partial a_i}(a_1,\ldots,a_6,t_k)\,\frac{\partial \dot{R}_c}{\partial a_j}(a_1,\ldots a_6,t_k). \tag{6}$$

In Equations (3) -(6), we have made the dependence of the covariance matrices upon the smoothing times notationally explicit by writing $\mathrm{Cov}\left(\Delta \hat{\hat{a}}\,(N_1)\right)$.. etc.

Now assume that N_1 observations are made first and that an estimator vector $\hat{\hat{a}}\,(N_1)$ is computed from the observations $\dot{R}_m\,(t_1)\ldots.$ $\dot{R}_m(t_{N_1})$, where the ith component of the estimator vector $\hat{\hat{a}}\,(N_1)$ is the maximum likelihood estimate of a_i. Then it follows from what has been said that the covariance matrix of the estimator vector $\hat{\hat{a}}\,(N_1)$ is given by the expression in (3).

Next assume that the same parameters are to be estimated from N_2 observations $\dot{R}_m\,(t_{N_1+1})\ldots.$, $\dot{R}_m(t_{N_1+N_2})$ without the knowledge of $\dot{R}_m\,(t_1)\ldots.\dot{R}_m\,(t_{N_1})$. Denote the resulting estimator vector based upon $\dot{R}_m\,(t_{N_1+1})\ldots\dot{R}_m\,(t_{N_1+N_2})$ by $\hat{\hat{a}}\,(N_2)$. Then if N_2 is sufficiently large so that the linearization in (2) holds, we may write:

$$\mathrm{Cov}\left(\Delta \hat{\hat{a}}\,(N_2)\right) = \sigma_n^2\, C^{-1}\,(N_2) \tag{7}$$

where:

$$C_{i,j}\,(N_2) = \sum_{k=N_1+1}^{N_1+N_2} \frac{\partial \dot{R}_c}{\partial a_i}\,(t_k)\ \frac{\partial \dot{R}_c}{\partial a_j}\,(t_k) \tag{8}$$

It is important to note that the estimator vector $\hat{\hat{a}}\,(N_2)$ was computed without assuming that the computed value of the estimator vector $\hat{\hat{a}}\,(N_1)$ was known and conversely. What we wish to show is that knowing only the computed estimator vectors $\hat{\hat{a}}\,(N_1)$ and $\hat{\hat{a}}\,(N_2)$ allows us to form a new estimator vector of the parameters such that the resultant accuracy is the same as if we were able to make the total number, N_1+N_2, of observations $\dot{R}_m(t_1)\ldots\dot{R}_m(t_{N_1})$, $\dot{R}_m\,(t_{N_1+1})\ldots$ $\dot{R}_m(t_{N_1+N_2})$ first and then estimate the parameters.

To show this, we assume that we have computed $\hat{\hat{a}}\,(N_1)$ and $\hat{\hat{a}}\,(N_2)$ as described above. Knowing the estimator vectors $\hat{\hat{a}}\,(N_1)$ and

$\hat{a}(N_2)$, we define the new estimator vector $\tilde{a}(N_1, N_2)$ by:

$$\tilde{a}(N_1, N_2) = \mathrm{Cov}\left(\Delta\hat{a}(N_1+N_2)\right)\left[\mathrm{Cov}^{-1}\left(\Delta\hat{a}(N_1)\right)\hat{a}(N_1) + \mathrm{Cov}^{-1}\left(\Delta\hat{a}(N_2)\right)\hat{a}(N_2)\right]. \tag{9}$$

Note that the new estimator $\tilde{a}(N_1, N_2)$ is obtained from linear operations on the vectors $\hat{a}(N_1)$ and $\hat{a}(N_2)$, and that $\tilde{a}(N_1, N_2)$ depends upon the observed data only through the estimator vectors $\hat{a}(N_1)$ and $\hat{a}(N_2)$. The proof of our assertion will consist of showing that:

$$\mathrm{Cov}\left(\Delta\tilde{a}(N_1, N_2)\right) = \mathrm{Cov}\left(\Delta\hat{a}(N_1+N_2)\right) \tag{10}$$

If we let a denote the column vector whose ith component is a_i, then subtracting a from both sides of (9) yields the following expression for the estimator error vector $\Delta\tilde{a}(N_1, N_2)$.

$$\Delta\hat{a}(N_1, N_2) = \mathrm{Cov}\left(\Delta\hat{a}(N_1+N_2)\right)\left[\mathrm{Cov}^{-1}\left(\Delta\hat{a}(N_1)\right)\Delta\hat{a}(N_1) + \mathrm{Cov}^{-1}\left(\Delta\hat{a}(N_2)\right)\Delta\hat{a}(N_2)\right] \tag{11}$$

The covariance matrix of the estimator errors $\Delta\tilde{a}(N_1, N_2)$ is given by:

$$\mathrm{Cov}\left(\Delta\tilde{a}(N_1, N_2)\right) = E\left[\Delta\tilde{a}(N_1, N_2)\left(\Delta\tilde{a}(N_1, N_2)\right)^T\right] \tag{12}$$

where T denotes matrix transposition and E is the expected value operator which is integration over the observation space with respect to the joint distribution of the components of $\Delta\hat{a}(N_1)$ and $\Delta\hat{a}(N_2)$. Using the symmetry of the matrix $\mathrm{Cov}\left(\Delta\hat{a}(N_1+N_2)\right)$ we may explicitly write:

$$\mathrm{Cov}\left(\Delta\tilde{a}(N_1, N_2)\right) = \mathrm{Cov}\left(\Delta\hat{a}(N_1+N_2)\right)\left[\mathrm{Cov}^{-1}\left(\Delta\hat{a}(N_1)\right) + \mathrm{Cov}^{-1}\left(\Delta\hat{a}(N_2)\right)\right]\mathrm{Cov}\left(\Delta\hat{a}(N_1+N_2)\right) \tag{13}$$

where in (13) we have used the fact that the maximum likelihood error

vectors $\Delta\hat{\hat{a}}(N_1)$, $\Delta\hat{\hat{a}}(N_2)$ are independently distributed with asymptotically multivariate normal distribution with zero means so that terms of the form:

$$E\left\{ Cov^{-1}\left(\Delta\hat{\hat{a}}(N_1)\right)\Delta\hat{\hat{a}}(N_1)\left(\Delta\hat{\hat{a}}(N_2)\right)^T Cov^{-1}\left(\Delta\hat{\hat{a}}(N_2)\right)\right\} = 0 \qquad (14)$$

thus yielding (13).

However, from Equations (4), (6), and (8), we see that:

$$Cov^{-1}\left[\Delta\hat{\hat{a}}(N_1+N_2)\right] = Cov^{-1}\left[\Delta\hat{\hat{a}}(N_1)\right] + Cov^{-1}\left[\Delta\hat{\hat{a}}(N_2)\right] \qquad (15)$$

so that

$$Cov\left(\Delta\tilde{\tilde{a}}(N_1,N_2)\right) = Cov\left(\Delta\hat{\hat{a}}(N_1+N_2)\right) \qquad (16)$$

which proves our assertion.

Intuitively we may say that a priori distributional knowledge obtained from prior observations has a modifying effect on our later data so that the effective sample size is increased. It is worthwhile to note that if the noise is auto-correlated, then quantities such as the expression given by (14) will not in general vanish and our assertion will no longer be true.

Next we consider the following situation. We assume that observations are made as before over a given interval of time -- say $\dot{R}_m(t_1), \ldots \dot{R}_m(t_N)$. On the basis of these observations we wish to estimate the values of the components of the position and velocity vectors at some initial time t = 0. Let these quantities be denoted by $x_i(0)$ where i = 1, ... 6.

The value of the quantities $x_i(t)$ at an arbitrary time t depends upon the quantities $x_i(0) \ldots x_i(0)$ and conversely. Thus there exist relations of the form:

$$x_i(t) = f_i\left(x_1(0), \ldots x_6(0)\, t\right) \qquad i=1, \ldots 6 \qquad (17)$$

and

$$x_i(0) = g_i\left(x_1(t), \ldots x_i(t)\right)$$

Having originally estimated the quantities $x_i(0)$ from our observations we may use (17) to predict values for the $x_i(t)$ based upon the estimators $\hat{x}_1(0) \ldots \hat{x}_2(0)$. Because of errors in the estimator state vector $\hat{x}(0)$, there will also be errors in the predicted quantities $\tilde{x}_1(t) \ldots \tilde{x}_2(t)$. Since:

$$\Delta \tilde{x}_i(t) = \sum_{k=1}^{6} \frac{\partial f_i}{\partial x_n(0)} \Delta x_n(0) \tag{18}$$

Then:

$$\Delta \tilde{x}_i(t) \, \Delta \tilde{x}_j(t) = \sum_{\ell=1}^{6} \sum_{k=1}^{6} \frac{\partial f_i}{\partial x_n(0)} \frac{\partial f_j}{\partial x_\ell(0)} \Delta x_k(0) \, \Delta x_\ell(0). \tag{19}$$

From (19) we see that the predicted covariance matrix for the quantities $\tilde{x}_i(t)$ may be written

$$\text{Cov} \left(\Delta \tilde{x}(t) \right) = J \; \text{Cov} \left(\Delta \hat{x}(0) \right) \; J^T \tag{20}$$

where J is the Jacobian matrix whose i, jth element is $\frac{\partial f_i}{\partial x_j(0)}$.

On the other hand, instead of first estimating $x_i(0)$ from the data and then predicting ahead to the $\tilde{x}_i(t)$ on the basis of the estimators $\hat{x}_i(0)$, we could have estimated the $x_i(t)$ quantities directly from the data. Let these direct estimates be denoted by $\hat{x}_i(t)$. We wish to show that under the assumptions of a linear propagation of errors that the two methods are equivalent, i.e., that

$$\text{Cov} \left(\Delta \hat{x}(t) \right) = \text{Cov} \left(\Delta \tilde{x}(t) \right) \tag{21}$$

To do this we recall that the i, jth element of the inverse of the matrix Cov $(\Delta \hat{x}(t)$ is given by:

$$\hat{C}_{i,j} = \frac{1}{\sigma_n^2} \sum_{k=1}^{N} \frac{\partial \dot{R}_c(t_k)}{\partial x_i(t)} \frac{\partial \dot{R}_c(t_k)}{\partial x_j(t)} \tag{22}$$

On the other hand, from Equation (20), the inverse of Cov $\left(\Delta \tilde{x}(t) \right)$ may be written:

$$\mathrm{Cov}^{-1}\left(\Delta\tilde{x}(t)\right) = \left(J^{T}\right)^{-1}\,\mathrm{Cov}^{-1}\left(\Delta\hat{x}(0)\right)\,J^{-1} \tag{23}$$

Since the inverse of the Jacobian matrix is the matrix whose i, jth element is $\frac{\partial g_i}{\partial x_j(t)}$ and since the i, jth element of $\mathrm{Cov}^{-1}\left(\Delta x(0)\right)$ is

$$\frac{1}{\sigma^2}\sum_{k=1}^{N}\frac{\partial \dot{R}_c(t_k)}{\partial x_i(0)}\;\frac{\partial \dot{R}_c(t_k)}{\partial x_j(0)}$$

then it follows that the i, jth element of $\mathrm{Cov}^{-1}\left(\Delta\tilde{x}(t)\right)$ may be written:

$$\tilde{C}_{i,j} = \frac{1}{\sigma^2}\sum_{\ell=1}^{6}\sum_{m=1}^{6}\sum_{n=1}^{N}\frac{\partial g_\ell}{\partial x_i(t)}\;\frac{\partial \dot{R}_c(t_n)}{\partial x_\ell(0)}\;\frac{\partial \dot{R}_c(t_n)}{\partial x_m(0)}\;\frac{\partial g_m}{\partial x_j(t)} \tag{24}$$

However, for fixed k, we note that

$$\sum_{\ell=1}^{6}\frac{\partial g_\ell}{\partial x_i(t)}\;\frac{\partial \dot{R}_c(t_n)}{\partial x_\ell(0)} = \frac{\partial \dot{R}_c(t_n)}{\partial x_i(t)}$$

and (25)

$$\sum_{m=1}^{6}\frac{\partial g_m}{\partial x_i(t)}\;\frac{\partial \dot{R}_c(t_n)}{\partial x_m(0)} = \frac{\partial \dot{R}_c(t_n)}{\partial x_j(t)}$$

thus: $\hat{C}_{i,j} = \tilde{C}_{i,j}$ and

$$\mathrm{Cov}\left(\Delta\tilde{x}(t)\right) = \mathrm{Cov}\left(\Delta\hat{x}(t)\right) \tag{26}$$

which completes the proof of equivalence.

APOLLO NOTE NO. 86

L. Horowitz
22 July 1963

OPTIMAL CONTROL THROUGH HAZARDOUS REGION IN A 3-DIMENSIONAL GRAVITATIONAL FIELD

INTRODUCTION

The Pontryagin Maximum Principle was sketched in Apollo Note No. 84 where the problem of optimum transfer of a vehicle between two points in phase space was considered. It was shown that under very general conditions there exists a point function H on the state variables x_i and the control variables u_i with the property that its absolute extrema completely characterize the desired optimal control functions $u_i(t)$.

This paper considers an American Rocket Society presentation (August 7-9, 1961) dealing with the Maximum Principle as it applies to the optimal control of a variable-mass vehicle moving in a central gravitational field.* It is shown that application of the maximum principle to the optimal selection of control functions yields a simultaneous system of non-linear two-point boundary value differential equations whose solution defines the desired optimal controls.

An interesting feature of this technique is that the "payoff function" to be optimized appears as an eclectic combination of the state variables with "weighting constants" chosen to best define the optimization criteria. We assume a maximum time T is specified for the transfer, as dictated by the maximum tolerable time in a hazardous radiation region.

SOLUTION OF THE PROBLEM

The following application of the Pontryagin Maximum Principle is essentially that of the American Rocket Society Conference (D. Lukes) presentation previously cited. Applications of the Pontryagin Maximum

---

* ARS Guidance, Control and Navigation Conference, Stanford, California August 7 - 9, 1961: Pontryagin Maximum Principle presented by D. Lukes

Principle are given in terms of references to Apollo Note Nos. 76 and 84.

Symbols used:

x_1, x_3, x_5: rectangular coordinates

$x_2 = \dot{x}_1$

$x_4 = \dot{x}_3$

$x_6 = \dot{x}_5$

x_7: mass

u_1, u_2, u_3: components of thrust

u_4: mass flow rate

c: constant exhaust velocity

G: gravitational constant

$||X|| = \sqrt{x_1^2 + x_3^2 + x_5^2}$

T: time to effect transfer

Equations of motion (84 - 1):

$$\dot{x}_1 = x_2$$

$$\dot{x}_3 = x_4$$

$$\dot{x}_5 = x_6$$

$$\dot{x}_2 = \frac{c u_1 u_4}{x_7} - \frac{G x_1}{||X||}$$

$$\dot{x}_4 = \frac{c u_2 u_4}{x_7} - \frac{G x_3}{||X||}$$

$$\dot{x}_6 = \frac{c u_3 u_4}{x_7} - \frac{G x_5}{\|X\|}$$

$$\dot{x}_7 = -u_4$$

Admissible controls (76-7):

$$u_1^2 + u_2^2 + u_3^2 = 1, \qquad 0 \le u_4 \le B$$

Payoff function:

We wish to satisfy the end conditions $x_i(T) = x_i^T$; $i = 1, 2, \cdots, 6$ and also minimize the net fuel expenditure $\int_0^T u_4(\tau)\, d\tau$. Thus D. Lukes suggests that the payoff function to be minimized is

$$S = x_8(T) = \sum_{i=1}^{6} \frac{1}{2} \lambda_i \left(x_i - x_i^T\right)^2 + \lambda_7 \int_0^T u_4(\tau)\, d\tau \qquad (1)$$

where λ_i are non-negative arbitrary weighting constants. Thus, we introduce the additional equation of motion

$$\dot{x}_8 = \sum_{i=1}^{6} \lambda_i \left(x_i - x_i^T\right) \dot{x}_i + \lambda_7 u_4 \qquad (2)$$

Adjoint variables:

Introduce $p_i(t)$: $\dot{p}_i = -\sum_{j=1}^{8} p_j \frac{\partial \dot{x}_j}{\partial x_i}$ by (84-8),

where $p_i(T) = 0$, $i = 1, 2, \cdots, 7$; $p_8(T) = -1$.

Pontryagin H-Function (84-11)

$$H = \sum_{i=1}^{8} p_i \dot{x}_i \qquad (3)$$

$$= \frac{c\, u_4}{x_7} \left[\underline{P} \cdot \underline{u} - \frac{x_7}{c} (p_7 + \lambda_7) \right] +$$

$$\left[p_1 - \lambda_1 (x_1 - x_1^T) \right] x_2 + \left[p_3 - \lambda_3 (x_3 - x_3^T) \right] x_4$$

$$+ \left[p_5 - \lambda_5 (x_5 - x_5^T) \right] x_6 - \frac{G\, \underline{P} \cdot \underline{X}}{\|X\|^3}$$

where $\underline{u} = (u_1, u_2, u_3)$

$\underline{X} = (x_1, x_3, x_5)$

$\underline{P} = \left(\left[p_2 - \lambda_2 (x_2 - x_2^T) \right], \left[p_4 - \lambda_4 (x_4 - x_4^T) \right], \left[p_6 - \lambda_6 (x_6 - x_6^T) \right. \right.$

and we define

$$\|P\| = \sqrt{\underline{P} \cdot \underline{P}} .$$

APPLICATION OF THE MAXIMUM PRINCIPLE

We wish to minimize $S = x_8(T)$. By the Pontryagin Maximum Principle (84-7), H must be maximized with respect to u. By examination of (3), we clearly require $\underline{u}$ to be parallel to $\underline{P}$ and select $u_4 = B$ when $\|P\| - \frac{x_7}{c} (p_7 + \lambda_7) > 0$, $= 0$ otherwise. Thus, the optimum controls (call them u_i^*) are:

$$u_1^* = \frac{\left| p_2 - \lambda_2 \left(x_2 - x_2^T \right) \right|}{\| P \|}$$

$$u_2^* = \frac{\left| p_4 - \lambda_4 \left(x_4 - x_4^T \right) \right|}{\| P \|}$$

$$u_3^* = \frac{\left| p_6 - \lambda_6 \left(x_6 - x_6^T \right) \right|}{\| P \|} \qquad (4)$$

$$u_4^* = \begin{cases} B, & \| P \| - \frac{x_7}{c} \left(p_7 + \lambda_7 \right) > 0 \\ 0, & \text{otherwise} \end{cases}$$

Denote u_4^* by B(t).

Optimization equations:

We calculate the adjoint equations from (84-13):

$$\dot{p}_i = - \frac{\partial H}{\partial x_i}$$

and obtain the desired simultaneous system:

$$\dot{x}_1 = x_2$$

$$\dot{x}_2 = \frac{c\,B(t)\left[p_2 - \lambda_2 (x_2 - x_2^T)\right]}{x_7 \|P\|} - \frac{G\,x_1}{\|X\|^3}$$

$$\dot{x}_3 = x_4$$

$$\dot{x}_4 = \frac{c\,B(t)\left[p_4 - \lambda_4 (x_4 - x_4^T)\right]}{x_7 \|P\|} - \frac{G\,x_3}{\|X\|^3}$$

$$\dot{x}_5 = x_6$$

$$\dot{x}_6 = \frac{c\,B(t)\left[p_6 - \lambda_6 (x_6 - x_6^T)\right]}{x_7 \|P\|} - \frac{G\,x_5}{\|X\|^3}$$

$$\dot{x}_7 = -B(t)$$

$$\dot{p}_1 = \lambda_1 x_2 + \frac{G}{\|X\|^3}\left(\left[p_2 - \lambda_2 (x_2 - x_2^T)\right] - \frac{3(\underline{P}\cdot\underline{X})\,x_1}{\|X\|^2}\right)$$

$$\dot{p}_2 = \lambda_2 \dot{x}_2 - \left[p_1 - \lambda_1 (x_1 - x_1^T)\right]$$

$$\dot{p}_3 = \lambda_3 x_4 + \frac{G}{\|X\|^3}\left(\left[p_4 - \lambda_4 (x_4 - x_4^T)\right] - \frac{3(\underline{P}\cdot\underline{X})\,x_3}{\|X\|^2}\right)$$

$$\dot{p}_4 = \lambda_4 \dot{x}_4 - \left[p_3 - \lambda_3 (x_3 - x_3^T)\right]$$

$$\dot{p}_5 = \lambda_5 x_6 + \frac{G}{\|X\|^3}\left(\left[p_6 - \lambda_6 (x_6 - x_6^T)\right] - \frac{3(\underline{P}\cdot\underline{X})\,x_5}{\|X\|^2}\right)$$

$$\dot{p}_6 = \lambda_6 \dot{x}_6 - \left[p_5 - \lambda_5 (x_5 - x_5^T)\right]$$

$$\dot{p}_7 = \frac{c\,B(t)\,\|P\|}{x_7^2}$$

As pointed out by D. Lukes, equation (2) can be dropped from the system once u^* has been determined, so the remaining problem is to solve the preceding non-linear simultaneous system with the boundary conditions

$$x_i(0) = x_i^o$$

$$p_i(T) = 0$$

for $i = 1, 2, \cdots, 7.$

The required controls $u_i^*(t)$ are then given by (4).

CONCLUSIONS

For optimal transfer through hazardous radiation regions, (4) provides optimal control for a variable mass vehicle traveling in a 3-dimensional gravitational field. The constants λ_i appearing in the payoff function (1) may be chosen to provide the best balance between minimum fuel consumption and maximum "terminal point" precision, where by terminal condition we mean the specified end condition in phase space.

APOLLO NOTE NO. 87 26 July 1963

RENDEZVOUS AIDS

1. RENDEZVOUS ERRORS WITH IMU AND OPTICAL SYSTEM

G. F. Floyd

In this section we assume that everything is working normally except the LEM radar. That is, the IMU, AGC and on-board optical system are functioning normally but there is no way to measure relative CSM/LEM range or range rate.

According to MIT Report E1212, IMU Error Data for Apollo Trajectories, p. 63, the 1 σ uncertainty in LEM velocity at the end of the lunar take-off trajectory will be 2.31 ft/sec. It is then reasonable to assume that on the basis of the long time available for CSM orbit determination, the error in CSM velocity at any time will be the order of 1 ft/sec. Therefore, at the end of the lunar take-off, if we assume that the LEM AGC is programmed to keep track of both LEM and CSM positions and velocities, the uncertainty in LEM/CSM relative range would be about

$$\sqrt{(2.3)^2 + (1.0)^2} \approx 3 \text{ ft/sec.}$$

?? = 2.5 ft/sec

This error will propagate on essentially a 1:1 basis during the 180° coast towards rendezvous, so as the LEM entered the terminal rendezvous stage, the inertially generated error in relative vector range rate (closing vector velocity) will still be about 3 ft/sec. At this time the closing velocity will be the order of 150 ft/sec., and the error in the inertially computed relative range may be several miles, leading to an error in the inertially predicted direction of the line-of-sight of perhaps 10° and the predicted line-of-sight is about 20° away from the relative velocity vector (see Grumman LMO-500-22, Figure 1, p. 6). Then the inertially predicted (1 σ) range rate error would be $150 (\cos 20^\circ - \cos 30^\circ) \simeq 150 (.94 - .86) = 150 (.08) = 12$ ft/sec.

However, with the use of the optical sight, the astronaut can accurately determine the real line-of-sight direction and with this information, the AGC can resolve the computed $\dot{\bar{r}}$ vector along the actual line-of-sight. In this case the error in the scalar $\dot{r}$ will involve only the error in the magnitude of $\dot{\bar{r}}$ and this has a 1 σ of 3 ft/sec.

Thus, with the inertial system and computation of CSM/LEM relative position, and the use of the angle pointing data in the computer, we would expect 1 σ errors in $\dot{r}$ during terminal phase of 3 ft/sec., hence 3 σ errors of 9 ft/sec. In addition, the inertial range data will be wrong by several miles and so not of much help.

The conclusion is then that the inertial, optical r and $\dot{r}$ data will not be satisfactory for docking and some assistance is needed.

2. WAYS OF USING DSIF IN TERMINAL RENDEZVOUS NAVIGATION

H. Engel

There are many ways in which the ground stations might be used to assist in the terminal phase of lunar rendezvous in the absence of a radar on board either of the two vehicles.

The parameters characterizing these techniques are the number of ground stations employed, the utilization of boost T/M data from the vehicles, the use of angular information from the vehicles and the use of ring-around. The angular information referred to is the direction relative to inertial space of the line-of-sight between the vehicles, determined optically using either the IMU or celestial objects for a reference system.

The discussion here is limited to the terminal portion of lunar rendezvous. In this terminal portion, the range between the two vehicles is assumed to be less than two nautical miles and the principal quantities of interest are the relative range and relative range rate.

Four second smoothing gives range and range rate of one vehicle from the observing station with standard deviations of 30 m and 0.1 m/sec., respectively.

As only the terminal phase of rendezvous is considered here, the CM/SM is assumed visible and the LEM capable of maintaining the line-of-sight angular rate zero without ground assistance.

Number of Stations	Boo T/M	Angular Information	Ring-Around	
1		✓		The simplest system uses only one ground station and a prescribed terminal rendezvous maneuver. It requires that the LEM place itself in line with the CM/SM and the Earth, either closer or farther from the Earth than the CM/SM, and by boosting normal to the line-of-sight preserve this configuration. In this situation, the ground station can determine the relative range and range rate in a very short time. Assuming that the CM/SM orbit is known, the relative range rate can be determined to 0.1 m/sec. in 4 seconds and the relative range to 10 m in half a minute. If the CM/SM orbit is not known accurately, then using transponders on both vehicles simultaneously, the relative range rate can be determined to 0.15 m/sec. in 4 seconds and the relative range to 14 m in half a minute. The propellant cost of this maneuver must still be calculated, but it certainly would seem to be within the 10% pad.
1	✓			If boosts are performed only in accordance with instructions from Earth or if the LEM transmits its estimates of the magnitude of such boosts, then the ground station(s) can use past observations together with estimates of the boost performed to obtain new values for relative range and relative range rate. This case has not yet been analyzed.
1				Using only ground station range and range rate rendezvous can be accomplished, but only with a <u>great</u> increase in the time required. In this mode it is necessary to observe the vehicle(s) for a significant fraction of an orbit following any boost to obtain relative velocity of 0.1 m/sec. Just how long these observations must be performed has not been determined.

Number of Stations	Boost T/M	Angular Information	Ring-Around	
IV 1		✓		If the LEM is required to drive the line-of-sight rate to zero, using the IMU or a celestial reference system, and transmits the direction of the line-of-sight to the ground, then the value of the ground assistance in terminal rendezvous is strongly dependent on the angle between the line-of-sight between the vehicles and the line-of-sight from the Earth to the CM/SM. If this angle is 0 or π, the situation is the same as the first case described. If this angle is approximately $\pi/2$, the relative range and range rate estimates are degraded by a factor of the order of 50 even when using three observing 4000 n. mi. apart simultaneously ($50 \approx$ [Earth-Moon Distance] / [Station Separation]).
IV 1	✓	✓		If the line-of-sight direction is transmitted to the ground, and if boosts are performed in accordance with instructions or telemetered to the ground, the ground can use this and past observation data to determine relative range and range rate to better accuracy than with boost telemetry alone.
1			✓	Using ring-around with one DSIF station, the relative range and range rate should be determined to better than 60 m and 0.2 m/sec. in 4 seconds, the errors decreasing inversely as the square root of the observation time.

3. RELATIVE RANGE AND RANGE RATE ERRORS USING THREE OBSERVING DSIF STATIONS

H. Engel

For this analysis an optimum configuration of vehicle and observing station is assumed, as shown in the accompanying figure.

Letting S_i be the distance from station i to a vehicle,,

$$S_i^2 = \sum_{j=1}^{3} (x_j - x_{ji})^2$$

$$S_i \, \delta S_i = \sum_{j=1}^{3} (x_j - x_{ji}) (\delta x_j - \delta x_{ji})$$

$$\sum_{j=1}^{3} (x_j - x_{ji}) \, \delta x_j = S_i \, \delta S_i + \sum_{j=1}^{3} (x_j - x_{ji}) \, \delta x_{ji}$$

Because of the symmetry of the chosen configuration, it is only necessary to consider errors in the location of one station and errors in measurement of one range and one range rate.

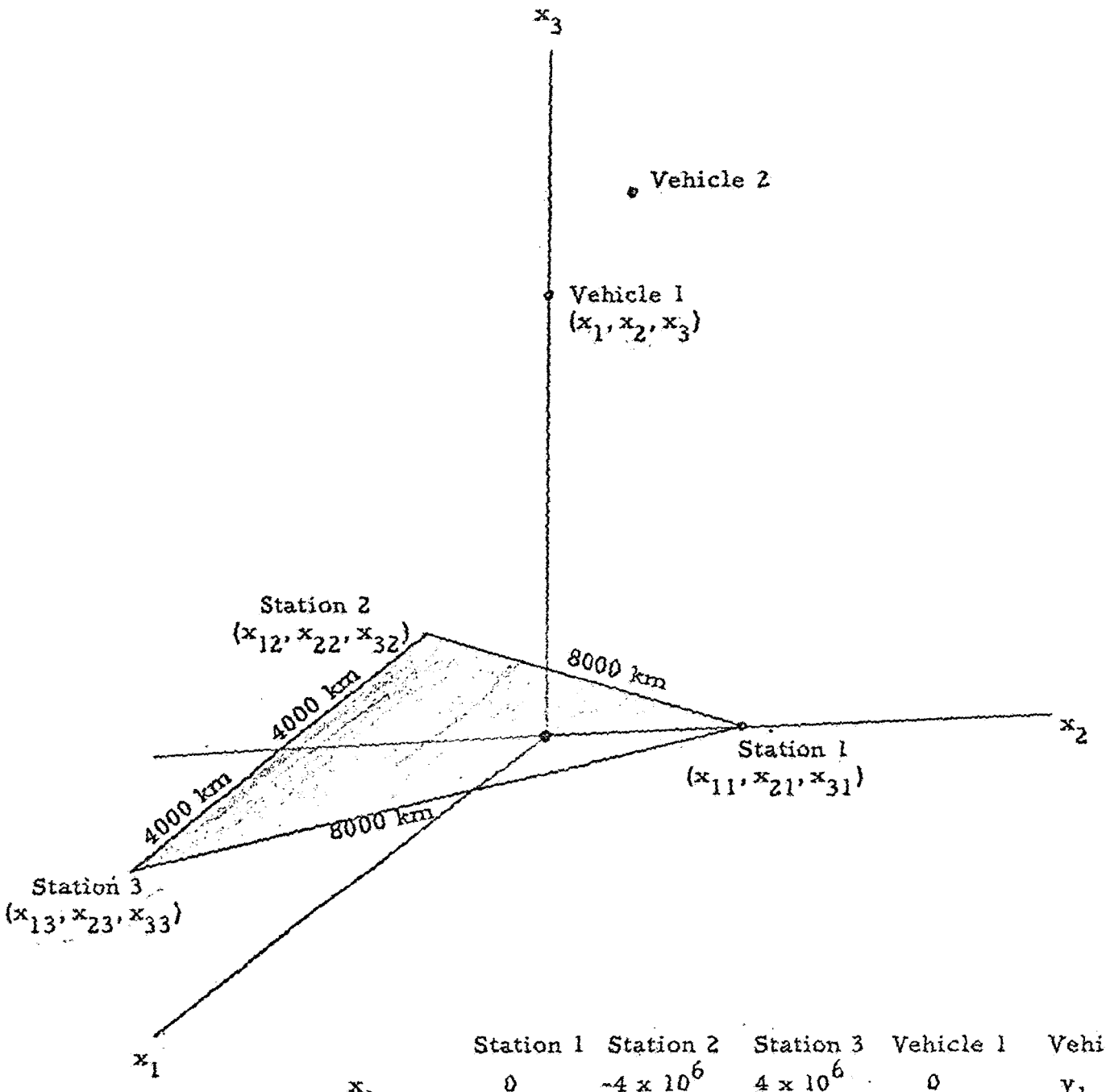

	Station 1	Station 2	Station 3	Vehicle 1	Vehicle 2
x_1	0	-4×10^6	4×10^6	0	y_1
x_2	$\frac{8 \times 10^6}{\sqrt{3}}$	$\frac{-4}{\sqrt{3}} \times 10^6$	$\frac{-4}{\sqrt{3}} \times 10^6$	0	y_2
x_3	0	0	0	4×10^8	$4 \times 10^8 + y_3$

(meters)

Considering errors $\delta x_{11}, \delta x_{21}, \delta x_{31}$ in the position of station 1,

$$0\,\delta x_1 - x_{21}\delta x_2 + x_3\,\delta x_3 = 0\,\delta x_{11} - x_{21}\,\delta x_{21} + x_3\,\delta x_{31}$$

$$-x_{12}\,\delta x_1 - x_{22}\delta x_2 + x_3\,\delta x_3 = 0$$

$$-x_{13}\,\delta x_1 - x_{23}\,\delta x_2 + x_3\,\delta x_3 = 0$$

Using the facts that $x_{22} = x_{23}$ and $x_{12} = -x_{13}$, we find from the second and third equations that

$$\delta x_1 = 0.$$

$$\delta x_2 = \frac{x_3}{x_{22}}\,\delta x_3$$

From the first equation, then,

$$\delta x_3 = \frac{x_{22}\,(x_3\,\delta x_{31} - x_{21}\,\delta x_{21})}{x_3\,(x_{22} - x_{21})}$$

and then,

$$\delta x_2 = \frac{x_3\,\delta x_{31} - x_{21}\,\delta x_{21}}{(x_{22} - x_{21})}$$

δx_2 is obviously far larger than δx_3, and δx_2 is primarily dependent on δx_{31}. Substituting in values,

$$\delta x_2 \approx \frac{-4 \times 10^8}{\frac{4}{\sqrt{3}} \times 10^6 + \frac{8 \times 10^6}{\sqrt{3}}}\,\delta x_{31}$$

$$\delta x_2 = -\frac{1}{\sqrt{3}}(10^2)\,\delta x_{31} = -57.7\,\delta x_{31}$$

For the second vehicle, the same equations may be written, substituting $\delta x_j + \delta y_j$ for δx_j and $x_j + y_j$ for x_j. Subtracting one set of these equations from the other, the errors in vector range between the two vehicles, resulting from an error in station position can be found.

$$\delta y_1 = 0$$

$$\delta y_2 = \frac{y_1 \delta x_{11} + y_2 \delta x_{21} + y_3 \delta x_{31}}{x_{22} - x_{21}}$$

$$\delta y_3 = \frac{x_{22} - y_2}{x_3 + y_3} \left[\delta y_2 - \frac{(x_{22} y_3 + x_3 y_2)}{(x_{22} - y_2)} \frac{(x_3 \delta x_{31} - x_{21} \delta x_{21})}{x_3 (x_{22} - x_{21})} \right]$$

The error in y_2 is proportional to the component of station position error in the direction of y. Calling X_1 the magnitude of the position error of station 1,

$$\left| \delta y_2 \right| \leq \left| \frac{X_1 y}{x_{22} - x_{21}} \right| = \frac{\sqrt{3}}{1.2} \times 10^{-7} X_1 y$$

and is very small compared to y even for station position errors of 100 m. Then,

$$\delta y_3 \approx \frac{x_{22}}{x_3} \left[\delta y_2 - \frac{x_3 y_2 \delta x_{31}}{x_{22} (x_{22} - x_{21})} \right]$$

$$= \frac{x_{22}}{x_3} \delta y_2 - \frac{y_2}{x_{22} - x_{21}} \delta x_{31} \approx - \frac{y_2}{x_{22} - x_{21}} \delta x_{31}$$

$$\left| \delta y_3 \right| < \frac{\sqrt{3}}{1.2} \times 10^{-7} X_1 y$$

Thus station position errors are of no importance in determining

the relative position of the two vehicles.

Now consider the case of an error in the measurement of S_1,

$$0\delta x_1 - x_{21}\,\delta x_2 + x_3\,\delta x_3 = S_1\,\delta S_1 \approx x_3\,\delta S_1$$

$$-x_{12}\,\delta x_1 - x_{22}\,\delta x_2 + x_3\,\delta x_3 = 0$$

$$-x_{13}\,\delta x_1 - x_{23}\,\delta x_2 + x_3\,\delta x_3 = 0$$

These equations lead to

$$\delta x_1 = 0$$

$$\delta x_2 = \frac{x_3}{3x_{22}}\,\delta S_1$$

$$\delta x_3 = \frac{1}{3}\,\delta S_1$$

The largest error is δx_2. Substituting values,

$$\delta x_2 = \frac{1}{3}\,\frac{4 \times 10^8}{\frac{4}{\sqrt{3}} \times 10^6}\cdot \delta S_1$$

$$= \frac{1}{\sqrt{3}} \times 10^2\,\delta S_1 = 57.7\,\delta S_1$$

If the error in S_1 is 30 m, the error in x_2 is 173 m. In this case, the position errors for the second vehicle are independent, so for like errors in the measurement of S for the two vehicles the error in range between them will be of the order of 150 m. Thus, a single set of range

observations from three ground stations cannot determine the relative position of the two vehicles with sufficient accuracy for the terminal phase of lunar rendezvous.

For velocity errors we proceed as follows.

$$S_i^2 = \sum_{j=1}^{3} (x_j - x_{ji})^2$$

$$S_i \dot{S}_i = \sum_{j=1}^{3} (x_j - x_{ji})\, \dot{x}_j$$

$$\delta S_i \dot{S}_i + S_i \delta\dot{S}_i = \sum_{j=1}^{3} (\delta x_j - \delta x_{ji})\, \dot{x}_j + \sum_{j=1}^{3} (x_j - x_{ji})\, \delta\dot{x}_j$$

Now, considering only an error in $\dot{S}_1$,

$$0\ \delta\dot{x}_1 - x_2,\ \delta\dot{x}_2 + x_3\ \delta\dot{x}_3 = S_1\ \delta S_1 \approx x_3\ \delta S_1$$

$$-x_{12}\ \delta\dot{x}_1 - x_{22}\ \delta\dot{x}_2 + x_3\ \delta\dot{x}_3 = 0$$

$$-x_{13}\ \delta\dot{x}_1 - x_{23}\ \delta\dot{x}_2 + x_3\ \delta\dot{x}_3 = 0$$

it follows that

$$\delta\dot{x}_1 = 0$$

$$\delta\dot{x}_2 = \frac{x_3}{3x_{22}}\ \delta\dot{S}_1$$

$$\delta\dot{x}_3 = \frac{1}{3}\ \delta\dot{S}_1$$

The largest error is $\delta \dot{x}_2$. By substitution

$$\delta \dot{x}_2 = 57.7 \delta \dot{S}_1$$

If $\delta \dot{S}_1$ is 0.1 m/sec, then $\delta \dot{x}_2$ is 5.77m/sec. or about 20 ft/sec.(1 σ) which is far more than the allowable rendezvous impact velocity of 0.3 m/sec. (1 ft/sec). Hence, it does not appear that with a single set of range and range rate measurements from three ground stations the ground can direct the terminal phase of rendezvous.

Compared with the results of Section 1, we note that the on-board inertial with optical tracking calculated $\dot{r}$ to about 3 ft/sec. or better than the above value by a factor of 6.

4. ITEMS FOR FURTHER STUDY — H. Engel

The computation procedure described in Apollo Note No. 82 has been programmed and is currently being debugged. With this program it is possible to determine the covariance matrix of orbit parameters for various times of observation following any boost, assuming no a priori data, and using only range rate from one observing station. This will show whether under these conditions the IMCC can provide data for LEM midcourse corrections.

In accordance with the discussion in Apollo Note No. 83, this program with minor modifications can make the same determinations on the basis of range or independent range and range rate from one station.

Further, accordingly, the Apollo Note No. 77, minor changes in the program will permit the same computations to be performed on the basis of data from more than one ground station.

Still further, Apollo Note No. 77 indicates how minor changes in the program can be made to permit the inclusion of a priori date such as LEM position prior to takeoff and telemetered or voice-communicated boost data. Such data can also include nominal or telemetered midcourse boosts or boosts near rendezvous.

The analysis necessary to adapt the program to using angle measurements has not yet been performed.

The computations to be performed, using the "standard" ascent trajectory, are as follows:

1. Using range rate from one ground station, with no a priori information, determines orbit parameter accuracy as a function of total time LEM is visible.

2. Using range and range rate from one ground station, with no a priori information, determine orbit parameter accuracy as a function of total time LEM is visible.

3. Using range rate (and perhaps range) from two and three ground stations, with no a priori information, determine orbit parameter accuracy as a function of total time LEM is visible.

4. Repeat 1, 2, and 3 as necessary including a priori values of position velocity and covariance of these quantities at the end of boost. This will greatly improve the accuracy with which the position and velocity can be determined by the ground at a later time.

5. Repeat 4 including a priori (or telemetered) values of mid-course corrections and boost at the apolune of the Hohmann ascent trajectory to determine how well ground can compute position and velocity as LEM again becomes visible:

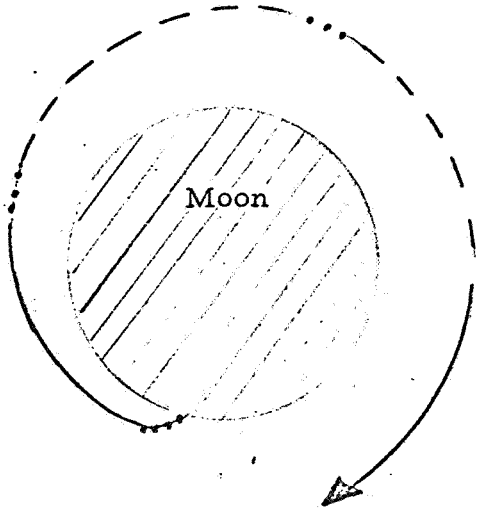

Solid Line = LEM visible

Dashed Line = LEM not visible

Dots = Boosts

6. Continue 5 with small telemetered boosts to determine how well the ground can assist in the terminal (docking) stage of rendezvous.

In addition to these computations an analysis will be performed to determine how long actual orbit calculations will take; that is, answers will be sought to the questions:

1. How long can the LEM be observed with the requirement that the observations be reduced and the trajectory data transmitted to the LEM before it is occultated by the Moon?

2. Can observations be reduced rapidly enough for the ground to be useful in aiding the terminal phase of rendezvous?

It appears that the Kalman-Schmidt method should be used in orbit determination in order to keep the processing time down. This is being investigated.

5. SOME "RING-AROUND" TECHNIQUES FOR DETERMINATION OF THE SCALAR RANGE AND RANGE RATE

H. Epstein

This portion is devoted to two basic techniques to quickly establish scalar range and range rate. Ring-around systems involving the DSIF and the use of other radar equipment available in the LEM are considered here.

The frequencies of interest for the CM transponder has been extracted from the unified S-band equipment specification for the CM. The normal mode is indicated below.

Normal Mode

Non-Coherent Mode	Crystal Frequency	$= \frac{2282.5}{120} = 19.0208333$ mc.
Coherent Mode	Frequency Received from DSIF	$= 2106.2$ mc. $(2287.5 \times \frac{221}{240})$
	Transponder Transmitted Frequency	$= 2282.5$ mc.

We will assume that the requirement exists for simultaneous communications between the DSIF and both spacecraft. We will further consider that essentially two transmitters (and possibly antenna systems) exist at each DSIF station. With the present frequency allocation, we will also assume that the CM/SM transponder will transmit at 2287.5 mc. for both modes and the LEM in both modes at 2282.5 mc. The corresponding DSIF frequencies are taken as approximately 2106.2 mc. and 2101.6 mc., respectively.

A. Ring-Around Systems For Scalar Range and Range Rate Between CM and LEM During Terminal Position of Rendezvous

Two basic types of ring-around systems are considered for this application. The first, in terms of measurements and computations made on earth and the second, by computations in the LEM. The basic geometry is indicated below. It should be indicated that this technique requires only one DSIF station to be employed.

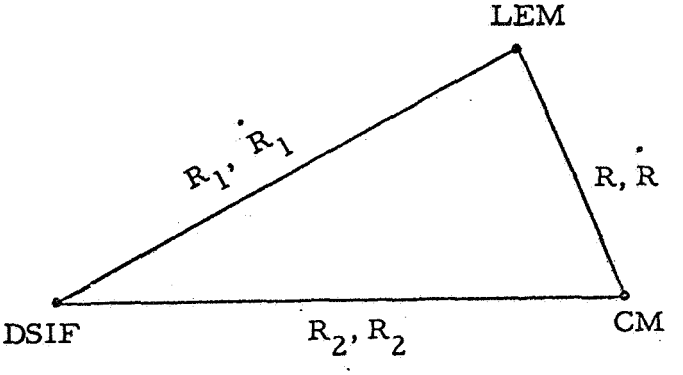

Prior measurements on the CM can be assumed sufficiently accurate that precise values for R_2 and $\dot{R}_2$ are known.

Case I. Earth Computation of R and $\dot{R}$

Let $R_3 = R_1 + R_2 + R$

and $\dot{R}_3 = \dot{R}_1 + \dot{R}_2 + \dot{R}$

then $R = R_3 - R_1 - R_2$

and $\dot{R} = \dot{R}_3 - \dot{R}_1 - \dot{R}_2$

One implementation for this technique would involve an additional transponder in either the LEM or the CM. The operation would be as follows.

Considering that the additional transponder is placed in the LEM - the DSIF would interrogate the LEM and measure R_1 and $\dot{R}_1$. At the same time the DSIF is interrogating the CM, which, in turn, would radiate a signal to the LEM or LEM and DSIF. The signal transmitted by the LEM as received from the CM (with the same ratio transponder) would be 2485 mc. This would require additional frequency allocation. A different ratio transponder could be used with a frequency range near the present DSIF if desired. The diplexing situation with the LEM transmitting at 2282.5 mc. and receiving at 2287.5 mc. would represent a serious r-f filtering problem. To circumvent this difficulty, a time-sharing mode would probably be necessary. An additional antenna receiving system to operate specailly with the CM received signal might conceivably possess adequate isolation from the directional antenna employed for the LEM transmitter if the present omni-antenna system is not suitable.

From a purely technique standpoint, the most desirable technique would involve essentially a special frequency allocation for the ring-around system. This would necessitate a new transponder in each the

LEM and CM. It might be practical to utilize the same antenna system with this technique with a somewhat more complex multiplexing network than presently employed.

One other alternate technique should be mentioned. For this mode the DSIF would transmit only to the LEM. The signals from the LEM would be received by the DSIF directly and, in addition, by the CM. An additional transponder in the CM could then retransmit this signal to the DSIF via its directional antenna at a frequency perhaps within the DSIF allowable transmission band (if required), suitable different from the transmission frequency to the LEM. If the same receiving antennas at the DSIF stations and the transmission antennas on the CM are required suitably broad-band antenna feeds would be required.

Other alternates could be indicated but these examples should provide suitable scope for the techniques involved.

In summary, the technique to be considered would be primarily determined by the following factors.

1. The allowable frequency allocation.
2. The additional equipment that can be placed on the CM, LEM, and at the DSIF stations.

Case II. Computation of R and $\dot{R}$ by the LEM aided by the DSIF

The basic concept involved here can best be explained with the aid of the pulsed waveforms as indicated below. To begin with the DSIF is considered to simultaneously transmit both the CM and LEM.

(a) Signal Transmitted by the DSIF

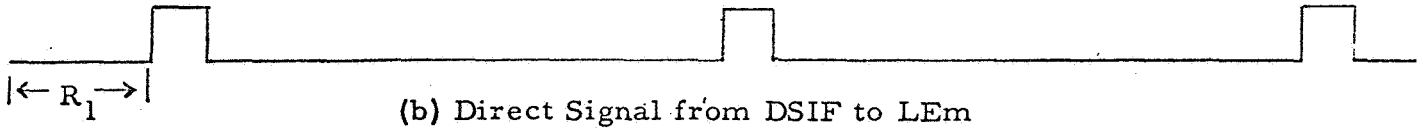

(b) Direct Signal from DSIF to LEm

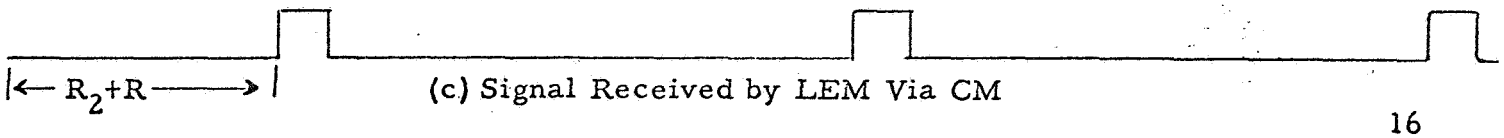

(c) Signal Received by LEM Via CM

In the LEM, one could measure $R_4 = R_2 + R - R_1$

If the transmission time of the DSIF to the LEM is delayed by $R_1 - R_2$ from the transmission of the DSIF to the CM then $R_4 = R$, (the desired range). Two techniques are suggested for this application: one, the above mentioned delay technique (and a similar frequency offset for $\dot{R}$ purposes) and, two, the transmission from the DSIF of $R_2 - R_1$ and $\dot{R}_2 - \dot{R}_1$ via a data link. Since the ephemeris of the CM should be well known, the delay and frequency offset would most appropriately be placed on the transmission to the DSIF. If the transponder in the CM is not modified, the diplexing problem mentioned earlier appears again. In addition, range and range rate processing equipment would be required in the LEM.

The factors which would determine the design of equipment for these purposes are as follows:

1. Frequency allocation.
2. Time synchronization problem.
3. The allowable additional equipment in the LEM, CM, and at the DSIF stations.

B. Using LEM Lunar Landing Radar for R and $\dot{R}$

The Lunar Landing Radar appears to possess interesting properties for this application. Basically, the optical system is presumed to place the LEM on a collision path with respect to the CM. It will probably be adequate to make occasional range, or range and range rate measurement with a high accuracy system. Since the lunar landing radar has fixed antennas, it is necessary to interrupt the optical tracking to orient the appropriate antenna to the CM. This difficulty could be circumvented if the antenna system for the LEM rendezvous radar could be employed with some rather simple modifications. This would require integration of some of the radar parameters for these equipments. The antenna system actually is one of the radar elements least likely to fail and as a consequence, this technique bears further consideration as perhaps the most attractive of the approaches indicated.

C. Power Calculations

The signal-to-noise ratio $(\frac{S}{N})$ for a one-way transmission system is given by:

$$\frac{S}{N} = \frac{P_T G_T G_R \alpha_z}{F R T B} \left(\frac{\lambda}{4\pi R}\right)^2$$

Standard values are given for the parameters to employ for scaling purposes as follows,

where:

P_T = transmitter power = 250 mw

$G_T G_R \alpha_z$ = - 6db

G_T = transmitting antenna gain

G_R = Receiving antenna gain

α_z = total system losses

λ = free-space wavelength = 13.5 cm

F = receiver noise figure = 11 db

B = receiver bandwidth = 1 mc

R = distance between transmitter and receiver

These values correspond to the most pessimistic situation for a range and range rate system with a solid-state transmitter only. $\frac{S}{N}$ as a function of range is given in a following graph.

A threshold signal occurs for a signal-to-noise ratio 0 db (quite frequently -2 db is employed by some). The strong signal condition is normally associated with signal-to-noise ratios of about 15 db. The corresponding ranges obtained for the standard system are about 12 KM and 2.1 KM respectively. Actually substantially greater ranges are obtained since the DSIF (or LEM) will have an effective bandwidth much more narrow. For example, the DSIF ring-around system requires that the phase-locked-loop properly operate. If we assume a 3000 cps bandwidth for the phase-locked-loop and a 10 db carrier suppression, the

corresponding ranges attained are 70 KM with a $\frac{S}{N}$ = 0 db and 12 KM with a $\frac{S}{N}$ = 15 db. Since interest here lies with comparatively short distances for the near locking phase, this performance level should easily be adequate. For other applications at much greater ranges, the power amplifier (20 watts) could be used which would increase these ranges by about an order of magnitude. In addition, use of the CM directional antenna for the CM to LEM link would increase ranges by more than an order of magnitude. Another alternate would be to employ a narrow band loop for the VCO (i.e., less than about 100 cps) for this application. This again would present a highly attractive solution. Recall that basically the minimum bandwidth in the phase-locked loop is limited by the rate of change of doppler frequency that must be accommodated.

In summary, the range requirement for this application does not appear to present a serious problem area.

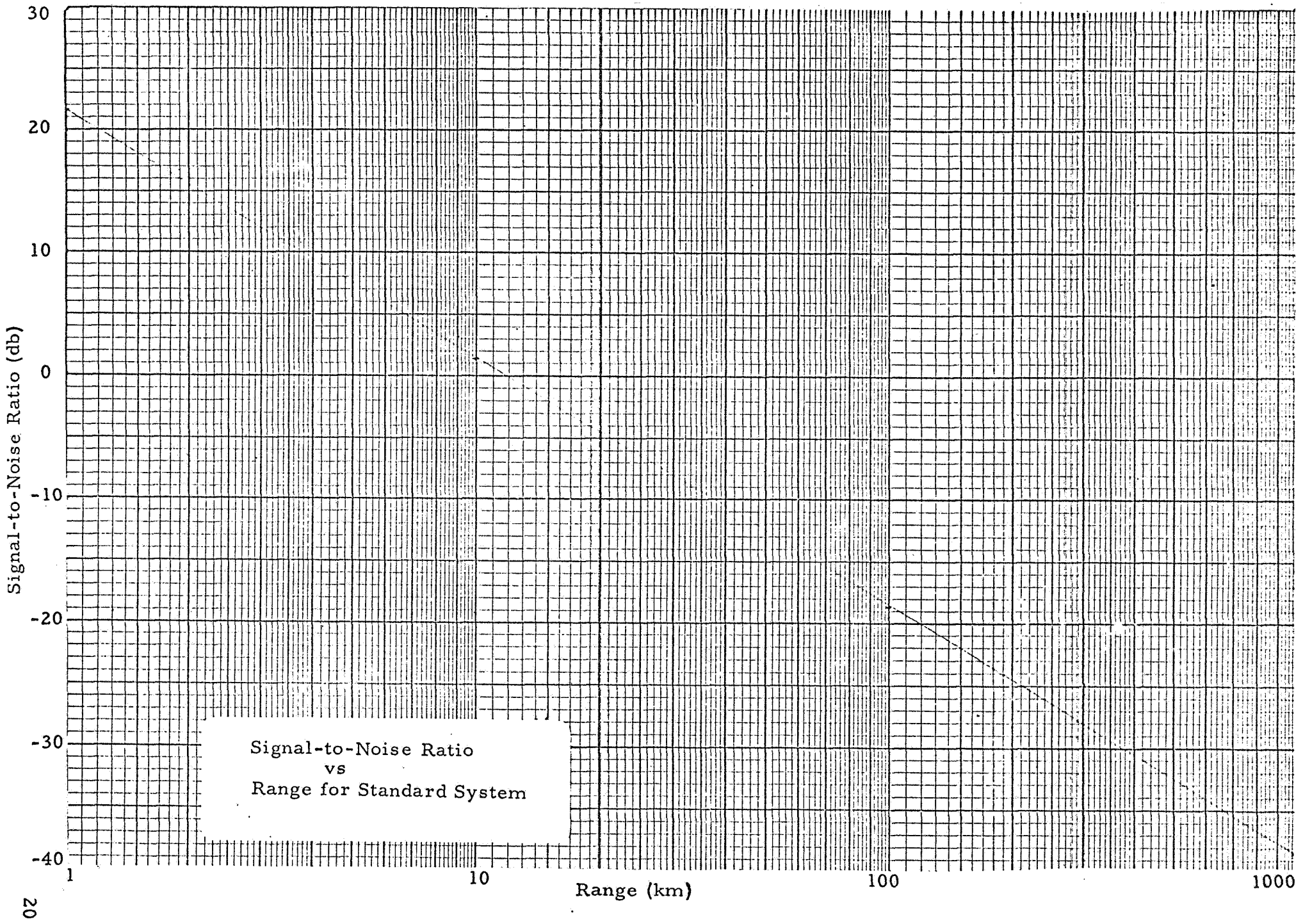
30
20
10
0
-10
-20
-30
-40
Signal-to-Noise Ratio (db)
1
10
100
1000
Range (km)
Signal-to-Noise Ratio
vs
Range for Standard System

6. SIMPLE RENDEZVOUS AID SENSOR — G. F. Floyd

The basic guidance scheme adopted by both Grumman and MIT for the terminal rendezvous phase consists of angle optical tracking and thrust application normal to the line-of-sight in order to drive the angular rate of the line-of-sight to zero, thus getting the LEM on a collision course with the CSM. In addition, thrusts are applied along the line-of-sight in order to maintain a schedule of range rate versus range. A typical schedule is given in Grumman Report, LMO-500-22, 1 April 1963, p. 5, and is as below.

Range (n.m.)	$\dot{R}$ ft/sec. Bounds	T (min) = $\frac{R}{\dot{R}}$	Percent Variation Allowed
40	350 - 250	11.6 - 16.2	16
35	325 - 225	10.8 - 15.8	19
30	300 - 200	10.3 - 15.2	19
20	200 - 120	10.3 - 16.8	24
10	120 - 70	8.4 - 14.5	26
4	70 - 30	5.8 - 13.5	40
1	30 - 10	3.5 - 10.3	51

The third column is simply the ratio of the range to the desired range rate and, in all probability, holding this ratio constant at approximately 10 minutes would give satisfactory results.

Since the command service module will be equipped with bright lights to aid the LEM in acquisition in angle tracking, this immediately suggests the use of an old idea originally studied in connection with back-up IR missile launching systems. The equipment involved would consist of a photocell mounted on the LEM optical tracker and a simple analog computer circuit. The received

optical power and its time derivative would be measured and their ratio computed. Since there is no atmosphere, received power as a function of range would be of the form:

$$P = \frac{K}{R^2}$$

Hence, its time derivative would be:

$$\dot{P} = \frac{-2K\dot{R}}{R^3}$$

leading to the ratio:

$$\boxed{\frac{2P}{\dot{P}} = \frac{R}{-\dot{R}} = T} \qquad (1)$$

Thus, this simple mechanization would yield the time to go and the LEM astronaut would control thrust along the line-of-sight to hold this measured time-to-go within acceptable limits. Again, we point out that this is an old idea borrowed from military programs that has been successfully used, and therefore the development program should be easy, the reliability should be good, and the total weight of the equipment could probably be kept less than a few pounds.

Preliminary Error Study

The main source of error is the ability of the sensor to detect changes in P. Thus from (1), we have:

$$\delta T = \frac{2 P \delta \dot{P}}{\dot{P}^2} \qquad (2)$$

where $\delta \dot{P} = \frac{\delta(\Delta P)}{\tau}$ (3)

and τ is the observation time. Using (1) and (3) in (2), we have

$$\delta T = \frac{2P\,\delta(\Delta P)}{\left(\frac{2P}{T}\right)^2 \tau}$$

$$\boxed{\frac{\delta T}{T} = \frac{T}{2\tau}\,\frac{\delta(\Delta P)}{P}} \qquad (4)$$

For preliminary calculations, we assume a 400 watt non-directional source with 10% of the energy in the photocell bandwidth or 40 watts of effective radiated power. The received power with an effective collector area of (A) at a range R in a vacuum is

$$P = \frac{P_t\, A}{4\pi R^2}$$

Assuming a 3" lens, ($A = 1/20$ ft.^{2}), and a range of 40 n.m. (24×10^4 ft.), we get:

$$P = \frac{(40)\quad(1/20)}{(12)\quad(580 \times 10^8} = 3 \times 10^{-12} \text{ watts}$$

The noise equivalent power of the photocell is about 10^{-15} watts so at a S/N of 10 the detectable power change is

$$\delta(\Delta P) \simeq 10^{-14} \text{ watts}$$

Using the value of T = 14 min. from the table and an observation time of 1/2 min., we get from (4)

$$\frac{\delta T}{T} = \frac{14\quad(10^{-14})}{(2)\quad(1/2)\,(3 \times 10^{-12})} = 5\%$$

which is much less than the 16% variation in T permitted by the $\dot{R}$ bounds.

Finally from (4), we see that the percent uncertainty in T will decrease with P, (T, τ, δ (ΔP) staying fixed), hence with the square of range so that by 20 n.m. the system would be good to 1% as compared with the 24% variation allowed at this range.

The conclusion is then that such a device works as though it would be useful, light and easy to develop, and therefore worthy of additional study.

In this connection items of planned-on-study include:

1. Determination of satisfactory (T) limits for easy control during the rendezvous.

2. Mechanization possibilities. For example, from Equation (1), we note that $\frac{d}{dt}$ (ln P) = $\frac{\dot{P}}{P}$ = $\frac{2}{T}$ so that a single loaded diode network to approximate the log function, with a differentiating circuit at the end may be sufficient to generate T.

3. Further error studies to establish the achievable accuracy to be expected.

7. FAR-SIDE RELAY

L. Lustick/
C. Siska

Additional trajectory calculations were made on the far-side relay to see if boost conditions could be established which would allow voice communication with the CM/LEM. It is desired to have voice communication capabilities during the portion of the mission from deboost into lunar orbit to rendezvous between LEM and CM (a period of approximately 32 hours). It is particularly important to have voice communication at the time of deboost of CM into lunar orbit.

The ground rules specified by Mr. Fordyce allowed boosts as large as 1000 ft/sec. to be applied within the first seven hours following translunar injection. The range between the relay and CM consistent with voice communication was given as 40,000 nautical miles.

Method

Nominal translunar injection conditions were established which were approximately consistent with the arrival of the CM at perilune (100 n.m.) 72 hours after injection. The effect of perturbations in the velocity vector, both at translunar injection and approximately 7 hours after injection were examined. The locus of the position of the relay relative to the CM/SM at the time when the CM/SM pierces the LSOI was established. These Loci are shown in Figure 1. The elongated ellipse is for a boost at translunar injection of 1000 ft/sec. The different points on the locus correspond to different boost directions relative to the reference velocity vector as indicated in the upper left diagram in Figure 1. The other ellipse shown in Figure 1 corresponds to applying a boost of 1000 ft/sec. approximately 7.6 hours after translunar injection.

In lunar space, each point on the locus is traveling roughly in a 45 degree direction from lower left to upper right, and therefore, one can quickly estimate which points will penetrate the lunar sphere of influence.

Results

The trajectories of several points on the loci of Figure 1 were examined briefly in lunar space and at first glance, it appears that the positions around $\alpha = -90^{\circ}$ for the 7.6 hr. delayed boost are the most promising to fulfill the mission requirements.

Figure 2 shows the trajectory for the $\alpha = -90$ boost in lunar space and also the reference lunar vehicle trajectory. The lunar vehicle enters the LSOI at 60 hours after translunar injection and arrives at perilune (for deboost into a circular orbit) approximately 12 hours later. Corresponding positions for the booster (Far-side Relay) are indicated. The perilune visibility limit shown in Figure 2, (i.e., the tangent to the lunar surface which passes through the perilune position) indicates that perilune is always visible to the booster position. Approximately thirty hours after lunar vehicle deboost, the Far-side Relay has approached the 40,000 n.mi. communications limit. Thus, it appears that the Far-side Relay will be within the voice communications limit for both lunar deboost and lunar rendezvous. Although it appears occultation by the moon occurs at 102 hours, this presents no problem since the trajectory can be shifted with slight changes in boost direction around $\alpha = -90^{\circ}$.

Far-side Relay trajectories going the other way around the moon (counter-clockwise), say for boosts slightly less than $\alpha = 90^{\circ}$, may also fulfill the mission requirement. This alternative procedure is yet to be investigated.

Conclusions

Assuming that a 1000 ft/sec. boost is available at approximately 7 hours after translunar injection, voice communications via the Far-side Relay appears feasible for both the lunar deboost and lunar rendezvous portions of the Apollo mission.

Future Tasks

1. Write a computer program based on the Egerov Model to facilitate the trajectory calculations so that a more complete evaluation of the far-side relay potential can be obtained.

2. Establish the nominal trajectory for the CM/SM more accurately. That is, what are translunar injection conditions that are consistent with a free return trajectory.

3. Investigate the effect of errors in the boost velocity on the far-side relay trajectory.

4. Determine expected orientation errors in the reference system at the time of boost and decide how the boost is to be executed.

5. Investigate the potential of the far-side relay as an aid to navigation.

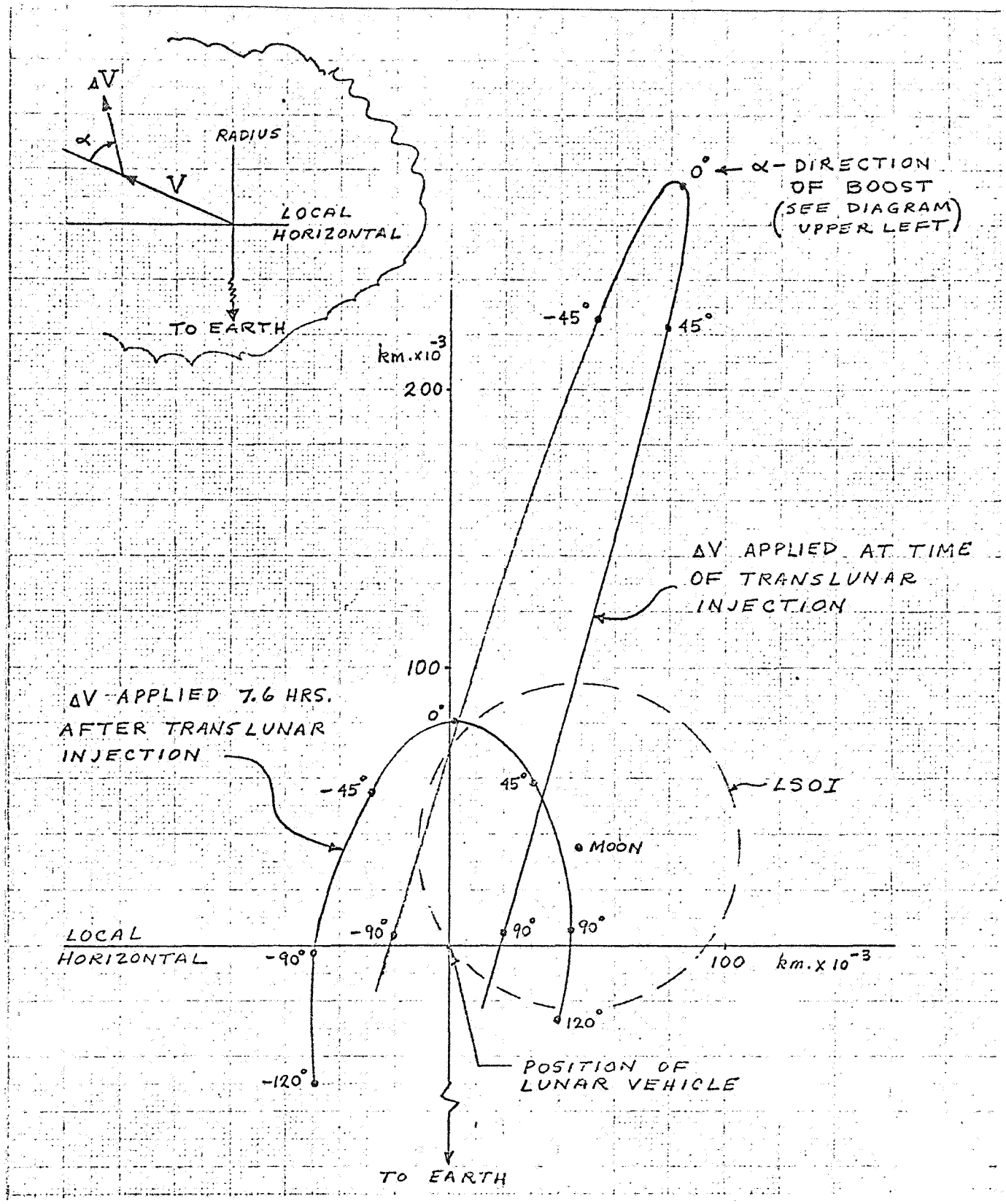

Figure 1. Relative Booster Positions At Time Lunar Vehicle Enters Lunar Sphere Of Influence - ΔV = 1000 ft/sec.

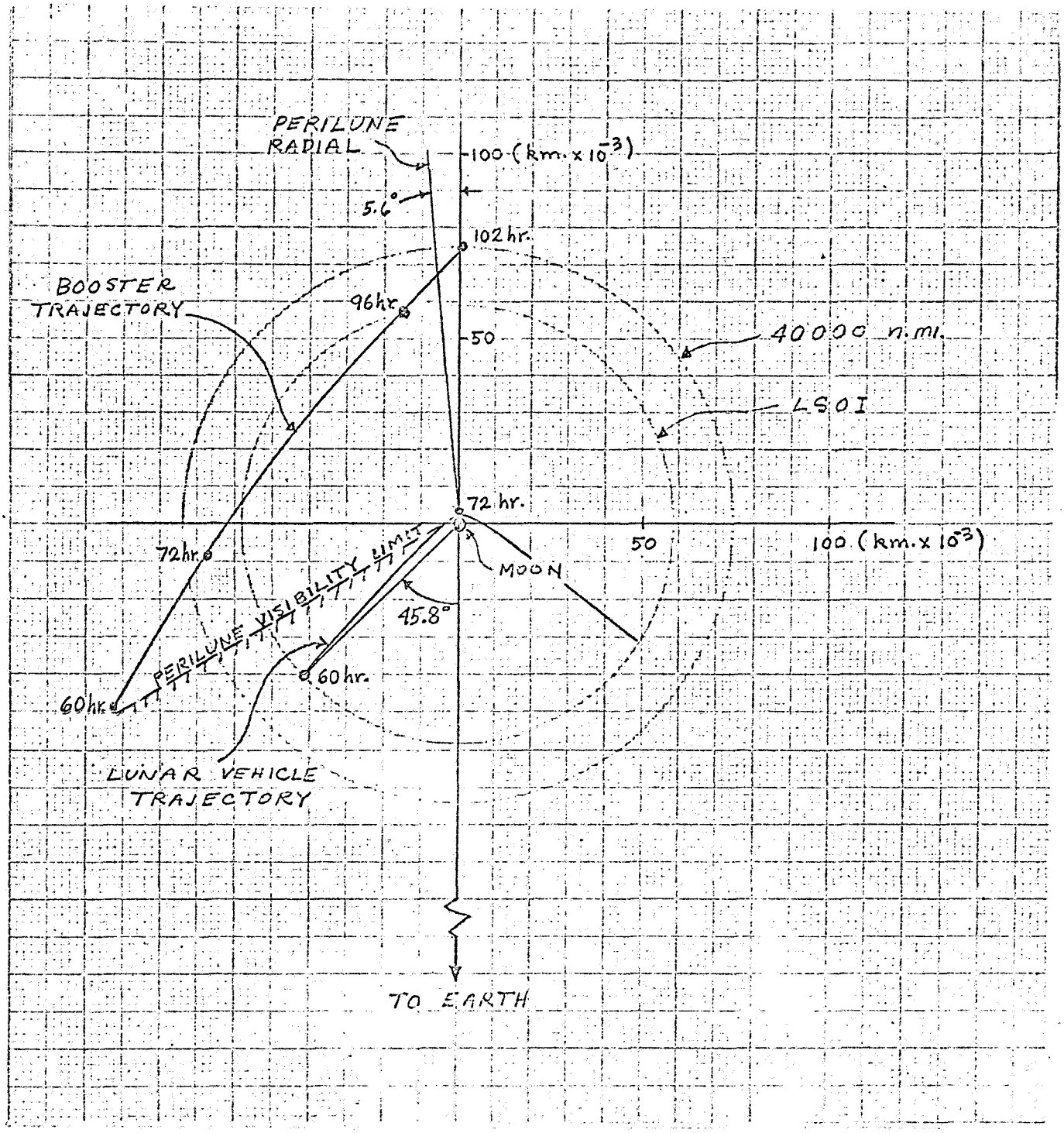

Figure 2. Booster Trajectory For ΔV_i = 1000 ft/sec. and $\alpha = -90^{\circ}$

APOLLO NOTE NO. 88

H. Engel
31 July 1963

KALMAN-SCHMIDT METHOD FOR ORBIT DETERMINATION

INTRODUCTION

This note on the Kalman-Schmidt method for orbit determination is intended primarily for internal Bissett-Berman Corporation distribution to acquaint those working on this project with the method. This note is based primarily on JPL Technical Memorandum 312-291, "Dynamic Filtering," by C. B. Solloway and on R. H. Battin's, "A Statistical Optimizing Navigation Procedure for Space Flight," appearing in the November 1962 ARS Journal.

As indicated in previous notes, it is possible to obtain a best linear estimate of the parameters of an orbit by varying these parameters until the estimated orbit best fits the observed data in the least-squares sense. The straightforward way of doing this requires that all the data be fitted in this manner, and since the problem is non-linear it is necessary to solve it by an iteration technique. These iterations are time-consuming.

In discussions with Tom Barker and Joe Pearey of JPL it was found that on the recent Venus probe shot the iterations (based, to be sure, on the reduction of far more data than we will have) required 20 to 25 minutes per iteration, and according to JPL three iterations are normally required for satisfactory convergence. No attempt was made to minimize the time required for these computations since time was not important in that application. It was estimated off-hand that the required time could have been reduced to ten minutes per iteration. Even ten minutes per iteration is too great for the LEM ascent problem.

The Kalman-Schmidt method, which improves the orbit parameters as each new observation is obtained, promises to provide estimates of orbit parameters with less delay.

METHOD

The Kalman-Schmidt method, as presented by Solloway and Battin, employs a reference trajectory to permit linearization of the equations to be solved; that is, there must be good a priori knowledge of the trajectory.

Let x_n be a column N-vector describing the deviation of the actual trajectory from the reference trajectory at time t_n. δx_n includes three position components $\bar{r}_n$, three velocity components $\dot{\bar{r}}_n$, and a number of components, α_n, corresponding to fixed but unknown biases in the observables. This same technique of including unknown fixed biases as orbit parameters has been employed previously in Apollo Note No. 43.

Let y_n be a column p-vector denoting the deviation of the measurements at time t_n resulting from the deviation δx_n. p is less than or equal to N. Since the fixed biases are included in x_n, the error in y_n is random with mean zero assumed. The random components, denoted by a column p-vector u_n are assumed to have a known p x p covariance matrix Q_n. The measured value of y_n is y_n^*

$$y_n^* = y_n + u_n$$

and

$$Q_n = E\left[u_n u_n^T\right]$$

Let M_n be the known p x N matrix that maps x_n into y_n, and let $\phi_{n+1,n}$ be the known N x N transition matrix that maps x_n into x_{n+1}.

$$y_{n+1} = M_n x_n$$

$$x_{n+1} = \phi_{n+1,n} x_n$$

Note well that the last equations above are linear in x_n. This

means that x_{n+1} and y_{n+1} can be computed by simple matrix multiplications based on the matrices M_n and $\phi_{n+1,n}$ that may be computed beforehand on the basis of the reference trajectory.

Let x_n^* be the best linear estimate of x_n prior to measurement y_n^*, and let P_n^* be the N x N covariance matrix of x_n^*. It is assumed that the expected of x_n^* is x_n.

$$P_n^* = E\left[(x_y^* - x_n)\ (x_n^* - x_n)^T\right]$$

Let $\bar{x}_{n+1}$ be predicted value of x_{n+1} based on all measurements prior to y_{n+1}^*, and let $\bar{y}_{n+1}$ be the predicted value of y_{n+1}^* based on all measurements prior to y_{n+1}^*. Making use of the linearity property described above,

$$\bar{x}_{n+1} = \phi_{n+1,n} x_n^*$$

$$\bar{y}_{n+1} = M_{n+1}\, x_{n+1}^*$$

Let $\hat{x}_n$ and $\hat{y}_n$ be the errors in the prediction of x_n and y_n^* prior to measurement y_n^*

$$\hat{x}_{n+1} = \bar{x}_{n+1} - x_{n+1}$$

$$\hat{y}_n = \bar{y}_n - y_n^*$$

Now, the expected value of $\hat{x}_{n+1}$ is zero, and its covariance matrix is:

$$E\left[\hat{x}_{n+1} \hat{x}_{n+1}^T \right] = E\left[(\bar{x}_{n+1} - x_{n+1}) (\bar{x}_{n+1} - x_{n+1})^T \right]$$

$$= E\left[\left\{ \phi_{n+1,n} (x_n^* - x_n) \right\} \left\{ \phi_{n+1,n} (x_n^* - x_n) \right\}^T \right]$$

$$= E\left[\phi_{n+1,n} (x_n^* - x_n) (x_n^* - x_n)^T \phi_{n+1,n}^T \right]$$

$$= \phi_{n+1,n} E\left[(x_n^* - x_n) (x_n^* - x_n)^T \right] \phi_{n+1,n}^T$$

$$= \phi_{n+1,n} P_n^* \phi_{n+1,n}^T$$

In like fashion, the expected value of $\hat{y}_n$ is zero and its covariance matrix is:

$$E\left[\hat{y}_n \hat{y}_n^T \right] = E\left[(\bar{y}_n - y_n^*) (\bar{y}_n - y_n^*)^T \right]$$

$$= E\left[\left\{ M_n (x_n^* - x_n) - u_n \right\} \left\{ M_n (x_n^* - x_n) - u_n \right\}^T \right]$$

$$= M_n P_n^* M_n^T + Q_n - E\left[u_n (x_n^* - x_n)^T \right] M_n^T - M_n E\left[(x_n^* - x_n) u_n^T \right]$$

$$= M_n P_n^* M_n^T + Q_n + 0 + 0$$

also,

$$E\left[\hat{x}_{n+1}\,\hat{y}_n^T\right] = E\left[(x^*_{n+1} - x_{n+1})\,(\bar{y}_n - y^*_n)\right]$$

$$= E\left[\left\{\phi_{n+1,n}(x^*_n - x_n)\right\}\left\{M_n\,(x^*_n - x_n) - u_n\right\}^T\right]$$

$$= \phi_{n+1,n}\;P^*_n M_n^T - \phi_{n+1,n}\,E\left[(x^*_n - x_n)\,u_n^T\right]$$

$$= \phi_{n+1,n}\;P^*_n\;M_n^T - 0$$

It is shown in the appendix that if α and β are two column vector random variables, not necessarily of the same dimension, with means zero and covariance matrices

$$\Lambda_\alpha = E\left[\alpha\,\alpha^T\right]$$

$$\Lambda_\beta = E\left[\beta\,\beta^T\right]$$

$$\Lambda_{\beta\alpha} = E\left[\beta\,\alpha^T\right]$$

then the "best" linear estimate β^* of β, given α, is:

$$\beta^* = \Lambda_{\beta\alpha}\,\Lambda_\alpha^{-1}\,\alpha$$

Now, letting $\hat{y}_{n-1}$ be α, and $\hat{x}_n$ be β, it follows that the best linear estimate of $\hat{x}_{n+1}$, given $\hat{y}_n$, is $\hat{x}^*_{n+1}$

$$\hat{x}^*_{n+1} = \Lambda_{\hat{x}_{n+1}\hat{y}_n}\,\Lambda_{\hat{y}_n}^{-1}\,\hat{y}_n$$

$$= (\phi_{n+1,n}\,P^*_n\,M_n^T)\;(M_n\,P^*_n\,M_n^T + Q_n)^{-1}\;\hat{y}_n$$

Letting

$$\Delta_n^* \triangleq \phi_{n+1,n} P_n^* M_n^T (M_n P_n^* M_n^T + Q_n)^{-1}$$

we have

$$\hat{x}_{n+1}^* = \Delta_n^* \hat{y}_n$$

Note that $(M_n P_n^* M_n^T + Q_n)$ is a p x p matrix. If only range rate from one station is measured, it is simply a number; if range and range rate from one station are measured, it is a 2 x 2 matrix; and so on.

Now the best estimate of x_{n+1}, given all measurements prior to y_{n+1}^* is

$$x_{n+1}^* = \bar{x}_{n+1} - \hat{x}_{n+1}^*$$

$$= \phi_{n+1,n} x_n^* - \Delta_n^* \hat{y}_n$$

$$= \phi_{n+1,n} x_n^* - \Delta_n^* (\bar{y}_n - y_n^*)$$

$$= \phi_{n+1,n} x_n^* - \Delta_n^* (M_n x_n^* - y_n^*)$$

$$= (\phi_{n+1,n} - \Delta_n^* M_n) x_n^* + \Delta_n^* y_n^*$$

$$= \phi^*_{n+1,n} x_n^* + \Delta_n^* y_n^*$$

where

$$\phi^*_{n+1,n} = \phi_{n+1,n} - \Delta_n^* M_n$$

If we now let $\tilde{x}_n$ be the error in the estimate of x_n,

$$\tilde{x}_n = x^*_n - x_n$$

then

$$\tilde{x}_{n+1} = \phi^*_{n+1,n}\, x^*_n + \Delta^*_n\, y^*_n - \phi_{n+1,n}\, x_n$$

$$= \phi^*_{n+1,n}\, x^*_n + \Delta^*_n (M_n\, x_n + u_n) - \phi_{n+1,n}\, x_n$$

$$= \phi^*_{n+1,n}\, x^*_n - (\phi_{n+1,n} - \Delta^*_n M_n)\, x_n + \Delta^*_n\, u_n$$

$$= \phi^*_{n+1,n}\, (x^*_n - x_n) + \Delta^*_n\, u_n$$

$$= \phi^*_{n+1,n}\, \tilde{x}_n + \Delta^*_n\, u_n$$

Now P^*_n is the covariance matrix of $\tilde{x}_n$, so

$$P^*_{n+1} = E\left[\, \tilde{x}_{n+1}\ \tilde{x}_{N+1}^{T}\, \right]$$

$$= E\left[\, (\phi^*_{n+1,n}\, \tilde{x}_n + \Delta^*_n\, u_n)\, (\phi^*_{n+1,n}\, \tilde{x}_n + \Delta_n\, u_n)^T\, \right]$$

$$= \phi^*_{n+1,n}\, P^*_n\ \phi^{*\,T}_{n+1,n} + \Delta^*_n\, Q_n\, \Delta^{*\,T}_n + 0 + 0$$

$$= \phi^*_{n+1,n}\, P^*_n\ (\phi_{n+1,n} - \Delta^*_n M_n)^T + \Delta^*_n\ Q_n\, \Delta^{*\,T}_n$$

$$= \phi^*_{n+1,n} P^*_n \phi^T_{n+1,n} + (\Delta^*_n Q_n - \phi^*_{n+1,n} P^*_n M^T_n) \Delta^{*T}_n$$

$$= \phi^*_{n+1,n} P^*_n \phi^T_{n+1,n} + (\Delta^*_n Q_n - \phi_{n+1,n} P^*_n M^T_n + \Delta^*_n M_n P^*_n M^T_n) \Delta^T_n$$

$$= \phi^*_{n+1,n} P^*_n \phi^T_{n+1,n} + (\Delta^*_n \left[M_n P^*_n M^T_n + Q_n \right] - \phi_{n+1,n} P^*_n M^T_n) \Delta^T_n$$

$$= \phi^*_{n+1,n} P^*_n \phi^T_{n+1;n} (\phi_{n+1,n} P^*_n M^T_n - \phi_{n+1,n} P^*_n M^T_n) \Delta^T_n$$

$$P^*_{n+1} = \phi^*_{n+1,n} P^*_n \phi^T_{n+1,n}$$

Thus, starting with the known Q_n, $\phi_{n+1,n}$, and M_n, and a priori estimates x^*_o and P^*_o, it is possible to find x^*_n and P^*_n by means of a single iteration technique:

$0 \rightarrow n$

$$\Delta^*_n = \phi_{n+1,n} P^*_n M^T_n (M_n P^*_n M^T_n + Q_n)^{-1}$$

$$\phi^*_{n+1,n} = \phi_{n+1,n} - \Delta^*_n M_n$$

$$P^*_{n+1} = \phi^*_{n+1,n} P^*_n \phi^T_{n+1,n}$$

$$x^*_{n+1} = \phi^*_{n+1,n} x^*_n + \Delta^*_n y^*_n$$

$n + 1 \rightarrow n$

APPENDIX

Theorem: Let α and β be two column vector random variables, not necessarily of the same dimension, with means zero and covariance matrices

$$\Lambda_{\alpha} = E\left[\alpha\ \alpha^{T}\right]$$

$$\Lambda_{\beta} = E\left[\beta\ \beta^{T}\right]$$

$$\Lambda_{\beta\,\alpha} = E\left[\beta\ \alpha^{T}\right]$$

Then the "best" linear estimate $\tilde{\beta}$ of β, given α, is

$$\tilde{\beta} = \Lambda_{\beta\,\alpha}\,\Lambda_{\alpha}^{-1}\,\alpha$$

where "best" means that the covariance matrix of the error in $\tilde{\beta}$ is such that variance in the estimate of any quantity, $\psi = a^{T}\beta$ is minimized. This can be shown as follows:

$$\sigma_{\psi}^{2} = E\left[(\psi - \tilde{\psi})(\psi - \tilde{\psi})^{T}\right]$$

$$= E\left[a^{T}(\beta - \tilde{\beta})(\beta - \tilde{\beta})^{T} a\right]$$

$$= a^{T}\,E\left[(\beta - \tilde{\beta})(\beta - \tilde{\beta})^{T}\right]\,a$$

$$= a^{T} R\, a$$

in which

$$R = E\left[(\beta - \tilde{\beta})(\beta - \tilde{\beta})^{T}\right]$$

To minimize σ_ψ^2, only R can be varied. Now since $\tilde{\beta}$ is a linear estimate of β, given α, write

$$\tilde{\beta} = A\alpha$$

$$R = E\left[(\beta - A\alpha)(\beta - A\alpha)^T\right]$$

$$= E\left[\beta\beta^T\right] - E\left[\beta(A\alpha)^T\right] - E\left[(A\alpha)\beta^T\right] + E\left[(A\alpha)(A\alpha)^T\right]$$

$$= \Lambda_\beta - E\left[\beta\alpha^T A^T\right] - E\left[A\alpha\beta^T\right] + E\left[A\alpha\alpha^T A^T\right]$$

$$= \Lambda_\beta - \Lambda_{\beta\alpha} A^T - A\Lambda_{\alpha\beta} + A\Lambda_\alpha A^T$$

Now vary A (and A_T) to obtain a stationary value.

$$\delta R = -\Lambda_{\beta\alpha}\delta A^T + A\Lambda_\alpha \delta A^T - \delta A\Lambda_{\alpha\beta} + \delta A\Lambda_\alpha A^T = 0$$

$$= (A\Lambda_\alpha - \Lambda_{\beta\alpha})\ \delta A^T + \delta A(\Lambda_\alpha A^T - \Lambda_{\alpha\beta}) = 0$$

Hence, for a stationary solution

$$A = A_s = \Lambda_{\beta\alpha}\Lambda_\alpha^{-1} \quad \text{and} \quad A^T = A_s^T = \Lambda_\alpha^{-1}\Lambda_{\alpha\beta}$$

and

$$R = R_s = \Lambda_\beta - \Lambda_{\beta\alpha}\Lambda_\alpha^{-1}\Lambda_{\alpha\beta} - \Lambda_{\beta\alpha}\Lambda_\alpha^{-1}\Lambda_{\alpha\beta} + \Lambda_{\beta\alpha}\Lambda_\alpha^{-1}\Lambda_\alpha\Lambda_\alpha^{-1}\Lambda_{\alpha\beta}$$

$$= \Lambda_\beta - \Lambda_{\beta\alpha}\Lambda_\alpha^{-1}\Lambda_{\alpha\beta}$$

It is "easily" shown that this stationary solution results in a <u>minimum</u> σ_ψ^2.

APOLLO NOTE NO. 89

L. Horowitz
26 July 1963

ON THE NUMERICAL COMPUTATION OF OPTIMUM CONTROLS

INTRODUCTION

The typical optimum control problem requires selection of bounded control functions $u_i(t)$ in such a way as to optimize some physical parameter (time, fuel expenditure, radiation hazard, etc.) over a transfer trajectory. In general, both initial and final position and velocity are specified as boundary conditions for the problem. Since the solution of differential equations of motion together with specified initial and final conditions is fundamental to the solution of this problem, we have every reason to expect to have to solve two-point boundary value problems somewhere along the line. Note that the two-point boundary value feature is introduced through the essential nature of the problem (i.e., a differential system with both initial and final boundary values explicitly specified) and is in no way induced by the particular optimization technique employed, be it variational calculus,[1] dynamic programming,[2] imbedding theory[3] or Pontryagin optimum control theory.[4]

In Apollo Note No. 86, the problem of minimum fuel transfer through a radiation hazard was considered. It was shown that the desired controls were provided through simultaneous solution of a two-point boundary value system of 14 non-linear differential equations.

This note sketches various techniques for mechanizing numerical solutions of such two-point boundary value problems as they apply to the synthesis of optimal controls.

SKETCH OF THE PROBLEM

As is well known, the digital computer is ideally suited to the

---

[1] A. Miele, Optimization Techniques, edited by G. Leitmann, Academic Press (1962), Chapter 4

[2] R. Bellman, Dynamic Programming, Princeton (1957), Chapter 3

[3] C. M. Kashmar; Leitmann (op. cit.), Chapter 10

[4] Apollo Note No. 84

simultaneous solution of initial value, non-linear differential systems. As R. Bellman points out, even the simultaneous solution of several hundred such differential equations is generally a matter of no great difficulty.[5] For given initial values of all variables, the differential system is readily converted into a finite-difference system. Then using an arbitrary "grid size", the computer steps along in discrete finite steps, computing values of the variables at step n + 1 by iteration on the system of finite-difference equations at step n. These techniques are well-documented and need not be repeated here.[6]

The problem occurs in the two-point boundary value case. For here, only some of the values are specified at the initial point; the remainder of the values are specified at the terminal point. Thus, simple iteration on the finite-difference system in discrete steps from the initial point is no longer possible, since all the required initial values are not known.

SUGGESTED TECHNIQUES

1. Direct Method

A direct technique is to guess initial values where necessary, then iterate forward to the terminal point. The derived terminal values are then compared with the given terminal values—new guesses for the initial values are then made by linear extrapolation and the process repeated until close terminal agreement is achieved. This may well be a long-winded process for the general case, so that special efforts to exploit any possible simplifications inherent in the particular problem should be carefully considered.

---

[5] R. Bellman, Adaptive Control Processes, (Princeton, 1961), p. 28

[6] See, e.g., Hildebrand, Introduction to Numerical Analysis (McGraw Hill, 1956), Chapter 6, or Milne, Numerical Calculus (Princeton, 1949) Chapter 5.

2. Large Grid

From the simultaneous system appearing on page 6 of Apollo Note No. 86, we see that the variables appear in a fairly simple fashion—this is to be expected, since the essential non-linearities are introduced through the $\frac{1}{r^2}$ gravitational field and the thrust constraint $u_1^2 + u_2^2 + u_3^2 \leq 1$; both simple algebraic forms. This suggests that the process outlined in 1 above be accelerated by choosing large grid sizes to localize the unknown initial values, since dramatic non-linear fluctuations should not occur in the region of interest. Finer resolution can then be attempted by narrowing the grid size.

3. Linearization

Were the original differential system linear, the general solution could be written parametrically in terms of the initial values (whether specified or not). Then evaluating the general (parametric) solution at the terminal point with the given terminal values imposed, the resulting algebraic system could then be solved directly for the unknown initial values appearing as parameters. Indeed, since linear differential systems are, in particular, linear in the boundary conditions, it suffices to choose any arbitrary values of the unknown initial conditions, solve the linear system at the terminal point and perform a single linear extrapolation to obtain the exact initial values directly as an immediate consequence of the linearity in the boundary values (courtesy of L. Lustick). This suggests as the first approximation, linearizing the original differential system (by linear truncation the Taylor Series expansions of the non-linear terms), solving the "parametric" initial-value linear system, evaluating the solution thus obtained at the terminal point, and then solving the resulting algebraic system for the unknown initial values. These values can then be used as first approximations for the unknown initial values of the non-linear case, and the non-linear system then solved in the ordinary fashion (e.g., Runge-Kutta method). The terminal values thus achieved can then be compared with the given terminal values and a linear extrapolation used as in method 1 above.

4. Replacement by Initial-Value Problem

Bellman provides a method for converting the two-point boundary value problem to an initial value problem by an iterative technique. Details are given in the literature.[7]

5. Time Reversal

Another possibility is to handle two-point systems like those in Apollo Note No. 86 by integrating the x_i equations forward in time, the p_i equations backward in time (assuming initial and final values where necessary), then extrapolating linearly as in 1. to obtain second approximations. Convergence should present no problem if the initial guesses are sufficiently close. The linearization technique 3. should suffice to obtain fairly good initial guesses since the physics of the problems under consideration dictate that the non-linear elements of the differential systems are generally slowly-varying quantities.

CONCLUSIONS

We have shown that two-point boundary value problems are inherent in the optimization problems under consideration and as such are in no way created by the particular optimization methods employed. Several possible techniques for mechanizing the numerical solutions have been suggested. We noted in particular that first-order linearization of the differential equations is eminently suitable for the problems under consideration in the earth return abort studies, since the intrinsic non-linearities are in general slowly-varying quantities. Finally, possible techniques for obtaining first-order approximations to the unknown initial and final boundary values were given. A better appraisal of the solution of two-point boundary value problems will be possible when actual computer solutions have been attempted.

---

[7] R. Bellman, Adaptive Control Processes (loc. cit.), p. 113

APOLLO NOTE NO. 90

C. Siska
6 August 1963

FURTHER EXAMINATION OF FAR-SIDE RELAY TRAJECTORIES

DISCUSSION

This note represents a continuation in the study of Far-side Relay trajectories as explored in Apollo Note No. 44 and Section 7 of Apollo Note No. 87.

There exists an interest for using the S IV booster as a voice communications relay between locations back of the Moon and the Earth during the times of lunar vehicle deboost from the translunar trajectory, and lunar rendezvous prior to Earth return. These periods of time occur approximately 72 and 100 hours, respectively, after translunar injection. A slant range limit of 40,000 n. mi. from the Moon has been adopted as consistent with the power requirement involved in the voice communication.

It is assumed that a velocity impulse of up to 1000 ft/sec. can be applied to the S IV booster at any time during a period of approximately 7 hours after translunar injection.

The feasibility of fulfilling the above-mentioned criteria is shown in Apollo Note No. 87, which illustrates a representative trajectory in the vicinity of the Moon.

In this note, the relation between boost velocity and direction, and the time of boost application is explored in a cursory manner, in order to indicate the operating region for these characteristics.

RESULTS

A graphical-analytic procedure has been used to determine the approximate lunar trajectories which appear in this note.

The particular combinations of operating characteristics which have been investigated are as follows:

t	ΔV	α
Time of Boost Application (hours after translunar injection)	Boost Velocity (ft/sec.)	Boost Direction Relative to Path Velocity
7.6	1,000	-120° to $+120^{\circ}$
7.6	500	-120° to $+120^{\circ}$
0	1,000	-120° to $+120^{\circ}$

It quickly became apparent that the range of boost directions, α, which might satisfy the mission requirement was approximately $-90^{\circ} < \alpha < -115^{\circ}$, as depicted in the following diagram.

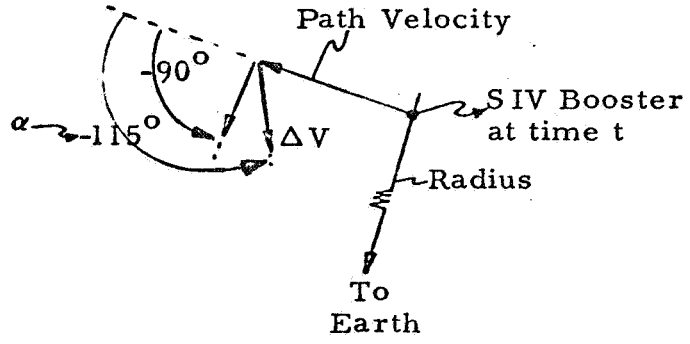

To approximate the range of admissible values of α for each combination of ΔV, and t, the $\alpha = -90^{\circ}$ trajectory was computed for each case to represent the one limit, and then the other limit of α was obtained by searching for the trajectory which yielded perilune visibility at t = 72 hours. These two trajectories for each combination of ΔV, t are illustrated in Figures 1, 2, and 3.

The vertical axis of the co-ordinate system has been chosen to be the Earth-Moon line at t = 60 hours. This line is moving around the Moon in a counterclock-wise direction at a rate of 0.55°/hour, and therefore, at some time part of the trajectory will not be visible to the Earth. Relative to the Earth, the path velocity is approximately 2 km/sec. so that the duration of occultation is approximately one-half hour.

Using Figures 1, 2, and 3, one can develop the operating region for given criteria as shown in Figure 4. Permissible values of ΔV and α for a given t lie within the region bounded by the specified t contour. This contour, as shown in Figure 4, consists of two segments; the left side is associated with the upper trajectory of Figures 1, 2, and 3 (leaving the 40,000 n. mi. circle at t = 100 hours), while the right side is for the lower trajectory (perilune visibility at t = 72 hours). A third segment which completes the contour is not shown and this would represent the situation when the t = 72 hour position lies on the 40,000 n. mi. circle.

Note that if the upper limit of ΔV is 1000 ft/sec., then applying the ΔV at t = 0 offers hardly any margin for error in thrust direction. Therefore, it appears preferable to apply ΔV sometime after translunar injection. However, thrust direction accuracy is expected to diminish with time because of gyro drift associated with the stable platform. Furthermore, evaporation of the residual fuel in the S IV booster may significantly lower the ΔV below the estimated value of 1000 ft/sec. for times after t = 0. These factors have not been given consideration up to the present time.

It can be noted that some combinations of ΔV and α yield counter-clock-wise lunar trajectories. However, none of these will simultaneously satisfy the criterion of observing the lunar vehicle perilune position at slant ranges of not more than 40,000 n. mi. for both t = 72 and t = 100 hours.

CONCLUDING REMARKS

A cursory analysis has shown that an operating region exists for the velocity impulse and direction for the S IV booster which will

satisfy the Far-side Relay voice communication requirement.

A precise definition of the boost conditions for the Far-side Relay should involve the following considerations:

1. A more extensive set of data to provide a more accurate and detailed delineation of the boost operating region (such as illustrated in Figure 4). This data can be most efficiently collected by means of a computer program using an Egorov Model.

2. Examination of the velocity impulse and thrust direction accuracy available with time after translunar injection.

3. A final check on the selected design operating point using three-body trajectory equations.

To the above should probably be added the consideration of possible secondary missions of the Far-side Relay which may influence the particular reference trajectory chosen. For example, the Far-side Relay might be used as a navigation aid, together with an Earth-based computer, for lunar rendezvous steering commands to the LEM.

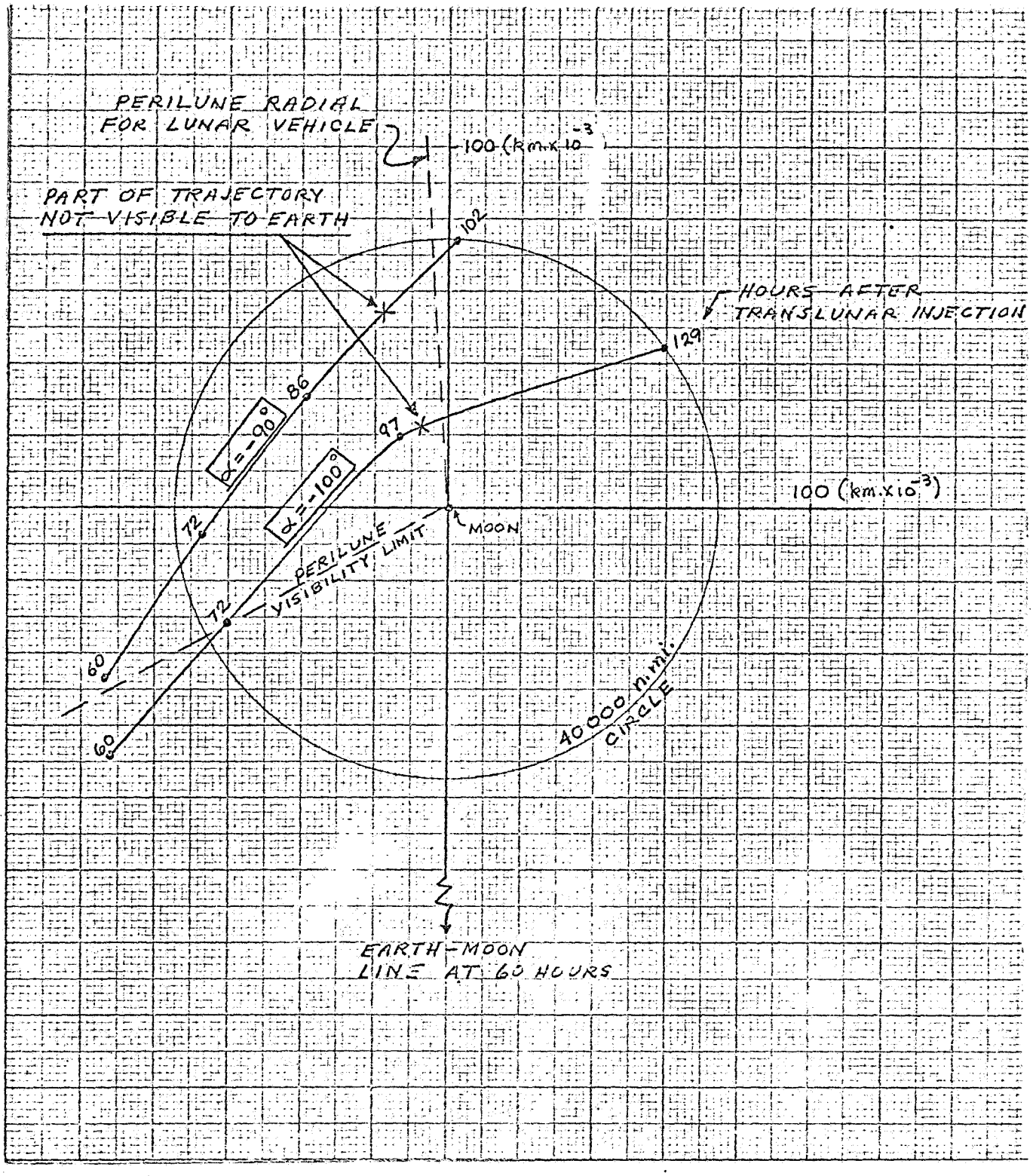

Figure 1. Far-side Relay Trajectories for ΔV = 1000 ft/sec. Applied 7.6 Hours After Translunar Injection.

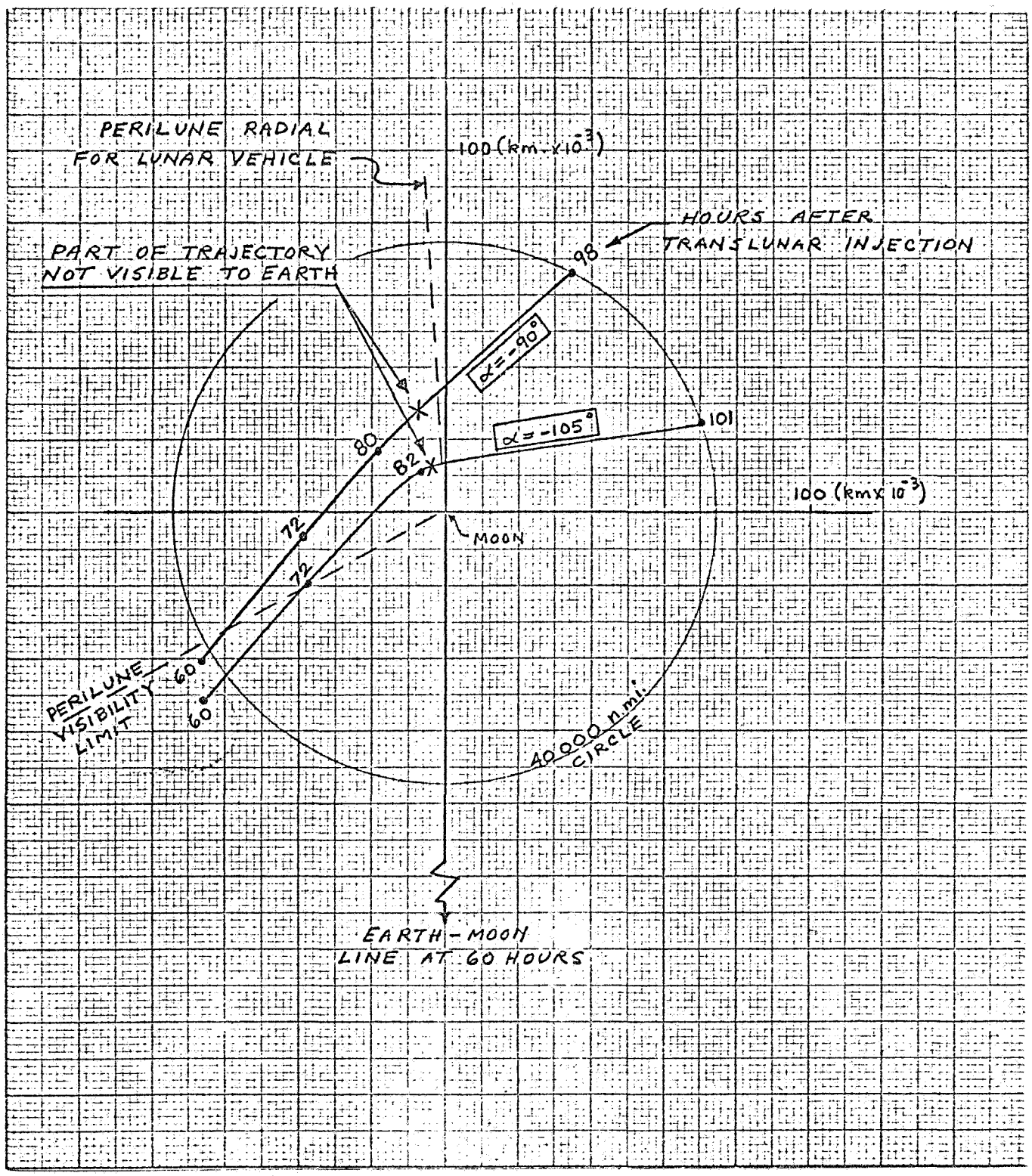

Figure 2. Far-side Relay Trajectories for ΔV = 500 ft/sec. Applied 7.6 Hours After Translunar Injection.

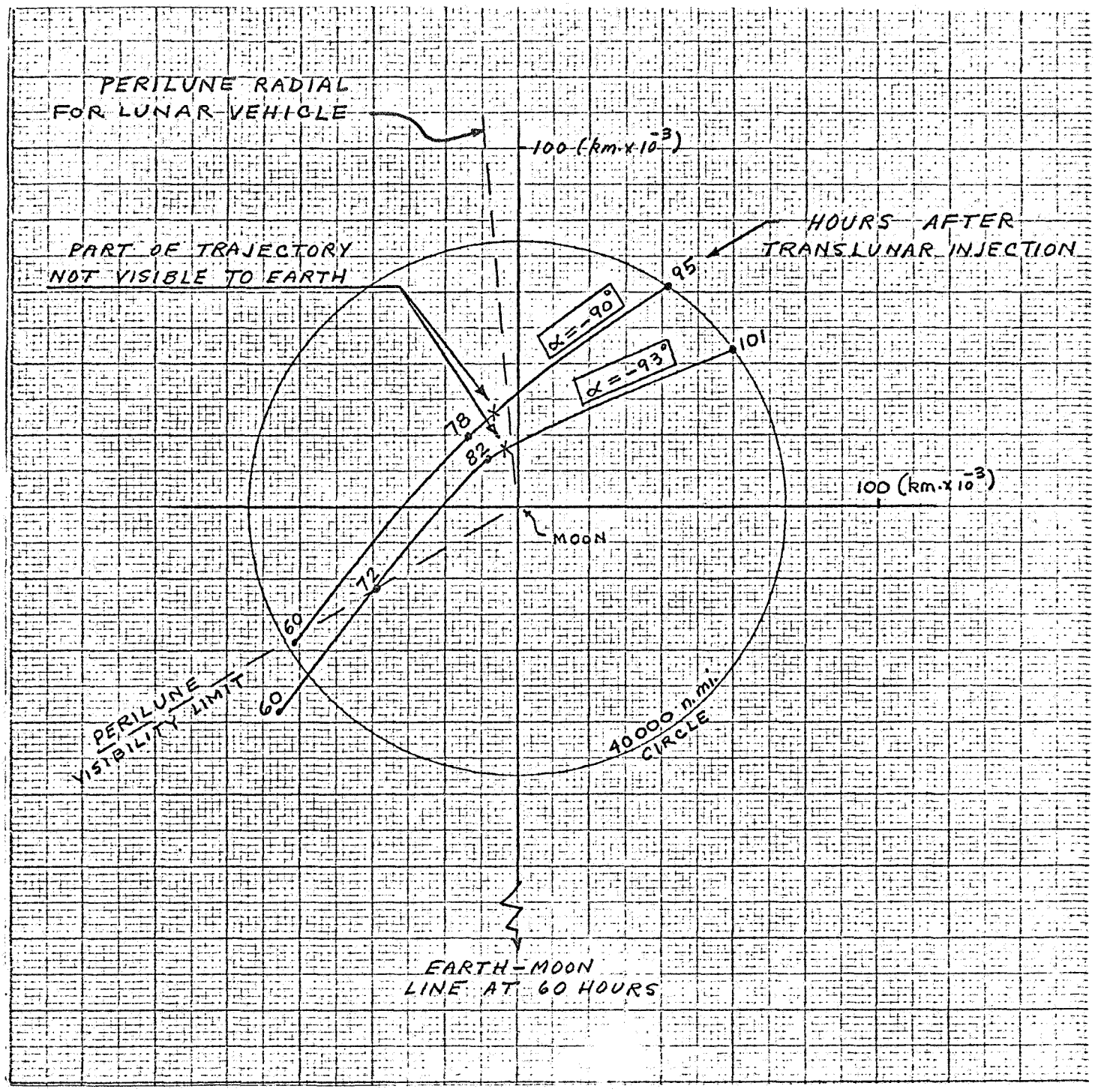

Figure 3. Far-side Relay Trajectories for ΔV = 1000 ft/sec. Applied at Time of Translunar Injection.

Limiting Criteria:

1. Lunar Vehicle Deboost Visible (t = 72 hours)
2. Lunar Rendezvous Visible (t = 100 hours and approx. same position as deboost)
3. Slant Range at Above Times $\leq$ 40,000 n. mi.

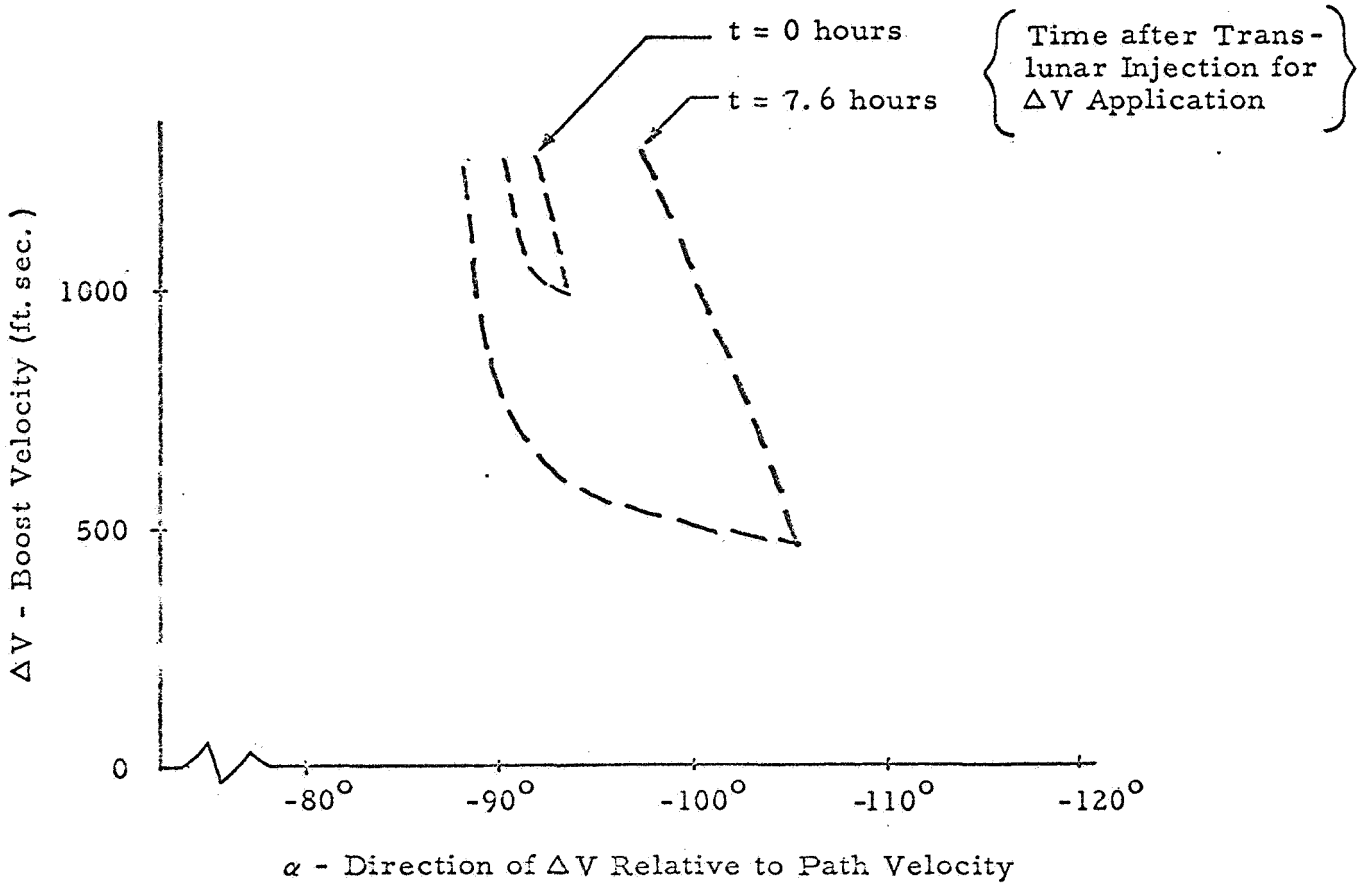

Figure 4. Approximate Operating Region for Far-side Relay Boost.

APOLLO NOTE NO. 91

L. Horowitz
5 August 1963

MINIMUM-TIME RENDEZVOUS

INTRODUCTION

Optimal control theory given in Apollo Note No. 84 is used here to develop a system of equations governing optimum thrust regulation for minimum-time rendezvous. Nonlinearities in the resulting differential system render closed form solutions untenable so that numerical computer solutions are ultimately needed. It has already been shown, however, that for the case under consideration, optimum control is always of the "bang-bang" type, with a maximum of three "switchings" over the entire optimal trajectory. [1]

Formulation of Problem

For simplicity, we take the case of planar motion in a constant gravitational field: [2]

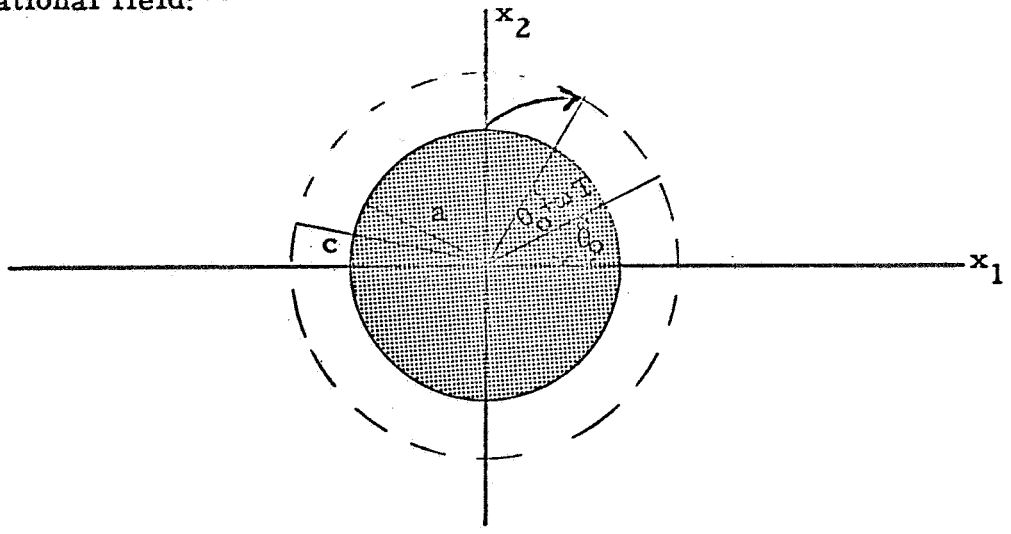

Figure 1.

---

[1] G. Leitmann, On a Class of Variational Problems in Rocket Flight, J. Aero/Space Science 26, 586-591 (1959).

[2] It has been shown that the optimum thrust schedule for this case is in fact always planar — see F. D. Faulkner, American Rocket Society Journal 31, 33-39 (1961).

notation:

x_1, x_2	:	position coordinates
x_3, x_4	:	$\dot{x}_1$, $\dot{x}_2$ respectively
x_5	:	time
u_1, u_2	:	normalized thrust components
b	:	maximum thrust magnitude
G	:	gravitational constant
$\|\|x\|\|$	:	$\sqrt{x_1^2 + x_2^2}$
T	:	total time for rendezvous (to be minimized)
V	:	constant tangential speed of target

equations of motion:

$$\begin{aligned} \dot{x}_1 &= x_3 \\ \dot{x}_2 &= x_4 \\ \dot{x}_3 &= -G\frac{x_1}{\|x\|} + b\,u_1 \\ \dot{x}_4 &= -G\frac{x_2}{\|x\|} + b\,u_2 \\ \dot{x}_5 &= 1 \end{aligned} \tag{1}$$

thrust constraint:

$$u_1^2 + u_2^2 = 1$$

boundary conditions:

initial:

$$x_1(0) = 0$$

$$x_2(0) = a$$

$$x_3(0) = 0$$

$$x_4(0) = 0$$

$$x_5(0) = 0$$

final:

$$x_1(T) = c \cos(\theta_o + \omega T)$$

$$x_2(T) = c \sin(\theta_o + \omega T)$$

$$x_3(T) = V \cos(\theta_o + \omega T)$$

$$x_4(T) = V \sin(\theta_o + \omega T)$$

$$x_5(T) = T$$

payoff function:

$$S = x_6(t) = \sum_{i=1}^{4} \lambda_i \left(x_i - x_i^T \right)^2 + \lambda_5 x_5(t),$$ where the

λ_i are non-negative, arbitrary weighting constants. We wish to minimize $x_6(T)$.

Adjoint variables:

Introduce new variables $p_i(t)$ (as in Apollo Note No. 84) by

the simultaneous system

$$\dot{p}_i = -\sum_{j=1}^{6} p_j \frac{\partial \dot{x}_j}{\partial x_i}, \quad \text{subject to the end conditions} \qquad (2)$$

$$p_i(T) = \begin{cases} 0, & i = 1, 2, 3, 4, 5 \\ -1, & i = 6 \end{cases}$$

H-function:

Introduce the Pontryagin H-function:

$$H = \sum_i p_i \dot{x}_i . \qquad (3)$$

Then by the Pontryagin Maximum Principle, H must be maximized with respect to u_i for optimum control.

Elimination of T:

We wish to eliminate the unknown T from the problem so that systems (1) and (2) can be solved simultaneously for the $x_i(t)$ and the $p_i(t)$ in terms of the $u_i(t)$; then (3) maximized with respect to u_i. To obtain an additional equation through which T may be eliminated, we consider a variation in the payoff function S:

$$S = x_6(t)$$

$$\delta S = \delta x_6 = \dot{x}_6 \, \delta t.$$

From (2), $\dot{p}_i(T) = \dfrac{\partial \dot{x}_6(T)}{\partial x_i}$ (since $p_i(T) = 0$ for $i = 1, 2, 3, 4, 5$).

Then from (3),

$$H(T) = -\dot{x}_6(T) \quad \text{so that}$$

$$\delta S = -H(T)\,\delta T.$$

For an optimum solution, we require the variation δS in the payoff function to be positive definite at time T. Since this must hold for any value of δt (positive or negative), we conclude H (t) must vanish identically at time T. This is then the required additional equation through which T may be eliminated:

$$H(T) = 0 \tag{4}$$

CONCLUSION

The desired optimal controls u_i (t) are obtained by solving the twelve simultaneous non-linear differential equations (1) and (2) subject to the initial boundary conditions in terms of the u_i. (3) is then maximized with respect to the u_i with $u_1^2 + u_2^2 = 1$. The final time T is then eliminated by (4). This yields the optimum controls u_i (t) for minimum-time rendezvous. As noted earlier, the optimum controls for this case will be "bang-bang" type, switching no more than three times over the entire trajectory. This technique has assumed ideal control so that no terminal error corrections have been considered here.

APOLLO NOTE NO. 92

L. Horowitz
6 August 1963

OPTIMUM ABORT TRAJECTORIES

INTRODUCTION

R. Roche has shown that to a first approximation, maximizing probability of safe earth return in an abort situation is tantamount to minimizing return time.[1] This note provides mechanization equations for effecting such minimum time transfers and shows how the desired optimum control is established. Two cases are treated:

I. Minimum time transfer in a gravitational field with initial and final conditions specified.

II. Minimum time transfer in a gravitational field with entry dive angle specified.

The optimization technique is that given in Apollo Note No. 84.

Case I:

Notation

x_1, x_3	:	rectangular coordinates
x_2, x_4	:	$\dot{x}_1$, $\dot{x}_3$ respectively
u_1, u_2	:	thrust components
G	:	gravitational constant
k	:	maximum thrust magnitude
S	:	payoff function

equations of motion (84-1):

$$\begin{aligned} \dot{x}_1 &= x_2 \\ \dot{x}_2 &= k u_1 - \frac{G x_1}{\|X\|} \\ \dot{x}_3 &= x_4 \end{aligned} \qquad (1)$$

[1] R. Roche, Apollo Note No. 71, p. 5

$$\dot{x}_4 = k u_2 - \frac{G x_3}{\|X\|}$$

$$\dot{x}_5 = 1 \quad , \text{ where } \|X\| = \sqrt{x_1^2 + x_3^2} \, .$$

thrust constraint (76-7):

$$u_1^2 + u_2^2 = 1$$

Payoff function:

We wish to satisfy the end conditions $x_i(t_f) = x_i^f$, $i = 1, 2, 3, 4$, for some (as yet unspecified) total transfer time t_f and at the same time minimize $x_5(t_f) = t_f$. Thus, a suitable payoff function is

$$S = x_6 = \sum_{i=1}^{4} \frac{1}{2} \lambda_i (x_i - x_i^f)^2 + x_5 , \qquad (2)$$

where the λ_i are arbitrary weighting constants ≥ 0. Thus, we require a minimum value of $S = x_6$ at $t = t_f$.

Boundary conditions:

Initial:

$$x_i(0) = x_i^o , \quad i = 1, 2, 3, 4, 5$$

Final:

$$x_i(t_f) = x_i^f , \quad i = 1, 2, 3, 4$$

Adjoint variables (84-8):

Introduce adjoint variables $p_i(t)$:

$$\dot{p}_i = - \sum_{j=1}^{6} p_j \frac{\partial \dot{x}_j}{\partial x_i} , \qquad (3)$$

where $p_i(t_f) = 0$, $i = 1, 2, 3, 4, 5$;

$$p_6(t_f) = -1 \; ;$$

as in Apollo Note No. 84, p. 6.

Pontryagin H-function (84-11):

$$H = \sum_{i=1}^{6} p_i \dot{x}_i \tag{4}$$

$$= p_1 x_2 + p_2 k u_1 - \frac{p_2 G x_1}{\|X\|} + p_3 x_4$$

$$+ p_4 k u_2 - \frac{p_4 G x_3}{\|X\|} + p_5 + p_6 \sum_{i=1}^{4} \lambda_i (x_i - x_i^f) \dot{x}_i + p_6$$

For an optimum solution, H must be maximized with respect to u_i. Therefore, the required optimum controls are:

$$\boxed{\begin{aligned} u_1 &= \frac{p_2 + \lambda_2 p_6 (x_2 - x_2^f)}{\|P\|} \\ u_2 &= \frac{p_4 + \lambda_4 p_6 (x_4 - x_4^f)}{\|P\|} \end{aligned}} \quad \text{, where} \tag{5}$$

$$\|P\| = \sqrt{\left[p_2 + \lambda_2 p_6 (x_2 - x_2^f)\right]^2 + \left[p_4 + \lambda_4 p_6 (x_4 - x_4^f)\right]^2}$$

Solution of I:

We now have the optimum controls u_1 and u_2 in terms of the $x_i(t)$ and the $p_i(t)$. These quantities are in turn obtained by simultaneous solution of (1) and (3) together with indicated boundary conditions $x_i(0) = x_i^o$ and $p_i(t_f) = 0$, $i = 1, 2, 3, 4, 5$; $p_6(t_f) = -1$. To eliminate the unknown quantity t_f from these equations, we use the additional relation

$$H(t_f) = 0 \tag{6}$$

since by (4), $H(t_f) = \sum_{i=1}^{6} p_i \dot{x}_i = -\dot{x}_6(t_f)$; just the time derivative of the payoff function S evaluated at time t_f. Hence, $\delta S(t_f) = H(t_f)\,\delta t$. For an optimum solution, $\delta S(t_f)$ must be non-negative for <u>any</u> variation δt, so that $H(t_f)$ must vanish identically for the optimum case. This eliminates t_f from (3) so that $x_i(t)$ and $p_i(t)$ can be determined by simultaneous solution of (1) and (3). Optimum controls $u_i(t)$ are then given by (5). This provides minimum time transfer in a gravitational field with initial and final conditions specified.

<u>Case II:</u>

Notation

Same as in Case I with following addition:

ψ_f : given entry dive angle

equations of motion:

Same as (1) in Case I

thrust constraint:

Same as Case I

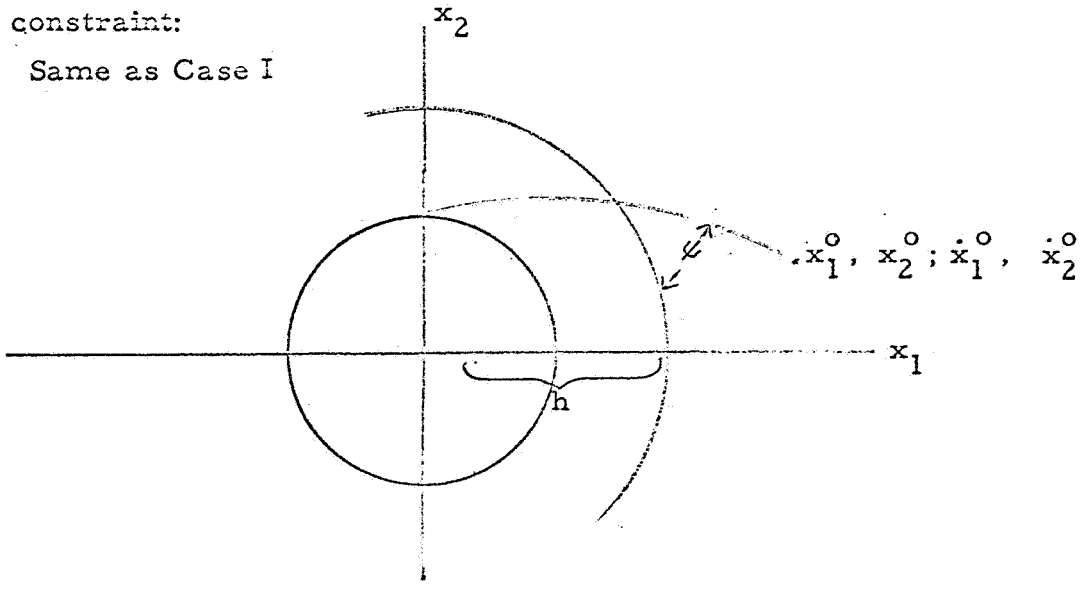

Figure 1.

boundary conditions:

Initial:

$$x_i(0) = x_i^o \quad \text{for } i = 1, 2, 3, 4$$

Final:

$$\psi_f = \arctan \left[\frac{x_2 \dot{x}_2 - x_1 \dot{x}_1}{x_1 \dot{x}_2 + x_2 \dot{x}_1} \right] \Bigg|_{x_1^2 + x_2^2 = h^2}$$

Payoff function:

We wish to satisfy the end condition $\psi = \psi_f$ when $x_1^2 + x_2^2 = h^2$ and also minimize transfer time. Thus, a suitable payoff function is

$$S = x_6 = x_5 + \lambda \left[\tan \psi_f - \frac{x_2 \dot{x}_2 - x_1 \dot{x}_1}{x_1 \dot{x}_2 + x_2 \dot{x}_1} \right], \tag{7}$$

where λ is an arbitrary non-negative weighting constant.

Adjoint variables:

Same as (3) of Case I.

$$H = \sum_{i=1}^{6} p_i \dot{x}_i \tag{8}$$

Optimum solution:

Optimum controls $u_i(t)$ are determined by maximizing H with respect to u_i, then solving (1) and (3) together with indicated boundary conditions to completely define the required optimum controls $u_i(t)$. The transfer time t_f is again eliminated from the problem by the additional relation $H(t_f) = 0$ as in Case I.

APOLLO NOTE NO. 93

H. Engel
14 August 1963

GROUND SYSTEM COMPUTATION OF LEM ORBIT

In the various schemes for ground support system computation of the LEM orbit on the basis of DSIF or MSFN radar data, there is the ever-present question of whether the computations can be performed rapidly enough to be of use. This note is intended to provide an answer to the question.

The conventional technique employed on deep-space shots is to acquire data for a long time, and then find the mean square error between the observations and the values of the quantity observed calculated on the basis of assumed or previously determined values of the trajectory parameters. The parameters are then adjusted and the computations repeated. The process continues until the mean square error is sufficiently small or can be reduced no further. The computation flow diagram is as follows for one kind of measurement only, say, Doppler velocity,

Given a priori values of orbit parameters $a_1, \ldots, a_s$

Obtain data measurements $M_1, M_2, \ldots, M_N$

Using a priori values of parameters

Compute expected values $E_1, E_2, \ldots, E_N$ of measurements, and $\partial E_1/\partial a_j, \ldots, \partial E_N/\partial a_j$ by integrating the differential equations of the orbit.

① ⟶ Compute $\sigma^2 = \frac{1}{N} \sum_{i=1}^{N} (M_i - E_i)^2$,

$$\frac{\partial \sigma^2}{\partial a_j} = \frac{2}{N} \sum_{i=1}^{N} \left(M_i - E_i - \sum_{k=1}^{s} \Delta a_k \frac{\partial E}{\partial a_k} \right) \frac{\partial E}{\partial a_j}$$

Is σ^2 small enough or as small as possible ?

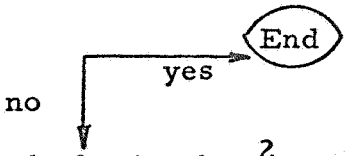

On the basis of σ^2 and $\frac{\partial \sigma^2}{\partial a_j}$ modify $a_1, \ldots, a_s$

Using these parameters compute E_i and $\partial E_i / \partial a_j$ $(i=1, \ldots, N)$ by integrating the differential equations of the orbit.

Go to (1) .

In this method of computation the computations up to the first yes-no decision can be performed concurrently with the receipt of data, but the computations necessary for the remaining computations can not be instituted until all the data is available. As a result in the case of deep-space shots, there is a long delay between receipt of the last data point and determination of the orbit parameters. According to JPL, the time required to perform an iteration is currently 20 to 25 minutes, and might possibly be reduced to 10 minutes by reprogramming. Two or three iterations have been found necessary. Further, the number of parameters considered by JPL is far more than 6, since the speed of light, the mass of the Moon and other quantities are considered as parameters. Still further, the number of observations used in the deep-space shots is far greater than will be used in ground support of the LEM.

Assuming that the gravitational field of the Moon and the ephemeris of the Moon have been determined to sufficient accuracy from previous lunar orbiting shots, and assuming that from burn-out to passing out of sight behind the Moon takes only 30 minutes, so that only 30 one-minute observations can be made, the time required to perform the necessary calculations for orbit parameter determination should be reduced by at least an order of magnitude. Use of the IBM 7094 instead of the IBM 7090 will reduce the time by almost another order of magnitude because of built-in double precision operations.

Since 30 observations is not a very large number of observations, it is not desirable to gain additional time for computation by decreasing the number of observations. Other means for reducing the time required for computation after receipt of the last data point can be found. Two approaches to this problem are possible.

The first approach starts the iteration procedure at, say, the 27th observation. The starting point for the second iteration, which uses 28 data points, is the orbit parameters determined in this fashion. In like manner the third iteration uses 29 observations, and the fourth 30 iterations, so the computations are completed with just one iteration after the last observation.

The second approach uses the Kalman-Schmidt method of parameter determination. This method is described in Apollo Note No. 88. The Kalman-Schmidt method employs a nominal or reference trajectory that has been pre-calculated in order to linearize the problem and to reduce the amount of real-time computation. If the actual trajectory is "close enough" to the reference trajectory, the Kalman-Schmidt method can be employed to produce orbit parameters within milliseconds after the final observation.

Using the lengthier procedure, the estimated time to find improved orbit parameters after the last observation is of the order of 3 seconds using range rate from one station with no biases, or 7 seconds using range, range rate and angle from three stations including biases in range and angle.

These computation times will be increased substantially if triple precision operations are required instead of double precision operations.

The computation times will increase slightly if more complete expressions for the gravitational field of the Moon must be employed.

The time to compute guidance instructions is negligible compared to the time required for orbit determination.

APPENDIX A

Encke's method is suitable for orbit calculations when near enough to one body that the effects of the gravitational fields of other bodies can be considered as small perturbations. This is the case for the LEM ascent and rendezvous trajectories.

Let $\overline{R} = \overline{R}(t)$ be the orbit relative to the Moon resulting from initial conditions of position and velocity, considering only the radially symmetric, inverse square component of the Moon's gravitational field.

$$\ddot{\overline{R}} = -\frac{\mu_M}{R^3}\,\overline{R}$$

in which μ_M is the gravitational constant of the Moon.

Let $\overline{r} = \overline{r}(t)$ be the actual motion relative to the Moon, and let

$$\overline{\rho} \triangleq \overline{r} - \overline{R}$$

Then

$$\ddot{\overline{r}} = -\frac{\mu_M}{r^3}\,\overline{r} + \overline{P}$$

and

$$\ddot{\overline{\rho}} = -\mu_M\left(\frac{\overline{r}}{r^3} - \frac{\overline{R}}{R^3}\right) + \overline{P}$$

in which $\overline{P}$ is the perturbing acceleration.

Letting

$$Q \triangleq \frac{1}{2}\left[\left(\frac{r}{R}\right)^2 - 1\right]$$

it is found that

$$Q = \frac{\overline{\rho}\cdot(\overline{R} + \overline{\rho}/2)}{R^2}$$

and

$$\ddot{\overline{\rho}} = \frac{-\mu_M}{R^3}\left[\overline{\rho} - \overline{r}\,F(Q)\right] + \overline{P}$$

where

$$F(Q) = 1 - (R/r)^3 = 1 - (1 + 2Q)^{-\frac{3}{2}}$$

$$= \sum_{j=1}^{\infty} C_j Q^j$$

For the orbits of interest, Q is a small quantity, R being of the order of 1.75×10^6 m and r differing from it by at most of the order of 10^4 m, so that $|Q| < 3 \times 10^{-5}$.

Further, the first few terms in the expansion for F (Q) are given by

$$F(Q) = 3Q - \frac{15}{2} Q^2 + \frac{35}{2} Q^3 - \frac{315}{8} Q^4 + \ldots$$

and since Q is of the order of 3×10^{-5} at most, it follows that the ratio of the third term to the first term in the above expression is between 0 and 5.25×10^{-9}. Still further the ratio of r F (Q) to ρ is

$$\frac{r\,F(Q)}{\rho} \doteq \frac{r\,3Q}{\rho} \doteq 3\,\frac{r\left(\frac{r-R}{R}\right)^2}{\rho}$$

$$< \frac{r}{\rho}\left(\frac{\rho}{R}\right)^2$$

$$< \frac{\rho}{R}$$

$$< 5.7 \times 10^{-3}$$

hence

$$\frac{r\,\frac{35}{2}\,Q^3}{\rho} < 5.7 \times 10^{-3} \times 5.25 \times 10^{-9}$$

$$< 3 \times 10^{-11}$$

Thus, the third and succeeding terms in F (Q) may be neglected, and

$$F(Q) \stackrel{\circ}{=} 3Q\left(1 - \frac{5}{2}Q\right)$$

The perturbing acceleration $\overline{P}$ may be written as

$$\overline{P} = \overline{P_1} + \overline{P_2} + \overline{P_3} + \overline{P_4}$$

in which

$\overline{P_1}$ = results from the remaining portion of the Moon's gravitational field.

$\overline{P_2}$ = results from the Earth's gravitational field.

$\overline{P_3}$ = results from the Sun's radiation pressure.

$\overline{P_4}$ = results from the Sun's gravitational field.

The gravitational potential of the Moon, in excess of its radially symmetric, inverse square portion, may be expressed as

$$U_M = \frac{G}{2r^3}\left(A_1 + A_2 + A_3 - 3I\right)$$

in which G is the universal gravitational constant, A_i is the moment of inertia about the principal axis u_i, and

$$I = \frac{1}{r^2}\left(A_1 u_1^2 + A_2 u_2^2 + A_3 u_3^2\right)$$

The corresponding acceleration has components

$$P_{1,j} = -\frac{\partial U}{\partial u_j} = \frac{3G}{2R^4}\,\frac{u_j}{R}\left(A_1 + A_2 + A_3 - 5I + 2A_j\right)$$

$$j = 1, 2, 3$$

The perturbing effect of the Earth is due to the difference in acceleration of the Moon and vehicle resulting from the Earth's gravitational field. Letting $\overline{R}_{EM}$ be the vector from the Earth to the Moon, then for the radially symmetric, inverse square portion of the field,

$$\overline{P_2} = \frac{\mu_E \, (\overline{R}_{EM} + \overline{r})}{\left|\overline{R}_{EM} + \overline{r}\right|^3} + \frac{\mu_E \, \overline{R}_{EM}}{R_{EM}^3}$$

$$= \frac{\mu_E}{R_{EM}^2} \left[\frac{\overline{R}_{EM} + \overline{r}}{R_{EM}} \left(1 + 2 \, \frac{\overline{R}_{EM} \cdot \overline{r}}{R_{EM}^2} - \frac{r^2}{R_{EM}^2} \right)^{-\frac{3}{2}} - \frac{\overline{R}_{EM}}{R_{EM}} \right]$$

Observe that r/R_{EM} is of the order of 5×10^{-3} or less. Letting

$$\alpha \triangleq \frac{2 \, \overline{R}_{EM} \cdot \overline{r}}{R_{EM}^2} + \frac{r^2}{R_{EM}^2}$$

it follows that

$$\left|\alpha\right| < 2 \, (5 \times 10^{-3})$$

$$< 10^{-2}$$

Further, μ_E / R_{EM}^2 is of the order of 3×10^{-6} m/sec ^{2}. Then

$$\overline{P_2} = \frac{-\mu_E}{R_{EM}^2} \left[\frac{\overline{r}}{R_{EM}} + \frac{\overline{R}_{EM} + \overline{r}}{R_{EM}} \left(- \frac{3}{2} \alpha + \frac{15}{8} \alpha^2 - \frac{35}{16} \alpha^3 + \frac{315}{128} \alpha_4 - \cdots \right) \right]$$

$$\doteq - 3 \times 10^{-6} \left[3 \times 10^{-5} + 1 \left(- \frac{3}{2} \, 10^{-2} + \frac{15}{8} \, 10^{-4} - \frac{35}{16} \, 10^{-6} + \cdots \right) \right]$$

so $\overline{P_2}$ can be represented adequately

$$\overline{P_2} = \frac{3\mu_E \overline{R}_{EM}}{2R_{EM}^3} \alpha$$

Thus,

$$P_{2,j} = R_{EM,j} \frac{3\mu_E}{2R_{EM}^5} \left[2\left(R_{EM,1} r_1 + R_{EM,2} r_2 + R_{EM,3} r_3 \right) + r_1^2 + r_2^2 + r_3^2 \right].$$

The effect of the higher order terms in the Earth's gravitational potential is obviously negligible.

The radiation pressure of the Sun at a distance of one astronomical unit is of the order of 4×10^{-5} dynes/m^2. With a LEM mass of 10 kg and a projected area of 10 m^2, the resultant acceleration is of the order of 10^{-12} m/sec^2, and may be neglected. Thus $\overline{P_3} \doteq 0$.

The acceleration of the vehicle relative to the Moon due to the Sun's gravitational field is

$$\overline{P_4} = \frac{\mu_s}{R_{SM}^2} \left[\frac{\overline{r}}{R_{SM}} + \frac{\overline{R}_{SM} + \overline{r}}{R_{SM}} \left(-\frac{3}{2}\alpha + \frac{15}{8}\alpha^2 - \ldots . \right) \right]$$

in which $\overline{R}_{MS}$ is the vector from the Sun to the Moon and $\alpha = r/R_{SM}$. Now μ_s/R_{SM}^2 is of the order of 10^{-11} m/sec^2, and the quantity in the brackets has magnitude less than unity, so for all practical purposes $\overline{P_4} \doteq 0$.

The differential equation for the unperturbed motion of the vehicle is most easily solved in the manner indicated in Apollo Note No. 82.

The solution of the differential equation for the perturbation $\overline{\rho}$ must be obtained by numerical integration. The method of Runge and Kutta can be used for the first few points, and then the methods of Adams and Moulton. According to JPL TR 32-223, one minute intervals of time may be used for the integration in the vicinity of the Moon. The equation to be integrated is:

$$\ddot{\overline{\rho}} = \frac{-\mu_M}{R^3} \left[\overline{\rho} + \overline{R} F(Q) \right] + \overline{P}$$

in which the right-hand side is a function of time and position only.

This equation may be rewritten as a set of simultaneous first order differential equations by letting

$$\xi_1 \triangleq \rho_1$$

$$\xi_2 \triangleq \rho_2$$

$$\xi_3 \triangleq \rho_3$$

$$\xi_4 \triangleq \dot{\rho}_1$$

$$\xi_5 \triangleq \dot{\rho}_2$$

$$\xi_6 \triangleq \dot{\rho}_3$$

Then

$$\dot{\xi}_{i+3} = \frac{-\mu_M}{R^3}\left[\xi_i + R_i\, F(Q)\right] + P_i \qquad i = 1, 2, 3$$

$$\dot{\xi}_i = \xi_{i+3} \qquad i = 1, 2, 3$$

The initial conditions are

$$\xi_{i,0} = 0. \qquad i = 1, \ldots, 6$$

The solution is started using the Runge-Kutta method, using

$$\xi_{i,n+1} = \xi_{i,n} + (k_{i,1} + 2k_{i,2} + 2k_{i,3} + k_{i,4}) / 6$$

where:

$$k_{i,1} = h\,\dot{\xi}_i\,(T_n, \xi_{1,n}, \xi_{2,n}, \ldots, \xi_{6,n})$$

$$k_{i,2} = h\,\dot{\xi}_i\,(T_n + h/2,\ \xi_{1,n} + k_{i,1}/2, \ldots, \xi_{6,n} + k_{6,1}/2)$$

$$k_{i,3} = h\,\dot{\xi}_i\,(T_n + h/2,\ \xi_{1,n} + k_{1,2}/2, \ldots,\ \xi_{6,n} + k_{6,2}/2)$$

$$k_{i,4} = h\,\dot{\xi}_i\,(T_n + h, \xi_{1,n} + k_{1,3}, \ldots, \xi_{6,n} + k_{6,3})$$

in which

$$h \triangleq T_{n+1} - T_n$$

and is independent of n.

The steps of the Runge-Kutta method are repeated five times to obtain initial differences for use in the methods of Adams and Moulton. These differences are $\nabla^j \xi_{i,5}$ in which

$$\nabla w_n \triangleq w_n - w_{n-1}$$

$$\nabla^{m+1} w_n \triangleq \nabla^m w_n - \nabla^m w_{n-1} = \nabla \nabla^m w_n$$

In the next and succeeding iterations, the method of Adams is employed to obtain first estimates of $\xi_{i,n+1}$, and then the method of Moulton is applied repeatedly to obtain better values for these quantities. It is assumed that three iterations each time are sufficient.

In Adam's method

$$\xi_{i,n+1} = \xi_{i,n} + h\left[1 + \frac{1}{2}\nabla + \frac{5}{12}\nabla^2 + \frac{3}{8}\nabla^3 + \frac{251}{720}\nabla^4 + \frac{95}{288}\nabla^5\right]\xi_{i,n}$$

and in Moulton's method the improved value of $\xi_{i,n+1}$ is obtained from:

$$\text{Improved } \xi_{i,n+1} = \xi_{i,n} + h\left[1 - \frac{1}{2}\nabla - \frac{1}{12}\nabla^2 - \frac{1}{24}\nabla^3 - \frac{19}{720}\nabla^4 - \frac{3}{160}\nabla^5\right]\xi_{i,n+1}$$

After obtaining $\bar{\rho}$ and $\dot{\bar{\rho}}$ in this manner for all the points in time at which data is to be taken, the computed values of the observed quantities are determined. Considering only range rate from one station as an example, the expected number of Doppler cycles in the one minute of observation must be computed, allowing for the motions of the vehicle and station during the signal transit time.

Using a co-ordinate system fixed in the station, a signal received by the station at time T_n must have been transmitted by the vehicle τ_n seconds earlier, where

$$\tau_n = \left| \bar{s}\,(T_n - \tau_n) \right| / c$$

in which $\bar{s}\ (T_n - \tau_n)$ is the position of the vehicle relative to the station at time $T_n - \tau_n$ and c is the speed of light. If this signal is a re-transmittal of a signal the vehicle received from the station, it must have been transmitted by the station at time $T_n - 2\tau_n$. Any relativistic corrections necessitated by the vehicle off-setting the re-transmitted frequency are neglected here. τ_n is determined by solution of the equation:

$$c\tau_n = \left| \bar{s}\ (T_n - \tau_n) \right| = s\ (T_n - \tau_n)$$

In the vicinity of T_n, s (T) can be expressed as a quadratic in T. Let s_n denote s (T_n). Then,

$$s\ (T_n - \tau_n) = s_n - \frac{s_{n+1} - s_{n-1}}{2h}\ \tau_n + \frac{s_{n+1} - 2\ s_n + s_{n-1}}{2h^2}\ \tau_n^2$$

$$= s_n + b_n\ \tau_n + c_n\ \tau_n^2$$

and

$$c\tau_n = s_n + b_n\ \tau_n + c_n\ \tau_n^2$$

so

$$\tau_n = \frac{(c - b_n) - \sqrt{(c - b_n)^2 - 4\ c_n\ s_n}}{2c_n}$$

$$= \frac{c - b_n}{2\ c_n} \left[1 - \sqrt{1 - \frac{4\ c_n\ s_n}{(c - b_n)^2}} \right]$$

$$\stackrel{o}{=} \frac{c - b_n}{2\ c_n}\ \frac{2\ c_n\ s_n}{(c - b_n)^2}$$

$$\stackrel{o}{=} \frac{s_n}{c - b_n}$$

or, more accurately,

$$\tau_n = \frac{s_n}{c - \dot{s}_n}$$

Letting f be the transmitting frequency of the station, the number of cycles received by the station between T_n and T_{n+1} is

$f \left[(T_{n+1} - 2\tau_{n+1}) - (T_n - 2\tau_n) \right]$ and the number of Doppler cycles between this and the signal transmitted in the interval $T_{n+1} - T_n$ is $-2f(\tau_{n+1} - \tau_n)$.

Let

$$\Gamma_n \triangleq -2f(\tau_n - \tau_{n-1})$$

and let γ_n be the measured value of this quantity. Then

$$\sigma^2 = \frac{1}{N} \sum_{i=1}^{N} (\gamma_i - \Gamma_i)^2$$

is to be minimized by choice of the six orbit parameters $a_1, \ldots, a_6$. This is accomplished by computing Γ_i and $\partial \Gamma_i / \partial a_j$ for the assumed set of six orbit parameters, and setting $\partial \sigma^2 / \partial a_j$ equal to zero. This gives six simultaneous linear equations for estimates of the changes in the parameters to minimize σ^2.

$$\sigma^2 = \frac{1}{N} \sum_{i=1}^{N} \left(\gamma_i - \Gamma_i - \frac{\partial \Gamma_i}{\partial a_1} \Delta a_1 - \ldots - \frac{\partial \Gamma_i}{\partial a_6} \Delta a_6 \right)^2$$

$$\frac{\partial \sigma^2}{\partial \Delta a_j} = 0 = \frac{2}{N} \sum_{i=1}^{N} \left(\gamma_i - \Gamma_i - \frac{\partial \Gamma_i}{\partial a_1} \Delta a_1 - \ldots - \frac{\partial \Gamma_i}{\partial a_6} \Delta a_6 \right) \frac{\partial \Gamma_i}{\partial a_j}$$

Letting

$$C_{jk} \triangleq \sum_{i=1}^{N} \frac{\partial \Gamma_i}{\partial a_j} \frac{\partial \Gamma_i}{\partial a_k}$$

and

$$e_k = \sum_{i=1}^{N} (\gamma_i - \Gamma_i) \frac{\partial \Gamma_i}{\partial a_k}$$

the above equations, $\partial \sigma^{-2} / \partial \Delta a_j = 0$, can be written as:

$$\left[C_{jk} \right] \left[\Delta a_j \right] = \left[e_k \right]$$

Inverting the C matrix, we find

$$\left[\Delta \alpha_j \right] = \left[C_{jk} \right]^{-1} \left[e_k \right].$$

The quantities $\partial \Gamma_i / \partial a_j$ to be used in the above equations are obtained as follows:

$$\Gamma_i = -2f (\tau_i - \tau_{i-1})$$

$$\frac{\partial \Gamma_i}{\partial a_j} = -2f \left(\frac{\partial \tau_i}{\partial a_j} - \frac{\partial \tau_{i-1}}{\partial a_j} \right)$$

Now,

$$\tau_i = \frac{s_i}{c - \dot{s}_i}$$

so

$$\frac{\partial \tau_i}{\partial a_j} = \frac{\tau_i}{s_i} \frac{\partial s_i}{\partial a_j} - \frac{\tau_i}{c - \dot{s}_i} \frac{\partial \dot{s}_i}{\partial a_j}$$

Thus $\partial \Gamma_i / \partial a_j$ can be computed. In calculating $\partial s_i / \partial a_j$ and $\partial \dot{s} / \partial a_j$, the unperturbed orbit may be used.

The orbit parameter estimates are changed in accordance with the Δa_j's obtained in this manner and the entire computation repeated.

The flow diagram for the computation could be as follows, although in practice a more efficient arrangement might be found. This flow diagram suffices for determining computation time.

Insert h and "a priori" parameters $a_1, \ldots, a_6$

Note: Parameters are position and velocity relative to the Moon.

(2) ⟶ Accept measurement γ_k

Is $k \geq 26$?

yes ↓ no ⟶ (2)

$\xi_{i,o} = 0 \qquad , i=1,\ldots,6$

$R_o^2 = a_1^2 + a_2^2 + a_3^2$

$R_o = \sqrt{R_o^2}$

$V_o^2 = a_4^2 + a_5^2 + a_6^2$

$-2E = \frac{\mu_M}{R_o} - V_o^2$

$\sqrt{-2E} = \sqrt{-2E}$

Note: $\overline{H} = \overline{R_o} \times \overline{V_o}$

$H_1 = a_2 a_6 - a_3 a_5$

$H_2 = a_3 a_4 - a_1 a_6$

$$H_3 = a_1 a_5 - a_2 a_4$$

$$H^2 = H_1^2 + H_2^2 + H_3^2$$

$$H = \sqrt{H^2}$$

$$\hat{H}_1 = H_1/H$$

$$\hat{H}_2 = H_2/H$$

$$\hat{H}_3 = H_3/H$$

$$\hat{R}_1 = a_1/R_o$$

$$\hat{R}_2 = a_2/R_o$$

$$\hat{R}_3 = a_3/R_o$$

Note: $\hat{L} = \hat{R}_o \times \hat{H}$

$$\hat{L}_1 = \hat{R}_2 \hat{H}_3 - \hat{R}_3 \hat{H}_2$$

$$\hat{L}_2 = \hat{R}_3 \hat{H}_1 - \hat{R}_1 \hat{H}_3$$

$$\hat{L}_3 = \hat{R}_1 \hat{H}_2 - \hat{R}_2 \hat{H}_1$$

Note: In the $\hat{R}_o$, $\hat{H}$, $\hat{L}$ co-ordinate system the unperturbed orbit is in the $\hat{R}_o \hat{L}$ - plane.

$$H_\mu = H/\mu_M$$

$$H_{2\mu} = H^2/\mu_M$$

$$H_\nu = H_{2\mu}/R_o$$

$$e \cos \theta_o = H_\nu - 1$$

$$e \sin \theta_o = H_\mu (\hat{R}_1 a_4 + \hat{R}_2 a_5 + \hat{R}_3 a_6)$$

$$e^2 = (e \cos \theta_o)^2 + (e \sin \theta_o)^2$$

$$e = \sqrt{e^2}$$

$$(1 - e^2)^{1/2} = \sqrt{-2E}\ H_\mu$$

$$e \sin \xi_o = \frac{(1-e^2)^{1/2} (e \sin \theta_o)}{H_\nu}$$

$$e \cos \xi_o = \frac{e^2 + (e \cos \theta_o)}{H_\nu}$$

$$\xi_o = \tan^{-1} \frac{(e \sin \xi_o)}{(e \cos \xi_o)}$$

Note: Branch path necessary, but not shown, if $H_\nu = 1$. Also, quadrant decision necessary but not shown to determine quadrant of ξ_o.

$$M_o = \xi_o - (e \sin \xi_o)$$

$$n = \frac{(-2E)\sqrt{-2E}}{\mu_M}$$

$$\alpha_5 = H/R_o$$

$$\alpha_4 = \sqrt{V_o^2 - \alpha_5^2}$$

$$\frac{\partial H}{\partial \alpha_j} = \delta_{1j} \alpha_5 - \delta_{2j} \alpha_4 + \delta_{5j} R_o \qquad j = 1, \ldots, 6$$

$$\frac{\partial E}{\partial \alpha_j} = \delta_{1j} \frac{\mu_M}{R_o^2} + \delta_{4j} \alpha_4 + \delta_{5j} \alpha_5$$

$$\frac{\partial e^2}{\partial \alpha_j} = 2 H_\mu^2 \left[\frac{\partial E}{\partial \alpha_j} + \frac{2E}{H} \frac{\partial H}{\partial \alpha_j} \right]$$

$$\frac{\partial (e \cos \theta_o)}{\partial \alpha_j} = \frac{\alpha_5}{\mu} \left[2 \frac{\partial H}{\partial \alpha_j} - \delta_{1j} \alpha_5 \right]$$

$$\frac{\partial (e \sin \theta_o)}{\partial \alpha_j} = \frac{\alpha_5}{\mu} (\delta_{4j} R_o + \delta_{2j} \alpha_5) + \frac{\alpha_4}{\mu} \frac{\partial H}{\partial \alpha_j}$$

$$\frac{\partial (e \sin \xi_o)}{\partial \alpha_j} = \frac{-(e \sin \xi_o)}{2 (1-e^2)} \frac{\partial e^2}{\partial \alpha_j} + \frac{(1-e^2)^{1/2}}{H_\nu} \frac{\partial (e \sin \theta_o)}{\partial \alpha_j} - \frac{(e \sin \xi_o)}{H_\nu} \frac{\partial (e \cos \theta_o)}{\partial \alpha_j}$$

$$\frac{\partial (e \cos \xi_o)}{\partial \alpha_j} = \frac{1}{H_\nu} \frac{\partial e^2}{\partial \alpha_j} + \left[\frac{(1-e)^{1/2}}{H_\nu} \right]^2 \frac{\partial (e \cos \theta_o)}{\partial \alpha_j}$$

$$\frac{\partial e}{\partial \alpha_j} = \cos \theta_o \frac{\partial (e \cos \theta_o)}{\partial \alpha_j} + \sin \theta_o \frac{\partial (e \sin \theta_o)}{\partial \alpha_j}$$

$$e \frac{\partial \xi_o}{\partial \alpha_j} = \cos \xi_o \frac{\partial (e \sin \xi_o)}{\partial \alpha_j} - \sin \xi_o \frac{\partial (e \cos \xi_o)}{\partial \alpha_j}$$

$$e \frac{\partial M_o}{\partial \alpha_j} = (1 - e \cos \xi_o) \left(e \frac{\partial \xi_o}{\partial \alpha_j} \right) - \frac{\sin \xi_o}{2} \frac{\partial e^2}{\partial \alpha_j}$$

$$\nu_o = \frac{\sin \xi_o \left(\frac{1 - e \cos \xi_o}{1 - e^2} + 1 \right) \frac{\partial e}{\partial \alpha_j}}{(1 - e \cos \xi_o)^2}$$

i= 0

③

(3)

$$M_{i+1} = M_i + n\,h$$

$$\tilde{\xi}_{i+1} = \xi_i + \frac{n\,h}{1 - e\cos\xi_i}$$

(4) $\longrightarrow$ $$\tilde{M} = \tilde{\xi}_{i+1} - e\sin\tilde{\xi}_{i+1}$$

Is $$\left|\frac{M_{i+1} - \tilde{M}}{1 - e\cos\tilde{\xi}_i}\right| \leq K_1 ?$$

yes

$$\xi_{i+1} = \tilde{\xi}_{i+1}$$

$$i = i + 1$$

$$\sin\xi_i = \sin\xi_i$$

$$\cos\xi_i = \cos\xi_i$$

$$\sin\theta_i = \frac{(1-e^2)^{1/2}\sin\xi_i}{1-e\cos\xi_i}$$

$$\cos\theta_i = \frac{\cos\xi_i - e}{1-e\cos\xi_i}$$

no

$$\tilde{\xi}_{i+1} = \tilde{\xi}_{i+1} + \left[\frac{M_{i+1} - \tilde{M}}{1-e\cos\tilde{\xi}_{i+1}}\right]$$

(4)

$$\sin(\theta_i - \theta_o) = \sin\theta_i\cos\theta_o - \sin\theta_o\cos\theta_i$$

$$\cos(\theta_i - \theta_o) = \cos\theta_i\cos\theta_o + \sin\theta_o\sin\theta_i$$

$$R_i = \frac{H_{2\mu}}{1 + e\cos\theta_i}$$

$$R_{i,R} = R_i\cos(\theta_i - \theta_o)$$

$$R_{i,L} = R_i \sin(\theta_i - \theta_o)$$

$$R_{i,1} = R_{i,R} \hat{R}_1 + R_{i,L} \hat{L}_1$$

$$R_{i,2} = R_{i,R} \hat{R}_2 + R_{i,L} \hat{L}_2$$

$$R_{i,3} = R_{i,R} \hat{R}_3 + R_{i,L} \hat{L}_3$$

$$\dot{R}_i = \frac{e \sin \theta_i}{H_\mu}$$

$$R_i \dot{\theta}_i = \frac{H}{R_i^2}$$

$$\dot{R}_{i,R} = \dot{R}_i \cos(\theta_i - \theta_o) - R_i \dot{\theta}_i \sin(\theta_i - \theta_o)$$

$$\dot{R}_{i,L} = \dot{R}_i \sin(\theta_i - \theta_o) + R_i \dot{\theta}_i \cos(\theta_i - \theta_o)$$

$$\dot{R}_{i,1} = \dot{R}_{i,R} \hat{R}_1 + \dot{R}_{i,L} \hat{L}_1$$

$$\dot{R}_{i,2} = \dot{R}_{i,R} \hat{R}_2 + \dot{R}_{i,L} \hat{L}_2$$

$$\dot{R}_{i,3} = \dot{R}_{i,R} \hat{R}_3 + \dot{R}_{i,L} \hat{L}_3$$

$i \geq k$

no → (3)

yes ↓

$\xi_{j,o} = 0 \qquad j = 1, \ldots, 6$

$i = 0$

$\ell = 1$

↓

(5)

(5)

$$r_{1,i} = R_{1,i} + \xi_{1,i}$$

$$r_{2,i} = R_{2,i} + \xi_{2,i}$$

$$r_{3,i} = R_{3,i} + \xi_{3,i}$$

$$r_i^2 = r_{1,i}^2 + r_{2,i}^2 + r_{3,i}^2$$

$$r_i = \sqrt{r_i^2}$$

$$I = \frac{\left(A_1 r_{1,i}^2 + A_2 r_{2,i}^2 + A_3 r_{3,i}^2\right)}{r_i^2}$$

$$\frac{3G}{2r_i^5} = \frac{3G}{2} \cdot \frac{1}{(r_i^2)^2 r_i}$$

$$A = A_1 + A_2 + A_3 - 5I$$

$$P_{1,1} = (A - A_1) \frac{3G}{2r_i^5} \xi_1$$

$$P_{1,2} = (A - A_2) \frac{3G}{2r_i^5} \xi_2$$

$$P_{1,3} = (A - A_3) \frac{3G}{2r_i^5} \xi_3$$

Look up $\overline{R}_{EM}$ in Ephemeris (assume 200 multiplications and 200 additions for each look-up and co-ordinate rotations).

$$R_{EM}^2 = R_{EM,1}^2 + R_{EM,2}^2 + R_{EM,3}^2$$

$$\bar{R}_{EM} \cdot \bar{r} = R_{EM,1}\, r_{1,i} + R_{EM,2}\, r_{2,i} + R_{EM,3}\, r_{3,i}$$

$$p_2 = \frac{3\mu_E}{2\left(R_{EM}^2\right)^2 \sqrt{R_{EM}^2}} \left(\bar{R}_{EM} \cdot \bar{r} + r_i^2 \right)$$

$$P_1 = P_{1,1} + p_2\, R_{EM,1}$$

$$P_2 = P_{1,2} + p_2\, R_{EM,2}$$

$$P_3 = P_{1,3} + p_2\, R_{EM,3}$$

$$Q = \frac{\xi_1 (R_1 + \xi_1/2) + \xi_2 (R_2 + \xi_2/2) + \xi_3 (R_3 + \xi_3/2)}{R^2}$$

$$F(Q) = 3Q\left(1 - \frac{5}{2} Q\right)$$

$$\dot{\xi}_1 = \xi_4$$

$$\dot{\xi}_2 = \xi_5$$

$$\dot{\xi}_3 = \xi_6$$

$$\dot{\xi}_4 = \frac{-\mu_M}{R^3} \left[\xi_1 + R_1 F(Q) \right] + P_1$$

$$\dot{\xi}_5 = \frac{-\mu_M}{R^3} \left[\xi_2 + R_2 F(Q) \right] + P_2$$

$$\dot{\xi}_6 = \frac{-\mu_M}{R^3} \left[\xi_3 + R_3 F(Q) \right] + P_3$$

$i \leq 5$?

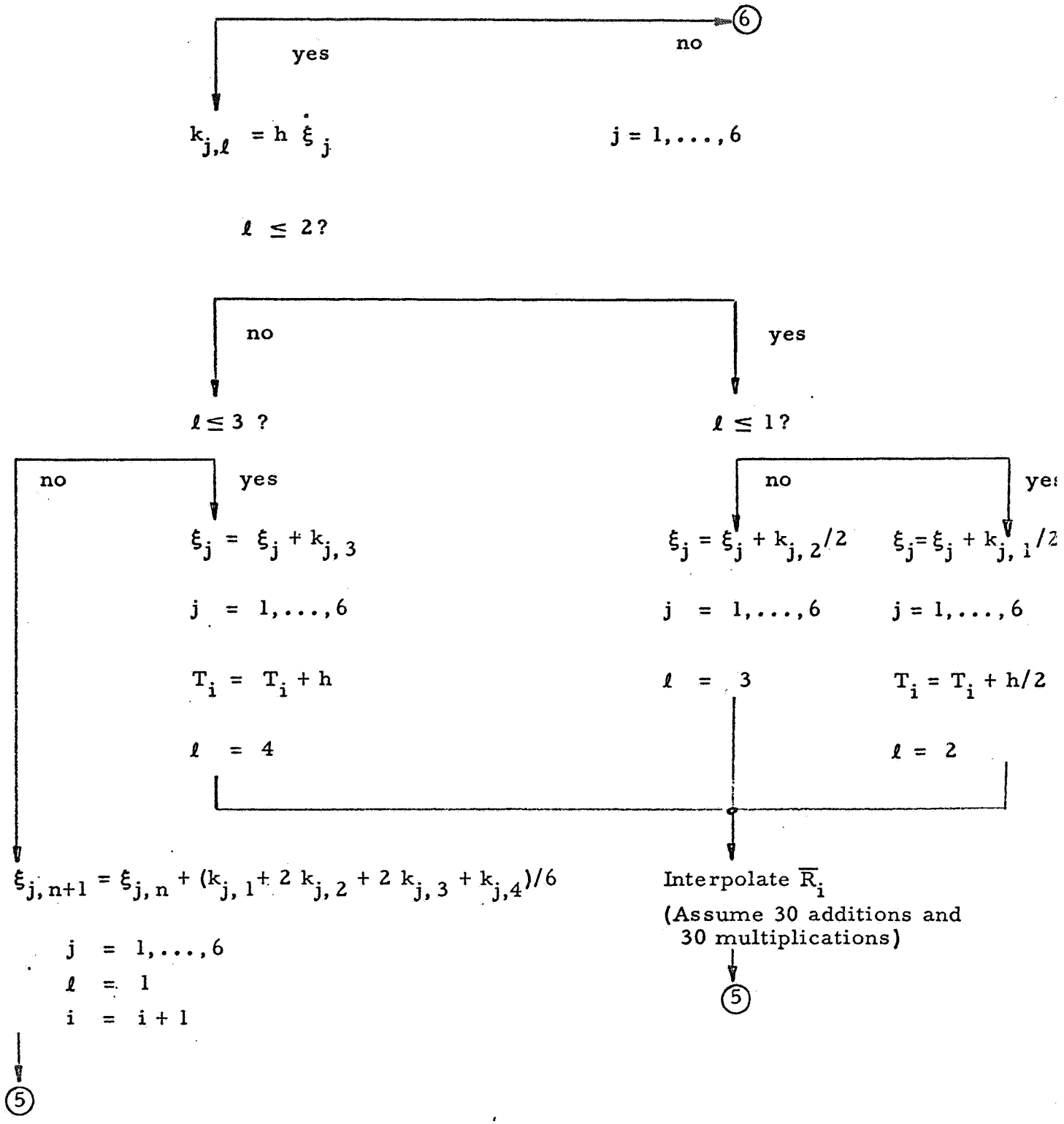
6
yes
no
$k_{j,\ell} = h \dot{\xi}_j$
$j = 1,\ldots,6$
$\ell \leq 2$?
no
yes
$\ell \leq 3$?
$\ell \leq 1$?
no
yes
no
yes
$\xi_j = \xi_j + k_{j,3}$
$j = 1,\ldots,6$
$T_i = T_i + h$
$\ell = 4$
$\xi_j = \xi_j + k_{j,2}/2$
$j = 1,\ldots,6$
$\ell = 3$
$\xi_j = \xi_j + k_{j,1}/2$
$j = 1,\ldots,6$
$T_i = T_i + h/2$
$\ell = 2$
$\xi_{j,n+1} = \xi_{j,n} + (k_{j,1} + 2\,k_{j,2} + 2\,k_{j,3} + k_{j,4})/6$
$j = 1,\ldots,6$
$\ell = 1$
$i = i + 1$
Interpolate $\overline{R}_i$
(Assume 30 additions and 30 multiplications)
5
5
6
$i \geq k$?

no → yes → (7)

$$\xi_{j,i+1} = \xi_{j,i} + h \left[\gamma_o \xi_{j,i} + \gamma_1 \xi_{j,i-1} + \gamma_2 \xi_{j,i-2} + \gamma_3 \xi_{j,i-3} + \gamma_4 \xi_{j,i-4} + \gamma_5 \xi_{j,i-5} \right] \qquad j=1,\ldots,6$$

$$m = 0$$

(8) → $$\xi_{j,i+1} = \xi_{j,i+1} + h \left[\beta_o \xi_{j,i+1} + \beta_1 \xi_{j,i} + \beta_2 \xi_{j,i-1} + \beta_3 \xi_{j,i-2} + \beta_4 \xi_{j,i-3} + \beta_5 \xi_{j,i-4} \right] \qquad j=1,\ldots,6$$

$$m = m + 1$$

$$m \geq 3 \ ?$$

no → (8)

yes → (5)

(7)

$$i = 0$$

(9) → $$R_{ED,I} = \zeta_1 \cos(\omega_e T_i + \ell_o)$$

$$R_{ED,II} = \zeta_1 \sin(\omega_e T_i + \ell_o)$$

$$R_{ED,III} = \zeta_2$$

$$R_{ED,1} = C_{11} R_{ED,I} + C_{12} R_{ED,II} + C_{13} R_{ED,III}$$

$$R_{ED,2} = C_{21} R_{ED,I} + C_{22} R_{ED,II} + C_{23} R_{ED,III}$$

$$R_{ED,3} = C_{31} R_{ED,I} + C_{32} R_{ED,II} + C_{33} R_{ED,III}$$

$$\dot{R}_{ED,I} = -\omega_e R_{ED,II}$$

$$\dot{R}_{ED,II} = \omega_e R_{ED,I}$$

$$\dot{R}_{ED,III} = 0$$

$$\dot{R}_{ED,1} = C_{11} \dot{R}_{ED,I} + C_{12} \dot{R}_{ED,II} + C_{13} \dot{R}_{ED,III}$$

$$\dot{R}_{ED,2} = C_{21} \dot{R}_{ED,I} + C_{22} \dot{R}_{ED,II} + C_{23} \dot{R}_{ED,III}$$

$$\dot{R}_{ED,3} = C_{31} \dot{R}_{ED,I} + C_{32} \dot{R}_{ED,II} + C_{33} \dot{R}_{ED,III}$$

$\dot{R}_{EM,1}$, $\dot{R}_{EM,2}$, $\dot{R}_{EM,3}$ from computed values of $R_{EM,1}$, $R_{EM,2}$, $R_{EM,3}$ by finite differences. (Assume 10 multiplications and 10 additions for each $\dot{R}_{EM,j}$).

$$\dot{r}_1 = \dot{R}_{i,1} + \dot{\xi}_4$$

$$\dot{r}_2 = \dot{R}_{i,2} + \dot{\xi}_5$$

$$\dot{r}_3 = \dot{R}_{i,3} + \dot{\xi}_6$$

$$s_{1,i} = R_{EM,1} + r_1 - R_{ED,1}$$

$$s_{2,i} = R_{EM,2} + r_2 - R_{ED,2}$$

$$s_{3,i} = R_{EM,3} + r_3 - R_{ED,3}$$

$$s^2 = s_{1,i}^2 + s_{2,i}^2 + s_{3,i}^2$$

$$s_i = \sqrt{s^2}$$

$$\dot{s}_{1,i} = \dot{R}_{EM,1} + \dot{r}_1 - \dot{R}_{ED,1}$$

$$\dot{s}_{i,2} = \dot{R}_{EM,2} + \dot{r}_2 - \dot{R}_{ED,2}$$

$$\dot{s}_{i,3} = \dot{R}_{EM,3} + \dot{r}_3 - \dot{R}_{ED,3}$$

$$s\,\dot{s} = s_{1,i}\,\dot{s}_{1,i} + s_{2,i}\,\dot{s}_{2,i} + s_{3,i}\,\dot{s}_{3,i}$$

$$\dot{s}_i = \frac{1}{s_i}\,(s\,\dot{s})$$

$$\tau_i = \frac{s_i}{c - s_i}$$

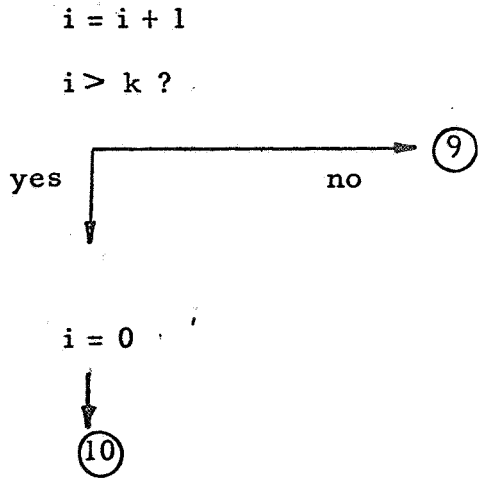

(10)

$$\gamma_i - \Gamma_i = \gamma_i - 2f(\tau_i - \tau_{i-1})$$

$$\sum(\gamma_i - \Gamma_i)^2 = \sum(\gamma_i - \Gamma_i)^2 + (\gamma_i - \Gamma_i)^2$$

$$e\frac{\partial\theta_i}{\partial\alpha_j} = \frac{(1-e^2)^{1/2}}{(1-e\cos\xi_i)^2}\left\{\frac{3(M_i-M_o)}{2E}\, e\frac{\partial E}{\partial\alpha_j} + \left(e\frac{\partial M_o}{\partial\alpha_j}\right) + \frac{\sin\xi_i}{2}\left(\frac{1-e\cos\xi_i}{1-e^2}+1\right)\frac{\partial e^2}{\partial\alpha_j}\right\}$$

$$\frac{\partial(\theta_i-\theta_o)}{\partial\alpha_j} = (1-e^2)^{1/2}\left\{\begin{array}{l}\dfrac{3(M_i-M_o)}{2E}\dfrac{\partial E}{\partial\alpha_j} + \sin\xi_i\left(\dfrac{1-e\cos\xi_i}{1-e^2}+1\right)\dfrac{\partial e}{\partial\alpha_j} \\ -\nu_o \\ +\dfrac{(\cos\xi_i-\cos\xi_o)\left(2-e\left[\cos\xi_i+\cos\xi_o\right]\right)}{(1-e\cos\xi_i)^2(1-e\cos\xi_o)^2}\left(e\dfrac{\partial M_o}{\partial\alpha_j}\right)\end{array}\right\}$$

$$\frac{\partial R_i}{\partial\alpha_j} = \frac{2R_i}{H}\frac{\partial H}{\partial\alpha_j} + \frac{R_i}{1+e\cos\theta_i}\left[\cos\theta_i\frac{\partial e}{\partial\alpha_j} - \sin\theta_i\left(e\frac{\partial\theta_i}{\partial\alpha_j}\right)\right]$$

$$\frac{\partial R_{i,R}}{\partial\alpha_j} = -R_{i,L}\frac{\partial(\theta_i-\theta_o)}{\partial\alpha_j} + \cos(\theta_i-\theta_o)\frac{\partial R_i}{\partial\alpha_j}$$

$$\frac{\partial R_{i,L}}{\partial \alpha_j} = R_{i,R} \frac{\partial(\theta_i - \theta_o)}{\partial \alpha_j} + \sin(\theta_i - \theta_o) \frac{\partial R_i}{\partial \alpha_j}$$

$$\frac{\partial R_{i,H}}{\partial \alpha_j} = \delta_{3j} \frac{\alpha_5 R_{i,R} - \alpha_4 R_{i,L}}{H} + \delta_{6j} \frac{R_{iL}}{\alpha_5}$$

$$\frac{\partial R_{i,1}}{\partial \alpha_j} = \frac{\partial R_{i,R}}{\partial \alpha_j} \hat{R}_1 + \frac{\partial R_{i,L}}{\partial \alpha_j} \hat{L}_1 + \frac{\partial R_{i,H}}{\partial \alpha_j} \hat{H}_1$$

$$\frac{\partial R_{i,2}}{\partial \alpha_j} = \frac{\partial R_{i,R}}{\partial \alpha_j} \hat{R}_2 + \frac{\partial R_{i,L}}{\partial \alpha_j} \hat{L}_2 + \frac{\partial R_{i,H}}{\partial \alpha_j} \hat{H}_2$$

$$\frac{\partial R_{i,3}}{\partial \alpha_j} = \frac{\partial R_{i,R}}{\partial \alpha_j} \hat{R}_3 + \frac{\partial R_{i,L}}{\partial \alpha_j} \hat{L}_3 + \frac{\partial R_{i,H}}{\partial \alpha_j} \hat{H}_3$$

$$A = \frac{1}{R_i} \frac{\partial H}{\partial \alpha_j} - \frac{H}{R_i^2} \frac{\partial R_i}{\partial \alpha_j} + \dot{R}_i \frac{\partial(\theta_i - \theta_o)}{\partial \alpha_j}$$

$$\frac{\partial \dot{R}_i}{\partial \alpha_j} = \frac{1}{H_\mu} \left[\sin\theta_i \frac{\partial e}{\partial \alpha_j} + \cos\theta_i \left(e \frac{\partial \theta_i}{\partial \alpha_j} \right) \right] - \frac{\dot{R}_i}{H} \frac{\partial H}{\partial \alpha_j}$$

$$B = -\frac{H}{R_i} \frac{\partial(\theta_i - \theta_o)}{\partial \alpha_j} + \frac{\partial \dot{R}_i}{\partial \alpha_j}$$

$$\frac{\partial \dot{R}_{i,R}}{\partial \alpha_j} = -A \sin(\theta_i - \theta_o) + B \cos(\theta_i - \theta_o)$$

$$\frac{\partial \dot{R}_{i,L}}{\partial \alpha_j} = A \cos(\theta_i - \theta_o) + B \sin(\theta_i - \theta_o)$$

$$\frac{\partial \dot{R}_{i,H}}{\partial \alpha_j} = \delta_{3j} \frac{\alpha_5 \dot{R}_{i,R} - \alpha_4 \dot{R}_{i,L}}{H} + \delta_{6j} \frac{\dot{R}_{i,L}}{\alpha_5}$$

$$\frac{\partial \dot{R}_{i,1}}{\partial \alpha_j} = \frac{\partial \dot{R}_{i,R}}{\partial \alpha_j} \hat{R}_1 + \frac{\partial \dot{R}_{i,L}}{\partial \alpha_j} \hat{L}_1 + \frac{\partial \dot{R}_{i,H}}{\partial \alpha_j} \hat{H}_1$$

$$\frac{\partial \dot{R}_{i,2}}{\partial \alpha_j} = \frac{\partial \dot{R}_{i,R}}{\partial \alpha_j} \hat{R}_2 + \frac{\partial \dot{R}_{i,L}}{\partial \alpha_j} \hat{L}_2 + \frac{\partial \dot{R}_{i,H}}{\partial \alpha_j} \hat{H}_2$$

$$\frac{\partial \dot{R}_{i,3}}{\partial \alpha_j} = \frac{\partial \dot{R}_{i,R}}{\partial \alpha_j} \hat{R}_3 + \frac{\partial \dot{R}_{i,L}}{\partial \alpha_j} \hat{L}_3 + \frac{\partial \dot{R}_{i,H}}{\partial \alpha_j} \hat{H}_3$$

$$\frac{\partial s}{\partial \alpha_j} = \frac{s_{1,i} \frac{\partial R_{i,1}}{\partial \alpha_j} + s_{2,i} \frac{\partial R_{i,2}}{\partial \alpha_j} + s_{3,i} \frac{\partial R_{i,3}}{\partial \alpha_j}}{s}$$

$$\frac{\partial \dot{s}}{\partial \alpha_j} = \frac{1}{s}\left[s_{1,i} \frac{\partial \dot{R}_{i,1}}{\partial \alpha_j} + s_{2,i} \frac{\partial \dot{R}_{i,2}}{\partial \alpha_j} + s_{3,i} \frac{\partial \dot{R}_{i,3}}{\partial \alpha_j} - \dot{s} \frac{\partial s}{\partial \alpha_j} \right.$$

$$\left. + \dot{s}_{i,1} \frac{\partial R_{i,1}}{\partial \alpha_j} + \dot{s}_{i,2} \frac{\partial R_{i,2}}{\partial \alpha_j} + \dot{s}_{i,3} \frac{\partial R_{i,3}}{\partial \alpha_j} \right]$$

$$\frac{\partial \tau_i}{\partial \alpha_j} = \frac{\tau_i}{s_i} \frac{\partial s_i}{\partial \alpha_j} - \frac{\tau_i}{c - \dot{s}_i} \frac{\partial \dot{s}_i}{\partial \alpha_j}$$

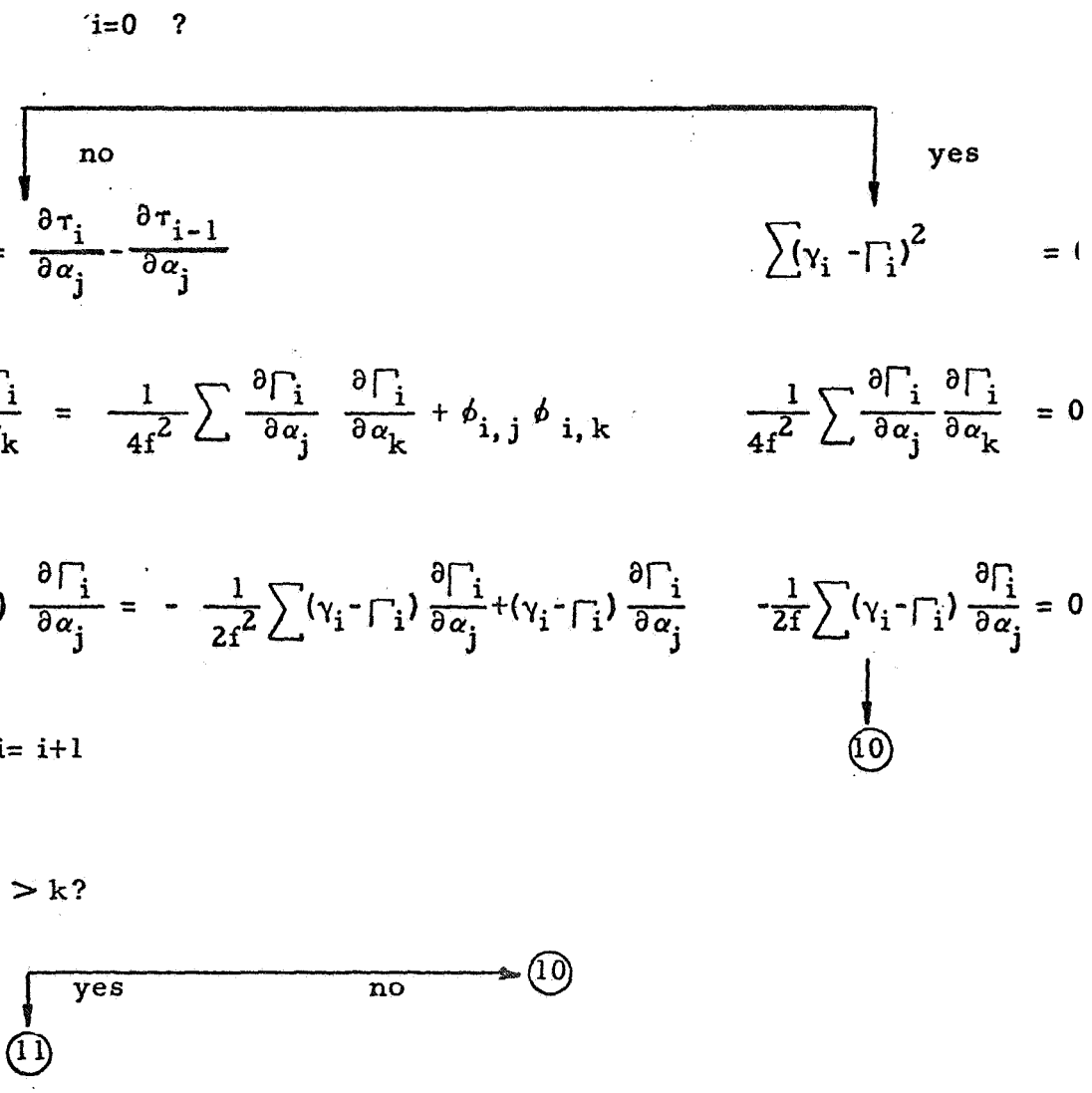

(11)

$$C_{jk} = 4f^2 \left(\frac{1}{4f^2} \sum \frac{\partial \Gamma_i}{\partial \alpha_j} \frac{\partial \Gamma_i}{\partial \alpha_k} \right)$$

$$e_k = -2f \left[\frac{-1}{2f} \sum (\gamma_i - \Gamma_i) \frac{\partial \Gamma_i}{\partial \alpha_k} \right]$$

Compute $\left[F_{kj} \right] = \left[C_{jk} \right]^{-1}$ using Jordan-Gauss method (assume 532 multiplications, 1064 additions, 72 divisions)

$$\Delta \alpha_j = \sum_{k=1}^{6} F_{kj} \cdot e_k$$

End

Computations Required

	Additions Subtraction	Multiplications	Divisions	Roots, Trigonometric	Load, Store
(1) → (2)	0	0	0	0	0
(2) → (3)	90	163	32	6	150
(3) → (4)	60	0	30	0	60
(4) → (5)	24	33	5	5	20
(5) → (6)	8,560	7,500	120	60	8,000
(6) → (7)	3,060	2,520	0	0	3,000
(7) → (10)	2,430	220	60	180	1,000
(10) → (11)	11,460	12,960	870	0	11,000
(11) → End	1,100	610	72		1,000
	26,784	34,006	1,189	251	24,230

The following mean times are allowed for the indicated double precision operations in the IBM 7094 computer (μ sec)

15	15	20	350	5

The total computation time is then 1.15 seconds. Allowing a factor of 2.5 for bookkeeping --indirect addressing, etc.-- the total computation time is still less than 3 seconds. Thus it appears that course correction instructions certainly can be given less than a minute after the last observation.

If range, range-rate and angle from three stations are to be used instead of just range rate from one, it is estimated that the following changes in computations will be needed.

	Additions Subtractions	Multiplications	Divisions	Roots, Trigonometric	Load, Store
(1)→(7)	0	0	0	0	0
(7)→(10)	7,300	700	200	600	3,000
(10)→(11)	20,000	24,000	1,500	0	20,000
(11)→(End)	13,400	6,700	550	0	10,000
	40,700	31,400	2,250	600	33,000

The additional computing time base on mean IBM 7094 times is 1.51 seconds. Allowing a factor of 2.5 this becomes 3.8 seconds.

Thus, even for range, range-rate and angle from three stations the total computation time is of the order of 7 seconds --far less than a minute.

APOLLO NOTE NO. 94

H. Engel
14 August 1963

USE OF ANGLE DATA

The observing station is at latitude λ North and longitude α East. The u, v, w coordinate system moves with the station. u points East, v points North and w points up. The unit vector $\hat{s}$ in the direction of the line-of-sight from the station to a vehicle can be resolved into u, v and w components. See Figure 1.

From Apollo Note No. 82, the components of $\bar{s}$ in the x'y'z' coordinate system are given by

$$X'_s = \begin{bmatrix} x' \\ y' \\ z' \end{bmatrix} = X' + L \left(\widetilde{X}_m - \widetilde{X}_d \right)$$

and

$$s^2 = x'^2 + y'^2 + z'^2$$

The components of $\hat{s}$ in the x, y, z coordinate system are then

$$Y_s = \frac{1}{s} X_s = \frac{1}{s} K^{-1} L^{-1} X'_s$$

and the components in the u, v, w system are

$$Y_s^w = \begin{bmatrix} u \\ v \\ w \end{bmatrix} = J Y_s$$

in which

$$J = \begin{bmatrix} 0 & 1 & 0 \\ -\sin\lambda & 0 & \cos\lambda \\ \cos\lambda & 0 & \sin\lambda \end{bmatrix} \begin{bmatrix} \cos(w_e T + \alpha) & \sin(w_e T + \alpha) & 0 \\ -\sin(w_e T + \alpha) & \cos(w_e T + \alpha) & 0 \\ 0 & 0 & 1 \end{bmatrix}$$

Let the u^*, v^*, w^* coordinate system be obtained by first rotating u, v, w through and angle ϕ_1 about u and then ϕ_2 about v displaced, the angles ϕ_1 and ϕ_2 being chosen so that w is along $\hat{s}$. These last two rotations correspond to the motions of an x-y antenna mount.

$$\begin{bmatrix} u^* \\ v^* \\ w^* \end{bmatrix} = \begin{bmatrix} \cos\phi_2 & 0 & -\sin\phi_2 \\ 0 & 1 & 0 \\ \sin\phi_2 & 0 & \cos\phi_2 \end{bmatrix} \begin{bmatrix} 1 & 0 & 0 \\ 0 & \cos\phi_1 & \sin\phi_1 \\ 0 & -\sin\phi_1 & \cos\phi_1 \end{bmatrix} \begin{bmatrix} u \\ v \\ w \end{bmatrix}$$

$$= \begin{bmatrix} \cos\phi_2 & \sin\phi_2 \sin\phi_1 & -\cos\phi_1 \sin\phi_2 \\ 0 & \cos\phi_1 & \sin\phi_1 \\ \sin\phi_2 & -\sin\phi_1 \cos\phi_2 & \cos\phi_1 \cos\phi_2 \end{bmatrix} \begin{bmatrix} u \\ v \\ w \end{bmatrix}$$

Since w^* is along $\hat{s}$, it follows that u^* and v^* are zero, giving two equations for ϕ_1 and ϕ_2.

$$0 = u\cos\phi_2 + v\sin\phi_2\sin\phi_1 - w\cos\phi_1\sin\phi_2$$

$$0 = v\cos\phi_1 + w\sin\phi_1$$

From the last of these equations

$$\tan\phi_1 = -\frac{v}{w}$$

and from the first,

$$\cot\phi_2 = -\frac{v}{u}\left(\sin\phi_1 - \frac{w}{v}\cos\phi_1\right)$$

$$= \frac{-v}{u\sin\phi_1}\left(\sin^2\phi_1 + \cos^2\phi_1\right)$$

so

$$\phi_1 = \tan^{-1} - \frac{v}{w}$$

$$\phi_2 = \tan^{-1}\left(\frac{-u \sin \phi_1}{v}\right)$$

Then taking derivatives of the first equation above,

$$\frac{d(\tan \phi_1)}{\tan \phi_1} = \frac{\sec^2 \phi_1 \, d\phi_1}{\tan \phi_1} = \frac{d(-v/w)}{-v/w}$$

or

$$\frac{d\phi_1}{\cos \phi_1 \sin \phi_1} = \frac{-dw}{w} + \frac{dv}{v}$$

From which the partials of ϕ_1 with respect to the orbit parameters, a_j, may be written

$$\frac{\partial \phi_1}{\partial a_j} = \sin \phi_1 \cos \phi_1 \left(\frac{1}{v} \frac{\partial v}{\partial a_j} - \frac{1}{w} \frac{\partial w}{\partial a_j}\right)$$

The following sketch

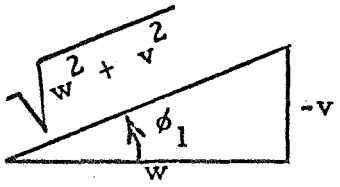

is useful in obtaining the auxillary equations

$$\sin \phi_1 = \frac{-v}{\sqrt{w^2 + v^2}} \quad ; \quad \cos \phi_1 = \frac{w}{\sqrt{w^2 + v^2}}$$

which may be used to reduce the derivative of ϕ_1 to

$$\frac{\partial \phi_1}{\partial a_j} = \frac{1}{w^2 + v^2} \left(v \frac{\partial w}{\partial a_j} - w \frac{\partial v}{\partial a_j} \right)$$

For the second radar angle, ϕ_2

$$\frac{d(\tan \phi_2)}{\tan \phi_2} = \frac{\sec^2 \phi_2 \, d\phi_2}{\tan \phi_2} = \frac{dv}{v} - \frac{du}{u} - \frac{\cos \phi_1 \, d\phi_1}{\sin \phi_1}$$

From this the partial of ϕ_2 with respect to the orbit parameters, may be written

$$\frac{\partial \phi_2}{\partial a_j} = \sin \phi_2 \cos \phi_2 \left(\frac{1}{v} \frac{\partial v}{\partial a_j} - \frac{1}{u} \frac{\partial u}{\partial a_j} - \cot \phi_1 \frac{\partial \phi_1}{\partial a_j} \right)$$

Again using a sketch

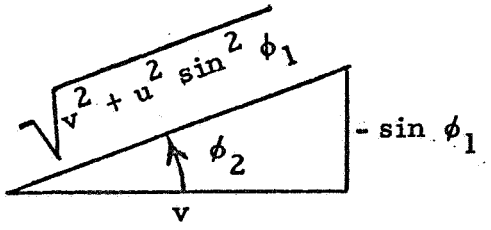

the partial equation may be reduced

$$\frac{\partial \phi_2}{\partial a_j} = \frac{-u v \sin \phi_1}{v^2 + u^2 \sin^2 \phi_1} \left[\frac{1}{v} \frac{\partial v}{\partial a_j} - \frac{1}{u} \frac{\partial u}{\partial a_j} + \frac{w/v}{w^2 + v^2} \left(v \frac{\partial w}{\partial a_j} - w \frac{\partial v}{\partial a_j} \right) \right]$$

$$= -\sqrt{w^2 + v^2} \left[\frac{\partial u}{\partial a_j} - \frac{u}{v} \frac{\partial v}{\partial a_j} - \frac{w u}{w^2 + v^2} \left(\frac{\partial w}{\partial a_j} - \frac{w}{v} \frac{\partial v}{\partial a_j} \right) \right]$$

Now $\partial u / \partial a_j$, $\partial v / \partial a_j$, and $\partial w / \partial a_j$ are equivalent to $\partial Y_s^w / \partial a_j$, and

$$\frac{\partial Y_s^w}{\partial a_j} = J \frac{\partial Y_s}{\partial a_j} = J\left[\frac{1}{s}\frac{\partial X_s}{\partial a_j} - \frac{X_s}{s^2}\frac{\partial s}{\partial a_j}\right]$$

$$= J\left[\frac{1}{s} K^{-1} L^{-1} \frac{\partial X'_s}{\partial a_j} - \frac{X_s}{s^2}\frac{\partial s}{\partial a_j}\right]$$

but $\partial X'_s / \partial a_j$ and $\partial s / \partial a_j$ are already available from Apollo Note No. 82, so the partials of u, v and w with respect to a_j are easily found.

Next, as in Apollo Note Nos. 43 and 83, the measured value of a quantity $f_m(t)$ can be expressed as

$$f_m(t) = f_c(t) + b + n(t)$$

in which $f_c(t)$ is the computed value of that quantity, b is a fixed bias and n (t) is a zero mean stationary Gaussean noise with variance σ^2.

The information matrix for each of the two groups of data, ϕ_1 and ϕ_2, are of the form

$$C_{ij} = \begin{cases} \sum_{k=1}^{N} \frac{1}{\sigma^2} \frac{\partial f_c(t_k)}{\partial a_i} \frac{\partial f_c(t_k)}{\partial a_j} \longrightarrow i, j = 1, \cdots, 6 \\ \sum_{k=1}^{N} \frac{1}{\sigma^2} \frac{\partial f_c(t_k)}{\partial a_j} \longrightarrow i = 7, j = 1, \cdots, 6 \\ \sum_{k=1}^{N} \frac{1}{\sigma^2} \longrightarrow i, j = 7 \end{cases}$$

$$C_{ij} = C_{ji}$$

where the computed quantities, f_c, are separately either ϕ_1 or ϕ_2. σ is the mean expected noise and is

$$\text{for } \phi_2: \quad \sigma_{\phi_2} = k \text{ a constant}$$

$$\text{for } \phi_1: \quad \sigma_{\phi_1} = k/\cos \phi_2$$

This last point is explained by the geometry of the definition of the angles, ϕ_1 and ϕ_2, and by the fact that the actual radar errors are assumed to be symmetrically distributed about the boresight axis. See Figure 2.

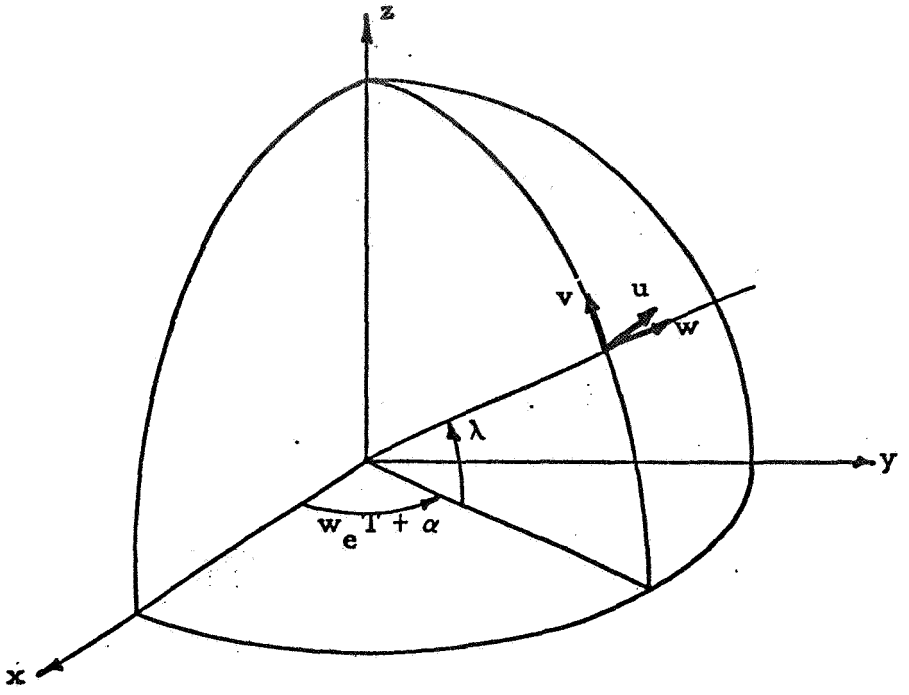

Figure 1.

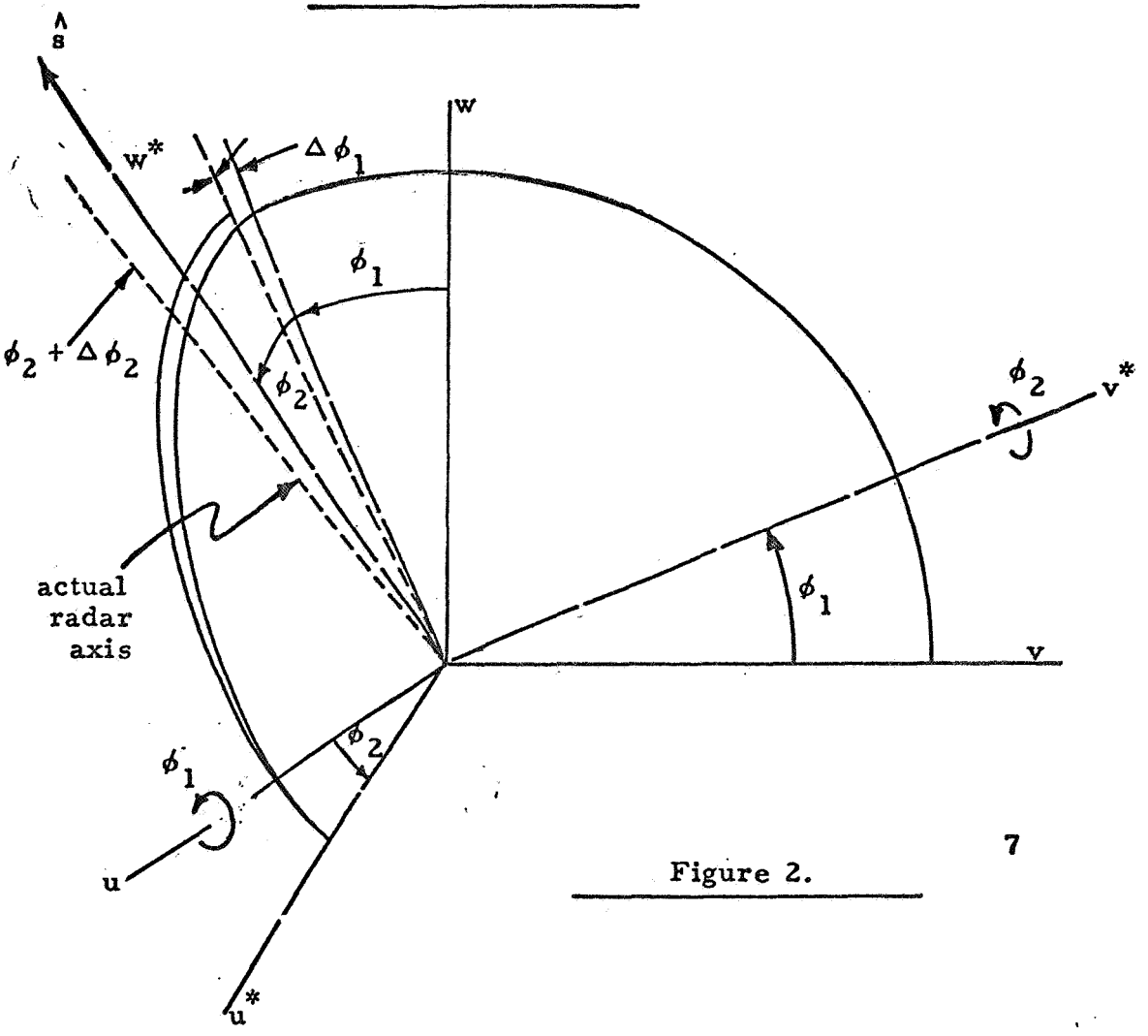

Figure 2.

APOLLO NOTE NO. 95

H. Engel
15 August 1963

GROUND ASSISTANCE TO LEM, INCLUDING MID-COURSE CORRECTION

Assume that at time $T = 0$ a priori orbit data are available and observations start. Assume further that at time T_1 the vehicle boosts for a mid-course correction based on the data up to that time, and the variance of the boost is known. The vehicle is observed until T_2, at which time the covariance matrix of the errors in the orbit parameters is calculated.

Let C_j denote the j-th information matrix and V_j the j-th covariance matrix, $C_j V_j = I$.

Let V_o be the covariance matrix of errors in initial position and velocity of the a priori data, and C_1 the corresponding information matrix of observations up to time T_1. Then

$$C_o = V_o^{-1}$$

$$C_2 = C_o + C_1$$

and

$$V_2 = C_2^{-1}$$

in which V_2 is the covariance matrix of errors in initial position and velocity resulting from the use of both sets of data.

The corresponding covariance matrix V_3 of errors in position and velocity at time T_1 is

$$V_3 = Q_1 V_2 Q_1^T$$

in which Q_1 is the Jacobian of the components at time T_1 with respect to those at time 0.

Assume that at time T_1 a boost with zero mean and covariance matrix V_4 is applied. In the simplest case, all the components of this

matrix are zero except for the three main diagonal element corresponding to the velocity components, which are σ_r^2.

The covariance matrix of errors in position and velocity after boost at time T_1 is

$$V_5 = V_3 + V_4$$

The corresponding covariance matrix at time zero is

$$V_6 = Q_1^{-1} \; V_5 \, Q_1^{-1T}$$

and

$$C_6 = V_6^{-1}$$

The information matrix of the observations from T_1 to T_2 is C_7. The information matrix from combining this with previous observations is C_8.

$$C_8 = C_6 + C_7$$

and the corresponding covariance matrix is

$$V_8 = C_8^{-1}$$

The covariance matrix of errors in position and velocity at time T_2 is V_9

$$V_9 = Q_2 \, V_8 \, Q_2^T$$

in which Q_2 is the Jacobian of the components at time T_2 with respect to those at time zero.

Combining all these intermediate stages, we find

$$C_o = V_o^{-1}$$

$$V_3 = Q_1 \left[C_o + C_1\right]^{-1} \; Q_1^T$$

$$C_6 = \Omega_1^T \left[V_3 + V_4 \right]^{-1} \Omega_1$$

$$V_9 = \Omega_2 \left[C_6 + C_7 \right]^{-1} \Omega_2^T$$

APOLLO NOTE NO. 96

L. Horowitz
15 August 1963

USE OF LEM/CM OBSERVATIONS

L. Lustick has pointed out a simple way to determine the information matrix (inverse of covariance matrix) resulting from observations of the LEM by the CM: If the CM orbit is circular, the necessary computations are the same as for an observing station on the surface of the earth (Apollo Note No. 82) with the earth-moon distance reduced to zero, the station latitude zero, the radius of the earth changed to the radius of the CM orbit, and the angular rate of the earth set equal to the angular rate of the CM in its orbit. The calculations may be performed for the same kinds of observables as already done for observations from earth—range, range rate and angle.

Some care is necessary in selecting angles to be used. For the nominal ascent (Hohmann transfer), the orbits of the CM and LEM are coplanar. Then a mechanization for defining the relative orientations of the three coordinate systems X, X' and $\widetilde{X}$ of Apollo Note No. 82 is simply to take all three systems coincident. Thus, X' is a right-handed, non-rotating, moon-centered coordinate system in which x' is along the initial position vector $(x'_o, 0, 0)$ of the LEM, vehicle motion is in the x'-y' plane, and y' is directed so that $\dot{y}'_o$ is positive. $\widetilde{X}$ and X are then taken to coincide with X' so that $(\widetilde{x}, \widetilde{y}, \widetilde{z}) = (x, y, z) = (x', y', z')$. We introduce the initial central angle α between the two vehicles as what was originally the DSIF station longitude in the X system. This mechanization treats the CM as a "pseudo-DSIF" to permit full utilization of the existing computer program for calculating information matrices. In this formulation, the rotation matrices L and K transforming between the 3 coordinate systems will reduce to the identity matrix. The resulting input data for the program can then be taken as follows:

$\beta = 0$ (since no earth involved)

$XI = 0$

$\eta = 0$

$ZETA = 0$

$\lambda = 0$ (latitude of DSIF)

α = central angle between LEM and CM, where α is positive for CM leading LEM

$\omega_e = \omega_{cm} = \sqrt{\frac{\mu}{R^3}} = 8.5463 \times 10^{-4}$ rad/sec

based upon: altitude = 80 n. mi.,

$R_m = 1.7373 \times 10^3$ km and $\mu = 4.896 \times 10^3$ km^3/sec^2

$\omega_m = 0$ (not relevant since $\rho_m \longrightarrow 0$)

ρ_e = moon radius + 80 n. mi. = 1.8855×10^6 meters

$\rho_m = 0$ (since earth-moon distance = 0)

$\mu = 4.896 \times 10^{12}$ m^3/sec^2

$L = 0$, $\ell = 0$ } latitude and longitude of sublunar point

The initial values for nominal lunar trajectories can then be selected as desired.

BB Fl

APOLLO NOTE NO. 97

C. Siska
20 August 1963

MINIMUM BOOST VELOCITY REQUIREMENT FOR FAR-SIDE RELAY

PURPOSE

This note presents data which augments the data appearing in Apollo Note No. 90.

RECAPITULATION

There is an interest in using the S-IV booster as a far-side relay to facilitate voice communications "back of the moon" to earth during the lunar deboost and lunar rendezvous operations. In principle, after the S-IV booster injects the lunar vehicle into a translunar orbit and is jettisoned, an additional boost can be applied to send the booster on its own translunar trajectory. To fulfill the far-side relay requirements, as presently defined, the S-IV booster must be within a slant range of 40,000 n. mi. from the lunar vehicle deboost position at a time approximately 72 and 100 hours after translunar injection (or, equivalently, S-IV booster jettison).

Apollo Note No. 90 indicates the operating region for the boost velocity, ΔV, and its direction α, relative to the path velocity, in order to fulfill far-side relay requirements when the ΔV is applied at 0 and 7.6 hours after translunar injection. Representative far-side relay trajectories are also shown in the note.

The present note examines the case when ΔV is applied at 4.15 hours after translunar injection and shows the resulting compilation of data.

RESULTS

Figures 1. and 2. show representative far-side relay trajectories in lunar space for ΔV values of 1000 and 700 ft/sec respectively. The direction of ΔV, denoted by α, is measured relative to the path

velocity existing at 4.15 hours after translunar injection; $\alpha = 0$ indicates that ΔV is directed along the path velocity and negative α values decrease the angle the path velocity makes with the local horizontal.

By combining results such as shown in Figures 1. and 2., one can develop limiting contours in the ΔV, α plane as shown in Figure 3. Combinations of ΔV and α which satisfy the indicated limit criteria lie within a specified contour. The left hand side of each contour is dictated by the criterion that the t = 100 hour positions lie on the 40,000 n. mi. circle (see Figures 1. and 2.), while the right hand side is associated with seeing the lunar vehicle deboost position at t = 72 hours.

Now the time when ΔV is applied will have an influence on the magnitude of ΔV which is available at that time, because of fuel "boil-off".

Thus, it would appear that from the consideration of boost velocity availability and boost requirements, there exists an upper limit to the time for applying the boost. The minimum ΔV required, as a function of time, can be obtained from Figure 3. and the resulting curve is shown in Figure 4.

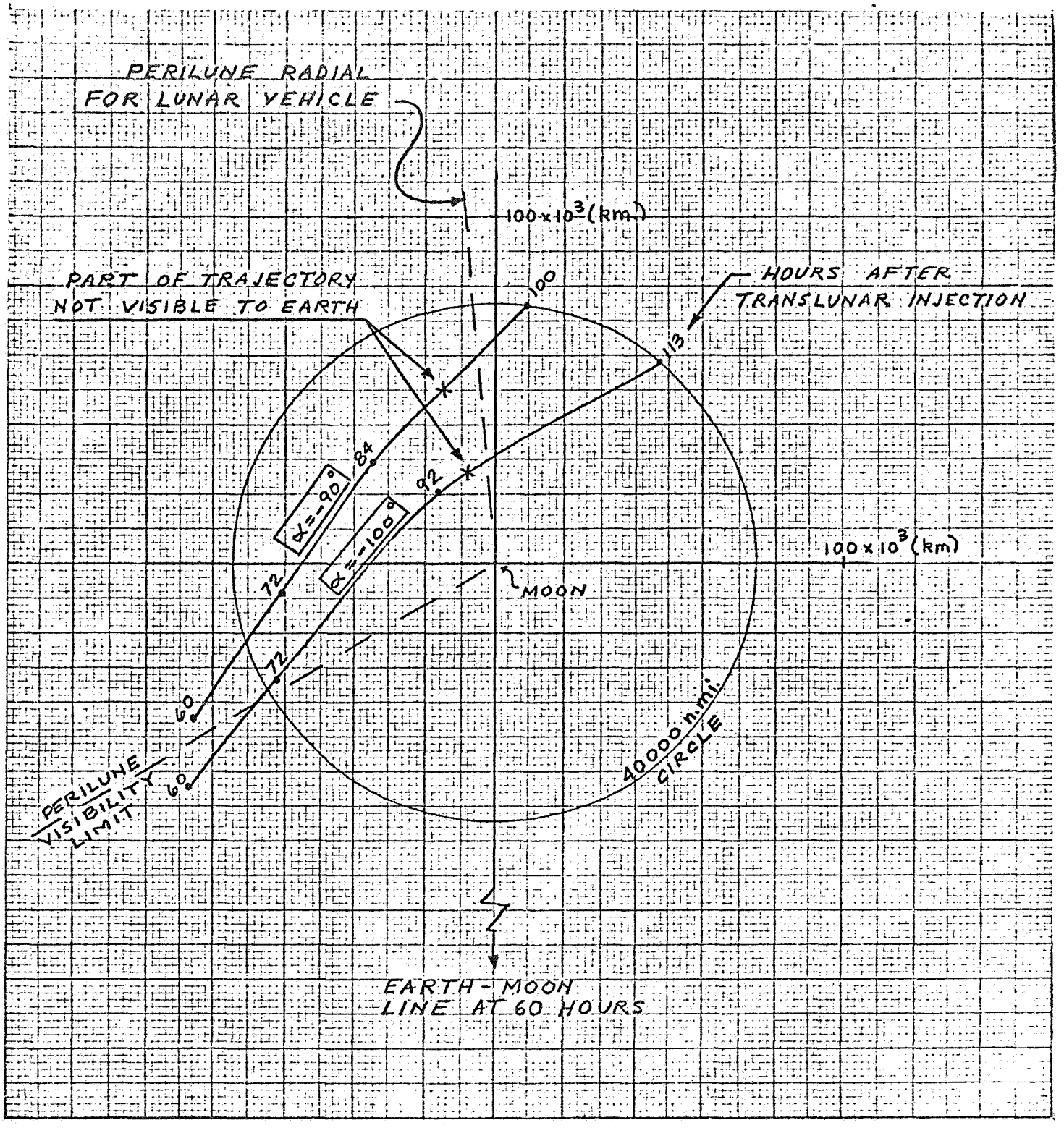

Figure 1. Far-side Relay Trajectories for ΔV = 1000 ft/sec. Applied 4.15 Hours After Translunar Injection.

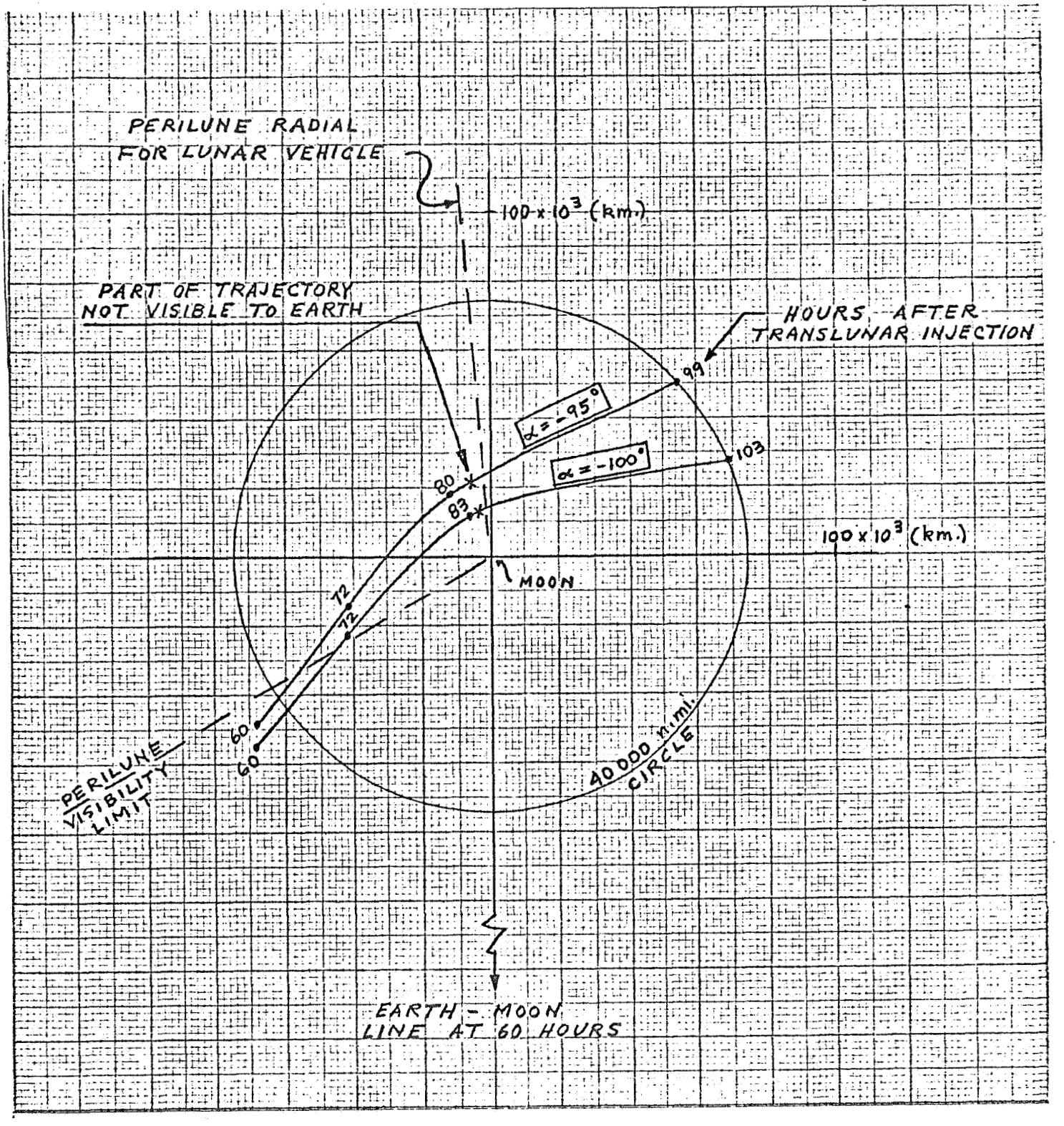

Figure 2. Far-side Relay Trajectories for ΔV = 700 ft/sec. Applied 4.15 Hours After Translunar Injection.

Limiting Criteria:

1. Lunar vehicle deboost visible (t = 72 hours)
2. Lunar rendezvous visible (t = 100 hours)
3. Slant range at above times $\leq$ 40,000 n. mi.

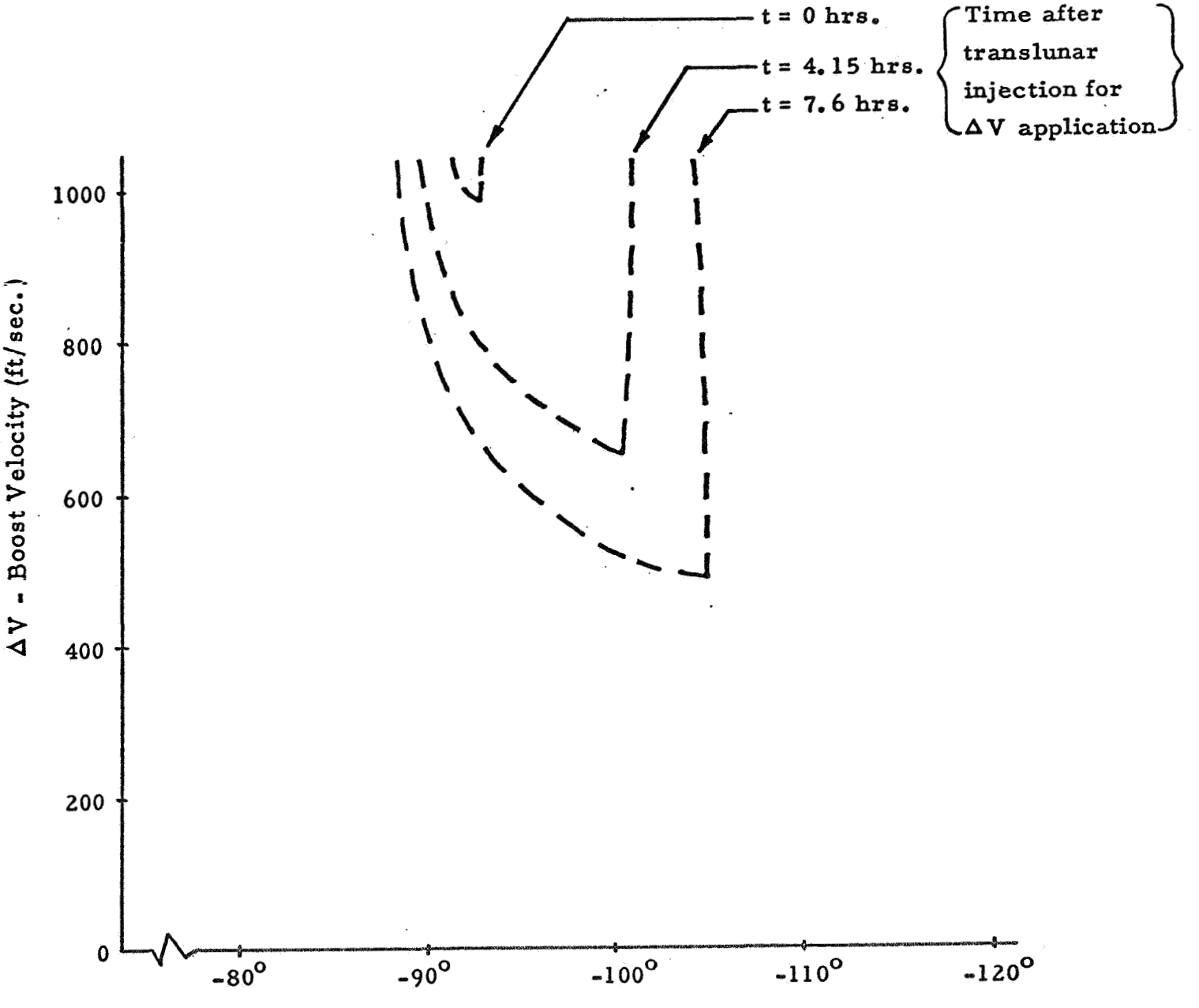

Figure 3. Approximate Operating Region for Far-side Relay Boost

Limiting Criteria:

1. Lunar vehicle deboost visible (t = 72 hours)
2. Lunar rendezvous visible (t = 100 hours)
3. Slant range at above times $\leq$ 40,000 n. mi.

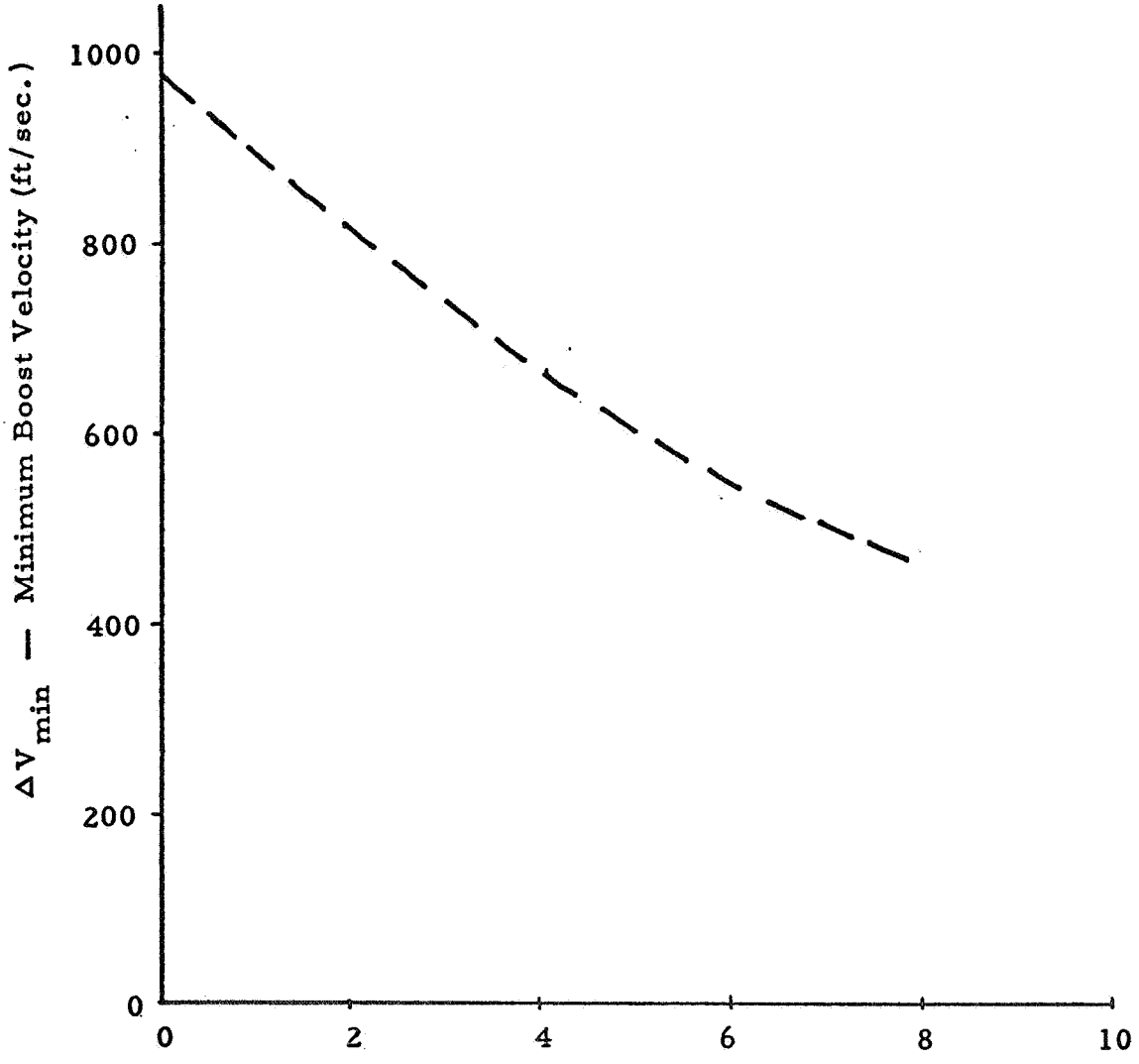

Figure 4. Minimum Boost Velocity Requirement for Far-side Relay

BBE:6

APOLLO NOTE NO. 98

H. Engel
21 August 1963

MULTIPLE DATA SOURCES WITH FIXED BIASES

Apollo Note No. 43 has shown how to treat biased data from a single source. Other notes have shown how to handle unbiased data from multiple sources. This note considers the case of data with fixed biases from multiple, uncorrelated sources.

It is assumed that each observed quantity, f_{jm}, may be expressed as

$$f_{jm}(t) = f_{jc}(t) + b_j + n_j(t)$$

in which f_{jc} is the computed value of the quantity, b_j is a fixed bias and n_j is zero mean Gaussian noise with correlation time small compared to the time between measurements. The standard deviation of the noise is assumed to be a known function of time: $\sigma_j = \sigma_j(t)$.

We may replace $f_{jc}(t) + b_j$, in which $f_{jc}(t)$ is a function of six parameters $a_1, \cdots, a_6$ by

$$F_{jc}(t) \triangleq f_{jc}(t) + b_j$$

in which $F_{jc}(t)$ is a function of seven parameters $a_1, \cdots, a_6, a_6 + j$

The measurements are made at times t_i, and rather than writing everything as functions of t_i, we shall simply write them as functions of i. Further, we shall assume all the different measurables are measured at the same instants. Then, the likelihood function of the data may be written as

$$L = \frac{1}{(2\pi)^{\frac{J}{\prod_{j=1}} \frac{N}{\prod_{i=1}} \sigma_j(i)}} \exp(-\mathcal{L})$$

where

$$\mathcal{L} = \frac{1}{2} \sum_{i=1}^{N} \sum_{j=1}^{J} n_j^2(i) \Big/ \sigma_j^2(i)$$

$$= \frac{1}{2} \sum_{i=1}^{N} \sum_{j=1}^{J} \left[f_{mj}(i) - \hat{F}_j(i) \right]^2 \Big/ \sigma_j^2(i)$$

in which $\hat{F}_j(i)$ is the estimated value of $F_j(i)$.

The maximum likelihood estimators of the parameters a_1, $\cdots$, a_6, $\cdots$, a_{6+J} and those which maximize the likelihood function, and are those found by solving the set of 6 + J simultaneous equations that result from setting the partial derivatives of $\mathcal{L}$ with respect to each of the parameters equal to zero.

$$\sum_{i=1}^{N} \sum_{j=1}^{J} \frac{1}{\sigma_j^2(i)} \left[f_{mj}(i) - \hat{F}_j(i) \right] \frac{\partial \hat{F}_j(i)}{\partial a_k} = 0 \qquad k = 1, \cdots, 6 + J$$

These equations are nonlinear, but for a sufficiently large number of independent observations, the estimators $\hat{a}_k$ may be written as

$$\hat{a}_k = a_k + \Delta a_k$$

where the random error terms Δa_k are negligible except where they appear as first order terms. Then

$$\hat{F}_j(i) = F_j(\hat{a}_1, \cdots, \hat{a}_{6+J}, i) = F_j(a_1, \cdots, a_{6+J}, i) + \sum_{\ell=1}^{6+J} \frac{\partial F_j}{\partial a_\ell} \Delta a_\ell$$

Making this substitution, we find

$$\sum_{i=1}^{N} \sum_{j=1}^{J} \frac{1}{\sigma_j^2(i)} \left[f_{mj}(i) - F_j(i) - \sum_{\ell=1}^{6+J} \frac{\partial F_j}{\partial a_\ell} \Delta a_\ell \right] \frac{\partial F_j}{\partial a_k} = 0$$

This last equation may in turn be written in matrix form as

$$C \Delta a = e$$

where

$$\Delta a = \begin{Bmatrix} \Delta a_1 \\ \Delta a_2 \\ \vdots \\ \Delta a_{6+J} \end{Bmatrix}$$

$$e = \begin{Bmatrix} \sum_{i=1}^{N} \sum_{j=1}^{J} \frac{\partial F_j}{\partial a_1} n_j(i) \Big/ \sigma_j^2(i) \\ \vdots \\ \sum_{i=1}^{N} \sum_{j=1}^{J} \frac{\partial F_j}{\partial a_{6+J}} n_j(i) \Big/ \sigma_j^2(i) \end{Bmatrix}$$

$$C_{k\ell} = \sum_{i=1}^{N} \sum_{j=1}^{J} \frac{\partial F_j}{\partial a_k} \frac{\partial F_j}{\partial a_\ell} \Big/ \sigma_j^2(i)$$

As in previous notes,

$$\text{Cov}\left(\hat{a}_k, \hat{a}_\ell\right) = C^{-1} E\left[e\ e^T\right] C^{-1}$$

Now, the expected value of $n_j(i)\, n_r(s)$ is given by

$$E\left[n_j(i)\, n_r(s)\right] = \delta_{jr}\, \delta_{is}\, \sigma_j^2(i)$$

so the expected value of $e_k e_\ell$ is

$$E\left[e_{k\ell}\right] = E\left[e_k\, e_\ell\right] = \sum_{i=1}^{N} \sum_{j=1}^{J} \frac{\partial F_j}{\partial a_k} \frac{\partial F_j}{\partial a_\ell} \frac{\sigma_j^2(i)}{\sigma_j^4(i)}$$

$$= C_{k\ell}$$

Thus

$$\text{Cov}\left(\hat{a}_k, \hat{a}_\ell\right) = C^{-1}.$$

Now, other expressions can be obtained for the elements of matrix C,

$$C_{k\ell} = \sum_{i=1}^{N} \sum_{j=1}^{J} \frac{1}{\sigma_j^2(i)} \frac{\partial F_j}{\partial a_k} \frac{\partial F_j}{\partial a_\ell} \qquad k, \ell = 1, \cdots, 6$$

$$C_{k\ell} = \sum_{i=1}^{N} \frac{1}{\sigma_{\ell-6}^2(i)} \frac{\partial F_{\ell-6}}{\partial a_k} \qquad \begin{array}{l} k = 1, \cdots, 6 \\ \ell = 7, \cdots, 6+J \end{array}$$

$$C_{k\ell} = \sum_{i=1}^{N} \frac{1}{\sigma_{\ell-6}^2(i)} \delta_{k\ell} \qquad k, \ell = 7, \cdots, 6+J$$

$$C_{k\ell} = C_{\ell k}$$

Further for σ_j stationary, these expressions reduce to

$$C_{k\ell} = \sum_{j=1}^{J} \frac{1}{\sigma_j^2} \sum_{i=1}^{N} \frac{\partial F_j}{\partial a_k} \frac{\partial F_j}{\partial a_\ell} \qquad k, \ell = 1, \cdots, 6$$

$$C_{k\ell} = \frac{1}{\sigma_{\ell-6}^2} \sum_{i=1}^{N} \frac{\partial F_{\ell-6}}{\partial a_k} \qquad \begin{matrix} k = 1, \cdots, 6 \\ \ell = 7, \cdots, 6+J \end{matrix}$$

$$C_{k\ell} = \frac{N}{\sigma_{\ell-6}^2} \delta_{k\ell} \qquad k, \ell = 7, \cdots, 6+J$$

$$C_{k\ell} = C_{\ell k}$$

Of course it is also possible to include the case where the observations at different stations are taken at different times by taking subsets of the observations from t_1 to t_n corresponding to each station.

APOLLO NOTE NO. 99

H. Engel
13 September 1963

PRELIMINARY RESULTS OF COMPUTER ANALYSES

Introduction

A problem susceptible to verification by a separate analysis has been run, and indicates that the computer program is correct.

In addition, a number of successful computer runs to determine the errors in future vehicle position have been accomplished.

These are all reported in this note.

Check Problem

The problem of determining vehicle position and velocity and probable errors in these quantities on the basis of one range and one range-rate measurement from each of three stations simultaneously is capable of direct analytic solution, and serves as a check on the computer program and on the more elaborate analysis on which it depends.

The distance s_i from station i to the vehicle is given by:

$$s_i^2 = \sum_{j=1}^{3} (x_j - x_{ji})^2$$

in which (x_1, x_2, x_3) is the vehicle position and (x_{1i}, x_{2i}, x_{3i}) is the position of the i-th station. Following Apollo Note No. 87,

$$\frac{\partial s_i}{\partial x_j} = \frac{1}{s_i} (x_j - x_{ji})$$

$$\frac{\partial \dot{s}_i}{\partial x_j} = \frac{\dot{x}_j}{s} - \frac{\dot{s}_i}{s_i} \frac{\partial s_i}{\partial x_j}$$

and

$$\frac{\partial \dot{s}_i}{\partial \dot{x}_j} = \frac{\partial s_i}{\partial x_j}$$

Now consider a configuration of vehicle and stations such as shown in Figure 1, which corresponds to a possible situation with the vehicle orbiting the Moon. The stations are all in the yz-plane, at the vertices of an equilateral triangle centered on the origin. The vehicle is on the x axis at a distance ℓ from the origin. ℓ is equal to the Earth-Moon distance less the Earth radius, less the Moon radius. The vehicle has a velocity

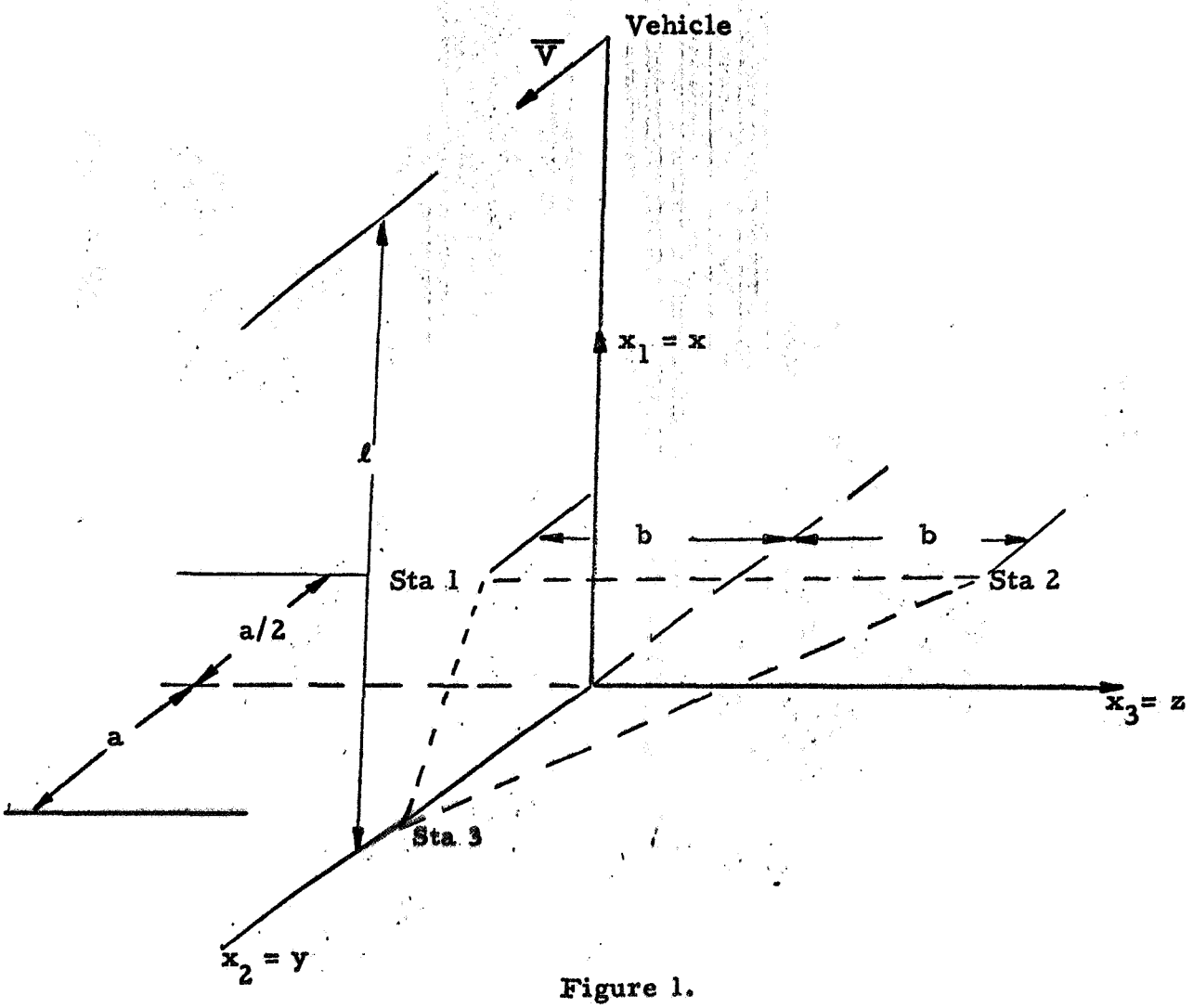

Figure 1.

V equal to 1.7017×10^3 m/sec in the y direction.

$$s = s_1 = s_2 = s_3$$

$$\bar{V} = 0\,\hat{x} + V\,\hat{y} + 0\,\hat{z}$$

$$\hat{s}_1 = \frac{\ell}{s}\,\hat{x} - \frac{a}{s}\,\hat{y} + 0\,\hat{z}$$

$$\hat{s}_2 = \frac{\ell}{s}\,\hat{x} + \frac{a}{2s}\,\hat{y} - \frac{b}{s}\,\hat{z}$$

$$\hat{s}_3 = \frac{\ell}{s}\,\hat{x} + \frac{a}{2s}\,\hat{y} + \frac{b}{s}\,\hat{z}$$

Then,

$$\dot{s}_i = \bar{V} \cdot \hat{s}_i$$

$$\dot{s}_1 = -\frac{aV}{s}$$

$$\dot{s}_2 = \frac{aV}{2s}$$

$$\dot{s}_3 = \frac{aV}{2s}$$

a_1 through a_6 are the parameters that describe the vehicle orbit in the computer calculations. a_1 through a_3 are vehicle position relative to the Moon, and a_4 through a_6 are vehicle velocity relative to the Moon the direction of a_1 and a_4 is $-\hat{x}$

direction of a_2 and a_5 is $\hat{y}$

direction of a_3 and a_6 is $-\hat{z}$.

Then the partial derivatives of s_i and $\dot{s}_i$ with respect to the vehicle orbit parameters are:

$$\frac{\partial s_i}{\partial a_j} = \begin{bmatrix} -\ell/s & -\ell/s & -\ell/s \\ a/(2s) & a/(2s) & -a/s \\ -b/s & b/s & 0 \\ 0 & 0 & 0 \\ 0 & 0 & 0 \\ 0 & 0 & 0 \end{bmatrix}$$

$$\frac{\partial \dot{s}_i}{\partial a_j} = \begin{bmatrix} a\dot{V}\ell/(2s^3) & a\dot{V}\ell/(2s^3) & -a\dot{V}\ell/s^3 \\ \frac{V}{s}\left(1-\left[\frac{a}{2s}\right]^2\right) & \frac{V}{s}\left(1-\left[\frac{a}{2s}\right]^2\right) & \frac{V}{s}\left(1-\left[\frac{a}{s}\right]^2\right) \\ ab\dot{V}/(2s^3) & -ab\dot{V}/(2s^3) & 0 \\ -\ell/s & -\ell/s & -\ell/s \\ a/(2s) & a/(2s) & -a/s \\ -b/s & b/s & 0 \end{bmatrix}$$

The information matrix corresponding to range measurements from station i has components

$$C^{i,R}_{jk} = \frac{\partial s_i}{\partial a_j} \frac{\partial s_i}{\partial a_k}$$

The corresponding information matrix elements for range-rate measurements are:

$$C_{jk}^{i,\dot{R}} = \frac{\partial \dot{s}_i}{\partial a_j} \frac{\partial \dot{s}_i}{\partial a_j}$$

All may be calculated from the $\partial s_i/\partial a_j$ and $\partial \dot{s}_i/\partial a_j$ matrices already given. We show, below, these $C^{i,R}$ and $C^{i,\dot{R}}$ matrices as computed in this fashion together with the values determined from the computer program (in parentheses). The small differences can be attributed to slightly different geometrics employed in the two calculations.

$$C_{jk}^{1,R} = \begin{bmatrix}
(1.0+0) & (-.41-2) & (.78-2) & (-.20-14) & (-.91-12) & (0) \\
1.0+0 & -.41-2 & .78-2 & 0 & 0 & 0 \\
(.41-2) & (.17-4) & (-.32-4) & (.82-17) & (.37-14) & (0) \\
-.41-2 & .16-4 & -.32-4 & 0 & 0 & 0 \\
(.78-2) & (-.32-4) & (.61-4) & (-.16-16) & (-.71-14) & (0) \\
0 & 0 & 0 & 0 & 0 & 0 \\
(-.20-14) & (.82-17) & (-.16-16) & (.40-29) & (.18-26) & (0) \\
0 & 0 & 0 & 0 & 0 & 0 \\
(-.91-12) & (.37-14) & (-.71-14) & (.18-26 & (.82-24) & 0 \\
0 & 0 & 0 & 0 & 0 & 0 \\
(0) & (0) & (0) & (0) & (0) & (0) \\
0 & 0 & 0 & 0 & 0 & 0
\end{bmatrix}$$

$$C^{2,R}_{jk} =$$

(1.0 + 0) 1.0 + 0	(-.41-2) -.45-2	(-.78-2) -.78-2	(-.20-14) 0	(-.91-12) 0	(0) 0
(-.41-2) .45-2	(.17-4) .20-4	(.32-4) .33-4	(.82-17) 0	(.37-14) 0	(0) 0
(-.78-2) -.78-2	(.32-4) .33-4	(.61-4) .61-4	(.16-16) 0	(.71-14) 0	(0) 0
(-.20-14) 0	(.82-17) 0	(.16-16) 0	(.40-29) 0	(.18-26) 0	(0) 0
(-.91-12) 0	(.37-14) 0	(.71-14) 0	(.18-26) 0	(.83-24) 0	(0) 0
(0) 0	(0) 0	(0) 0	(0) 0	(0) 0	(0) 0

$$C^{3,R}_{jk} =$$

(1.0 + 0) 1.0 + 0	(.89-2) .89-2	(-.18-8) 0	(.44-14) 0	(-.91-12) 0	(0) 0
(.89-2) .89-2	(.79-4) .81-4	(-.16-10) 0	(.39-16) 0	(-.81-4) 0	(0) 0
(-.18-08) 0	(-.16-10) 0	(.32 -17) 0	(-.78-23) 0	(.16-20) 0	(0) 0
(.44-14) 0	(.39-16) 0	(-.80-23) 0	(.19-28) 0	(-.40-26) 0	(0) 0
(-.91-12) 0	(-.81-14) 0	(.16-20) 0	(-.40-26) 0	(.83-24) 0	(0) 0
(0) 0	(0) 0	(0) 0	(0) 0	(0) 0	(0) 0

$$C^{1,\dot{R}}_{jk} = \begin{bmatrix}
(.34-15) & (.83-13) & (.26-17) & (-.18-7) & (.75-10) & (-.14-9) \\
.40-15 & .90-13 & .30-17 & -.20-7 & .90-10 & -.16-9 \\
(.83-13) & (.20-10) & (.65-15) & (-.45-5) & (.18-7) & (-.35-7) \\
.90-13 & .20-10 & .71-15 & -.45-5 & .20-7 & -.35-7 \\
(.26-17) & (.65-15) & (.21-19) & (-.14-9) & (.59-12) & (-.11-11) \\
.30-17 & .71-15 & .25-19 & -.16-9 & .70-12 & -.12-12 \\
(-.18-7) & (-.45-5) & (-.14-9) & (1.0+0) & (-.41-2) & (.78-2) \\
-.20-7 & -.45-5 & -.16-9 & 1.0+0 & -.45-2 & .78-2 \\
(.75-10) & (.18-7) & (.59-12) & (-.41-2) & (.17-4) & (-.32-4) \\
.90-10 & .20-7 & .70-12 & -.45-2 & .20-4 & -.35-4 \\
(-.14-9) & (-.35-7) & (-.11-11) & (.78-2) & (-.32-4) & (.61-4) \\
-.16-9 & -.35-7 & -12-11 & .78-2 & -.35-4 & .61-4
\end{bmatrix}$$

$$C^{2,\dot{R}}_{jk} = \begin{bmatrix}
(.34-15) & (.83-13) & (-.26-17) & (-.18-7) & (.75-10) & (.14-9) \\
.40-16 & .90-13 & -.32-17 & -.20-7 & .90-10 & .16-9 \\
(.83-13) & (.20-10) & (-.65-15) & (-.45-5) & (.18-7) & (.35-7) \\
.90-13 & .20-10 & -.70-15 & -.45-5 & .20-7 & .35-7 \\
(-.26-17) & (-.65-15) & (.21-19) & (.14-9) & (-.59-12) & (-.11-11) \\
-.32-17 & -.70-15 & .25-19 & .16-9 & -.70-12 & -.12-11 \\
(-.18-7) & (-.45-5) & (.14-9) & (1.0+0) & (-.41-2) & (-.78-2) \\
-.20-7 & -.45-5 & .16-9 & 1.0+0 & -.45-2 & -.78-2 \\
(.75-10) & (.18-7) & (-.59-12) & (-.41-2) & (.17-4) & (.32-4) \\
.90-10 & .20-7 & -.70-12 & -.45-2 & .20-4 & .35-4 \\
(.14-9) & (.35-7) & (-.11-11) & (-.78-2) & (.32-4) & (.61-4) \\
.16-9 & .35-7 & -.12-11 & -.78-2 & .35-4 & .61-4
\end{bmatrix}$$

$$C^{3,\dot{R}}_{jk} = \begin{bmatrix}
(.16\text{-}14) & (-.18\text{-}12) & (-.28\text{-}23) & (.40\text{-}7) & (.35\text{-}9) & (-.71\text{-}16) \\
.16\text{-}14 & -.18\text{-}12 & 0 & .40\text{-}7 & .35\text{-}9 & 0 \\
(-.18\text{-}12) & (.20\text{-}10) & (-.32\text{-}21) & (-.45\text{-}5) & (-.40\text{-}7) & (.80\text{-}14) \\
-.18\text{-}12 & .20\text{-}10 & 0 & -.45\text{-}5 & -.40\text{-}7 & 0 \\
(-.28\text{-}23) & (.32\text{-}2) & (0) & (-.71\text{-}16) & (-.63\text{-}18) & (.13\text{-}24) \\
0 & 0 & 0 & 0 & 0 & 0 \\
(.40\text{-}7) & (-.45\text{-}5) & (-.71\text{-}16) & (1.0 + 0) & (.89\text{-}2) & (-.18\text{-}8) \\
.40\text{-}7 & -.45\text{-}5 & 0 & 1.0 + 0 & .90\text{-}2 & 0 \\
(.35\text{-}9) & (-.40\text{-}7) & (-.63\text{-}18) & (.89\text{-}2) & (.79\text{-}4) & (-.16\text{-}10) \\
.35\text{-}9 & -.40\text{-}7 & 0 & .90\text{-}2 & .80\text{-}4 & 0 \\
(-.71\text{-}16) & (.80\text{-}14) & (.13\text{-}24) & (-.18\text{-}8) & (-.16\text{-}10) & (.32\text{-}17) \\
0 & 0 & 0 & 0 & 0 & 0
\end{bmatrix}$$

In the above, the notation a + b stands for $a \times 10^b$.

In addition, several values of the Jacobian matrix $\partial x_i(t)/\partial a_j$ were checked for t equal to one-half period and were found to be correct. Further, the covariance matrix obtained using all the $C^{i,R}$ and $C^{i,\dot{R}}$ with $\sigma_R = 15$ m and $\sigma_{\dot{R}} = 3$ cm/sec. were checked for reasonableness and found to be very nearly equal to the estimated values.

Computations Without Boost

The following computations have been performed, and the results are presented graphically. In all these cases the parameters used are:

$a_1 = 1.7525 \times 10^6$ m

$a_4 = 0$ m/sec

$a_5 = 1.70172 \times 10^3$ m/sec

$\xi = 0^\circ$

$\eta = 180^\circ$

$\zeta = 180^\circ$

$\omega_e = .7291160 \times 10^{-4}$ rad/sec

$\omega_m = .42360 \times 10^{-6}$ rad/sec

$\rho_e = 6.3781 \times 10^6$ m

$\rho_m = 3.85 \times 10^8$ m

$\mu = 4.896 \times 10^{12}$ m^3/sec^2

$L = 15^\circ$

$\ell = 90^\circ$

These conditions correspond to a vehicle at perilune of a Hohmann transfer from 8 n. mi. altitude to 80 n. mi. altitude, the nominal lunar rendezvous maneuver. Perilune is on the Earth-Moon line, and the orbit of the vehicle is in the plane of Earth-Moon rotation.

The orbit period is 116.2 minutes. Half a period is 58.09 minutes. Through a minor error, the time used for prediction of errors at time of nominal rendezvous was 59.08 minutes. This has a negligible effect upon the results of the computations since error in position and not position is calculated. Error in position is a slowly varying quantity, while position of the LEM or position of the LEM relative to the CM/SM is not. The error was discovered early in the computations, but because of its very small effect and because of the desire to obtain results in time for the final report, it was not corrected.

Three stations are used

Station	λ (latitude)	α (longitude)
Madrid	41°	-4°
Johannesburg	-26°	28°
Woomera	-30°	138°

Information matrices for range and range-rate from these stations have been computed for 1, 4, 9, 16 and 25 successive 1 minute observations after the initial conditions. The Jacobian matrix for computing the errors at rendezvous was computed for 59.08 minutes as described above.

Using σ_R = 15 m and $\sigma_{\dot{R}}$ = 3 cm/sec for one minute observations, the covariance matrices of errors at 59.08 minutes have been computed for the following conditions.

Stations			Data			Total Observation Time (minutes)					Remarks
M	J	W	R	$\dot{R}$	A priori	1	4	9	16	25	
x	x	x	x	x		x	x	x	x	x	
			x	x	x	x	x	x	x	x	Note 1
			x				x	x	x	x	Note 2
			x		x	x	x	x	x	x	Note 1
				x			x	x	x	x	Note 2
				x	x	x	x	x	x	x	Note 1
x	x		x	x			x	x	x	x	Note 2
			x	x	x	x	x	x	x	x	Note 1
			x				x	x	x	x	Note 2
			x		x	x	x	x	x	x	Note 1
				x			x	x	x	x	Note 2
				x	x	x	x	x	x	x	Note 1
x			x	x			x	x	x	x	Note 2
			x	x	x	x	x	x	x	x	Note 1
			x					x	x	x	Note 2
			x		x	x	x	x	x	x	Note 1
				x				x	x	x	Note 2
				x	x	x	x	x	x	x	Note 1
				x	x	x	x	x	x	x	Note 3
				x	x	x	x	x	x	x	Note 4

Note 1:

A priori data

$$\sigma_{a_1} = \sigma_{a_2} = \sigma_{a_3} = 10^3 \text{m}$$

$$\sigma_{a_4} = \sigma_{a_5} = \sigma_{a_6} = \sqrt{10} \text{ m/sec.}$$

Note 2:

The number of minutes of observations to be able to determine a_1 through a_6 depends on the number of stations and whether range, range-rate or both are used. The total number of independent observations must be at least 6. For this reason, the covariance matrix of the errors at rendezvous starts with other than 1 minute of observations in some instances.

Note 3:

A priori data

$$\sigma_{a_1} = \sigma_{a_2} = \sigma_{a_3} = \sqrt{10}^{1} \quad 10^3 \text{ m}$$

$$\sigma_{a_4} = \sigma_{a_5} = \sigma_{a_6} = \sqrt{10} \quad 10 \text{ m/sec.}$$

Note 4:

A priori data

$$\sigma_{a_1} = \sigma_{a_2} = \sigma_{a_3} = 10^4 \text{ m}$$

$$\sigma_{a_5} = \sigma_{a_6} = \sigma_{a_7} = \sqrt{10} \quad 10^2 \text{ m/sec.}$$

On the basis of these error covariance matrices σ_x, σ_y and σ_z have been plotted, as has $(\sigma_x^2 + \sigma_y^2 + \sigma_z^2)^{1/2}$ which is referred to as the RMS error at 59.08 minutes.

Further, a major portion of the error is in the y direction (along the direction of motion). Now, the CM/SM is in a circular orbit, and the LEM is near apolune in a near-circular orbit. Thus, the relative motion is in the y direction, and for small errors in velocity is approximately 29.7 m/sec. As a consequence, a short time before or after the nominal rendezvous time the error in the y direction becomes zero while the errors in the x and z directions remain essentially unchanged. The RMS time between nominal rendezvous and this time of minimum miss is $\sigma_y/29.7$ seconds

and has been plotted for those cases in which the velocity errors are small. The corresponding minimum RMS misses have also been plotted.

Computations With Boost

Additional information matrices corresponding to range and range-rate measurements from Madrid, Johannesburg and Woomera at one minute intervals from 17 to 25 minutes has been computed; so has the Jacobian matrix $\partial x_i / \partial a_j$ corresponding to 16 minutes. With these additional matrices, the following problem has been solved, according to the method outlined in Apollo Note No. 95.

The vehicle has the orbit parameters described under "Computations Without Boost," above. The vehicle is observed in range and range-rate from Madrid, Woomera, and Johannesburg for 16 minutes. An orbit correcting boost is then made with RMS errors of 1.0 m/sec. in the x, y and z directions. The actual boost is assumed zero; this does not substantially affect the errors in estimated position at future time. Then the vehicle is observed for another 9 minutes, and the error covariance matrix at rendezvous computed.

From this the RMS errors at 59.08 minutes (1250m), the RMS difference between the nominal time of rendezvous and the time of minimum RMS miss (32.4 sec) and the minimum RMS miss (790m) are computed.

In performing the calculations for determining the errors with boost, it has been necessary to "fool" the program to obtain the desired results since the modifications to make these computations simple and routine have not yet been completed. At present these computations require several computer passes performed at least a half day apart, with a consequent lengthy throughput time.

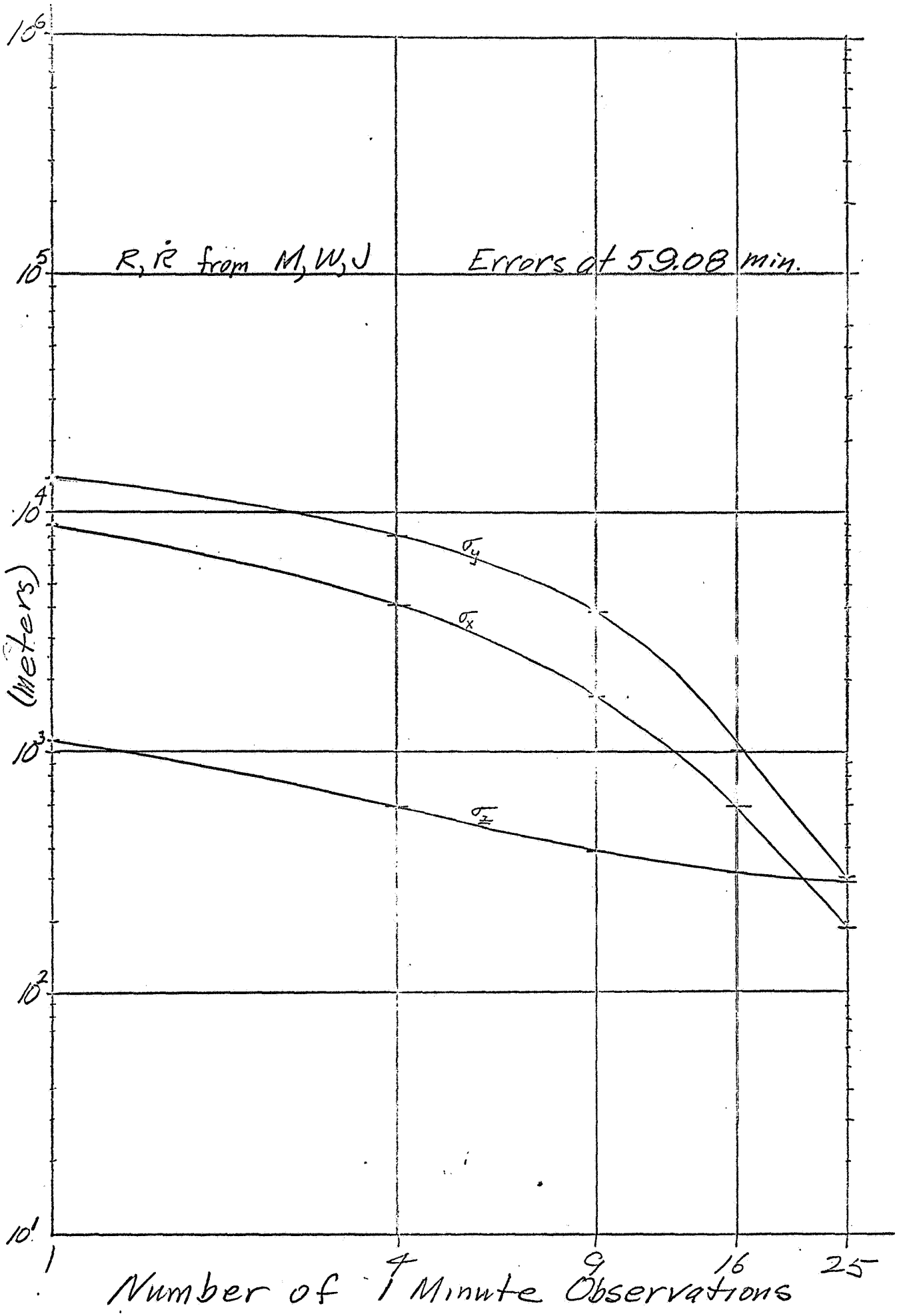
R, Ṙ from M, W, J
Errors at 59.08 min.
10^6
10^5
10^4
10^3
10^2
10^1
(meters)
σ_y
σ_x
σ_z
1
4
9
16
25
Number of 1 Minute Observations

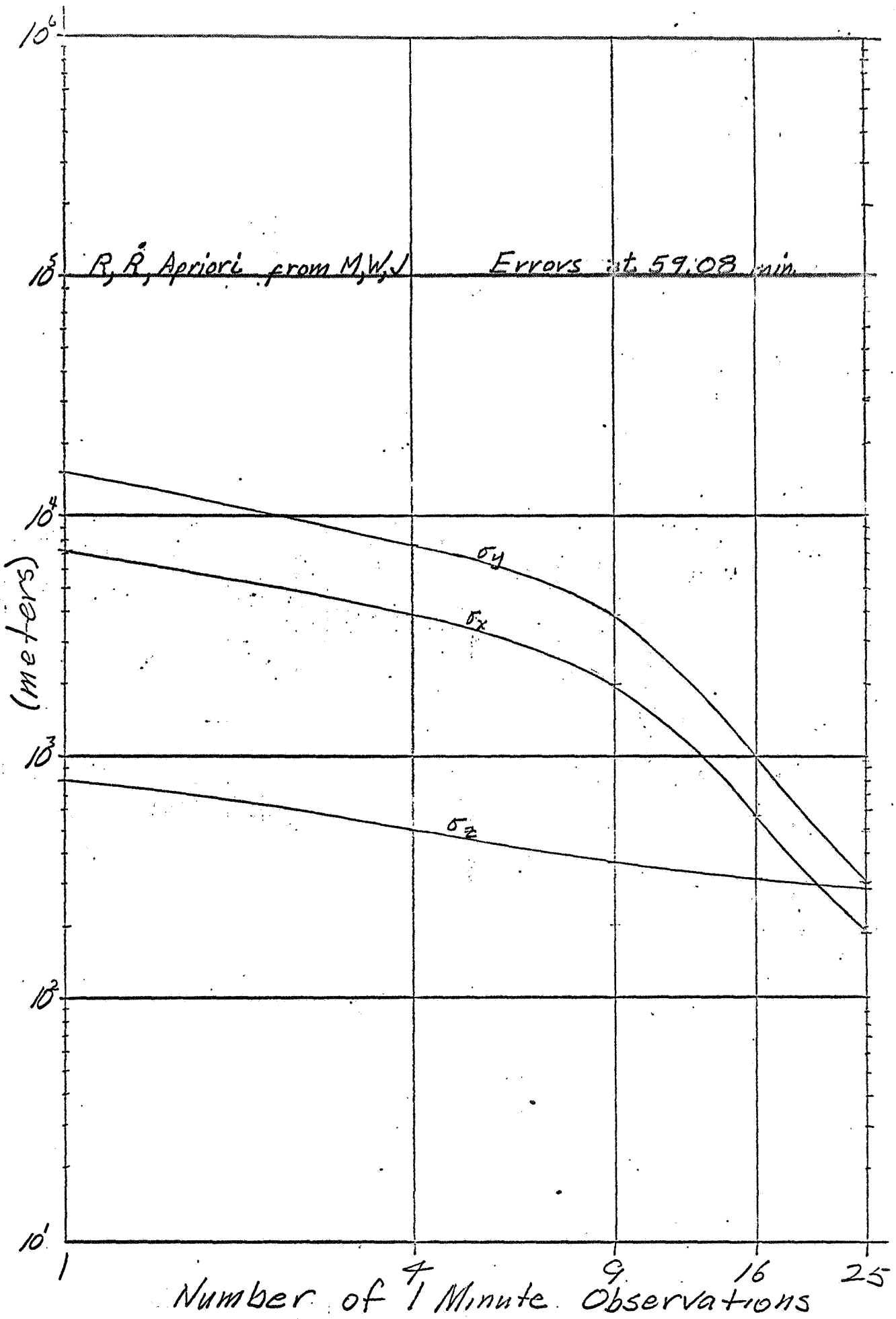
10^6
10^5
R, Ṙ, Apriori from M,W,J
Errors : t, 59.08 min.
10^4
10^3
10^2
10^1
(meters)
σ_y
σ_x
σ_z
1
4
9
16
25
Number of 1 Minute Observations

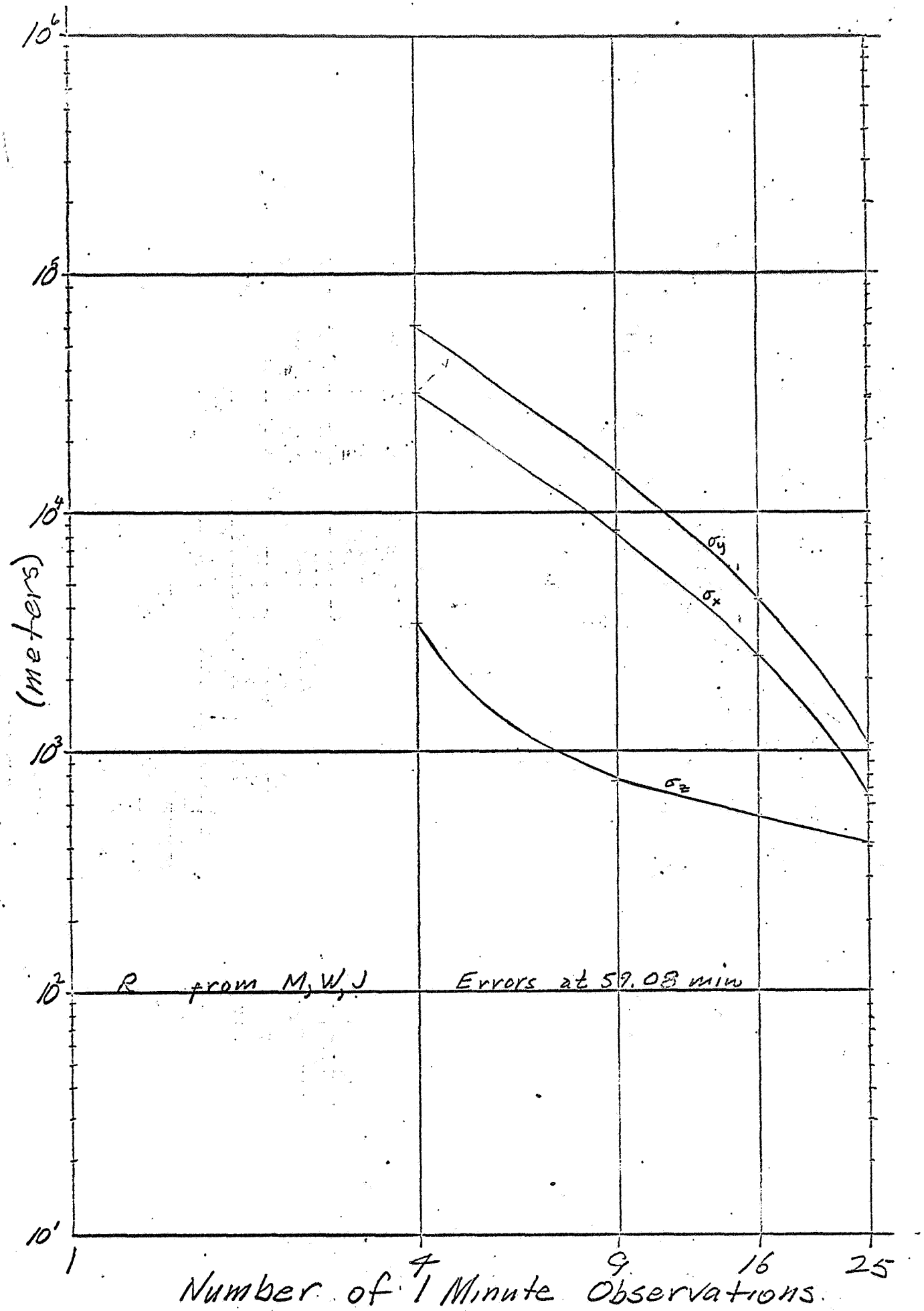
10^6
10^5
10^4
10^3
10^2
10^1
(meters)
σ_y
σ_x
σ_z
R from M, W, J
Errors at 59.03 min
1
4
9
16
25
Number of 1 Minute Observations

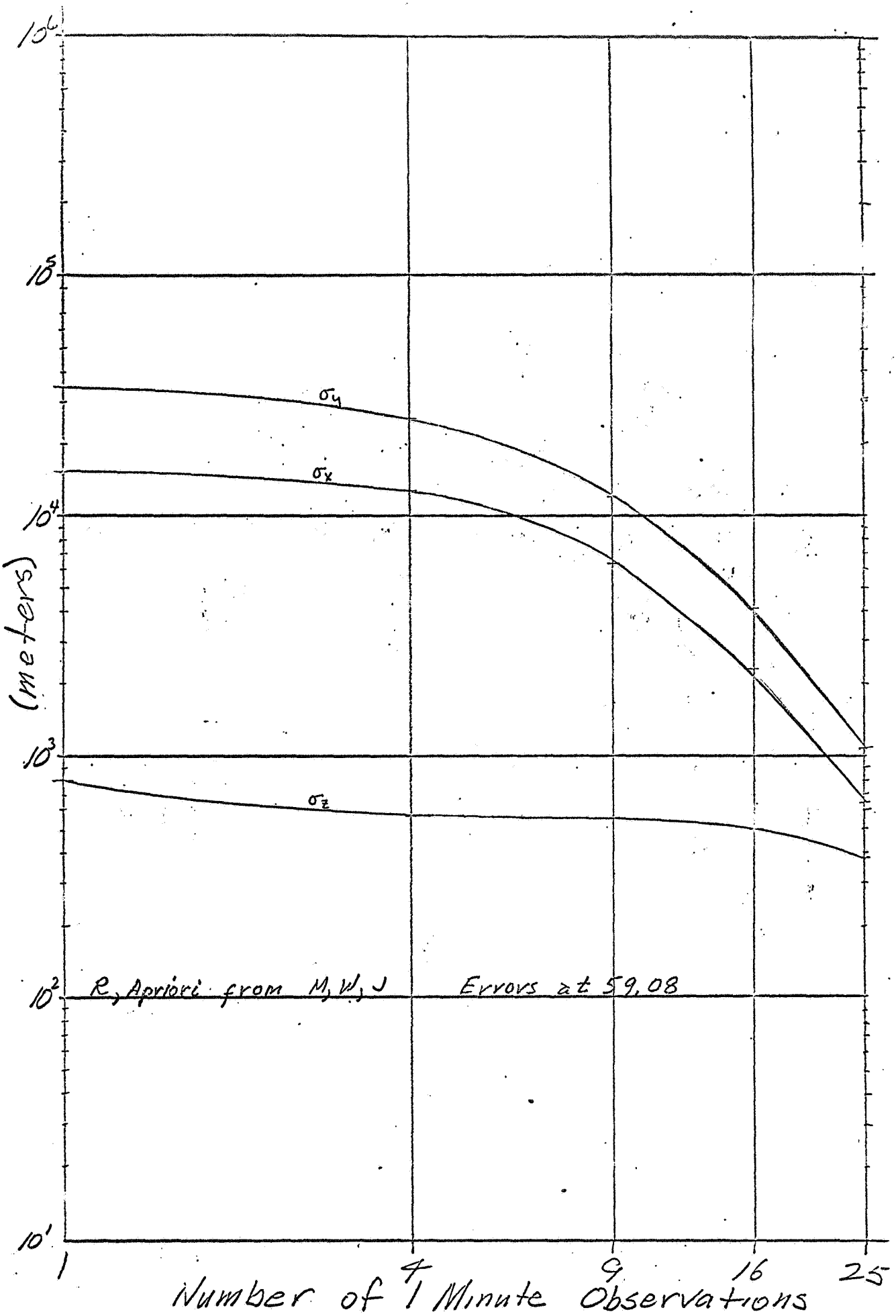
10^6
10^5
10^4
10^3
10^2
10^1
σ_y
σ_x
σ_z
(meters)
R, Apriori from M, W, J
Errors at 59.08
1
4
9
16
25
Number of 1 Minute Observations

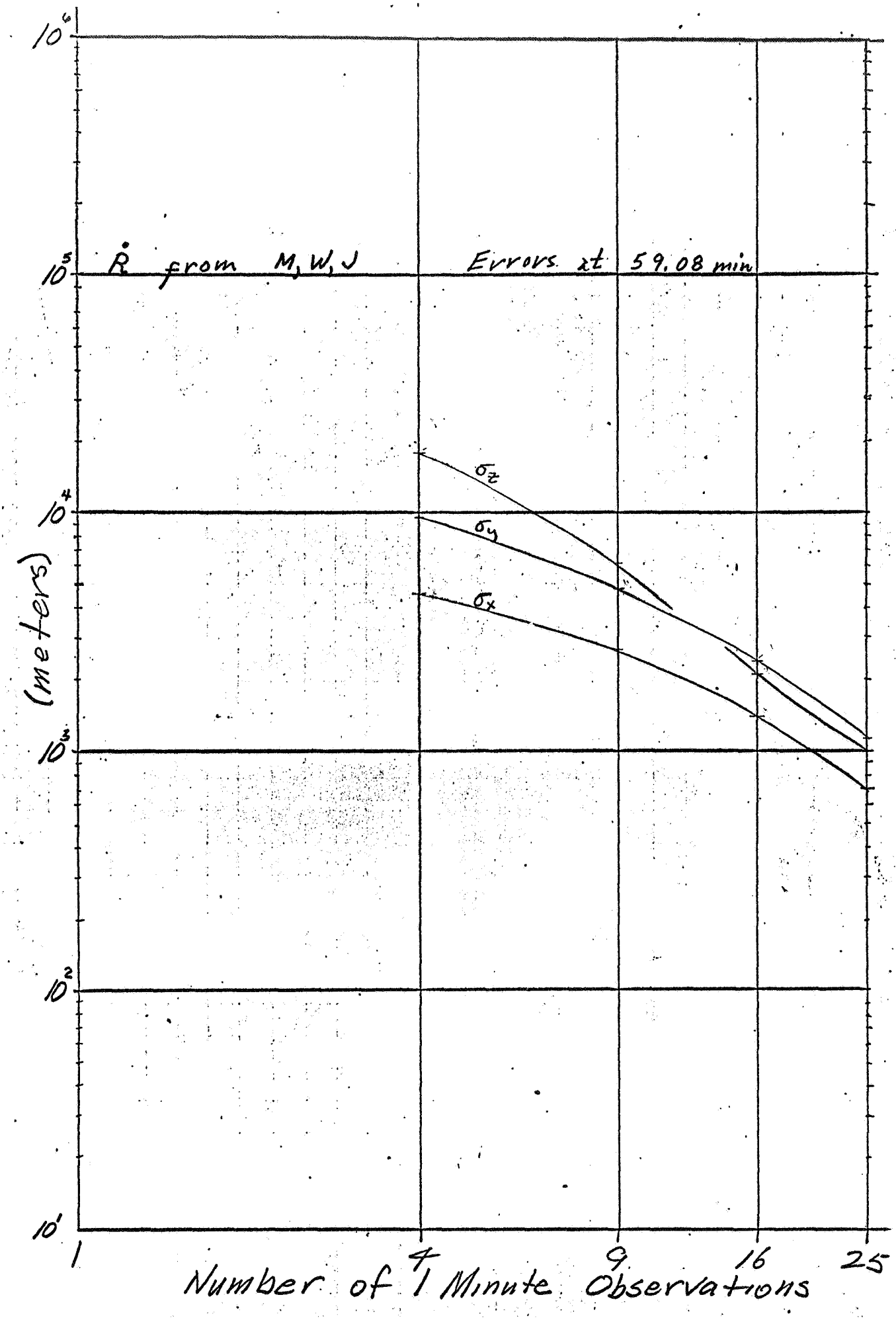
$\dot{R}$ from M, W, J
Errors at 59.08 min
σ_z
σ_y
σ_x
10^6
10^5
10^4
10^3
10^2
10^1
(meters)
1
4
9
16
25
Number of 1 Minute Observations

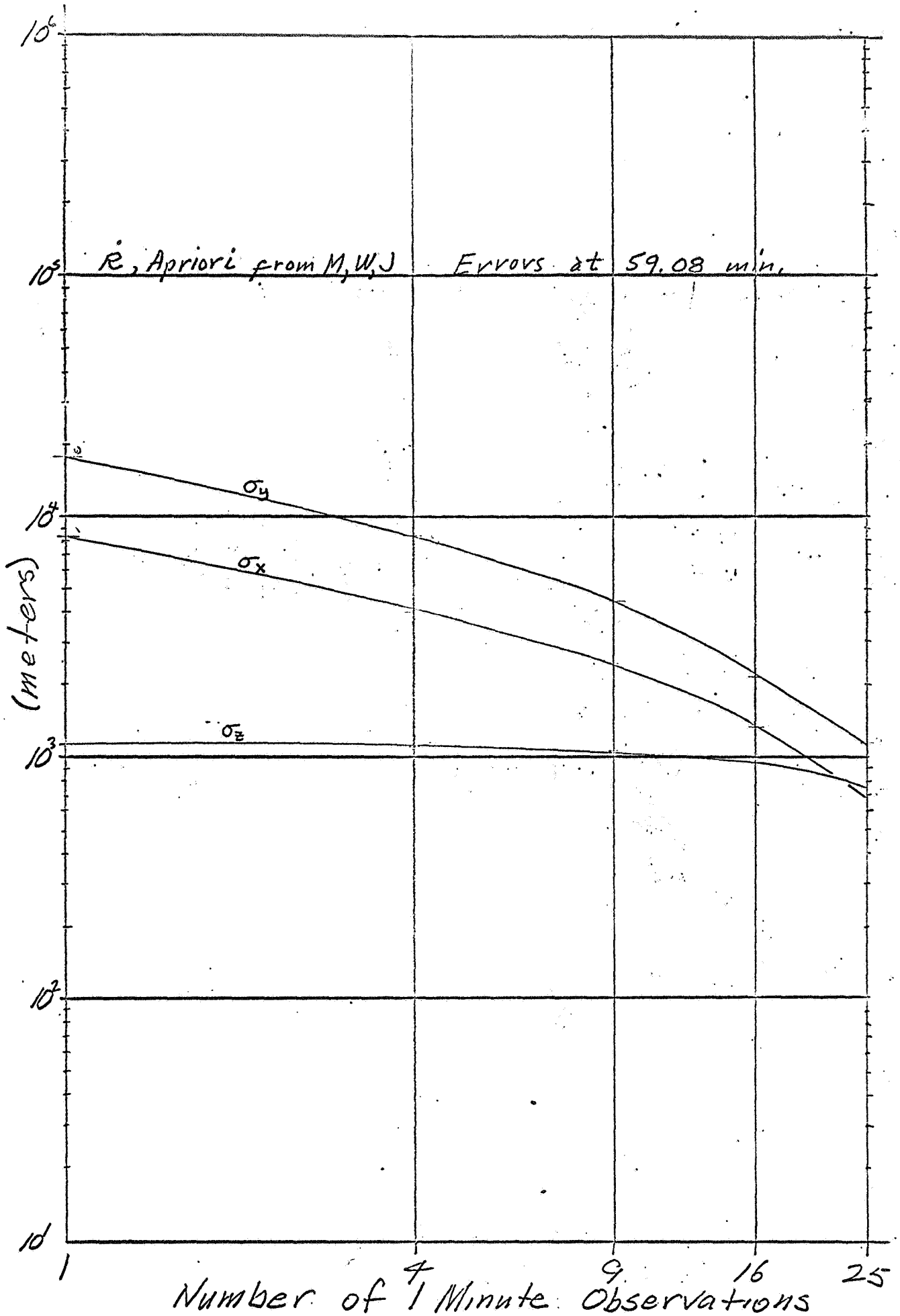
10^6
10^5
$\dot{R}$, Apriori from M, W, J Errors at 59.08 min.
10^4
σ_y
σ_x
σ_z
10^3
10^2
10^1
(meters)
1
4
9
16
25
Number of 1 Minute Observations

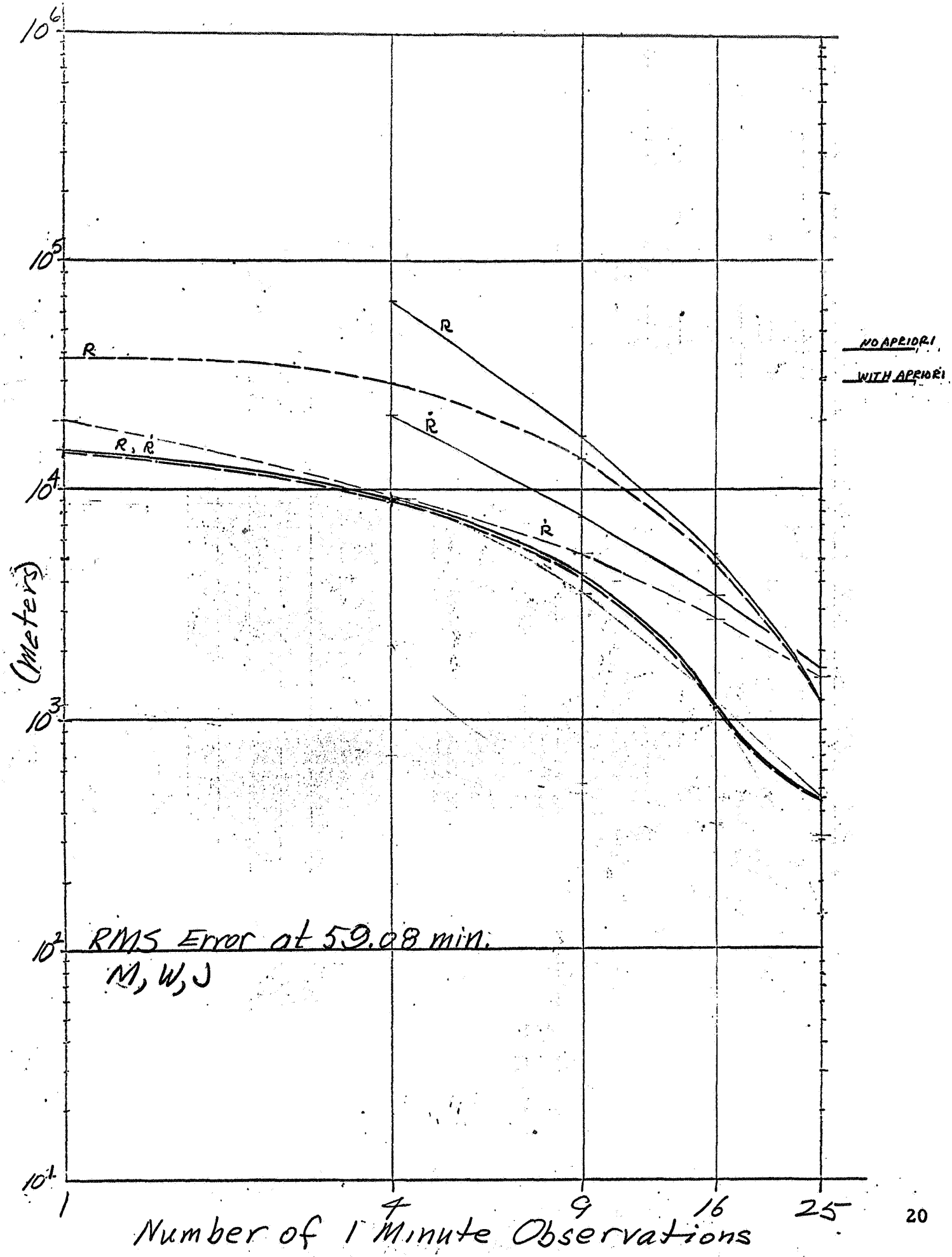
10^6
10^5
10^4
10^3
10^2
10^1
(Meters)
R
R
R, Ṙ
Ṙ
Ṙ
NO APRIORI
WITH APRIORI
RMS Error at 59.08 min.
M, W, J
1
4
9
16
25
Number of 1 Minute Observations

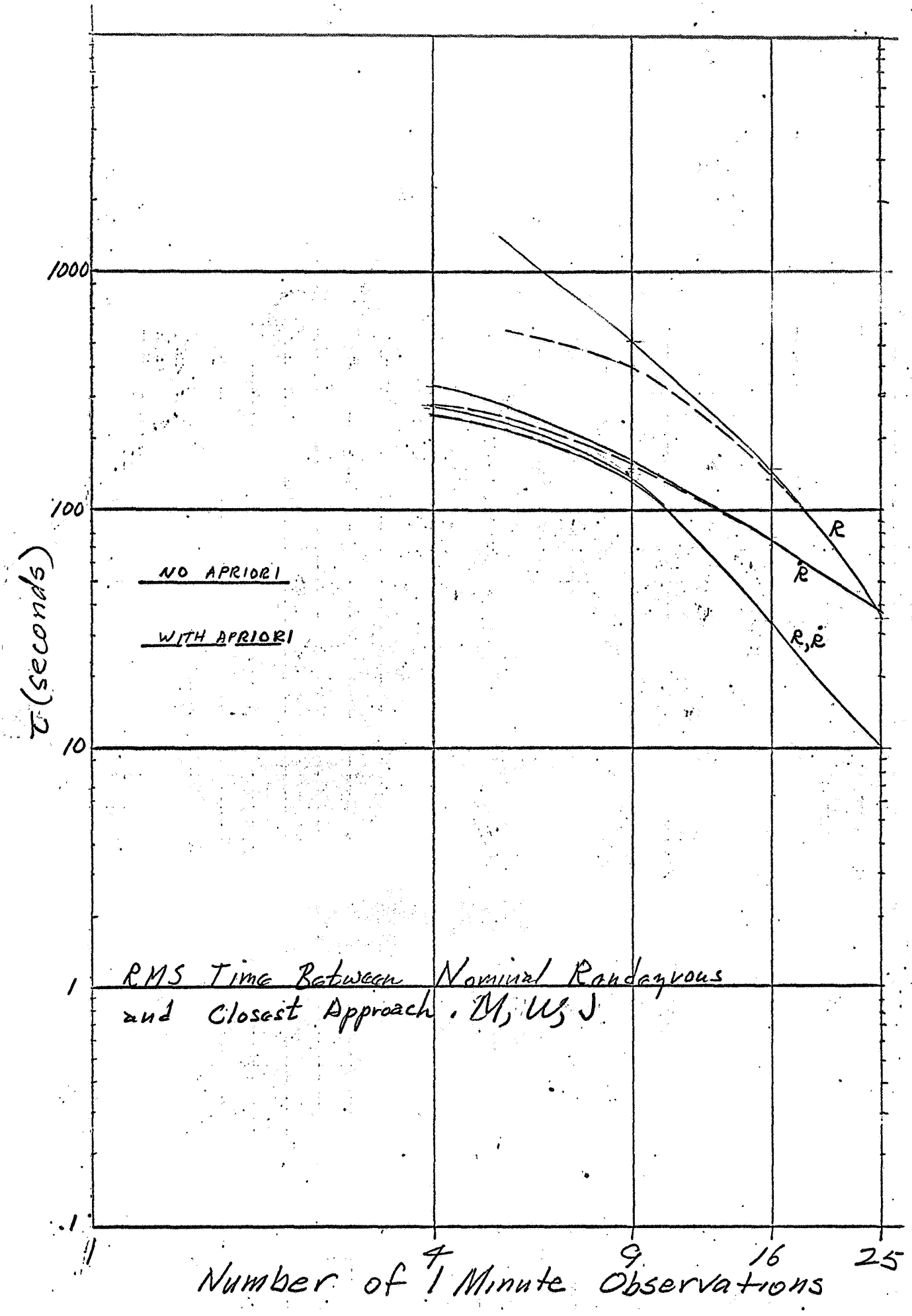

RMS Time Between Nominal Rendezvous and Closest Approach. M, W, J.

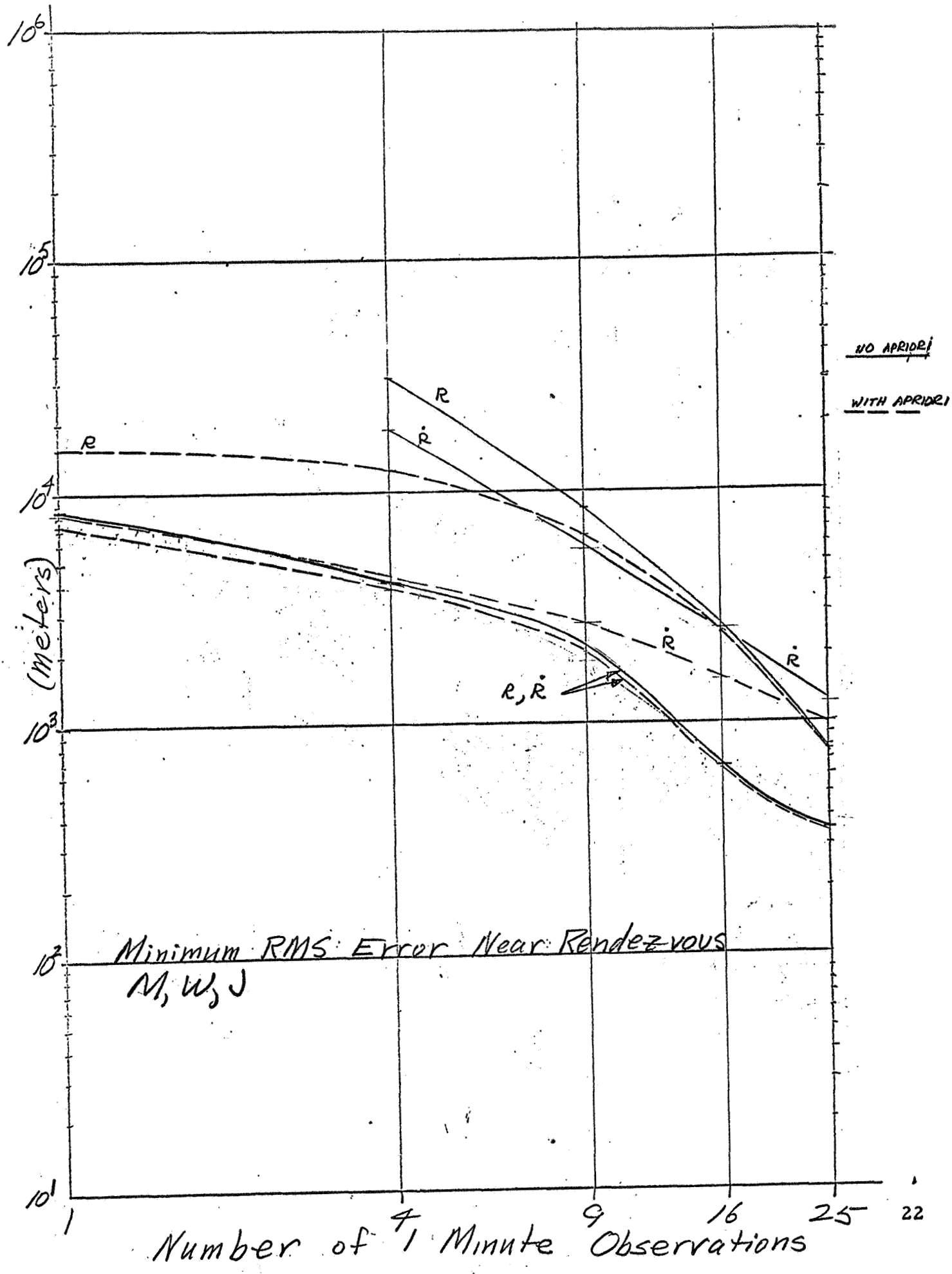
10^6
10^5
10^4
10^3
10^2
10^1
(Meters)
NO APRIORI
WITH APRIORI
R
$\dot{R}$
R
$\dot{R}$
$\dot{R}$
R, $\dot{R}$
Minimum RMS Error Near Rendezvous
M, W, J
1
4
9
16
25
Number of 1 Minute Observations

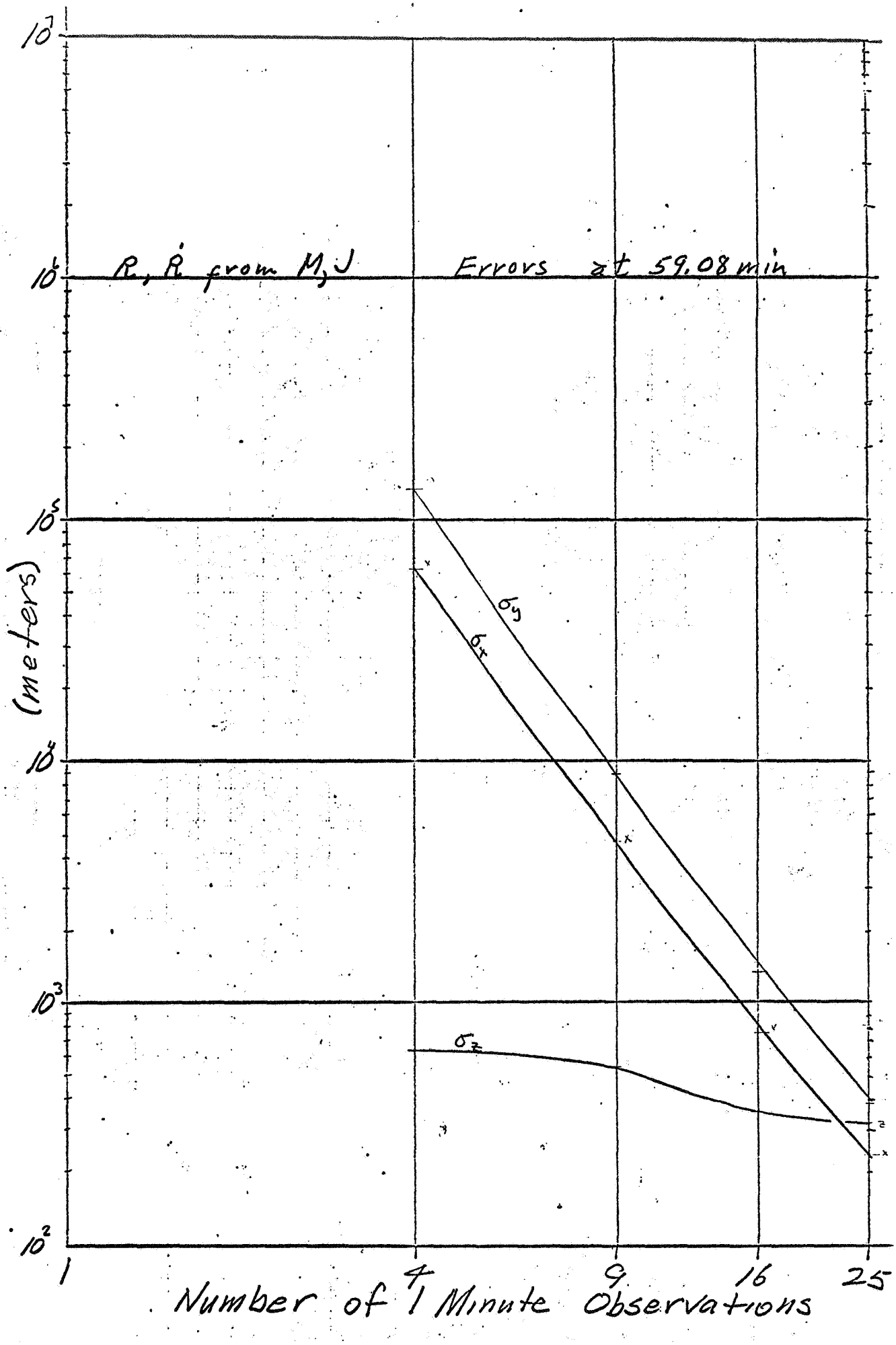
R, Ṙ from M, J
Errors at 59.08 min
10^7
10^6
10^5
10^4
10^3
10^2
(meters)
σ_y
σ_x
σ_z
1
4
9
16
25
Number of 1 Minute Observations

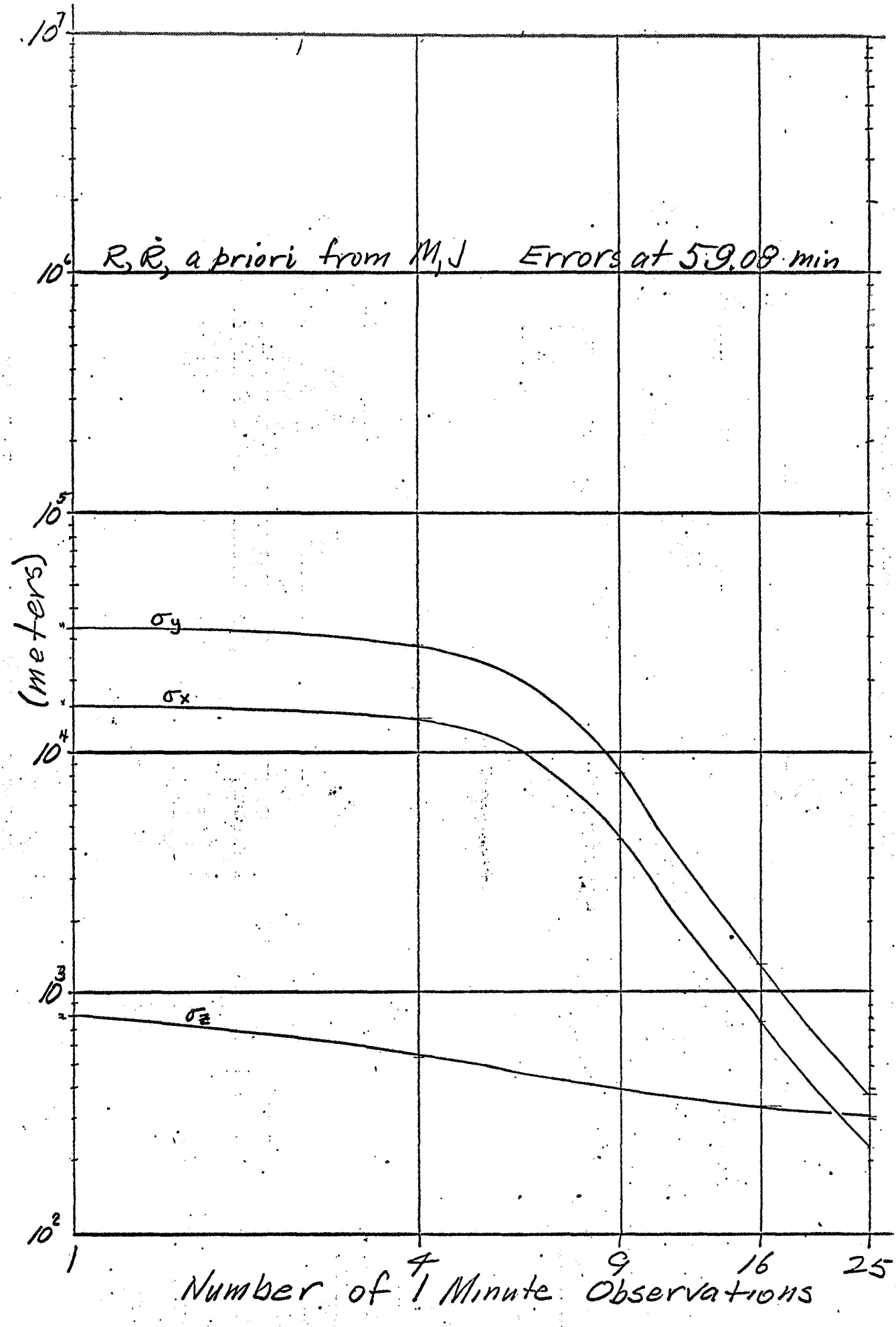
R, Ṙ, a priori from M, J Errors at 59.08 min
(meters)
10^7
10^6
10^5
10^4
10^3
10^2
σ_y
σ_x
σ_z
1
4
9
16
25
Number of 1 Minute Observations

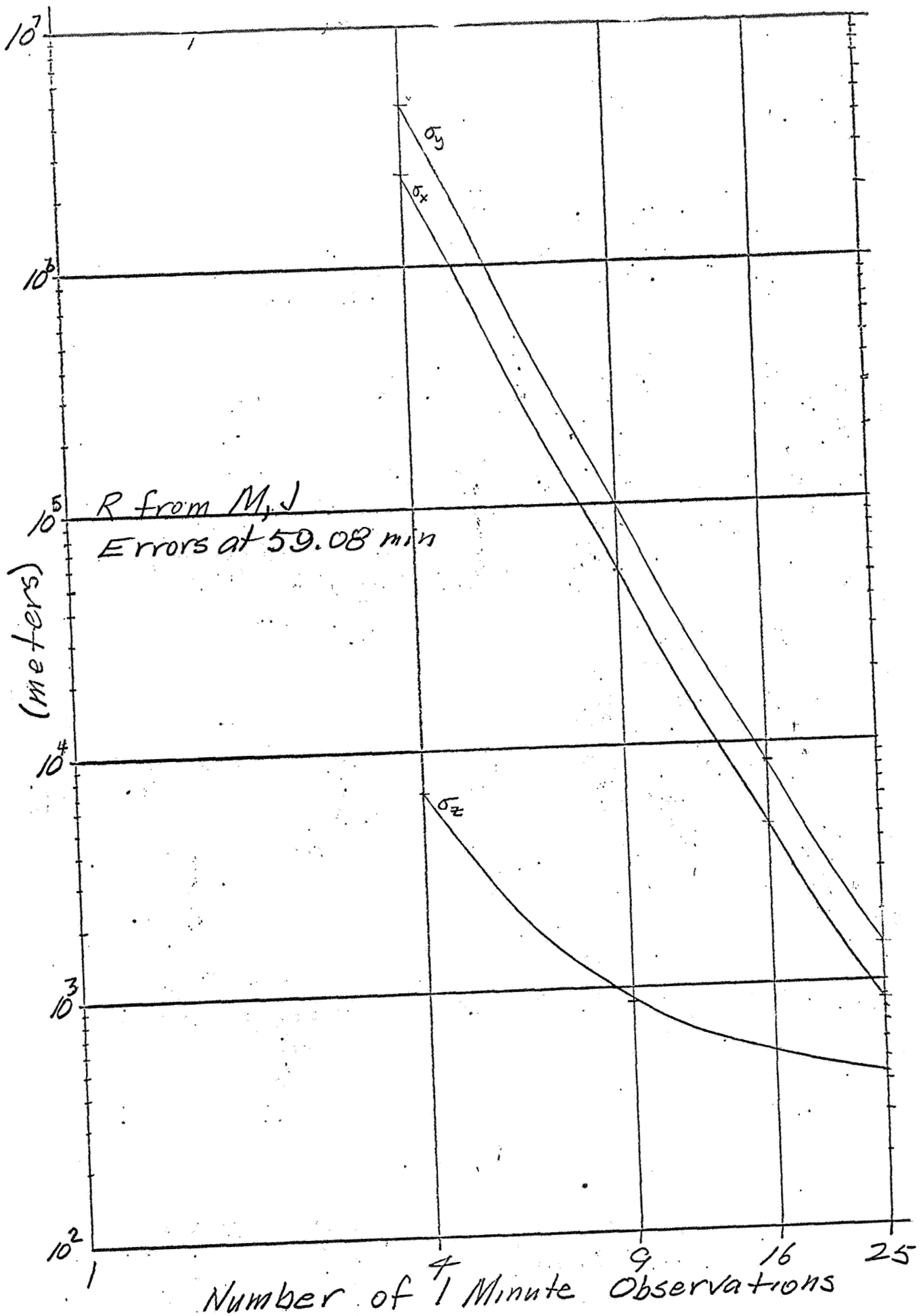
10^7
10^6
10^5
10^4
10^3
10^2
σ_y
σ_x
σ_z
R from M, J
Errors at 59.08 min
(meters)
1
4
9
16
25
Number of 1 Minute Observations

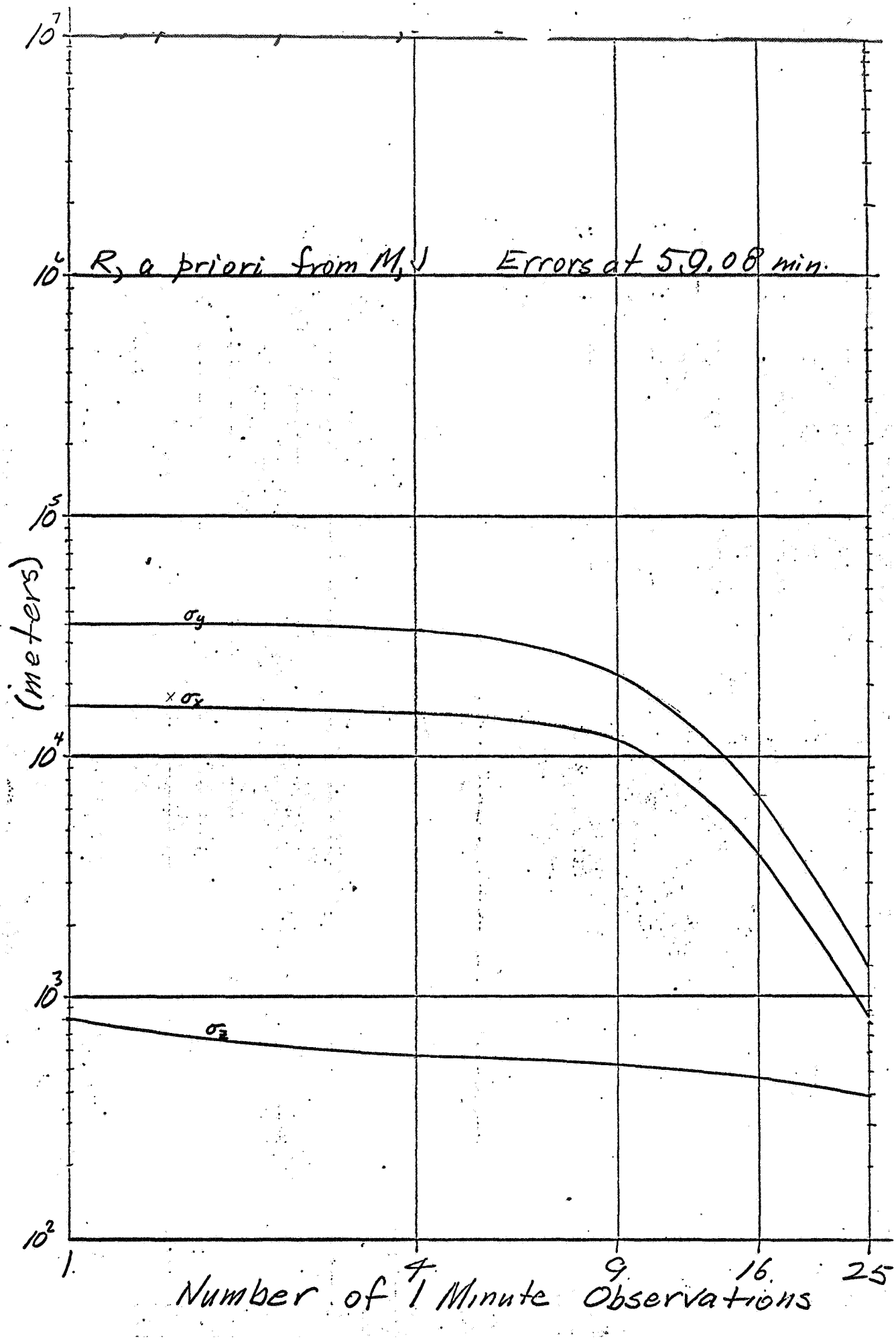
R, a priori from M, J
Errors at 5.9.08 min.
10^7
10^6
10^5
10^4
10^3
10^2
(meters)
σ_y
σ_x
σ_z
1
4
9
16
25
Number of 1 Minute Observations

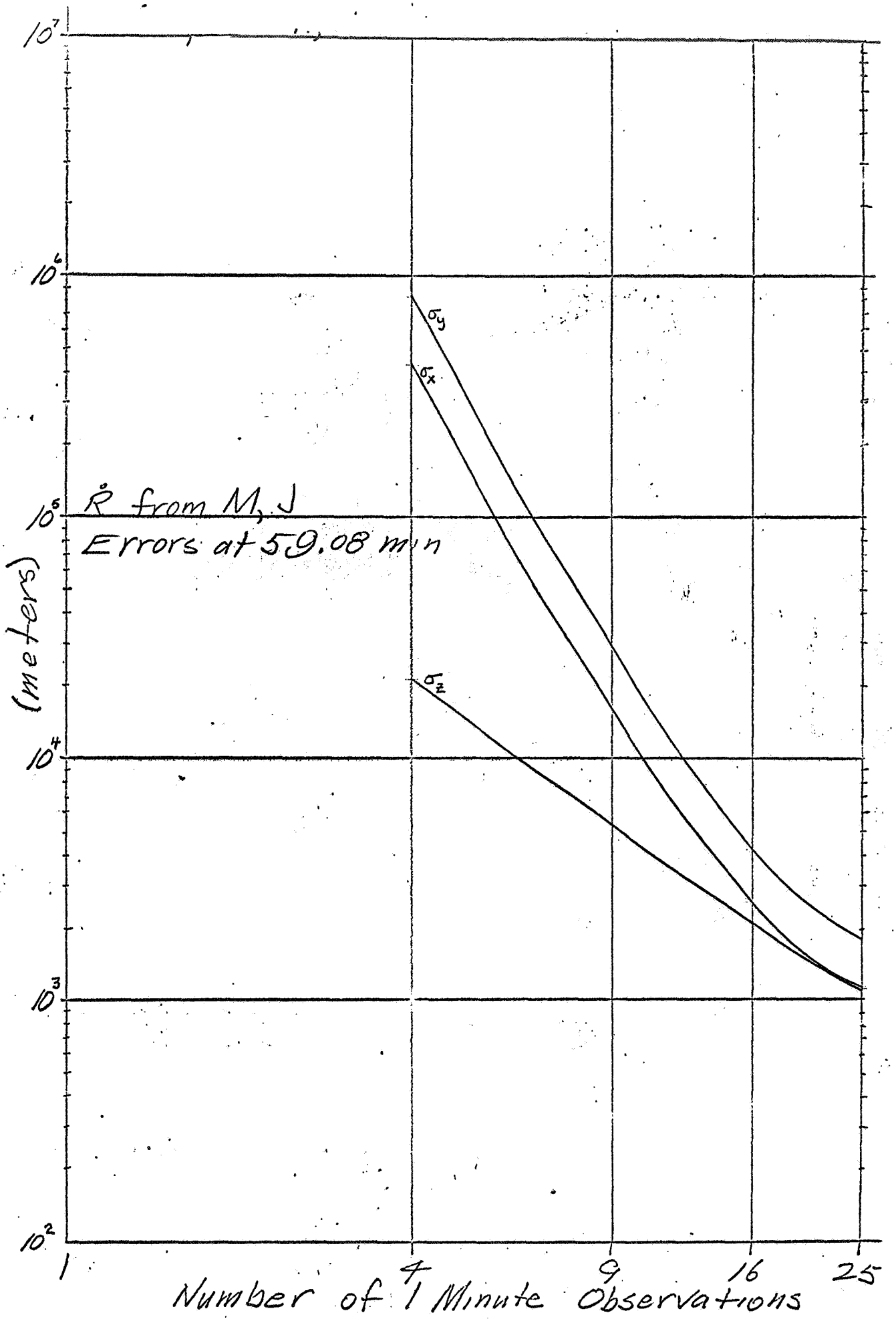
10^7
10^6
10^5
10^4
10^3
10^2
σ_y
σ_x
σ_z
$\dot{R}$ from M, J
Errors at 59.08 min
(meters)
1
4
9
16
25
Number of 1 Minute Observations

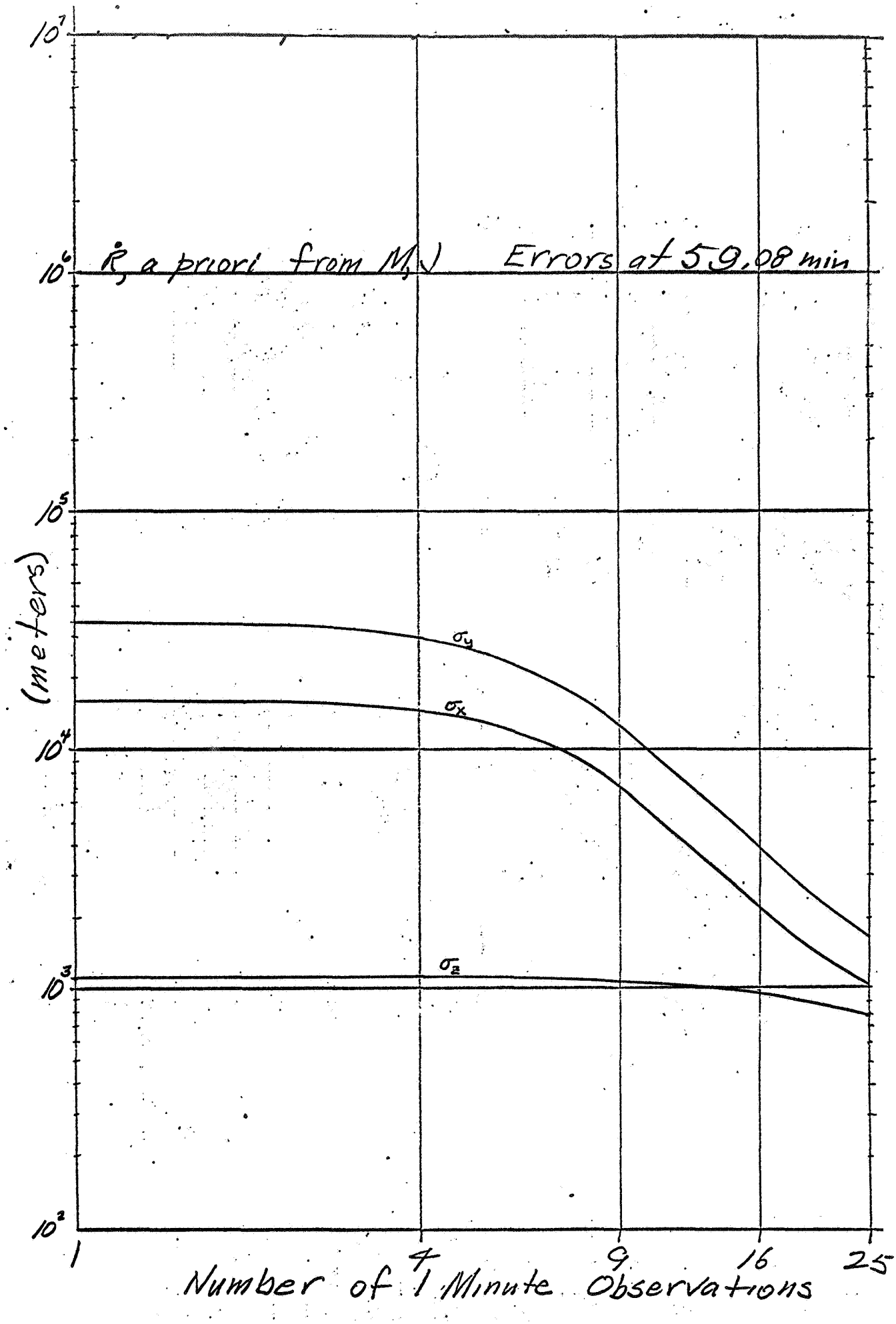
$\dot{R}$, a priori from M, J Errors at 59.08 min
10^7
10^6
10^5
10^4
10^3
10^2
(meters)
σ_y
σ_x
σ_z
1
4
9
16
25
Number of 1 Minute Observations

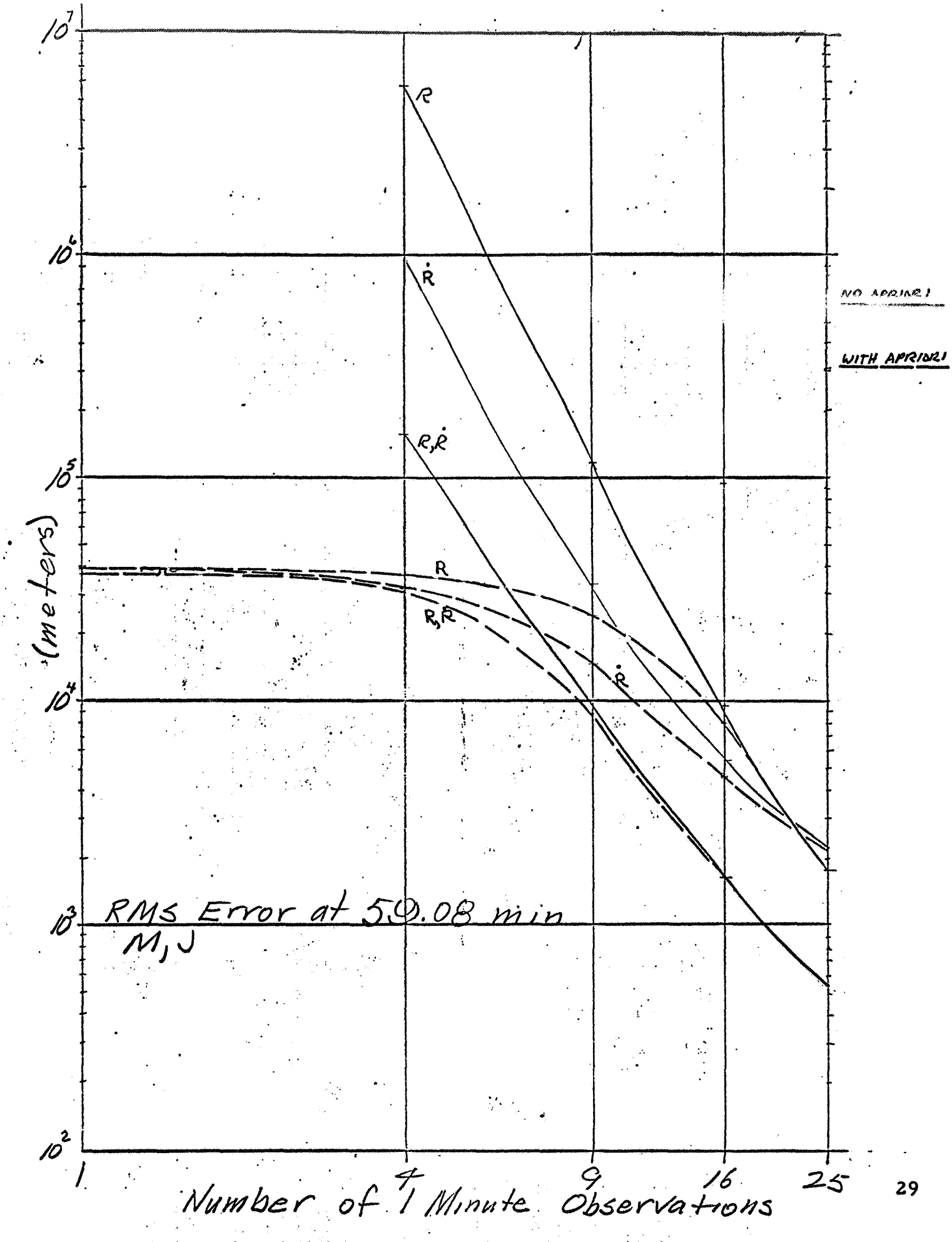
10^7
10^6
10^5
10^4
10^3
10^2
R
$\dot{R}$
R,$\dot{R}$
R
R,$\dot{R}$
$\dot{R}$
NO APRIORI
WITH APRIORI
RMS Error at 59.08 min
M, J
(meters)
1
4
9
16
25
Number of 1 Minute Observations

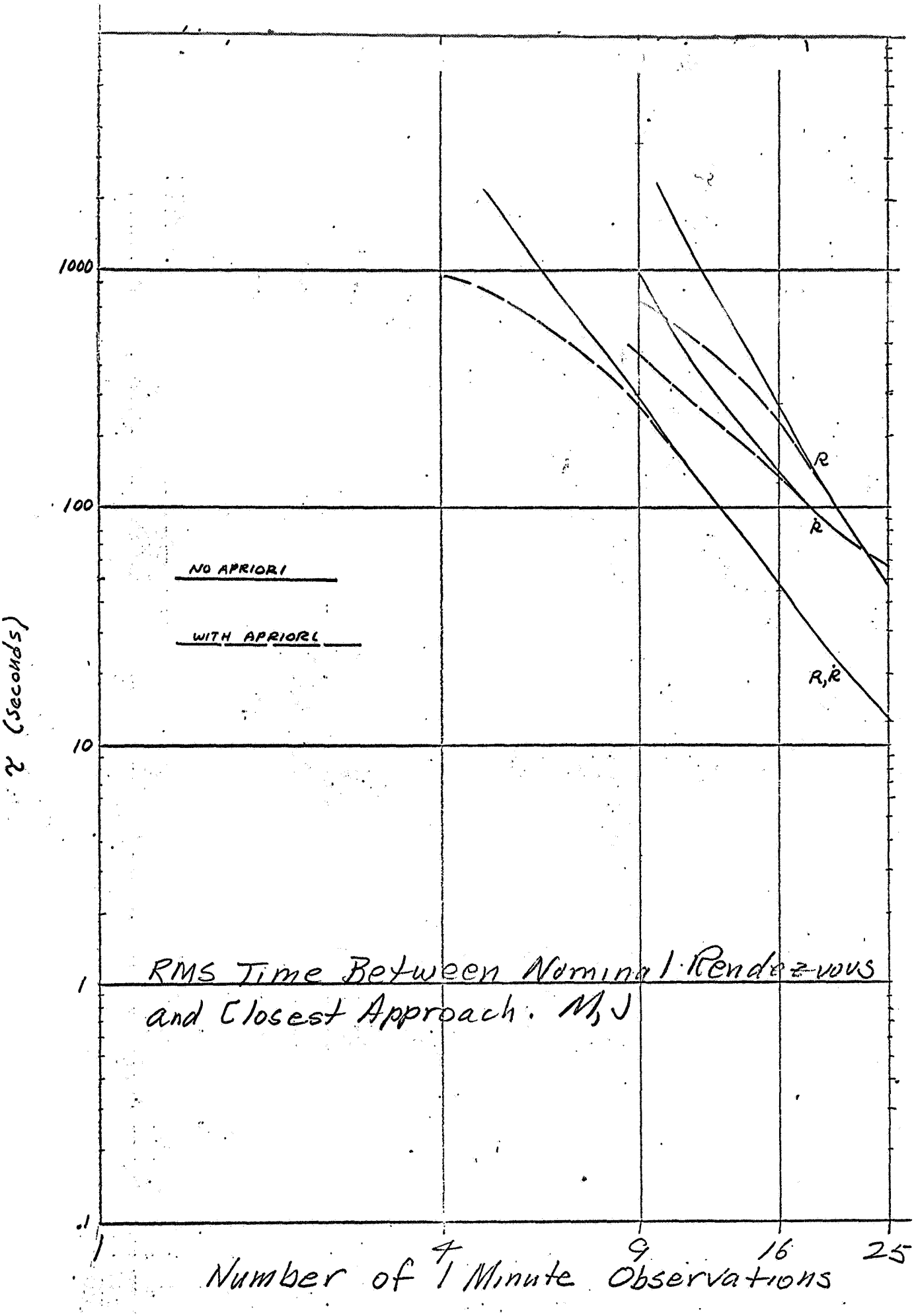

RMS Time Between Nominal Rendezvous and Closest Approach. M, J

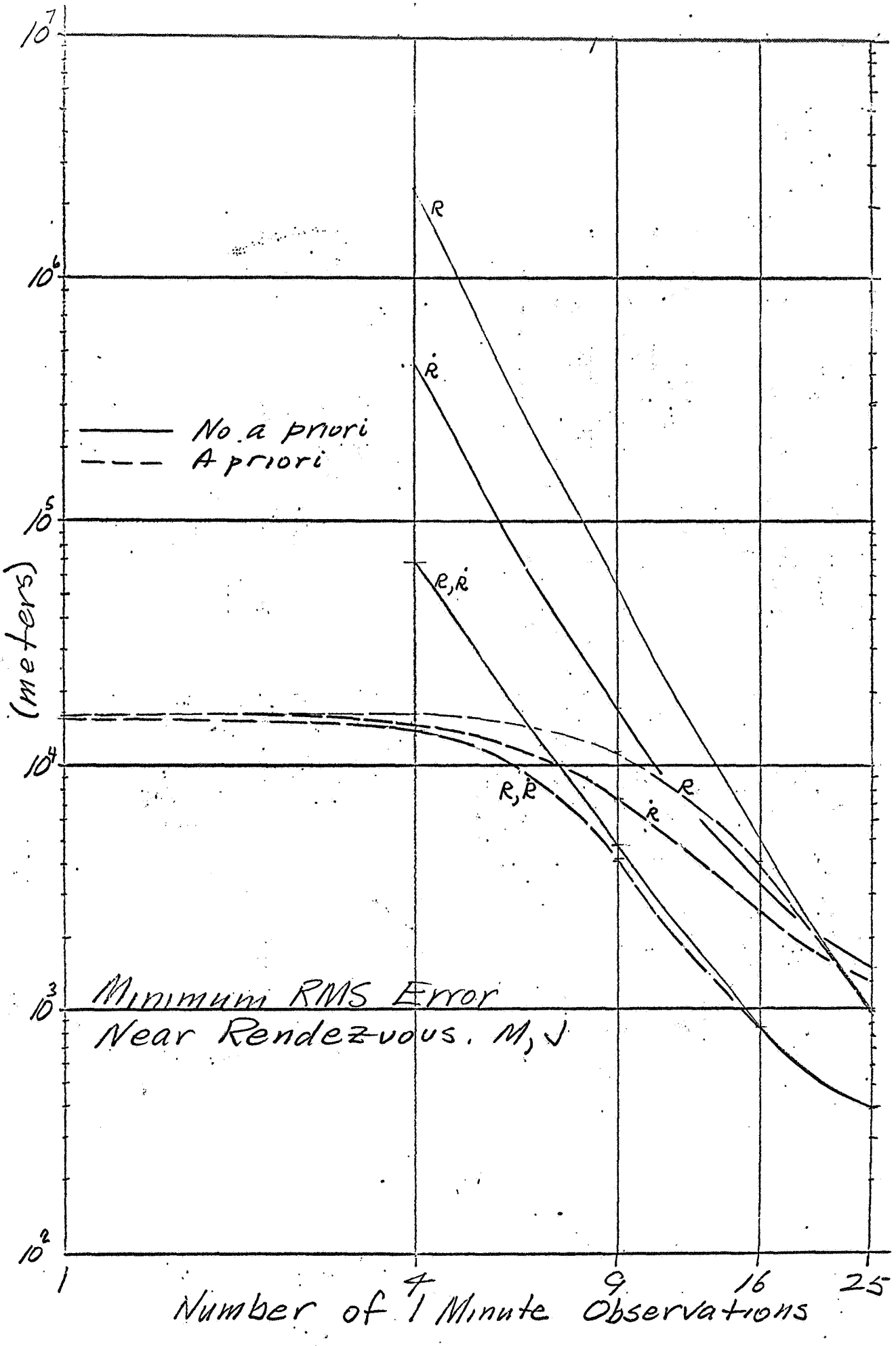
10^7
10^6
10^5
10^4
10^3
10^2
(meters)
R
$\dot{R}$
R,$\dot{R}$
R,$\dot{R}$
R
$\dot{R}$
No a priori
A priori
Minimum RMS Error
Near Rendezvous. M, J
1
4
9
16
25
Number of 1 Minute Observations

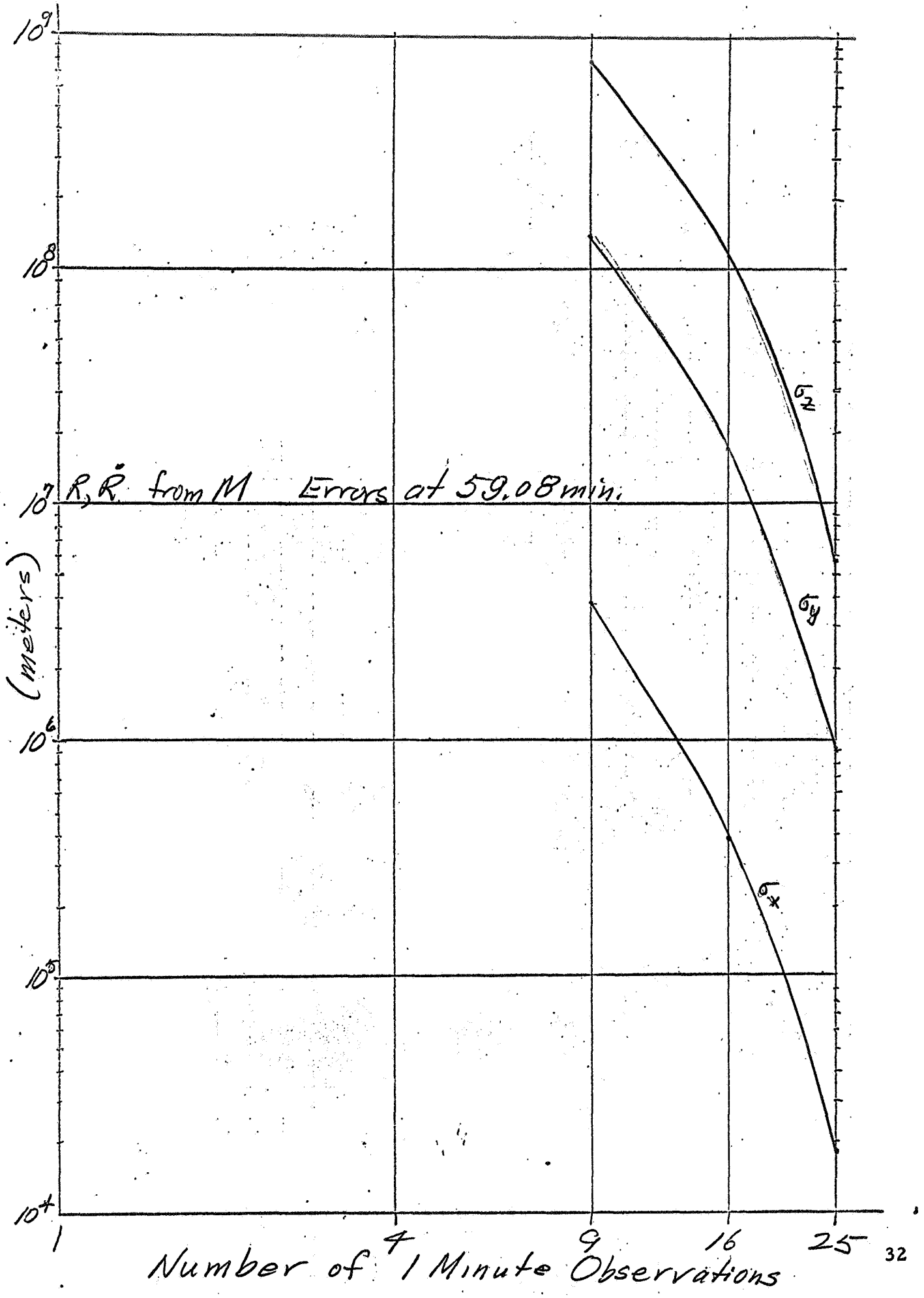
R, Ṙ from M Errors at 59.08 min.
(meters)
10^9
10^8
10^7
10^6
10^5
10^4
σ_N
σ_y
σ_*
1
4
9
16
25
Number of 1 Minute Observations

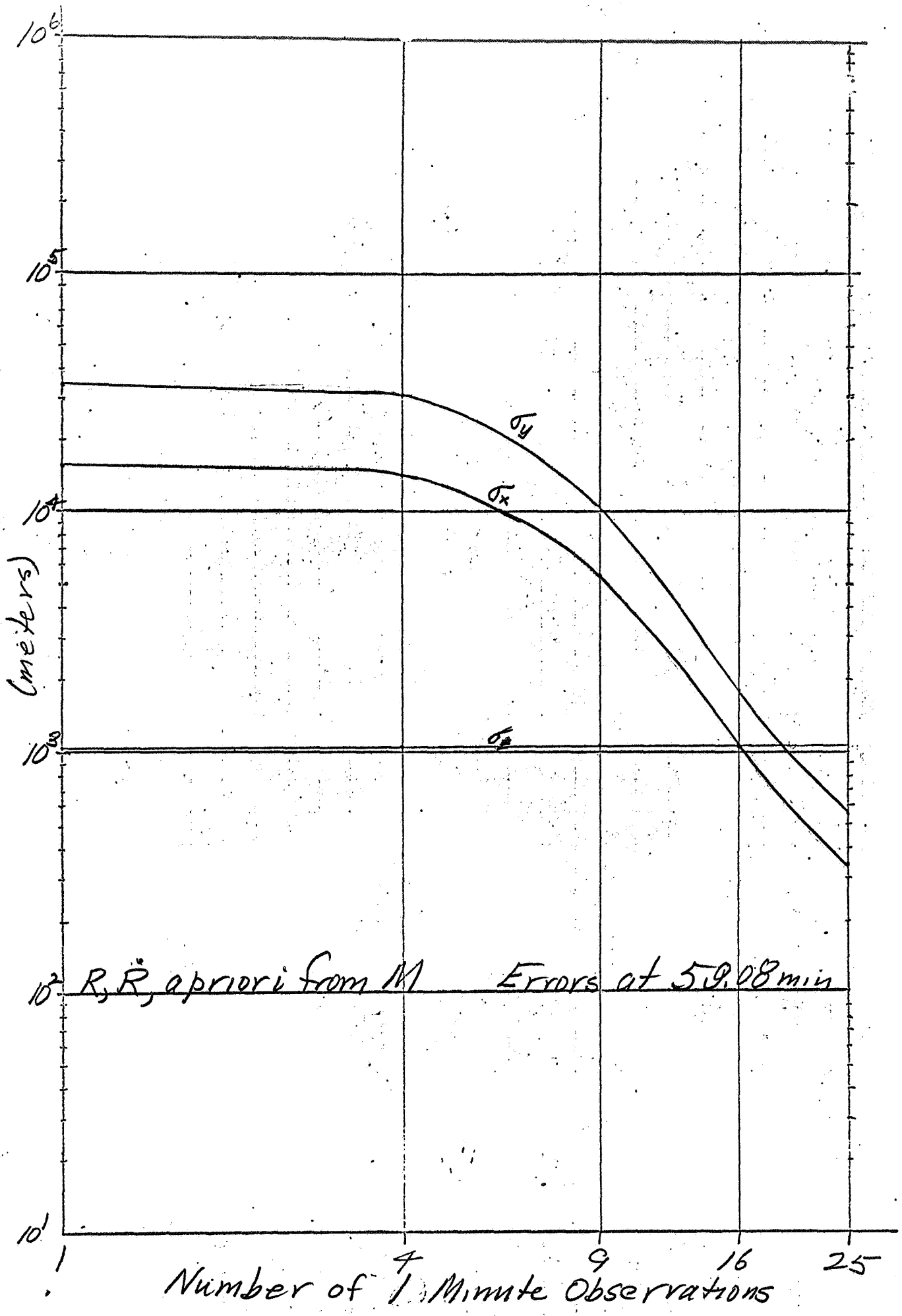
10^6
10^5
10^4
10^3
10^2
10^1
σ_y
σ_x
σ_z
(meters)
R, $\dot{R}$, $\ddot{R}$, a priori from M
Errors at 59.08 min
1
4
9
16
25
Number of 1 Minute Observations

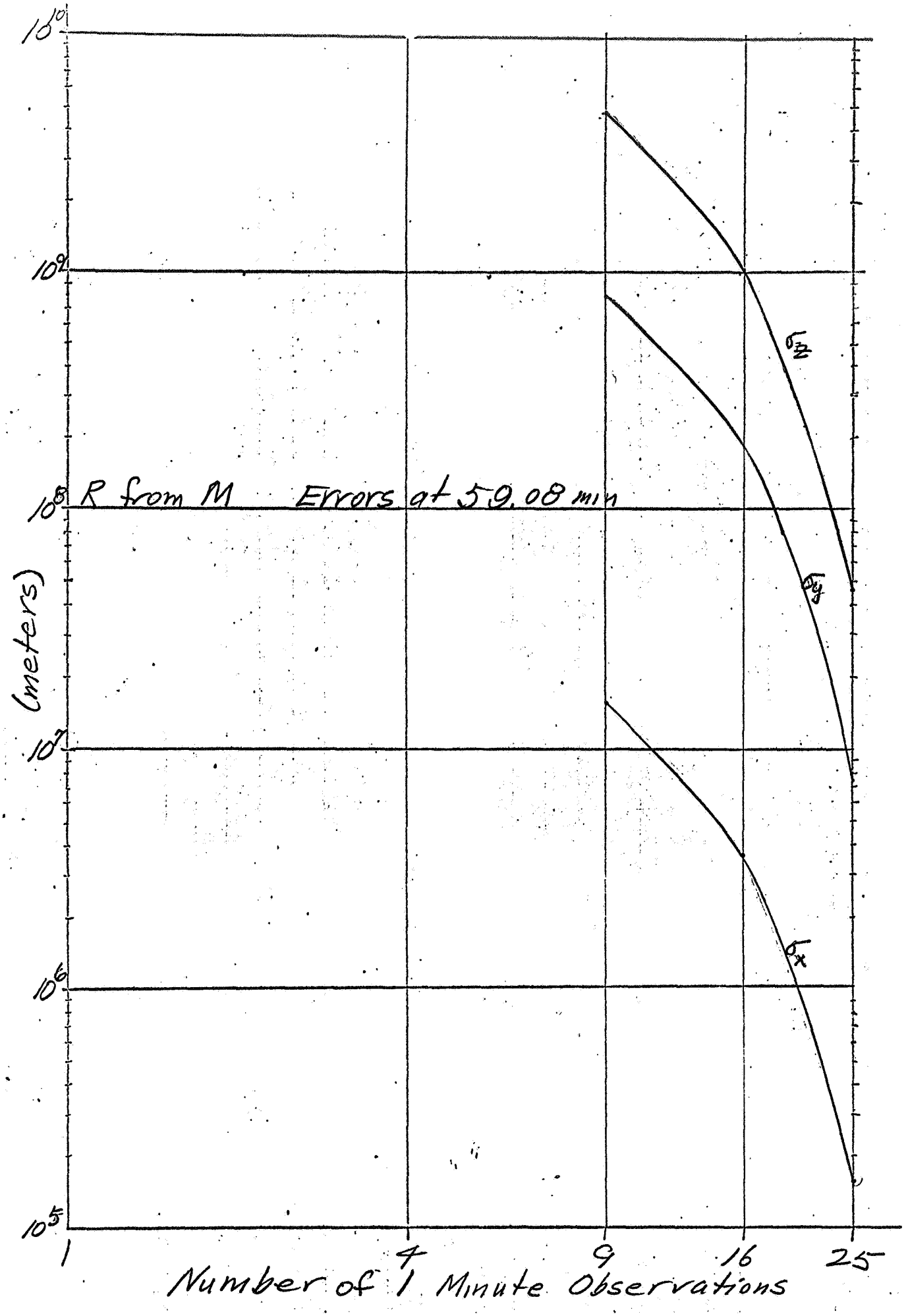
R from M Errors at 59.08 min
(meters)
10^{10}
10^{9}
10^{8}
10^{7}
10^{6}
10^{5}
σ_z
σ_y
σ_x
1
4
9
16
25
Number of 1 Minute Observations

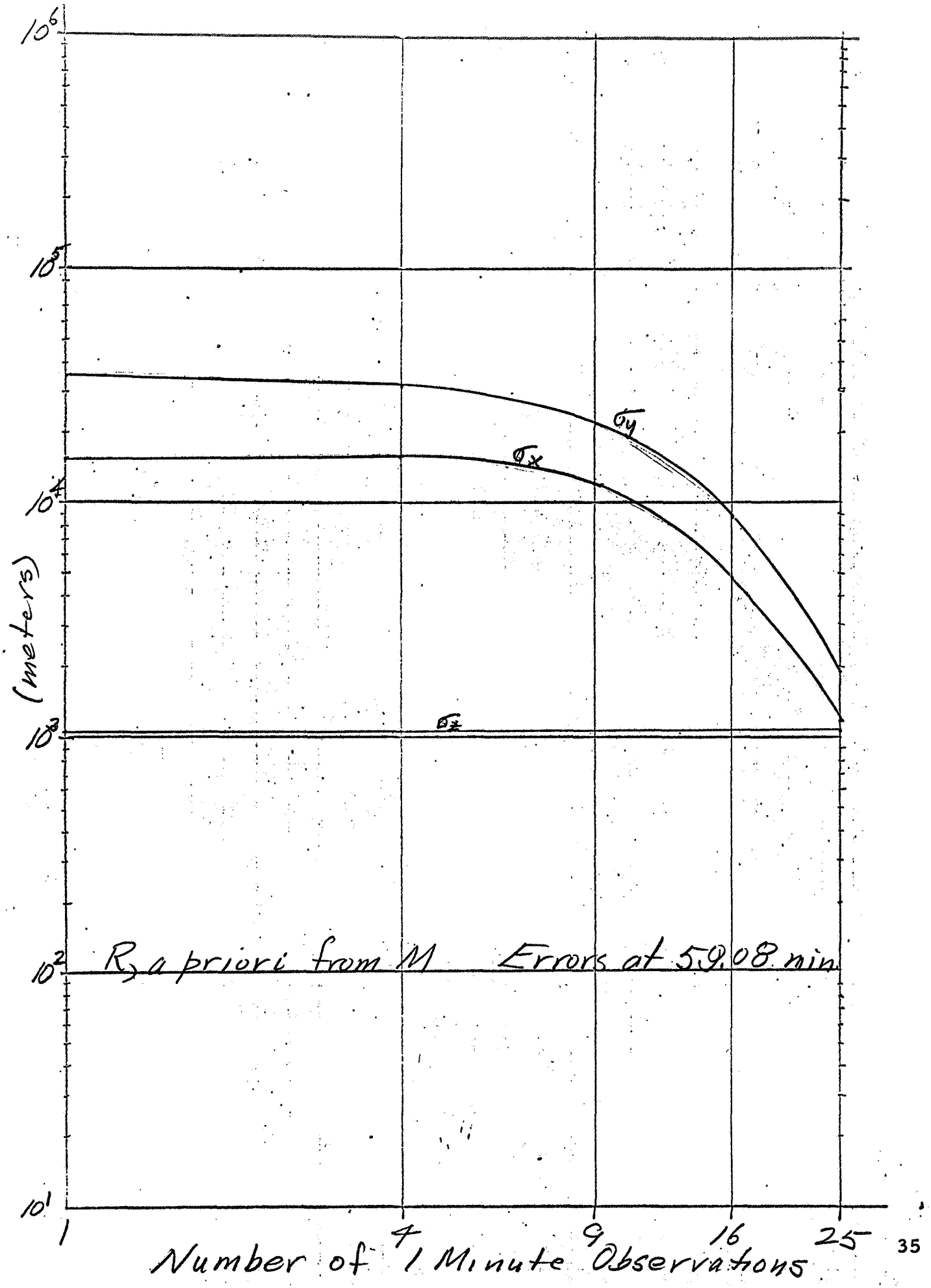
10^6
10^5
10^4
10^3
10^2
10^1
(meters)
σ_y
σ_x
σ_z
R, a priori from M
Errors at 59.08 min.
1
4
9
16
25
Number of 1 Minute Observations

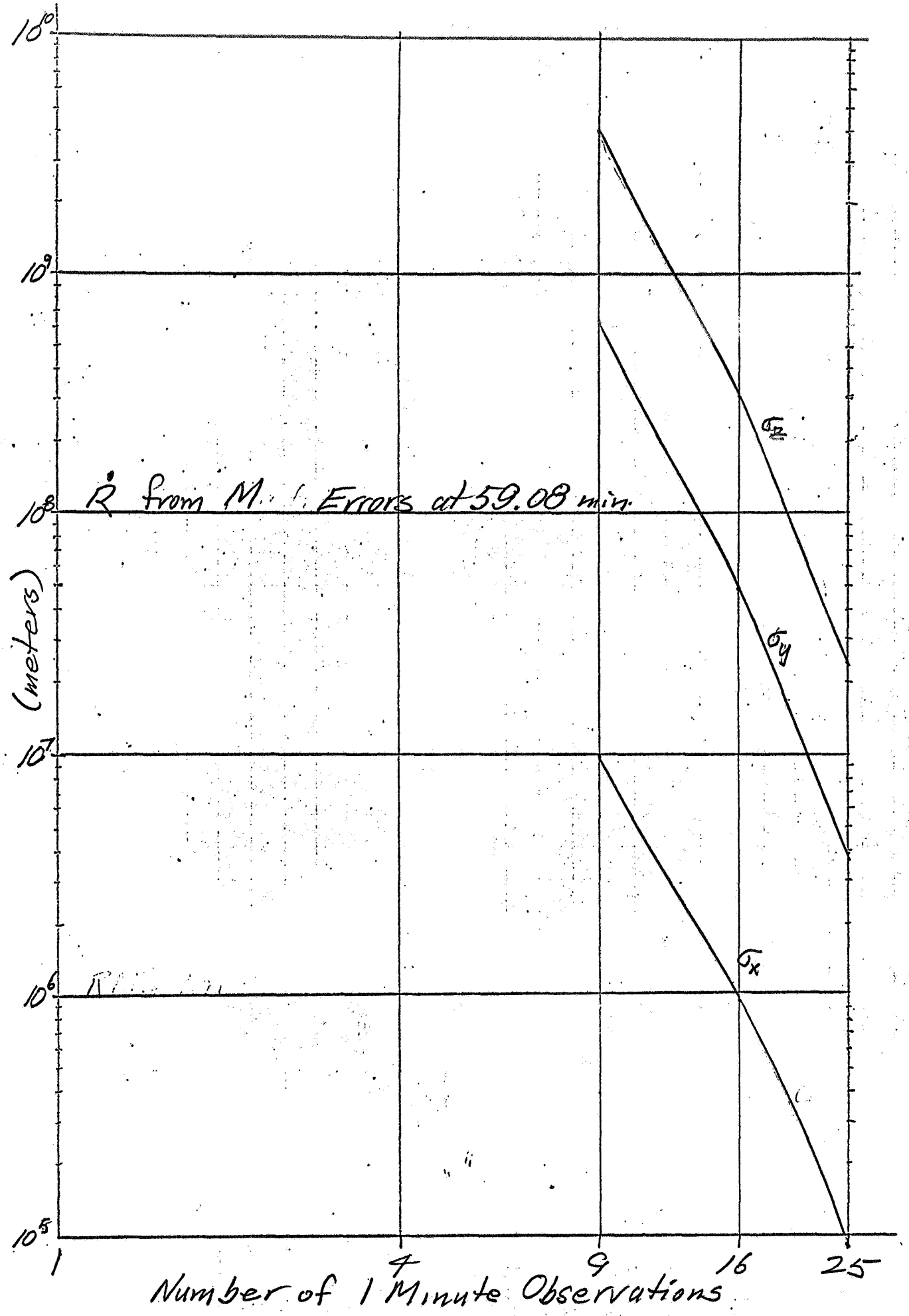
10^{10}
10^{9}
10^{8}
10^{7}
10^{6}
10^{5}
(meters)
$\dot{R}$ from M. C. Errors at 59.08 min.
σ_z
σ_y
σ_x
1
4
9
16
25
Number of 1 Minute Observations

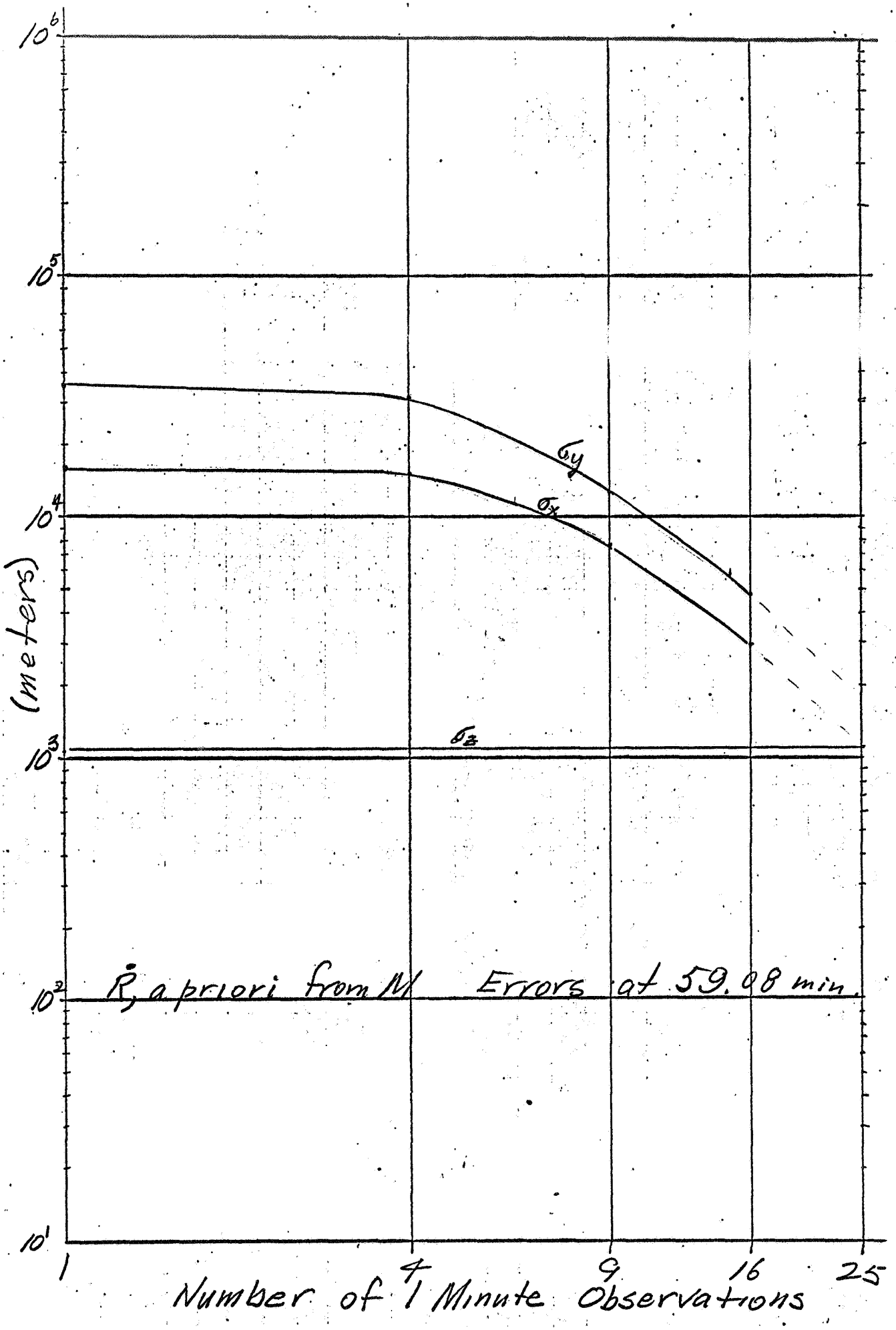
10^6
10^5
10^4
10^3
10^2
10^1
(meters)
σ_y
σ_x
σ_z
$\dot{R}$, a priori from M
Errors at 59.98 min.
1
4
9
16
25
Number of 1 Minute Observations

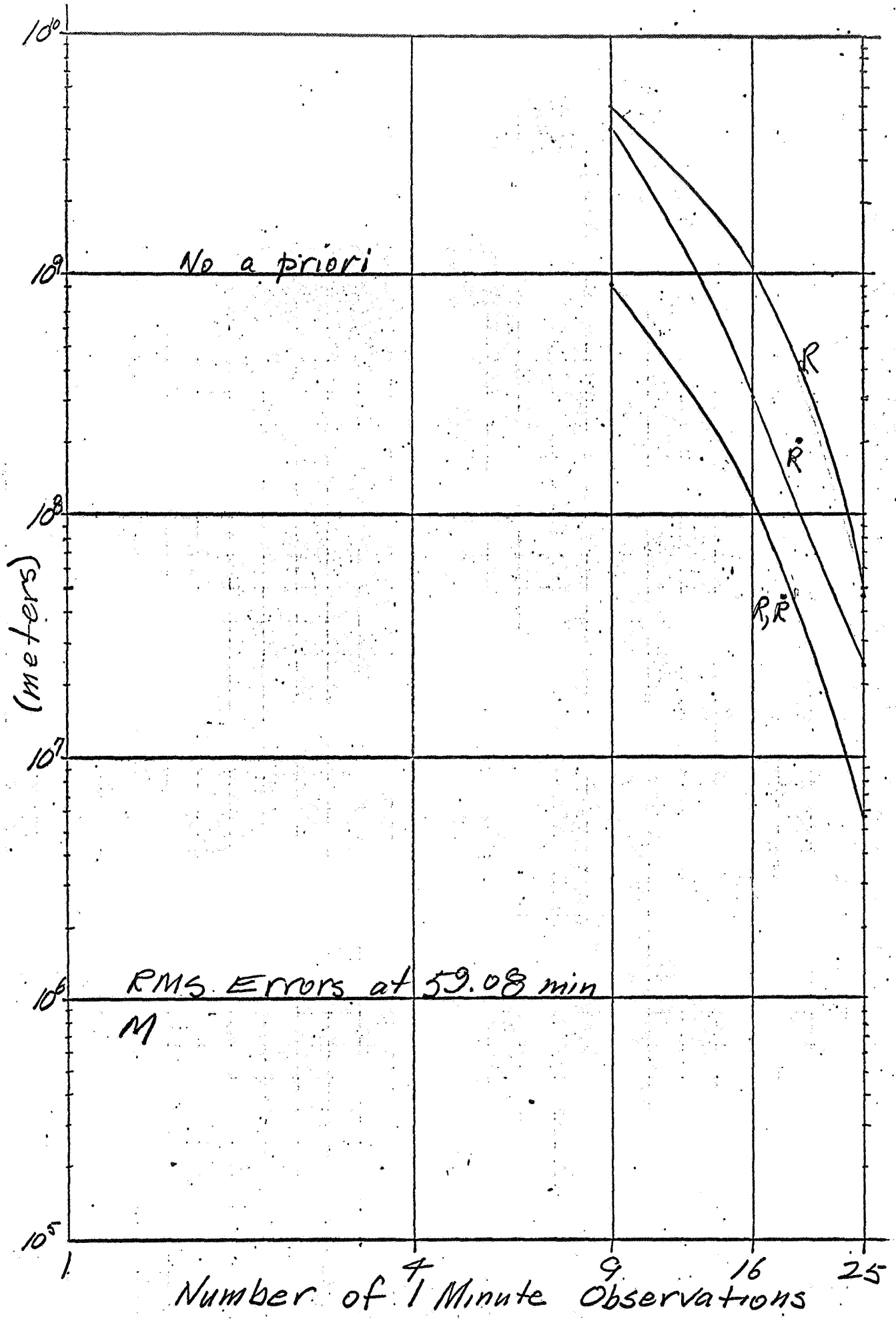
No a priori
R
Ṙ
R, Ṙ
RMS Errors at 59.08 min
M
(meters)
Number of 1 Minute Observations
1
4
9
16
25

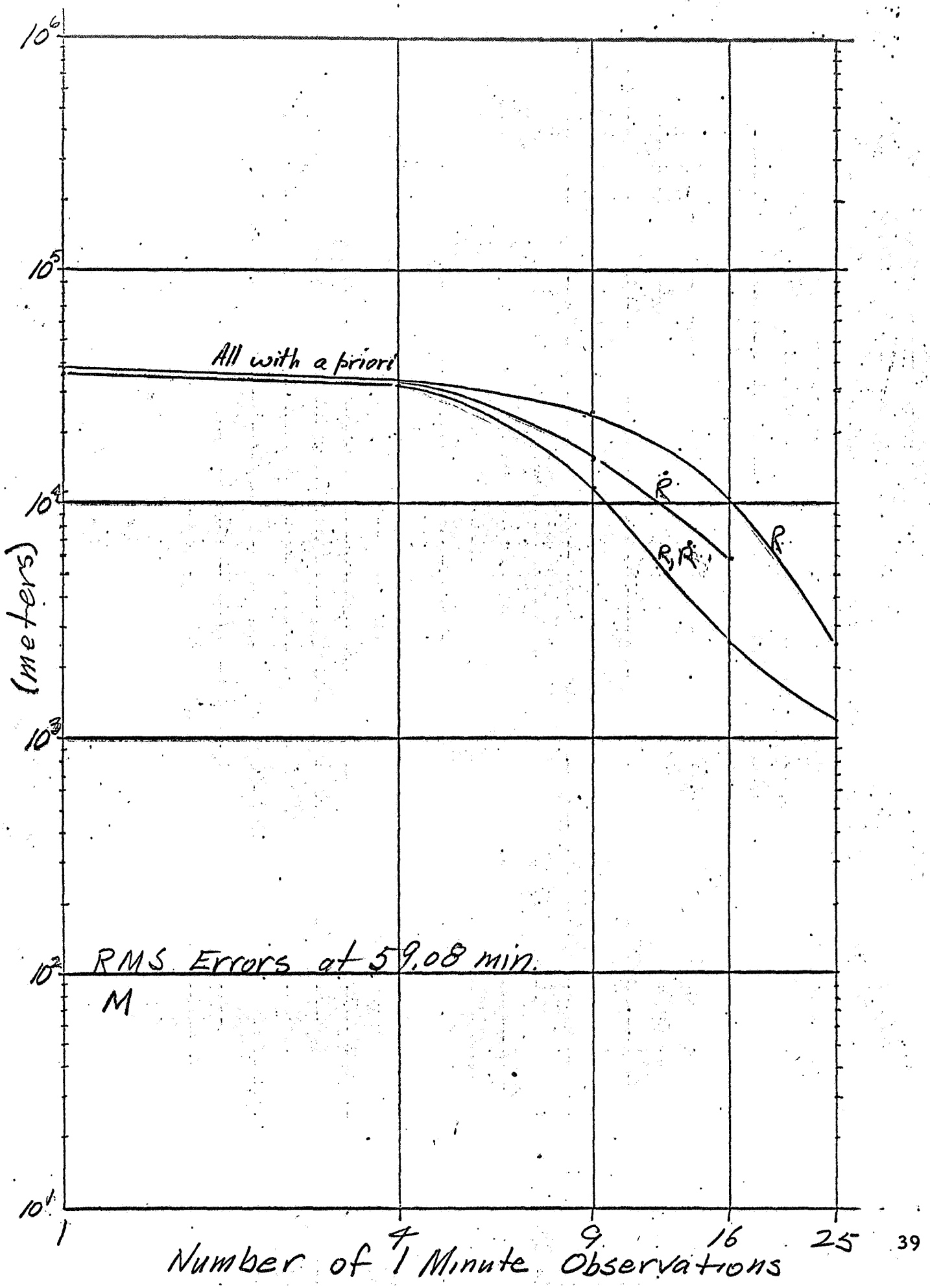
All with a priori
$\dot{R}$
R, $\dot{R}$
R
RMS Errors at 59.08 min.
M
(meters)
10^6
10^5
10^4
10^3
10^2
10^1
1
4
9
16
25
Number of 1 Minute Observations

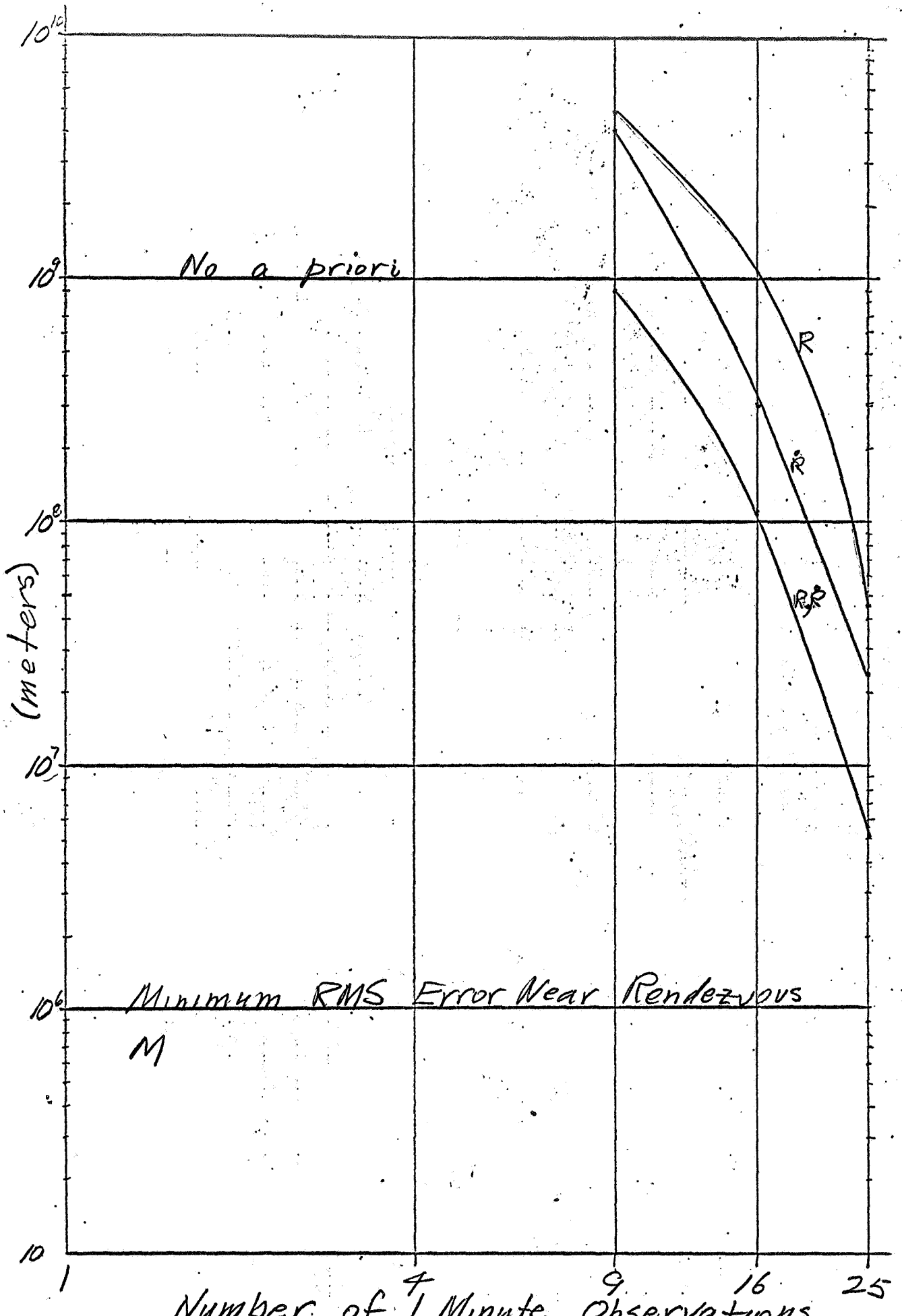
10^{10}
10^{9}
10^{8}
10^{7}
10^{6}
10
No a priori
R
$\dot{R}$
$R_{\dot{R}}$
Minimum RMS Error Near Rendezvous
M
(meters)
1
4
9
16
25
Number of 1 Minute Observations

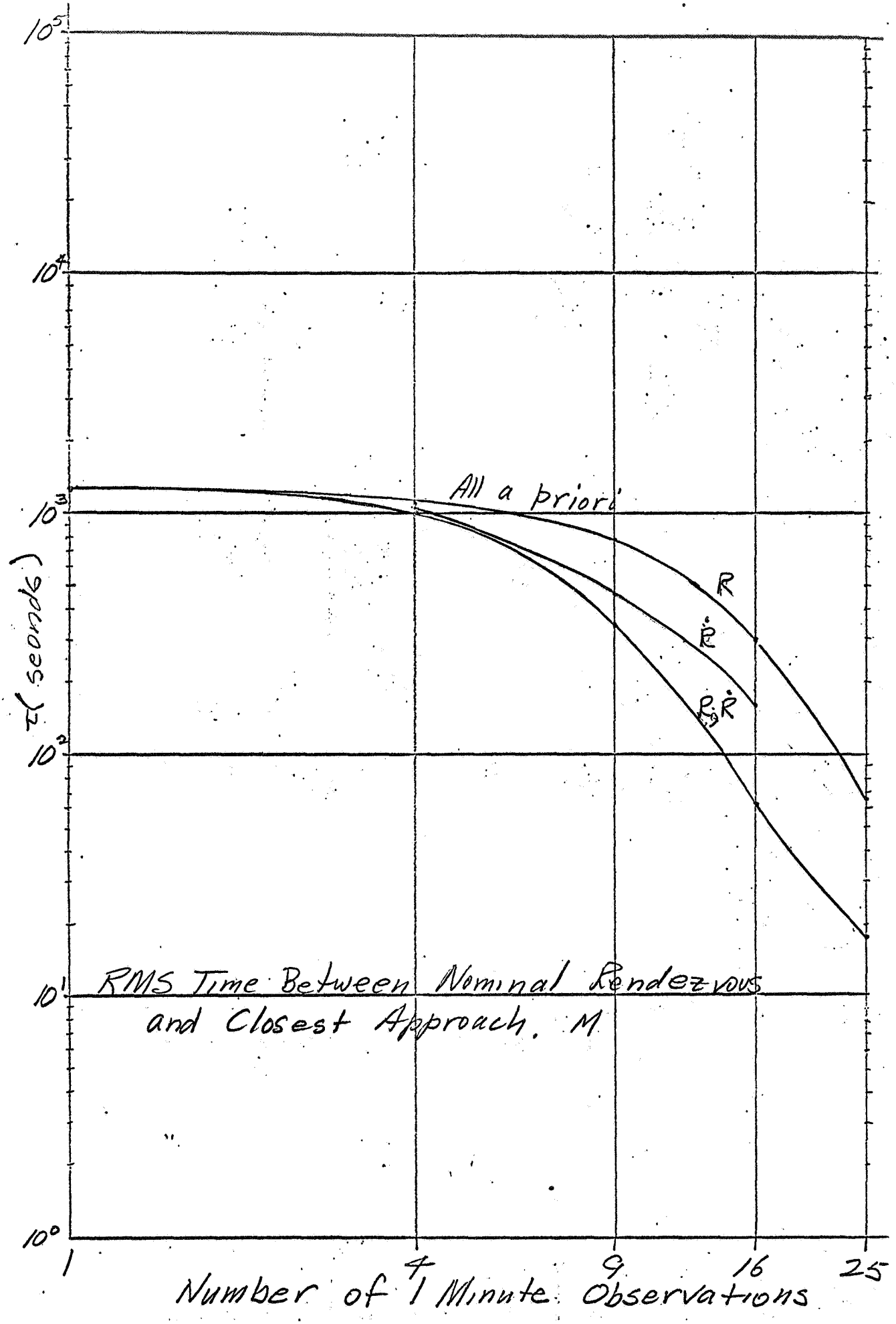
10^5
10^4
10^3
10^2
10^1
10^0
All a priori
R
$\dot{R}$
$R, \dot{R}$
τ (seconds)
RMS Time Between Nominal Rendezvous and Closest Approach, M
1
4
9
16
25
Number of 1 Minute Observations

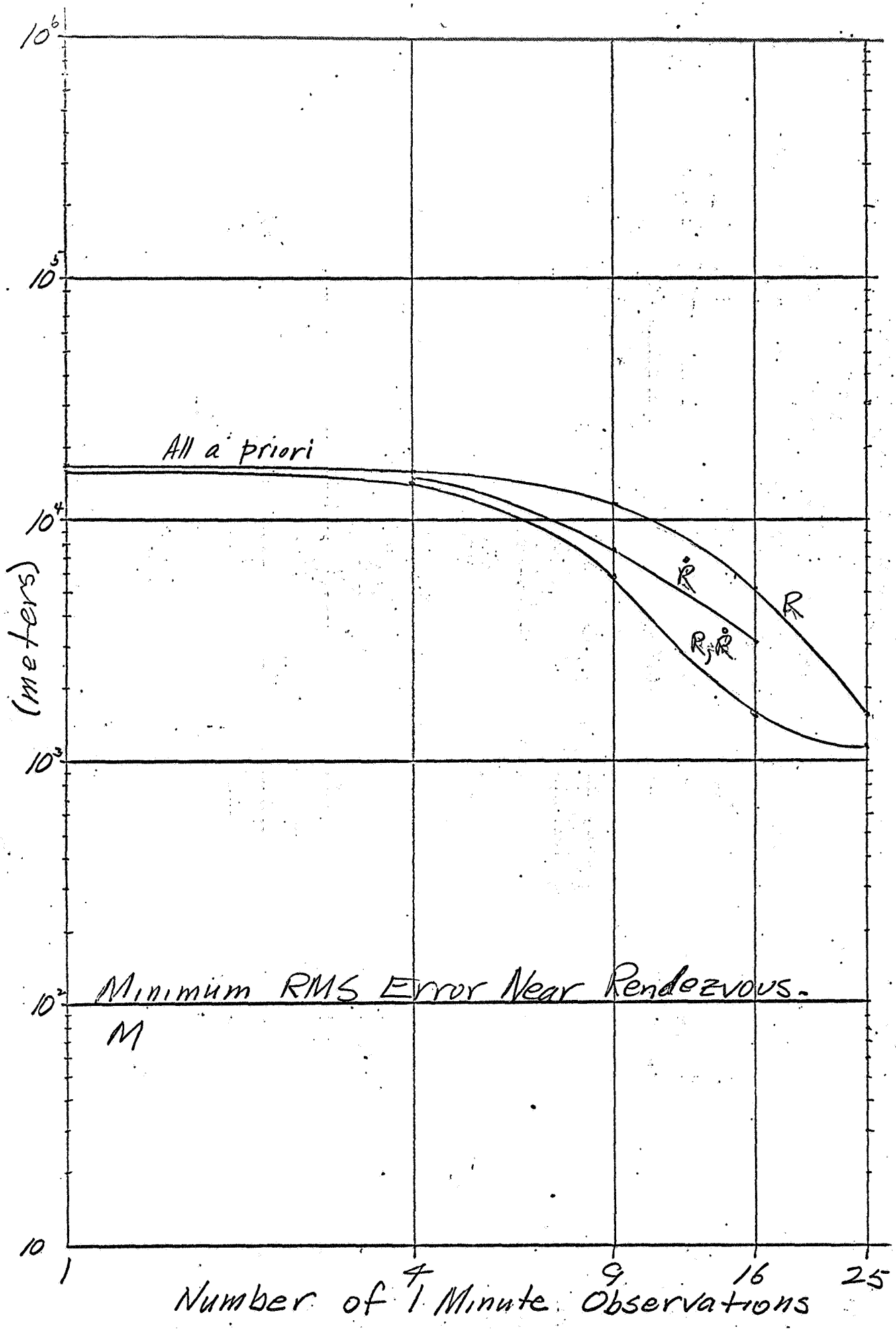
10^6
10^5
10^4
10^3
10^2
10
(meters)
All a priori
$\dot{R}$
R
R, $\dot{R}$
Minimum RMS Error Near Rendezvous.
M
1
4
9
16
25
Number of 1 Minute Observations

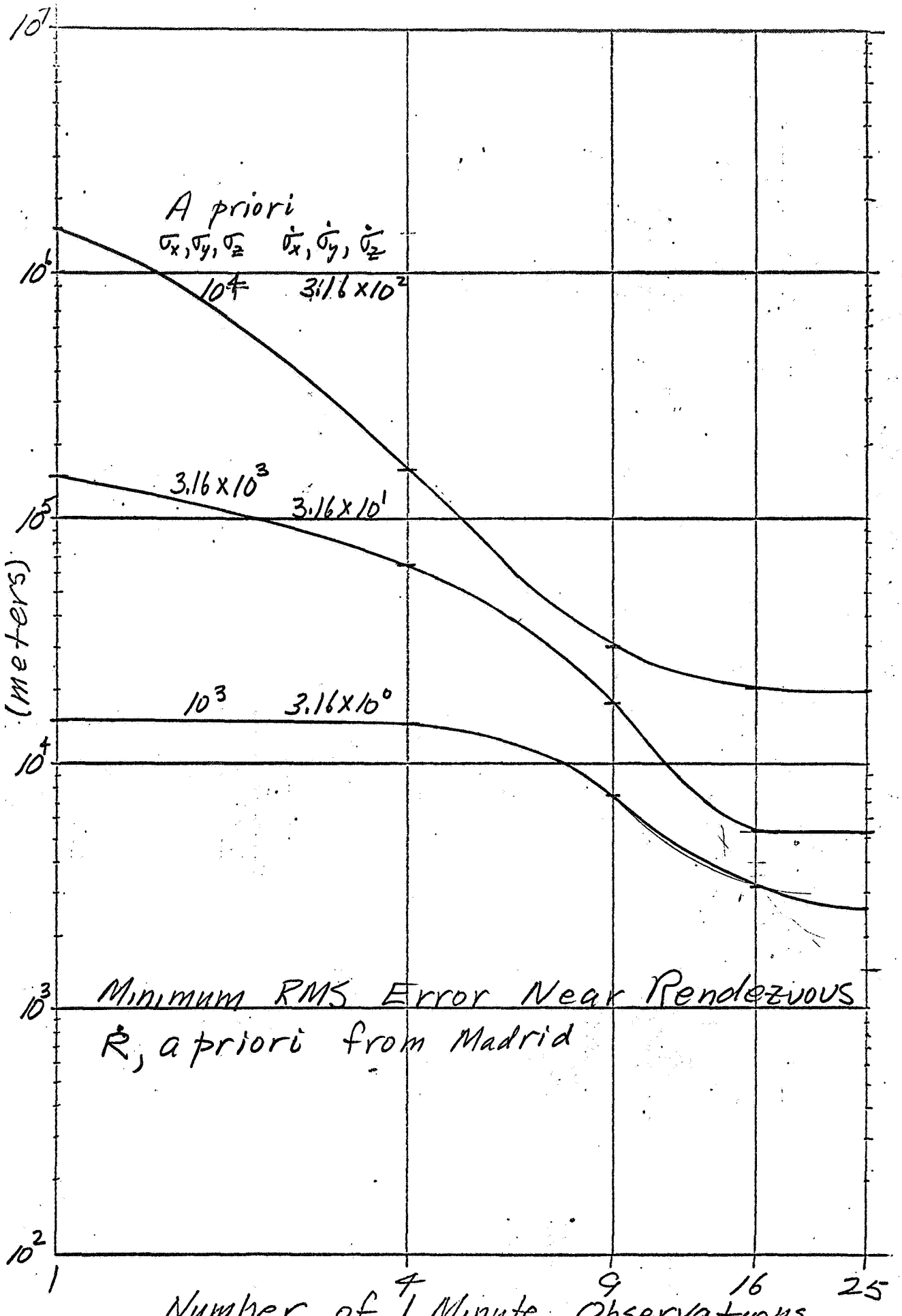
A priori
$\sigma_x, \sigma_y, \sigma_z$ $\dot{\sigma}_x, \dot{\sigma}_y, \dot{\sigma}_z$
10^4 3.16×10^2
3.16×10^3 3.16×10^1
10^3 3.16×10^0
10^7
10^6
10^5
10^4
10^3
10^2
(meters)
Minimum RMS Error Near Rendezvous
$\dot{R}$, a priori from Madrid
1
4
9
16
25
Number of 1 Minute Observations

APOLLO NOTE NO. 100

H. Dale
23 August 1963

ORBIT PARAMETERS FROM THREE STATIONS USING RANGE AND RANGE-RATE

Apollo Note No. 87 discusses the effect of measuring the position of the LEM by taking range and range-rate measurements from three stations equally spaced upon an Earth-based triangle. Three stations that could be used are those at Madrid, Johannesburg and Woomera. They are positioned upon the Earth as shown in the following sketch:

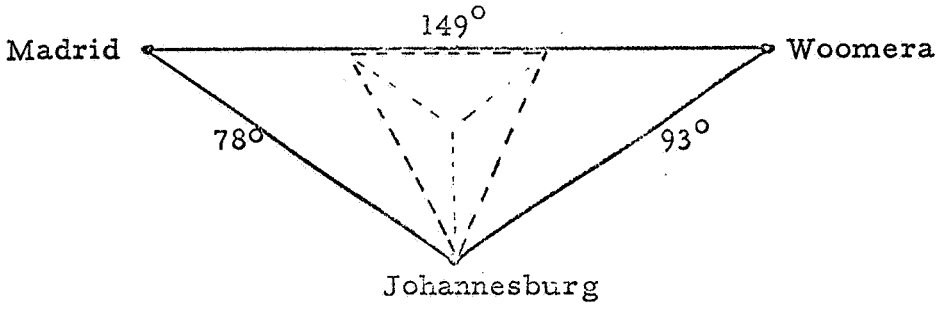

A conservatively placed 55° equalateral triangle is constructed within the above sketch. This triangle can be used along with Apollo Note No. 87 to estimate the expected error in position and velocity. From Apollo Note No. 87, page 9:

$$\delta x_2 = \frac{x_3}{3 x_{22}} \delta S_1$$

where x_3 = Earth-Moon Distance = 3.85×10^8 m.

x_{22} = $\frac{1}{\sqrt{3}}$ (half edge of triangle)

= $\frac{1}{\sqrt{3}} (R_e \sin 27^\circ) = \frac{.45\ (6.38 \times 10^6)}{1.732} = 1.67 \times 10^6$

δS_1 = error in measuring range from a single station

$\therefore \delta x_2 = 77\ \delta S_1$

From Apollo Note No. 87, it can be seen that δx_2 is an error in non-orthogonal three-dimensional planar co-ordinates, each axis at 60° to each other axis. Thus for equally likely errors in each of the range measuring stations

$$\overline{\sigma^2_{x_2}} = \left(\frac{1}{2}\delta x_2\right)^2 + \left(\frac{1}{2}\delta x_2\right)^2 + (\delta x_2)^2$$

$$= 1.5\,(\delta x_2)^2$$

Thus the expected error in position normal to the line-of-sight (in all directions)

$$\sigma_{x_{1,2}} = \sqrt{1.5\,(77\,\sigma S_1)^2} = 94\,\sigma S_1$$

where σS_1 is the estimated single station error in measuring range over some short smoothing time.

On page 11 of the referenced note, it is seen that the same sort of equation applies to $\dot{S}$ measurements. Thus

$$\sigma_{\dot{x}_{1,2}} = 94\,\sigma\dot{S}_1$$

With one-shot measurements of S and $\dot{S}$ expected errors are:

$$\sigma\dot{S} = 3 \text{ cm/sec} \Rightarrow \sigma_{\dot{x}_{1,2}} = 3 \text{ m/sec.}$$

$$\sigma_S = 15 \text{ meters} \Rightarrow \sigma_{x_{1,2}} = 1500 \text{ meters}$$

From Apollo Note 7, expressions exist for predicting the future positional error due to initial errors in a satellites velocity and position. Using equations (11) and (12) from Apollo Note No. 7 and realizing that range errors (corresponding to y in Note No. 7) are insignificant, then after 180° of travel:

$$x = \frac{4\dot{x}_o}{\omega} \sin \pi - \frac{3\dot{x}_o}{\omega} \pi + x_o$$

$$y = \frac{2\dot{x}_o}{\omega} \cos \pi + \frac{2\dot{x}_o}{\omega}$$

and at 180° $z = 0$, $\dot{z} = \dot{z}_o$. But since $\dot{x}_o$, x_o and $\dot{z}_o$ are actually random variables, then

$$\sigma_x = (\theta = 180^\circ) = \pm \left[\left(\frac{3\pi \dot{x}_o}{\omega} \right)^2 + x_o^2 \right]^{1/2}$$

$$\sigma_y = (\theta = 180^\circ) = \pm \frac{4\dot{x}_o}{\omega}$$

where ω is the nominal LEM angular rate ($.9 \times 10^{-3}$ rad/sec) and $\dot{x}_o = \sigma_{\dot{x}_{1,2}}$ and $x_o = \sigma_{x_{1,2}}$. Thus for the assumed numbers involved:

$\sigma_x (\theta = 180^\circ)$ = 31,000 meters (along the orbit path)

$\sigma_y (\theta = 180^\circ)$ = 13,000 meters (altitude)

$\sigma_z (\theta = 180^\circ)$ = 1,500 meters (out of track)

And it is interesting to note that the major error (along the orbit path) is strongly a function of range-rate measurements alone. Velocity errors at 180° were not calculated but will be small.